UNIVERSITÀ DEGLI STUDI DI MILANO

PhD course in Veterinary and Animal Science

Equine and bovine microvesicles derived from amniotic progenitor cells in regenerative and reproductive topics

PhD Supervisor:

Prof. Dr. Fausto Cremonesi

PhD Added Supervisor:

Dr. Anna Lange-Consiglio

PhD Student:

Claudia Perrini

Matr. R10416

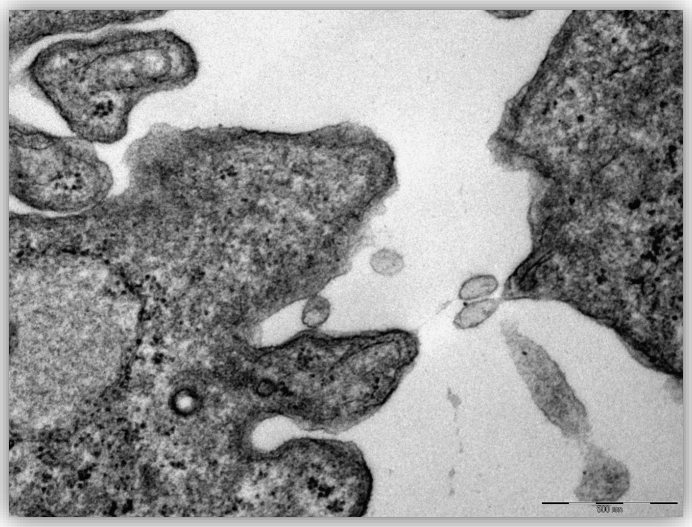

XXIX cycle VAS

Supervisors

Professor Fausto Cremonesi

Università degli Studi di Milano

Reproduction Unit

Centro Clinico-Veterinario e Zootecnico-Sperimentale di Ateneo

Via dell'Università 6 – 26900 Lodi (Italy)

Department of Veterinary Medicine,

Via Celoria 10 – 20133 Milano (Italy)

E-mail: fausto.cremonesi@unimi.it

Tel: +39 02 503 31150 Fax: +39 02 503 31115

http://www.veterinaria.unimi.it/Facolta/2605_ITA_HTML.html

Doctor Anna Lange-Consiglio

Università degli Studi di Milano

Head of Reproduction Laboratory

Centro Clinico-Veterinario e Zootecnico-Sperimentale di Ateneo

Via dell'Università 6 – 26900 Lodi (Italy)

E-mail: anna.langeconsiglio@unimi.it

Tel: +39 02 503 31150 Fax: +39 02 503 31115

http://www.veterinaria.unimi.it/Facolta/2605_ITA_HTML.html

RIASSUNTO

Durante questo progetto di dottorato sono stati condotti studi per comprendere la capacità delle cellule mesenchimali amniotiche (AMCs) di agire attraverso meccanismi paracrini. La prima fase del disegno sperimentale ha valutato l'efficacia delle AMCs sulla proliferazione delle cellule endometriali (EDCs) in assenza di un contatto cellula-cellula. Le EDCs sono state co-coltivate in un sistema trans-well con le AMCs o sono state coltivate in presenza del loro *medium* condizionato (CM). In entrambe le condizioni sperimentali è stato osservato un aumento del tasso di proliferazione delle EDCs definendo, così, il ruolo cruciale dei fattori secreti dalle AMCs come mediatori dell'azione delle cellule staminali. Il CM è composto da fattori solubili e non-solubili rappresentati da microvescicole (MVs). Per capire il ruolo delle MVs e del loro contenuto nell'azione paracrina, la seconda fase del disegno sperimentale è stata incentrata sull'individuazione del tipo di MVs secrete dalle AMCs e sulla loro efficacia in processi infiammatori *in vitro* su due importanti modelli sperimentali nella specie equina quali l'endometrio ed il tendine. La produzione di MVs è stata ottimizzata attraverso un'ultracentrifugazione del CM a 100.000 g per 1 ora. Attraverso lo strumento Nanosight è stato calcolato che la produzione di MVs da AMCs equine è di circa 2550±71 particelle/cellula, con una dimensione media di 258±55 nm. La microscopia elettronica a trasmissione ha confermato la presenza di vescicole cellulari che per dimensioni e modalità di secrezione sono state classificate come shedding vesicles. Per capire se le cellule endometriali (EDCs) e tendinee (TNCs) fossero target delle MVs secrete dalle AMCs, è stata studiata l'incorporazione delle medesime dopo marcatura con un fluorocromo lipofilico quale il PKH-26. Dopo uno studio di una curva dose-risposta è stato osservato che la dose ottimale per l'incorporazione di MVs in EDCs è stata di $50x10^6$ MVs/ml a 72 h e per le TNCs di $50x10^6$ MVs/ml a 24-48h. Per esaminare l'abilità delle MVs nel contrastare un processo infiammatorio, entrambe le linee cellulari sono state stressate *in vitro* con LPS e trattate con MVs. La vitalità cellulare, l'espressione di alcuni geni pro-infiammatori ed il rilascio delle rispettive citochine sono stati i parametri impiegati per valutare l'efficacia delle MVs. Per entrambe le linee cellulari, il tasso di apoptosi è drammaticamente salito nelle cellule trattate con LPS, rispetto al controllo (CTR). LPS ha indotto un aumento significativo dell'espressione di *TNF-α*, *IL-6* e *IL-1β* in EDCs e di *MMP-1*, *MMP-9*, *MMP-13* e *TNF-α* in TNCs. Le MVs sono state in grado di contrastare l'effetto di LPS, diminuendo il tasso di apoptosi in entrambe le linee cellulari e riducendo il livello di espressione dei geni pro-infiammatori. Una conferma di questi dati è stata ottenuta attraverso l'analisi delle

citochine pro-infiammatorie (TNF-β and IL-6) ed anti-infiammatorie (TGF-α) rilasciate dalle EDCs nel terreno di coltura, confermando l'abilità delle MVs di trasportare molecole capaci di contrastare la risposta infiammatoria in cellule stressate con LPS.
Data l'importanza del contenuto in miRNA delle MVs, sia nelle AMCs sia nelle loro MVs è stata studiata la presenza di tre miRNA (miR-335, miR-146a, and miR-26a-2) coinvolti nella regolazione dei processi infiammatori. Questi tre miRNA sono stati identificati sia nelle AMCs sia nelle MVs, di conseguenza, è possibile ipotizzare che l'espressione genica dopo infiammazione con LPS e trattamento con MVs possa essere stato modulato dal trasferimento di miRNAs dalle MVs alle cellule target.
Successivamente a questi studi, si è tentato di capire quanto in un processo rigenerativo possa essere imputato alle MVs e quanto ai fattori solubili presenti nel CM e, a questo proposito, è stata valutata l'abilità delle MVs di inibire la proliferazione delle cellule periferiche mononucleate del sangue (PBMC). La loro azione è stata comparata a quello del CM e del sovranatante (SN) ottenuto dal CM dopo scorporazione delle MVs. Il CM ed il SN hanno manifestato capacità immunosoppressiva ma, anche dopo un trattamento di sonicazione al fine del rilascio del loro contenuto, le MVs non hanno dimostrato quest'abilità. Questi risultati portano a dedurre che le MVs sono in grado di trasportare informazioni alle cellule target attraverso molecole capaci di contrastare l'effetto infiammatorio dovuto all'uso di LPS ma, tenendo in considerazione la mancanza di effetto immunomodulatorio, probabilmente *in vivo* la loro azione è integrata anche dalla presenza dei fattori solubili presenti nel CM.
I meccanismi paracrini materno-fetali sono di vitale importanza ai fini dell'instaurarsi di una gravidanza, per cui si è ritenuto interessante studiare questi meccanismi durante la produzione *in vitro* di embrioni bovini. Le differenti componenti del secretoma (CM, SN e MVs) ottenute da AMCs ed EDCs bovine sono state aggiunte al terreno di coltura embrionale a differenti giorni di coltura. I risultati hanno dimostrato che il giorno 5 è il migliore momento per la supplementazione e che le MVs di AMCs portano a migliori risultati qualitativi. Questi dati sono stati confermati dalla valutazione di alcuni geni coinvolti nell'apoptosi e nella protezione contro specie reattive dell'ossigeno. I motivi per i quali le MVs di AMCs si siano dimostrate migliori di quelle secrete dalle EDCs non sono ancora conosciuti ma è probabile che le EDCs coltivate in monostrato *in vitro* vadano incontro a de-differenziamento che altera la qualità del loro secreto.

In conclusione, è possibile affermare che le AMCs sono una linea cellulare affascinante in quanto derivano da materiale di scarto biologico, e quindi a basso costo, e possono essere impiegate in medicina rigenerativa per la loro capacità di trasportare informazioni alle cellule target. Le MVs possono offrire un nuovo strumento terapeutico privo di cellule nell'ambito della nanomedicina.

ABSTRACT

During this PhD project, studies were carried out to understand the ability of amniotic mesenchymal cells (AMCs) to act by paracrine mechanism. At first, AMCs and their conditioned *medium* (CM) were investigated in an *in vitro* model using equine endometrial cells (EDCs) as target. Proliferation of EDCs was studied co-culturing them with AMCs in a trans-well system or in presence of AMC-CM. In both conditions, there was a significant increase in EDC proliferation rate, defining the crucial role of factors secreted by AMCs in stem cells action. CM is composed of soluble factors and no-soluble factors as microvesicles (MVs). In this context, in the second step of this project, the presence and the type of AMC-MVs were identified to understand their role in regenerative medicine. The production of MVs was optimized through a CM ultracentrifugation at 100.000 g for 1 hour. Microvesicle production from equine AMCs was 2550±71 particles/cell, with a mean dimension of 258±55 nm. The transmission electron microscopy confirmed the presence of extra-cellular vesicles that were classified as shedding vesicles for their size and modality of secretion. In order to understand if endometrial cells (EDCs) tendon cells (TNCs) were target of these MVs, an incorporation study was performed labelling MVs with a lipophilic fluorochrome such as PKH-26. By a dose-response curve, the optimal conditions of incorporation were at 72 h at a concentration of $50x10^6$ MVs/ml for EDCs, and at 24-72 h at a concentration of $50x10^6$ MVs/ml for TNCs. In order to study MVs ability to counteract an *in vitro* inflammation, EDCs and TNCs challenged with LPS and treated with MVs were evaluated by viability cell tests, by expression of some pro-inflammatory genes, and by release of respective cytokines. For both cell types, the apoptosis rate increased dramatically in cells treated with LPS if compared to the control (CTR). LPS significantly upregulated the expression of *TNF-α, IL-6* and *IL-1β* in EDCs and of *MMP-1*, *MMP-9*, *MMP-13* and *TNF-α* in TNCs. MVs were able to counteract the action of LPS, decreasing the apoptosis rate and reducing in the expression levels of the pro-inflammatory genes in both cell lines. Coherent results were obtained through the analysis of pro-inflammatory (TNF-β and IL-6) and anti-inflammatory (TGF-α) cytokines released by EDCs in the culture *medium*, confirming the ability of MVs to transport molecules able to counteract the stress induced by LPS.

Since MVs contain various active molecules, the presence of three miRNAs (miR-335, miR-146a, and miR-26a-2) was investigated, as they are involved in the regulation of inflammation. The selected miRNAs have been found in both AMCs and their MVs, so the previously observed

downregulation of gene expression could be correlated to miRNA transfer from MVs to target cells. Moreover, the ability of MVs to inhibit peripheral blood mononuclear cell (PBMC) was evaluated, but MVs, also after lysis by sonication to release their content, were not able to inhibit PBMC proliferation despite to CM and SN. These results led to hypothesize that MVs brought to the target cells some molecules able to counteract the inflammatory situation due to the LPS but, taking into account the lack of their immunomodulatory action, probably, for an *in vivo* healing, soluble factor of CM are necessary too.

Paracrine mechanism are essential also in maternal-fetal communication. In this context, we studied these mechanisms during bovine *in vitro* embryo production. Different components of secretome (CM, SN and MVs) from bovine AMCs and EDCs were supplemented to the embryo culture *media* at different days of culture. The results demonstrated that the day 5 of culture is the best time point for the supplementation of these components and that AMCs-MVs provided the best environment for the embryo concerning the blastocyst quality. These data were confirmed by the evaluation of genes involved in apoptosis and reactive oxygen species protection. The reasons for which the MVs of AMCs have proved better than those secreted by EDCs are not yet known but it is likely that *in vitro* culture of EDCs in monolayer may induce a de-differentiation that alters the quality of their secretion.

As conclusion of this project, it is possible to speculate that AMCs are fascinating in view of producing off-the-shelf products, at low cost, and their use in regenerative medicine for their capacity to carry information to the target cells. The MVs may offer a new therapeutic cell-free tool in nanomedicine.

Structure of the work - The first section of this thesis gives a brief overview of the literature about the regenerative medicine, focusing the attention on the paracrine communication between cells. More details are provided on the description of extracellular vesicles that are supposed to be mainly involved in this paracrine action. The second section concerns some models for the study of the paracrine communication in regenerative veterinary medicine such as equine tendinitis and endometritis, and, furthermore, in bovine embryo production. Lastly, a list of the publications realized during my PhD project follows, within which it is possible to find the protocols used to study the mechanisms involved in these communications and the original results of the research of the 3-academic-year–period (2014-2016).

This thesis is based on the following papers:

I. Corradetti B, Correani A, Romaldini A, Marini MG, Bizzaro D, **Perrini C**, Cremonesi F, Lange-Consiglio A. *Amniotic membrane-derived mesenchymal cells and their conditioned media: potential candidates for uterine regenerative therapy in the horse.* 2014 PLoS One. 9(10):e111324.

II. **Perrini C**, Strillacci MG, Bagnato A, Esposti P, Marini MG, Corraddetti B, Bizzaro D, Idda A, Ledda S, Capra E, Pizzi F, Lange-Consiglio A, Cremonesi F. *Microvesicles secreted from equine amniotic-derived cells and their potential role in reducing inflammation in endometrial cells in an in vitro model.* 2016 Stem Cell Res Ther doi: 10.1186/s13287-016-0429-6

III. Lange-Consiglio A, **Perrini C**, Tasquier R, Deregibus MC, Camussi G, Pascucci L, Marini MG, Corradetti B, Bizzaro D, De Vita B, Romele P, Parolini O, Cremonesi F. *Equine amniotic microvesicles and their anti-inflammatory potential in a tenocyte model in vitro.* 2016 Stem Cell Dev 15;25(8):610-21.

IV. **Perrini C**, Esposti P, Compagnoni D, Treglia S, Cremonesi F, Lange Consiglio A. *Secretome derived from different cell lines in bovine in vitro embryo production*. 2016 Submitted to PlosOne

Other papers published during the PhD project include the following:

I. Lange-Consiglio A, Corradetti B, **Perrini C**, Bizzaro D, Cremonesi F. *Leptin and leptin receptor are detectable in equine spermatozoa but are not involved in in vitro fertilization.* 2014 Reprod Fertil Dev 28(5):574-85.

II. Lange-Consiglio A, Cazzaniga N, Garlappi R, Spelta C, Pollera C, **Perrini C**, Cremonesi F.

Platelet concentrate in bovine reproduction: effects on in vitro embryo production and after intrauterine administration in repeat breeder cows. 2015 Reprod Biol Endocrinol 13:65.

III. Lange-Consiglio A, Corradetti B, Bertani S, Notarstefano V, **Perrini C**, Marini MG, Arrighi S, Bosi G, Belloli A, Pravettoni D, Locatelli V, Cremonesi F, Bizzaro D. *Peculiarity of porcine amniotic membrane and its derived cells: a contribution to the study of cell therapy from a large animal model.* 2015 Cell Reprogram 17(6):472-83.

IV. Lange-Consiglio A, Romaldini A, Correani A, Corradetti B, Esposti P, Cannatà MF, **Perrini C**, Marini MG, Bizzaro D, Cremonesi F. *Does the bovine pre-ovulatory follicle harbor progenitor stem cells?* 2016 Cell Reprogram 18(2):116-26.

V. Marini MG, **Perrini C**, Esposti P, Corradetti B, Bizzaro D, Riccaboni P, Fantinato E, Urbani G, Gelati G, Cremonesi F, Lange-Consiglio A. *Effects of platelet-rich plasma in a model of bovine endometrial inflammation in vitro.* 2016 Reprod Biol Endocrinol doi: 10.1186/s12958-016-0195-4

VI. Lange-Consiglio A, **Perrini C**, Bertero A, Esposti P, Cremonesi F, Vincenti L. *Isolation, molecular characterization and in vitro differentiation of bovine Wharton's jelly-derived multipotent mesenchymal cells.* 2016 Theriogenology doi: 10.1016/j.theriogenology.2016.09.042.

VII. Andrade GM, da Silveira JC, **Perrini C**, del Collado M, Gebremedhn S, Tesfaye D, Meirelles FV, Perecin F. *MicroRNA mediated regulation and role of PI3K-Akt pathway in bovine oocyte developmental competence.* 2016 Submitted to Scientific Reports.

Table of contents

LIST OF ABREVIATION

AKI: acute kidney inflammation

AMC-MVs: amniotic mesenchymal cells derived microvesicles

AMCs: amniotic mesenchymal cells

bp: base pair

CD: cluster of differentiation

CM: conditioned *medium*

c-MYC: v-myc avian myelocytomatosis viral oncogene homolog

CTR: control

DNA: deoxyribonucleic acid

dsRNA: double strand RNA

EDCs: endometrial cells

EGF: epidermal growth factor

ESCs: embryonic stem cells

GTP: guanosine triphosphate

GTPase: GTP hydrolase enzymes

HLA-DR: human leukocyte antigen - D related

ICM: inner cell mass

IGF: insulin-like growth factor

IL: interleukine

iPS: induced pluripotent stem cells

ISCT: International society for cellular therapy

IVC: *in vitro* culture

IVP: *in vitro* production

lncRNA: long noncoding RNA

Log FC: logarithm of fold change

LPS: lipopolysaccharide

miRNA: micro RNA

MMP: metalloprotease

mRNA: messenger RNA

MSC-MVs: mesenchymal stromal cells derived microvesicles

MSCs: mesenchymal stromal cells

MVs: microvesicles

NANOG: Nanog homebox

NK: natural killer

OCT 4: octamer-binding transcription factor 4

p53: tumor protein p53

PDGF: platelet derived growth factor

piRNA: piwi-interacting RNAs

Piwi: p-element induced wimpy testis

PMNs: polymorphnuclear neutrophils

pre-miRNA: precursor miRNA

pri-miRNA: primordial miRNA

PRP: platelet-rich plasma

PTEN: phosphatase and tensin homolog

Rho-A: ras homolog family member A

RISC: RNA-induced silencing complex

RNA: ribonucleic acid

RNAi: RNA interference

rRNA: ribosomal RNA

RT-qPCR: quantitative reverse transcription polimerase chain reaction

SCF: stem cell factor

SN: supernatant

snoRNA: smal nucleolar RNA

snRNA: small nuclear RNA

TGFβ1: transforming growth factor beta-1

TEM: transmission electron microscopy

TNCs: tendon cells

TNF- α : tumor necros factor α

tRNA: transfer RNA

VEGF: vascular endothelial growth factor

1. INTRODUCTION

Regenerative medicine is a newly emerging and multidisciplinary field based on biology, medicine and genetic manipulation for the development of strategies aimed to restore, maintain, or enhancing the function of tissues or organs that have been compromised through disease, pathology or injury. Many treatments have been proposed for the regenerative medicine, but stem cell based therapies, nowadays, represent promising opportunities to repair or replace diseased or damaged tissues otherwise not treatable by conventional pharmaceutical remedies.

The use of adult stem cells, such as mesenchymal stromal cells (MSCs), have represented a good therapeutic approach to the study and the treatment of many injuries. Unfortunately, stem cells derived from adult tissues are considered more limited in their potential and growth as compared to embryonic stem cells (Paris and Stout, 2010). Moreover, the risk of the immunological rejection of the transplanted cells by the recipient is another important limiting factor. For the effective application of stem cells in regenerative medicine, a large number of cells should be non-invasively collected without risk for the donor and with the ability to cryogenically bank and expand the cells. In human medicine, placenta-derived amniotic mesenchymal cells (AMCs) have been reported as an alternative and novel class of stem cells with intermediate characteristics between embryonic and adult stem cells. Firstly, placental tissues are generally discarded after parturition overcoming any ethical issues. Secondly, the amount of the tissue is so abundant that a large number of cells can be easily collected. The origin of these tissues supports the possibility that they may contain cells with the plasticity typical of the early embryonic cells. Lastly, since placenta is involved in the maintenance of fetal-maternal immune tolerance during pregnancy, AMCs should have higher immunomodulatory capacities than adult MSCs (Arnhold et al., 2007).

After isolation, stem cell can be administered into the organism intravenously, or directly into the lesioned tissue. This last route, when possible, allows to use a lower amount of cells with the highest concentration into the area of interest. In any case, recently, it has been demonstrated that the inhospitable environment of the lesion, due to the presence of inflammation cells and molecules, could lead to a premature cell death of the injected cells (Leung et al., 2006). For these reasons, researchers hypothesized that cells could not directly be responsible of the healing, but products released from the cells themselves could intervene in the regenerative process, instead. Conditioned *medium* (CM) is defined as the culture *medium*

enriched of soluble factors and microvesicles (MVs) released by the cultured cells. CM has been already demonstrated to have the same *in vivo* effect of the administration of the stem cells of origin, when injected into spontaneous equine tendon lesions (Lange-Consiglio et al., 2013a). For this reason, recently, the paracrine effect involving CM and MVs is subject of further studies. This PhD work aimed to better understand the mechanism of paracrine communication involving MVs derived from amniotic progenitor cells in two *in vitro* model studies: tendon lesion and endometritis in the equine species. In addition, paracrine mechanisms of communication between bovine embryos and amniotic and endometrial cells secretome were studied.

2. SOURCE OF STEM CELLS

Stem cells are primitive cells with the capacity of self-renewal and the ability to give rise to other cell types in a process known as differentiation. Differentiation can be toward specific lineage progenitors, which have the capacity to grow, or toward a terminal and highly specialized state no longer capable to grow (Morrison et al., 1997; Lovell-Badge, 2010). Stem cells have been isolated from all stages of life, from preimplantation embryos to adulthood. Categories of stem cells have been described based on their tissue of origin (Igura et al., 2004; Zhang et al., 2006)

- embryonic stem cells (ESCs) derived from in the inner cell mass (ICM) of the early preimplantation embryo (Evans and Kaufman, 1981; Martin, 1981)
- fetal stem cells isolated from fetal tissues (Guillot et al., 2006)
- extra-fetal cells isolated from extra-fetal tissues, such as amniotic membranes (Marcus and Woodbury, 2008; Lange-Consiglio et al., 2012)
- adult stem cells isolated from mature tissues such as, for example, bone marrow (Pittenger et al., 1999), adipose tissue (Zuk et al.,2001), periosteum (Hanada et al., 2001), brain (Mackay et al., 1998), muscle (Williams et al., 1999).
- induced pluripotent stem cells (iPS) that represent a newest category, since they are stem cells obtained by reprogramming of adult cells into ESC-like cells.

According to their differentiation potential, stem cells have been classified mainly into four categories: totipotent, pluripotent, multipotent and unipotent. The best known totipotent cell is the zygote that has the ability to give rise to an entire living organism. Once the blastocyst stage is reached, embryonic stem cells isolated from the ICM lose the totipotency of the zygote but are still able to differentiate into the three germ layers, so they are pluripotent. Based on their self-renewal and differentiation abilities, ESCs are hierarchically higher than other cell types that have more restricted properties, but it is important to take into account potential problems in clinical applications aroused by their high tumorigenic rate after transplantation (Kooreman and Wu, 2010) and ethical issues. Adult stem cells represent a population with more restricted differentiation potential respect to ESCs, because they are considered multipotent. Multipotent progenitors exist in a variety of tissues, including fetal, extra-fetal and adult tissues. Among stem cells, there are mature cells committed only for a single cell line and for this reason are defined unipotent (Mathur and Martin, 2004).

The international society for cellular therapy (ISCT) has proposed the following minimum

criteria for the definition of the MSCs (Dominici et al., 2006):

- adherence to plastic surfaces under standard cell culture conditions
- expression of cell surface markers, such as cluster of differentation (CD) CD90, CD73 and CD105, and lack of expression of CD14, CD34, CD45, CD79, CD19 and human leukocyte antigen - D related, HLA-DR
- capability to differentiate into chondrocytes, osteoblasts and adipocytes

3. AMNIOTIC MESENCHYMAL CELLS: THE HUMAN LESSON

The requirement for extended self-renewal capacity becomes less important when, as in fetal and extra-fetal tissues, abundant multipotent cells can be obtained from the starting material for regenerative medicine applications. Extra-fetal tissues, such as amniotic membranes, are routinely discarded at parturition, so there is less ethical controversy attending the harvest of the resident stem cell populations. Amnion is a thin avascular membrane composed of an inner epithelial layer and an outer connective tissue layer. To obtain cells from term delivered amnion, this membrane is separated from allantois by peeling them apart. The elastin lamina in the loose connective tissue of the amnion facilitates the separation of the membranes. Typically, human amnion stromal cells, called amniotic mesenchymal cells (AMCs), are obtained after complete removal of the epithelial layer using trypsin followed by digestion in collagenase (Donofrio et al., 2005). Because human amniotic membrane differentiates from the epiblast at a time when it retains pluripotency, it is reasonable to speculate that AMCs may have escaped the specification that accompanies gastrulation and that these cells may preserve some or all of the characteristics of the epiblast such as pluripotency (Miki and Strom, 2006). Immunohistochemical and quantitative PCR analysis demonstrated that AMCs express typical MSC phenotypical markers (*CD105*, *CD90* and *CD73*) and stem cell marker (octamer-binding transcription factor 4, *OCT4*; Nanog homebox, *NANOG*; stem cell factor, *SCF*; v-myc avian myelocytomatosis viral oncogene homolog, *c-MYC*; keratinocyte marker 19 and 8; and β1-integrin) (Bilic et al., 2008; Yu et al., 2015; Kwon et al., 2016). These data, taken together, indicate that some stem cell marker-positive cells are conserved over the course of pregnancy. These cells possess immune suppressive activity on T-lymphocytes (Magatti et al., 2008; Alikarami et al., 2015), multipotent differentiation ability (Barzilay et al., 2008; Carraro et al., 2008; Sun and Ji, 2009; Connell et al., 2013; Moussavou et al., 2013; Jiawen et al., 2014) low immunogenicity (Kubo et al., 2001) and anti-inflammatory activity (Toda et al., 2007).

Several clinical trials demonstrated prolonged survival of human amniotic membrane or human AMCs after xenogeneic transplantation into immunocompetent animals, including rabbits (Avila et al., 2001) and rats (Kubo et al., 2001), suggesting active migration and integration into specific organs, and indicating active tolerance of the xenogeneic cells (Evangelista et al., 2008).

Amniotic membrane has been used in ocular surface reconstruction for substrate transplantation to promote the development of normal corneal or conjunctival epithelium without acute rejection in absence of immunosuppressive treatment (Gomes et al., 2005).

Amniotic membrane transplantation is an effective clinical therapy for reconstruction of the ocular surface also in veterinary patients such as horses (Lassaline et al., 2005; Ollivier et al., 2006; Plummer, 2009) and dogs (Arcelli et al., 2009) because it is avascular and strong, promotes re-epithelialization, decreases inflammation and fibrosis (Solomon et al., 2005) and modulates angiogenesis (Dua et al., 2004). Several growth factors, such as transforming growth factor, keratinocyte growth factor and hepatocyte growth factors, produced from amniotic membrane are involved in these processes (Koizumi et al., 2000).

4. PARACRINE MECHANISMS OF COMMUNICATION

Communication between cells is required for proper development and functioning of tissues, either via direct interactions or via secreted factors (Tetta et al., 2013). In the past, these secreted factors included small soluble molecules (neurotransmitters, chemokines, cytokines and hormones) that could behave in a paracrine manner (short distances) or in an endocrine manner (long distances) (Morhayim et al., 2014). Nowadays, the molecules and vesicles produced and secreted from a cell are commonly defined “secretome”. This concept born from the hypothesis that after the administration of stem cells into the damaged area, the regeneration is due to secretome rather than to the presence of the cells themselves. In fact, some studies reported beneficial effects of stem cell therapy in degenerative diseases or lesions and revealed that stem cells led to tissue repair due to their ability to secrete trophic factors that exert beneficial impact on the damaged tissue, rather than their capacity to differentiate into the needed cells (Lange-Consiglio et al., 2013a; Yang et al., 2013). Various studies on stem cell-derived secreted factors showed that these products alone without the stem cells themselves might led to tissue repair in various conditions that involved tissue/organ damage. Secretome can be identified as the culture *medium*, called conditioned *medium* (CM) (Kim and Choi, 2013) where the stem cells are cultured.

4.1 CONDITIONED *MEDIUM*

The use of CM has several advantages compared to the use of stem cells, as it can be manufactured, freeze-dried, packaged and transported more easily. Moreover, as it is a cell free product, there is no need to match the donor and the recipient to avoid rejection problems. Therefore, CM have a promising prospect to be produced as pharmaceuticals for regenerative medicine. So far, CM has been produced from several cells type, such as mesenchymal stem cells (derived from adipose tissue, bone marrow), embryonic and extra-fetal stem cells and iPS.

The process to produce CM is easy: cells need to be cultured in their typical culture *medium* added or not with supplements. Some authors add fetal bovine serum to the *medium*, while others use serum-free media. Culture *medium* represents a microenvironment that mimic the *in vivo* conditions and may determine cell fate and thus cell secretion (Goswami and Kaplan, 2011). The timing for the CM production varies in culture duration from sixteen hours to five days (Mirabella et al., 2011; Ho et al., 2012). The production of CM can also differ from cell culture in normoxia (oxygen level of 20-21%) and variable oxygen deprived (hypoxia with

oxygen level from 0.5% to 2%) condition. Conditioned *medium* contains various growth factors and tissue regenerative agents, which are secreted by the stem cells. Each stem cell type, depending on its very typical nature, can secrete different factors. Some anti-inflammatory cytokines that have been described to be secreted by stem cells are transforming growth factor beta-1 (TGFβ1), interleukine (IL) 6, 10, 27, 17E, 13, while the secreted pro-inflammatory cytokines are IL-8, IL-9, and IL-1β (Mirabella et al., 2011). In CM, various factors may be present and act in concert to promote regeneration in several pathological conditions. Most of the stem cells secrete vascular endothelial growth factor (VEGF) that plays a role on angiogenesis that is important in regeneration of injured/damaged tissues/organs (Sadat et al., 2007). In addition, VEGF may prevent apoptosis in hypoxic condition, preventing further damage. Other growth factors contribute in the regeneration of injured/damaged tissue organs, with special emphasis on proliferation, such as platelet derived growth factor (PDGF) for connective tissue, glial and other cells, epidermal growth factor (EGF) for mesenchymal, glial and epithelial cells, and insulin-like growth factor (IGF) I and II for various kinds of cells (Litwack, 2008). Pro-inflammatory cytokines that play a role in regeneration are IL-1β due to its liver protective role, IL-8 due to its angiogenic activity, and IL-9 due to wound healing promotion activity (di Santo et al., 2009). In addition, anti-inflammatory cytokines prevent inflammation, promote liver regeneration, promote tissue repair, prevent apoptosis, induce vasodilatation, reduce cellular oxidative stress and apoptosis and induce bone marrow stem cell proliferation (Zagoura et al., 2012).

The use of CM for therapy is very appealing and may be booming in the near future, as studies on the use of CM for various diseases are accumulating. Conditioned *medium* have already been tested in various kinds of human diseases/conditions, for example alopecia (Fukuoka et al., 2012), acute and chronic hind limb ischemia (Mirabella et al, 2011), acute and chronic wound healing (Lee et al., 2011), myocardial infarct (Yang et al., 2013), acute liver injury/failure (Zagoura et al., 2012), cerebral injury/ischemia/stroke (Inoue et al., 2013), spinal cord injury (Cantinieaux et al., 2013), and showed improvement of these conditions. A study in mice demonstrated that dental pulp-derived stem cell CM protects the heart from injury in response to ischemia/reperfusion through at least two mechanisms, improvements in myocardial cell viability and suppression of inflammatory cytokines (Yamaguchi et al., 2015). Another example is the application of implants treated with CM secreted by human deciduous teeth stem cells to promote bone morphogenesis during the early stages of osseo-integration, facilitating the bone

regeneration around dental implants (Omori et al., 2015). Concerning other stem cell source, CM secreted by human notochordal cells restored chondrocyte cartilage matrix production to healthy chondrocyte baseline levels in a model of osteoarthritic articular, significantly counteracts by the production of potent pro-inflammatory cytokines (Müller et al., 2016). Again, human bone marrow MSCs-CM has been reported to have partly protective effects against induced nephrotoxicity in a model of rat acute kidney injury (Abedi et al., 2016).

In veterinary medicine, CM has only been tested *in vivo* in spontaneous tendon lesions in sportive horses with results, in term of relapses, overlapping those obtained by the use of stem cells of origin (Lange-Consiglio et al., 2013a,b).

4.2 EXTRACELLULAR VESICLES

A specific route of cell-to-cell communication that has gained more and more attention is the communication via extracellular vesicles, also called microvesicles (MVs). They have been studied in several biological processes and are discovered now as novel mediators of intercellular communication both in health system and during disease evolution (Yoon et al., 2014). Extracellular vesicles are membrane-bound vesicles that transfer information such as lipids, proteins and nucleic acids from one cell to another, thereby influencing the recipient cell function (Raposo and Stoorvogel, 2013; Yanez-Mo et al., 2015). They form a heterogeneous group of small particles commonly categorized in three main classes (Hristov et al., 2004; Cocucci et al., 2009; Simons and Raposo, 2009; Morhayim et al., 2014; Yanez-Mo et al., 2015):

- exosomes, formed within the endosomal network and released after the fusion of multivesicular bodies with the plasma membrane (10–100 nm dimension)
- microvesicles/microparticles/ectosomes/shedding vesicles/matrix vesicles produced by outward budding of the plasma membrane (100–1000 nm dimension)
- apoptotic bodies that are released when dying cells fragment (0.8–5 μm dimension)

Unfortunately, the terminology in the literature is a bit confounding, because the term “microvesicles” identify either the whole vesicles group or the specific 100-1000 nm dimension category. For this reason, in order to simplify the comprehension of the reader, from now on, the term “microvesicles” will be used as synonymous of “extracellular vesicles”.

4.3 ISOLATION AND CHARACTERIZATION METHODS OF MICROVESICLES

One major challenge in the expanding field of MV research is to improve and standardize

methods for MV isolation and characterization. Currently, differential centrifugation is the “gold standard” procedure for this purpose (Thery et al., 2006). In this method, biological fluids or supernatants of cultured cells undergo multiple sequential centrifugations, starting from low speed to remove cellular debris, followed by increasing speeds to isolate smaller particles. Apoptotic bodies and big microvesicles are commonly pelleted at around 10.000 g, whereas small shedding vesicles and exosomes require high-speed centrifugation (≥100.000 g) (Thery et al., 2006). Microvesicles-depleted serum and/or serum-free *medium* incubation before MVs collection are essential for cell cultures to eliminate MVs and protein contaminants from bovine fetal calf serum (Morhayim et al., 2014). Other isolation methods for MVs, which have been developed to date, include ultrafiltration, sucrose density gradient, size-exclusion chromatography and immune-affinity capture (Taylor and Shah, 2015). The most used methods to characterize MVs include biochemical, fluidic and imaging analyses. Western blot and flow cytometry are also used to study MVs with known vesicle markers (Wubbolts et al., 2003). The analysis of smaller sized MVs is difficult with conventional flow cytometry as it cannot distinguish particles <250 nm. This led to the recent development of a high-resolution flow cytometry that could quantify immune-labeled MVs in the range of 100–200 nm (van der Vlist et al., 2012). Nanoparticle tracking analysis is another method that allows quantification and determination of size distribution of MVs as small as 50 nm, based on their Brownian motion in fluids (van der Pol et al., 2010; Zheng et al., 2013).

4.4 MOLECULAR COMPOSITION OF MICROVESICLES

Microvesicles contain a specific composition of nucleic acids, proteins, as well as lipids in a functionally active form. Because of the increasing interest in MV research, public online databases that document the molecular content of MVs are available. These include Vesiclepedia (www.microvesicle.org) (Kalra et al., 2012), Evpedia (www.evpedia.info) (Kim et al., 2013) and ExoCarta (www.exocarta.org) (Simpson et al., 2012) which are based on proteomic, lipidomic, microarray and deep sequencing analyses of different MV populations described in literature. Knowledge on the molecular composition of MVs is pivotal to understand the relation with cellular origin, biogenesis and interactions with target cells. The role of MVs in intercellular communication is supported by the fact that nucleic acids are found to be enriched in MVs. In 2006, the presence of functional ribonucleic acid (RNA) in murine stem cell derived-MVs was described for the first time (Ratajczak et al., 2006). Microvesicles do not only contain messenger

RNA (mRNA) (Baj-Krzyworzeka et al., 2006) but also micro RNA (miRNA), long noncoding RNA (lncRNA), piwi-interacting RNA (piRNA), ribosomal RNA (rRNA), transfer RNA (tRNA), small nuclear RNA (snRNA), and small nucleolar RNA (snoRNA) (Huang et al., 2013). The presence or absence of genomic deoxyribonucleic acid (DNA) fragments into MVs is still debated. In addition to nucleic acids, MVs are also highly abundant in proteins. Most predominantly, MVs are enriched in cytoskeletal, cytosolic, heat shock, plasma membrane, and vesicular trafficking proteins (Mathivanan and Simpson, 2009; Morhayim et al., 2014). These proteins are involved in a broad range of function including MV biogenesis, selection of cargo, as well as binding and uptake by target cells (Hemler, 2003; Perez-Hernandez et al., 2013). Among MV protein, tetraspanins are the best described proteins and have been widely used as markers for MVs (Andreu and Yanez-Mo, 2014). Tetraspanins may be coupled to chaperones such as heat shock proteins that aid in the sorting machineries of vesicular cargo (Hegmans et al., 2004). Markers, such as CD9, CD63, CD81, CD82 and CD151 are shared among MV groups from various cellular sources, while others are restricted to particular cells. For instance, CD37 and CD53 are characteristic for hematopoietic cells-derived MVs (Andreu and Yanez-Mo, 2014). The bilayer membrane of MVs is formed by lipids, which provide structure and protect MV cargo from degradation before they reach their targets. MVs are generally enriched in cholesterol, sphingomyelin, phosphatidylserine and glycosphingolipids, compared to their parent cells (Record et al., 2014). Besides providing structure, MV lipids play pivotal role in vesicular formation, release and intercellular communication (Llorente et al., 2007; Subra et al., 2010; Record et al., 2014).

4.5 BIOGENESIS AND UPTAKE MECHANISMS OF MICROVESICLES

At least three distinct mechanisms of MV biogenesis are known: 1) exocytosis, 2) direct budding from the plasma membrane and 3) fragmentation of dying cells, each leading to the release of the three different MV groups described above. Exosomes, which are the smallest-sized MV class, are released from exocytosis of multivesicular bodies (de Gassart et al., 2004). However, the process by which these bodies fuse with plasma membrane and release of exosomes in the extracellular environment is still unknown. It has been proposed that cytoskeleton and tumor protein p53 (p53) play an important role in these processes, as well as guanosine triphosphate (GTP) hydrolase enzymes (GTPases) (Yu et al., 2006; Simpson et al., 2009). On the other hand, shedding vesicles direct bud from the plasma membrane. Apoptotic bodies are formed from

cellular degradation of dying cells and are immediately phagocytosed in order to prevent their contents spilling out and cause damage to the surrounding cells. However, they can also escape phagocytosis and target specific cells, but the function of apoptotic body targeting is still under investigation (Bergsmedh et al., 2001). MV uptake by recipient cells generally depends on the type of target cells. In most cases, MV internalization appears to occur via endocytosis including phagocytosis, micropinocytosis, clathrin-dependent, caveolin-dependent, and lipid raft-mediated endocytosis (Mulcahy et al., 2014). Besides endocytosis, MVs uptake can also occur via membrane fusion. However, direct fusion of MVs with the plasma membrane may be limited to acidic environments, such as those found in tumor microenvironments, because at neutral pH, the rigidity of the membraneprevents fusion (Parolini et al., 2009).

4.6 MICROVESICLES IN REGENERATIVE MEDICINE

Recent findings indicate a pro-regenerative role for MVs released by MSCs in several models of tissue regeneration, including regeneration of kidney, heart, liver and nervous tissues.

Kidney regeneration mediated by MVs produced by human bone marrow-derived stem cells has been studied in an acute kidney inflammation (AKI) models induced by cisplatin. The injury of cultured renal tubular epithelial cells is mitigated after the addition of MVs, increasing the amount of proliferation, while decreasing the number of apoptotic cells (Camussi et al., 2010). In addition, microarray analysis of the MV mRNA detected 239 species of mRNA molecules, with specific enrichment of mRNAs involved in cell proliferation, transcription and immune regulation, providing another example of selective uptake of RNA species into MVs. These processes appear to be mediated, at least in part, by the transfer of RNA by MSC-MVs, as indicated by the loss of regenerative effects after RNase treatment of the MVs. In addition to mRNAs, the transfer of miRNAs by MVs is important in the context of kidney regeneration. In a rat model of AKI, intravenously injected endothelial progenitor cells-MVs localize mainly in the peritubular capillaries and renal tubular cells, and subsequently promote tissue repair and reduce functional impairment (Cantaluppi et al., 2012). Their protective effects can be inhibited by the knockdown of Dicer, essential for the processing of miRNA. These data indicate an important and potential role of MVs transferred miRNA in stimulating tissue regeneration.

Concerning the heart tissue, the intravenous injection of MVs in a mouse model reduces the infarct size caused by ischemia and reperfusion and improves left ventricular function drastically observed as early as 4 hours after reperfusion (Lai et al., 2010).

For the hepatic tissue, an example is represented by the ability of MVs to reduce tetrachloride-induced liver fibrosis, by inhibiting the epithelial-to-mesenchymal transition of hepatocytes and the collagen production (Li et al., 2013). In another study, human liver stem cells have been used as a MV source to stimulate liver regeneration after physical and chemical injury in a rat model. These stem cells produce MVs that protect cultured hepatocytes from D-galactosamine-induced apoptosis. In parallel with the *in vitro* data, administration of these MVs to hepatectomized rats contributed significantly to structural and functional hepatic recovery. Specifically, the amounts of the hepatic enzymes aspartate aminotransferase and alanine aminotransferase in the serum diminished, and the production of albumin increased (Herrera et al., 2010).

A role for MVs has also been proposed in an ischemic model of neural regeneration. Treatment of healthy primary rat cortical neurons with MVs derived from the brain extract-treated MSCs increases the total number of neurites and the neurite length. The changes in neurite number and length seem to result from the targeting and inhibition, by specific transported miRNAs, of ras homolog family member A (Rho-A), a small GTPase, suppressor of neurite growth (Xin et al., 2012).

Many other studies have been already performed on the ability of MVs to carry information between cells, with the result to ameliorate a pathological situation. Eventually, some studies demonstrated that MVs from different cell source have immunological activity, since they are able to differentially modulate T, B and natural killer (NK) cell functions (Di Trapani et al., 2016).

5. MICROVESICLES AND NON CODING RNAs: miRNAs AND piRNAs

Micro RNA (miRNA) sequences are distributed all throughout the genome, being localized in exonic or intronic regions, as well as intergenic locations. The biogenesis of miRNAs starts with their transcription by RNA polymerase II, although some other miRNAs are transcribed by RNA polymerase III, resulting in a primary transcript known as primordial mi-RNA (pri-miRNA) which contains a 33 base pair (bp) hairpin stem, a terminal loop and a flanking single stranded sequence of hundreds of bases. In general, pri-miRNAs are capped at the 5' end and polyadenylated at the 3' end. After transcription, a specific RNase III, called Drosha, processes the pri-miRNA by cleaving. Drosha digestion can occur co-transcriptionally or before splicing, and the product of this digestion is an intermediary RNA molecule known as precursor miRNA (pre-miRNA). Following pre-miRNA generation, Exportin-5, a double strand RNA (dsRNA) binding protein, transports the pre-miRNAs to the cytoplasm in a GTP dependent process. Once in the cytoplasm, Dicer, another RNase III, digests the pre-miRNA into a 22 bp mature duplex miRNA (miRNA:miRNA*, where miRNA* is called passenger strand). Dicer is an essential protein of miRNA maturation and its down-regulation decreases the mature miRNA levels. After generation of the miRNA duplex, the strands are unwound: one strand (the miRNA-guide strand) is loaded onto the RNA-induced silencing complex (RISC), formed by Dicer and its cofactors. The resultant complex between mature miRNA and RISC is denominated miRISC. The remaining passenger strand is excluded and generally degraded. Finally, miRISC acts as a guide to recognize the mRNA targets, based on complementarity rules, to negatively regulate mRNAs. There are at least three possible mechanisms by which miRNA mediate repression of gene expression: 1) mRNA target hybridization and degradation, 2) inhibition during the mRNA initiation or elongation phases and 3) mRNA decay by its recruitment to P bodies (Romero-Cordoba et al., 2014). As a result, mRNA molecule target is set to silent.

Recently, noncoding RNAs able to associate with P-element Induced WImpy testis (Piwi) proteins have been discovered and named piRNAs (Piwi-interacting RNAs). First identified in germ cells and more recently in somatic cells, piRNAs differ greatly from miRNA and small-interfering RNA in their structure and origin. piRNAs are considerably longer than mature miRNA and are derived from single stranded precursors that originate largely from repetitive sequences in the genome. piRNAs are believed to act as sequence-specific guides for Piwi protein complexes to mediate what seems to be their primary function: transcriptional gene silencing of retrotransposons and other genetic elements. Extensive analyses of piRNAs

associated with Piwi proteins have identified the genomic origins of piRNAs and led to the proposal of two biogenesis pathways: the primary processing pathway and the ping-pong amplification loop. Both mechanisms are important for mounting an effective defense against transposable elements. First, the primary piRNA biogenesis pathway results in production of primary piRNA. Next, the ping-pong cycle further shapes the piRNA population by using the initial pool of piRNAs, which associate with specific Piwi proteins, to target and cleave multiple transposable elements transcripts thereby further amplifying production of piRNAs (Bamezai et al., 2012).

Recently, researchers demonstrated that MVs can be carrier of small non coding RNAs, and that these MVs can ameliorate situation in different pathology models, such as myocardium ischemia (Wang et al., 2015), or atherosclerotic lesion (Hergenreider et al., 2011). These finding support the hypothesis that MVs carry information into the target cells, which can capture the miRNA content in order to reduce the stress induced by the pathological environment.

6. MODELS FOR THE STUDY OF PARACRINE COMMUNICATION

While the predominant interest in this field is normally focused on human application, stem cells can benefit high value animal species. Investigations in these species also provide opportunities for preclinical optimization of therapeutic strategies in humans.

6.1 IMPORTANT PATHOLOGIES IN EQUINE SPECIES: ENDOMETRITIS AND TENDON LESIONS

Endometritis is an important cause of reduced fertility in large animals, also in mares in which artificial insemination by fresh or frozen semen may induce acute endometrial inflammatory reactions. If these conditions are not promptly resolved, infections become chronic mainly in old mares that, if pregnant, show a pregnancy loss rate higher than expected (Hurtgen, 2006). The regular uterine environment promotes normal embryo development but clinical or subclinical disorders could contribute to pregnancy failure. Cytological endometritis emerged as a problem of remarkable importance for equine reproduction because animals suffering of this disorder present a persistent inflammatory uterine environment leading to reduced conception rate and increased foaling-to-conception intervals. Equine endometritis is characterized by the expression of pro-inflammatory cytokines and an influx of polymorphnuclear neutrophils (PMNs) into the uterus. Mares resistant to persistent endometritis clear the inflammation within hours after exposure to microorganisms or semen. In contrast, mares that are susceptible to persistent endometritis fail to clear the inflammation in a timely fashion. They have an imbalanced of pro- and anti- inflammatory cytokine and, consequently, these mares establish a chronic inflammation, which interferes with the establishment of pregnancy (Troedsson and Woodward, 2016). Many treatments have been proposed to treat or prevent endometritis. In mares, post-mating endometritis is treated with uterine irrigation and ecbolics, and acute endometritis with systemic or intrauterine antibiotics but these therapies are not always effective for resolving chronic uterine inflammation. The prevention include nutritional supplements and hygienic conditions during parturition. Commonly, therapies in use include hormonal treatments with GnRH, exogenous gonadotrophins and prostaglandins (Perez-Marin et al., 2011). However, in view of the enhancement of embryo-maternal interactions, a different approach to restore or ameliorate uterine receptivity in case of infertility due to endometrial damages could be represented by regenerative medicine. One example of new treatment for equine endometritis is represented by the use of platelet-rich plasma (PRP). The latter has an effect in modulating the exacerbated uterine inflammatory response to semen in mares with

chronic degenerative endometritis (Reghini et al., 2016) and also *in vitro* study on endometrial cells stressed by lipopolysaccharide (LPS) confirmed the effect of PRP (Marini et al., 2016). The following and more innovative step is the use of stem cells. Researchers already demonstrated that the endometrial hysteroscopy injection of autologous bone marrow-MSCs in mares is a safe procedure (Alvarenga et al., 2016).

In addition to endometritis, also the tendon lesion is an important disease in equine species. In this large animal, injuries affecting tendons are the most common causes of lost training days or premature retirement in the equine athlete. Standard treatments are not effective and the tendon healing is a prolonged process, with a high risk of re-injury during athletic performance.

Tendons and ligaments heal slowly after injury and rarely regain their original strength and elastic qualities. Suboptimal healing, prolonged rehabilitation time and a high incidence of recurrence make degenerative injuries difficult to treat successfully. The prognosis for patients with tendon or joint injuries is often poor (Lange-Consiglio et al., 2013b). Despite a short inflammatory phase after the injury incident, the healing process is dominated by fibroplasia and can be referred to repair rather than regeneration, with the formation of hyper-cellular scar tissue with poor extracellular matrix organization, in which stiffness is increased but elasticity is decreased compared with the original tendon tissue (Richardson et al., 2007). Standard treatment for orthopaedic injuries are not effective, and tendons require a long healing time, with high risk of re-injury during athletic performances. For this reason, a regenerative medicine could bring to a regeneration of the original tissue, restoring the functionality of the system. Researchers demonstrated that PRP treatment in some cases leads to the formation of tendon with normal morphology and functionality, which translate in the resumption of the agonistic activity (Scala et al., 2015).

6.2. BOVINE *IN VITRO* EMBRYO PRODUCTION

It is known that, usually, *in vitro* produced (IVP) embryos are of a poorer quality when compared with *in vivo* ones (Wrenzycki and Stinshoff, 2013). Fertilization of eutherian animals occurs in the maternal oviduct, which is the natural and unique environment to achieve the necessary requirements for embryo life in its early and late development. The *in vitro* conceived embryo is manipulated and cultured in very different conditions and today a huge amount of information point out the alterations that can occur in IVP embryos because of the manipulation and artificial environmental conditions associated with these techniques (Lucas,

2013). Some researchers reported that the culture system and the *medium* composition can affect the embryo quality (Abe et al., 2002; Rizos et al., 2002) and that the *in vitro* culture (IVC) of embryo is probably the most relevant factor in the alterations of epigenetic reprogramming and development of IVP embryos. In fact, while the innate feature of the oocyte is the major factor determining the blastocyst yield, it is evident that post-fertilization culture environment is critical in defining the quality of the blastocyst (Costa Pereira et al., 2005; Lonergan et al., 2006). This underline the key effect of the maternal microenvironment on the success of early embryonic development in terms of viability (Schmaltz-Panneauet al., 2015). In mammals, during the pre-implantation stage, the exchange of different types of signals between the mother and the embryo is thought to be critical for embryo development and implantation (Fazeli, 2008). In cattle, it has been considered that the absence of communication between a receptive endometrium and a viable embryo could be an important cause of the low efficiency of pregnancies (Thatcher et al., 2001). These considerations led to the hypothesis that paracrine communication between the mother and the embryo/fetus must exists.

6.2.1. BOVINE MATERNAL-FETAL COMMUNICATION

A myriad of locally produced factors into the microenvironment of the reproductive tract is regulated not one-way but, rather, through embryonic–maternal cross talk. Both embryonic and maternal counterpart have been described to secrete MVs involved in paracrine communication.

Microvesicles can be secreted from maternal side and bioinformatics of endometrium-derived MVs miRNAs revealed that these miRNAs have potential targets in biological pathways highly relevant for embryo implantation (Ng et al., 2013). On the other hand, it has been revealed that IVP embryos release MVs whose amount increase with developmental stage and whose size correlates with embryo quality (Gardiner et al., 2013). These considerations led the hypothesis that a successful implantation is dependent on coordination between the embryo and the endometrium, and MVs may participate in this required cross-talk. Endometrial epithelium release MVs involved in the transfer of signaling miRNAs and of adhesion molecules to the blastocyst that in turn can affect endometrial receptivity and implantation. Analysis of these vesicles revealed miRNAs and proteins expressed both by the conceptus trophectoderm and by the endometrial epithelium. In human studies, MVs have been isolated from uterine fluid from women in different phases of the menstrual cycle. Both the luminal and glandular apical

surfaces of endometrial epithelial cells express CD9 and CD63 exosomal markers, thereby showing that the endometrial epithelium is a possible source of the exosomes found in the uterine cavity (Ng et al., 2013). The identification of MVs in the uterine fluid suggests a possible role of MVs in transferring information from the endometrium during implantation.

6.2.2. CO-CULTURE SYSTEMS IN BOVINE EMBRYO PRODUCTION

To mimic the *in vivo* cross-talk environment, co-culture systems are largely used in IVP embryos in different species and, in some mammalian species, somatic cell co-cultures improved the development of IVP embryos (Li et al., 2001). Indeed, co-culture system with bovine oviduct epithelial cells, used for the development of bovine zygotes, enhanced blastocyst formation and quality of the resulting embryos, inducing also specific transcriptomic changes (Schmaltz-Panneau et al., 2015). This suggests that paracrine mechanisms of communication exist between "helper" cells and embryos. In fact, various growth factors, receptors and binding proteins are secreted by cells in the *medium*, but the embryos themselves produce them too. Conditioned *media* were already developed and used in bovine embryo IVP. Some of these cell-free media, produced, for example, by culturing granulosa, cumulus or oviduct cells, demonstrated a similar effect in development of embryos produced by co-culture systems (Rieger et al., 1995). In addition to the reputation of CM, as already said in this thesis, the existence of MVs inside CM could be assumed as key factor for the beneficial effect of the use of cell-free media.

6.2.3 EMBRYONIC BI-DIRECTIONAL COMMUNICATION: AMNIOTIC MESENCHYMAL CELLS AND ENDOMETRIAL CELLS

Placenta is a transient organ that mediates not only hormonal, nutritional and oxygen support to the fetus but also actively secretes signal substances and immune regulatory factors that modulate maternal immune response during pregnancy. For the first time, Sabapatha et al. (2006) described circulating placental exosomes and studied their role in the down regulation of T-cell responses of pregnant women. Successful implantation is dependent on coordination between the embryo and the endometrium, so it has been suggested that the endometrial epithelium releases MVs that are involved in the transfer of signaling miRNAs and adhesion molecules to the blastocyst, which in turn can affect endometrial receptivity and implantation (Burns et al., 2014). Further experiments have shown that these MVs can pass through the zona

pellucida and can be internalized by blastomeres (Saadeldin et al., 2014). *In vitro* studies have shown that MVs isolated from the uterine fluid of pregnant sheep can transfer RNAs to other cells. These findings indicate that these MVs likely have a biological role in the interaction between the embryo and the endometrium (Burns et al., 2014). A fundamental study described that syncytiotrophoblast secretes miRNAs in the maternal circulation by exosomes (Chim et al., 2008) supporting the opposite direction of communication, from embryos to maternal environment, by microvesicles.

7. SUMMARY OF THE PROJECT

During my PhD project, studies were carried out to understand the already known ability of MSCs to ameliorate pathological situation in animal models in *in vitro* studies. Results of these studies produced during the 3-year project are described in some publications that are attached in the following chapter.

The first paper, entitled “Amniotic membrane-derived mesenchymal cells and their conditioned *media*: potential candidates for uterine regenerative therapy in the horse” by Corradetti et al. (2014) was aimed to investigate if AMCs and their CM could be a potential tool for the regeneration of damaged uteri in a *vitro* model. The paracrine action of the AMCs was investigated comparing the potential of AMCs in toto and AMC-conditioned *medium* (AMC-CM) in an *in vitro* model using endometrial cells (EDCs) as target. The experiment was designed to study the endometrial regeneration, analyzing EDC proliferation by co-culturing them with AMCs in a trans-well system or in presence of AMC-CM. In both conditions, there was a significant increase in EDC proliferation rate, defining the crucial role of soluble factors as mediators of stem cells action. These preliminary findings revealed that AMCs, via their derived CM, have the potential to improve endometrial cell replenishment. It is possible to speculate that the beneficial effects in tissue regeneration is due to the release of soluble factors indicating CM as a novel therapeutic cell-free product for regenerative medicine applications (Corradetti et al., 2014).

The second study, published in the paper entitled “Microvesicles secreted from equine amniotic-derived cells and their potential role in reducing inflammation in endometrial cells in an *in vitro* model” by Perrini et al. (2016), aimed to study MVs as anti-inflammatory tool in an *in vitro* model of equine endometritis. The production of CM and MVs from cultures of equine AMCs was optimized. Conditioned *media* were produced by culturing AMCs in a serum-free *medium* for 5 days, collecting the culture *medium* and centrifuging it to remove cell debris. From the CM, it was possible to obtain MVs through an ultracentrifugation at 100.000 g for 1 hour. The supernatant (SN) obtained after this step can be considered as the ensemble of soluble factors of the CM deprived of MVs. Microvesicle production from equine AMCs was 2550±71 particles/cell. Next step was the characterization of AMC-derived MVs by Nanosight Instrument: the size of MVs ranged from 50 nm to 670 nm, with a mean size of 258±55 nm for three samples. The transmission electron microscopy (TEM) revealed the presence of variably-

sized extra-cellular membranous roughly spherical vesicles, budding from or lying near AMCs, characterized by an electron-lucent or moderately electron-dense content. The size of MVs varied from about 100 nm to 1000 nm, with a predominance of vesicles between 100 and 200 nm. Because of the size and morphological characteristics, the vesicles observed were considered mainly shedding vesicles, rather than exosomes.

Then, some experiments of incorporation and action of MVs into LPS challenged-target cells, represented by EDCs, as model of equine endometrial injury, were performed. In order to obtain the optimal concentration of MVs for their application in the following experiments, a dose/response curve at different concentrations of MVs and different exposure times was studied. Endometrial cell internalization and accumulation of MVs peaked at 72 h at a concentration of $50x10^6$ MVs. At this point, the effect of LPS and MVs on EDCs was evaluated by viability cell tests (apoptotic and prolificacy tests), by expression of some pro-inflammatory genes, studied by quantitative reverse transcription polimerase chain reaction (RT-qPCR), and by release of respective cytokines.

Considering that the MV uptake by EDCs was visible by fluorescence signal only after 6 hours, MVs were used simultaneously to LPS or three hours after the treatments by LPS or 24 hours before the LPS. The rate of apoptosis increased dramatically in cells treated with LPS if compared to the EDCs CTR. The results of prolificacy test had the opposite trend. MVs were able to counteract the action of LPS either when used simultaneously to LPS or when incorporated by endometrial cells 24 h before the treatment with LPS, because cells pre-treated with MVs or treated with MVs and LPS together had an apoptotic rate lower than the EDCs CTR. LPS upregulated significantly the expression of *TNF-α, IL-6* and *IL-1β*. In the condition where LPS and MVs were used simultaneously, the action of LPS was counteracted by MVs, indeed, the expression of *IL-6* and *IL-1β* fell significantly. The expression of *TNF-α* was independent by presence of MVs. Coherent results were obtained through the analysis of pro-inflammatory (TNF-β and IL-6) and anti-inflammatory (TGF-α) cytokines released by EDCs in the culture *medium*, confirming the ability of MVs to transport molecules capable to counteract the inflammatory response of cell stressed with LPS.

Since MVs contain various active molecules, such as lipids, proteins, mRNA, and miRNA, we studied the presence of three miRNAs in MVs involved in the regulation of pro-inflammatory genes (miR-335, miR-146a, and miR-26a-2) that have been demonstrated to regulate the expression of some pro-inflammatory genes in human and bovine species. We found the

presence of these three miRNAs in both AMCs and their MVs, so the downregulation of gene expression shown in this study could be correlated to miRNA transfer from MVs to EDCs (Perrini et al., 2016).

After these results, a similar experimental design was performed to study the ability of MVs to counteract an *in vitro* inflammation, leading to the third publication entitled "Equine amniotic microvesicles and their anti-inflammatory potential in a tenocyte model *in vitro*" by Lange-Consiglio et al. (2016). Also for tendon cells (TNCs), in order to obtain the optimal concentration of MVs for their application in the following experiments, a dose/response curve at different concentrations of MVs and different exposure times was studied. For TNCs, internalization and accumulation of MVs suddenly increased at 24-72 h at a concentration of $50x10^6$ MVs/ml. At this point, knowing the optimal dose of MVs, their ability to counteract an *in vitro* inflammation was studied in TNCs challenged with LPS. After exposure to LPS, a moderate but significant increased gene expression of metalloproteinase (*MMP) 1* and *9* was observed if compared to TNCs CTR. Expression of *MMP-13* and tumor necrosis factor α (*TNF-α)* were noticed significantly higher after LPS exposure if compared to TNCs CTR. The presence of MVs had a significant effect on gene expression, with a striking reduction in the expression levels for *MMP-1*, *MMP-9*, *MMP-13*, and *TNF-α*, when compared to TNCs CTR.
Moreover, in this study, the ability of MVs to inhibit peripheral blood mononuclear cell (PBMC) proliferation when stimulated with phytohemagglutinin (PHA) was evaluated, but MVs, also after lysis by sonication to release their content, were not able to inhibit PBMC proliferation.
These results led to conclude that MVs brought to the target cells some molecules able to counteract the inflammatory situation due to the LPS but, taking into account the lack of their immunomodulatory action, probably, for an *in vivo* tendon lesions healing, soluble factor of CM are necessary too (Lange-Consiglio et al., 2016).

Since paracrine communication seems to be regulated by cell secretome represented by CM, SN and MVs, we thought it could be interesting to study these mechanisms during *in vitro* embryo production, considering that usually the *in vitro* production rate is lower than *in vivo* one. The results of this study are collected in the fourth paper entitled "Secretome derived from different cell lines in bovine *in vitro* embryo production" by Perrini et al. that has been submitted to Plos One (November 2016). Different components of secretome from bovine AMCs and EDCs were

supplemented to the embryo culture *media* at different days of culture. Endometrium and amnion were studied because they have a role in the establishment of pregnancy. Endometrial cells were evaluated at the early luteal phase, which correspond to the period when these cells, *in vivo,* interact with early stage embryos. Amnion was chosen because Lange-Consiglio et al. (2010) used a monolayer of equine amniotic epithelial cells as feeder to culture bovine embryos with good results in term of blastocyst rate, compared to the bone marrow derived cells and cumulus cells. These authors suggested that EGF, produced by monolayer of amniotic epithelial cells, could have been one of most representative candidate to play a positive role in the embryonic development as it happens *in vivo* for the endometrium. Indeed, EGF is produced *in vivo* by endometrial cells and the embryo possesses receptors for it. In this context, in our study, the amniotic cells were further investigated and compared to endometrial cells through the effect of their secretome. The results demonstrated that the day 5 of culture is the best time point for the supplementation of these components and that AMCs-MVs provided the best environment for the embryo concerning the blastocyst quality, rather than blastocyst rate, since the number of alive blastomeres and the ICM/trophoblast ratio were higher than in the CTR condition. These data were confirmed by the evaluation of genes involved in apoptosis and reactive oxygen species protection. Probably, AMC-MVs bring information that led to the production of embryos with better qualities respect to the standard embryo production.

7.1 PUBLICATIONS

OPEN ACCESS Freely available online

PLOS ONE

Amniotic Membrane-Derived Mesenchymal Cells and Their Conditioned Media: Potential Candidates for Uterine Regenerative Therapy in the Horse

Bruna Corradetti[1], Alessio Correani[1], Alessio Romaldini[1], Maria Giovanna Marini[1], Davide Bizzaro[1], Claudia Perrini[2], Fausto Cremonesi[2,3]*, Anna Lange-Consiglio[2]

1 Department of Life and Environmental Sciences, Università Politecnica delle Marche, Ancona, Italy, **2** Large Animal Hospital, Reproduction Unit, Università degli Studi di Milano, Lodi, Italy, **3** Department of Veterinary Science for Animal Health, Production and Food Safety, Università degli Studi di Milano, Milan, Italy

Abstract

Amniotic membrane-derived mesenchymal cells (AMCs) are considered suitable candidates for a variety of cell-based applications. In view of cell therapy application in uterine pathologies, we studied AMCs in comparison to cells isolated from the endometrium of mares at diestrus (EDCs) being the endometrium during diestrus and early pregnancy similar from a hormonal standpoint. In particular, we demonstrated that amnion tissue fragments (AM) shares the same transcriptional profile with endometrial tissue fragments (ED), expressing genes involved in early pregnancy (*AbdB-like Hoxa* genes), pre-implantantion conceptus development (*Erα, PR*, *PGRMC1* and *mPR*) and their regulators (*Wnt7a*, *Wnt4a*). Soon after the isolation, only AMCs express *Wnt4a* and *Wnt7a*. Interestingly, the expression levels of prostaglandin-endoperoxide synthase 2 (*PTGS2*) were found greater in AM and AMCs than their endometrial counterparts thus confirming the role of AMCs as mediators of inflammation. The expression of nuclear progesterone receptor (PR), membrane-bound intracellular progesterone receptor component 1 (*PGRMC1*) and membrane-bound intracellular progesterone receptor (*mPR*), known to lead to improved endometrial receptivity, was maintained in AMCs over 5 passages *in vitro* when the media was supplemented with progesterone. To further explore the potential of AMCs in endometrial regeneration, their capacity to support resident cell proliferation was assessed by co-culturing them with EDCs in a transwell system or culturing in the presence of AMC-conditioned medium (AMC-CM). A significant increase in EDC proliferation rate exhibited the crucial role of soluble factors as mediators of stem cells action. The present investigation revealed that AMCs, as well as their derived conditioned media, have the potential to improve endometrial cell replenishment when low proliferation is associated to pregnancy failure. These findings make AMCs suitable candidates for the treatment of endometrosis in mares.

Citation: Corradetti B, Correani A, Romaldini A, Marini MG, Bizzaro D, et al. (2014) Amniotic Membrane-Derived Mesenchymal Cells and Their Conditioned Media: Potential Candidates for Uterine Regenerative Therapy in the Horse. PLoS ONE 9(10): e111324. doi:10.1371/journal.pone.0111324

Editor: Eric Asselin, University of Quebec at Trois-Rivieres, Canada

Received May 21, 2014; **Accepted** September 29, 2014; **Published** October 31, 2014

Data Availability: The authors confirm that all data underlying the findings are fully available without restriction. All relevant data are within the paper.

Funding: General funding from Università degli Studi di Milano and Università Politecnica delle Marche is gratefully acknowledged. The funders had no role in study design, data collection and analysis, decision to publish, or preparation of the manuscript.

Competing Interests: The authors have declared that no competing interests exist.

* Email: fausto.cremonesi@unimi.it

Introduction

Embryo-maternal communication is a pre-requisite for successful implantation that facilitates the establishment, recognition, and maintenance of pregnancy. Studies of early pregnancy in different mammalian species have shown that the majority of embryo losses occurs during the pre-implantation phase: in the horse, this phase is very critical [1,2]. During this period, the conceptus (the embryo and the associated extra-embryonic membranes) interacts with the uterine environment via paracrine signaling to coordinate attachment and implantation. Disruption of the integrity of the endometrial tissue and of the capacity to support its functions are the responsible factors in determining a subfertile phenotype [3]. As such, the development of chronic endometritis followed by degenerative and abnormal changes of the endometrium, like fibrosis (scarring) around the glands, might inhibit the regeneration of traumatized endometrium. The damage then leads to an impairment of the progenitor cell ratio that reduces the endometrial tissue's ability to regenerate and thus future foaling rates as well. This mainly results in the inability of the tissue to support embryo implantation.

Given the potential role of these cells have in remodeling the endometrium, it may be reasonable to suggest cell therapies based on mesenchymal stem cells (MSCs) as suitable strategies to restore and maintain normal function in damaged reproductive tissues.

With this in mind, we recently retrieved MSCs from extra-fetal tissues in the equine species [4]. For the first time, we compared the proliferative and differentiative potential of amniotic membrane-derived MSCs (AMCs) with bone marrow derived MSCs (BM-MSCs). together with their possible application in the treatment of horse tendon injuries [5,6]. We next demonstrated the potential immunomodulatory properties of AMCs and their conditioned medium (AMC-CM) *in vitro*, and proved the efficacy of AMC-CM in the treatment of spontaneous horse tendon and ligament injuries *in vivo* [7]. Data obtained in this study demonstrated the crucial role of soluble factors in inhibiting

peripheral blood mononucleated cell proliferation *in vitro* and in improving healing *in vivo*. Taken together, the AMCs features described so far by our group suggest this cell type as the most suitable for regenerative medicine approaches [5] and its derived conditioned media (CM) as a novel, cell-free therapeutic product in regenerative medicine.

For these reasons, the aim of the present study was to better understand the nature of AMCs, so that we may exploit their potential role in uterine replacement therapy. AMCs were further characterized for the expression of early pregnancy-associated genes in view of their potential application in endometrial regeneration or in stimulating the proper preparation of the endometrium for embryo implantation.

The AbdB-like Hoxa gene (Hoxa9) and the wingless type genes (Wnt7a, Wnt4a), which influence pre-implantantion conceptus development, the classical oestrogen (ERα and ERβ) and progesterone (PR) receptors, and the more recently characterized membrane-bound intracellular progesterone receptors (PGRMC1 and mPR), were evaluated on amniotic membrane fragment (AM) or AMCs (at different passages) in comparison to endometrial tissue fragments (ED) or isolated endometrial cells (EDCs) at diestrus. We also looked at the expression of other genes, including the cyclooxygenase prostaglandin E2 synthase (*PTGS2*), forkhead box 01 (*FOXO1*), serum/glucocorticoid regulated kinase 1 (*SGK1*), and tumor protein p53 inducible protein3 (*TP53*) whose transcriptional activity has been associated with luteo-protective action [8], protection of the feto-maternal unit against oxidative damage [9], improved reproductive outcome [10], and epithelial ion transport and cell survival responses [11] during early pregnancy, respectively. Since the endometrial stromal and epithelial cells proliferation and differentiation through the period of embryo preimplantation are controlled by ovarian steroid hormones (progesterone and estrogen) [12,13], we aimed to recreate the endometrial environment, thus culturing AMCs for different passages in the presence of progesterone.

We further hypothesized that AMCs might induce tissue-resident endometrial cells to proliferate or, alternatively, to modulate the local immune response and promote endometrial regeneration. MSCs, in general, are believed to play their role as mediators of tissue repair through the release of paracrine factors [14]. To test this hypothesis EDCs were cultured either with AMCs in a transwell system or with their conditioned media, in order to evaluate the capability of AMCs to increase the proliferative potential of endometrial cells.

Materials and Methods

Materials

Samples were collected from horses slaughtered in a national slaughterhouse (Titbit Srl, Bagnolo in Piano, Reggio Emilia, Italy) with legal regulations.

Chemicals were obtained from Sigma-Aldrich Chemical (Milan, Italy) unless otherwise specified, and tissue culture plastic dishes were purchased from Euroclone (Milan, Italy).

Tissue collection and isolation

Three amniotic membranes were obtained at term of normal pregnancies after vaginal delivery from three mares. Clean collected portions of allanto-amnion were kept at 4°C in PBS with 100 U/ml penicillin, 100 μg/ml streptomycin and 4 μg/ml amphotericin B and were processed within 8 h. The amniotic membrane was stripped from the overlying allantois and cut into small pieces (about 9 cm^2 each) before starting the enzymatic digestion. Endometrial tissues were collected from 3 different horses aged between 8 and 10 years, after euthanasia unrelated to our experiments. Endometrial samples were obtained during the reproductive season from normal-cycling mares at diestrus (early-mid luteal phase). Before euthanasia, 5 ml of blood were collected in heparinized tubes from all mares. After centrifugation, plasma was separated, kept refrigerated and immediately transported to the laboratory for progesterone determination by a quantitative Enzyme Linked Fluorescent Assay (ELFA) based on the MiniVidas (Biomerieux, Firenze, Italy) technology. According to the manufacturer, the measurement range of the assay varied from 0.25 to 80 ng/ml with an intra-assay variability of 4.12% and an inter-assay variability of 6.32%.

Only uteri belonging to mares with an obvious corpus luteum on the ovary and progesterone levels between 6 to 20 ng/ml, indicative of the early/mid diestral phase of the estrous cycle [15], were used for endometrial fragment collection and ensuing cell culture.

Tissue fragments for RNA isolation were immediately immersed in RNA Later solution, whereas those destined for cell isolation and expansion procedure were kept at 4°C in saline solution supplemented with 4 μg/ml amphotericin B, 100 IU/ml penicillin and 100 μg/ml streptomycin and were processed within 8 h.

Cell isolation

Amniotic membrane-derived mesenchymal cells were isolated as previously reported [4]. Briefly, amnion fragments were incubated for 9 min at 38.5°C in PBS containing 2.4 U/mL dispase (Becton Dickinson, Milan, Italy). After a resting period (5–10 min) at room temperature in high-glucose Dulbecco's modified Eagle's medium (HG-DMEM; EuroClone, Milan, Italy), supplemented with 10% heat inactivated fetal bovine serum (FBS) and 2 mM L-glutamine, the fragments were digested with 0.93 mg/mL collagenase type I and 20 mg/mL DNAse (Roche, Mannheim, Germany) for approximately 3 h at 37°C. The amnion fragments were then removed, and mobilized cells were passed through a 100 μm cell strainer before being collected by centrifugation at 200×g for 10 min.

Endometrial cells from diestrus mare's uteri were obtained according to the protocol described by Donofrio et al. [16] and slightly modified for equine cells. Briefly, the endometrium was digested in sterile filtered Hank's buffered salt solution supplemented with 2 mg/ml collagenase II, 4 mg/ml bovine serum albumine, and 0.4 mg/ml DNase I for 90 minutes at 38.5°C in a shaking bath. Cells were then filtered through a membrane with a pore size of 80 μm, centrifuged at 200×g for 10 minutes, and then washed twice in PBS. This protocol allowed for the isolation of the endometrial stromal portion.

Fibroblasts (used as a control for AMCs) were isolated from skin specimens collected from three horses after euthanasia unrelated to our experiments. Samples (2 mm^3) were taken by excision and fragments of approximately 1 mm were incubated with 40 mg/ml collagenase IV for 3 h at 38.5°C. After digestion, cells were washed and allowed to grow to confluence in 60-mm culture dishes.

Before seeding, the primary cultures (P0) obtained from the amnion, endometrium and skin were counted using a Burker chamber with the trypan blue dye exclusion assay.

Cell expansion

Endometrial and fibroblast cells cultures were established in HG-DMEM supplemented with 10% FBS, penicillin (100 UI/ml)-streptomycin (100 μg/ml), 0.25 μg/ml amphotericin B and 2 mM L-glutamine. Medium was supplemented with 10 ng/ml epidermal growth factor (EGF) for AMC cultures.

To remove non-adherent cells, the medium was replaced for the first time after 72 h, and then changed either twice per week thereafter or according to the experiment requirements. For maintenance of cultures, cells were plated in flasks of 25 cm^2 at the density of 1×10^5 cells/cm^2 and incubated at 38.5°C in a humidified atmosphere with 5% CO_2. Adherent cells were detached with 0.05% trypsin-EDTA just prior to reaching confluence (80%) and then reseeded for culture maintenance at the density of 1×10^4 cells/cm^2.

Molecular characterization of EDCs was performed only at P0 as *de facto* control for gene expression, whereas AMCs were studied from P0 to P5.

Preparation of conditioned medium

AMCs and fibroblasts, at P3, were plated in 24-well plates at a density of 1×10^5 cells/well in DMEM standard complete medium. To obtain AMC-CM and fibroblast-CM, cells were cultured for 5 days at 38.5°C in a humidified atmosphere with 5% CO_2. Supernatants from each plate were then collected, pooled, centrifuged at 700×g, filtered (0.2 μm), and stored at −80°C. This procedure was performed for cells obtained from three different placentas and from three different samples of skin.

The collected supernatants were lyophilized and stored at 4°C until use, at which point they were dissolved in sterile cell culture water to one-quarter of the initial volume.

Molecular characterization

Total RNA was extracted from tissues (AM and ED) and cells (AMCs and EDCs) immediately after isolation (P0) using TRI Reagent® Solution (Life Technologies, Monza, Italy). Total RNA was also extracted from AMCs at different passages (P1, P3 and P5) and after culture in the presence of progesterone. Samples were then treated with DNase in order to avoid DNA contamination. RNA concentration and purity were measured by Nanodrop Spectrophotometer (Nanodrop® ND1000). The cDNA was synthesized from total RNA (500 ng) using a Taqman Reverse Transcription reagents kit (Applied Biosystems, Branchburg, NJ). The gene expression evaluation was performed using specific sequences; equine-specific oligonucleotide primers were designed using open source PerlPrimer software v. 1.1.17, based on available NCBI *Equus caballus* sequences or on mammal multi-aligned sequences. Primers were designed across an exon–exon junction in order to avoid genomic DNA amplification and their sequence conditions and the references used are shown in Table 1. Equine glyceraldehyde-3-phosphate dehydrogenase (*GAPDH*) was employed as a reference gene in each sample in order to standardize the results by eliminating variation in mRNA and cDNA quantity and quality.

Conventional RT-PCR was performed in a 25 μl final volume with RBC Taq DNA Polymerase (RBC Bioscience) under the following conditions: initial denaturation at 95°C for 2 minutes, 32 cycles at 95°C for 30 seconds (denaturation), 55–60°C for 30 seconds (annealing), 72°C for 1 minute (elongation) and final elongation at 72°C for 7 minutes. For conventional PCR, primers were used at 300 nM final concentrations.

Quantitative PCRs were performed with SYBR green method in a MyiQ iCycler thermal cycler (Biorad). Triplicate PCR reactions were carried out for each sample analyzed. The reactions were set on a strip in a final volume of 25 μl by mixing, for each sample, 1 μl of cDNA, 12.5 μl of 2X concentrated Power Sybr®Green PCR Master Mix (Applied Biosystems) containing SYBR Green as a fluorescent intercalating agent, 0.2 μm forward primer, 0.2 μm of reverse primer and MQ water. PCR efficiencies were tested and found to be close to 1. The thermal profile for all reactions was 10 minutes at 95°C and then 40 cycles of 15 seconds at 95°C, 1 minute at 60°C. Fluorescence monitoring occurred at the end of each cycle. Additional dissociation curve analysis was per- formed and in all cases showed one single peak. The data thus obtained were analyzed using the iQ5 optical system software version 2.0 (BioRad). Gene expression levels found in AM and AMCs were normalized and represented with respect to ED and EDCs, respectively.

Proliferation studies

Growth curves. To obtain growth curves at P1 and P5, AMCs and EDCs were plated at the density of 9×10^3 cells into six-well tissue culture plates. Every three days, over the 15 days of culture, cells from one well of each plate were detached and counted.

Doubling time (DT). Cell proliferation was determined as previously reported [4]. DT for passages 1–5 was assessed plating 9×10^3 cells into six-well tissue culture plates. Every 4 days cells were trypsinized, counted and reseeded at the same density. Mean DT was calculated from day 0 to day 4. The DT value was obtained for each passage according to the formula DT = CT/CD, where CT represents the culture time and CD = $\log(N_c/N_o)$/log2 represents the number of cell generations (N_c represents the number of cells at confluence, N_o represents the number of seeded cells). Data representative of three independent experiments are reported.

EDC proliferation in presence of AMCs or AMC-CM. To assess the potential of AMCs to increase EDCs proliferation (evaluated as growth curves and DT) 24-well plates with 0.4 μm-pore transwell inserts were used to physically separate the two cell populations. EDCs were plated at 1×10^4 cells/well in standard complete medium and AMCs were added at the same density on top of the inserts.

To evaluate the effect of AMC-CM on EDCs proliferation, growth and DT were studied plating 9×10^3 cells into six-well tissue culture plates. For this experiment, cultures were established in standard complete medium supplemented with 10% AMC-CM. As a control group, EDCs were studied in the presence of either fibroblasts separated with a transwell system or fibroblast-derived CM.

AMCs culture in the presence of progesterone

To determine whether AMCs would be effective in replacement therapy we cultured them in the presence of progesterone. Cultures at P1 were established in HG-DMEM supplemented with 10% FBS, 10 ng/ml EGF, 1% penicillin (100 UI/ml)/streptomycin (100 μg/ml), 0.25 mg/ml amphotericin B, 2 mM L-glutamine (standard complete medium) and 20 ng/ml of progesterone. For maintenance of the cultures, cells were plated at 1×10^4 cells/cm^2 and incubated at 38.5°C in a humidified atmosphere with 5% CO_2. Just prior to reaching confluence (80%), adherent cells were detached with 0.05% trypsin-EDTA and then reseeded for culture maintenance at the density of 1×10^4 cells/cm^2. The medium was changed twice per week. Cells at P5 were the last time point included for the molecular characterization studies.

Statistical analysis

For proliferation data, statistical analysis was performed using GraphPad Instat Software version 3.00 for Windows (La Jolla, CA, US). Three replicates for each experiment were performed. Results are reported as mean ± standard deviation (SD). One-way analysis of variance (ANOVA) for multiple comparisons by Student-Newman-Keuls multiple comparison tests was used. Differences were considered statistically significant for P values

Table 1. Oligonucleotide sequences used for RT-PCR analysis.

REF SEQ	Markers	Forward (5′→3′)	Reverse (5′→3′)	$T_{Annealing}$	bp
XM_001498494.3	Progesteron Receptor (PR)	GTCAGTGGACAGATGCTGTA	CGCCTTGATGAGCTCTCTAA	55°C	255
NM_001081772.1	Estrogen receptor a (ERa)	TCCATGATCAGGTCCACCTTCT	GGTGTCTGTCATCTTGTCCA	55°C	341
XM_001915519.2	Estrogen receptor b (ERb)	TCAGCCTGTTCGACCAAGTG	CCTTGAAGTCGTTGCCAGGA	60°C	194
NM_001256979.1	Membrane-associated progesterone receptor (MPR)	GCCAAGTATCGTTACCGGAG	AAGAGGATCTGGAGCGTGTG	55°C	173
XM_001914705.2	Membrane-associated progesterone receptor (PGRMC1)	TCAACGGCAAGGTGTTCGAC	GGCTCTTCCTCATCTGAGTA	58°C	280
XM_003364827.1	Homeobox protein Hox-A9-like (Hoxa9)	ACGCTGGAACTGGAGAAAGA	CTTTCGCTCGGTCCTTATTG	55°C	160
NM_001163856.1	Glyceraldehyde-3-phosphate dehydrogenase (GAPDH)	AGATCAAGAAGGTGGTGAAG	TTGTCATACCAGGAAATGAGC	59°C	178
XM_001501510.2	Wingless-type MMTV integration site family, member 4 (Wnt7a)	TTTCGGATTCCCGCAGTCTC	CATCTGCACCTGCCTCTGAA	55°C	177
XM_001489623.2	Wingless-type MMTV integration site family, member 7A(Wnt7a)	CATGGTCTACCTCCGGATCG	TATGACGATGATGGCGTCGG	55°C	134
XM_005600181.1	Tumor protein p53 inducible protein3 (TP53)	TCGCATTTCAAGCCAAACCG	CTTCCTTCTCCTTCCCGTCG	60°C	110
XM_005601179.1	Forkhead box 01 (FOX01)	ATTGAGCGCTTGGACTGTG	CGTTGTCTTGACACTGTGC	60°C	126
XM_005609749.1	Prostaglandin-endoperoxide synthase 2 (PTGS2)	GATCCTAAGCGAGGTCCAGC	AGGCGCAGTTTATGCTGTCT	60°C	101
XM_001504377	Serum/glucocorticoid regulated kinase 1 (SGK1)	CTGCACTCCCTGAACATCGT	ATGTTCTCCTTGCAGAGCCC	60°C	107

doi:10.1371/journal.pone.0111324.t001

<0.05. For quantitative PCR data, non-parametric tests were used. The Kruskal-Wallis test was used for comparison between multiple groups whereas Mann-Whitney U-test was employed to compare two groups. $P<0.05$ was considered significant.

Results

Cells isolation and expansion

Cells were selected purely on their ability to adhere to plastic. For AMCs, initial viability was >90%, whereas for EDCs it was >80%. All cell lines displayed the typical fibroblast-like morphology (Figs 1A and 1B). AMCs observed at the early stages of culture organised as tridimensional clusters (Fig 1C).

Molecular characterization

As previously reported, molecular studies demonstrated that at P3 AMCs display a typical mesenchymal stromal phenotype, expressing pluripotent and MSC-specific markers [4]. For further information, see Supplementary Information. When the expression of genes associated to pre-implantantion conceptus development was investigated, conventional RT-PCR analysis demon-

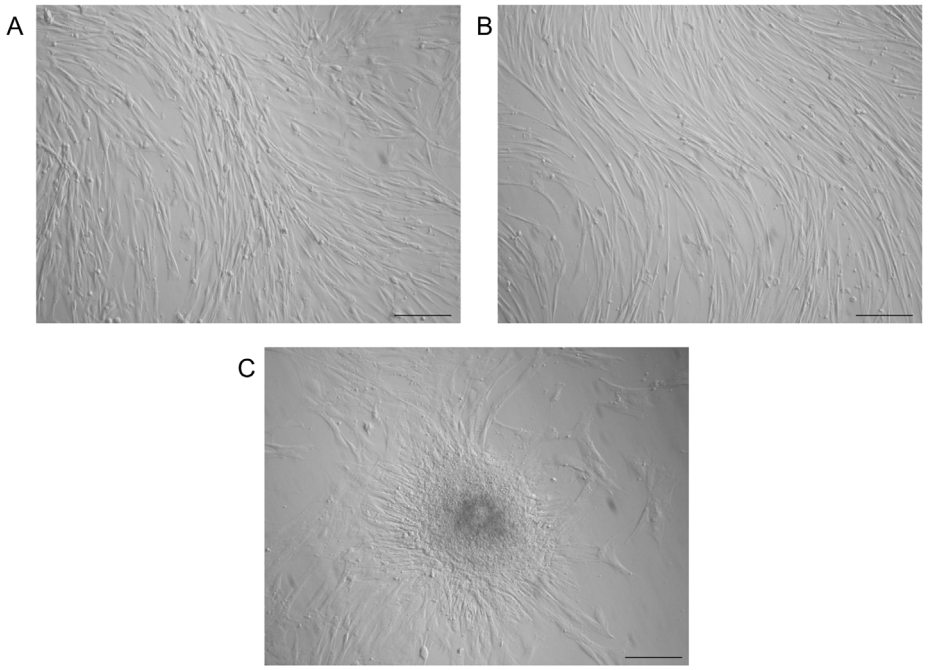

Figure 1. Cell morphology. Monolayer of AMCs (A) and EDCs (B); tridimensional cluster of AMCs (C). Magnification, x 20; scale bar = 20 μm.
doi:10.1371/journal.pone.0111324.g001

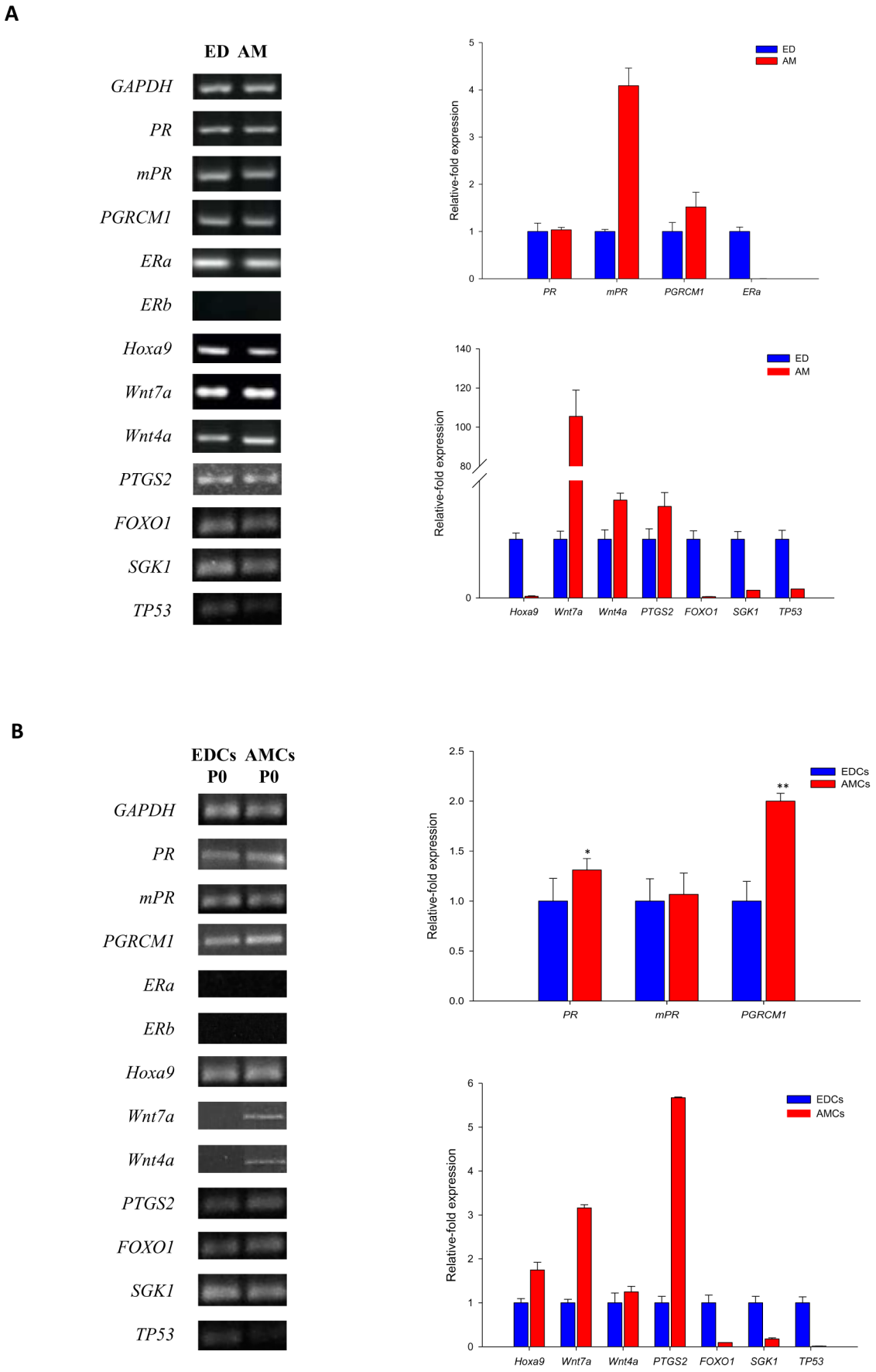
A
ED AM
GAPDH
PR
mPR
PGRCM1
ERa
ERb
Hoxa9
Wnt7a
Wnt4a
PTGS2
FOXO1
SGK1
TP53
Relative-fold expression
ED
AM
PR
mPR
PGRCM1
ERa
Hoxa9
Wnt7a
Wnt4a
PTGS2
FOXO1
SGK1
TP53
B
EDCs AMCs
P0 P0
EDCs
AMCs

Figure 2. Molecular characterization of endometrial tissue (ED) and amnion (AM) (A), and endometrial cells at diestrus stage (EDCs) and amniotic-derived stem cells (AMCs) (B). Qualitative and quantitative RT–PCR analysis for the expression of genes associated to differentiation of uterine stromal cells during early pregnancy (*Hoxa9*), those influencing pre-implantantion conceptus development (*ERα, ERβ, PR, PGRMC1* and *mPR*) and their regulators (*Wnt7a*, *Wnt4a*), and prostaglandin E_2 synthase (*PTGS2*), *FOXO1*, *SGK1*, and *TP53*. *GAPDH* was used as reference gene.
doi:10.1371/journal.pone.0111324.g002

strated that *PR, mPR, PGRMC1, Hoxa9, Wnt7a, Wnt4a*, as well as *PTGS2, FOXO1*, *SGK1* and *TP53* were expressed in ED and AM. While *ERα* was expressed by AM and ED, *ERβ* was not detected in both tissues.

Quantitative RT-PCR showed a statistically significant increase in the expression of *mPR* (4.08±0.37; P<0.01), *PGRCM1* (1.52±0.3; P<0.05), *Wnt7a* (105.41±13.27), *Wnt4a* (1.66±0.11; P<0.05), and *PTGS2* (1.55±0.23; P<0.05) in the comparison of AM to ED (Fig 2A). Although *ERα* expression was demonstrated by conventional RT-PCR, when quantitatively analyzed it was found to be statistically lower when comparing AM to ED.

At P0, right after cell isolation, AMCs expressed all the genes studied with only the exception of *ERα* and *ERβ*. When cells from the amniotic membrane and endometrial tissue were quantitatively compared, data showed a significant upregulation in the expression of *PR* (1.3±0.11; P<0.05), *PGRCM1* (2±0.07; P< 0.01), *Hoxa9* (1.74±0.17; P<0.05), *Wnt7a* (3.16±0.7; P<0.01), and *PTGS2* (5.66±0.015) in AMCs (Fig 2B).

Despite being qualitatively detected in ED and AM and in cells derived from both sources, the levels of *FOXO1*, *SGK1* and *TP53* found in AM and AMCs were significantly lower in comparison to those observed in ED and EDCs (Fig 2B). No expression for the genes of interest was detected in further passages with only the exception of *Hoxa9* whose mRNA was found at P1 (data not shown). AMCs cultured in the presence of supplemented progesterone, expressed *Hoxa-9*, *PGRMC1* and *mPR* until the last passage studied (Fig 3).

Proliferation studies

Growth curve and DT. At P1, EDCs and AMCs demonstrated a growth curve with an initial lag phase of 3 days that decreased at P5 with AMCs growing more rapidly than EDCs during this phase (Figs 4A and 4B). The proliferative potential of EDCs was higher at P1 than at P5 in contrast with the results of AMCs.

The DT values at P1 were similar between the two cell lines (Fig 4C). In EDCs, it significantly increased (P<0.05) toward P5. On the contrary, the greater proliferative ability associated to AMCs was found between P3 and P5, and was further confirmed by the growth curve at passage 5. At each passage, the differences observed between the DT values observed for AMCs and EDCs was statistically significant (P<0.05). The mean DT value for the EDCs was 2.19±0.65 days, while it was 0.88±0.22 days for AMCs.

EDCs proliferation in presence of AMCs or AMC-CM. *In vitro* studies demonstrated that co-culture with AMCs significantly increased EDCs proliferation in all passages studied (Figs 4 A, B, C). The mean DT value for EDCs in the transwell experiment (1.78 days) had a decrease of ~1.23-fold in comparison to baseline EDCs proliferation in standard complete medium (2.19 days; P<0.05 for all comparisons). The culture in the presence of AMC-CM was able to stimulate EDCs proliferation to the same level of that obtained when cells were grown in the transwell system (DT value of 1.63 days with a decrease of ~1.34-fold). Co-culture with fibroblasts, physically separated through a transwell system or in presence of their CM, did not induce any change in the proliferative potential of EDCs (Figs 4 D, E, F).

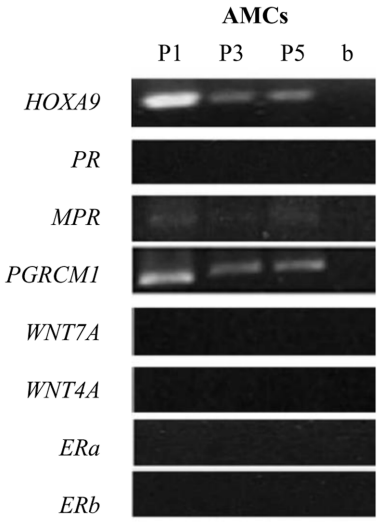

Figure 3. Molecular characterization of AMCs. Conventional RT-PCR analysis of evaluated genes in AMCs after culture with progesterone from passage 1 (P1) to passage (P5).
doi:10.1371/journal.pone.0111324.g003

Discussion

As in humans, equine fetal adnexa have been recently suggested as appealing candidates for the derivation of MSCs to be used in cell-based therapies [4,17–26] due to their higher proliferation capacity, longer telomeres, broader differentiation, and extensive proliferative potential in comparison to cells obtained from adult tissues [5,17,27].

We previously isolated AMCs from the equine amniotic membranes confirming that these cells share specific characteristics with embryonic and adult stem cells; they express representative mesenchymal (*CD105*, *CD44*, *CD29*, *CD166*) and pluripotent (Tra-1-60, SSEA-4, Oct-4) markers, are highly proliferative and retain high plasticity [4,5]. We also provided evidence of their superior efficacy in tendon regeneration compared to their bone marrow counterparts when allogeneically transplanted *in vivo* [4,6].

Taken together, these characteristics make AMCs suitable candidates for endometrial regeneration. To test this hypothesis we further characterized AMCs comparing them to uterine stromal cells collected at diestrus, due to the similarities found in the hormonal profile between early pregnancy and the diestrous stage. Both stages are characterized by high blood progesterone level [28].

Our data demonstrates that at P0, AM and AMCs are similar to ED and EDCs, respectively, for the expression of some endometrial-specific genes. Although our study only assayed a few genes, we selected the ones that are crucial in the process of conceptus-endometrium interaction. In particular, we found the expression of *Wnt4a* statistically higher in AM than ED and with similar results between AMCs and EDCs. This data can be explained with the role that the wingless type genes play in reproductive events:

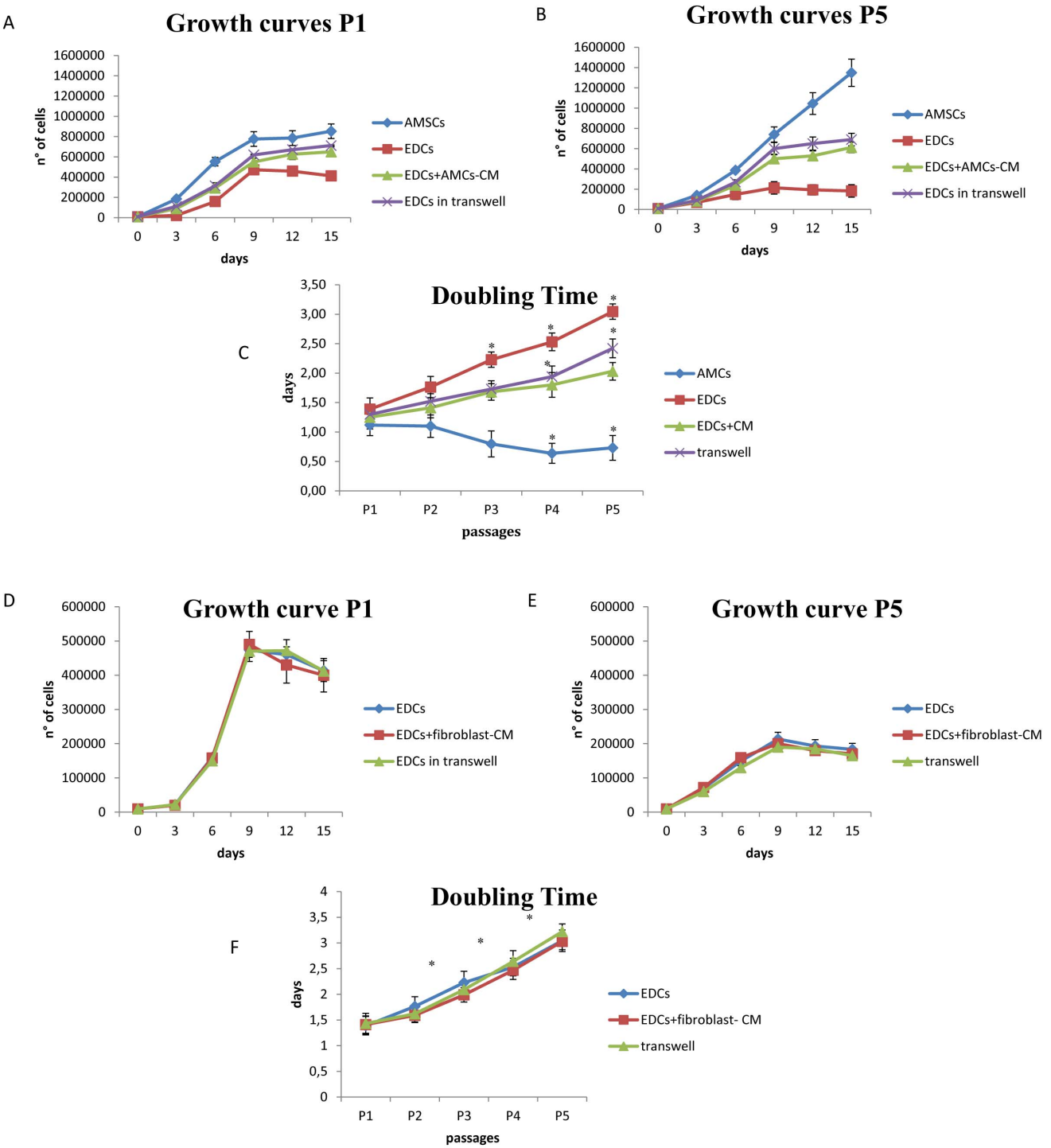

Figure 4. Proliferation studies. Growth curve at P1 (A) and P5 (B) for AMCs and EDCs alone or in co-culture with AMCs by transwell system or by AMC-conditioned medium (AMC-CM). Doubling times at different passages during cell culture for both AMCs and EDCs (C) in different culture conditions. Asterisks represent statistically different doubling times with respect to P1 ($P<0.01$). Growth curve at P1 (D) and P5 (E) for EDCs alone or in co-culture with fibroblast by transwell system or by fibroblast-conditioned medium. Doubling times at different passages during cell culture for EDCs (E) in different culture conditions with fibroblast. Asterisks represent statistically different doubling times with respect to P1 ($P<0.01$).
doi:10.1371/journal.pone.0111324.g004

including the establishment and maintenance of pregnancy, implantation, proliferation, and secretion activity of endometrium during the estrous cycle and pregnancy [29–32].

According to this, we can hypothesize that in horses *Wnt7a* and *Wnt4a* regulation allows the synchronization of the uterus and embryo development during the pre-implantation period of the mare as proposed in sheep and mice [28,33,34].

The AbdB-like Hoxa family includes a second class of genes differentially expressed during early pregnancy and primarily confined to the mesenchymal cell compartment during in utero

development [35,36]. Among these genes, AMCs and EDCs share the expression of *Hoxa-9*, which is specifically involved in the Müllerian duct cell patterning into oviducts, uterus, and vagina [35], as well as uterine function during early pregnancy [36,37]. In particular, this gene is considered as one of the primary steroid hormone-responsive genes in the uterine stroma of humans and mice [35]. Its expression is regulated by factors such as ovarian steroids, interferons, and embryonic oestrogen in human [38], mouse [31], sheep [39], pig [40], and recently in equine endometrium [28]. As in humans, equine proliferation and secretion of endometrial cells, implantation of embryo, renewal of endometrial layers, and configuration of endometrial gland morphogenesis [29,33,41] are essential processes for the establishment of pregnancy [42] controlled by ovarian steroid hormones and local growth factors [43]. Among these, progesterone and estrogens are at the forefront of the cascade that could play a critical role in endometrial maturation and receptivity [44] and are thought to influence pre-implantation conceptus development [45,46]. These hormones are thought to act indirectly via the endometrium. As mentioned above, progesterone mediates endometrial maturity and receptivity through specific nuclear receptors [47]. Data obtained herein demonstrate that the levels of expression of *mPR* and *PGRMC1* detected in AM and AMCs respectively, are even higher than those found in ED and EDCs. These findings may indicate the differential biological effect exerted by progesterone on the amniotic membrane and on the cells derived from it. While in ED it acts through a relatively slow 'genomic pathway' [45,46], in the amniotic tissues progesterone seems to work via ligand-specific steroid receptors, including the non-classical membrane-associated receptors we analysed (*PGRMC1* and *mPR*) [48,49].

The co-expression of *Wnt* and *Hoxa9* as well as the progesterone receptors in AMCs, suggests that these cells share similar cellular and molecular characteristics with uterine stromal cells. For some of the genes studied, our results confirm those obtained in humans, showing the same pattern of expression [50]. The loss of expression of some markers observed soon after AMCs isolation, as well as in EDCs, could depend on the culture conditions employed in this study with the consequent changes induced during the expansion.

When the expression of *FOXO1*, *SGK1*, and *TP53* was investigated the levels found in AM and AMCs were significantly lower than those observed in ED and EDCs. So far, no data has been published regarding these markers as crucial players in the process of conceptus-endometrium interaction in the equine species, and only one paper reports the link between TP53 transcriptional activity and cattle reproduction (10). Further studies are required to elucidate the role of *FOXO1*, *SGK1*, and *TP53* regulation in horses. At a molecular level, this study reinforces our previous findings regarding the immunomodulatory potential of the amniotic membrane and the cells derived from them (7) and further highlights their potential use in cell-based therapies. This observation comes from the higher levels of *PTGS2* expression found in AM and AMCs compared to their endometrial counterparts. It is important to point out that prostaglandin E_2 not only exerts a crucial role as immunosuppressive molecules during pro-inflammatory events, but are also known to be actively involved at the onset of pregnancy as temporary luteo-protective factors [51].

To recreate the biochemical cues found during gestation, characterized by high progesterone levels, we optimized the AMCs culture system supplementing the media with progesterone. The presence of progesterone in the culture media was sufficient to preserve the expression of membrane-bound intracellular progesterone receptors and *Hoxa-9* along the 5 passages *in vitro*. Since endometrial receptivity depends on the number of progesterone receptors in epithelial and stromal cells [52], our data provide an intriguing indication of the possible application of AMCs in endometrial regeneration.

Whether the major contribution of AMCs to the healing process depends on their ability to differentiate, the immunomodulatory and trophic factors they release, or is a combination of the two mechanisms is still under debate [53,54]. The present study also provides evidence of the role that soluble signals produced by AMCs may have in promoting EDC proliferation. Indeed, the presence of AMCs by transwell system or the effect of AMC-CM increased the EDCs proliferation.

In conclusions, the present work lays the foundation for *in vivo* studies on the potential application of AMCs in the treatment of horse uterine diseases. A substantial overlap was found between equine amnion and endometrium based on gene expression profiling, indicating that AMCs are ideal therapeutic candidates for uterine cells replenishment when scarcity or low proliferation of uterine endometrial cells is associated with pregnancy failure. Besides this, our data reinforce the idea that MSCs obtained from gestational tissues exert their beneficial effects in tissue regeneration through the release of soluble factors and indicates the conditioned media as novel therapeutic cell-free products for regenerative medicine applications.

Supporting Information

Figure S1 Characterization of AMCs. (A) Flow cytometric analysis for the evaluation of pluripotency-associated markers (Oct-4, c-Myc and SSEA-4). Histograms represent relative number of cells vs. fluorescence intensity. Gray histograms indicate background fluorescence intensity of cells labelled with isotype control antibodies only; green histograms show positivity for the marker of interest. (B) RT–PCR analysis of mesenchymal (*CD29, CD44, CD166* and *CD105*), haematopoietic (*CD34*) specific gene expression at P1. Major histocompatibility complex (*MHC*) I and II gene expression is also reported.
(TIF)

Materials S1
(DOC)

References S1
(DOC)

Results S1
(DOC)

Author Contributions

Conceived and designed the experiments: ALC FC BC DB. Performed the experiments: ALC BC AC AR MGM CP FC. Analyzed the data: ALC BC AC AR MGM. Contributed reagents/materials/analysis tools: DB FC. Wrote the paper: ALC BC FC DB.

References

1. Merkt H, Gunzel AR (1979) A survey of early pregnancy losses in West German thoroughbred mares. Equine Vet J 11: 256–258.

2. Ginther OJ, Bergfelt DR, Leith GS, Scraba ST (1985) Embryonic loss in mares: incidence and ultrasonic morphology. Theriogenology 24: 73–86.

3. LeBlanc MM (2010) Advances in the diagnosis and treatment of chronic infectious and post–mating-induced endometritis in the mare. Reprod Dom Anim 45 (Suppl. 2): 21–27.
4. Lange-Consiglio A, Corradetti B, Bizzaro D, Magatti M, Ressel L, et al. (2012) Characterization and potential applications of progenitor-like cells isolated from horse amniotic membrane. J Tissue Eng Regen Med 6: 622–635.
5. Lange-Consiglio A, Corradetti B, Meucci A, Bizzaro D, F . Cremonesi (2013a) Characteristics of equine mesenchymal stem cells derived from amnion and bone marrow: *in vitro* proliferative and multilineage potential assessment Equine Vet J 45(6): 737–744.
6. Lange-Consiglio A, Tassan S, Corradetti B, Meucci A, Bizzaro D, et al. (2013b) Investigating the potential of equine mesenchymal stem cells derived from amnion and bone marrow in equine tendon diseases treatment in vivo. Cytotherapy 15: 1011–1020.
7. Lange-Consiglio A, Rossi D, Tassan S, Perego R, Cremonesi F, et al. (2013c) Conditioned medium from horse amniotic membrane-derived multipotent progenitor cells: immunomodulatory activity in vitro and first clinical application in tendon and ligament injuries in vivo. Stem Cells Dev 22(22): 3015–3024.
8. Dorniak P, Spencer TE (2013) Biological roles of progesterone, prostaglandins, and interferon-tau in endometrial function and conceptus elongation in ruminants. Anim Reprod: 10: 239–251.
9. Kajihara T, Brosens JJ, Ishihara O (2013) The role of FOXO1 in the decidual transformation of the endometrium and early pregnancy. Medical Molecular Morphology 46: 61–68.
10. Ponsuksili S, Murani E, Schwerin M, Schellander K, Tesfaye D, et al. (2012) Gene expression and dna-methylation of bovine pretransfer endometrium depending on its receptivity after in vitro-produced embryo transfer. PLOS ONE 7: e42402.
11. Feroze-Zaidi F, Fusi L, Takano M, Higham J, Salker MS et al. (2007) Role and Regulation of the Serum- and Glucocorticoid- Regulated Kinase 1 in Fertile and Infertile Human Endometrium. Endocrinology 148: 5020–5029.
12. Bigsby RM, Cunha GR (1986) Estrogen stimulation of deoxyribonucleic acid synthesis in uterine epithelial cells which lack estrogen receptors. Endocrinology 119: 390–396.
13. Kurita T, Young P, Brody JR, Lydon JP, O'Malley BW, et al. (1998) Stromal progesterone receptors mediate the inhibitory effects of progesterone on estrogen-induced uterine epithelial cell deoxyribonucleic acid synthesis. Endocrinology 139: 4708–4713.
14. Hwang NS, Zhang C, Hwang YS Varghese S (2009) Mesenchymal stem cell differentiation and roles in regenerative medicine. Wiley Interdiscip Rev Syst Biol Med 1: 97–106.
15. Daels PF, Hughes JP (2005) The normal estrous cycle. In: Equine reproduction. A.O McKinnon and J.L. Voss Eds, 6th edition, Wiley-Blackwell Publishing, USA 121–132.
16. Donofrio G, Franceschi V, Capocefalo A, Cavirani S, Sheldon IM (2008) Bovine endometrial stromal cells display osteogenic properties. Reproductive Biology and Endocrinology 6: 65–73.
17. Kern S, Eichler H, Stoeve J, Kluter H, Bieback K (2006) Comparative analysis of mesenchymal stem cells from bone marrow, umbilical cord blood, or adipose tissue. Stem Cells 24: 1294–1301.
18. Koch TG, Heerkens T, Thomsen PD, Betts DH (2007) Isolation of mesenchymal stem cells from equine umbilical cord blood. BMC Biotechnol 30: 7–26.
19. Guest DJ, Ousey IC, Smith MRW (2008) Defining the expression of marker genes in equine mesenchymal stromal cells. Stem Cells Clon Adv Appl 1: 1–9.
20. Reed SA, Johnson SE (2008) Equine umbilical cord blood contains a population of stem cells that express Oct4 and differentiate into mesodermal and endodermal cell types. J Cell Physiol 215: 329–336.
21. Bartholomew S, Owens SD, Ferraro GL, Carrade DD, Lara DJ, et al. (2009) Collection of equine cord blood and placental tissues in 40 thoroughbred mares. Equine Vet J 41: 724–728.
22. Hoynowski SM, Fry MM, Gardner BM, Leming MT, Tucker JR, et al. (2007) Characterization and differentiation of equine umbilical cord-derived matrix cells. Biochem Biophys Res Commun 362: 347–353.
23. Cremonesi F, Violini S, Lange Consiglio A, Ramelli P, Ranzenigo G, et al. (2008) Isolation, in vitro culture and characterization of foal umbilical cord stem cells at birth. Vet Res Commun 32: 139–142.
24. Passeri S, Nocchi F, Lamanna R, Lapi S, Miragliotta V, et al. (2009) Isolation and expansion of equine umbilical cord-derived matrix cells (EUCMCs) Cell Biol Int 33: 100–105.
25. Iacono E, Cunto M, Zambelli D, Ricci F, Tazzari PL, Merlo B (2012) Could fetal fluid and membranes be an alternative source for Mesenchymal Stem Cells (MSCs) in the feline species? A preliminary study. Vet Res Commun 36(2): 107–118.
26. Corradetti B, Lange-Consiglio A, Barucca M, Cremonesi F, Bizzaro D (2011) Size-Sieved subpopulations of mesenchymal stem cells from intervascular and perivascular equine umbilical cord matrix. Cell Proliferation 44: 330–342.
27. Kogler G, Sensken S, Airey JA, Trapp T, Muschen M, et al. (2004) A new human somatic stem cell from placental cord blood with intrinsic pluripotent differentiation potential. J Exp Med 200: 123–135.
28. Atli MO, Guzeloglub A, Dincb DA (2011) Expression of wingless type (WNT) genes and their antagonists at mRNA levels in equine endometrium during the estrous cycle and early pregnancy. Animal Reproduction Science 125: 94–102.
29. Chen Q, Zhang Y, Lu J, Wang Q, Wang S, et al. (2009) Embryo-uterine cross-talk during implantation: the role of Wnt signaling. Mol Hum Reprod 15: 215–221.
30. Miller C, Pavlova A, Sassoon DA (1998) Differential expression patterns of Wnt genes in the murine female reproductive tract during development and the estrous cycle. Mech Dev 76: 91–99.
31. Hayashi K, Erikson DW, Tilford SA, Bany BM, Maclean JA, et al. (2009) WNT genes in the mouse uterus: potential regulation of implantation. Biol Reprod 80: 989–1000.
32. Nusse R (accessed 18.12.09), http://www.stanford.edu/~rnusse/wntwindow.
33. Mohamed OA, Jonnaert M, Labelle-Dumais C, Kuroda K, Clarke H (2005) Uterine Wnt/Beta-catenin signaling is required for implantation. Proc Natl Acad Sci USA 102: 8579–8584.
34. Hayashi K, Burghardt RC, Bazer FW, Spencer TE (2007) WNTs in the ovine uterus: potential regulation of peri-implantation ovine conceptus development. Endocrinology 148: 3496–3506.
35. Ma L, Benson GV, Lim H, Dey SK, RL Maas (1998) Abdominal B (AbdB) Hoxa Genes: regulation in adult uterus by estrogen and progesterone and repression in Müllerian duct by the synthetic estrogen diethylstilbestrol (DES) Dev Biol 15: 141–154.
36. Lim H, Ma L, Ma W, Maas RL, KS Dey (1999) Hoxa-10 regulates uterine stromal cell responsiveness to progesterone during implantation and decidualization in the mouse. Mol Endocrinol 3: 1005–1017.
37. Benson GV, Lim H, Paria BC, Satokata I, Dey SK, et al. (1996) Mechanisms of reduced fertility in Hoxa-10 mutant mice: uterine homeosis and loss of maternal Hoxa-10 expression. Development 122: 2687–2696.
38. Tulac S, Nayak NR, Kao LC, Van Waes M, Huang J, et al (2003) Identification, characterization, and regulation of the canonical Wnt signaling pathway in human endometrium. J Clin Endocrinol Metab 88: 3860–3866.
39. Kim S, Choi Y, Bazer FW, Spencer TE (2003) Identification of genes in the ovine endometrium regulated by interferon tau independent of signal transducer and activator of transcription 1. Endocrinology 144: 5203–5214.
40. Kiewisz J, Kczmarek MM, Blitek A, Bodek G, Ziecik AJ (2008) Expression profile of the Wnt5a, Wnt7a, beta-catenin and E-cadherin genes in the endometrium during peri-implantation period in pigs. Reprod Dom Anim 43: 92.
41. Mericskay M, Kitajewski J, Sassoon D (2004) Wnt5a is required for proper epithelial–mesenchymal interactions in the uterus. Development 13: 2061–2072.
42. Hess AP, Nayak NR, Giudice LC (2006) Oviduct and endometrium: cyclic changes in the primate oviduct and endometrium. In: Neill, J.M. (Ed.), Knobil and Neill's Physiology of Reproduction, 3rd edition. Elsevier Academic Press Inc., United States of America 9: 337–382.
43. Paria BC, Lim H, Das SK, Reese J, Dey SK (2000) Molecular signalling in uterine receptivity for implantation. Cell Dev Biol 11: 67–76.
44. de Ziegler D, Fanchin R, de Moustier B, Bulletti C (1998) The hormonal control of endometrial receptivity: estrogen (E2) and progesterone. J Reprod Immunol 39: 149–166.
45. Beato M (1989) Gene regulation by steroid hormones. Cell 56: 335–344.
46. Tuohimaa P, Blauer M, Pasanen S, Passinen S, Pekki A (1996) Punnonen R. Mechanisms of action of sex steroid hormones: basic concepts and clinical correlations. Maturitas 23(Suppl): S3–12.
47. Suzuki T, Schirra F, Richards SM, Jensen RV, Sullivan DA (2008) Estrogen and progesterone control of gene expression in the mouse meibomian gland. Invest Ophthalmol Vis Sci 49: 1797–1808.
48. Falkenstein E, Norman AW, Wehling M (2000) Mannheim classification of nongenomically initiated (rapid) steroid action(s) J Clin Endocrinol Metab 85: 2072–2075.
49. Rambags BP, van Tol HT, van den Eng MM, Colenbrander B, Stout TA (2008) Expression of progesterone and oestrogen receptors by early intrauterine equine conceptuses. Theriogenology 69: 366–375.
50. Han K, Lee JE, Kwon SJ, Park SY, Shim SH, et al. (2008) Human amnion-derived mesenchymal stem cells are a potential source for uterine stem cell therapy. Cell Prolif 41(5): 709–725.
51. Fischer C, Drillich M, Odau S, Heuwieser W, Einspanier R, et al. (2010) Selected pro-inflammatory factor transcripts in bovine endometrial epithelial cells are regulated during the oestrous cycle and elevated in case of subclinical or clinical endometritis. Reprod Fertil Dev 22: 818–829.
52. Diedrich K, Fauser BC, Devroey P, Griesinger G (2007) The role of the endometrium and embryo in human implantation. Hum Reprod Update 13: 365–377.
53. Chong AK, Chang J, Go JC (2009) Mesenchymal stem cells and tendon healing. Front Biosci 14: 4598–4605.
54. Yagi H, Soto-Gutierrez A, Parekkadan B, Kitagawa Y, Tompkins RG, et al. (2010) Mesenchymal stem cells: Mechanisms of immunomodulation and homing. Cell Transplant 19: 667–679.

Perrini et al. Stem Cell Research & Therapy (2016) 7:169
DOI 10.1186/s13287-016-0429-6

Stem Cell Research & Therapy

RESEARCH Open Access

Microvesicles secreted from equine amniotic-derived cells and their potential role in reducing inflammation in endometrial cells in an in-vitro model

Claudia Perrini[1], Maria Giuseppina Strillacci[2], Alessandro Bagnato[2], Paola Esposti[1], Maria Giovanna Marini[3], Bruna Corradetti[3], Davide Bizzaro[3], Antonella Idda[4], Sergio Ledda[4], Emanuele Capra[5], Flavia Pizzi[5], Anna Lange-Consiglio[1*] and Fausto Cremonesi[1,2]

Abstract

Background: It is known that a paracrine mechanism exists between mesenchymal stem cells and target cells. This process may involve microvesicles (MVs) as an integral component of cell-to-cell communication.

Methods: In this context, this study aims to understand the efficacy of MVs in in-vitro endometrial stressed cells in view of potential healing in in-vivo studies. For this purpose, the presence and type of MVs secreted by amniotic mesenchymal stem cells (AMCs) were investigated and the response of endometrial cells to MVs was studied using a dose-response curve at different concentrations and times. Moreover, the ability of MVs to counteract the in vitro stress in endometrial cells induced by lipopolysaccharide was studied by measuring the rate of apoptosis and cell proliferation, the expression of some pro-inflammatory genes such as tumor necrosis factor-α (*TNF-α)*, interleukin-6 (*IL-6)*, interleukin 1β (*IL-1β),* and metalloproteinases (*MMP*) 1 and 13, and the release of some pro- or anti-inflammatory cytokines.

Results: MVs secreted by the AMCs ranged in size from 100 to 200 nm. The incorporation of MVs was gradual over time and peaked at 72 h. MVs reduced the apoptosis rate, increased cell proliferation values, downregulated pro-inflammatory gene expression, and decreased the secretion of pro-inflammatory cytokines.

Conclusion: Our data suggest that some microRNAs could contribute to counteracting in-vivo inflammation of endometrial tissue.

Keywords: Microvesicles, Endometrium, Inflammation, LPS, Regenerative medicine

Background

The regular uterine environment promotes normal embryo development, but clinical or subclinical disorders could contribute to pregnancy failure. As reviewed by Hurtgen [1], endometritis is an important cause of reduced fertility in mares in which artificial insemination by fresh or frozen semen may induce acute endometrial inflammatory reactions. If these conditions are not promptly resolved, infections become chronic and, in old pregnant mares, often result in higher pregnancy loss. A similar clinical endometritis also occurs in dairy cows following parturition [2, 3]. Furthermore, cytological endometritis emerged as a problem of remarkable importance for dairy cattle reproduction because animals suffering from this disorder present a persistent inflammatory uterine environment even in the absence of clinical symptoms. A reduced conception rate and increased calving-to-conception intervals are consequences of these uterine diseases [4–7].

Successful implantation requires a complex sequence of signaling events that are crucial to the establishment of pregnancy, and a large number of molecular mediators, influenced by the level of ovarian hormones, have been involved in this early embryo-maternal interaction.

* Correspondence: anna.langeconsiglio@unimi.it
[1]Large Animal Hospital, Reproduction Unit, Università degli Studi di Milano, Via dell'Università 6, 26900 Lodi, Italy
Full list of author information is available at the end of the article

These mediators include adhesion molecules, cytokines, growth factors, lipids, and others [8, 9]. Koot et al. [10] underlined that infertility could occur after the early phases of implantation as a malfunction of the endometrium-embryo 'dialogue'. The degree of endometrial production of these mediators could be impaired by persistent endometritis. Indeed, pro-inflammatory factors transcripted in bovine endometrial epithelial cells are elevated in cases of subclinical or clinical endometritis [11]. Repeat-breeding cows (animals that after three or more inseminations do not get pregnant because of fertilization failure or early embryonic death) show abnormalities in the growth factor-cytokine network, specifically in endometrial epidermal growth factor (EGF) concentration [12]. The EGF family acts on the trophectoderm, promoting cell attachment and embryo development [13], and its impairment could explain the pregnancy failure in these animals.

Many therapies have been proposed to treat or prevent mare endometritis. Post-mating endometritis is usually treated with uterine irrigation and ecbolic, while the acute endometritis treatment is performed with systemic or intra-uterine antibiotics. However, these therapies are not always effective for resolving chronic uterine inflammation. The prevention, mainly in cattle, includes nutritional supplements and hygienic conditions during parturition. Commonly, therapies in use include hormonal treatments with GnRH, exogenous gonadotrophins, and prostaglandins [14], or the exploitation of assisted reproductive techniques, such as in vitro embryo production and embryo transfer. However, in case of infertility due to endometrial damage, the embryo-maternal interaction and the restoration of uterine receptivity could be improved by regenerative medicine treatment.

Regenerative medicine has several applications in the treatment of many pathologies in both human and veterinary medicine. Treatments are based on mesenchymal stem cell (MSC) transplantation but, although engraftment of the transplanted MSCs has been documented in some cases [15–17], only a small percentage of the injected MSCs engraft successfully in various disease models [18–21]. In an irradiated murine model, endometrial regeneration by bone marrow-derived MSCs has been studied showing a low number of cells engrafted in the regenerating endometrium [22]. Consistent with these findings, some studies recently showed that the regenerative ability of MSCs could be attributed to the production of molecules and mediators capable of activating the intrinsic repair processes in the damaged tissues. To date, the conditioned medium (CM) obtained from in vitro cultured MSCs has been proven to be sufficient to stimulate the structural and functional regeneration of cardiac [20, 23], renal [19, 24], spinal cord [25], and tendon [26] tissues. These results indicate that the beneficial effects of MSCs can be attributed to the activation of paracrine mechanisms enabling stimulation of endogenous stem cells. These cells are responsible for the bioactive soluble factors (lipids, growth factors, and cytokines) known to inhibit apoptosis and fibrosis, enhance angiogenesis, stimulate mitosis and/or differentiation of tissue-resident progenitor cells, and modulate the immune response [27]. In addition to soluble factors, recent findings indicate that extracellular vesicles are released from MSCs inside the CM and that these can be involved as important mediators in cell-to-cell communication [28]. Microvesicles (MVs) have been categorized into exosomes (EXs), released from the endosomal compartment, and shedding vesicles (SVs), which bud directly from the cell membrane. MVs contain various active molecules such as lipids, proteins, mRNA, and microRNA (miRNA) [29]. It has been demonstrated that CM and MVs can be used in vitro and in vivo to repair tissue damage, increasing the healing rate [26, 29, 30]. MVs are involved in a dynamic mutual paracrine communication between the embryonic and the maternal environment at the early stage of pre-implantation embryo development [31]. Equine embryos at day 8 are thought to secrete MVs that can modulate the functions of the oviduct epithelium through transfer of early pregnancy factor (HSP10) and miRNAs [32]. On the other hand, MVs can be secreted from the maternal side, and endometrium-derived MV miRNAs are revealed to have potential targets in biological pathways highly relevant for embryo implantation [33]. Uterine miRNAs are suggested to play a potential regulatory role in the development and progression of bovine subclinical endometritis. Indeed, Hailemariam et al. [34] demonstrated that there is an aberrant expression of 23 miRNAs in cows with subclinical endometritis compared with healthy cows. Furthermore, they observed a similar expression of miRNA patterns in cytobrush samples from sick cows and in vitro cultured endometrial cells challenged by lipopolysaccharide (LPS). This suggests that in vitro endometrial cell culture, treated with LPS, could be an excellent model to test potential regenerative medicine treatments for endometritis. In human medicine, the different pattern of miRNAs between women with and without endometriotic disease have been proposed as biomarkers that could underpin the development of a noninvasive diagnostic test for endometriosis [35].

In this context, the aims of this study were to identify the presence and type of MVs secreted by amniotic mesenchymal progenitor cells (AMCs), and to elucidate whether equine endometrial cells could be targeted by MVs in vitro. In addition, we considered whether MVs are able to counteract an in vitro endometrial cell inflammatory process induced by LPS.

Methods

Materials

Uteri samples were collected from horses slaughtered in a national slaughterhouse under legal regulation. Chemicals were obtained from Sigma-Aldrich Chemical (Milan, Italy) unless otherwise specified, and tissue culture plastic dishes were purchased from Euroclone (Milan, Italy).

Study design

Initially, amniotic cells were isolated and cultured to produce MVs that were characterized using a Nanosight instrument (Nanoparticle tracking analysis, NTA; NanoSight Ltd., Amesbuty, UK). Endometrial cells were isolated, and specific endometrial genes were identified by qualitative reverse transcription polymerase chain reaction (RT-PCR). Isolated endometrial cells were used as the target for different concentrations of MVs. Furthermore, the effect of MVs on endometrial cells treated by LPS was analyzed by quantitative RT-PCR (qRT-PCR) expression of inflammatory genes, evaluation of the release of different cytokines, and viability cell tests. Finally, the presence of some miRNAs, regulating inflammation, inside the MVs was evaluated.

Tissue collection

Allanto-amniotic membranes were obtained at term from normal pregnancies in three mares. Samples of allanto-amnion were transported at 4 °C in calcium- and magnesium-free phosphate-buffered saline (PBS; Euroclone, Milan, Italy) supplemented with 4 mg/mL amphotericin (Euroclone), 100 UI/mL penicillin and 100 mg/mL streptomycin (Euroclone), and were processed within 12 h of collection. The amniotic membrane was mechanically separated from the allantois and the isolation of AMCs was performed as previously reported by Lange-Consiglio et al. [36].

Endometrial samples were obtained during the reproductive season from normal-cycling mares at diestrus stage (early-mid luteal phase). Before slaughtering, 5 ml of blood was collected in heparinized tubes from all mares. After centrifugation, plasma was separated, kept refrigerated, and immediately transported to the laboratory for progesterone determination by a quantitative enzyme linked fluorescent assay (ELFA) based on the MiniVidas (Biomerieux, Firenze, Italy) technology. According to the manufacturer, the measurement range of the assay varied from 0.25 to 80 ng/ml with an intra-assay variation of 4.12 % and an inter-assay variability of 6.32 %.

Only uteri belonging to mares with an obvious corpus luteum on the ovary and progesterone levels between 6 and 20 ng/ml, indicative of the early/mid diestral phase of the estrous cycle [37], were used for endometrial fragment collection and ensuing cell culture.

Tissue fragments for RNA isolation were immediately immersed in RNA Later solution, whereas those destined for cell isolation and the expansion procedure were kept at 4 °C in saline solution supplemented with 4 μg/ml amphotericin B, 100 IU/ml penicillin, and 100 μg/ml streptomycin and processed within 8 h.

Cell isolation

Amniotic membrane-derived mesenchymal cells were isolated as recently reported by Lange-Consiglio et al. [36]. Briefly, amnion fragments were incubated for 9 min at 38.5 °C in PBS containing 2.4 U/mL dispase (Becton Dickinson, Milan, Italy). After a resting period (5–10 min) at room temperature in high-glucose Dulbecco's modified Eagle's medium (HG-DMEM; EuroClone, Milan, Italy), supplemented with 10 % heat-inactivated fetal bovine serum (FBS) and 2 mM L-glutamine, the fragments were digested with 0.93 mg/mL collagenase type I and 20 mg/mL DNAse (Roche, Mannheim, Germany) for approximately 3 h at 37 °C. The amnion fragments were then removed, and mobilized cells were passed through a 100-μm cell strainer before being collected by centrifugation at 200 × g for 10 min.

Endometrial cells from diestrum uteri of mares were obtained according to the protocol described by Donofrio et al. [38] and slightly modified for equine cells. Briefly, the endometrium was digested in sterile filtered Hank's buffered salt solution supplemented with 2 mg/ml collagenase II, 4 mg/ml bovine serum albumin, and 0.4 mg/ml DNase I for 90 min at 38.5 °C in a shaking bath. Cells were then filtered through a membrane with a pore size of 80 μm and centrifuged at 200 × g for 10 min, then washed twice in PBS. This protocol allowed for the isolation of the endometrial stromal portion. Before seeding, cells were counted using a Burker chamber with the Trypan Blue dye exclusion assay.

Cell expansion

Endometrial cell (EDC) cultures were established in HG-DMEM supplemented with 10 % FBS, penicillin (100 UI/ml), streptomycin (100 μg/ml), 0.25 μg/ml amphotericin B, and 2 mM L-glutamine. Medium was supplemented with 10 ng/ml EGF for AMC cultures.

To remove non-adherent cells for both cell lines the medium was replaced for the first time after 72 h, and then changed either twice per week thereafter or according to the experiment requirements. For maintenance of cultures, cells were plated in flasks of 25 cm^2 at a density of 1×10^5 cells/cm^2 and incubated at 38.5 °C in a humidified atmosphere with 5 % CO_2. Adherent cells were detached with 0.05 % trypsin-EDTA just prior to reaching confluence (80 %) and then reseeded for culture maintenance at a density of 1×10^4 cells/cm^2.

A detailed characterization of these cells was performed in the paper of Corradetti et al. [39]. In this study, a molecular characterization of EDCs was performed only at passage (P)0 as a de facto control for gene expression.

Isolation and measurements of MVs

MVs were obtained from the culture media of AMCs derived from three different placentas, cultured for 1 week with HG-DMEM supplemented with 10 % MV-deprived FCS and overnight in HG-DMEM deprived of FCS and supplemented with 0.5 % BSA (Sigma). The overnight culture media were pooled and centrifuged at 2000 × g for 20 min to remove debris, then at 100,000 × g (Beckman Coulter Optima L-100 K ultracentrifuge) for 1 h at 4 °C, washed in serum-free medium 199 containing N-2-hydroxyethylpiperazine-N-2-ethanesulfonic acid (HEPES; 25 mM) and submitted to a second ultracentrifugation under the same conditions. After ultracentrifugation, the pellet was immediately resuspended in HG-DMEM, and a fraction of the resuspended pellet was taken for measurements of MV size and concentration. A second fraction was labeled with fluorochrome PKH-26 and the remaining part of the pellet was cryopreserved with 1 % dimethylsulfoxide at −80 °C and used for the in vitro test. The size and concentration of MVs were evaluated by the Nanosight LM10 instrument, which permits discrimination of microparticles less than 1 μm in diameter. The software (NTA 2.0 analytic software) allows the analysis of video images of particle movement under Brownian motion and the calculation of diffusion coefficient, sphere equivalent, and hydrodynamic radius of particles by using the Strokes–Einstein equation. This instrument was configured with a 405-nm laser and a high-sensitivity sCMOS camera (OrcaFlash2.8, Hamamatsu C11440, NanoSight Ltd). Videos were collected and analyzed using the NTA software with the minimal expected particle size, minimum track length, and blur setting all set to automatic. Ambient temperature was recorded manually and did not exceed 25 °C. Each sample (5 μl) was diluted in sterile physiological solution to a final volume of 1 ml. Samples were analyzed within 15 min of the initial dilution with a delay of 10 s between sample introduction and the start of the measurement. For each sample, multiple videos of 30 s duration were recorded generating replicate histograms that were averaged.

MVs labeling with PKH-26

To trace in vitro MVs by fluorescence microscopy, MVs from AMCs were labeled with the red fluorescence aliphatic chromophore intercalating into lipid bilayers PKH26 dye (Sigma). Briefly, after ultra-centrifugation, the MV pellet was diluted to 1 ml with PKH-26 kit and 2 μl of fluorochrome was added to this suspension and incubated for 30 min at 38.5 °C. At the end of the reaction, 7 ml of serum-free DMEM was added to the suspension that was ultra-centrifuged again at 100,000 g for 1 h at 4 °C. The final pellet was immediately resuspended in HG-DMEM.

Incorporation of MVs in endometrial cells

To study the incorporation capacity of MVs into endometrial cells, a dose-response growth was performed in three replicates. Endometrial cells were seeded at a density of 60×10^3 on culture slides (13 mm; Nalgen Nunc International, Rochester, NY, USA) in 24 wells and co-cultured with 10, 20, 30, 40, and 50×10^6 MVs/ml labeled with PKH-26 dye, and pre-incubated or not with trypsin (0.5 mM) for 24, 48, and 72 h at 38.5 °C. At the end of each experimental condition, cells were nuclear stained with 10 μg/ml Hoechst 33343 for 15 min at 38 °C. The uptake of MVs was evaluated by an Olympus BX51 microscope equipped with a Scion Corporation 1394 video camera interfaced with a computer provided with software for image acquisition and analysis (Image-Pro Plus 5.1-Media Cybernetics, Immagini & Computer, Bareggio, Italy). Excitation wavelength was positioned at 550 nm while emission wavelength was set at 567 nm. Hoechst 33342 dye (Sigma) was excited at 353–365 nm while the emission wavelength was set at 460 nm. To detect the intensity of fluorescence, a semi-quantitative analysis was performed. Different images were acquired for each condition and then, for each image, the area of interest (AOI; where the signal was present) was manually defined by the user. Inside the AOI, up to three different background signals were sampled. The background areas were positioned by the user only where the fluorescent signal was not specific. The maximum value collected from the background areas was then used to define the threshold. Only fluorescence with an intensity above the threshold was considered to indicate fluorescence due to labeled MVs. Finally, the program measured the signal intensity expressed in arbitrary units (a.u.).

Confocal microscopy analysis to assess internalization of MVs was performed using a Leica SP2 laser scanning confocal microscope (Leica Microsystems Srl, Italy) equipped with a PL Fluotar 20× AN 0.5 Dry objective.

In vitro effect of MVs on endometrial cells treated with LPS

The dose-response curve of LPS on endometrial cells was studied showing that 10 ng/ml and 12–24 h were the dose and the times most effective in inducing cellular stress evaluated by an apoptotic study (data not shown). Sixty thousand cells were incubated at the same time with LPS 10 ng/ml and 40×10^6 MVs/ml for 3, 12, and 24 h. In another experimental condition,

endometrial cells were treated first for 3 h with LPS and then with MVs at the same concentrations and times. In the last experiment, endometrial cells were treated first for 24 h with MVs and then with LPS 10 ng/ml. Endometrial cells alone or endometrial cells with LPS or MVs only were used as controls at different times. At the end of each experimental condition, the MTT reduction assay method and apoptotic test were used to analyze cell proliferation and viability of cells on some samples. Cells from other samples were detached with 0.05 % trypsin-EDTA, centrifuged, and cryopreserved for molecular biology studies in liquid nitrogen using standard cryopreservation protocols. The supernatants were destined for the evaluation of cytokines released from endometrial cells. All experiments were performed in three replicates.

Viability cell tests

Cell proliferation test by MTT reduction assay method

The MTT reduction assay method (Chemicon, Temecula, CA, USA) estimates the activity of the enzyme dehydrogenase by converting the MTT compound (3-(4,5-dimethylthiazol- 2-yl)-2,5-diphenyletrazolium bromide) into formazan by the mitochondria. The measurement was performed with a spectrophotometer (Perking Elmer HTS 700 plus; Boston, MA, USA) at the absorbance reading of 570 nm for each sample. Briefly, at each experimental condition of in vitro effect of MVs on endometrial cells treated with LPS, cells were washed twice in PBS, and 1 ml of 5 mg/l MTT solution was added to each well. Avoiding light, plates were then placed in a humidified incubator at 37 °C for 4 h. The supernatant was discarded, 1 ml of dimethylsulfoxide was added as an extracting solution, and plates were incubated for 2 h until the precipitations were resolved completely for spectrophotometric reading. This test was performed in three replicates.

Apoptotic test

The percentage of apoptotic cells was assessed using an Annexin-V-FITC Apoptosis Detection KIT (Sigma) following the manufacturers' instructions; 500 μl of cells (5×10^5 cells) were incubated with 5 μl of Annexin V solution and with 10 μl propidium iodide for 1 h at room temperature while protected from light. Apoptosis rates were evaluated by conventional fluorescence analysis using a BX 51 microscope (Olympus) equipped with a DMU filter set. One hundred cells were analyzed using a combination of 488/560 nm emission. Cells at the early stage of apoptosis stained with the annexin V-FITC alone. Live cells showed no staining with either propidium iodide or Annexin V-FITC. Cells dead for apoptosis were stained by both propidium iodide and Annexin V-FITC, and cells dead for necrosis were stained by propidium iodide alone. The apoptotic test was performed in three replicates.

Molecular biology studies

Characterization of endometrial cells

After isolation from endometrial tissue, cells were analyzed to detect the expression of specific endometrial genes as previously reported [39]. Total RNA was extracted from endometrial cells immediately after isolation (P0) using TRI Reagent Solution (Life Technologies, Monza, Italy) and conventional RT-PCR was performed with RBC Taq DNA Polymerase (RBC Bioscience) using previously optimized primers [39]. The primer sequences and conditions are shown in Tables 1 and 2. Glyceraldehyde-3-phosphate dehydrogenase gene (*GAPDH*) was employed as a reference gene.

Gene expression of pro-inflammatory cytokines

Genes involved in the inflammatory process, such as interleukin-1β (*IL-1β*), interleukin-6 (*IL-6*) and tumor necrosis factor α *(TNF-α*), were analyzed by qRT-PCR under all experimental conditions. The mRNA expression levels of all genes were measured in three samples (biological replicates). Total RNA was isolated using the mirVana™ miRNA isolation Kit (Life Technologies) according to the manufacturer's protocol and stored at −20 °C. The concentration and purity of RNAs were evaluated three times by the NanoQuant spectrophotometer (Thermo Scientific, USA) and, in order to verify the integrity of extracted RNA, eight samples that were randomly chosen were analyzed on a Bioanalyzer 2100 using the Agilent RNA 6000 Pico Kit (Agilent). According to the RNA quantity, each sample was normalized to the final RNA concentration of 10 ng/μl.

RT-PCRs were performed with the High Capacity cDNA Reverse Transcription Kit (Applied Biosystems/Life Technologies, Carlsbad, CA, USA) using 100 ng of RNA per reaction.

All the qPCR experiments were run in triplicates (technical replicates) using the qPCR protocol described by TaqMan Fast Gene Expression Assays (Life Technologies™) on a 7500 Fast Real-time PCR System instrument (Applied Biosystems by Life Technologies™). To assess gene expression, each target gene and the *GAPDH*, as the housekeeping control gene, were co-amplified. The assay primers were available and synthesized by Life Technologies™.

Average target gene threshold cycle (ΔCt_g) for each sample (calculated using the CT values of the technical replicates within each experimental conditions) were normalized to the average GAPDH values (ΔCt_{GAPDH}) of the same cDNA sample. Then the expression variations calculated were normalized to the internal control (i.e., control cell at 3 h) using the ΔΔCt method.

Table 1 Oligonucleotide sequences used for reverse transcription polymerase chain reaction analysis

Reference sequence	Markers	Forward	Reverse	Annealing temperature	bp
XM_001498494.3	Progesteron Receptor (*PR*)	GTCAGTGGACAGATGCTGTA	CGCCTTGATGAGCTCTCTAA	55 °C	255
NM_001256979.1	Membrane-associated progesterone receptor (*MPR*)	GCCAAGTATCGTTACCGGAG	AAGAGGATCTGGAGCGTGTG	55 °C	173
XM_001914705.2	Progester one receptor membrane component 1 (*PGRMC1*)	TCAACGGCAAGGTGTTCGAC	GGCTCTTCCTCATCTGAGTA	58 °C	280
XM_003364827.1	Homeobox protein Hox-A9-like (*Hoxa9*)	ACGCTGGAACTGGAGAAAGA	CTTTCGCTCGGTCCTTATTG	55 °C	160
NM_001163856.1	Glyceraldehyde-3-phosphate dehydrogenase (*GAPDH*)	AGATCAAGAAGGTGGTGAAG	TTGTCATACCAGGAAATGAGC	59 °C	178
NM_001081847.2	Matrix metallopeptidase 1 (*MMP-1*)	ACTGCCAAATGGACTTCAAGCTGC	TCTTCACAGTGCTAGGAAAGCCG	60 °C	158
NM_001081804.1	Matrix metallopeptidase 13 (*MMP-13*)	CTCTGGTCTGCTGGCTCACGC	CCAAACTCGTGTGCAGCGAC	60 °C	132

Finally, the fold-change expression of each gene was calculated as $2^{-\Delta\Delta CT}$ [40].

Gene expression of metalloproteinases

Matrix metalloproteinase 1 (*MMP-1*) and matrix metalloproteinase 13 (*MMP-13)* were selected to evaluate the effect of MVs to contrast LPS activity. Gene expression was performed with the SYBR green method in a MyiQ iCycler thermal cycler (Biorad). Triplicate PCR reactions were carried out for each sample, analyzed using primer sequences reported in Table 1. The reactions were set on a strip in a final volume of 25 μl by mixing, for each sample, 1 μl of cDNA, 12.5 μl of 2× concentrated SYBR Premix Ex Taq II (Takara Bio) containing SYBR Green as a fluorescent intercalating agent, 0.2 μM forward primer, 0.2 μM of reverse primer, and MQ water. PCR efficiencies were tested and found to be close to 1. The thermal profile for all reactions was 30 s at 95 °C and then 40 cycles of 5 s at 95 °C, and 30 s at 60 °C. Fluorescence monitoring occurred at the end of each cycle. The efficiency of amplification for each primer was monitored through the analysis of serial dilution. Additional dissociation curve analysis was performed, and in all cases showed a single peak. The data thus obtained were analyzed using the iQ5 optical system software version 2.0 (BioRad). The expression of each gene was normalized to the reference gene *GAPDH* in order to standardize the results by eliminating variation in cDNA quantity. Sequences used are listed in Table 1.

miRNA analyses by RNA extraction and PCR amplification

The MV pellet was subjected to RNase digestion to remove extraneous ribonucleic acids [41]. Total RNA was isolated from a pool of different MVs and amniotic-derived cell preparations using the NucleoSpin® mRNA kit (Macherey-Nagel, Germany), in combination with TRIzol® lysis and purification of small and large RNA in one fraction (total RNA). RNAs were quantified using a NanoDrop ND-1000 spectrophotometer (NanoDrop Technologies, Wilmington, DE, USA). RNA quality was checked using the Agilent Bioanalyser 2100 (Agilent, Santa Clara, CA, USA), where the presence of small RNAs was verified in both MV and cell samples.

RNAs from all samples were reverse transcribed with the miScript Reverse Transcription Kit and the cDNA was then pre-amplified using the miScript PreAMP PCR Kit (all from Qiagen, Valencia, CA, USA), following the manufacturer's instruction with some modification: miScript PreAMP Primer Mix was replaced with miR-specific primers: hsa-miR-26a-2, -335, -146a, and SNORD95 as forward primer, and miScript Universal Primer as reverse primer in separate reactions. *Homo sapiens* hsa miRNA were perfectly homologous with *Equus caballus* eca miRNA sequence. PCR was performed on pre-amplified products using the PCR Master Mix (2×) (Thermo Fisher Scientific Inc., Waltham, MA, USA), with the same primer couple: hsa-miR-26a-2, -335, -146a, SNORD95 in combination with miScript Universal Primer. The small nucleolar snoRNA, C/D Box 95 SNORD95 was used as the positive control.

Table 2 Oligonucleotide sequences synthesized by Life Technologies

Assay ID	Gene symbol	Entrez gene ID	NCBI assembly	CHR	Location on NCBI genome assembly	Location on transcript or gene
Ec03467871_m1	*TNF*	100033834	2.1	20	31359792	318
Ec03468680_m1	*IL-6*	100034196	2.1	4	54424314	468
Ec04260298_s1	*IL-1B*	100034237	2.1	Un|NW_001871813.1	5795	254

Negative controls using water in place of the pre-Amp product were performed alongside each reaction. The cycling conditions were 3 min at 95 °C, followed by 35 cycles of 30 s at 95 °C, 30 s at 58 °C, 1 min at 72 °C, and finally 7 min at 72 °C. The amplified PCR products were separated electrophoretically on 2.5 % agarose gels, and visualized under UV, using the GeneRuler 50 bp as a DNA ladder (Thermo Fisher Scientific Inc.).

Cytokines

Cytokine release (IL-6, transforming growth factor (TGF)-β, and TNF-α) was measured in cell-free supernatants obtained by centrifugation at 1200 rpm for 5 min and stored at −80 °C until measurement. Cytokine production was assessed by commercially available sandwich ELISAs (Bioptis SA, Liege, Belgium). ELISAs were performed according to the supplier's instructions. Results are expressed in pg/ml. The limit of detection was 15.6 pg/ml for all cytokines tested.

Statistical analysis

For quantitative PCR experiments, data were analyzed by one-way analysis of variance (ANOVA). Also, cell viability data were analyzed by one-way ANOVA applying a Bonferroni correction.

For cytokines, statistical differences were determined using ANOVA followed by Dunnett's multiple comparison test, the Tukey–Kramer multiple comparisons test or unpaired *t* test.

Differences were considered statistically significant if the value of *P* was <0.05.

Results

Tissue collection and cell isolation

Cells were selected for their ability to adhere to plastic. For AMCs, the initial viability was >90 %, whereas for EDCs it was >85 %. EDCs (Fig. 1a) and AMCs (Fig. 1b) displayed fibroblast-like morphology. Molecular biology analyses at P3 showed that AMCs showed a typical mesenchymal stromal phenotype, with the expression of markers such as CD29, CD44, CD106, CD105, and MHCI, but not CD34 and MHCII. Moreover, AMCs showed differentiative potential in mesenchymal (osteogenic, adipogenic, and chondrogenic) and ectodermic lines (neurogenic) as reported by Lange-Consiglio et al. [36].

The molecular biology study on endometrial cells at P0 confirmed that these cells were endometrial cells because of the expression of *PR, MPR, PGRMC1, HOXA-9* (Fig. 1c).

Isolation and measurement of MVs

In all the studied samples, the viability of AMCs at the time of MV collection was 99 % as detected by trypan blue exclusion. By Nanosight, the size of MVs ranged from 50 to 670 nm, with a mean size of 258 ± 55 nm for three samples. The number of MVs ranged from 800 to 4700 particles/cell, with a mean value of 2550 ± 71 particles/cell (corresponding to 540×10^6 particles/ml of medium). In a previous study [42], transmission electron microscopy (TEM) analysis revealed the presence of variably sized extracellular membranous vesicles budding from, or lying near, the cell of origin. The size of MVs ranged from 100 nm to 1000 nm, with a predominance of vesicles between 100 and 200 nm. Because of the size, by Nanosight and TEM, and morphological characteristics, the vesicles observed were mainly considered as shedding vesicles.

Incorporation of MVs in endometrial cells

As seen by fluorescence microscopy, in all the studied samples no fluorescence signal was detectable up to the sixth hour of co-incubation of MVs with endometrial cells, and only nuclei stained with Hoechst 33342 were visible (Fig. 2a). The increase in uptake of 40×10^6 MVs/ml by endometrial cells between 24 h and 72 h is showed in Fig. 2b, c, d and e. No signal was detected after treatment of MVs with trypsin. The incorporation of MVs is gradual and constant at 24 h with a concentration of 40×10^6 MVs/ml, and suddenly increases at a concentration of 50×10^6 MVs/ml. The uptake of MVs drastically increased at 48 h at a concentration of 40×10^6 MVs/ml and decreased at a concentration of 50×10^6 MVs/ml. The internalization and accumulation of MVs peaked at 72 h for all the different concentrations but, once again, decreased at a concentration of 50×10^6 MVs/ml (Fig. 3a).

As seen by confocal microscopy, after 24 h of incubation with MVs, endometrial cells showed a fine granular fluorescent pattern within their cytoplasm, indicating incorporation of MVs (Fig. 3b and c).

In vitro effect of MVs on endometrial cells treated with LPS

Viability cell tests The effect of LPS and MVs was evaluated by apoptotic and cell proliferation tests. The rate of cells at the early stage of apoptosis increased dramatically on treatment with LPS; indeed, the percentage of apoptotic cells reached 55 ± 4.1 % at 12 h of stress, decreasing to 40.48 ± 4.82 % at 24 h. The rate of apoptosis due to MVs is not statistically different from endometrial cells alone (Fig. 4a). The results of the cell proliferation test showed the opposite trend to the apoptotic test, confirming the effect of LPS and MVs (Fig. 4b).

MVs were able to counteract the action of LPS either when used simultaneously with LPS or when incorporated from endometrial cells 24 h before the treatment

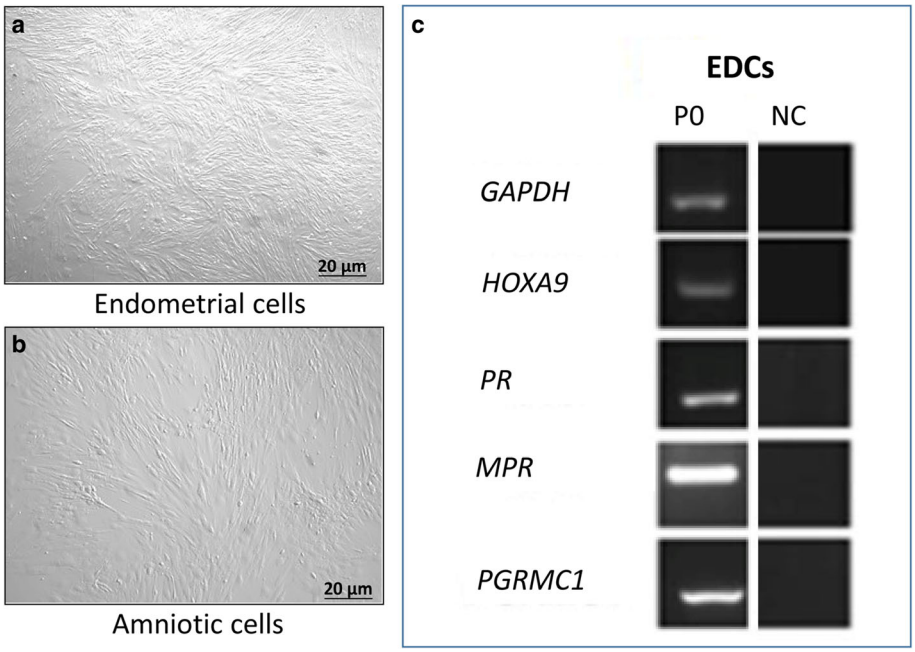

Fig. 1 Morphology of **a** endometrial (*EDCs*) and **b** amniotic cells. **c** Expression of specific endometrial markers revealed by qualitative PCR on endometrial cells at passage 0 (*P0*). *GAPDH* glyceraldehyde-3-phosphate dehydrogenase, *HOXA9* homeobox protein Hox-A9-like, *MPR* membrane-associated progesterone receptor, *NC* negative control, *PGRMC1* progesterone receptor membrane component 1, *PR* progesterone receptor

with LPS. In this condition, cells previously treated with MVs and after being exposed to LPS had a lower apoptotic rate ($P < 0.05$) than the control cells, at both 12 and 24 h of experiment (12.01 ± 1.38 % vs 18.05 ± 1.34 % at 12 h and 15.56 ± 1.5 % vs 24.5 ± 2.78 % at 24 h). On the other hand, the stress induced by LPS exposure before the treatment with MVs was not contrasted by MVs and the apoptotic rate increased up to 63.16 ± 6.8 % at 24 h (Fig. 4c). The results of the cell proliferation test showed the opposite trend to the apoptotic test (Fig. 4d).

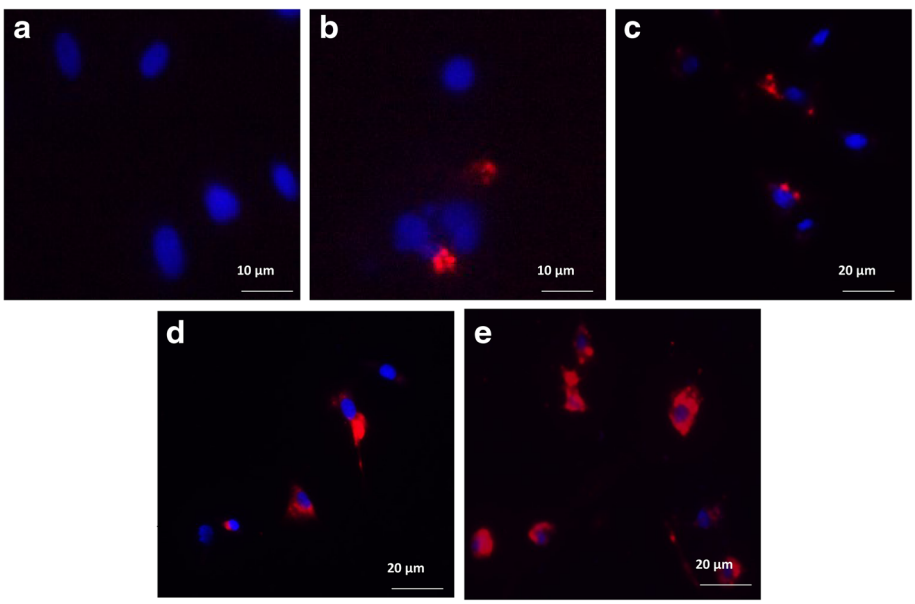

Fig. 2 Representative micrographs of internalization by endometrial cells of MVs labeled with PKH-26. Under a fluorescent microscope, the endometrial cell nuclei are *blue* and the MVs are *red*. **a** No incorporation of MVs pre-incubated with trypsin. Incorporation of 40×10^6 MVs/ml into the target cells from **b** 24 h, **c** 36 h, **d** 48 h, and **e** 72 h, respectively

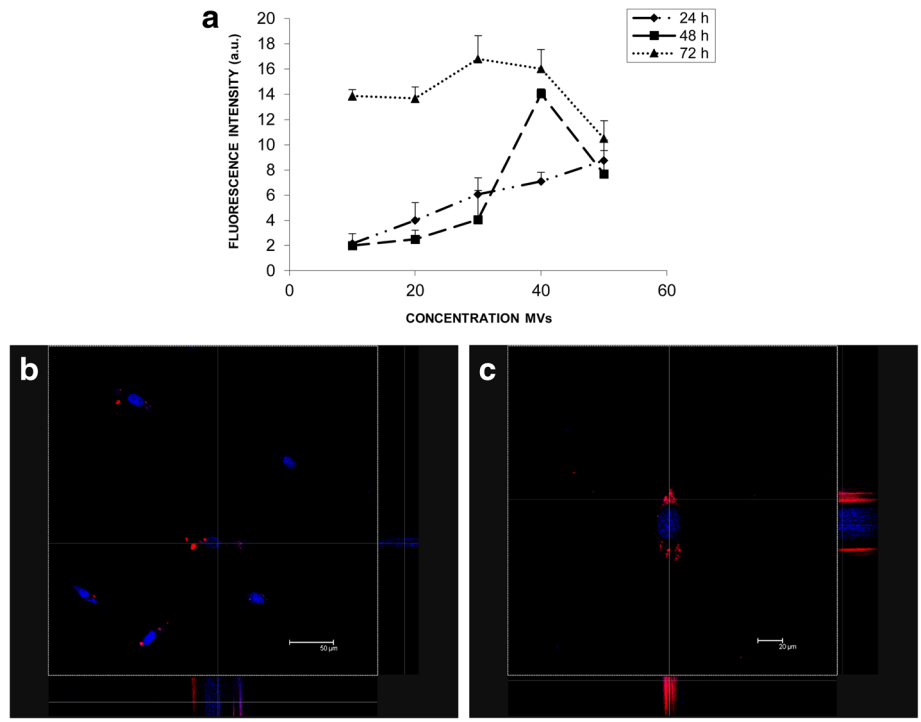

Fig. 3 MV uptake. **a** Graph of dose/exposure time for microvesicle (*MV*) incorporation. The uptake of MVs drastically increased at 72 h for all concentration but decreased at 50×10^6/ml MVs. Data represent the mean and SD of three independent experiments. **b**, **c** Representative z-stack orthogonal projection micrographs showing the internalization of MVs as detected by confocal microscopy in two group of endometrial cells co-cultured with MVs for 24 h. The images were taken at different plans scanned every 0.5 μm from top to bottom of the nucleus and showed at different magnification. *a.u.* arbitratry units

Molecular biology study

The expression of some pro-inflammatory genes was evaluated by qRT-PCR. Endometrial cells, LPS, and MVS were tested alone. Data were obtained from three samples and are shown in Fig. 5. LPS at 3 h significantly upregulated ($P < 0.05$) the expression of *TNF-α* and *IL-6* ($0.0019 \pm 0.317^{E-6}$ and 10.54 ± 0.014, respectively) and of *ILβ-1* at 24 h (9.91 ± 0.017). Endometrial cells used as controls (CTR) and MVs did not induce expression of pro-inflammatory genes. In the experiment with simultaneous use of LPS and MVs, the action of LPS was counteracted by MVs; indeed, the expression of *IL-6* at first increased significantly ($P < 0.05$) at 3 h by LPS and then fell significantly in the presence of MVs either at 12 h (2.41 ± 0.039) or at 24 h (1.15 ± 0.081). *IL-1β* at 24 h was completely and significantly ($P < 0.05$) downregulated (0.22 ± 0.0008). The expression of *TNF-α* is not dependent on the presence of MVs.

When LPS was used for 3 h before adding the MVs, the action of LPS was neutralized by the presence of MVs. Indeed, the expression of *IL-6* at 3 h, 12 h, and 24 h was 2.08 ± 0.0019, 1.75 ± 0.0033, and 2.65 ± 0.0013, respectively, compared to the treatment with LPS only. In addition, the expression of *IL-1β* was significantly ($P < 0.05$) downregulated at 24 h (0.21 ± 0.0016).

Under the final condition of MVs for 24 h and then LPS, the expression of all genes was downregulated. *TNF-α* expression at 3 h fell 0.0002-fold compared to the treatment with LPS. *IL-6* expression was statistically ($P < 0.05$) downregulated at each time point, and *IL-1β* was statistically ($P < 0.05$) downregulated at 24 h.

A moderate but significant ($P < 0.05$) increase in the expression was observed for *MMP-1* (5.18 ± 0.44) and *MMP-13* (2.69 ± 0.19) compared to untreated cells when endometrial cells were exposed to LPS for 24 h (Fig. 5d and e). The presence of MVs, simultaneously to LPS, significantly counteracted the effect of LPS on the expression of metalloproteinases as shown by the striking reduction in the expression levels for *MMP-1* (1.67 ± 0.14) and *MMP-13* (0.36 ± 0.11).

miRNA analyses by RNA extraction and PCR amplification

Expression of specific miRNA was determined by PCR assay that showed the presence of miR-26a-2, miR-335, and miR-146a in both MVs and cells isolated from the amniotic membrane (Fig. 5f).

Cytokines

The results of the release over time (3, 12, and 24 h) of pro-inflammatory (TNF-α and IL-6) and anti-inflammatory

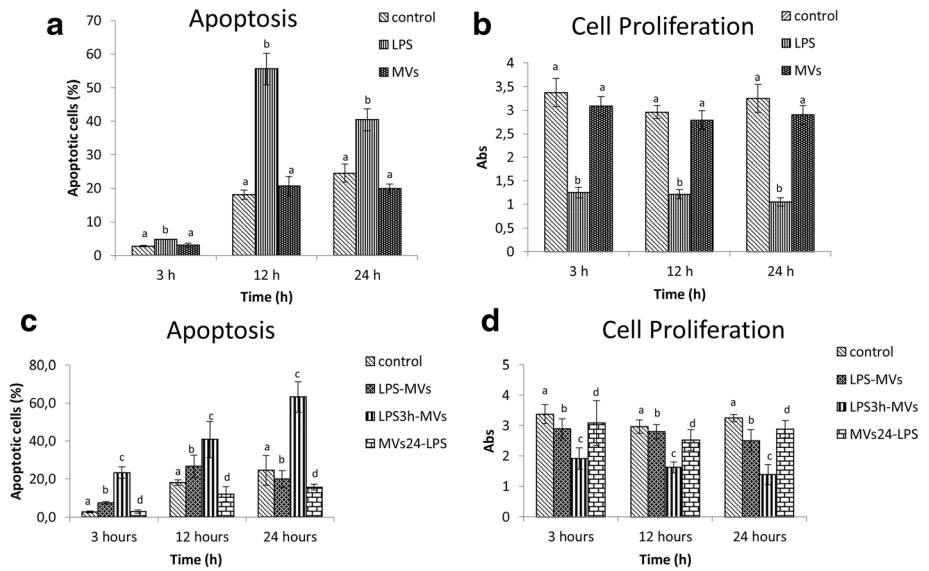

Fig. 4 Results of viability and proliferation. The rate of cells at **a** the early stage of apoptosis and **b** absorbance values of the cell proliferation test in control cells. **c** Early apoptosis rate and **d** absorbance values of the cell proliferation test in treated cells. Data represent the mean and SD of three independent experiments. Values labeled with different letters are statistically different within each time point (3 h, 12 h and 24 h) ($P < 0.05$). *MV* microvesicle, *LPS* lipopolysaccharide

(TGF-β) cytokines by endometrial cells stimulated with 10 ng/ml of LPS and treated with MVs are shown graphically in Fig. 6.

Cells stressed with LPS secreted significantly ($P < 0.05$) more TNF-α and IL-6 at 3 h and 12 h, respectively, when compared to control cells and cells treated by MVs. The MVs, used simultaneously or incorporated from endometrial cells 24 h before the treatment with LPS, were able to counteract the action of LPS and significantly ($P < 0.05$) and equally decreased the production of TNF-α and IL-6, mainly between 12 h and 24 h. Cells incubated with LPS for 3 h before the treatment with MVs secreted significantly more TNF-α and IL-6 when compared to all the other experimental conditions.

TGF-β was constitutively produced by control cells but the treatment with MVs induced a higher release ($P < 0.05$) of TGF-β, mainly when used simultaneously with LPS or incorporated from endometrial cells 24 h before the treatment with LPS. No efficacy of MVs was evident after LPS-induced stress of cells for 3 h before the addition of MVs.

Discussion

MVs are secreted by MSCs. Although bone marrow represents the most widely investigated source of MSCs, cells harvested from bone marrow have limited potential in terms of in vitro proliferation capability [43, 44] and do not appear to noticeably improve long-term functionality [45] compared to those from extra-fetal tissues. AMCs have already been demonstrated to be an excellent source for the treatment of tendon diseases in horse [26]. Furthermore, Lange-Consiglio et al. [46] used the conditioned medium derived from AMCs for the treatment of horse tendon diseases and showed that the positive evolution of spontaneous tendon injuries in competition horses was comparable to that achieved with AMCs, thereby showing that AMC-CM had angiogenic and immunomodulatory properties mediated by paracrine mechanisms. Corradetti et al. [39] demonstrated that equine AMCs share the same transcriptional profile as endometrial cells and express genes that are involved in early pregnancy, pre-implantation, and conceptus development. In addition, co-culture of endometrial cells by transwell in the presence of AMCs, or incubated with CM, showed a significant increase in the proliferation rate of endometrial cells compared to fibroblasts and the CM secreted by them. All these preliminary data suggest that AMCs and CM exert regenerative effects through paracrine mechanisms, and that AMCs and their CM may have the potential to improve endometrial cell replenishment. Since MVs are contained in the CM, the aim of the present study was to investigate the role of MVs produced by AMCs in in-vitro cell-to-cell communication that could ultimately lead to endometrium repair. We ultimately aim to demonstrate that they could be used as effective tools for regenerative medicine purposes, especially in the reproduction field.

Our results show that AMCs secrete MVs (with a mean size of 258 nm) as detected by a Nanosight instrument, and this size allows us to categorize them as shedding vesicles. Moreover, we found that MVs are easily internalized by endometrial cells. Fluorescent microscopy analysis

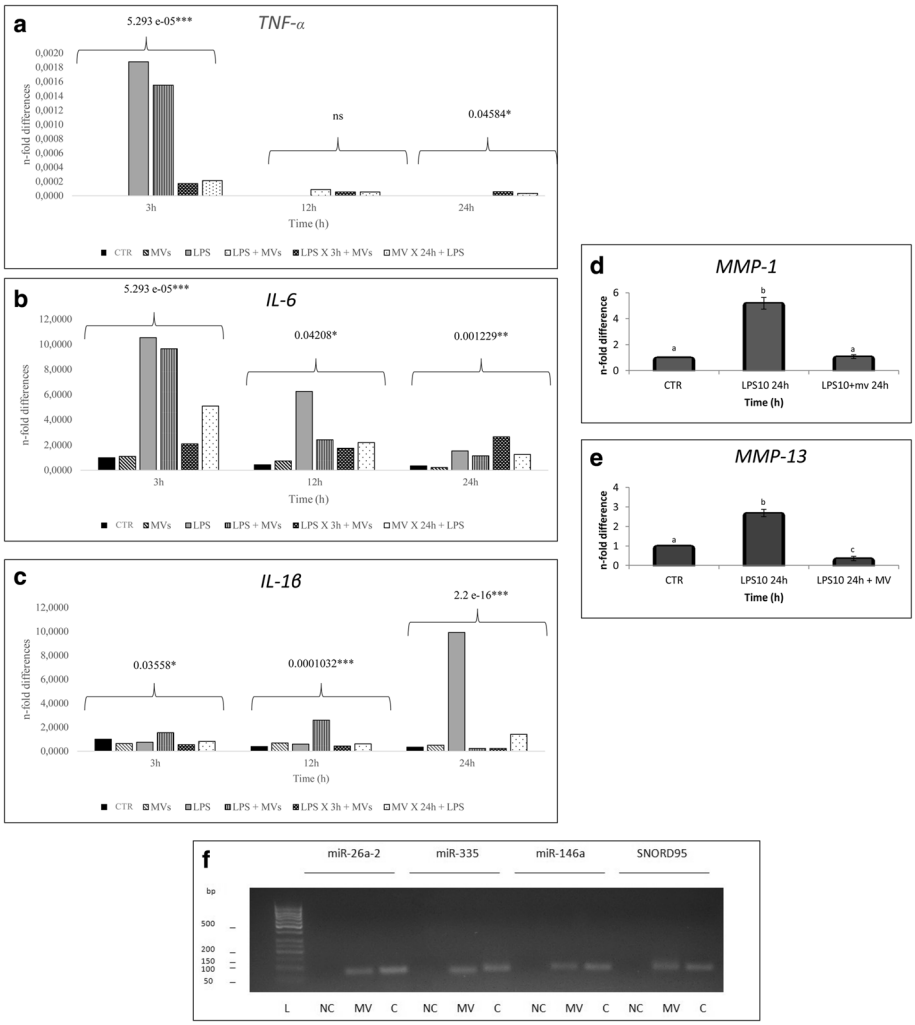

Fig. 5 Quantitative RT-PCR analysis for the expression of **a** *TNF-α*, **b** *IL-6*, and **c** *IL-1β* in endometrial cells in different experimental conditions. Expression of **d** *MMP-1* and **e** *MMP-13* in endometrial cells exposed to 10 ng/ml LPS (*LPS10 24h*) and simultaneously to 10 ng/ml LPS and MVs (*LPS10 24h + MV*). Expression levels have been normalized to the reference gene (*GAPDH*). Data are represented as fold-change compared with the expression observed in endometrial cells (control, CTR). Values are mean ± SD ($n = 3$). *P* values of expression levels in respect to control are shown above groups when significant in panels **a–c**, and the values labeled with different letters are statistically different ($P < 0.05$) in panels **d** and **e**. **f** PCR assays to determine the presence of different miRNA (miR-26a-2, miR-335, miR146a), and small nucleolar snoRNA, C/D Box 95 (*SNORD95*; positive control) in MVs and cells (*C*) isolated from amniotic membrane. *CTR* control, *IL* interleukin, *L* molecular weight ladder, *LPS* lipopolysaccharide, *MMP* matrix metalloproteinase, *MV* microvesicle, *NC* negative control, *ns* not significant, *TNF* tumor necrosis factor

suggests that the uptake of MVs by endometrial cells starts at 6 h after co-culture and increases gradually at 24 h, rising to the maximum internalization at 72 h at all different concentrations. At a concentration of 50×10^6 MVs/ml, a decrease at 48 h and 72 h was detected. We hypothesize that after 48 h and 72 h of exposure at 40×10^6/ml, the cells are saturated and phagocytosis of MVs, for the release of their contents into the cell cytoplasm, begins. This phagocytosis probably results in the destruction of the MV membranes and, consequently, in the loss of fluorescence signal. Cocucci et al. [47] demonstrated that the internalization of MVs is the result of the direct fusion or endocytic uptake by target cells. Once internalized, the MVs fuse their membrane with that of endosomes, making a horizontal transfer of their contents into the cytoplasm of the recipient cells. Alternatively, MVs can remain segregated inside the endosomes and be phagocytized by lysosomes or eliminated from the cells after fusion with the plasma membrane through a mechanism of transcytosis [47]. Our data show that horizontal transfer of the contents of MVs within endometrial cells could be one of the mechanisms of action of MVs, although other methods of interaction may occur simultaneously. The process of uptake and internalization of MVs by the endometrial cells could also be facilitated by the presence of surface cell receptors. This hypothesis is confirmed by the results of

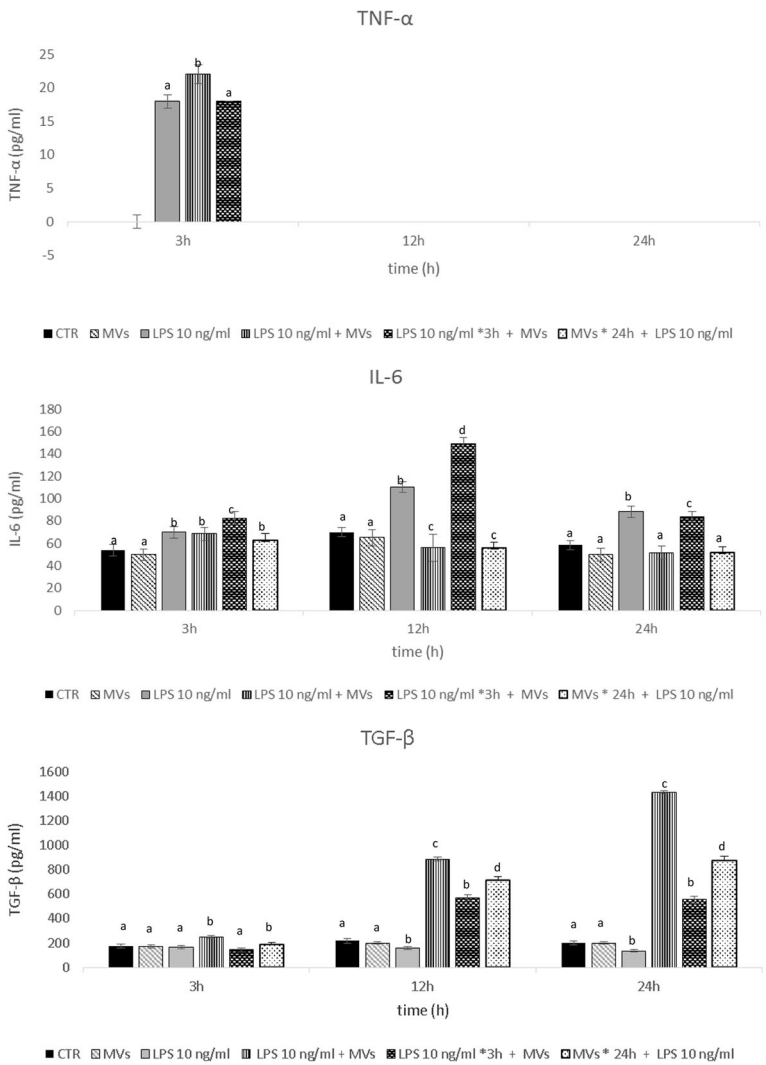

Fig. 6 Effect of LPS and MVs under different experimental conditions on the release of TNF-α, IL-6, and TGF-β in endometrial cells. Each value represents the mean ± SD of three samples. Values labeled with different letters are statistically different within each time point (3 h, 12 h and 24 h) ($P < 0.05$) *CTR* control, *IL* interleukin, *LPS* lipopolysaccharide, *MV* microvesicle, *TGF* transforming growth factor, *TNF* tumor necrosis factor

experiments in which MVs were treated with trypsin before being incubated with endometrial cells. Having identified that the endometrial cells represent target cells for MVs secreted by equine AMCs, a further aim of this study was to understand whether MVs might be involved in the regeneration of endometrial diseases. Obviously, due to the difficulty of studying the repair systems of endometritis in vivo, we recapitulated in vitro the inflammatory process by stimulating cells with LPS.

The inflammatory response is a complex process involving many signaling cascades and cytokines have a significant role in the recruitment of inflammatory cells [48]. In the genital tract, the initial response of the endometrium against infection is dependent on innate immunity and mucosal defense systems [49, 50]. The uterine immune response is generated not only by professional immune cells but also by endometrial epithelial and stromal cells, which can respond to LPS through the Toll-like receptors (TLRs) [51]. Activated TLRs subsequently stimulate the production of pro-inflammatory cytokines and chemokines [52].

To understand the mechanism of action of MVs, a single concentration of 40×10^6 MVs/ml was used after stress induced with LPS. This concentration was chosen because, during the study of internalization, endometrial cells at 24 h of culture were not saturated with MVs and no MV degradation started.

In these experiments, we used LPS and MVs under different conditions. In control cells, even if the apoptosis is higher than expected, the cell proliferation of 80 % remaining cells was very high during the 24 h of experimentation, as proven by MTT values. Indeed,

viability was constantly high over the different times of culture, and values of absorbance also did not statistically change in the presence of MVs. When the cells were stressed with LPS, the viability decreased with respect to control cells and cells cultured in the presence of MVs. Indeed, apoptosis increased drastically after treatment with LPS and, vice versa, the proliferation declined to the same intensity. The dose of LPS (10 ng/ml) was chosen on the basis of data obtained by Herath et al. [53]. These authors found that this value is present in cows with clinical endometritis. Also, over a short time, this dose of LPS is probably also deleterious for endometrial cells in a static system in vitro if compared to in vivo environments, where this effect can be modulated. These results underscored the stressor effect of LPS that has been reduced by the beneficial effect of MVs on the vitality of cells. When LPS and MVs were used at the same time, the viability of cells was high without significant differences compared to control cells. These results confirm the anti-inflammatory properties of MVs. However, the beneficial effect of MVs is time-dependent. In fact, MVs did not counteract the action of LPS if the cells were previously exposed to LPS (3 h LPS exposure). On the other hand, LPS does not show any detrimental effect if the internalization of MVs in the endometrial cells occurred 24 h before LPS treatment.

The expression of pro-inflammatory genes supports these data. LPS induces overexpression of *IL-1β* at 24 h and MVs are able to counteract this action. Indeed, at 24 h this expression is downregulated in all three experimental conditions (LPS and MVs simultaneously, LPS for 3 h and then MVs, MVs for 24 h and then LPS). This downregulation is observed even in the experiment where cells were previously exposed to LPS. The cells surviving the apoptotic process are probably able to incorporate MVs that, at 24 h, are capable of counteracting the action of LPS. The overexpression of *IL-6* and *TNF-α* induced by LPS occurs at 3 h and, at this time, MVs used either simultaneously or added after the action of LPS are not able to block the action of LPS. This seems to indicate that the downregulation of these genes could occur only when the cells are incubated with MVs for a longer time to guarantee the necessary incorporation of MVs. Indeed, we found that MVs were visible only after 6 h and increased up to 24 h.

In parallel with gene expression, the release of cytokines was studied, confirming the observations regarding gene regulation. LPS was demonstrated to be capable of inducing the release of *TNF-α* the peak of which was obtained 24 h after stimulation with LPS. The release of *IL-6* appeared earlier and reached the highest level 12 h after stimulation with LPS, and then gradually decreased over the subsequent observation period. MVs reduce the release of these pro-inflammatory cytokines and the maximum modulatory activity was observed between 12 h and 24 h, both when MVs were used simultaneously or 24 h before LPS treatment. In both cases, no contrasting action of MVs was obtained within the first 3 h, confirming that the internalization had yet to begin.

MMP-1 and *MMP-13* expression is induced by *IL-1β*, so the expression of these two genes was investigated at 24 h after treatment with 10 ng/ml LPS, taking into account the higher expression of *IL-1β* at this time. *MMP-1* and *MMP-13* expression was statistically higher compared to the control, confirming the inflammatory effect induced by LPS. Matrix metalloproteinases (MMPs) are a family of structurally related zinc/calcium-dependent proteinases with a pivotal role in the extracellular matrix degradation during both normal and pathological tissue remodeling processes [54, 55]. In addition, the MMP collagenases are key participants in extracellular matrix remodeling and are important for the separation of bovine placental tissues from the endometrium at term [56]. *MMP*-1, -2, -3, -9, and -13 are all highly expressed in the bovine endometrium in late gestation [57], while *MMP-1* and *MMP-13* expression levels are downregulated in postpartum endometrium. Our study demonstrated that MVs downregulated the expression of *MMP-1* and *MMP-13* at 24 h of LPS treatment.

It is well known that miRNA-containing microvesicles can regulate the inflammation process [58]. In this context, from our results it is possible to assume that the cargo of MVs contributed to the anti-inflammatory effect. Since MVs contain various active molecules, such as lipids, proteins, mRNA, and miRNA [29], we studied the presence of three miRNAs in MVs involved in the regulation of pro-inflammatory genes in our in vitro model (miR-335, miR-146a, and miR-26a-2). miR-335 has been demonstrated to regulate the expression of *TNF-a* and *IL-6* during human adipose cell inflammation [59]. miR-146a has been demonstrated to decrease the expression of *IL-1β* and, as an indirect effect, to suppress the level of *MMP* in intervertebral discs in bovine species [60]. miR-26a-2 has been widely studied and it has been correlated with human inflammation, cell proliferation, and apoptosis [61]. The DIANA tool confirmed that these miRNAs have predicted targets also in horse inflammation. The downregulation of gene expression shown in this study could be correlated to miRNA transfer from MVs to endometrial cells.

Conclusion

These data provide a critical starting point for beginning to dissect how equine amniotic MVs respond to and alter an inflammatory situation, shown to be a promising approach for the treatment of endometritis. Much research is still needed to establish the true biological role

of miRNAs in endometrial disease with a view to translating this knowledge into clinically effective outcomes.

Abbreviations

a.u.: Arbitrary units; AMC: Amniotic mesenchymal stem cell; AOI: Area of interest; CM: Conditioned medium; EDC: Endometrial cell; EGF: Epidermal growth factor; EX: Exosome; FBS: Fetal bovine serum; GAPDH: Glyceraldehyde-3-phosphate dehydrogenase gene; HEPES: N-2-hydroxyethylpiperazine-N-2-ethanesulfonic acid; HG-DMEM: High-glucose Dulbecco's modified Eagle's medium; Hoxa9: Homeobox protein Hox-A9-like; IL: Interleukin; LPS: Lipopolysaccharide; miRNA: MicroRNA; MMP: Matrix metalloproteinase; MPR: Membrane-associated progesterone receptor; MSC: Mesenchymal stem cell; MTT: 3-(4,5-dimethylthiazol- 2-yl)-2,5-diphenyletrazolium bromide; MV: Microvesicle; P: Passage; PBS: Phosphate-buffered saline; PGRMC1: Membrane-associated progesterone receptor; PR: Progesterone Receptor; qRT-PCR: Quantitative reverse transcription polymerase chain reaction; RT-PCR: Reverse transcription polymerase chain reaction; SV: Shedding vesicle; TEM: Transmission electron microscopy; TGF: Transforming growth factor; TLR: Toll-like receptor; TNF: Tumor necrosis factor

Acknowledgments

This study was supported by grants from Università degli Studi di Milano, Milano, Italy and Università Politecnica delle Marche, Ancona, Italy. We thank Dott.ssa Maria Chiara Deregibus and Prof. Giovanni Camussi (Department of Internal Medicine and Molecular Biotechnology Center, University of Torino, Torino, Italy) for their assistance in measurements of MVs and Dott.ssa Miriam Ascagni (Department of Bioscience, Universita'degli Studi di Milano, Italy) for her skilled assistance in confocal microscopy.

Funding

The research was financially supported by Università degli Studi di Milano.

Authors' contributions

CP: isolation of amniotic cells, conditioned medium and microvesicles, collection and assembly of data on vitality, cell proliferation, and LPS experiments, and final approval of the manuscript. MGS: molecular biology study, data analysis, and final approval of the manuscript. AB: molecular biology study, collection and assembly of data, financial support, and final approval of the manuscript. PE: isolation of endometrial cells, collection and assembly of data of vitality, cell proliferation and LPS experiments, and final approval of the manuscript. MGM: molecular biology study, collection and assembly of data, and final approval of the manuscript. BC: molecular biology study, collection and assembly of data, and final approval of the manuscript. DB: molecular biology study, collection and assembly of data, financial support, and final approval of the manuscript. AI: collection and assembly of data of release of cytokines, and final approval of the manuscript. SL: collection and assembly of data of release of cytokines, financial support, and final approval of the manuscript. EC: molecular biology study on miRNA, and final approval of the manuscript. FP: molecular biology study on miRNA, and final approval of the manuscript. FC: conceptions and design, financial support, and final approval of the manuscript. AL-C: conceptions and design, in vitro study of MV uptake, coordination of all experiments, collection and assembly of all data analysis and interpretation, manuscript writing, and final approval of the manuscript.

Competing interests

The authors declare that they have no competing interests.

Ethics approval

The study was approved by the University of Milan Ethics Committee (Protocol Number 41/15). All procedures were conducted following standard veterinary practice and in accordance with the 2010/63 EU directive on animal protection. Informed client consent was obtained for collection of placenta at term of the mares' pregnancy.

Author details

[1]Large Animal Hospital, Reproduction Unit, Università degli Studi di Milano, Via dell'Università 6, 26900 Lodi, Italy. [2]Department of Veterinary Medicine, Università degli Studi di Milano, Milano, Italy. [3]Department of Life and Environmental Sciences, Università Politecnica delle Marche, Ancona, Italy. [4]Department of Veterinary Medicine, Università degli Studi di Sassari, Sassari, Italy. [5]Institute of Biology and Agricultural Biotechnology-CNR, Milano, Italy.

Received: 31 August 2016 Revised: 22 September 2016
Accepted: 21 October 2016 Published online: 18 November 2016

References

1. Hurtgen JP. Pathogenesis and treatment of endometritis in the mare: a review. Theriogenology. 2006;66(3):560–6.
2. Markusfeld O. Periparturient traits in seven high dairy herds. Incidence rates, association with parity, and interrelationships among traits. J Dairy Sci. 1987;70(1):158–66.
3. Zwald NR, Weigel KA, Chang YM, Welper RD, Clay JS. Genetic selection for health traits using producer-recorded data. II. Genetic correlations, disease probabilities, and relationships with existing traits. J Dairy Sci. 2004;87(12):4295–302.
4. Borsberry S, Dobson H. Periparturient disease and their effect on reproductive performance in five dairy herds. Vet Rec. 1989;124:217–9.
5. McDougall S. Effect of intrauterine antibiotic treatment on reproductive performance of dairy cows following periparturient disease. N Z Vet J. 2001;49:150–8.
6. LeBlanc SJ, Duffield TF, Leslie E, Bateman KG, Kefe GP, Walton JS, Johnson H. Defining and diagnosing postpartum clinical endometritis and its impact on reproductive performance in dairy cows. J Dairy Sci. 2002;85:2223–36.
7. Vieira-Neto A, Gilbert RO, Butler WR, Santos JEP, Ribeiro ES, Vercouteren MM, Bruno RG, Bitta JHJ, Galvão KN. Individual and combined effects of anovulation and cytological endometritis on the reproductive performance of dairy cows. J Dairy Sci. 2014;97:5415–25.
8. Lessey BA, Damjanovich L, Coutifaris C, Castelbaum A, Albelda SM, Buck CA. Integrin adhesion molecules in the human endometrium. Correlation with the normal and abnormal menstrual cycle. J Clin Invest. 1992;90:188–95.
9. Simon C, Martin JC, Pellicer A. Paracrine regulators of implantation. Baillieres Clin Obstet Gynaecol. 2000;14(5):815–26.
10. Koot YEM, Boomsma CM, Eijkemans MJC, Lentjes EGW, Macklon NS. Recurrent pre-clinical pregnancy loss is unlikely to be a 'cause' of unexplained infertility. Hum Reprod. 2011;26:2636–41.
11. Fischer C, Drillich M, Odau S, Heuwieser W, Einspanier R, Gabler C. Selected pro-inflammatory factor transcripts in bovine endometrial epithelial cells are regulated during the oestrous cycle and elevated in case of subclinical or clinical endometritis. Reprod Fertil Dev. 2010;22:818–29.
12. Katagiri S, Takahashi Y. Changes in EGF concentrations during estrous cycle in bovine endometrium and their alterations in repeat breeder cows. Theriogenology. 2004;62:103–12.
13. Castro-Rendón WA, Castro-Álvarez JF, Guzmán-Martinez C, Bueno-Sanchez JC. Blastocyst-endometrium interaction: intertwining a cytokine network. Braz J Med Biol Res. 2006;39:1373–85.
14. Perez-Marin CC, Molina Moreno L, Vizuete CG. Clinical approach to the repeat breeder cow syndrome. A Bird's-Eye View of Veterinary Medicine. 2011;18:337–62.
15. Kotton DN, Ma BY, Cardoso WV, Sanderson EA, Summer RS, Williams MC, Fine A. Bone marrow-derived cells as progenitors of lung alveolar epithelium. Development. 2001;128:5181–8.
16. Ortiz LA, Gambelli P, Gaupp D, Baddoo M, Kaminski N, Phinney DG. Mesenchymal stem cell engraftment in lung is enhanced in response to bleomycin exposure and ameliorates its fibrotic effects. Proc Natl Acad Sci U S A. 2003;100:840–51.
17. Liu Y, Yan X, Sun Z, Chen B, Han Q, Li J, Zhao RC. Flk-1+ adipose-derived mesenchymal cells differentiate into skeletal muscle satellite cells and ameliorate muscular dystrophy in mdx mice. Stem Cells Dev. 2007;16:695–706.
18. Duffield JS, Park KM, Hsiao LL, Kelley VR, Scadden DT, Ichimura T, Bonventre JV. Restoration of tubular epithelial cells during repair of the postischemic kidney occurs independently of bone marrow-derived cells. J Clin Invest. 2005;115:1743–55.
19. Togel F, Hu Z, Weiss K, Isaac J, Lange C, Westenfelder C. Administered mesenchymal stem cells protect against ischemic acute renal failure through differentiation-independent mechanism. Am J Physiol Cell Physiol. 2005;289:F31–42.
20. Bi B, Schmitt R, Israilova M, Nishio H, Cantley LG. Stromal cells protect against acute tubular injury via an endocrine effect. J Am Soc Nephrol. 2007;18:2486–96.
21. Chimenti I, Smith RR, Li TS, Gerstenblith G, Messina E, Giacomello A, Marbán E. Relative roles of direct regeneration versus paracrine effects of human

cardiosphere-derived cells transplanted into infarcted mice. Circ Res. 2010; 106:971–80.
22. Gil-Sanchis C, Cervelló I, Khurana S, Faus A, Verfaillie C, Simón C. Contribution of different bone marrow-derived cell types in endometrial regeneration using an irradiated murine model. Fertil Steril. 2015;103(6): 1596–605.
23. Gnecchi M, He H, Noiseux N, Liang OD, Zhang L, Morello F, Mu H, Melo LG, Pratt RE, Ingwall JS, Dzau VJ. Evidence supporting paracrine hypothesis for Akt-modified mesenchymal stem cell-mediated cardiac protection and functional improvement. FASEB J. 2006;20:661–9.
24. Timmers L, Lim SK, Arslan F, Armstrong JS, Hoefer IE, Doevendans PA, Piek JJ, El Oakley RM, Choo A, Lee CN, Pasterkamp G, de Kleijn DP. Reduction of myocardial infarct size by human mesenchymal stem cell conditioned medium. Stem Cell Res. 2007;1:129–37.
25. Quertainmont R, Cantinieaux D, Botman O, Sid S, Schoenen J, Franzen R. Mesenchymal stem cell graft improves recovery after spinal cord injury in adult rats through neutrophic and pro-angiogenic actions. PLoS One. 2012; 7:e39500.
26. Lange-Consiglio A, Tassan S, Corradetti B, Meucci A, Perego R, Bizzaro D, Cremonesi F. Investigating the potential of equine mesenchymal stem cells derived from amnion and bone marrow in equine tendon diseases treatment in vivo. Cytotherapy. 2013;10:1016–23.
27. Yagi H, Soto-Gutierrez A, Parekkadan B, Kitagawa Y, Tompkins RG, Kobayashi N, Yarmush ML. Mesenchymal stem cells: mechanisms of immunomodulation and homing. Cell Transplant. 2010;19:667–79.
28. Sabin K, Kikyo N. Microvesicles as mediators of tissue re-generation. Transl Res. 2014;163:286–95.
29. Biancone L, Bruno S, Deregibus MC, Tetta C, Camussi G. Therapeutic potential of mesenchymal stem cell-derived microvesicles. Nephrol Dial Transplant. 2012;27(8):3037–42.
30. Bruno S, Grange C, Collino F, Deregibus MC, Cantaluppi V, Biancone L, Tetta C, Camussi G. Microvesicles derived from mesenchymal stem cells enhance survival in a lethal model of acute kidney injury. PLoS One. 2012;7(3):e33115.
31. Saadeldin IM, Oh HJ, Lee BC. Embryonic-maternal cross-talk via exosomes: potential implications. Stem Cells Cloning. 2015;8:103–7.
32. Bemis LT, McCue PM, Hatzel JN, Bemis J, Ferris RA. Evidence for production of early pregnancy factor (Hsp10), micro RNAs and exosomes by day 8 equine embryos. J Equine Vet Sci. 2012;32(7):398.
33. Ng YH, Rome S, Jalabert A, Forterre A, Singh H, Hincks CL, Salamonsen LA. Endometrial exosomes/microvesicles in the uterine microenvironment: a new paradigm for embryo-endometrial cross talk at implantation. PLoS One. 2013;8(3):e58502.
34. Hailemariam D, Ibrahim S, Hoelker M, Drillich M, Heuwieser W, Looft C, Cinar MU, Tholen E, Schellander K, Tesfaye D. MicroRNA-regulated molecular mechanism underlying bovine subclinical endometritis. Reprod Ferti Dev. 2014;26(6):898–913.
35. Hull ML, Nisenblat V. Tissue and circulating microRNA influence reproductive function in endometrial disease. Reprod Biomed Online. 2013;27:515–29.
36. Lange-Consiglio A, Corradetti B, Bizzaro D, Magatti M, Ressel L, Tassan S, Parolini O, Cremonesi F. Characterization and potential applications of progenitor-like cells isolated from horse amniotic membrane. J Tissue Eng Regen Med. 2012;6:622–35.
37. Daels PF, Hughes JP. The normal estrous cycle. In: McKinnon AO, Voss JL, editors. Equine reproduction. 6th ed. USA: Wiley-Blackwell Publishing; 2005.
38. Donofrio G, Franceschi V, Capocefalo A, Cavirani S, Sheldon IM. Bovine endometrial stromal cells display osteogenic properties. Reprod Biol Endocrinol. 2008;6:65–73.
39. Corradetti B, Correani A, Romaldini A, Marini MG, Bizzaro D, Perrini C, Cremonesi F, Lange-Consiglio A. Amniotic membrane-derived mesenchymal cells and their conditioned media: potential candidates for uterine regenerative therapy in the horse. PLoS One. 2014;9(10):e111324.
40. Livak KJ, Schmittgen TD. Analysis of relative gene expression data using real-time quantitative PCR and the 2-ΔΔCT method. Methods. 2001;25:402–8.
41. Skog J, Würdinger T, van Rijn S, Meijer DH, Gainche L, Sena-Esteves M, Curry Jr WT, Carter BS, Krichevsky AM, Breakefield XO. Glioblastoma microvesicles transport RNA and proteins that promote tumour growth and provide diagnostic biomarkers. Nat Cell Biol. 2008;10:1470–6.
42. Lange-Consiglio A, Perrini C, Tasquier R, Deregibus MC, Camussi G, Pascucci L, Marini MG, Corradetti B, Bizzaro D, De Vita B, Romele P, Parolini O, Cremonesi F. Equine amniotic microvesicles and their anti-inflammatory potential in a tenocyte model in vitro. Stem Cells Dev. 2016;15(8):610–21. doi:10.1089/scd.2015.0348.
43. Guest DJ, Smith MR, Allen WR. Equine embryonic stem-like cells and mesenchymal stromal cells have different survival rates and migration patterns following their injection into damaged superficial digital flexor tendon. Equine Vet J. 2010;42:636–42.
44. Lange-Consiglio A, Corradetti B, Meucci A, Bizzaro D, Cremonesi F. Characteristics of equine mesenchymal stem cells derived from amnion and bone marrow: in vitro proliferative and multilineage potential assessment. Equine Vet J. 2013;45:737–44.
45. Paris DB, Stout TA. Equine embryos and embryonic stem cells: defining reliable markers of pluripotency. Theriogenology. 2010;74:516–24.
46. Lange-Consiglio A, Rossi D, Tassan S, Perego R, Cremonesi F, Parolini O. Conditioned medium from horse amniotic membrane-derived multipotent progenitor cells: immunomodulatory activity in vitro and first clinical application in tendon and ligament injuries in vivo. Stem Cell Dev. 2013; 22(22):3015–24.
47. Cocucci E, Racchetti G, Podini P, Meldolesi J. Enlargeosome traffic: exocytosis triggered by various signals is followed by endocytosis, membrane shedding or both. Traffic. 2007;8:742–57.
48. Woodward EM, Christoffersen M, Horohov D, Squires EL, Troedsson MH. The effect of treatment with immune modulators on endometrial cytokine expression in mares susceptible to persistent breeding-induced endometritis. Equine Vet J. 2015;47(2):235–9.
49. Sheldon IM, Price SB, Cronin J, Gilbert RO, Gadsby JE. Mechanisms of infertility associated with clinical and subclinical endometritis in high producing dairy cattle. Reprod Domest Anim. 2009;44 Suppl 3:1–9.
50. Wira CR, Grant-Tschudy KS, Crane-Godreau MA. Epithelial cells in the female reproductive tract: a central role as sentinels of immune protection. Am J Reprod Immunol. 2005;53:65–76.
51. Davies D, Meade KG, Herath S, Eckersall PD, Gonzalez D, White JO, Conlan RS, O'Farrelly C, Sheldon IM. Toll-like receptor and antimicrobial peptide expression in the bovine endometrium. Reprod Biol Endocrinol. 2008;6:53.
52. Akira S, Takeda K. Toll-like receptor signalling. Nat Rev Immunol. 2004;4: 499–511.
53. Herath S, Williams EJ, Lilly ST, Gilbert RO, Dobson H, Bryant CE, Sheldon IM. Ovarian follicular cells have innate immune capabilities that modulate their endocrine function. Reproduction. 2007;134:683–93.
54. Sternlicht MD, Werb Z. How matrix metalloproteinases regulate cell behavior. Annu Rev Cell Dev Biol. 2001;17:463–516.
55. Mott JD, Werb Z. Regulation of matrix biology by matrix metalloproteinases. Curr Opin Chem Biol. 2004;16:558–64.
56. Eiler H, Hopkins FM. Bovine retained placenta: effects of collagenase and hyaluronidase on detachment of placenta. Biol Reprod. 1992;4:580–5.
57. Kizaki K, Ushizawa K, Takahashi T, Yamada O, Todoroki J, Sato T, Ito A, Hashizume K. Gelatinase (MMP-2 and -9) expression profiles during gestation in the bovine endometrium. Reprod Biol Endocrinol. 2008;6:66.
58. Hulsmans M, Holvoet P. MicroRNA-containing microvesicles regulating inflammation in association with atherosclerotic disease. Cardiovasc Res. 2013;100:7–18.
59. Zhu L, Chen L, Shi CM, Xu GF, Xu LL, Zhu LL, Guo XR, Ni Y, Cui Y, Ji C. MiR-335, an adipogenesis-related microRNA, is involved in adipose tissue inflammation. Cell Biochem Biophys. 2014;68:283–90.
60. Gu SX, Li X, Hamilton JL, Chee A, Kc R, Chen D, An HS, Kim JS, Oh C, Ma YZ, van Wijnen AJ, Ima HJ. MicroRNA-146a reduces IL-1 dependent inflammatory responses in the intervertebral disc. Gene. 2015;555(2):80–7.
61. Gao J, Liu QG. The role of miR-26 in tumors and normal tissues (Review). Oncol Lett. 2011;2:1019–23.

STEM CELLS AND DEVELOPMENT
Volume 25, Number 8, 2016

DOI: 10.1089/scd.2015.0348

Equine Amniotic Microvesicles and Their Anti-Inflammatory Potential in a Tenocyte Model In Vitro

Anna Lange-Consiglio,[1] Claudia Perrini,[1] Riccardo Tasquier,[1] Maria Chiara Deregibus,[2] Giovanni Camussi,[2] Luisa Pascucci,[3] Maria Giovanna Marini,[4] Bruna Corradetti,[4] Davide Bizzaro,[4] Bruna De Vita,[5] Pietro Romele,[6] Ornella Parolini,[6] and Fausto Cremonesi[1,7]

Administration of horse amniotic mesenchymal cells (AMCs) and their conditioned medium (AMC-CM) improves the in vivo recovery of spontaneous equine tendon lesions and inhibits in vitro proliferation of peripheral blood mononuclear cells (PBMC). This process may involve microvesicles (MVs) as an integral component of cell-to-cell communication during tissue regeneration. In this study, the presence and type of MVs secreted by AMCs were investigated and the response of equine tendon cells to MVs was studied using a dose–response curve at different concentrations and times. Moreover, the ability of MVs to counteract in vitro inflammation of tendon cells induced by lipopolysaccharide was studied through the expression of some proinflammatory genes such as metallopeptidase (*MPP*) *1*, *9*, and *13* and tumor necrosis factor-α (*TNFα*), and expression of transforming growth factor-β (*TGF-β*). Lastly, the immunomodulatory potential of MVs was investigated. Results show that AMCs secrete MVs ranging in size from 100 to 200 nm. An inverse relationship between concentration and time was found in their uptake by tendon cells: the maximal uptake occurred after 72 h at a concentration of 40×10^6 MVs/mL. MVs induced a downregulation of *MMP1*, *MMP9*, *MMP13*, and *TNFα* expression without affecting PBMC proliferation, contrary to CM and supernatant. Our data suggest that MVs contribute to in vivo healing of tendon lesions, alongside soluble factors in AMC-CM.

Introduction

There are three regenerative mechanisms ascribed to mesenchymal stem cells (MSCs): (i) differentiation toward reparative or replacement cell types, (ii) enhancement of the nutrient supply, and (iii) improvement of the survival and function of endogenous cells through paracrine actions [1–3]. It is known that the inhospitable microenvironment of injured or degenerating tissues may result in the death or apoptosis of a large proportion of implanted MSCs in the short period immediately posttransplantation [4]. This raises the need to identify other mechanisms than differentiation of transplanted cells for the promotion of regeneration. This notion is supported by a recent study of Lange-Consiglio et al. [5] in which a conditioned medium (CM), derived from amniotic mesenchymal cells (AMCs), was injected into spontaneous injuries of equine tendons and ligaments and produced results consistent, and overlapping (in terms of time to complete healing), with the beneficial effects of transplanted AMCs as observed in the same animal model [6]. These results suggest that it may be possible to substitute cell treatment with the use of CM derived from the culture of these cells as the in vivo effects are mainly exerted by factors released from cells rather than through the direct cell-to-cell contact. This hypothesis was further supported by the evaluation of the immunosuppressive properties of AMC-CM, as peripheral blood mononuclear cell (PBMC) proliferation was inhibited by AMC-CM [5].

Secreted bioactive molecules may act as paracrine or endocrine mediators directly activating target cells and/or causing neighboring cells to secrete functionally active agents [7]. However, little is known about how the MSCs might release these secretions. Many of the secreted molecules cannot freely cross cell membranes, and a carrier is needed to facilitate the crossing [8]. It has recently been demonstrated that extracellular vesicles, or microvesicles

[1]Large Animal Hospital, Reproduction Unit, Università degli Studi di Milano, Lodi, Italy.
[2]Department of Internal Medicine and Molecular Biotechnology Center, University of Torino, Torino, Italy.
[3]Department of Veterinary Medicine, University of Perugia, Perugia, Italy.
[4]Biochemistry, Biology and Genetics, Università Politecnica delle Marche, Ancona, Italy.
[5]Department of Animal Reproduction and Radiology, FMVZ, UNESP, Botucatu, San Paolo, Brazil.
[6]Centro di Ricerca E. Menni, Fondazione Poliambulanza, Istituto Ospedaliero, Brescia, Italy.
[7]Department of Veterinary Medical Science, Università degli Studi di Milano, Milano, Italy.

(MVs), released from cells are an integral component of cell-to-cell communication in tissue regeneration [9,10] and therefore may contribute to the paracrine action of MSCs. These vesicles can be categorized into exosomes and shedding vesicles. Exosomes arise from the endosomal membrane cell compartment and are released into the extracellular space after fusion of multivesicular bodies with the plasma membrane [11–13]. Shedding vesicles, also known as ectosomes or microparticles, originate from direct budding and 'blebbing' of the plasma membrane of many different cell types [11–13]. Exosomes tend to be homogeneous in size (30–120 nm), while shedding vesicles are more heterogeneous (ranging from 100 nm to 1 μm). MVs express surface receptors and contain biologically active molecules such as proteins and lipids, as well as mRNA and microRNA [14].

Some in vivo studies have indicated that MVs could accelerate the recovery from acute kidney injury induced by glycerol in SCID mice [15], or significantly improve the recovery of blood flow in a rat hind limb ischemia model [16] suggesting that the therapeutic potential of MSC-derived MVs was similar to that of MSCs. Considering the in vivo results in spontaneous equine tendon lesions treated with AMC-CM and the in vitro results on inhibition of PBMC proliferation [5], it appears reasonable to assume that MSC-derived MVs act as mediators in the repair of tendon lesions. In this context, the aims of this study were to identify the presence and type of MVs secreted by AMCs and elucidate whether equine tendon cells can be the target of MVs in vitro. In addition, in an explorative study, we considered whether MVs are able to counteract an in vitro equine tendon cell inflammatory process induced by lipopolysaccharide (LPS) and their effect on inhibition of PBMC proliferation.

Materials and Methods

Materials

Tendon samples were collected from horses slaughtered in a national slaughterhouse under legal regulation. Chemicals were obtained from Sigma-Aldrich Chemical unless otherwise specified, and tissue culture plastic dishes were purchased from Euroclone.

Study design

Initially, amniotic cells were isolated and cultured to produce MVs that were characterized using Nanosight and transmission electron microscopy (TEM). Tendon cells were then isolated and specific tendon genes were identified by qualitative PCR. Isolated tendon cells were used as the target for different concentrations of MVs. Furthermore, the effect of MVs was analyzed by quantitative PCR expression of inflammatory genes on tendon cells treated by LPS and, last, the effect of MVs on inhibition of PBMC proliferation was also investigated.

Tissues collection and cell isolation

This study was approved by the Ethics Committee of the University of Milan and written owner consent was obtained. All procedures were conducted following standard veterinary practice and in accordance with 2010/63 EU directive on animal protection and Italian Law (D.L. No. 116/1992). Allanto-amniotic membranes were obtained at term from normal pregnancies in three mares. Samples of allanto-amnion were transported at 4°C in calcium- and magnesium-free phosphate-buffered saline (Euroclone) supplemented with 4 mg/mL amphotericin (Euroclone), 100 UI/mL penicillin–100 mg/mL streptomycin (Euroclone), and were processed within 12 h of collection. The amniotic membrane was mechanically separated from the allantois and the isolation of AMCs was performed as previously reported by Lange-Consiglio et al. [17].

Superficial digital flexor tendon samples were aseptically collected from the mid-metacarpal region from three horses within 2 h of slaughtering (mean age: 7 ± 3 years). Tendon cells were isolated by stripping off the sheath and paratenon from tendon samples to obtain 2–3 g of trimmed tissue cut into small pieces with scalpel and scissors and then digested in HG-DMEM supplemented with 0.075% collagenase type I at 37.5°C overnight (about 16–20 h). The digested suspension was filtered on an 80 μm strainer, centrifuged at 400 *g* for 10 min, and washed twice in PBS. Before seeding, cells were counted using a Burker chamber with the Trypan Blue dye exclusion assay.

Cell culture and expansion

Amniotic and tendon cell cultures were established in the HG-DMEM standard medium composed of 10% fetal calf serum (FCS), penicillin (100 UI/mL)–streptomycin (100 μg/mL), 0.25 μg/mL amphotericin B, and 2 mM glutamine. The medium was supplemented with 10 ng/mL epidermal growth factor for AMC cultures. Cultures were established at a density of 1×10^5 cells/cm^2 in T75 culture flasks. The flasks were incubated at 38.5°C with 5% CO_2 and 90% humidity. The medium was replaced after 72 h to remove nonadherent cells and then replaced twice weekly until cells reached approximately 80% confluence. Cells were then detached with 0.05% trypsin-EDTA (Euroclone), counted, and redistributed at a density of 1×10^4 cells/cm^2 into new culture flasks to maintain and expand the culture for three passages (P). Previous molecular biology analyses at P3 showed that these AMCs display a typical mesenchymal stromal phenotype, with the expression of markers such as CD29, CD44, CD106, CD105, and MHCI, but not of CD34 and MHCII, as reported by Lange-Consiglio et al. [17]. At P3, AMCs were used to obtain the CM or MVs and for the TEM analysis. At P3, tendon cells were used for the in vitro experiment with MVs and LPS, or cryopreserved in liquid nitrogen, using standard cryopreservation protocols, for the molecular biology study to confirm the characteristics of isolated cells.

Preparation of AMC-CM

AMCs at P3 were plated into 24-well plates at a density of 5×10^4 cells/mL/well in DMEM standard medium. To generate AMC-CM, cells were cultured for 5 days at 37°C in a humidified atmosphere of 5% CO_2. Supernatants (SN) from each plate were then collected, pooled, centrifuged at 700 *g*, and stored at +4°C until use. This procedure was performed for cells obtained from three different placentas. The final AMC-CM was obtained pooling the media obtained from different amniotic samples.

Isolation and measurements of MVs

MVs were obtained from the culture media of AMCs derived from three different placentas, cultured for a week with HG-DMEM supplemented with 10% MV-deprived FCS and overnight in HG-DMEM deprived of FCS, and supplemented with 0.5% of BSA (Sigma). The overnight culture media were centrifuged at 2,000 *g* for 20 min to remove debris, then at 100,000 *g* (Beckman Coulter Optima L-100K ultracentrifuge) for 1 h at 4°C, washed in serum-free medium 199 containing N-2-hydroxyethylpiperazine-N-2-ethanesulfonic acid (HEPES) 25 mM (Sigma), and submitted to a second ultracentrifugation under the same conditions. After ultracentrifugation, SN were stored at +4°C until use for lymphocyte proliferation test, while the pellets were immediately resuspended in HG-DMEM, and a sample of the resuspended pellet was taken for measurements of MV size and concentration. A second fraction was labeled with fluorochrome PKH-26 and the remaining part of pellet was cryopreserved with 1% of dimethylsulfoxide at −80°C and used for the in vitro test. Size and concentration of MVs were evaluated by the Nanosight LM10 instrument (Nanoparticle tracking analysis, NTA; Nano-Sight Ltd.), which permits discrimination of microparticles less than 1 μm in diameter. The software (NTA 2.0 analytic software) allows the analysis of video images of particle movement under Brownian motion and the calculation of diffusion coefficient, sphere equivalent, and hydrodynamic radius of particles by using the Strokes–Einstein equation. This instrument was configured with a 405 nm laser and a high-sensitivity sCMOS camera (OrcaFlash2.8, Hamamatsu C11440; NanoSight Ltd.). Videos were collected and analysed using the NTA software with the minimal expected particle size, minimum track length, and blur setting, all set to automatic. Ambient temperature was recorded manually and did not exceed 25°C. Five microliters of each sample was diluted in sterile physiological solution to a final volume of 1 mL. Samples were analyzed within 15 min of the initial dilution with a delay of 10 s between sample introduction and the start of the measurement. For each sample, multiple videos of 30 s duration were recorded generating replicate histograms that were averaged.

TEM of MVs

For TEM analysis, AMCs were detached from the well by trypsin-EDTA and centrifuged at 600 *g* for 10 min to remove the culture medium. Cells were then fixed with 2.5% glutaraldehyde in 0.1 M cacodylate buffer (CB) pH 7.3, for 1 h at 4°C. The pellet was subsequently washed twice in CB, postfixed in 2% osmium tetroxide, dehydrated in a graded series of ethanol up to absolute, preinfiltrated, and embedded in Epon 812. Ultrathin sections (90 nm) were sectioned and mounted on 200-mesh copper grids, stained with uranyl acetate and lead citrate, and examined under a Philips EM 208 transmission electron microscope (TEM) equipped with a digital camera [University Centre for Electron Microscopy (CUME)—Perugia].

MV labeling with PKH-26

To trace in vitro MVs by fluorescence microscopy, MVs from AMCs were labeled with the red fluorescence aliphatic chromophore intercalating into lipid bilayers PKH26 dye (Sigma). Briefly: after ultracentrifugation, the MV pellet was diluted to 1 mL with the PKH-26 kit, and 2 μL of fluorochrome were added to this suspension and incubated for 30 min at 38.5°C. Thereafter, 7 mL of serum-free DMEM were added to the suspension that was ultracentrifuged again at 100,000 *g* for 1 h at 4°C. The final pellet was immediately resuspended in HG-DMEM.

Incorporation of MVs in tendon cells

To study the capacity of MVs to be incorporated into tendon cells, a dose–response growth was performed in three replicates. Tendon cells were seeded at a density of 60×10^3 on culture slides (13 mm; Nalgen Nunc International) in 24 wells and cocultured with 10-20-30-40-50 $\times 10^6$ MVs/mL labeled with PKH-26 dye, and preincubated or not with trypsin (0.5 mM) for 24, 48, and 72 h at 38.5°C. At the end of each experimental condition, cells were nuclear stained with 10 μg/mL of Hoechst 33343 for 15 min at 38°C. The uptake of MVs was evaluated by an Olympus BX51 microscope equipped with a Scion Corporation 1394 video camera interfaced with a computer provided with software for image acquisition and analysis (Image-Pro Plus 5.1-Media Cybernetics; Immagini & Computer). Excitation wavelength was positioned at 550 nm, while emission wavelength was set at 567 nm. Hoechst 33342 dye (Sigma) was excited at 353–365 nm, while the emission wavelength was set at 460 nm. To detect the intensity of fluorescence, a semiquantitative analysis was performed. Different images were acquired for each condition then, for each image, the area of interest (AOI; where the signal was present) was manually defined by the user. Inside the AOI, up to three different background signals were sampled. The background areas were positioned by the user only where the fluorescent signal was not specific. The maximum value collected from the background areas was then used to define the threshold. Only fluorescence with an intensity above the threshold was considered to indicate fluorescence due to labeled MVs. Finally, the program measured the signal intensity expressed in arbitrary unit (a.u.).

Confocal microscopy analysis to assess internalization of MVs was performed using a Leica SP2 laser scanning confocal microscope (Leica Microsystems Srl) equipped with a PL Fluotar 20x AN 0.5 Dry objective.

In vitro effect of MVs on tendon cells treated with LPS

Dose/response curve of LPS on tendon cells was studied showing that 100 ng/mL and 48 h were the dose and the time most effective in inducing cellular stress evaluated by apoptotic study (data not shown). Sixty thousand cells were incubated with and without LPS (100 ng/mL) in the presence or absence of 40×10^6 MVs/mL for 24 and 48 h. Tendon cells at different times were used as control. At the end of each experimental condition, cells were detached with 0.05% trypsin-EDTA, centrifuged, and cryopreserved, for molecular biology studies, in liquid nitrogen using standard cryopreservation protocols.

Molecular biology study

After isolation from tendon tissue, cells were analyzed to detect the expression of specific tendon genes. Total RNA

was extracted from tendon cells immediately after isolation (P0) using TRI Reagent Solution (Life Technologies). Samples were then treated with DNase to avoid DNA contamination. RNA concentration and purity were measured by Nanodrop Spectrophotometry (NanodropH ND1000). The cDNA was synthesized from total RNA (500 ng) using the PrimeScript RT reagent Kit (Takara Bio). The gene expression evaluation was performed using specific sequences; equine-specific oligonucleotide primers were designed using open source PerlPrimer software v. 1.1.17 based on available NCBI Equus caballus sequences or on mammal multialigned sequences. Primers were designed across an exon–exon junction to avoid genomic DNA amplification and their sequence conditions and the references used are shown in Table 1.

Conventional reverse transcription-PCR (RT-PCR) on tendon genes as tenascin (*TN*), tenomodulin (*TNDT*), decorin (*DCN*), and collagen type I (*COL1A1*) was performed in a 25 μL final volume with RBC Taq DNA Polymerase (RBC Bioscience) under the following conditions: initial denaturation at 95°C for 2 min, 32 cycles at 95°C for 30 s (denaturation), 55–60°C for 30 s (annealing), 72°C for 1 min (elongation), and final elongation at 72°C for 7 min. For conventional PCR, primers were used at 300 nM final concentrations.

After treatment of cells with LPS and MVs or CM, some specific genes involved in the inflammatory process were analyzed by RT-quantitative PCR (RT-qPCR) that was performed with SYBR green method in a MyiQ iCycler thermal cycler (Biorad). Matrix metallopeptidase 1 (*MMP1*), matrix metallopeptidase 9 (*MMP9*), matrix metallopeptidase 13 (*MMP13*), and tumor necrosis factor-α (TNFα) were proinflammatory genes selected for this study. Transforming growth factor-β (TGFβ) was evaluated as anti-inflammatory gene. Triplicate PCR reactions were carried out for each sample analyzed. The reactions were set on a strip in a final volume of 25 μL by mixing, for each sample, 1 μL of cDNA, 12.5 μL of 2X concentrated SYBR Premix Ex Taq II (Takara Bio) containing SYBR Green as a fluorescent intercalating agent, 0.2 μm forward primer, 0.2 μm of reverse primer, and MQ water. PCR efficiencies were tested and found to be close to 1. The thermal profile for all reactions was 30 s at 95°C and then 40 cycles of 5 s at 95°C and 30 s at 60°C. Fluorescence monitoring occurred at the end of each cycle. Efficiency of amplification for each primer was monitored through the analysis of serial dilution. Additional dissociation curve analysis was performed and in all cases showed a single peak. The data thus obtained were analyzed using the iQ5 optical system software version 2.0 (BioRad). The expression of each gene was normalized to the reference gene glyceraldehyde-3-phosphate dehydrogenase (*GAPDH*) (internal control) to standardize the results by eliminating variation in cDNA quantity.

PBMC isolation

Horse PBMCs were obtained from heparinized whole blood samples, after informed consent was obtained from the owners, using density gradient centrifugation (Lymphoprep; Axis-Shield) at 500 *g* without brakes for 20 min at room temperature.

PBMC proliferation test

Proliferation was induced by stimulating PBMC (2×10^5 horse PBMC/well in a 96-well flat-bottomed plate) through the addition of phytohemagglutinin (PHA; Sigma) at a final concentration of 2 μg/mL in a final volume of 200 μL/well of RPMI complete medium. To study the effects of MVs on PBMC proliferation, MVs were used in different amounts: 100×10^6, 50×10^6, and 5×10^6 in 100 μL of DMEM supplemented with 0.1% penicillin/streptomycin and 10% FCS. The same concentrations of MVs were tested after sonication by Soniprep 150 instrument (MSE). PBMC proliferation was tested also with 170, 120, and 80 μL/well of CM in its entirety and its SN obtained after centrifugation to separate the MVs.

All cultures were carried out in triplicate.

In all cases, PBMC proliferation was assessed after 3 days of culture by adding 0.67 μCi per well (96-well tissue culture plates) of [3H]-thymidine (INC Biomedicals) for 16–18 h. Cells were then harvested with a Filtermate Harvester (PerkinElmer), and thymidine incorporation was measured using a microplate scintillation and luminescence counter (Top Count NXT; PerkinElmer).

Table 1. Primer Sequences and Characteristics

Markers	*Forward*	*Reverse*	*bp*
Decorin (*DEC*)	CCAATGTTCTGATTTGGGTCTG	GTTGTTGACAAGAATCAACGC	152
Tenomodulin (*TNMD*)	CCATGCTGGATGAGAGAGGT	GTTGCAAGGCATGATGACAC	152
Tenascin-C (*TEN*)	CAAGTTCACAACAGACCTC	AGGTCGTGTCTCCATTCAG	184
Collagen type I (*COL1A1*)	CTACGATGGCTGCACGAGTC	GACAGGGCCAATGTCGATGC	151
Matrix metallopeptidase 1 (*MMP1*)	ACTGCCAAATGGACTTCAAGCTGC	TCTTCACAGTGCTAGGAAAGCCG	158
Matrix metallopeptidase 9 (MMP9)	CGACGAAGAGTTGTGGTCTCTGG	GCGGTCGGTGTCATAGTAGGC	184
Matrix metallopeptidase 13 (*MMP13*)	CTCTGGTCTGCTGGCTCACGC	CCAAACTCGTGTGCAGCGAC	132
Tumor necrosis factor-α (*TNFα*)	GCCTCAGCCTCTTCTCCTTC	GGCTTGTCACTTGGGGTTC	172
Transforming growth factor-β (*TGFβ*)	GGAATGGCTGTCCTTTGATG	CGGAGTGTGTTATCTTTGCTGTC	120
glyceraldehyde-3-phosphate dehydrogenase (*GAPDH*)	TAACGTGTCAGTCGTGGATC	TTGTCATACCAGGAAATGAGC	234

Statistical analysis

For quantitative PCR data, nonparametric tests were used. The Mann–Whitney U-test was employed to compare two groups (treated vs. untreated). Results were considered statistically significant if the value of P was <0.05.

For PBMC proliferation test, paired t-test, baseline corrected unpaired t-test, and ANOVA plus Tukey's test were used with GraphPad Prism software, version 6. Results were considered statistically significant if the value of P was <0.05.

Results

Tissue collection and cell isolation

Cells were selected purely on their ability to adhere to plastic. For AMCs, initial viability was >90%, whereas for tendon cells it was >80%. Amniotic cells (Fig. 1A) and tendon cells (Fig. 1B) displayed typical fibroblast-like morphology. AMCs observed at the early stages of culture were organized as three-dimensional clusters (Fig. 1C).

The molecular biology study on tendon cells confirmed that these cells were tendon cells because of the expression of *TN*, *TNMD*, *DCN*, and *COL1A1*.

Isolation and measurements of MVs

In all studied samples, the viability of AMCs at the time of MV collection was 99% as detected by trypan blue exclusion. By Nanosight, the size of MVs ranged from 50 to 670 nm, with a mean size of 258 ± 55 nm for three samples. The number of MVs ranged from 800 to 4,700 particles/cell, with a mean value of $2{,}550 \pm 71$ particles/cell (corresponding to 540×10^6 particles/mL of medium).

TEM of MVs

TEM revealed the presence of variably sized, extracellular membranous vesicles budding from or lying near the source cell and characterized by an electron-lucent or moderately electron-dense content (Fig. 2A, B). The size of MVs varied from about 100 to 1,000 nm, with a predominance of vesicles between 100 and 200 nm. The vesicles were roughly spherical.

Although active budding was not frequently observed, it is believed that, because of size and morphological characteristics, the vesicles observed were mainly shedding vesicles (microvesicles), rather than exosomes. Multivesicular bodies in the early stages of maturation were occasionally detected (Fig. 2C). This suggests that the production of exosomes by these cells is less relevant compared with shedding vesicles.

Incorporation of MVs in tendon cells

As seen by fluorescence microscopy, in all studied samples, no fluorescence signal was detectable up to the sixth hour of coincubation of MVs, and tendon cells and only

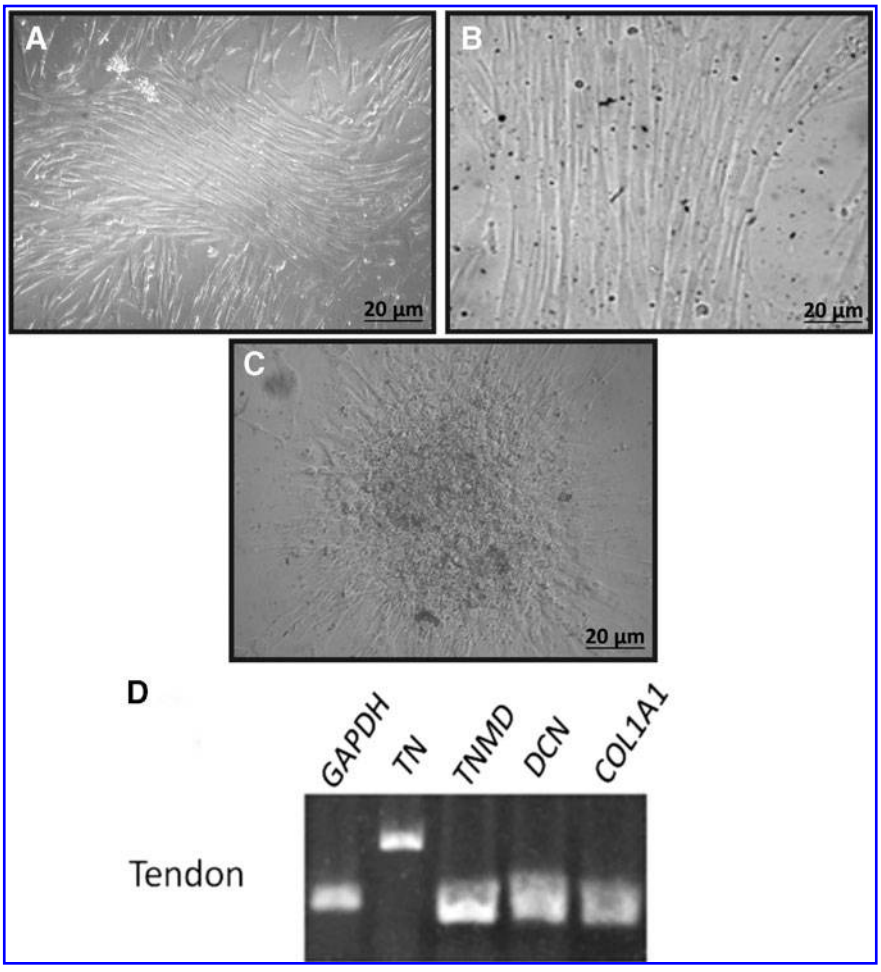

FIG. 1. Morphology of amniotic **(A)** and tendon cells **(B)**. AMCs observed at the early stages of culture organized as three-dimensional clusters **(C)**. Results of molecular biology study on tendon cells **(D)**. AMC, amniotic mesenchymal cell.

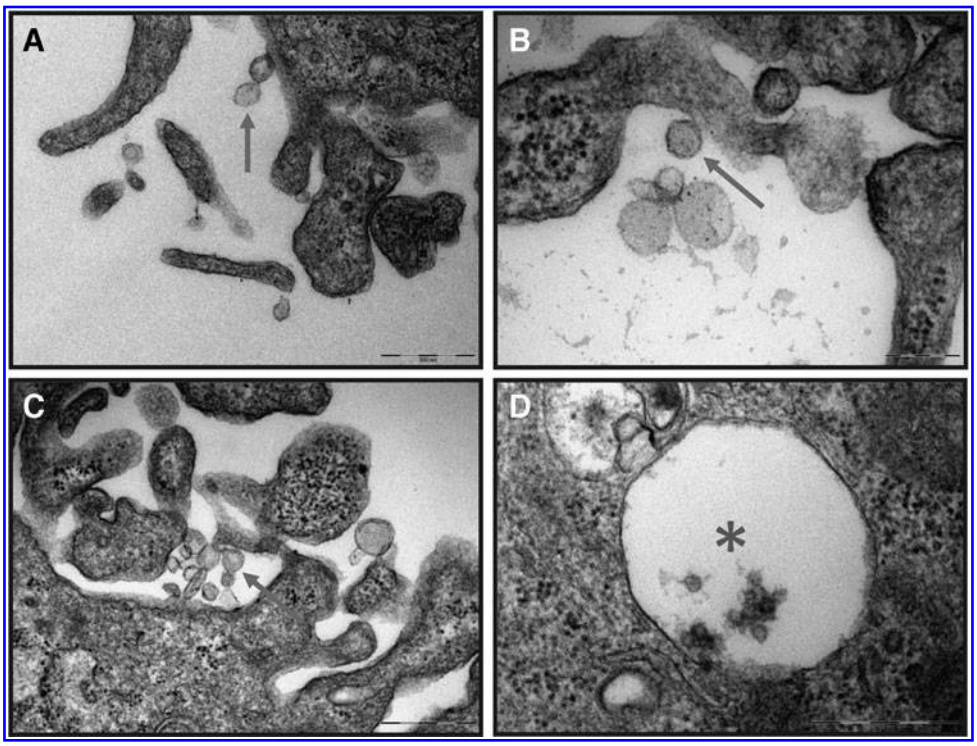

FIG. 2. Electron microscopy analysis of MVs. **(A–C)** *Arrows* show the release of MVs from the surface of an AMC. *Asterisk* shows a multivesicular body in the early stage of maturation **(D)**. Scale bar: 500 nm for **(A, C, and D)**, 200 nm for **(B)**. MV, microvesicle.

nuclei stained with Hoechst 33342 were visible (Fig. 3A). Neither was any signal detected after treatment of MVs with trypsin. When MVs were incorporated into cells, a fine granular fluorescent pattern was detectable within the cytoplasm, indicating the incorporation of labeled MVs. Under a fluorescent microscope, the tendon cell nuclei (blue), the MVs (red), and the merged image, show the incorporation of MVs into the target cells (Fig. 3B–D). The internalization and accumulation of MVs peaked between 24 (Fig. 3E) and 72 (Fig. 3F) h.

As seen by confocal microscopy, after 24 h of incubation with MVs, tendon cells showed a fine granular fluorescent pattern within their cytoplasm, indicating incorporation of MVs (Fig. 4).

At higher concentrations, uptake rate was faster: 50×10^6 MVs were incorporated in 24 h, 40×10^6 MVs in 48 h, and 30×10^6 MVs in 72 h (Fig. 5). Moreover, the uptake of MVs drastically increased at 72 h at a concentration of 40×10^6 MVs and decreased at the concentration of 50×10^6 MVs (Fig. 6).

In vitro effect of MVs on tendon cells treated with LPS

The expression of some proinflammatory genes was evaluated by RT-qPCR and nonstimulated tendon cells were used as a control. Data were obtained from three samples. A moderate, but significantly ($P<0.05$) increased gene expression of *MMP1* (1.6 ± 0.14) and *MMP9* (4.4 ± 0.14) was observed compared to tendon cells 48 h after exposure to LPS (Fig. 6). A significantly higher expression of *MMP13* (16.7 ± 0.12) and TNFα (8.47 ± 0.42) were noticed 48 h after LPS exposure compared to baseline levels (Fig. 7). The presence of MVs had a significant effect on the gene expression of metallopeptidases when compared to expression levels of control. In particular, a striking reduction in the expression levels for *MMP1* (0.77 ± 0.2), *MMP9* (2.4 ± 0.18), *MMP13* (7.22 ± 0.18), and *TNFα* (3.42 ± 0.21) was found at 48 h after addition of MVs. At 24 h, the combination of LPS and MVs increased the expression of *MMP9*. Tendon cells constitutively express *TGFβ* that decreased after LPS treatment, but it is restored from MVs.

PBMC proliferation test

Through in vitro studies, we demonstrated that MVs did not inhibit PBMC proliferation after activation with PHA even after sonication of them (Fig. 8). The only inhibitor effect was evident with CM in its entirety and its SN obtained after centrifugation to isolate MVs (Fig. 8), without a statistical difference between them. The inhibitory effect was dose dependent either with the CM or its SN with significant effect at 170 and 120 μL, but not with 80 μL.

Discussion

AMCs are the focus of great interest in veterinary regenerative medicine for their in vitro multilineage differentiation potential, their great in vitro expansion, and for their potential therapeutic applications in vivo in spontaneous equine tendon lesions [5]. Their paracrine effects have been demonstrated in in vitro and in vivo [6] studies, suggesting that soluble factors are implicated in the AMC effects and cell-cell contact is not necessary for their action. Cell-derived MVs were described as a new mechanism for cell-to-cell communication [18], indeed, MVs are released by a variety of cell types, [18,19] including stem cells and progenitor cells [9,20]. In this study, we investigated whether equine AMCs produce MVs and if tendon cells could be targeted by them. Our results show that AMCs secret MVs

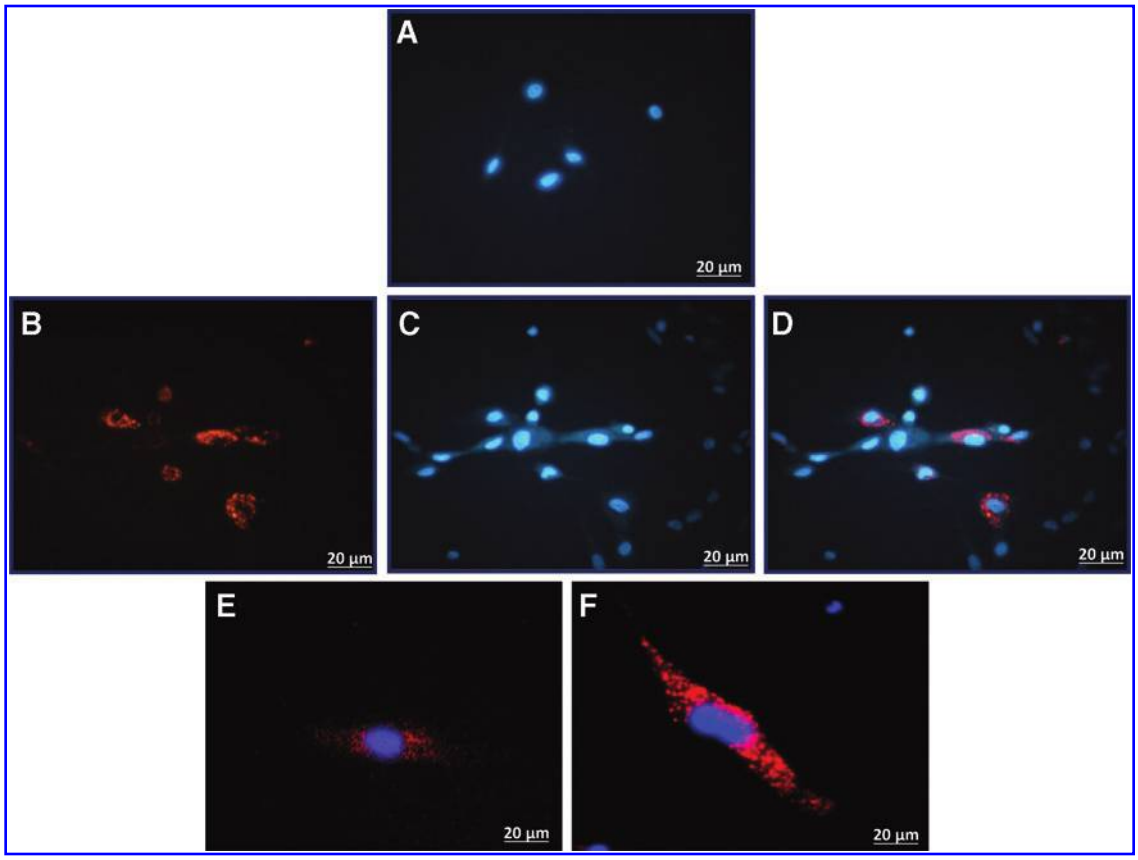

FIG. 3. Representative micrographs of internalization by tendon cells of MVs labeled with PKH-26. Under a fluorescent microscope, the tendon cell nuclei (*blue*), the MVs (*red*), and the merged image, which show incorporation of MVs into the target cells. **(A)** No incorporation of MVs preincubated with trypsin. MVs **(B)**, tendon cell nuclei **(C)** and merged image **(D)** show the incorporation of MVs into the target cells. **(E)** Internalization in tendon cell at 24 h and **(F)** 72 h. Color images available online at www.liebertpub.com/scd

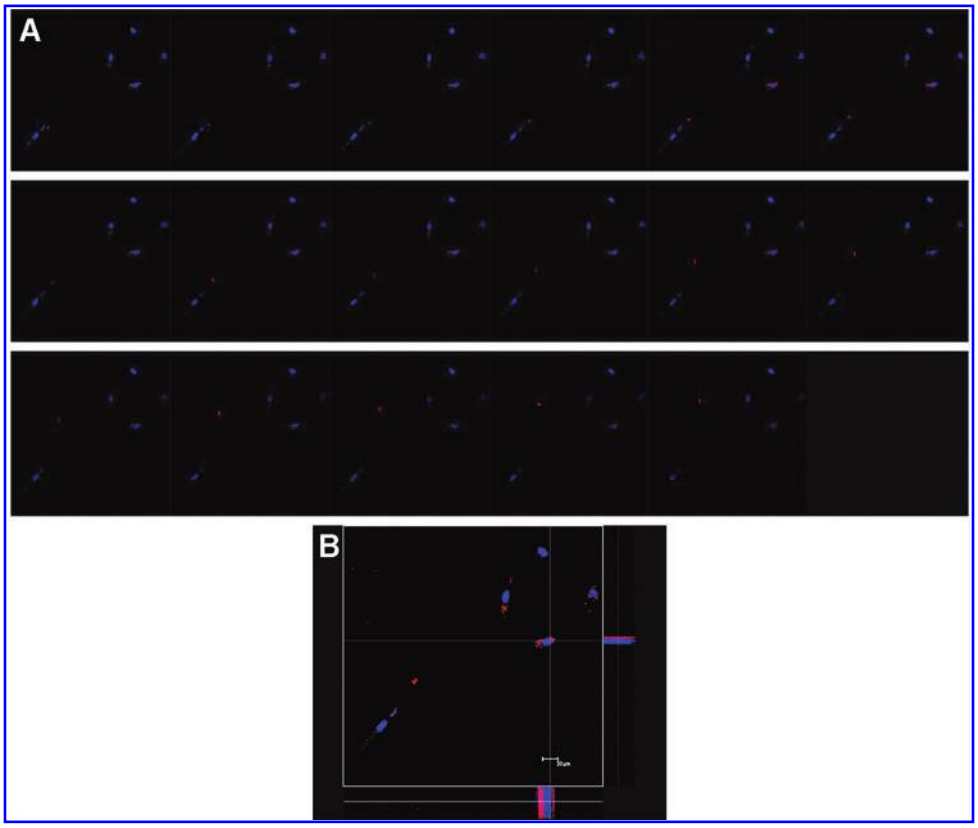

FIG. 4. Representative z-stack micrographs showing the internalization of MVs as detected by confocal microscopy in tendon cells co-cultured with MVs for 24 h. **(A)** The images were taken at different plans scanned every 0.5 µm from top to bottom of the nucleus. **(B)** Orthogonal projection of the same group of cells. Color images available online at www.liebertpub.com/scd

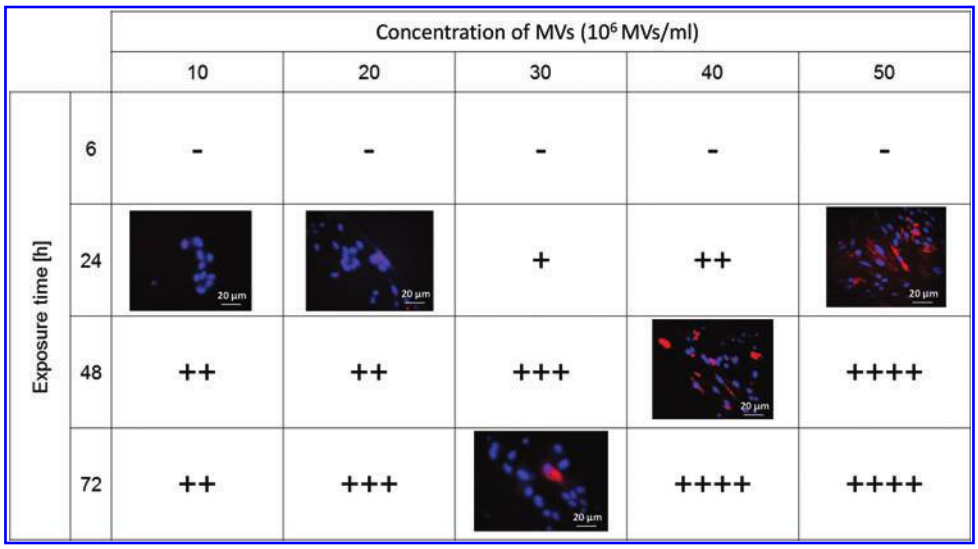

FIG. 5. Micrographs of dose/exposition time for MV incorporation. No fluorescence signal was detectable up to the sixth hour of coincubation of MVs and tendon cells. At higher concentrations, the uptake rate was higher: 50×10^6 MVs were incorporated in 24 h, 40×10^6 MVs in 48 h, and 30×10^6 MVs in 72 h. Color images available online at www.liebertpub.com/scd

(with a mean size of 258 nm) as detected by a Nanosight instrument. The TEM analysis confirmed this size, underlining that the vesicles observed are mainly shedding vesicles or MVs. Indeed, the production of exosomes by these cells was more rarely detected. An interesting finding is the number of MVs that these cells are capable of secreting. In our experimental conditions, each amniotic cell, plated at a density of 1×10^4 cells/cm^2, is able to secrete approximately 2,550 MVs, corresponding to about 540×10^6 particles/mL of SN. Moreover, we found that MVs are easily internalized by tendon cells. Fluorescent microscopy analysis suggests that the uptake of MVs by tendon cells shows an inverse relationship between concentration and time. Indeed, the highest concentrations are internalized in a shorter time and, vice versa. The behavior of the cells stimulated with MVs for 72 h is surprising. More MVs (determined by semiquantitative analysis) are incorporated at 72 h when compared to other studied times, but after a peak of internalization with 40×10^6 MVs/mL, there is an abrupt decrease of fluorescence intensity detected at 50×10^6 MVs/mL. Obviously, the target cell is able to incorporate MVs, but it must be able to use their contents too. We hypothesize that after 72 h of exposure at 40×10^6/mL, the cells are saturated and phagocytosis of MVs, for the release of their contents into the cell cytoplasm, begins. This phagocytosis probably results in the destruction of the MV membranes and, consequently, in the loss of fluorescence signal. A mechanism for internalization as a result of the direct fusion or endocytic uptake by target cells was demonstrated by Cocucci et al. [21]. Once internalized, the MVs can fuse their membrane with that of endosomes, making a horizontal transfer of their contents into the cytoplasm of the recipient cells. Alternatively, MVs can remain segregated inside the endosomes and be phagocytized by lysosomes or eliminated from the cells after fusion with the plasma membrane through a mechanism of transcytosis [21]. Our data show that horizontal transfer of the contents of MVs within tendon cells could be one of the mechanisms of action of MVs, although other methods of interaction may occur simultaneously. Indeed, the lack of MV internalization by tenocytes after treatment with trypsin is interesting. Presumably, the interaction between membrane receptors of

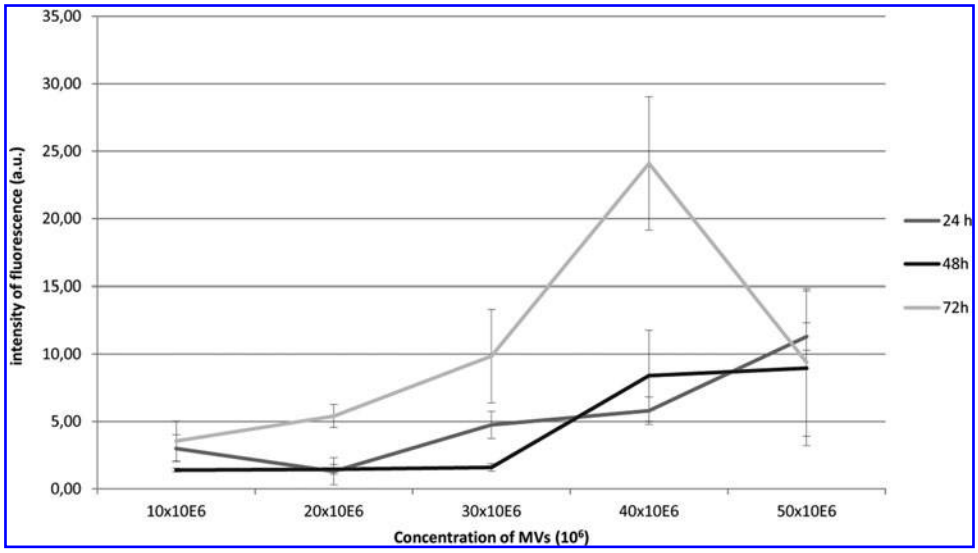

FIG. 6. Graph of dose/exposition time for MV incorporation. The uptake of MVs drastically increased at 72 h at 40×10^6 MVs and decreased at 50×10^6 MVs. Data represent the mean and SD of at least three independent experiments. In the curve of 72 h, values labeled with different letters are statistically different ($P<0.05$).

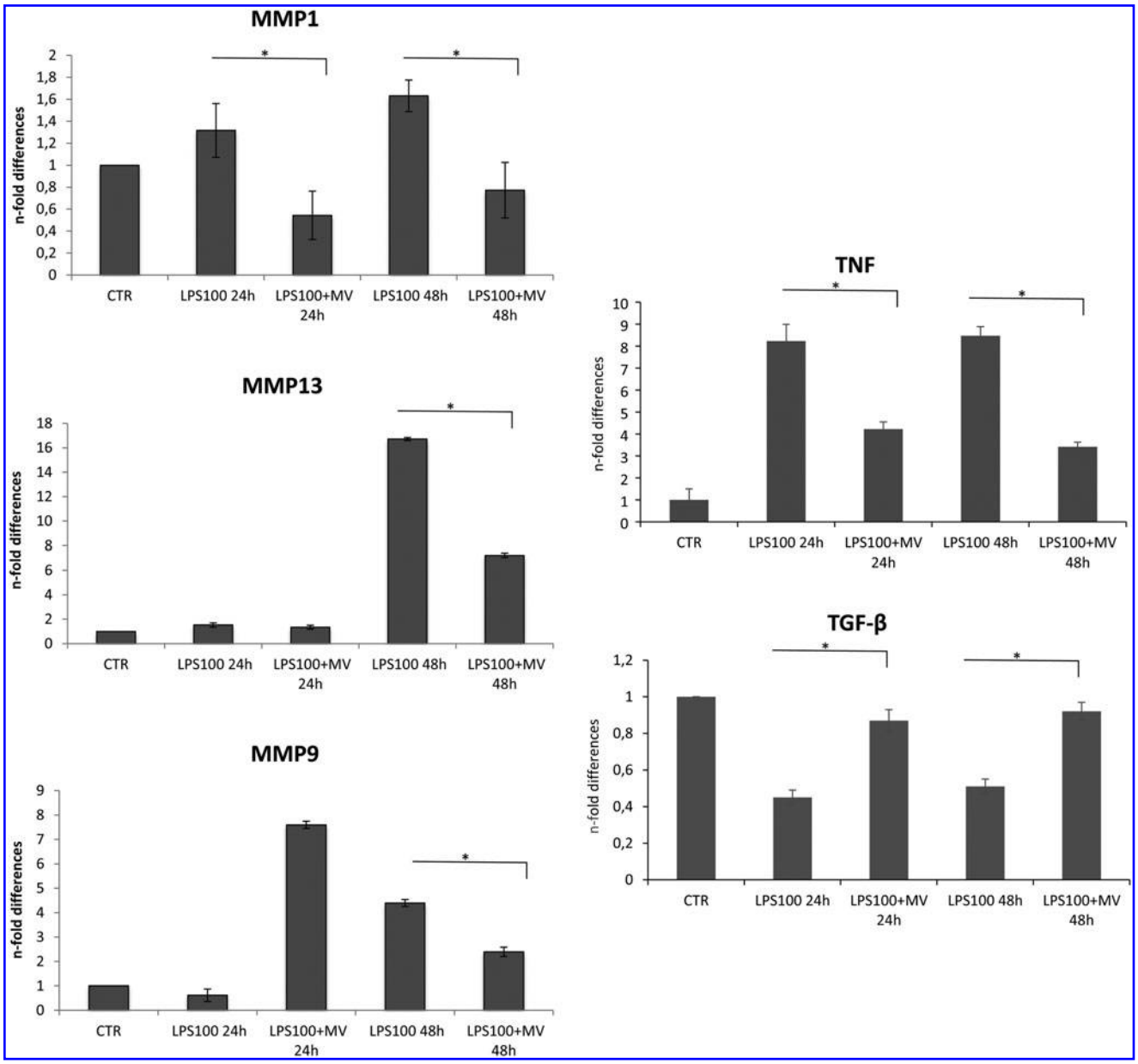

FIG. 7. Quantitative RT-PCR analysis for the expression of *MMP1, MMP9, MMP13, TNFα,* and *TGFβ* genes. Cells were cultured in presence of 100 ng/mL LPS with or without MVs at 24 and 48 h. Expression levels have been normalized to the reference gene (*GAPDH*). Data are represented as fold change compared with the expression observed in tendon cells (control). Values are mean ± SD ($n = 3$). *Asterisks* depict significant ($^*P < 0.05$) differences. LPS, lipopolysaccharide; RT-PCR, reverse transcription-PCR.

the MVs and target cell surface receptors is required for the process of internalization. The removal of surface molecules by trypsin treatment inhibits their incorporation, confirming the importance of surface molecules in the internalization of MVs. Bruno et al. [15] found that MSC-derived MVs expressed several adhesion molecules of MSCs such as CD44, CD29 (α1-integrin), α4- and α5 integrins, and CD73, but not α6 integrin. Some of these molecules, namely CD44 and CD29, were found to be instrumental in MV internalization into tubular endothelial cells, as treatment with anti-CD44 and anti-CD29 blocking antibodies prevented MV incorporation. In our study, the simple treatment with trypsin and the subsequent failure of incorporation of MVs into tendon cells confirm a process of interaction between the receptor and the target cells before internalization of MVs.

Having identified that the tendon cells represent target cells for MVs secreted by equine AMCs, a further aim of this study was to understand whether or not these MVs might be involved in the regeneration of tendon injuries previously treated in vivo with AMC-CM [6]. Obviously, due to the difficulty of studying the repair systems of spontaneous tendon pathology in vivo, we recapitulated in vitro the inflammatory process by stimulating cells with LPS. The inflammatory process is essential because the activation of the inflammatory cascade is an important stimulus for tendon healing, although persistent inflammation is believed to be the

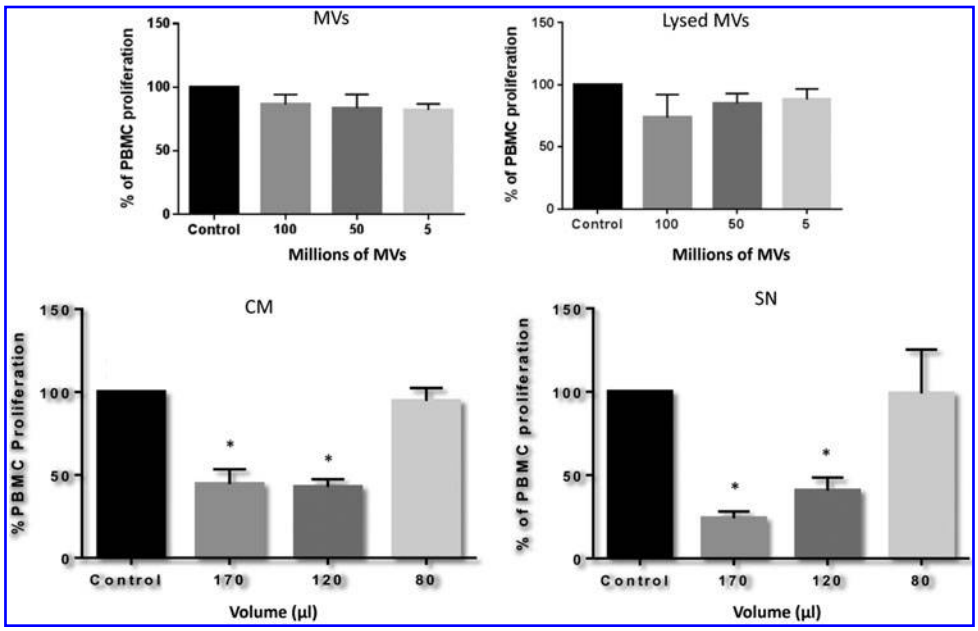

FIG. 8. Lymphocyte proliferation test. Effects of different amounts (100-50-5×10^6) of MVs per mL and different amount of CM and SN on the proliferation of PHA-stimulated lymphocytes (PBMC + PHA). Data represent the mean and SD of at least three independent experiments. $^*P<0.05$ versus Control (PBMC + PHA). CM, conditioned medium; PBMC, peripheral blood mononuclear cell; SN, supernatant.

cause of fibrosis that is counterproductive to achieve a successful healing [22]. In physiological conditions, inflammation becomes self-regulating within the first 24–48 h following an insult [23]. For this reason, the in vitro experiment was set at 48 h. In this explorative study, we analyzed TNF-α, which it is a proinflammatory cytokine that mediates inflammation [24] and genes involved in tendon extracellular matrix degradation. In addition, expression of TGFβ was assessed. Following 48 h treatment with LPS at 100 ng/mL, *MMP1* and *MMP9* expression increased moderately, while *MMP13* and *TNFα* expression increased more than control. The MMPs are a family of structurally related zinc-/calcium-dependent proteinases that play a central role in the extracellular matrix degradation during both normal and pathological tissue remodeling processes [25,26]. Nomura et al. [27] demonstrated that in equine superficial digital flexor tendinitis, *MMP1* was not detected at mRNA level, while *MMP13* was upregulated in the tendinitis compared to normal tendon, suggesting that MMP13 plays an important role in tendon injuries in the racehorse. Although the origin of these MMP13-expressing cells in the tendinitis is still not clear, we hypothesize that this enzyme could be involved in the process of superficial digital flexor tendinitis development. Expression of *MMP9* has been reported to increase in horses with insulin-induced laminitis compared with control horses [28], so it is plausible that in our static in vitro system, with LPS treatment, the *MMP9* is moderately expressed. These data confirm our results regarding the moderate increase of *MMP1* and *MMP9* compared to *MMP13* in the LPS treatment.

Since treatment with LPS induced an inflammatory response, an explorative study to understand the mechanism of action by MVs was performed. The single concentration of 40×10^6 MVs/mL was used because, during the study of internalization, neither were tendon cells saturated with MVs at this concentration at 48 h of culture nor did MV degradation start. In this experiment, MVs downregulated the expression of *MMP1, MMP9*, *MMP13*, and *TNFα* genes at 48 h of LPS treatment and restored the expression of *TGFβ* that is constitutively expressed by tendon cells. At 24 h, the combination of LPS and MVs increased unexpectedly the expression of *MMP9*. This behavior was consistent in all three experiment replicates. From our data not shown, MVs alone do not induce an upregulation of the genes studied at different time, but apparently, the combination of LPS and MVs induced an inflammatory process. In tendon lesion, the presence of MMP9 is remarkable, but its presence is probably related to invading cells and their factors [29]. In our in vitro context at 24 h, MVs could have introduced factors (such as miRNA) that, acting as an inflammatory process, temporarily enhanced the expression of *MMP9* that is reinstated at 48 h by MVs themselves.

The last study was the PBMC proliferation inhibition by MVs to confirm that the inhibition obtained by AMC-CM [5] was due to the paracrine factors that communicate with immune cells. However, the finding that inhibition of PBMC proliferation was induced only by whole CM or by its SN and not by MVs suggests that this competence is imputable to factors (growth factors) not contained in MVs. This hypothesis was further supported by our findings that PBMC proliferation was not inhibited by the sonicated or lysed MVs. A similar effect was recently reported by Del Fattore et al. [30] with bone marrow-derived extravesicle (EV) that induced T-cell apoptosis without significantly suppressing T-cell proliferation, even if EV treatment increased the Treg/Teff ratio and the immunosuppressive cytokine IL-10 concentration in the culture medium. The divergent effects of AMC-CM and MVs on PBMC stimulated with PHA are at present unexplained. Even though it is generally accepted that MSCs from amniotic membrane or other sources act in a paracrine manner (for review [31–33]), from our study, it is possible to hypothesize that the effect of these mechanisms is mainly due to soluble factors and not the cargo of MVs. Although many studies failed to detect those cytokines and growth factors that are present in low concentrations [34], TGF-β1, hepatocyte growth factor, prostaglandin E2, interleukin-10, haem oxygenase-1, interleukin-6, and human leukocyte antigen-G5 are all known to be constitutively produced by MSCs [35–37]. Recently, Rossi et al. [38] suggested that prostaglandins as one of the key effector

molecules of the antiproliferative activity of human amniotic membrane-derived cells. However, the divergent effects of AMC-CM and MVs on PBMC stimulated with PHA are at present unexplained and, as demonstrated by Del Fattore et al. [30], appear to be different from those exhibited by their cells of origin. In this context, the immunosuppressive effects of MVs cannot be ruled out since more studies are required regarding MVs and lysed MV influence on the different lymphocytic subpopulations.

Conclusion

Our preliminary results demonstrate that AMCs produce MVs that are able to target tendon cells. Moreover, these MVs, in our explorative experimental conditions, exerted anti-inflammatory effects although they were not able to suppress immune cell activity in vitro. This let us assume that in therapeutic in vivo administration of CM, for the treatment of spontaneous equine tendon injuries [6], both MVs' cargo and soluble factors contributed to the regenerative effect. Additional works will be needed to better understand both, the efficacy and the mechanisms of action of this novel potential tool, which will change the perspective of the therapeutic use of MSCs in tendon lesions, or in inflammatory process-based diseases, considering the MVs as a cell-free therapy.

Acknowledgments

This study was supported by grants from Università degli Studi di Milano, Milano, Italy; Università Politecnica delle Marche, Ancona, Italy; and by Centro di Ricerca E. Menni, Fondazione Poliambulanza, Istituto Ospedaliero, Brescia, Italy. The authors wish to thank Dott.ssa Miriam Ascagni (Department of Bioscience, Università degli Studi di Milano, Italy) for her skilled assistance in confocal microscopy.

Author Disclosure Statement

The authors declare that no competing financial interests exist in relation to this article.

References

1. Dazzi F and NJ Horwood. (2007). Potential of mesenchymal stem cell therapy. Curr Opin Oncol 19:650–655.
2. Hwang NS, C Zhang, YS Hwang and S Varghese. (2009). Mesenchymal stem cell differentiation and roles in regenerative medicine. Wiley Interdiscip Rev Syst Biol Med 1: 97–106.
3. Satija NK, VK Singh, YK Verma, P Gupta, S Sharma, F Afrin, M Sharma, P Sharma, RP Tripathi and GU Gurudutta. (2009). Mesenchymal stem cell-based therapy: a new paradigm in regenerative medicine. J Cell Mol Med 13: 4385–4402.
4. Leung VY, D Chan and KM Cheung. (2006). Regeneration of intervertebral disc by mesenchymal stem cells: potentials, limitations, and future direction. Eur Spine J 15 Suppl 3:S406–S413.
5. Lange-Consiglio A, S Tassan, B Corradetti, A Meucci, R Perego, D Bizzaro and F Cremonesi. (2013). Investigating the potential of equine mesenchymal stem cells derived from amnion and bone marrow in equine tendon diseases treatment in vivo. Cytotherapy 10:1016–1023.
6. Lange-Consiglio A, D Rossi, S Tassan, R Perego, F Cremonesi and O Parolini. (2013). Conditioned medium from horse amniotic membrane-derived multipotent progenitor cells: immunomodulatory activity in vitro and first clinical application in tendon and ligament injuries in vivo. Stem Cell Dev 22:3015–3024.
7. Caplan AI and JE Dennis. (2006). Mesenchymal stem cells as trophic mediators. J Cell Biochem 98:1076–1084.
8. Huang YC, O Parolini and L Deng. (2013). The potential role of microvesicles in mesenchymal stem cell-based therapy. Stem Cells Dev 15:841–844.
9. Ratajczak J, K Miekus, M Kucia, J Zhang, R Reca, P Dvorak and MZ Ratajczak. (2006). Embryonic stem cells-derived microvesicles reprogram hematopoietic progenitors: Evidence for horizontal transfer of mRNA and protein delivery. Leukemia 20:847–856.
10. Camussi G, MC Deregibus, S Bruno, V Cantaluppi and L Biancone. (2010). Exosomes/microvesicles as a mechanism of cell-to-cell communication. Kidney Int 78:838–848.
11. Théry C, M Ostrowski and E Segura. (2009). Membrane vesicles as conveyors of immune responses. Nat Rev Immunol 9:581–593.
12. Mathivanan S, H Ji and RJ Simpson. (2010). Exosomes: extracellular organelles important in intercellular communication. J Proteomics 73:1907–1920.
13. György B, TG Szabó, M Pásztói, Z Pál, P Misják, B Aradi, V László, E Pállinger, E Pap, et al. (2011). Membrane vesicles, current state-of-the-art: emerging role of extracellular vesicles. Cell Mol Life Sci 68:2667–2688.
14. Biancone L, S Bruno, MC Deregibus, C Tetta and G Camussi. (2012). Therapeutic potential of mesenchymal stem cell-derived microvesicles. Nephrol Dial Transplant 27: 3037–3042.
15. Bruno S, C Grange, MC Deregibus, RA Calogero, S Saviozzi, F Collino, L Morando, A Busca, M Falda, et al. (2009). Mesenchymal stem cell-derived microvesicles protect against acute tubular injury. J Am Soc Nephrol 20:1053–1067.
16. Zhang HC, XB Liu, S Huang, XY Bi, HX Wang, LX Xie, YQ Wang, XF Cao, J Lv, et al. (2012). Microvescicles derived from human umbilical cord mesenchymal stem cells stimulated by hypoxia promote angiogenesis both in vitro and in vivo. Stem Cells Dev 21:3289–3297.
17. Lange-Consiglio A, B Corradetti, D Bizzaro, M Magatti, L Ressel, S Tassan, O Parolini and F Cremonesi. (2012). Characterization and potential applications of progenitor-like cells isolated from horse amniotic membrane. J Tissue Eng Regen Med 6:622–635.
18. Schorey JS and S Bhatnagar. (2008). Exosome function: from tumor immunology to pathogen biology. Traffic 9: 871–881.
19. Morel O, F Toti, B Hugel and JM Freyssinet. (2004). Cellular microparticles: A disseminated storage pool of bioactive vascular effectors. Curr Opin Hematol 11:156–164.
20. Deregibus MC, V Cantaluppi, R Calogero, M Lo Iacono, C Tetta, L Biancone, S Bruno, B Bussolati and G Camussi. (2007). Endothelial progenitor cell-derived microvescicles activate an angiogenic program in endothelial cells by a horizontal transfer of mRNA. Blood 110:2440–2448.
21. Cocucci E, G Racchetti, P Podini and J Meldolesi. (2007). Enlargeosome traffic: exocytosis triggered by various signals is followed by endocytosis, membrane shedding or both. Traffic 8:742–757.

22. Dowling BA, AJ Dart and DR Hodgson. (2000). Superficial digital flexor tendonitis in the horse. Equine Vet J 32: 369–378.
23. Traub-Dargatz JL, MD Salman and JL Voss. (1991). Medical problems of adult horses, as ranked by equine practitioners. J Am Vet Res 198:1745–1747.
24. Prasanna SJ, D Gopalakrishnan, SR Shankar, AB Vasandan. (2010). Pro-inflammatory cytokines, IFN-γ and TNFα, influence immune properties of human bone marrow and Wharton jelly mesenchymal stem cells differentially. PLoS One 5:1–16.
25. Sternlicht MD and Z Werb. (2001). How matrix metalloproteinases regulate cell behavior. Ann Rev Cell Dev Biol 17:463–516.
26. Mott JD and Z Werb. (2004). Regulation of matrix biology by matrix metalloproteinases. Curr Opin Cell Biol 16:558–564.
27. Nomura M, Y Hosaka and Y Kasashima. (2007). Active expression of matri metalloptoinase-13 mRNA in Granulation Tissue of Equine Superficial Digital Flexor Tendinitis. J Vet Med Sci 69:637–639.
28. deLaat MA, MT Kyaw-Tanner, AR Nourian, CM McGowan, MN Sillence and CC Pollitt. (2011). The developmental and acute phases of insulin-induced laminitis involve minimal metalloproteinase activity. Vet Immunol Immunopathol 140:275–281.
29. Karousou E, M Ronga, D Vigetti, A Passi and N Maffulli. (2008). Collagens, proteoglycans, MMP-2, MMP-9 and TIMPS in human Achilles tendon rupture. Clin Orthop Relat Res 466:1577–1582.
30. Del Fattore A, R Luciano, L Pascucci, BM Goffredo, E Giorda, M Scapaticci, A Fierabracci and M Muraca. (2015). Immunoregulatory effects of mesenchymal stem cell-derived extracellular vesicles on T lymphocytes. Cell Transplant 24:2615–2627.
31. Magatti M, S De Munari, E Vertua, L Gibelli, G Wengler and O Parolini. (2008). Human amnion mesenchyme harbors cells with allogeneic T-cell suppression and stimulation capabilities. Stem Cells 26:182–192.
32. Engela AU, CC Baan, FJ Dor, W Weimar and MJ Hoogduijn. (2012). On the interactions between mesenchymal stem cells and regulatory T cells for immunomodulation in transplantation. Front Immunol 3:126.
33. Nauta AJ and WE Fibbe. (2007). Immunomodulatory properties of mesenchymal stromal cells. Blood 110:3499–3506.
34. Galderisi U and A Giordano. (2014). The gap between the physiological and therapeutic roles of mesenchyma stem cells. Med Res Rev 34:1100–1126.
35. Aggarwal S and MF Pittenger (2005). Human mesenchymal stem cells modulate allogeneic immune cell responses. Blood 105:1815–1822.
36. Chabannes D, M Hill, E Merieau, J Rossignol, R Brion, JP Soulillou, I Anegon and MC Cuturi. (2007). A role for heme oxygenase-1 in the immunosuppressive effect of adult rat and human mesenchymal stem cells. Blood 110:3691–3694.
37. Selmani Z, A Naji, I Zidi, B Favier, E Gaiffe, L Obert, C Borg, P Saas, P Tiberghien, et al. (2008). Human leukocyte antigen- G5 secretion by human mesenchymal stem cells is required to suppress T lymphocyte and natural killer function and to induce CD4 + CD25highFOXP3 + regulatory T cells. Stem Cells 26:212–222.
38. Rossi D, S Pianta, M Magatti, P Sedlmayr and O Parolini. (2012). Characterization of the conditioned medium from amniotic membrane cells: prostaglandins as key effectors of its immunomodulatory activity. PLoS One 7:e46956.

Address correspondence to:
Prof. Fausto Cremonesi
Large Animal Hospital
Reproduction Unit
Università degli Studi di Milano
Via dell'Università 6
Lodi 26900
Italy

E-mail: fausto.cremonesi@unimi.it

Received for publication November 11, 2015
Accepted after revision February 24, 2016
Prepublished on Liebert Instant Online February 25, 2016

Secretome derived from different cell lines in bovine *in vitro* embryo production

Claudia Perrini[1], Paola Esposti[1], Diego Compagnoni[1], Sara Treglia[1], Fausto Cremonesi[1,2], Anna Lange Consiglio[1*]

Perrini C.[1]: Reproduction Unit, Large Animal Hospital, Università degli Studi di Milano, Via dell'Università 6, 26900 Lodi, Italy. E-mail: claudia.perrini@unimi.it; phone n.: +390250331150; fax: +390250331115

Esposti P.[1]: Reproduction Unit, Large Animal Hospital, Università degli Studi di Milano, Via dell'Università 6, 26900 Lodi, Italy. E-mail: paolaesposti.dvm@gmail.com; phone n.: +390250331150; fax: +390250331115

Compagnoni D.[1]: Reproduction Unit, Large Animal Hospital, Università degli Studi di Milano, Via dell'Università 6, 26900 Lodi, Italy. E-mail: diego.compagnoni@studenti.unimi.it; phone n.: +390250331150; fax: +390250331115

Treglia S.[1]: Reproduction Unit, Large Animal Hospital, Università degli Studi di Milano, Via dell'Università 6, 26900 Lodi, Italy. E-mail: sara.treglia@studenti.unimi.it; phone n.: +390250331150; fax: +390250331115

Cremonesi F.[1]: Reproduction Unit, Large Animal Hospital, Università degli Studi di Milano, Via dell'Università 6, 26900 Lodi, Italy. E-mail: fausto.cremonesi@unimi.it; phone n.: +390250331150; fax: +390250331115. [2]Department of Veterinary Medicine, Università degli Studi di Milano, Via Celoria 10, 20133 Milano, Italy. phone n.: +390250318146; fax: +390250318148.

Lange-Consiglio A.[1]: Reproduction Unit, Large Animal Hospital, Università degli Studi di Milano, Via dell'Università 6, 26900 Lodi, Italy. E-mail: anna.langeconsiglio@unimi.it; phone n.: +390250331150; fax: +390250331115

Running Title: Secretome and *in vitro* embryo production

*Correspondence should be addressed to Anna Lange-Consiglio, Reproduction Unit, Large Animal Hospital, Università degli Studi di Milano, Italy; E-mail: anna.langeconsiglio@unimi.it

ABBREVIATIONS

AMCs: amniotic epithelial derived cells

BAX: Bcl-2–associated X protein

BSA: bovine serum albumin

CM: conditioned medium

COCs: cumulus–oocyte complexes

CTR: control

EDCs: epithelial endometrial cells

EGF: epidermal growth factor

FCS: fetal calf serum

GPX1: glutathione peroxidase 1

HEPES: N-2-hydroxyethylpiperazine-N-2-ethanesulfonic acid

HG-DMEM: high-glucose Dulbecco's modified Eagle's medium

ICM: inner cell mass

IVC*: in vitro* culture

IVF: *in vitro* fertilization

IVM: *in vitro* maturation

IVP: *in vitro* embryo production

miRNA: microRNA

MVs: microvesicles

No-CM: no-conditioned medium

PBS: phosphate-buffered saline

ROS: reactive oxygen species

SN: supernantant

SOFaa: synthetic oviductal fluid with aminoacids

TALP: Tyrode's-albumin-lactate-pyruvate

ABSTRACT

Conditioned media (CM), secreted by cells during their culture, brings to results similar to co-culture systems in *in vitro* embryo production. CM is composed of microvesicles (MVs) and soluble factors that are present in supernatant (SN) after removal of MVs. The effect of different component of CM has not been studied yet, so we tried to study these interactions *in vitro*. Secretome of bovine endometrial and amniotic cells on embryo rate and quality was investigated. Presumptive zygotes were randomly transferred in SOFaa (control, CTR) or cultivated by adding 20% endometrial or amniotic CM or SN or $100x10^6$ MVs/ml on day 1, 3 and 5 post fertilization. Embryos were evaluated on day 7. Results showed that on day 1, only MVs of both cell lines allowed embryo development but with rate lower than CTR. On day 3, amniotic and endometrial CM and MVs provided blastocyst, but the rate of CM is statistically lower than those obtained by MVs in both cell lines. On day 5, all the fractions of secretome of both cell lines provided embryos but only amniotic MVs gave a rate of embryos comparable to CTR. Qualitatively, only amniotic CM and MVs on day 5 provided values statistically higher of inner cell mass than CTR. These data were confirmed by evaluation of genes involved in apoptosis and reactive oxygen species protection. In conclusion, MVs gave results equivalent or better than CM, and amniotic CM and MVs resulted in a blastocyst rate comparable to CTR, but with a better embryo quality.

Key words: embryo quality, bovine, microvesiscles, amniotic cells, endometrial cells

INTRODUCTION

It is known that, usually, embryos produced *in vitro* are of a poorer quality when compared with *in vivo* ones [1]. Fertilization of eutherian animals occurs in the maternal oviduct. This is the natural and unique environment to achieve the necessary requirements for embryo life in its early and late development. The embryo conceived *in vitro* is manipulated and cultured in very different conditions and today a huge amount of information, mostly derived from animals, point out the

alterations that can occur in embryos produced *in vitro* because of the manipulation and artificial environmental conditions associated with these techniques [2]. It is quite difficult to define the degree of influence of the different factors implicated in the *in vitro* embryo production technique, such as superovulation, gametes and embryo culture and absence of maternal embryo-signaling [3]. Some researchers reported that the culture system and the medium composition can affect embryo quality [4,5] and that the *in vitro* culture (IVC) of embryo is probably the most relevant factor in the alterations of epigenetic reprogramming and development of animal embryos produced *in vitro*. As a direct result embryo physiology, gene expression and development are compromised [6]. In fact, while the innate feature of the oocyte is the major factor determining the blastocyst yield, it is evident that post-fertilization culture environment is critical in defining the quality of the blastocyst [5,7-9]. This underline the key effect of the maternal microenvironment on the success of early embryonic development in terms of viability [10]. In mammals, during the pre-implantation stage, the exchange of different types of signals between the mother and the embryo is thought to be critical for embryo development and implantation [11].

Thus, successful pregnancy in mammals involves synchronization between a receptive endometrium and a viable embryo [11-13]. In cattle, it has been considered that the absence of these signals could be an important cause of the low efficiency of IVF [14].

To mimic the *in vivo* cross-talk environment, co-culture systems are largely used in in vitro embryo production (IVP) in different species and, in some mammalian species, somatic cell co-cultures improved the *in vitro* development of embryos [15-18]. Indeed, co-culture system with bovine oviduct epithelial cells used for the development of bovine zygotes produced *in vitro* enhanced blastocyst formation and quality of the resulting embryos, inducing also specific transcriptomic changes [10]. This suggests that paracrine mechanisms of communication exist between “helper” cells and embryos. In fact, various growth factors, receptors and binding proteins are secreted by cells in the medium, but the embryos themselves also produce them. Conditioned media (CM), composed of factors secreted by cells during their culture, were developed and used in bovine

embryo IVP. Some of these cell-free media, produced, for example, by culturing granulosa, cumulus or oviductal cells demonstrated a similar effect in development of embryos produced by co-culture systems [19]. In addition to the reputation of CM, recent studies have uncovered the existence of MVs, which are released by cells into the extracellular environment. As consequence, we can define the CM as a composition of soluble factors plus MVs. These MVs have been shown to contain proteins, lipids (specifically high levels of sphingomyelins), a variety of RNA species, including microRNAs (miRNAs) and mRNA fragments [20], but researchers are still debating the presence/absence of DNA inside them. MVs could serve as vehicles for the transfer of these molecules between cells both locally (autocrine and paracrine) and remotely [21,22]. MVs are secreted by most of the cells and can be found in organic fluids, for example, MVs have been isolated from the uterine luminal fluid of cyclic and pregnant sheep [23]. Analysis of these vesicles revealed miRNAs and proteins expressed both by the conceptus trophectoderm and by the endometrial epithelium, such as cathepsin L1 and prostaglandin synthase 2. *In vitro* studies have shown that these MVs, isolated in pregnant sheep, can transfer RNAs to other cells [23]. These findings indicate that these MVs likely have a biological role in the interaction between the embryo and the endometrium, transferring information from the latter supporting early embryo development, although this hypothesis still needs to be proven. The successful ontogenesis is dependent on coordination between the embryo and the microenvironments that *in vivo* is represented by endometrium, and *in vitro* by different culture conditions. The *in vitro* use of feeder cell or CM probably involve MVs that may participate in this required cross-talk. The effect of different component of feeder cells secretome has never been studied and, since it is difficult to study these communications *in vivo*, we tested these interactions *in vitro*. Endometrium and amnion have a role in the establishment of pregnancy, then, their secretome, composed of CM *in toto*, MVs and supernatant (SN), composed of CM soluble factors after removal of MVs, was investigated to know which of these components, if not all, have effects on embryo production, in terms of blastocyst rate and quality.

MATERIALS AND METHODS

Chemicals were obtained from Sigma-Aldrich Chemical (Milan, Italy) unless otherwise specified, and tissue culture plastic dishes were purchased from Euroclone (Milan, Italy).

Samples of endometrial tissue and ovaries were collected from bovine slaughtered in a slaughterhouse (INALCA, Ospedaletto Lodigiano, Lodi, Italy) under legal regulations.

Allanto-amniotic membranes were obtained at term of normal pregnancies and after vaginal delivery from three cows (*bos taurus*). All procedures were performed according to approved animal care and use protocols of the institutional ethics committee and to good veterinary practice for animal welfare as to European directive 2010/63/UE. Moreover, written farmers' consent was obtained at the beginning of the study.

Cell isolation and culture

Portions of allanto-amnion were kept at 4 °C in phosphate-buffered saline (PBS; EuroClone, Milan, Italy) with 100 U/ml penicillin-100 mg/ml streptomycin and amphotericin B and were processed within 12 h. The amniotic membrane was stripped from the overlying allantois and cut into small pieces (about 9 cm^2 each) before enzymatic digestion.

Amniotic epithelial derived cells (AMCs) were isolated and characterized as previously reported [24]. Briefly, amnion fragments were incubated for 9 min at 38.5 °C in PBS containing 2.4 U/mL dispase (Becton Dickinson, Milan, Italy). After a resting period (5-10 min) at room temperature in high-glucose Dulbecco's modified Eagle's medium (HG-DMEM; EuroClone, Milan, Italy), supplemented with 10% heat inactivated fetal calf serum and 2 mM L-glutamine, the fragments were digested with 0.05% trypsin/EDTA for 45 min at 38.5 °C for approximately 45 min. Then, the amnion fragments were removed and mobilized cells were passed through a 100 µm cell strainer before being collected by centrifugation at 250 g for 10 min.

Epithelial endometrial cells (EDCs) at early luteal phase (day 4-8, considering day 0 = estrus) were

isolated according to Donofrio et al. [25]. Shortly, the endometrium was digested in sterile filtered Hank's buffered salt solution supplemented with 2 mg/ml collagenase II, 2 mg/ml trypsin III (Roche), 4 mg/ml bovine serum albumine, and 0.4 mg/ml DNase I for 90 minutes at 38.5 °C in a shaking bath. Then, cells were filtered through a membrane with a pore size of 80 µm, centrifuged at 250 g for 10 minutes, and washed twice in PBS. To obtain separate stromal and epithelial cell populations, the cell suspension was removed 18 h after plating, which allowed selective attachment of stromal cells. The removed cell suspension was then reseeded and incubated allowing epithelial cells to adhere. Stromal and epithelial cell populations were distinguished by cell morphology.

Both cell lines were cultured in a medium composed of HG-DMEM supplemented with 10% fetal calf serum (FCS), 1% penicillin (100 UI/ml)–streptomycin (100 mg/ml), 0.25 mg/ml amphotericin B and 2 mM L-glutamine. In AMCs culture medium, 10 ng/ml epidermal growth factor (EGF) was also added. Both cell lines were incubated at 38.5 °C in a humidified atmosphere of 5% CO_2, until they reached passage (P) 3.

Conditioned medium, microvesicles and supernatant production

For CM production, cells at P3 at confluence were cultured for 5 days in a serum-free medium. Conditioned media of three samples from each cell line were collected, pooled, centrifuged at 3500 g for 20 min to remove cellular debris. Control medium, no-conditioned medium (no-CM), was generated in the same way as above, except that no cells were cultured in the plates.

A portion of CM *in toto* was stored at -80 °C. To obtain MVs and SN, another portion of CM was ultra-centrifuged (Beckman Coulter Optima L - 100K) at 100,000 g for 1h at 4 °C. SN was collected and stored at – 80 °C for later use. The pellet was washed in serum-free medium 199 containing N-2-hydroxyethylpiperazine-N-2-ethanesulfonic acid (HEPES) 25 mM and submitted to a second ultra-centrifugation under the same conditions. The resulting pellet, composed of MVs, was fractionated for MVs analysis or used for the *in vitro* test.

Measurements of MVs

Size and concentration of MVs were evaluated by Nanosight LM10 instrument (Nanoparticle tracking analysis, NTA, Nano-Sight Ltd., Amesbuty, U.K.), which permits discrimination of microparticles less than 1 µm in diameter. The software (NTA 2.0 analytic software) allows the analysis of video images of particle movement under Brownian motion and the calculation of diffusion coefficient, sphere equivalent and hydrodynamic radius of particles by using the Strokes–Einstein equation. This instrument is equipped with a 405 nm laser and a high-sensitivity sCMOS camera (OrcaFlash2.8, Hamamatsu C11440, NanoSight Ltd). Videos were collected and analysed using the NTA software with the minimal expected particle size, minimum track length and blur setting, all set to automatic. Ambient temperature was recorded manually and did not exceed 25 °C. Five µl of each sample were diluted in sterile physiological solution to a final volume of 1 ml. Samples were analyzed within 15 min of the initial dilution with a delay of 10 seconds between sample introduction and the start of the measurement. For each sample, multiple videos of 30 seconds duration were recorded generating replicate histograms that were averaged.

MVs labeling with PKH-26

To trace MVs *in vitro* by fluorescence microscopy, MVs from AMCs and ECs were labeled with the red fluorescence aliphatic chromophore intercalating into lipid bilayers PKH-26 dye. Briefly, after ultra-centrifugation, the MV pellet was diluted to 1 ml with PKH-26 kit solution and 2 µl of fluorochrome were added to this suspension and incubated for 30 min at 38.5 °C. Thereafter, 7 ml of serum free DMEM were added to the suspension that was ultra-centrifuged again at 100,000 g for 1 h at 4 °C. The final pellet was immediately resuspended in HG-DMEM and cryopreserved with 1% of dimethylsulfoxide at -80 °C.

In vitro embryo production in different IVC media

Collection of oocytes and in vitro maturation (IVM)

Ovaries were collected from slaughtered Holstein-Fresian cows (*bos taurus*) whose age, genealogy, and physiological status were unknown. Ovaries were transported in sterile saline solution (0.9% NaCl) supplemented with 150 mg/l kanamycin and maintained at 30 °C. About 5940 oocytes were used to produce embryos to submit to IVC with different culture system. Oocytes were retrieved by aspiration of 3-5 mm diameter follicles with 18 G needle. Cumulus–oocyte complexes (COCs) were selected and washed tree times in pre-incubated TCM 199-Hepes buffered supplemented with 10% FCS.

IVM was performed for 24 h in TCM 199 Earl's Salt medium supplemented with 10% FCS, 5 μg/ml LH (Lutropin, Vetoquinol, France), 0.5 μg/ml FSH (Folltropin, Vetoquinol) 0.2 mM sodium pyruvate, 5 μl/ml gentamycin and 1 mg/ml estradiol 17β. Cultures were performed in 70 μl droplets (up to 20 oocytes/droplet) of the medium under mineral oil, at 38.5 °C in 5% CO_2.

In vitro fertilization (IVF)

IVF was performed in Tyrode's-albumin-lactate-pyruvate (TALP) medium containing 2 mM penicillamine, 1 mM hypotaurine, 250 mM epinephrine, 20 μg/ml heparin, 114 mM NaCl, 3.2 mM KCl, 0.4 mM NaH2PO4, 10mM sodium lactate, 25mM NaHCO3, 0.5mM MgCl2-6H20, 2.0 mM CaCl2-2H2O, 6mg/ml bovine serum albumin (BSA, Sigma), 5 μl /ml gentamicin, 0.2mM sodium pyruvate. Frozen-thawed semen of only one bull of proved fertility was prepared by Percoll density gradient (Amersham Pharmacia Biotec) (45/90%). Semen was thawed at 37 °C for 30 s, placed on the top of the Percoll gradient and centrifuged for 30 min at 300 g. Semen suspension was diluted in the appropriate volume of fertilization medium to obtain a final concentration of 10^7 spermatozoa per ml. An aliquot of 10 μl of semen was co-incubated with matured oocytes for 18 h at 38.5 °C in 5% CO_2. At the end of gamete co-culture, cumulus cells were completely removed and cumulus-free presumptive zygotes were randomly transferred into different culture system and cultured up to day 7.

In vitro culture (IVC)

The standard medium for IVC was synthetic oviductal fluid with aminoacids (SOFaa) composed of 1.1 M NaCl, 72 mM KCl, 12 mM KH_2PO_4, 7.4 mM $MgSO_4$, 50 mM DL-lactate, 250 mM $NaHCO_3$, 260 mM fenol red, 100 mM sodium pyruvate, 178 mM $CaCl_2$-$2H_2O$, 125 mM Hepes sodium salt, 125 mM Hepes, 30.8 mM glutamine, 500 mM glycine, 84.2 mM alanine, 100X MEM non essential, 100X BME, 2.8 mM Myo-Inositol, 340 mM trisodium citrate, 2% FCS, 0.005 gr/ml BSA, 0.2mM sodium pyruvate, 5 µl/ml gentamicin.

At the beginning of the culture in SOFaa, presumptive zygotes were randomly assigned to a control group (CTR, no supplementation), or to one of the experimental groups in which SOFaa was supplemented with one of the a-cellular extracts on day 1 or 3 or 5. Experimental groups were as follows:

SOFaa supplemented with 20% of CM obtained by AMCs or EDCs (SOF+CM) added on day 1, 3 or 5;

SOFaa supplemented with 20% of no-CM (SOF+ no-CM) added on day 1, 3 or 5;

SOFaa supplementd with 20% of SN obtained by AMCs or EDCs (SOF+SN) added on day 1, 3 or 5;

SOFaa additioned of $100x10^6$ MVs obtained by AMCs or EDCs (SOF+MVs) added on day 1, 3 or 5.

In every culture condition, IVC was performed for 7 days in 5% O_2, 5% CO_2 and 90% N_2 in humidified atmosphere at 38.5 °C. Usually, the half of the medium is renewed on day 3 and 6 during culture period. In this study, to avoid stress to the embryo and to allow the action of secretome, the medium was renewed on day 3 and 5 and these time points (includind day 1 as culture starting) were chosen to add different components of secretoma to SOF.

Evaluation of MVs uptake by blastocysts

To confirm MVs incorporation into blastocyst, a group of IVC embryos was cultured in SOF

supplemented with AMCs- and EDCs-MVs previously stained with PKH-26. A dose–response curve was studied with different concentration of MVs (10-20-40-60-80-100-150 $x10^6$ MVs/ml). On day 7, blastocysts were stained with Hoechst 33343 (10 µg/mL) and MVs incorporation was evaluated under fluorescent microscopy BX71 (Olympus). Labeled MVs were excited at 550 nm while emission wavelength was set at 567 nm. Hoechst 33342 dye was excited at 353-365 nm while the emission wavelength was set at 460 nm. In addition, confocal microscopy analysis to assess internalization of MVs was performed using a Leica SP2 laser scanning confocal microscope (Leica Microsystems Srl, Italy) equipped with a PL Fluotar 20x AN 0.5 Dry objective.

Blastocyst production rate and viability evaluation

On day 7, embryos of control and experimental groups were counted out of the initial oocytes, for the evaluation of blastocyst rate. A portion of the blastocyst was used for the analysis of viability, which was assessed by Hoechst 33342 and propidium iodide staining. Blastocyst were retrieved from the IVC drops, washed with PBS supplemented with 2% BSA and incubated with Hoechst 33342 (10 µg/ml) and propidium iodide (1 µg/ml) for 15 min at 38.5 °C. Then, they were observed under fluorescent Olympus BX51 microscope at a magnification of 40x, analyzing the images with Image-Pro Plus 5.1-Media Cybernetics software. Hoechst 33342 dye was excited at 353-365 nm while the emission wavelength was set at 460 nm. Propidium iodide was excited at 535 nm while the emission wavelength was set at 617 nm.

Differential staining

Another portion of the cultured embryos of control and experimental groups was used for differential staining. The latter was performed with propidium iodide and Hoechst 33342 after disrupting the membrane integrity of the surface trophectoderm cells with detergent (Triton X-100), which permits penetration of propidium iodide into the trophectoderm cells, but not into the inner cell mass cells. Since all the cells were stained with Hoechst 33342, in this way, the inner cell mass

(ICM) stained blue and the trophectoderm purple. The staining was performed according to Thouas et al. [26] with some modifications. Briefly, prior to differential staining, embryo were washed in PBS supplemented with 5% FCS, then were permeabilised for 30 seconds in PBS containing 0.04% Triton X-100 and 0.1 mg/ml of propidium iodide. After that, embryos were staining with 10 µg/ml of Hoechst for 15 min at 38.5 °C and mounted on a glass slide in a small drop of PBS. Four small pillars of wax were applied and a cover glass was laid over the drop applying a suitable pressure to visualize cell for counting. Cell counting was performed from digital photographs obtained by a fluorescent Olympus BX51 microscope at a magnification of 40x at the wavelength previously described. The images were analysed, using Image Pro-Plus software, by a single operator in a blinded manner.

Gene expression assessment in IVP bovine embryos on day 5 of treatment

Genes involved in apoptosis (*BAX;* Bcl-2–associated X protein) and reactive oxygen species (ROS) protection (*GPX1;* glutathione peroxidase 1) were analyzed by reverse transcription-quantitative PCR (RT-qPCR) in embryos treated on day 5 with CM, MVs, and SN of both cell lines. The mRNA expression levels of all genes were measured in three samples (biological replicates). Fifteen blastocyst for each group on day 7 of culture were collected, washed in sterile PBS and immediately placed in sterile RNAse DNAse–free eppendorf tubes. Samples were kept at -80 °C until RNA extraction. RNA extraction was performed using Trizol and the concentration of RNAs were evaluated three times using a NanoDrop ND-1000 spectrophotometer (NanoDrop Technologies, Wilmington, DE, USA). RNAs quality was checked using the Agilent Bioanalyser 2100 (Agilent, Santa Clara, CA). RT-PCRs were performed with the High Capacity cDNA Reverse Trascription Kit (Applied Biosystems/Life Technologies, Carlsbad, CA, USA) using 100 ng of RNA per reaction. All the qPCR experiments were run in triplicates (technical replicates) using the qPCR protocol described by TaqMan Fast Gene Expression Assays (Life Tecnologies™) on 7500 Fast Real-time PCR System instrument (Applied Biosystems by Life Technologies™). To assess gene

317 expression, each target gene and the *GAPDH*, as the housekeeping control gene, were co-amplified.
318 Conditions of amplifications were an initial step of 95 °C (3 minutes), followed by 40 cycles of 95
319 °C (30 seconds), 60 °C (30 seconds), and 72 °C (20 seconds), followed by the acquisition of the
320 melting curve (fluorescence acquisition every 0.5 °C). PCR efficiencies were tested and found to be
321 close to 1. Efficiency of amplification for each primer was monitored through the analysis of serial
322 dilution. Additional dissociation curve analysis was performed and in all cases showed a single
323 peak.
324 Average target gene threshold cycle (ΔCt_g) for each sample (calculated using the CT values of the
325 technical replicates within each experimental conditions), were normalised to the average GAPDH
326 values (ΔCt_{GAPDH}) of the same cDNA sample. Then, the expression variations calculated were
327 normalized to internal control (i.e. CTR) using the ΔΔCt method. Finally, the fold change
328 expression of each gene was calculated as $2^{-\Delta\Delta CT}$ [27] Primers from each gene were designed using
329 Primer3 web interface (www. primer3plus.com). The assay primers were available and synthesized
330 by Life technologies™.
331 **BAX:** Forward AGAGGATGATCGCAGCTGTGGA;
332 Reverse CAAAGATGGTCACTGTCTGCCATGT; (bp = 300); Gene Bank access NM_173894.1
333 **GPX1**: Forward GCAACCAGTTTGGGCATCA; Reverse CTCGCACTTTTCGAAGAGCATA;
334 (bp = 116); Gene Bank access NM_174076.3.
335
336 **Statistical analysis**
337 Development on day 7 was assessed using Chi-square test. Cell counts were compared using one-
338 way ANOVA and the non-parametric Kruskall-Wallis test with Dunn's pairwise multiple
339 comparison.
340 For quantitative PCR expression, Kruskal–Wallis and Mann–Whitney nonparametric tests were
341 performed to analyze relative mRNA abundance. Differences were considered statistically
342 significant at the 95% confidence level and $P<0.05$. Data were analyzed with GraphPad Instat 3.00

for Windows (GraphPad software, Inc. La Jolla, CA, USA).

RESULTS

Cell isolation

Cells were selected purely on their ability to adhere to plastic. The initial viability of EDCs and AMCs was >90%. EDCs and AMCs show typical polygonal epithelial morphology (Figure 1 A,B). Previous molecular biological analyses on AMCs at P3 showed that these cells display a typical stem cell phenotype, with the expression of markers, such as CD29, CD44, CD106, CD105, and MHCI, but not CD34 and MHCII, as reported by Corradetti et al. [24].

Previously molecular biology study on EDCs confirmed their endometrial nature due to the expression of *ER-A*, *ER-B*, *PR* and *TP53* [28].

MVs identification and uptake in bovine blastocyst

The 100,000 g fractions isolated in this study measured using Nanosight Instruments, showed a major peak in each preparation between 226-363 nm for EDCs (Fig 2A) and 220-295 for AMCs (Fig 2B). NanoSight analysis determined that amniotic MVs had a dimension between 50 nm and 670 nm, with a mean of 258±55 nm. Considering the seeding density and the amount of MVs obtained it possible to speculate that AMCs produced about 800 to 4700 MVs/cell, with a mean of 2550±71 MVs/cell, corresponding to $540x10^6$ MVs/ml of CM. Endometrial cell instead produced MVs with a dimension between 199 nm and 337 nm with a mean of 238±40 nm. Endometrial cells produced about 2762 to 3414 MVs/cell with a mean of 3166±329 MVs/cell, corresponding to $670x10^6$ MVs/ml of CM.

Fluorescent microscope analysis demonstrated that both amniotic and endometrial MVs were internalized into blastomeres. Blastomers nuclei were stained in blue by Hoechst 33342 (Fig 3A) and MVs in red by PKH-26 (Fig 3B). MVs incorporation is better evaluable by the merging of blue and red images (Fig 3C). A dose–response curve showed that the concentration of $100x10^6$ MVs/ml

provided the more intense fluorescence signal (data not shown). We calculated that $100x10^6$ MVs are present in about 20% of CM of both cell lines and, for this reason, SOF was supplemented with 20% of CM or SN.

As seen by confocal microscopy, after incubation with labeled MVs, blastomeres showed a fine granular fluorescent pattern within their cytoplasm at the same plane of nuclei, indicating incorporation of MVs (Figure 3D).

Blastocyst rate

A total of 2820 oocytes were fertilized over the course of this experiment that consisted of three replicates.

Embryo morphology was evaluated on day 7 after fertilization under a stereomicroscope (Leica) and the embryos were grouped according to stage (morula, compact morula and blastocyst). Poor quality morulas/compact morulas were classified as degenerate if there was loss of plasma membrane integrity (lysis) and/or generalized loss of cell forms.

Blastocyst rate obtained from the different fractions of secretome are showed in Fig 4. In CTR, blastocyst rate was 35.45±2.53%.

The use of no-CM (control medium) on different days did not provide blastocyst.

CM and SN of both cell lines on day 1 did not provide blastocysts. Amniotic and endometrial MVs on day 1 gave 24.24±2.75% and 26.19±2.82% of blastocysts, respectively, that were not statistically different ($P>0.05$) between them but different ($P<0.05$) compared to the CTR.

On day 3, CM and MVs, but not SN, of both cell lines provided embryos. Only amniotic MVs gave a rate comparable to CTR, while the other experimental conditions provided lower results statistically different ($P<0.05$) compared to CTR.

On day 5, amniotic CM and MVs provided respectively 34.17±3.29% and 34.85±3.66% of blastocyst, without statistical difference ($P<0.05$) between them and CTR. The 25.80±2.83% rate obtained by amniotic SN on day 5 was statistically lower ($P<0.05$) than the other groups previously

395 described. All the blastocyst rates obtained by endometrial CM, SN or MVs used on day 5 were
396 statistically lower than amniotic secretome and CTR (21.69±1.87, 13.70±2.05 and 29.27±2.44%,
397 respectively).
398
399 **Embryo viability evaluation**
400 Results of embryo viability by different fractions of secretome are showed in Fig 5. The Fig. 6 A,B
401 point out an embryo on day 7 and the corresponding viability staining.
402 The rate of blastomeres viability in CTR was 92.36±4.48%.
403 Almost all experimental conditions that gave embryos provided a rate of viability not statistically
404 different ($P<0.05$) compared to the CTR. Three conditions, namely endometrial CM added on day
405 3, (83.61±5.18), endometrial SN added on day 5 (84.29±2.71) and endometrial MVs added on day
406 5 (85.98±2.77) provided statistically significant lower values of vitality compared to CTR. The only
407 treatments that gave a statistically significant ($P<0.05$) higher rate of viable blastomeres than the
408 CTR were amniotic CM and MVs added on day 5 (99.4±4.83and 98.56±3.27% respectively).
409
410 **Embryo quality evaluation**
411 Results of embryo quality by different fractions of secretome are showed in Table 1, 2, 3. The Fig. 6
412 C shows the differential staining in an embryo on day 7, while the Fig 7 display the number of ICM.
413 The rate of ICM/trophoblast in CTR was 29.65±2.03.
414 When blastocysts were differentially stained to permit the cell counting of inner cell mass and
415 trophectoderm, the rate of ICM/trophoblast was statistically similar ($P>0.05$) to CTR for all the
416 experimental condition with two exceptions. Namely, amniotic and endometrial MVs, added on day
417 1, gave a lower rate ($P<0.05$) than the CTR, while amniotic CM and MVs added on day 5, provided
418 a quality of embryos that was statistically better ($P<0.05$) than the control and the other groups. This
419 increase is due to the statistically higher number ($P<0.05$) of ICM cells of the amniotic CM and
420 MVs treated embryos compared to the CTR (33.66±1.93 and 34.42±1.27 vs 27.6±1.44,

respectively). On the contrary, the number of trophoblast cell in these experimental conditions was similar.

Table 1: Effect of conditioned medium secreted by amniotic or endometrial cells on embryo quality evaluated by differential staining

Conditioned media (CM)	**day**	**Differential staining**			
		Total cells	**Inner cell mass**	**Troph**	**Ratio ICM:troph**
SOF (CTR)		120.69±5.43	27.6±1.44[a]	93.09±5.62	29.65±2.03[a]
SOF + no-CM	1	-	-	-	-
SOF + no-CM	3	-	-	-	-
SOF + no-CM	5	-	-	-	-
SOF + CM-AMCs	1	-	-	-	-
SOF + CM-AMCs	3	115.43±8.82	25.6±2.72[a]	86.12±4.55	29.75±3.46[a]
SOF + CM-AMCs	5	128.66±3.52	32.4±1.83[b]	96.26±5.82	33.66±1.93[b]
SOF + CM-EDCs	1	-	-	-	-
SOF + CM-EDCs	3	101.66±7.55	20.82±2.98[c]	76.44±8.37	26.7±5.67[b]
SOF + CM-EDCs	5	102.91±3.58	25.41±1.03[a]	87.5±7.54	29.04±2.88[a]

Different small letters superscripts (a,b,c) indicate statistically different comparisons ($P<0.05$).

Table 2: Effect of supernatant secreted by amniotic or endometrial cells on embryo quality evaluated by differential staining

Supernatant (SN)	day	Total cells	Differential staining		
			Inner cell mass	Troph	Ratio ICM:troph
SOF (CTR)		120.69±5.43	27.6±1.44[a]	93.09±5.62	29.65±2.03[a]
SOF + SN-AMCs	1	-	-	-	-
SOF + SN-AMCs	3	-	-	-	-
SOF + SN-AMCs	5	105.54±2.51	22.33±2.58[b]	83.21±5.86	26.84±2.89[b]
SOF + SN-EDCs	1	-	-	-	-
SOF + SN-EDCs	3	-	-	-	-
SOF + SN-EDCs	5	98.98±2.26	20.29±1.17[b]	78.69±5.56	25.78±2.83[b]

Different small letters superscripts (a,b,c) indicate statistically different comparisons (P<0.05).

Table 3: Effect of microvesicles secreted by amniotic or endometrial cells on embryo quality evaluated by differential staining

Microvesicles (MVs)	day	Total cells	Differential staining		
			Inner cell mass	Troph	Ratio ICM:troph
SOF (CTR)		120.69±5.43	27.6±1.44 [a]	93.09±5.62	29.65±2.03[a]
SOF + MVs-AMCs	1	108.15±8.49	20.87±1.64 [b]	87.28±3.23	23.91±2.41[b]
SOF + MVs-AMCs	3	107.83±8.41	25.71±2.16 [a]	82.12±4.37	31.31±3.33[a]
SOF + MVs-AMCs	5	132.98±8.42	34.42±1.27 [c]	98.56±4.66	34.92±2.98[c]
SOF + MVs-EDCs	1	115.72±7.55	23.92±2.66 [a]	91.78±3.95	26.06±2.37[a]
SOF + MVs-EDCs	3	105.77±8.57	20.98±1.14 [b]	84.79±6.12	24.74±2.85[b]
SOF + MVs-EDCs	5	104.42±7.21	23.18±2.83 [a]	81.22±6.65	28.54±2.51[a]

Different small letters superscripts (a,b,c) indicate statistically different comparisons (P<0.05).

Embryo gene expression

Regarding gene related to apoptosis, *BAX* was significantly (P<0.05) downregulated in groups treated with CM and MVs secreted by AMCs (0.5±0.12 and 0.5±0.13, respectively) but up-regulated with SN of both cell lines compared to CTR group (P<0.05, Fig 8A). *GPX1* (Fig 8B), was significantly upregulated (P<0.05) for treatments with CM and MVs secreted by AMCs compared to CTR group (3.2±0.27 and 4.0±0.37). *GPX1* expression in AMC-MVs was statistically different (P<0.05) compared to AMC-CM.

DISCUSSION

As already stated, IVP embryos have a lower development, a lower number of blastomeres and a higher apoptosis rate compared to the ones produced *in vivo* in various animal species [29-31]. In addition, it is known that their implantation rate after transfer is low [32-34].

To date, to improve embryo quality, the *in vitro* blastocysts production is still based on using feeder cells, mainly oviduct and uterine epithelia cells, to mimic *in vivo* conditions. This suggests that paracrine or autocrine trafficking between helper cells and embryos is present. Many growth factors, receptors and binding proteins are secreted into the culture medium by helpers cells [35,36] and the potential of these medium, called CM, is already known for a long time. Ijaz et al. [37] and Zhu et al. [38] defined the CM as a complex matrix of secreted products from cells, in particular growth factors, cytokines and glycoproteins that may influence the development of early embryos pre-implantation. Some experiments have shown that the use of CM provides embryo developmental rates similar to those obtained in the co-culture systems [39-41], with the benefit of not having animal cells in the embryo culture. To date, the effect of all components of CM on *in vitro* embryo development has not been investigated. Lopera-Vásquez et al. [42] evaluated the effect of conditioned media (CM) and extracellular vesicles (EVs) derived from bovine oviduct epithelial cell but they did not studied the effect of soluble factors (SN) only and the incorporation of MVs inside the blastomeres. Since the embryo interacts with the uterus for implantation and with

509 the placenta, this study investigated the effect of different components of endometrial and amniotic
510 cell secretome on the IVP embryos development.
511 Endometrial cells were isolated at early luteal face (day 4-8, considering day 0 = estrus) because
512 only in this case these cells are in contact with the early embryo *in vivo* up to the blastocyst stage.
513 The amnion was chosen because Lange-Consiglio et al. [43] used the monolayer of equine amniotic
514 epithelial cells as feeder to culture bovine embryos with good results, in term of blastocyst rate,
515 compared to the bone marrow derived cells and control cells, represented by monolayer of cumulus
516 cells. These authors suggested that EGF, produced by monolayer of amniotic epithelial cells, could
517 have been one of most representative candidate to play a positive role in the embryonic
518 development as it happens *in vivo* for the endometrium. Indeed, EGF is produced *in vivo* by
519 endometrial cells and the embryo possesses receptors for it. In this context, in our study, the
520 amniotic cells were further investigated and compared to endometrial cells through the effect of
521 their secretoma
522 In this study, at first, we identified the presence of MVs in CM produced by both amniotic and
523 endometrial cell culture. By their size it is possible to classify these MVs as shedding vesicles, also
524 known as ectosomes or microparticles, that originate from direct budding and 'blebbing' of the
525 plasma membrane. These shedding vesicles are different from exosomes that arise from the cell
526 membrane endosomal compartment and are released into the extracellular space after fusion of
527 multivesicular bodies with the plasma membrane. Exosomes tend to be homogeneous in size (30-
528 120 nm) while shedding vesicles are more heterogeneous (ranging from 100 nm to 1 μm). MVs
529 found in amniotic and endometrial CM are similar in size (258±55 nm for AMCs and 238±40 nm
530 for EDCs) even if, in the same culture conditions and density of seeding, the EDCs produced more
531 MVs than AMCs ($670x10^6$ MVs/ml vs $540x10^6$ MVs/ml). Obviously, these data refer to *in vitro*
532 study and no information about their production in *in vivo* conditions are available.
533 In this study, at first, the control medium (no-CM) was tested to verify that components of the
534 original medium used to culture had no effect on *in vitro* embryo production. No embryos were

obtained, probably for dilution of SOF with medium no containing growth factors.

After that, the CM *in toto* and its different components, MVs and SN, were used on different days during the embryo culture to study the temporal effect, considering the changing nutritional requirements of the embryo during its development.

The results of our study suggest that the exposition of bovine embryos at different time of culture to the various fractions of secretome of both cell lines provide dissimilar rates of blastocysts. Among the different experimental conditions, the best results were obtained when supplementation started on day 5, corresponding also, in the case of amniotic CM and MVs, to the better culture conditions for embryo quality. Indeed, this condition did not improve the blastocyst rate compared to the CTR but enhanced the quality of embryos as observed by the increase of ICM/trophoblast rate and by the rate of blastomere vitality. In all the other conditions, the rate of blastocysts was lower than CTR and, mostly, all the results obtained by endometrial CM, SN or MVs used on day 5 were lower than those obtained by amniotic secretome and CTR groups. In almost all the experimental conditions that reduced the total number of cells, or that of the inner mass cells, a decrease in embryo viability was noted. Moreover, the data obtained by addition of amniotic CM *in toto* or MVs were equivalent while blastocysts number and quality provided by SN were always scarce or insignificant.

These data were confirmed by gene expression evaluation performed on day five of treatment. Studies are still not completely in accordance regarding the set of genes capable of reflecting accurately the effect of different culture conditions on embryo quality [44]. Therefore, we selected two genes related to apoptosis and ROS protection, respectively. Melka et al. [45] reported that *Bax* pro-apoptotic gene expression could be a potential quality marker as they found an upregulation of this gene in poor quality 4-cell preimplantation embryos with a higher DNA fragmentation, compared with morphologically good quality embryos at the same stage. Our study, indeed, found a downregulation of this gene in groups treated by CM and MVs secreted by AMCs compared to CTR group ($P<0.05$) and up-regulation in groups treated by SN of both cell lines.

Because embryo protection against oxidative stress relies on the activity of certain antioxidant

enzymes [46], we have evaluated mRNA expression of *GPX1* gene to investigate the effect of different components of secretome on embryo defense mechanisms against ROS. GPX1 deficiencies can have an effect on the cells, making them more susceptible to possible stressors leading to an increase in apoptosis. In accordance with this study, our CTR group has less abundant *GPX1* mRNA compared to groups treated by CM and MVs secreted by AMCs, suggesting its susceptibility to ROS damage. Moreover, the expression of *GPX1* in amniotic MVs is higher compared to amniotic CM

The reasons of the good result on day 5 of supplementation are not clear, and can only be hypothesized. The beginning of the activation of the genome takes place, in the bovine, between the 8 and 16 cell stage, corresponding, to the embryonic stage attained, in *vitro*, between day 2 and 4 of culture. The embryo at this stage may be more susceptible to the influence of culture conditions compared to other developmental stages [47]. Environmental changes at this stage could unsettle the activation of the embryonic genome and this would explain why amniotic and endometrial secretome have not favored embryonic development. On the contrary, the supplementations on the 5^{th} day increased the development of blastocysts. Moreover, probably as in the mouse, two periods, during which embryos are more responsive to the culture conditions, are recognized which coincide with the time elapsing between 48 and 72 hours, and between 72 and 120 hours [47]. Furthermore, day 5 mimics the time of the bovine embryo entrance into the uterus following fertilization and this would confirm the positive results obtained by supplementation on day 5. It is important to underline that amniotic secretome appears more suitable than the endometrial one. This might indicate that the amniotic and endometrial secretome contain different components and that these differences cause different degrees of development. At this stage of the experiment we did not investigated the composition of secretome but it is known that CM contain many factors secreted by the somatic cells. Indeed, some studies have shown that many factors, such as EGF, PDGF, LIF, IL6, IL1, bFGF, VEGF [39,48,49], and embryotrofic factors [47] are secreted from the cells in co-culture and, therefore, are consequently also present in the CM. Up to our knowledge, as indicated

587 in the present study, it is our believe that soluble factors should not be called up for the better
588 embryo development compared to CTR, because we do not obtained the same results by the use of
589 SN that is only constituted by soluble factors. As a matter of fact, MVs were able to produce best
590 results when, added either alone or as components of CM *in toto,* while the only soluble factors in
591 CM deprived of MVs did not provide positive results. Moreover, our study evidenced the ability of
592 embryos to uptake labeled MVs and this could suggests that there may be a mechanism of transfer
593 of the MVs contents within the blastomeres.
594 To date, no works in the literature relating to the incorporation of MVs of any origin into the
595 blastocyst have been traced. A question of particular interest relates to what kind of molecules
596 contained in MVs is involved in this communication. Recently, several studies have focused on
597 miRNAs. These small non-coding RNA molecules are present in many biological fluids such as in
598 follicular fluid or culture media [50]. While total miRNAs in human biofluids or supernatants from
599 cell cultures may be released from apoptotic cells or cell debris, MVs miRNAs are actively released
600 by viable cells and are expected to represent an active means of communication between cells and
601 tissues locally or systemically. MV-encapsulated miRNAs, in particular, are shielded from
602 degradation and are remarkably stable in biological fluids. Specifically, miRNAs that are
603 encapsulated by MVs might have a different role compared with miRNAs in biofluids as they
604 transfer biological information to recipient cells [51].
605 Certainly, amniotic MVs induced improvement of embryo quality, compared to endometrial MVs,
606 by transfer of specific amniotic progenitor cell signals or material. At this stage, we could not
607 investigate the different expression profile of miRNAs between amniotic and endometrial MVs. In
608 our study, we can only see their functional influence on embryo development. MiRNAs play an
609 essential regulatory role during development, indeed, aberration of blastocyst miRNA expression is
610 associated with human infertility [52]. It could be that miRNAs, transferred by MVs route within
611 the blastocyst, contribute to the miRNA content of the blastocyst itself promoting their development
612 and quality. Moreover, it is likely that amniotic secretome promote embryo development in a more

physiological way than endometrial one, but further experiments are planned to better explain these data and to better understand MVs cargo of both cell lines.

In conclusion, it is known that co-culture systems improved the *in vitro* development of embryos, but after our results, we suggest that in this system, probably, MVs along with their miRNA contents are involved in this effect. Indeed, the present study demonstrated that the brief *in vitro* exposition of embryo to amniotic CM and MVs, but not to soluble factors (SN), improved embryo quality. Blastocyst rate from IVP is essential and, in this study, culture with amniotic MVs gave similar rate to CTR. On the other hand, it is mandatory that IVP embryos at the blastocyst stage should be of the highest possible quality to ensure optimal pregnancy rates after transfer, especially after freezing and thawing. Amniotic MVs induced increase of ICM and changes in the profile of expression of some genes known to be related to embryo quality, suggesting reduced apoptosis and increased capacity to struggle against oxidative stress. Once that relevant miRNAs and functional targets will identified, a possible clinical use for these molecules will represent the next front line and may lead to novel strategies for better enhancing or manipulating reproductive efficiency. Moreover, this study may provide a useful starting point for further studies related to paracrine mechanisms of communications between embryo and culture medium.

ACKNOWLEDGEMENTS

The authors wish to thank Dott.ssa Maria Chiara Deregibus and Prof. Giovanni Camussi (Department of Internal Medicine and Molecular Biotechnology Center, University of Torino, Torino, Italy) for their skilled assistance in Nanosight instrument use, and Dott.ssa Miriam Ascagni (Department of Biology, Università degli Studi di Milano, Milano, Italy) for her skilled assistance in confocal microscopy.

Authors wish to thank Vetoquinol for providing the Lutropin used in the IVM protocol.

AUTHORS' CONTRIBUTIONS

ALC conceived the study, carried out the isolation, culture and expansion of amniotic and endometrial cells, prepared the conditioned medium, performed the statistical analysis, coordinated the experiments and draft the manuscript.

CP participated in isolation of amniotic and endometrial cells and in the preparation of conditioned medium. Moreover, CP carried out the isolation and labeled of MVs, and performed molecular studies. PE and DC participated in the *in vitro* embryo production. ST carried out the count of viability evaluation and differential. FC conceived the study, collected amnion at delivery and critically read the manuscript. All authors have read and approved the final manuscript.

AUTHOR DISCLOSURE STATEMENT

The authors declare that no competing financial interests exist in relation to this manuscript.

REFERENCES

1. Wrenzycki C, Stinshoff H. Maturation environment and impact on subsequent development al competence of bovine oocytes. Reprod Domest Anim. 2013;48(Suppl 1): 38-43.
2. Lucas E. Epigenetic effects on the embryo as a result of periconceptional environment and assisted reproduction technology. Reprod BioMed Online. 2013;27: 477-485.
3. Ventura‐Junca P, Irarrázaval I, Rolle AJ, Gutiérrez JI, Moreno RD, Santos MJ. In vitro fertilization (IVF) in mammals: epigenetic and developmental alterations. Scientific and bioethical implications for IVF in humans. Biol Res. 2015;48: 68.
4. Abe H, Yamashita S, Satoh T, Hoshi H. Accumulation of cytoplasmic lipid droplets in bovine embryos and cryotolerance of embryos developed in different culture systems using serum-free or serumcontaining media. Mol Reprod Dev. 2002;61: 57-66.
5. Rizos D, Ward F, Duffy P, Boland MP, Lonergan P. Consequences of bovine oocyte maturation, fertilization or early embryo development in vitro versus in vivo: implications for blastocyst yield and blastocyst quality. Mol Reprod Dev. 2002;61: 234-248.

665 6. Gardner DK, Lane M. Ex vivo early embryo development and effects on gene expression and
666 imprinting. Reprod Fertil Dev. 2005;17: 361-370.
667 7. Rizos D, Gutierrez-Adan A, Perez-Garnelo S, de la Fuente J, Boland MP, Lonergan P. Bovine
668 embryo culture in the presence or absence of serum: implications for blastocyst development,
669 cryotolerance, and messenger RNA expression. Biol Reprod. 2003;68: 236-243.
670 8. Costa Pereira D, Nunes Dodeb MA, Rumpf R. Evaluation of different culture systems on the in
671 vitro production of bovine embryos. Theriogenology. 2005;63: 1131-1141.
672 9. Lonergan P, Fair T, Corcoran D, Evans ACO. Effect of culture environment on gene expression
673 and developmental characteristics in IVF-derived embryos. Theriogenology. 2006;65: 137-152.
674 10. Schmaltz-Panneau B, Locatelli Y, Uzbekova S, Perreau C, Mermillod P. Bovine oviduct
675 epithelial cells dedifferentiate partly in culture, while maintaining their ability to improve early
676 embryo development rate and quality. Reprod Domest Anim. 2015;50(5): 719-729.
677 11. Fazeli A. Maternal communication with gametes and embryos. Theriogenology. 2008;70: 1182-
678 1187.
679 12. Robertson SA, Chin PY, Glynn DJ, Thompson JG. Peri-conceptual cytokines—setting the
680 trajectory for embryo implantation, pregnancy and beyond. Am J Reprod Immunol.
681 2011;66(Suppl 1): 2-10.
682 13. Rottmayer R, Ulbrich SE, Kölle S, Prelle K, Neumueller C, Sinowatz F et al. A bovine oviduct
683 epithelial cell suspension culture system suitable for studying embryo-maternal interactions:
684 morphological and functional characterization. Reproduction. 2006;132: 637-648.
685 14. Thatcher WW, Guzeloglu A, Mattos R, Binelli M, Hansen TR, Pru JK. Uterine-conceptus
686 interactions and reproductive failure in cattle. Theriogenology. 2001;56: 1435-1450.
687 15. White KL, Hehnke K, Rickords LF, Southern LL, Thompson Jr DL, Wood TC. Early embryonic
688 development in vitro by co-culture with oviductal epithelial cells in pigs. Biol Reprod. 1989;41:
689 425-430.
690 16. Rexroad Jr CE, Powell AM. Development of ovine embryos co-cultured on oviductal cells,

691 embryonic fibroblasts, or STO cell monolayers. Biol Reprod. 1993;49: 789-793.
692 17. Park JS, Han YM, Lee CS, Kim SJ, Kim YH, Lee KJ et al. Improved development of DNA-
693 injected bovine embryos co-cultured with mouse embryonic fibroblast cells. Anim Reprod Sci.
694 2000;59: 13-22.
695 18. Li X, Morris LHA, Allen WR. Influence of coculture during maturation on the developmental
696 potential of equine oocytes fertilized by intracytoplasmic sperm injection (ICSI). Reproduction.
697 2001;121: 925-932.
698 19. Rieger D, Grisart B, Semple E, Van Langendonckt A, Betteridge K, Dessy F. Comparison of the
699 effects of oviductal cell co-culture and oviductal cell-conditioned medium on the development
700 and metabolic activity of cattle embryos. J Reprod Infertil. 1995;105(1): 91-98.
701 20. Thery C, Ostrowski M, Segura E. Membrane vesicles as conveyors of immune responses. Nat
702 Rev Immunol. 2009;9: 581-593.
703 21. Zhang M, Ouyang H, Xia G. The signal pathway of gonadotrophins-induced mammalian oocyte
704 meiotic resumption. Mol Hum Reprod. 2009;15: 399-409.
705 22. Raposo G, Stoorvogel W. Extracellular vesicles: exosomes, microvesicles, and friends. J Cell
706 Biol. 2013;200: 373-383.
707 23. Burns G, Brooks K, Wildung M, Navakanitworakul R, Christenson LK, Spencer TE.
708 Extracellular vesicles in luminal fluid of the ovine uterus. PLoS One. 2014;9: e90913.
709 24. Corradetti B, Meucci A, Bizzaro D, Cremonesi F, Lange Consiglio A. Mesenchymal stem cells
710 from amnion and amniotic fluid in bovine. Reproduction. 2013;14: 391-400.
711 25. Donofrio G, Franceschi V, Capocefalo A, Cavirani S, Sheldon IM. Bovine endometrial stromal
712 cells display osteogenic properties. Reprod Biol Endocrinol. 2008;6: 65-73.
713 26. Thouas GA, Korfiatis NA, French AJ, Jones GM, Trounson AO. Simplified technique for
714 differential staining of inner cell mass and trophectoderm cells of mouse and bovine blastocysts.
715 Reprod BioMed Online. 2001;3: 25-29.
716 27. Livak KJ, Schmittgen TD. Analysis of relative gene expression data using realtime quantitative

717 PCR and the 2-ΔΔCT method. Methods. 2001;25: 402-408.
718 28. Marini MG, Perrini C, Esposti P, Corradetti B, Bizzaro D, Riccaboni P et al. Effects of platelet-
719 rich plasma in a model of bovine endometrial inflammation *in vitro* Reprod Biol Endocrinol.
720 2016;14: 58.
721 29. Booth PJ, Holm P, Callesen H. The effect of oxygen tension on porcine embryonic development
722 is dependent on embryo type. Theriogenology. 2005;63: 2040-2052.
723 30. Gjorret JO, Wengle J, Maddox-Hyttel P, King WA. Chronological appearance of apoptosis in
724 bovine embryos reconstructed by somatic cell nuclear transfer from quiescent granulosa cells.
725 Reprod Domest Anim. 2005;40: 210-216.
726 31. Pomar FJ, Teerds KJ, Kidson A, Colenbrander B, Tharasanit T, Aguilar B et al. Differences in
727 the incidence of apoptosis between in vivo and in vitro produced blastocysts of farm animal
728 species: a comparative study. Theriogenology. 2005;63: 2254-2268.
729 32. Kikuchi K, Onishi A, Kashiwazaki N, Iwamoto M, Noguchi J, Kaneko H et al. Successful piglet
730 production after transfer of blastocysts produced by a modified in vitro system. Biol Reprod.
731 2002;66: 1033-1041.
732 33. Berg DK, van Leeuwen J, Beaumont S, Berg M, Pfeffer PL. Embryo loss in cattle between Days
733 7 and 16 of pregnancy. Theriogenology. 2010;15: 250-260.
734 34. Bakri NM, Ibrahim SF, Osman NA, Hasan N, Jaffar FHF, Rahman ZA et al. Embryo apoptosis
735 identification: Oocyte grade or cleavage stage? Saudi J Biol Sci. 2016;23: S50-S55.
736 35. Van Langendonckt A, Vansteenbrugge A, Donnay I, Van Soom A, Berg U, Semple E et al.
737 Three-year results of in vitro production of bovine embryos in serum-poor bovine oviduct
738 conditioned medium. An overview. Reprod Nutr Dev. 1996;36: 493-502.
739 36. Zquierdo D, Villamediana P, Paramio MT. Effect of culture media on embryo development
740 from prepubertal goat IVM-IVF oocytes. Theriogenology. 1999;52: 847-861.
741 37. Ijaz A, Lambert RD, Sirard MA. In vitro cultured bovine granulosa and oviductal cells secrete
742 sperm motility maintaining factor(s). Mol Reprod Dev. 1994;37(1): 54-60.

743 38. Zhu J, Barrat CL, Lippes J, Pacey AA, Cooke ID. The sequential effects of human cervical
744 mucus, oviductal fluid, and follicular fluid on sperm function. Fertil Steril. 1994,61: 1129-1135.
745 39. Kobayashi K, Takagi Y, Satoh T, Hoshi H, Oikawa T. Development of early bovine embryos to
746 the blastocyst stage in serum-free conditioned medium from bovine granulosa cells. In Vitro Cell
747 Dev Biol. 1992;28: 255-259.
748 40. Mermillod P, Vansteenbrugge A, Wils C, Mourmeaux JL, Massip A, Dessy F. Characterization
749 of the embryotrophic activity of exogenous protein-free oviduct-conditioned medium used in
750 culture of cattle embryos. Biol Reprod. 1993;49: 582-587.
751 41. Lee YL, Lee KF, Xu JS, Kwok KL, Luk JM, Lee WM et al. Embryotrophic factor-3 from
752 human oviductal cells affects the messenger RNA expression of mouse blastocyst. Biol Reprod.
753 2003;68: 375-382.
754 42. Lopera-Vásquez R, Hamdi M, Fernandez-Fuertes B, Maillo V, Beltrán-Breña P, Calle A et al..
755 Extracellular vesicles from BOEC in in vitro embryo development and quality. PLoS One.
756 2016;Feb 4,11(2): e0148083.
757 43. Lange-Consiglio A., Maggio V., Pellegrino L., Cremonesi F. Equine bone marrow mesenchymal
758 or amniotic epithelial stem cells as feeder in a model for the in vitro culture of bovine embryos.
759 Zygote. 2010;20: 45-51.
760 44. Cordova A, Perreau C, Uzbekova S, Ponsart C, Locatelli Y, Mermillod P. Development rate and
761 gene expression of IVP bovine embryos cocultured with bovine oviduct epithelial cells at early
762 or late stage of preimplantation development. Theriogenology. 2014;81: 1163-1173.
763 45. Melka MG, Rings F, Holker M, Tholen E, Havlicek V, Besenfelder U et al. Expression of
764 apoptosis regulatory genes and incidence of apoptosis in different morphological quality groups
765 of in vitroproduced bovine pre-implantation embryos. Reprod Domest Anim. 2010;45: 915-921.
766 46. Harvey MB, Arcellana-Panlilio MY, Zhang X, Schultz GA, Watson AJ. Expression of genes
767 encoding antioxidant enzymes in preimplantation mouse and cow embryos and primary bovine
768 oviduct cultures employed for embryo coculture. Biol Reprod. 1995;53: 532-540.

769 47. Xu JS, Cheung TM, Chan STH, Ho PC, Yeung WSB. Temporal effect of human oviductal cell
770 and its derived embryotrophic factors on mouse embryo development. Biol Reprod. 2001;65:
771 1481-1488.
772 48. Baranao RI, Piazza A, Rumi LS, Polak de Fried E. Determination of IL-1 and IL-6 levels in
773 human embryo culture-conditioned media. Am J Reprod Immunol. 1997;37: 191-194.
774 49. Ishiwata I, Tokieda Y, Kiguchi K, Sato K, Ishikawa H. Effects of embryotrophic factors on the
775 embryogenesis and organogenesis of mouse embryos in vitro. Hum Cell. 2000;13: 185–195.
776 50. Rosenbluth EM, Shelton DN, Wells LM, Sparks AET, Van Voorhis BJ. Human embryos secrete
777 microRNAs into culture media—a potential biomarker for implantation. Fertil Steril. 2014;101:
778 1493-1500.
779 51. Machtinger R, Laurent LC, Baccarelli AA. Extracellular vesicles: roles in gamete maturation,
780 fertilization and embryo implantation. Hum Reprod Update. 2016;22: 182-193.
781 52. McCallie B, Schoolcraft W, Katz-Jaffe MG. Aberration of blastocyst microRNA expression is
782 associated with human infertility. Fertil Steril. 2010;93: 2374-2382.

783 **FIGURE LEGENDS**
784

785 **Figure 1.** Cell morphology. Monolayer of epithelial endometrial (A) and amniotic epithelial cells
786 (B). Scale bar = 20µm. Original magnification x20.

787

788 **Figure 2.** Nanosight analysis. Results of MVs purified from endometrial (A) and amniotic epithelial
789 cells (B). The mean size and particle concentration values are calculated by the Nanoparticle
790 Tracking Analysis software that allows the analysis of video images of the particle movement. The
791 curve describes the relationship between particle number distribution (left Y-axis) and particle size
792 (X-axis).

793

794 **Figure 3.** Incorporation of MVs. Representative micrographs of internalization by blastomeres of
795 MVs labeled with PKH-26. Under a fluorescent microscope, the blastomeric nuclei are blue (A) and
796 the MVs are red (B). Merge image (C). Representative z-stack orthogonal projection micrographs
797 showing the internalization of MVs as detected by confocal microscopy in blastocyst co-cultured
798 with MVs for 24 h (D). The images were taken at different plans scanned every 5 µm from top to
799 bottom of the blastocyst.

800

801 **Figure 4.** Graphic representation of effect of secretome produced by amniotic or endometrial cells
802 on blastocyst rate. Different small letters superscripts (a,b,c) indicate statistically different
803 comparisons ($P<0.05$).

804

805 **Figure 5.** Graphic representation of effect of secretome produced by amniotic or endometrial cells
806 on embryo viability. Different small letters superscripts (a,b,c) indicate statistically different
807 comparisons ($P<0.05$).

808

809 **Figure 6.** Evaluation of blastocyst. Blastocyst at 7 day of culture observed at optical microscopy
810 (A). Vitality staining (B) and differential staining (C).
811
812 **Figure 7.** Graphic representation of effect of secretome produced by amniotic or endometrial cells
813 on inner cell mass. Different small letters superscripts (a,b,c) indicate statistically different
814 comparisons ($P<0.05$).
815
816 **Figure 8.** Quantitative PCR analysis for the expression *BAX* and *GPX1* in blastocysts treated on day
817 5 with secretome of both cell lines. Expression levels normalized to the reference gene *GAPDH*.
818 Data are represented as fold-change compared with expression observed in CTR blastocysts. Values
819 are mean ± SD (n=3). Different letters depict significant ($P<0.05$) differences between treatments.

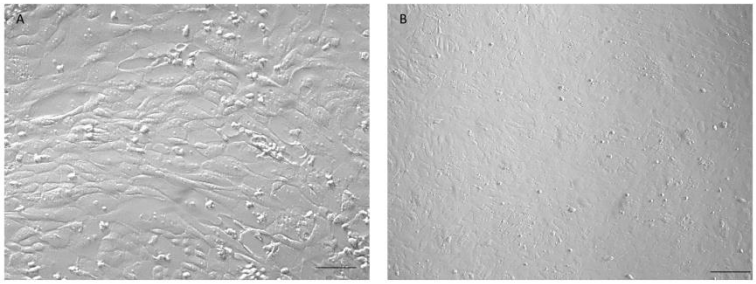

Figure 1

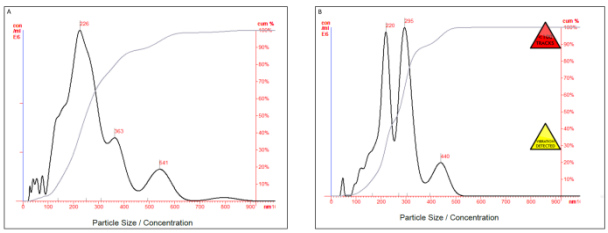

Figure 2

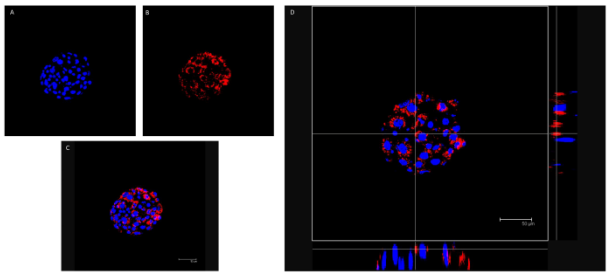

Figure 3

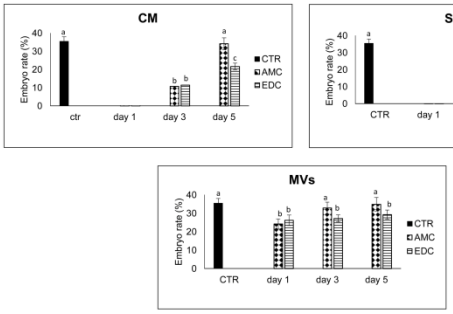

Figure 4

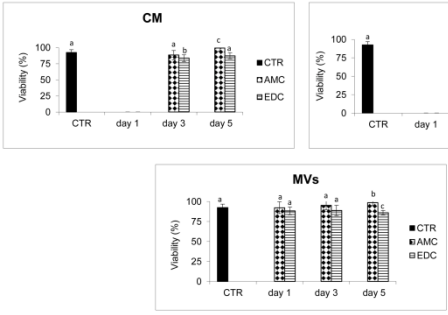

Figure 5

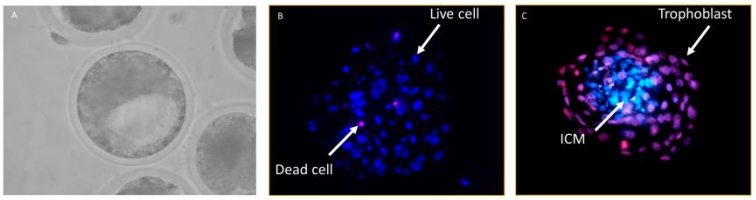

Figure 6

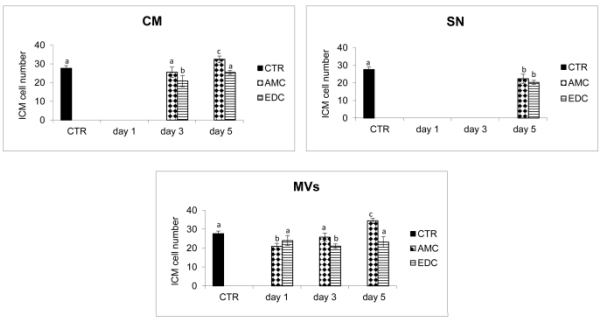

Figure 7

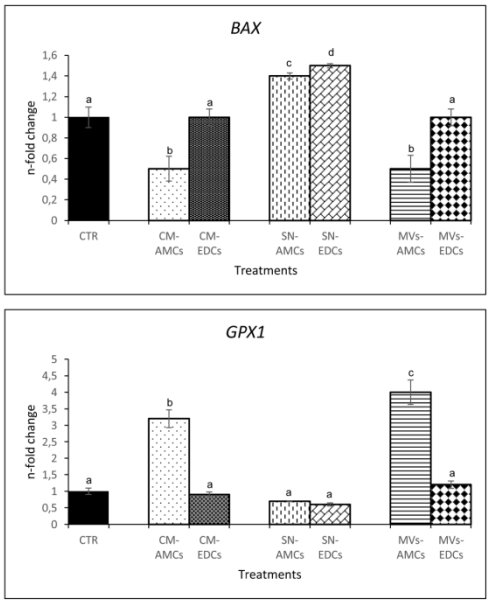

Figure 8

8. DISCUSSIONS

In veterinary, as in human medicine, fetal adnexa have been recently suggested as appealing candidates for the derivation of MSCs to be used in cell-based therapies (Kern et al., 2006; Lange-Consiglio et al., 2012) due to their higher proliferation capacity, longer telomeres, broader differentiation, and extensive proliferative potential in comparison to cells obtained from adult tissues (Lange-Consiglio et al., 2013c). Amniotic mesenchymal cells isolated from the equine amniotic membranes share specific characteristics with embryonic and adult stem cells. They express representative mesenchymal and pluripotent markers, are highly proliferative and retain high plasticity. Taken together, these characteristics make AMCs suitable candidates as tool for regenerative medicine, as previously demonstrated by my research group in the treatments of equine spontaneous tendon lesions (Lange-Consiglio et al., 2012; Lange-Consiglio et al., 2013b).

In the context of paracrine communication between cells, and considering the inhospitable environment of the lesion, due to the presence of inflammation cells and molecules, that lead to a premature cell death of the injected cells (Leung et al., 2006), our previous studies tested the effect of CM in *in vivo* equine spontaneous tendon lesions (Lange-Consiglio et al., 2013a). The results showed the same effect, in term of rate of relapses, compared to the administration of the original stem cells (Lange-Consiglio et al., 2013b). For this reason, in our laboratory, recently, the paracrine effect involving CM and MVs in tendon lesions and other pathologies, or in paracrine mechanism of cell communication, has been subjected to further studies. All data presented in the appended publications provided evidence of the role of the soluble signals produced by AMCs.

At first, we found that AMC-CM promoted *in vitro* EDCs proliferation demonstrating the potential application of this secretome to improve endometrial cell replenishment when low endometrial regenerationis associated to pregnancy failure. The cell-cell contact was not necessary for the action of AMCs on EDCs proliferation and, since cell-derived MVs have been recently described as a new mechanism for cell-to-cell communication (Schorey and Bhatnagar, 2008), we investigated their presence inside the AMC-CM. We found that AMCs secrete MVs, mainly shedding vesicles, and that these MVs are incorporated in both cell lines studied (TNCs and EDCs). An interesting finding is the number of MVs that these cells are capable of secreting. In our experimental conditions, each amniotic cell, plated at a density of $1x10^4$ cells/cm^2, is able to secrete approximately 2.550 MVs, corresponding to about $540x10^6$ particles/mL of CM.

These values are important in the perspective of MVs application in the *in vivo* treatment of diseases.

Moreover, we demonstrate that TNCs and EDCs are *in vitro* target of MVs because these MVs are incorporated in both studied cell lines and their fluorescence signal (after labeling by PKH-26) is visible inside the cells at the same plane of the nucleus. We do not know the mechanism for their internalization by target cells but the hypothesis is that, once internalized, MVs can fuse their membrane with that of endosomes or, alternatively, MVs can remain segregated inside the endosomes and be phagocytized by lysosomes (Cocucci et al., 2007). In any case, their contents is transferred into the cytoplasm of the target cells. We observed the effect of MV cargo on cells stressed by LPS. It is known that the stimulation with LPS leads to a modification of gene expression of various cytokines and interleukins (*TNF-α*, *IL-1β, IL-8,* and *IL-6*) revealing, thus, the ability of LPS to contribute to inflammation during the early acute stages (Vèzina-Audette et al., 2013). In our explorative study, the expression of *TGF-β*, *TNF-α, MMP*-1, *MMP-9* and *MMP-13* genes were investigated for the study on TNCs, whereas *TNF-α*, *IL-6*, *IL-1β*, *MMP-1* and *MMP-13* genes were investigated for endometrial studies. Our results showed that, in TNCs, a concentration of $40x10^6$ MVs/mL downregulates the expression of *MMP-1*, *MMP-9*, *MMP-13*, and *TNF-α* genes, and restores the expression of *TGF-β* that is constitutively expressed by TCs.

Considering that inside target cells the fluorescence signal of labeled MVs was visible only after the 6^{th} hours of incubation, our question was if the time required by the MVs to transfer the signal after their incorporation was enough to counteract the stress effect of LPS. In this context, three different experimental conditions were used for EDCs: 1) LPS and MVs were administered simultaneously, 2) LPS was administered for 3 h and then MVs were added, 3) MVs were administered for 24 h and then LPS was added. Results showed that LPS induced an over-expression of *IL-6* and *TNF-α*, and MVs were able to counteract this action when they were used either simultaneously or 24 h before the action of LPS. MVs added 3 h after LPS were not able to neutralize the action of this stressor. In parallel with gene expression, the release of cytokines studied by ELISA confirmed the observations about gene regulation. Indeed, LPS induced the release of TNF-α and IL-6, whereas, MVs reduced the release of these pro-inflammatory cytokines, both when used simultaneously or 24 h before LPS treatment. In both cases, no contrasting action of MVs was obtained when MVs were added after LPS. In addition, MVs were not able to counteract the action of LPS within the first 3 h, confirming that their

internalization has yet to begin. This seems to indicate that the downregulation of these genes could occur only when the cells are incubated with MVs for enough time to guarantee their necessary incorporation.

Another important aim of our study was to understand the efficacy of MVs on PBMC proliferation inhibition, in order to confirm the presence of paracrine factors as mediators for communication with immune cells. However, compared to the data of Lange-Consiglio et al. (2013a), where equine AMC-CM showed this potential, MVs were not able to inhibit the PBMC proliferation even after their sonication to release their content. Since the whole CM or its SN, composed of soluble factor after removal of MVs, showed this competence, we hypothesize that this ability is imputable to soluble factors and not to molecules contained in MVs. This let us assume that in therapeutic *in vivo* administration of CM for the treatment of spontaneous equine tendon injuries (Lange-Consiglio et al., 2013a), both MVs cargo and soluble factors had contributed to the regenerative effect.

Our results are promising despite the limits just described, that are the time of MVs uptake and the lack of immunomodulatory effect. Our studies were performed in *in vitro* systems which are static and, to confirm or not these data, we need to test the effect of these MVs *in vivo*. Indeed, increasing numbers of reports in human medicine indicate that MVs show therapeutic effects similar to those that can be achieved by the MSCs themselves. Recently, Zhang et al. (2014) elegantly demonstrated that MVs induce recovery from skin burns, promoting skin cell proliferation. Katsuda and Ochiya (2015) investigated the *in vivo* therapeutic potential of MVs using animal models of Alzheimer's disease. These findings, as well as ours, suggest a novel therapeutic strategy using MVs as drugs for future regenerative medicine.

However, MVs and their cargo may play key roles in numerous aspects of biology, including reproduction. Gametogenesis, fertilization, implantation and early embryo development are complex processes that are highly dependent on communication between cells and organs. After the development, embryo migrates into the uterus, and the subsequent adherence of the blastocyst to the endometrial luminal epithelium must occur to result in a successful implantation (Cuman et al., 2014). Detection of MVs in the reproductive biofluids, including plasmastic, seminal, follicular and uterine luminal fluids, points to possible roles of MVs in the intercellular communication necessary for and after the conception. In this context, we tried to study the effect of amniotic and endometrial secretome on *in vitro* embryo production. MVs were able to produce better results when added either alone or as components of CM in toto

during the bovine embryo culture. On the other hand, the soluble factors in CM deprived of MVs, which is SN, did not provide positive results. Moreover, our study evidenced the ability of embryos to uptake labeled MVs and this could suggests that there may be a mechanism of transfer of the MV content within the blastomeres. Surprisingly, amniotic MVs induced improvement of embryo quality but further experiments will be needed to better explain these data.

The main question to explain all our data is "how do MVs act?" One of the most attractive characteristics of MVs is their ability to transfer RNAs (mRNA, miRNA, piRNA) from one cell to another, thereby allowing the transferred RNAs to affect the target cells. Between 2006 and 2007, a sensational finding demonstrated that MV-contained mRNAs could be transferred in recipient cells and translated to proteins (Ratajczak et al., 2006; Valadi et al., 2007). Furthermore, in 2010, MVs were shown to transfer miRNAs between cells, and these miRNAs displayed RNA interference (RNAi) effects in the recipient cells (Pegtel et al., 2010; Kosaka et al., 2010; Zhang et al., 2010). In recent years, MVs containing RNAs have been shown to be transferred from MSCs to injured cells and to contribute to tissue recovery (Katsuda and Ochiya, 2015).

MicroRNAs are also proposed to be key molecules responsible for MSC-MVs-mediated therapeutic potential. For example, miR-335 has been demonstrated to regulate the expression of *TNF-α* and *IL-6* during human adipose cell inflammation (Zhu et al., 2014). MiR-146a has been demonstrated to decrease the expression of *IL-1β* and, as an indirect effect, to suppress the level of *MMP* in intervertebral discs in bovine species (Gu et al., 2015) while miR-26a-2 has been widely studied and it has been correlated with human inflammation, cell proliferation, and apoptosis (Gao and Liu, 2011). In my PhD project, we investigated the presence of these three miRNA and we found their presencein both equine AMCs and their derived MVs. The miRBase tool (http://www.mirbase.org/) confirmed that these miRNAs have predicted targets also in horse inflammation. The downregulation of pro-inflammatory gene expression showed in our studies could be correlated to miRNA transfer from MVs to target cells.

It is important to say that we expanded the miRNAs cargo of equine amniotic cells and their MVs (unpublished data). RNA was extracted from three different samples of AMCs and their respective AMC-MVs using Trizol® and purified by NucleoSpin® miRNA kit. RNA concentration and quality were determined by Agilent 2100. MicroRNA libraries were generated using the TruSeq Small RNA Library Preparation kits. The libraries were pooled and purified on a Pippin

Prep system to recover the fractions containing mature miRNAs. The libraries obtained were quantified by RT-PCR with KAPA Library Quantification Kits. MicroRNA detection and discovery was carried out with Mirdeep2. Equuss caballus miRNAs available at miRBase (http://www.mirbase.org/) were used to accomplish known miRNA detection on the trimmed sequences. The Mirdeep2 quantifier module was used to quantify expression and retrieve counts for the detected miRNAs. Fold change in miRNA expression was calculated based on the normalized mean differences between cells, cells and MVs or between cells and the corresponding MVs. Statistical analysis were performed by using the t test or ANOVA with Newman-Keuls multicomparison test, where appropriate. A p value < 0.05 was considered significant.

Table 1 shows the list of miRNAs presents in the AMC-MVs and their abundancy is referred as the average number of the count of the sequences in three samples.

Table 1. List of all the miRNAs present in AMC-MVs listed in ascending order referring to the average number of counts of the sequences in three samples.

miRNA	Count	miRNA	Count	miRNA	Count
eca-miR-22	299833	eca-miR-130a	2064	eca-miR-107b	464
eca-miR-21	178114	eca-miR-381	1851	eca-miR-148b-3p	445
eca-miR-10b	62999	eca-miR-25	1805	eca-miR-323-3p	436
eca-miR-143	41528	eca-let-7d	1771	eca-miR-451	433
eca-miR-127	30627	eca-miR-23a	1609	eca-miR-1388	432
eca-miR-27b	21340	eca-miR-125b-5p	1482	eca-miR-188-5p	411
eca-miR-24	20906	eca-miR-28-5p	1466	eca-miR-19b	391
eca-miR-26a	17766	eca-miR-432	1425	eca-miR-1379	369
eca-miR-16	15046	eca-miR-423-3p	1378	eca-miR-301a	363
eca-let-7a	14543	eca-miR-146b-5p	1162	eca-miR-193a-3p	352
eca-let-7f	13408	eca-miR-31	1104	eca-miR-370	328
eca-miR-411	10592	eca-let-7g	1101	eca-miR-342-3p	322
eca-miR-221	10497	eca-miR-23b	1097	eca-miR-450b-5p	269
eca-miR-423-5p	10019	eca-miR-196b	1061	eca-miR-503	255
eca-miR-186	9874	eca-miR-660	1036	eca-miR-361-5p	246
eca-miR-30d	9665	eca-miR-486-5p	1010	eca-miR-34a	246
eca-miR-148a	7823	eca-miR-146a	1007	eca-miR-101	243
eca-miR-92a	7744	eca-miR-199a-5p	970	eca-miR-132	243
eca-miR-28-3p	7585	eca-miR-424	961	eca-miR-502-3p	241
eca-miR-181a	6611	eca-miR-3958	921	eca-miR-134	235
eca-let-7c	6310	eca-miR-532-5p	921	eca-miR-130b	228
eca-miR-199a-3p	5456	eca-miR-487b	910	eca-miR-656	226
eca-miR-199b-3p	5302	eca-miR-30b	890	eca-miR-145	221
eca-miR-27a	4761	eca-miR-103	822	eca-miR-340-5p	218
eca-miR-99b	4473	eca-miR-379	808	eca-miR-15b	206
eca-miR-30e	4104	eca-miR-193b	741	eca-miR-450c	203
eca-miR-29a	4004	eca-miR-380	738	eca-miR-744	202
eca-miR-10a	3820	eca-miR-107a	737	eca-miR-125a-3p	201
eca-miR-100	3531	eca-miR-155	702	eca-miR-122	196
eca-miR-191a	3361	eca-miR-214	664	eca-miR-99a	196
eca-miR-378	3254	eca-miR-93	649	eca-miR-485-3p	190
eca-miR-222	3041	eca-miR-181b	636	eca-miR-17	183
eca-miR-199b-5p	3032	eca-miR-128	625	eca-miR-487a	180
eca-miR-125a-5p	2816	eca-miR-369-3p	597	eca-miR-1271a	179
eca-miR-494	2692	eca-miR-15a	520	eca-miR-485-5p	179
eca-miR-409-3p	2674	eca-miR-98	520	eca-miR-204b	176
eca-let-7e	2442	eca-miR-382	520	eca-miR-3548	160
eca-miR-410	2225	eca-miR-889	509	eca-miR-431	160
eca-miR-151-5p	2096	eca-miR-30c	490	eca-miR-376c	145

miRNA	Count	miRNA	Count	miRNA	Count
eca-miR-126-5p	142	eca-miR-18a	56	eca-miR-582-3p	22
eca-miR-433	139	eca-miR-708	56	eca-miR-140-5p	21
eca-miR-1307	136	eca-miR-138	52	eca-miR-324-3p	21
eca-miR-330	136	eca-miR-324-5p	52	eca-miR-331	21
eca-miR-106a	128	eca-miR-192	50	eca-miR-140-3p	20
eca-miR-758	127	eca-miR-193a-5p	46	eca-miR-144	19
eca-miR-20a	122	eca-miR-542-5p	46	eca-miR-676	19
eca-miR-329b	122	eca-miR-671-5p	46	eca-miR-1468	17
eca-miR-542-3p	122	eca-miR-532-3p	45	eca-miR-9055	17
eca-miR-425	118	eca-miR-301b-3p	44	eca-miR-628a	17
eca-miR-502-5p	117	eca-miR-126-3p	43	eca-miR-34c	17
eca-miR-1180	115	eca-miR-362-5p	41	eca-miR-142-3p	15
eca-miR-7	115	eca-miR-377	41	eca-miR-490-5p	15
eca-miR-454	114	eca-miR-182	39	eca-miR-545	15
eca-miR-299	112	eca-miR-1	38	eca-miR-340-3p	14
eca-miR-29b	92	eca-miR-3200	38	eca-miR-872	14
eca-miR-495	92	eca-miR-500	38	eca-miR-218	14
eca-miR-374a	91	eca-miR-450a	36	eca-miR-342-5p	14
eca-miR-505	88	eca-miR-345-3p	35	eca-miR-329a	14
eca-miR-9021	88	eca-miR-369-5p	35	eca-miR-374b	13
eca-miR-543	87	eca-miR-148b-5p	34	eca-miR-8946	13
eca-miR-196a	86	eca-miR-361-3p	33	eca-miR-9080	13
eca-miR-133a	84	eca-miR-363	33	eca-miR-376a	12
eca-miR-136	83	eca-miR-296	32	eca-miR-6529	12
eca-miR-142-5p	83	eca-miR-335	32	eca-miR-150	11
eca-miR-3959	81	eca-miR-493b	30	eca-miR-671-3p	11
eca-miR-106b	77	eca-miR-32	28	eca-miR-9163	10
eca-miR-365	77	eca-miR-1296	27	eca-miR-190a	10
eca-miR-652	77	eca-miR-501-5p	27	eca-miR-1842	10
eca-miR-154a	76	eca-miR-409-5p	25	eca-miR-7177b	10
eca-miR-497	76	eca-miR-539	25	eca-miR-1197	9
eca-miR-19a	72	eca-miR-184	24	eca-miR-1193	8
eca-miR-376b	70	eca-miR-350	24	eca-miR-483	8
eca-miR-1839	68	eca-miR-655	24	eca-miR-185	7
eca-miR-195	61	eca-miR-194	23	eca-miR-590-3p	6
eca-miR-197	61	eca-miR-496	23	eca-miR-190b	6
eca-miR-29c	60	eca-miR-8992	23	eca-miR-8917	6
eca-miR-92b	59	eca-miR-328	22	eca-miR-1185	6
eca-miR-149	57	eca-miR-345-5p	22	eca-miR-183	5

miRNA	Sample	miRNA	Sample
eca-miR-615-3p	5	eca-miR-9174	3
eca-miR-215	5	eca-miR-9180	3
eca-miR-3065	5	eca-miR-337-5p	2
eca-miR-874	5	eca-miR-3613	2
eca-miR-223	4	eca-miR-188-3p	2
eca-miR-490-3p	4	eca-miR-205	2
eca-miR-154b	4	eca-miR-212	2
eca-miR-187	4	eca-miR-491-5p	2
eca-miR-326	4	eca-miR-541	2
eca-miR-8986b	4	eca-miR-8920	2
eca-miR-9060	4	eca-miR-9a	2
eca-miR-139-5p	4	eca-miR-34b-5p	2
eca-miR-362-3p	3	eca-miR-323-5p	1
eca-miR-582-5p	3	eca-miR-1249	1
eca-miR-8951	3	eca-miR-33b	1
eca-miR-9178	3	eca-miR-9159	1
eca-miR-1301	3	eca-miR-8986a	1
eca-miR-449a	3	eca-miR-129a-5p	1
eca-miR-504	3	eca-miR-129b-3p	1
eca-miR-450b-3p	3	eca-miR-129b-5p	1
eca-miR-873	3	eca-miR-8914	1
eca-miR-9182	3	eca-miR-8977	1
eca-miR-200a	3	eca-miR-9126	1
eca-miR-200b	3	eca-miR-95	1
eca-miR-675	3		

Surprisingly, we found 24 miRNAs enriched in the MVs respect to the original AMCs. Table 2 shows these miRNA, referred as average of fold change in three samples.

Table 2. List of the 24 top miRNAs differentially expressed in the MVs versus the original AMCs expressed as logarithm of fold change (Log FC). The p value is $p < 0.002$ for all the data.

miRNA	Log FC
eca-miR-144	11,48
eca-miR-490-5p	10
eca-miR-223	9,41
eca-miR-150	9,04
eca-miR-451	8,37
eca-miR-486-5p	6,37
eca-miR-142-3p	5,39
eca-miR-142-5p	5,39
eca-miR-146a	4,07
eca-miR-126-3p	4,02
eca-miR-122	4,02
eca-miR-423-5p	3,21
eca-miR-126-5p	3,2
eca-miR-125a-3p	3,07
eca-miR-132	2,94
eca-miR-9055	2,79
eca-miR-1468	2,35
eca-miR-140-3p	2,06
eca-miR-1180	1,83
eca-miR-22	1,67
eca-miR-342-5p	1,53
eca-miR-323-3p	1,46
eca-miR-188-5p	1,42
eca-miR-370	1,05

These results demonstrated that AMCs-MVs contain miRNAs specific of the origin cell that may serve as a signature when MVs are administrated to target cells. Twenty-four miRNAs were found to be selectively accumulated inside the AMC-MVs suggesting a dynamic regulation of

miRNA compartmentalization in the MVs released from amniotic stem cells. These selective miRNAs may be transferred and accumulated into target cells where they may downregulate specific genes.

For this reason, through Ingenuity software (http://www.ingenuity.com/products/ipa/microrna-regulatory-analysis) we studied the pathways in which these 24 miRNAs could be involved, showing that these pathways are mainly those involved in the inflammatory and immune response (table 3).

Table 3. Functional enrichments in the network of the 24 selected miRNAs

BIOLOGICAL PROCESS (GO)		
pathway ID	**pathway description**	**count in gene set**
GO:0006952	defense response	62
GO:0006955	immune response	59
GO:0045087	innate response	51
GO:0002376	immune system precess	67
GO:0051707	response to other organism	39

MOLECULAR FUNCTION (GO)		
pathway ID	**pathway description**	**count in gene set**
GO:0005126	cytokine receptor binding	22
GO:0005515	protein binding	90
GO:0005102	receptor binding	38
GO:0070851	growth factor receptor binding	13
GO:0005149	interleukin-1 receptor binding	7

The recent finding that MVs may carry selected patterns of mRNAs and miRNAs suggests that MVs may represent a new mechanism of genetic exchange between cells. Ratajczak et al. (2006) demonstrated that MVs released from embryonic stem cells may reprogram hematopoietic progenitors by delivering mRNAs and proteins. The mechanism of mRNA and miRNA compartmentalization and in particular whether RNAs are accumulated into MVs in a random or organized manner, remain to be defined. However, some studies (Collino et al., 2010; Chen et al., 2010), as well as the present results, suggest a selective mechanism of RNA packaging into MVs.

Obviously, the work is in progress because it will be necessary to monitor the ribonucleoproteins involved in the intracellular traffic of RNAs and to compare the species of

miRNAs contained in the MVs and in the origin cells to obtain information on the mechanism of RNA accumulation within MVs. Moreover, it should be demonstrated that the miRNAs contained inside MVs are transferred to target cells. This will require the study of miRNAs cargo inside the target cells to find the presence of transferred miRNAs and to understand if these miRNAs are functional.

9. CONCLUSIONS

Microvesicles display a cell-free approach to regenerative medicine overlapping the potential of origin cells, but limiting concerns of using active replicating cells that may undergo mal-differentiation or mutation. Mesenchymal derived MVs have beneficial effects on the recovery from a variety of tissue injuries mainly tested in human medicine. Our results are the first indication of their importance also in veterinary medicine. Amniotic derived MVs showed ability to down-regulated pro-inflammatory genes expression and apoptosis on cells stressed by LPS. Probably, the MSC-MVs content of molecules, including proteins and non coding RNAs, such miRNAs and piRNA, are able to mediate these effects, and elucidations on the mechanisms of these actions are now in progress. For the realization of clinical applications of MSC-MVs, two concerns are important. At first, for future considerations, it will be necessary to improve the standardization of the protocols used for their isolation and storage, and to define the criteria for characterization and quality control. Moreover, it is important to underline that, in addition to preliminary *in vitro* studies (as in this PhD project), whenever possible, representative animal models should be identified and applied in advance of clinical studies investigating MV-based therapeutics. Safety, toxicity and immunogenicity need to be monitored in the course of early phase clinical trials. Reliable information concerning efficacy and long-term side effects of autologous or allogeneic MVs must be obtained before their clinical application.

Lastly, it is important to underline that our study was performed with amniotic cells that represent an alternative and promising source of MSCs. The amniotic membrane, as a MSC source, is fascinating in view of producing off-the-shelf products from biological waste. If the safety and efficacy of these cells can be proven comparable, or better than MSC from other sources, the amnion could become an important and unforeseen cell source of MSCs and their secretome.

10. FUTURE PERSPECTIVES

In the next few years, the therapeutic effects of MSC-MVs should be explore and better understand. Specifically, proteome analysis of MSC-MVs, and proposed signalling pathways that are expected, could predict a single MV molecule as therapeutic effector.

In our context, once that relevant miRNAs contents in equine and bovine AMC-MVs and functional targets are identified, a possible clinical use for these molecules may represent the next front line and may lead to novel strategies, for example, for tendon and endometrial diseases or for better enhancing or manipulating reproductive efficiency. In this respect, MVs, as endogenous carriers of biomolecules, may be particularly advantageous. MVs are naturally present in human biofluids, but may also be engineered for tissue-specific transfers. MVs could be loaded with a range of molecules and serve as drug delivery vesicles, which provide new options in antitumor and immune therapy for targeted drug delivery, for example, or to transfer selected compounds into gametes and embryos to increase reproductive success. In this regard, the application of synthetic or semisynthetic MVs for therapeutic drug delivery is still in its infancy. Issues regarding the understanding of MVs biogenesis, large-scale production, and *in vivo* interactions need to be addressed to develop successful and cost-effective MVs-based drug delivery systems. Given their reduced size, their potential to express targeting ligands in native conformations, and their deformable structure, MVs offer a logical biological vesicle platform for adapting and producing semisynthetic vesicles with excellent potential for nanomedicine applications. Undoubtedly, progress in synthetic biology to harnessing MVs for therapeutic nucleic acid delivery is crucial to mimic the physicochemical properties of naturally occurring MVs to overcome delivery challenges and to establish robust technology platforms. If successful, MVs could then transport nucleic acids into a subsequent population of cells, including embryos, to obtain the desired effect.

11. REFERENCES

- Abe H, Yamashita S, Satoh T and Hoshi H. 2002. Accumulation of cytoplasmic lipid droplets in bovine embryos and cryotolerance of embryos developed in different culture systems using serum-free or serumcontaining media. Molecular Reproduction and Development 61:57–66.
- Abedi A, Azarnia M, Jamali Zahvarehy M, Foroutan T, Golestani S. 2016. Effect of Different Times of Intraperitoneal Injections of Human Bone Marrow Mesenchymal Stem Cell Conditioned *Medium* on Gentamicin-Induced Acute Kidney Injury. Urol J. 28(3):2707-16.
- Alikarami F, Yari F, Amirizadeh N, Nikougoftar M, Jalili MA. 2015. The Immunosuppressive Activity of Amniotic Membrane Mesenchymal Stem Cells on T Lymphocytes. Avicenna J Med Biotechnol 7(3):90-966.
- Alvarenga MA, do Carmo MT, Sgabinazzi LG, Guastali MD, Maia L, Landim FC. 2016. Feasibility and Safety of Endometrial Injection of Autologous Bone Marrow Mesenchymal Stem Cells in Mares. Journal of equine veterinary science 42:12-18.
- Andreu Z and Yanez-Mo M. 2014. Tetraspanins in extracellular vesicle formation and function. Front Immunol 5:442.
- Arcelli R, Tibaldini P, Angeli G and Bellezza E. 2009. Equine amniotic membrane transplantation in some ocular surface diseases in the dog and cat: a preliminary study. Vet Res Commun 33:169-171.
- Arnhold SJ, Goletz I, Klein H, Stumpf G, Beluche LA, Rohde C, Addicks K, Litzke LF. 2007. Isolation and characterization of bone marrow-derived equine mesenchymal stem cells. Am J Vet Res 68:1095-1105.
- Avila M, Espana M, Moreno, Pena C. 2001. Reconstruction of ocular surface with heterologous limbal epithelium and amniotic membrane in a rabbit model. Cornea 20:414-420.
- Baj-Krzyworzeka M, Szatanek R, Weglarczyk K, Baran J, Urbanowicz B, Brański P, Ratajczak MZ, Zembala M. 2006. Tumour derived microvesicles carry several surface determinants and mRNA of tumour cells and transfer some of these determinants to monocytes. Cancer ImmunolImmunother 55:808–18.
- Bamezai S, Rawat VP, Buske C. 2012. Concise review: The Piwi-piRNA axis: pivotal beyond transposon silencing. Stem Cells 30(12):2603-11.
- Barzilay R, Kan I, Ben-Zur T, Bulvik S, Melamed E, Offen D. 2008. Induction of human mesenchymal stem cells into dopamine-producing cells with different differentiation

protocols. Stem Cells and Development 17:547–554.

- Bergsmedh A, Szeles A, Henriksson M, Bratt A, Folkman MJ, Spetz AL, Holmgren L. 2001. Horizontal transfer of oncogenes by uptake of apoptotic bodies. Proc Natl AcadSci U S A 98:6407–11.
- Bilic G, Zeisberger SM, Mallik AS, Zimmermann R, Zisch AH. 2008. Comparative Characterization of Cultured Human Term Amnion Epithelial and Mesenchymal Stromal Cells for Application in Cell Therapy. Cell Transplantation 17(8):955-968.
- Burns G, Brooks K, Wildung M, Navakanitworakul R, Christenson LK, Spencer TE. 2014. Extracellular vesicles in luminal fluid of the ovine uterus. PLoS One 9:e90913.
- Camussi G, DeregibusMC, TettaC. 2010. Paracrine/endocrine mechanism of stem cells on kidney repair: role of microvesicle-mediated transfer of genetic information. Curr Opin Nephrol Hypertens 19:7–12.
- Cantaluppi V, Gatti S, Medica D, Figliolini F, Bruno S, Deregibus MC, Sordi A, Biancone L, Tetta C, Camussi G. 2012. Microvesicles derived from endothelial progenitor cells protect the kidney from ischemiareperfusion injury by microRNA-dependent reprogramming of resident renal cells. Kidney Int 82:412–27.
- Cantinieaux D, Quertainmont R, Blacher S, Rossi L, Wanet T, Noël A, Brook G, Schoenen J, Franzen R. 2013. Conditioned *medium* frombone marrow-derived mesenchymal stem cells improves recovery after spinal cord injury in rats: an original strategy to avoid cell transplantation. PLoS ONE 8(8):e69515.
- Carraro G, Perin L, Sedrakyan S, Giuliani S, Tiozzo C, Lee J, Turcatel G, De Langhe SP, Driscoll B, Bellusci S, Minoo P, Atala A, De Filippo RE, Warburton D. 2008. Human amniotic fluid stem cells can integrate and differentiate into epithelial lung lineages. Stem Cells 26:2902–2911.
- Cocucci E, G Racchetti, P Podini, J Meldolesi. 2007. Enlargeosome traffic: exocytosis triggered by various signals is followed by endocytosis, membrane shedding or both. Traffic 8:742–757.
- Cocucci E, Racchetti G, Meldolesi J. 2009. Shedding microvesicles: artefacts no more. Trends Cell Biol 19:43–51.
- Connell JP, Camci-Unal G, Khademhosseini A, Jacot JG. 2013. Amniotic Fluid-Derived Stem Cells for Cardiovascular Tissue Engineering Applications. Tissue Engineering Part B-Reviews 19:368–379.
- Costa Pereira D, Nunes Dodeb MA, Rumpf R. 2005. Evaluation of different culture systems on the *in vitro* production of bovine embryos. Theriogenology 63:1131–1141.

- Cuman C, Menkhorst E, Winship A, Van Sinderen M, Osianlis T, Rombauts LJ, Dimitriadis E. 2014. Fetal-maternal communication: the role of Notch signalling in embryo implantation. Reproduction 147:R75–R86.
- de Gassart A, Geminard C, Hoekstra D, Vidal M. 2004. Exosome secretion: the art of reutilizing nonrecycled proteins? Traffic 5:896–903.
- del Conde I, Shrimpton CN, Thiagarajan P, Lopez JA. 2005. Tissue factor-bearing microvesicles arise from lipid rafts and fuse with activated platelets to initiate coagulation. Blood 106(5):1604–11.
- di Santo S, Yang Z, Wyler von Ballmoos M, Voelzmann J, Diehm N, Baumgartner I, Kalka C. 2009. Novel cell-free strategy for therapeutic angiogenesis: *in vitro* generated conditioned *medium* can replace progenitor cell transplantation. PLoS ONE4(5)e5643.
- di Trapani M, Bassi G, Midolo M, Gatti A, TakamKamga P, Cassaro A, Carusone R, AdamoA, Krampera M. 2016. Differential and transferable modulatory effects of mesenchymal stromal cell-derived extracellular vesicles on T, B and NK cell functions. Sci Rep 13(6):24120.
- Dominici M, Le Blanc K, Mueller I, Slaper-Cortenbach I, Marini F, Krause D, Deans R, Keating A, Prockop Dj, Horwitz E. 2006. Minimal criteria for defining multipotent mesenchymal stromal cells. The International Society for Cellular Therapy position statement. Cytotherapy 8(4):315–317.
- Donofrio G, Colleoni S, Galli C, Lazzari G, Cavirani S, Flammini CF. 2005. Susceptibility of bovine mesenchymal stem cells to bovine herpesvirus 4. J Virol Methods 127:168-170.
- Dua HS, Gomes JA, King AJ, Maharajan VS. 2004. The amniotic membrane in ophthalmology. Surv Ophthalmol 49:51-77.
- Evangelista M, Soncini M, Parolin, O. 2008. Placenta-derived stem cells: new hope for cell therapy? Cytotechnology 58:33-42.
- Evans MJ and Kaufman MH. 1981. Establishment in culture of pluripotential cells from mouse embryos. Nature 292:154-156.
- Fazeli A. 2008. Maternal communication with gametes and embryos. Theriogenology 70:1182–7.
- Fukuoka H, Suga H, Narita K, Watanabe R, Shintani S. 2012. The latest advance in hair regeneration therapy using proteins secreted by adipose-derived stem cells. American Journal of Cosmetic Surgery 29(4):273–28.
- Gao J and Liu QG. 2011. The role of miR-26 in tumors and normal tissues. Oncol Lett 2:1019-

23.

- Gardiner CF, Ferriera JF, Poli M, Turner K, Child T, Sargent IL. 2013. IVF embryos release extracellular vesicles which may act as an indicator of embryo quality. J Extracell Vesicles 2:20826.
- Gomes JA, Romano A, Santos MS, Dua HS. 2005. Amniotic membrane use in ophthalmology. Curr Opin Ophthalmol 16:233-240.
- Goswami R and Kaplan MH. 2011. A brief history of IL-9. The Journal of Immunology 186(6):3283–3288.
- Gu SX, Li X, Hamilton JL, Chee A, Kc R, Chen D, An HS, Kim JS, Oh C, Ma YZ, van Wijnen AJ, Ima HJ. 2015. MicroRNA-146a reduces IL-1 dependent inflammatory responses in the intervertebral disc. Gene 555(2):80–7.
- Guillot PV, O'Donoghue K, Kurata H, Fisk NM. 2006. Fetal stem cells: betwixt and between. Semin Reprod Med 24(5):340-7.
- Hanada K, Solchaga LA, Caplan AI, Hering TM, Goldberg VM, Yoo JU, Johnstone B. 2001. BMP-2 induction and TGF-beta 1 modulation of rat periosteal cell chondrogenesis. J Cell Biochem 81:284-294.
- Hegmans JP, Bard MP, Hemmes A, Luider TM, Kleijmeer MJ, Prins JB, Zitvogel L, Burgers SA, Hoogsteden HC, Lambrecht BN. 2004. Proteomic analysis of exosomes secreted by human mesothelioma cells. Am J Pathol 164:1807–15.
- Hergenreider E, Heydt S, Tréguer K, Boettger T, Horrevoets AJ, Zeiher AM, Scheffer MP, Frangakis AS, Yin X, Mayr M, Braun T, Urbich C, Boon RA, Dimmeler S. 2012. Atheroprotective Communication Between Endothelial Cells and Smooth Muscle Cells via KLF2-Dependent Enrichment of miRNAs. Circulation 124(21):22-26
- Herrera MB, Fonsato V, Gatti S, Deregibus MC, Sordi A, Cantarella D, Calogero R, Bussolati B, Tetta C, Camussi G. 2010. Human liver stem cellderived microvesicles accelerate hepatic regeneration in hepatectomized rats. J Cell Mol Med 14:1605–18.
- Ho JC, Lai WH, Li MF, Au KW, Yip MC, Wong NL, Ng ES, Lam FF, Siu CW, Tse HF. 2012. Reversal of endothelial progenitor cell dysfunction in patients with type 2 diabetes using a conditioned *medium* of human embryonic stem cellderived endothelial cells. Diabetes Metabolism Research and Reviews 28(5):462–473.
- Hristov M, Erl W, Linder S, Weber PC. 2004. Apoptotic bodies from endothelial cells enhance the number and initiate the differentiation of human endothelial progenitor cells *in vitro*.

Blood 104:2761–6.

- Igura K, Zhang X, Takahashi K, Mitsuru A, Yamaguchi S, Takashi TA. 2004. Isolation and characterization of mesenchymal progenitor cells from chorionic villi of human placenta. Cytotherapy 6:543-553.
- Inoue T, Sugiyama M, Hattori H, Wakita H, Wakabayashi T, Ueda M. 2013. Stem cells from human exfoliated deciduous tooth-derived conditioned *medium* enhance recovery of focal cerebral ischemia in rats. Tissue Engineering A 19(1-2):24–29.
- Jiawen S, Jianjun Z, Jiewen D, Dedong Y, Hongbo Y, Jun S, Xudong W, Shen SG, Lihe G. 2014. Osteogenic differentiation of human amniotic epithelial cells and its application in alveolar defect restoration. Stem Cells Transl Med 3(12):1504-13.
- Kalra H, Simpson RJ, Ji H, Aikawa E, Altevogt P, Askenase P, Bond VC, Borràs FE, Breakefield X, Budnik V, Buzas E, Camussi G, Clayton A, Cocucci E, Falcon-Perez JM, Gabrielsson S, Gho YS, Gupta D, Harsha HC, Hendrix A, Hill AF, Inal JM, Jenster G, Krämer-Albers EM, Lim SK, Llorente A, Lötvall J, Marcilla A, Mincheva-Nilsson L, Nazarenko I, Nieuwland R, Nolte-'t Hoen EN, Pandey A, Patel T, Piper MG, Pluchino S, Prasad TS, Rajendran L, Raposo G, Record M, Reid GE, Sánchez-Madrid F, Schiffelers RM, Siljander P, Stensballe A, Stoorvogel W, Taylor D, Thery C, Valadi H, van Balkom BW, Vázquez J, Vidal M, Wauben MH, Yáñez-Mó M, Zoeller M, Mathivanan S. 2012. Vesiclepedia: a compendium for extracellular vesicles with continuous community annotation. PloS Biol 10:e1001450.
- Katsuda T and Ochiya T. 2015. Molecular signatures of mesenchymal stemcell-derived extracellular vesicle-mediatedtissue repair. Stem Cell Research & Therapy 6:212.
- Kern S, Eichler H, Stoeve J, Kluter H, Bieback K. 2006. Comparative analysis of mesenchymal stem cells from bone marrow, umbilical cord blood, or adipose tissue. Stem Cells 24:1294–1301.
- Kim HO and Choi S. 2013. Mesenchymal stem cell-derived secretome and microvesicles as a cell-free therapeutics for neurodegenerative disorders. Tissue Engineering and Regenerative Medicine 10(3)93–101.
- Kwon A, Kim Y, Kim M,Kim J, Choi H, Jekarl DW, Lee S, Kim JM, Shin JC, IY Park. 2016. Tissue-specific differentiation potency of mesenchymal stromal cells from perinatal tissues. Scientific Reports 6:23544.
- Koizumi NJ, Inatomi TJ, Sotozono CJ, Fullwood NJ, Quantock AJ, Kinoshita S. 2000. Growth factor mRNA and protein in preserved human amniotic membrane. Curr Eye Res 20:173-177.

- Kooreman NG and Wu JC. 2010. Tumorigenicity of pluripotent stem cells: biological insights from molecular imaging. J R Soc Interface 7(Suppl6):S753-763.
- Kosaka N, Iguchi H, Yoshioka Y, Takeshita F, Matsuki Y, Ochiya T. 2010. Secretory mechanisms and intercellular transfer of microRNAs in living cells. J Biol Chem 285:17442–52.
- Kubo M, Sonoda Y, Muramatsu R, Usui M. 2001. Immunogenicity of human amniotic membrane in experimental xenotransplantation. Invest Ophthalmol Vis Sci 42:1539–1546.
- Lai RC, Arslan F, Lee MM, Sze NS, Choo A, Chen TS, Salto-Tellez M, Timmers L, Lee CN, El Oakley RM, Pasterkamp G, de Kleijn DP, Lim SK. 2010. Exosome secreted by MSC reduces myocardial ischemia/reperfusion injury. Stem Cell Res 4:214–22.
- Lange-Consiglio A, Corradetti B, Bizzaro D, Magatti M, Ressel L, Tassan S, Parolini O, Cremonesi F. 2012. Characterization and potential applications of progenitor-like cells isolated from horse amniotic membrane. J Tissue Eng Regen Med 6:622–635.
- Lange-Consiglio A, Corradetti B, Meucci A, Bizzaro D, F . Cremonesi. 2013c. Characteristics of equine mesenchymal stem cells derived from amnion and bone marrow: *in vitro* proliferative and multilineage potential assessment. Equine Vet J 45(6):737–744.
- Lange-Consiglio A, Maggio V, Pellegrino L, Cremonesi F. 2010. Equine bone marrow mesenchymal or amniotic epithelial stem cells as feeder in a model for the *in vitro* culture of bovine embryos. Zygote 20:45-51.
- Lange-Consiglio A, Rossi D, Tassan S, Perego R, Cremonesi F, Parolini O. 2013a. Conditioned *medium* from horse amniotic membrane-derived multipotent progenitor cells: immunomodulatory activity *in vitro* and first clinical application in tendon and ligament injuries *in vivo*. Stem Cells Dev 22(22):3015–3024.
- Lange-Consiglio A, Tassan S, Corradetti B, Meucci A, Perego R, Bizzaro D, Cremonesi F. 2013b. Investigating the efficacy of amnion-derived compared with bone marrow-derived mesenchymal stromal cells in equine tendon and ligament injuries. Cytotherapy 15(8):1011-20.
- Lassaline ME, Brooks DE, Ollivier FJ, Komaromy AM, Kallberg ME, Gelatt KN. 2005. Equine amniotic membrane transplantation for corneal ulceration and keratomalacia in three horses. Vet Ophthalmol 8:311-317.
- Lee J, Kim J, Lee KI, Shin JM, Chae JI, Chung HM. 2011. Enhancement of wound healing by secretory factors of endothelial precursor cells derived from human embryonic stem cells Cytotherapy 13(2):165–178.

- Leung VYL, Chan D, Cheung KMC. 2006. Regeneration of intervertebral disc by mesenchymal cells: potentials, limitations and future direction. Eur Spine J 15(Suppl3):S406–S413.
- Li T, Yan Y, Wang B, Qian H, Zhang X, Shen L, Wang M, Zhou Y, Zhu W, Li W, Xu W. 2013. Exosomes derived from human umbilical cord mesenchymal stem cells alleviate liver fibrosis. Stem Cells Dev 22:845–54.
- Li X, Morris LHA, Allen WR. 2001. Influence of coculture during maturation on the developmental potential of equine oocytes fertilized by intracytoplasmic sperm injection (ICSI). Reproduction 121:925–932.
- Litwack G. 2008. Growth factors and cytokines. in Human Biochemistry and Disease pp. 587–683, Elsevier Academic Press.
- Llorente A, van Deurs B, Sandvig K. 2007. Cholesterol regulates prostasome release from secretory lysosomes in PC-3 human prostate cancer cells. Eur J Cell Biol 86:405–15.
- Lonergan P, Fair T, Corcoran D, Evans ACO. 2006. Effect of culture environment on gene expression and developmental characteristics in IVF-derived embryos. Theriogenology 65:137–152.
- Lovell-Badge R. 2001. The future for stem cell research. Nature 414:88-91.
- Lucas E. 2013. Epigenetic effects on the embryo as a result of periconceptional environment and assisted reproduction technology. Reproductive BioMedicine Online 27:477–485.
- Mackay AM, Beck SC, Murphy JM, Barry FP, Chichester CO, Pittenger MF. 1998. Chondrogenic differentiation of cultured human mesenchymal stem cells from marrow. Tissue Eng 4:415-428.
- Magatti M, De Munari S, Vertua E, Gibelli L, Wengler GS, Parolini O. 2008. Human amnion mesenchyme harbors cells with allogeneic T-cell suppression and stimulation capabilities. Stem Cells 26:182-192.
- Marcus AJ and Woodbury D. 2008. Fetal stem cells from extra-embryonic tissues: do not discard. Journal of cellular and molecular medicine 12(3):730-742.
- Martin GR. 1981. Isolation of a pluripotent cell line from early mouse embryos cultured in *medium* conditioned by teratocarcinoma stem cells. Proc Natl Acad Sci USA 78:7634-7638.
- Mathivanan S and Simpson RJ. 2009. ExoCarta: A compendiumof exosomal proteins and RNA. Proteomics 9:4997–5000.
- Mathur A and Martin JF. 2016. Stem cells and repair of the heart. Lancet 364:183-192.
- Miki T and Strom SC. 2006. Amnion-derived pluripotent/multipotent stem cells. Stem Cell

Rev 2:133-142.

- Mirabella T, Cilli M, Carlone S, Cancedda R, Gentili C. 2011. Amniotic liquid derived stem cells as reservoir of secreted angiogenic factors capable of stimulating neo-arteriogenesis in an ischemic model," Biomaterials 32(15):3689–3699.
- Morhayim J, Baroncelli M, van Leeuwen JP. 2014. Extracellular vesicles: specialized bone messengers. Arch BiochemBiophys 561:38–45.
- Morrison SJ, Shah NM, Anderson DJ. 1997. Regulatory mechanisms in stem cell biology. Cell 88:287-298.
- Moussavou G, Kwak DH, Lim MU, Kim JS, Kim SU, Chang KT, Choo YK. 2013. Role of gangliosides in the differentiation of human mesenchymal-derived stem cells into osteoblasts and neuronal cells. BMB Rep 46:527–532.
- Mulcahy LA, Pink RC, Carter DR. 2014. Routes and mechanisms of extracellular vesicle uptake. J Extracell Vesicles 4:3.
- Müller S, Acevedo L, Wang X, Karim Z, Matta A, Mehrkens A, Schaeren S, Feliciano S, Jakob M, Martin I, Barbero A, Erwin M. 2016. Notochordal cell conditioned *medium* (NCCM) regenerates end-stage human osteoarthritic articular chondrocytes and promotes a healthy phenotype. Arthritis Research & Therapy 18:125.
- Ng YH, Rome S, Jalabert A, Forterre A, Singh H, Hincks CL, Salamonsen LA. 2013. Endometrial exosomes/microvesicles in the uterine microenvironment: a new paradigm for embryo-endometrial cross talk at implantation. PLoS One 8(3):e58502.
- Ollivier FJ, Kallberg ME, Plummer CE, Barrie KP, O'Reilly S, Taylor DP, Gelatt KN, Brooks DE. 2006. Amniotic membrane transplantation for corneal surface reconstruction after excision of corneolimbal squamous cell carcinomas in nine horses. Vet Ophthalmol 9:404-413.
- Omori M, Tsuchiya S, Hara K, Kuroda K, Hibi H, Okido M and Ueda M. 2015. A new application of cell-free bone regeneration: immobilizing stem cells from human exfoliated deciduous teeth-conditioned *medium* onto titanium implants using atmospheric pressure plasma treatment. Stem Cell Research & Therapy 6:124.
- Paris DB and Stout TA. 2010. Equine embryosand embryonic stem cells: defining reliablemarkers of pluripotency. Theriogenology 74: 516–524.
- Parolini I, Federici C, Raggi C, Lugini L, Palleschi S, De Milito A, Coscia C, Iessi E, Logozzi M, Molinari A, Colone M, Tatti M, Sargiacomo M, Fais S. 2009. Microenvironmental pH is a key factor for exosome traffic in tumor cells. J Biol Chem 284:34211–22.

- Pegtel DM, Cosmopoulos K, Thorley-Lawson DA, van Eijndhoven MA, Hopmans ES, Lindenberg JL, de Gruijl TD, Würdinger T, Middeldorp JM. 2010. Functional delivery of viral miRNAs via exosomes. Proc Natl Acad Sci U S A 107:6328–33.
- Perez-Hernandez D, Gutiérrez-Vázquez C, Jorge I, López-Martín S, Ursa A, Sánchez-Madrid F, Vázquez J, Yáñez-Mó M. 2013. The intracellular interactome of tetraspanin-enriched microdomains reveals their function as sorting machineries toward exosomes. J Biol Chem 288:11649–61.
- Perez-Marin CC, Molina Moreno L, Vizuete CG. 2011. Clinical approach to the repeat breeder cow syndrome. A Bird's-Eye View of Veterinary Medicine 18:337-362.
- Pittenger MF, Mackay AM, Beck SC, Jaiswal RK, Douglas R, Mosca JD, Moorman MA, Simonetti DW, Craig S, Marshak DR. 1999. Multilineage potential of adult human mesenchymal stem cells. Science 284:143-147.
- Plummer CE. 2009. The use of amniotic membrane transplantation for ocular surface reconstruction: a review and series of 58 equine clinical cases (2002–2008). Veterinary Ophthalmology 12:17-24.
- Raposo G and Stoorvogel W. 2013. Extracellular vesicles: exosomes, microvesicles, and friends. J Cell Biol 200:373–83.
- Ratajczak J, Miekus K, Kucia M, Zhang J, Reca R, Dvorak P, Ratajczak MZ. 2006. Embryonic stem cellderived microvesicles reprogram hematopoietic progenitors: evidence for horizontal transfer of mRNA and protein delivery. Leukemia 20:847–56.
- Record M, Carayon K, Poirot M, Silvente-Poirot S. 2014. Exosomes as new vesicular lipid transporters involved in cell-cell communication and various pathophysiologies. Biochim Biophys Acta 1841:108–20.
- Reghini MF, Ramires Neto C, Segabinazzi LG, Castro Chaves MM, Dell'AquaCde P, Bussiere MC, Dell'Aqua JA Jr, Papa FO, Alvarenga MA. 2016. Inflammatory response in chronic degenerative endometritis mares treated with platelet-rich plasma. Theriogenology 86(2):516-22.
- Richardson LE, Dudhia J, Clegg PD, Smith R. 2007. Stem cells in veterinary medicine-attempts at regenerating equine tendon after injury. Trends Biotechnol 25:409–416.
- Rieger D, Grisart B, Semple E, Van Langendonckt A, Betteridge KJ, Dessy F. 1995. Comparison of the effects of oviductal cell co-culture and oviductal cell-conditioned *medium* on the development and metabolic activity of cattle embryos. Journal of Reproduction & Infertility

105(1):91–98.

- Rizos D, Ward F, Duffy P, Boland MP, Lonergan P. 2002. Consequences of bovine oocyte maturation, fertilization or early embryo development *in vitro* versus *in vivo*: implications for blastocyst yield and blastocyst quality. Molecular Reproduction and Development 61:234–248.
- Romero-Cordoba SL, Salido-Guadarrama I, Rodriguez-Dorantes M, Hidalgo-Miranda A. 2014. miRNA biogenesis: biological impact in the development of cancer. Cancer BiolTher 15(11):1444-55.
- Saadeldin IM, Kim SJ, Choi YB, Lee BC. 2014. Improvement of cloned embryos development by co-culturing with parthenotes: a possible role of exosomes/microvesicles for embryos paracrine communication. Cell Reprogram 16:223–234.
- Sabapatha A, Gercel-Taylor C, Taylor D. 2006. Specific isolation of placenta-derived exosomes from the circulation of pregnant women and their immunoregulatory consequences. Am J ReprodImmunol 56:345–355.
- Sadat S, Gehmert S, Song YH, Yen Y, Bai X, Gaiser S, Klein H, Alt E. 2007. The cardioprotective effect of mesenchymal stem cells is mediated by IGF-I and VEGF," Biochemical and Biophysical Research Communications 363(3)674–679.
- Scala M, Lenarduzzi S, Spagnolo F, Trapasso M, Ottonello C, Muraglia A, Barla A, Squillario M, Strada P. 2015. Regenerative medicine for the treatment of Teno-desmic injuries of the equine. A series of 150 horses treated with platelet-derived growth factors. *In Vivo* 28(6):1119-23.
- Schmaltz-Panneau B, Locatelli Y, Uzbekova S, Perreau C, Mermillod P. 2015 Bovine oviduct epithelial cells dedifferentiate partly in culture, while maintaining their ability to improve early embryo development rate and quality. Reproduction in Domestic Animal 50(5):719–729.
- Schorey JS and S Bhatnagar. 2008. Exosome function: from tumor immunology to pathogen biology. Traffic 9:871–881.
- Simons M and Raposo G. 2009. Exosomes–vesicular carriers for intercellular communication. CurrOpin Cell Biol 21:575–81.
- Simpson RJ, Kalra H, Mathivanan S. 2012. ExoCarta as a resource for exosomal research. J Extracell Vesicles 16:1.
- Simpson RJ, Lim JW, Moritz RL, Mathivanan S. 2009. Exosomes: proteomic insights and

diagnostic potential. Expert Rev Proteomics 6:267–83.

- Solomon A, Wajngarten M, Alviano F, Anteby I, Elchalal U, Pe'er J, Levi-Schaffer F. 2005. Suppression of inflammatory and fibrotic responses in allergic inflammation by the amniotic membrane stromal matrix. ClinExp Allergy 35:941-948.
- Subra C, Grand D, Laulagnier K, Stella A, Lambeau G, Paillasse M, De Medina P, Monsarrat B, Perret B, Silvente-Poirot S, Poirot M, Record M. 2010. Exosomes account for vesicle-mediated transcellular transport of activatable phospholipases and prostaglandins. J Lipid Res 51:2105–20.
- Sun NZ and Ji HS. 2009 *In vitro* differentiation of human placenta-derived adherent cells into insulin-producing cells. J Int Med Res 37:400–406.
- Taylor DD and Shah S. 2015. Methods of isolating extracellular vesicles impact down-stream analyses of their cargoes. Methods 1(87):3-10.
- Tetta C, Ghigo E, Silengo L, Deregibus MC, Camussi G. 2013. Extracellular vesicles as an emerging mechanism of cell-to-cell communication. Endocrine 44:11–9.
- Thatcher WW, Guzeloglu A, Mattos R, Binelli M, Hansen TR, Pru JK. 2001. Uterine-conceptus interactions and reproductive failure in cattle. Theriogenology 56:1435–1450.
- Thery C, Amigorena S, Raposo G, Clayton A. Isolation and characterization of exosomes from cell culture supernatants and biological fluids. CurrProtoc Cell Biol 3(3):22.
- Toda A, Okabe M, Yoshida T, Nikaido T. 2007. The potential of amniotic membrane/amnion-derived cells for regeneration of various tissues. J Pharmacpò Sci 105(3):215-28.
- Troedsson MH and Woodward EM. 2016. Our current understanding of the pathophysiology of equine endometritis with an emphasis on breeding-induced endometritis. Reprod Biol 16(1):8-12.
- Valadi H, Ekström K, Bossios A, Sjöstrand M, Lee JJ, Lötvall JO. 2007. Exosome mediated transfer of mRNAs and microRNAs is a novel mechanism of genetic exchange between cells. Nat Cell Biol 9:654–9.
- van der Pol E, Hoekstra AG, Sturk A, Otto C, van Leeuwen TG, Nieuwland R. 2010. Optical and non-optical methods for detection and characterization of microparticles and exosomes. J Thromb Haemost 8:2596–607.
- van der Vlist EJ, Nolte-'t Hoen EN, Stoorvogel W, Arkesteijn GJ, Wauben MH. 2012. Fluorescent labeling of nano-sized vesicles released by cells and subsequent quantitative and qualitative analysis by high-resolution flow cytometry. Nat Protoc 7:1311–26

- Vézina-Audette R, Lavoie-Lamoureux A, Lavoie J-P, Laverty S. 2013. Inflammatory stimuli differentially modulate the transcription of paracrine signaling molecules of equine bone marrow multipotent mesenchymail stromal cells. Osteoarth Cartilage 21:1116-1124.
- Wang Y, Zhang L, Li Y, Chen L, Wang X, Guo W, Zhang X, Qin G, He SH, Zimmerman A, Liu Y, Kim IM, Weintraub NL, Tang Y. 2015. Exosomes/microvesicles from induced pluripotent stem cells deliver cardioprotective miRNAs and prevent cardiomyocyte apoptosis in the ischemic myocardium. International journal of cardiology 192:61-69.
- Williams JT, Southerland SS, Souza J, Calcutt AF, Cartledge RG. 1999. Cells isolated from adult human skeletal muscle capable of differentiating into multiple mesodermal phenotypes. Am Surg 65:22-26.
- Wrenzycki C and Stinshoff H. 2013. Maturation environment and impact on subsequent development al competence of bovine oocytes. Reproduction in Domestic Animal 48(Suppl1):38–43.
- Wubbolts R, Leckie RS, Veenhuizen PT, Schwarzmann G, Möbius W, Hoernschemeyer J, Slot JW, Geuze HJ, Stoorvogel W. 2003. Proteomic and biochemical analyses of human B cell-derived exosomes. Potential implications for their function and multivesicular body formation. J Biol Chem 278:10963–72.
- Xin H, Li Y, Buller B, Katakowski M, Zhang Y, Wang X, Shang X, Zhang ZG, Chopp M. 2012. Exosome-mediated transfer of miR- 133b from multipotent mesenchymal stromal cells to neural cells contributes to neurite outgrowth. Stem Cells 30:1556–64.
- Yamaguchi S, Shibata R, Yamamoto N, Nishikawa M, Hibi H, Tanigawa T, Ueda M, Murohara T, Yamamoto A. 2015. Dental pulp-derived stem cell conditioned *medium* reduces cardiac injury following ischemiareperfusion. Scientific reports 5:16295.
- Yanez-Mo M, Siljander PR, Andreu Z, Zavec AB, Borràs FE, Buzas EI, Buzas K, Casal E, Cappello F, Carvalho J, Colás E, Cordeiro-da Silva A, Fais S, Falcon-Perez JM, Ghobrial IM, Giebel B, Gimona M, Graner M, Gursel I, Gursel M, Heegaard NH, Hendrix A, Kierulf P, Kokubun K, Kosanovic M, Kralj-Iglic V, Krämer-Albers EM, Laitinen S, Lässer C, Lener T, Ligeti E, Linē A, Lipps G, Llorente A, Lötvall J, Manček-Keber M, Marcilla A, Mittelbrunn M, Nazarenko I, Nolte-'t Hoen EN, Nyman TA, O'Driscoll L, Olivan M, Oliveira C, Pállinger É, Del Portillo HA, Reventós J, Rigau M, Rohde E, Sammar M, Sánchez-Madrid F, Santarém N, Schallmoser K, Ostenfeld MS, Stoorvogel W, Stukelj R, Van der Grein SG, Vasconcelos MH, Wauben MH, De Wever O. 2015. Biological properties of extracellular vesicles and their physiological

functions. J Extracell Vesicles 14(4):27066.

- Yang D, Wang W, Li L, Peng Y, Chen P, Huang H, Guo Y, Xia X, Wang Y, Wang H, Wang WE, Zeng C. 2013. The relative contribution of paracine effect versus direct differentiation on adipose-derived stem cell transplantation mediated cardiac repair. PLoS ONE 8(3):e59020.
- Yoon YJ, Kim OY, Gho YS. 2014. Extracellular vesicles as emerging intercellular communicasomes. BMB Rep 47:531–9.
- Yu SC, Xu YY, Li Y, Xu B, Sun Q, Li F, Zhang XG. 2015. Construction of tissue engineered skin with human amniotic mesenchymal stem cells and human amniotic epithelial cells. Eur Rev Med Pharmacol Sci 19(23):4627-35.
- Yu X, Harris SL, Levine AJ. 2006. The regulation of exosome secretion: a novel function of the p53 protein. Cancer Res 66:4795–801.
- Zagoura DS, Roubelakis MG, Bitsika V, Trohatou O, Pappa KI, Kapelouzou A, Antsaklis A, Anagnou NP. 2012. Therapeutic potential of a distinct population of human amniotic fluid mesenchymal stem cells and their secreted molecules in mice with acute hepatic failure. Gut 61(6):894–906.
- Zhang B, Wang M, Gong A, Zhang X, Wu X, Zhu Y, Shi H, Wu L, Zhu W, Qian H, Xu W. 2014. HucMSC-exosome mediated-Wnt4 signaling is required for cutaneous wound healing. Stem Cells 33:2158–68.
- Zhang X, Soda Y, Takahashi K, Bai Y, Mitsuru A, Igura K, Satoh H, Yamaguchi S, Tani K, Tojo A, Takahashi TA. 2006. Successful immortalization of mesenchymal progenitor cells derived from human placenta and the differentiation abilities of immortalized cells. BiochemBiophys Res Commun 351:853-859.
- Zhang Y, Liu D, Chen X, Li J, Li L, Bian Z, Sun F, Lu J, Yin Y, Cai X, Sun Q, Wang K, Ba Y, Wang Q, Wang D, Yang J, Liu P, Xu T, Yan Q, Zhang J, Zen K, Zhang CY. 2010. Secreted monocytic miR-150 enhances targeted endothelial cell migration. Mol Cell 39:133–44.
- Zheng Y, Campbell EC, Lucocq J, Riches A, Powis SJ. 2013. Monitoring the Rab27 associated exosome pathway using nanoparticle tracking analysis. Exp Cell Res 319:1706–13.
- Zhu L, Chen L, Shi CM, Xu GF, Xu LL, Zhu LL, Guo XR, Ni Y, Cui Y, Ji C. 2014. MiR-335, an adipogenesis-related microRNA, is involved in adipose tissue inflammation. Cell Biochem Biophys 68:283–90.
- Zuk, Zhu M, Mizuno H, Huang J, Futrell JW, Katz AJ, Benhaim P, Lorenz HP, Hedrick MH. 2001. Multilineage cells from human adipose tissue: implications for cell-based therapies. Tissue

Eng 7:211-228.

12. APPENDIX: OTHER PUBLICATIONS

During the 3 year-project, the work performed in the laboratory was not only focused on the experiments designed for the present thesis. Some hours were spent also working on side projects. In this contest, since the laboratory investigates on the biology of the reproduction, a paper entitled “Leptin and leptin receptor are detectable in equine spermatozoa but are not involved in *in vitro* fertilization” was published.

Then, in the field of the regenerative medicine, some experiments were performed on the use of PRP as tool for the regeneration. On this basis, two papers entitled “Platelet concentrate in bovine reproduction: effects on *in vitro* embryo production and after intrauterine administration in repeat breeder cows” and “Effects of platelet-rich plasma in a model of bovine endometrial inflammation *in vitro*” emerged from the experiments.

In parallel with the characterization of equine and bovine AMCs, also the porcine ones were object of study; from that, a paper entitled “Peculiarity of porcine amniotic membrane and its derived cells: a contribution to the study of cell therapy from a large animal model” developed from the experiments.

Alongside the AMCs, other sources of stem cells were investigated and the paper entitled “Does the bovine pre-ovulatory follicle harbor progenitor stem cells?” is about the study of a potential niche of stem cells in the ovary, whereas the paper titled “Isolation, molecular characterization and *in vitro* differentiation of bovine Wharton's jelly-derived multipotent mesenchymal cells” is about the study of stem cells obtained from the Wharton's jelly.

Finally, during a project developed in Brazil with the team headed by Prof. Felipe Perecin, a study on the miRNA differential expression of cumulus-oocyte complexes and their derived extracellular vesicles was conducted. The article that emerged, entitled “MicroRNA mediated regulation and role of PI3K-Akt pathway in bovine oocyte developmental competence” has been submitted to Scientific Report on December, 2016. In this study, we tested the hypothesis that oocyte competence is associated with alterations of regulatory miRNAs during follicle development, then 348 miRNAs were screened in granulosa cells and cumulus-oocyte complexes and their derived MVs. Bioinformatics analyses revealed that PI3K-Akt pathway was highly regulated by exclusive miRNAs. Indeed, PI3K-Akt signalling pathway had different levels in follicular cells correlating with oocyte competence. This miRNA-modulated pathway was downregulated in follicular cells of lower quality oocytes, indicated by increased levels of phosphatase and tensin homolog (PTEN) and decreased

levels of PTEN regulators bta-miR-494 and bta-miR-20a. In conclusion, it was possible to assume that the miRNA expression profiles can be used as tool to identify molecular pathways involved in oocyte competence.

CSIRO PUBLISHING

Reproduction, Fertility and Development
http://dx.doi.org/10.1071/RD14130

Leptin and leptin receptor are detectable in equine spermatozoa but are not involved in *in vitro* fertilisation

Anna Lange-Consiglio[A], *Bruna Corradetti*[B], *Claudia Perrini*[A], *Davide Bizzaro*[B] *and Fausto Cremonesi*[A,C,D]

[A]Large Animal Hospital, Reproduction Unit, Università degli Studi di Milano, Via dell'Università 6, 26900 Lodi, Italy.
[B]Department of Life and Environmental Sciences, Università Politecnica delle Marche, Via Brecce Bianche, 60131 Ancona, Italy.
[C]Department of Veterinary Science for Animal Health, Production and Food Safety, Università degli Studi di Milano, Via Celoria, 20133 Milano, Italy.
[D]Corresponding author. Email: fausto.cremonesi@unimi.it

Abstract. In human and swine, leptin (OB) has been identified in seminal plasma and leptin receptors (OB-R) on the cell surface of spermatozoa, indicating that spermatozoa are a target for OB. This hormone has also been detected in follicular fluid (FF) in women and mares, although its role requires further study. The aims of this study were to investigate the immunolocalisation and the expression of OB and OB-R in equine spermatozoa and to evaluate the involvement of OB in equine *in vitro* fertilisation (IVF). Since progesterone (P) and OB are both found in FF, the individual and combined effects of these two hormones were studied in equine IVF and compared with the results obtained from the use of FF for *in vitro* sperm preparation. For the first time, we were able to identify OB and OB-R mRNA and their corresponding proteins in equine spermatozoa. When spermatozoa were treated with OB, there was a decrease in the three motility parameters VSL, STR and LIN, commonly associated with hyperactivation, whilst the acrosome reaction rate increased ($P < 0.05$). The fertilisation rate was 51% with FF, 46.15% with P, 43.64% with P+OB and 0% with OB alone. The percentage of eight-cell stage embryos was 18.7% with FF, 17.1% with P and 16.7% with OB+P. OB alone did not permit oocyte fertilisation, indicating that, in the horse, OB is involved in capacitation and hyperactivation but not in sperm penetration.

Additional keywords: follicular fluid, horse, hyperactivation, immunocytochemistry, progesterone.

Received 12 April 2014, accepted 15 August 2014, published online 13 October 2014

Introduction

In equine species, *in vitro* assisted reproduction techniques are challenging. Only two papers report the birth of foals from *in vitro* fertilisation (IVF). In both cases, *in vivo*-matured oocytes collected by ovum pick-up were used (Palmer *et al.* 1991; Bezard 1992). The main limiting factors appear to be the reliance on the zona pellucida for hardening of oocytes and reduced *in vitro* capacitation of stallion spermatozoa. Heparin, equine proteins present in zona pellucida (also called zona proteins), caffeine and lysophospholipids have been shown to increase the percentage of capacitated and acrosome-reacted spermatozoa, although they do not facilitate sperm penetration into *in vitro*-matured oocytes (Graham 1996). Following incubation of sperm–oocyte complexes for 1 h there is a low incidence (20%) of the acrosomal reaction (AR) in stallion spermatozoa bound to the zona pellucida (Ellington *et al.* 1993; Cheng *et al.* 1996; Meyers *et al.* 1996). The reported low incidence of AR in zona-bound spermatozoa suggests that several other localised biological agents contribute to induction of the AR required for successful fertilisation *in vivo*. Follicular fluid (FF) represents one of these agents as, at ovulation, it is transported, together with the cumulus–oocyte complex, from the follicle to the oviductal ampulla, where fertilisation occurs. Progesterone (P) has been suggested to be the main active component in FF responsible for the induction of the AR. When charcoal treatment is used to remove steroid hormones from FF it becomes inactive; efficacy is restored when the charcoal-treated FF is supplemented with P (Cheng *et al.* 1998). Furthermore, progesterone receptors have been detected on the surface of spermatozoa in different species including man (Kirkman-Brown *et al.* 2002) and horse (Cheng *et al.* 1998).

Another hormone found in the FF is leptin (OB). This hormone is the 167-amino acid product of *Ob* gene expression (Zhang *et al.* 1994) and is involved in the regulation of energy metabolism. OB is synthesised predominantly by adipocytes and has been shown to be involved in the regulation of various reproductive functions (Chehab *et al.* 1996). OB has been quantitatively assayed in human (De Placido *et al.* 2006), pig

(Lackey *et al.* 2002) and mare FF (Lange-Consiglio *et al.* 2013). Both P and OB have been reported to be involved in capacitation and acrosome reactions of spermatozoa. Many studies confirm that the effects of P on human spermatozoa are mediated by the increase of intracellular calcium concentrations (Blackmore *et al.* 1990), the stimulation of phospholipase activity (Murase and Roldan 1996), the phosphorylation of proteins (Tesarik *et al.* 1993; Luconi *et al.* 1995; Emiliozzi *et al.* 1996) and the efflux of chloride (Meizel 1997). It is known that OB is also involved in protein phosphorylation. Tyrosine phosphorylation of sperm proteins during capacitation has been reported in mice, human, bulls, hamsters (Visconti *et al.* 1995; Leclerc *et al.* 1996; Galantino-Homer *et al.* 1997), pigs (Kaláb *et al.* 1998; Flesch *et al.* 1999; Tardif *et al.* 2003) and horses (González-Fernández *et al.* 2013). Furthermore, the Janus kinases and signal transducers and activators of transcription pathways (JAK/STAT) represent the main signalling cascades activated by OB (Thomas 2004). The binding between OB and OB receptors (OB-R) activates JAK2 kinase, causing phosphorylation of several tyrosine residues including those on the functional OB-R. These phosphorylative mechanisms provide binding sites for STAT3 protein, which, following activation, is translocated to the nucleus where transcription of target genes is stimulated.

By this mechanism it is conceivable that OB increases protein tyrosine phosphorylation and affects both the capacitation and the acrosome reactions (Lampiao and du Plessis 2008). In pigs and horses, as in man, OB has been found in seminiferous tubules and in seminal plasma (Lackey *et al.* 2002; Aquila *et al.* 2005*a*). OB-R were detected on the cell surface of human spermatozoa, indicating that these may be a possible target for OB in the male genital tract (Jope *et al.* 2003). In the horse, there are as yet no reports of the presence of OB-R on the surface of spermatozoa, nor any on the effects of OB on capacitation and fertilisation. In this context, we investigated whether OB and OB-R are detectable at a molecular level and by immunocytochemistry in equine spermatozoa. Since OB and P are found in FF, we also aimed to assess the individual and combined effect of OB and P in comparison to FF to better understand the role of OB in equine IVF.

Materials and methods

Materials and animals

All reagents were purchased from Sigma Aldrich Chemical (Milano, Italy) unless otherwise specified.

Fresh semen was collected by means of an artificial vagina from three adult stallions of proven fertility. All collections were performed according to approved animal care and following protocols of the Bioethics Committee of Milan University.

Equine epididymides ($n = 6$) and ovaries ($n = 375$) were collected at a local abattoir from horses slaughtered for reasons other than the present study.

Experimental design

There were three parts to this study: in the first, OB and OB-R on equine spermatozoa were assessed by immunocytochemistry, western blot analysis and molecular biology; in the second, the effect of OB on capacitation and hyperactivation of equine spermatozoa was studied by motility assessment, fluorescent staining and detection of apoptosis. In this step, the individual effect of OB was compared with that induced by P or by the combination of OB and P (OB+P), or by FF. In the third part, IVF was performed using media supplemented with OB, P, OB+P or FF.

Experiment 1: detection of OB and OB-R on equine spermatozoa by immunocytochemistry, western blot analysis and molecular biology

Immunocytochemistry

Immunocytochemical detection of OB and OB-R was performed on fresh ejaculated spermatozoa selected by a swim-up procedure and on spermatozoa collected from the caput epididymidis of three different stallions, pooled and washed three times with Tris-buffered saline (TBS; 0.05 M Tris/HCl, 0.15 M NaCl; pH 7.5). Ten µL of concentrated cell suspension were smeared onto clean glass slides. The smears were dried and fixed in cold absolute methanol for 7 min at −20°C. After methanol removal, spermatozoa were washed in TBS and placed in a blocking solution overnight. The blocking solution consisted of 0.1 M glycine, 1% goat serum, 0.01% Triton X-100, 1% powdered non-fat dry milk, 0.5% bovine serum albumin (BSA) and 0.02% sodium azide in phosphate-buffered saline (PBS; Euroclone, Milan, Italy). After blocking, OB and OB-R staining were carried out overnight using anti-OB (A-20) and anti-OB-R (M-18) affinity-purified rabbit polyclonal antibodies (Santa Cruz Biotechnology Inc., Santa Cruz, CA, USA) diluted 1 : 100 in PBS containing 1% Triton X-100 (PBS-T).

The specificity of the immunostaining was proven using non-immune rabbit serum (DakoCytomation, Glostrup, Denmark) instead of specific antiserum or omission of the primary antibody.

Spermatozoa were then washed four times for 15 min in PBS-T and incubated for 4 h with goat anti-rabbit fluorescein isothiocyanate (FITC)-conjugated secondary antibody (Santa Cruz Biotechnology Inc.), diluted 1 : 100 in PBS-T. Slides were examined by conventional fluorescence analysis using a BX 51 microscope (Olympus, Sintak S.r.l., Corsico, Mi, Italy) equipped with dichroic mirror ultraviolet (DMU) filter set. Three hundred spermatozoa per slide were analysed by a combination of 488/650 nm emission wavelength (100× objective). Similar staining on histological slides of equine adipose tissue was used as positive control.

Western blot analysis

Swim-up purified spermatozoa were washed and centrifuged for 5 min at 5000*g* at room temperature and the pellet was shaken in lysis buffer (60 mM Tris-HCl (pH 6.8), 50 mM dithiothreitol (DTT), 2% sodium dodecyl sulfate (SDS), 10% glycerol, 1 mM of phenylmethylsulfonyl fluoride (PMSF) for 15 min. Protein concentration was evaluated using Bradford's assay and an equal quantity of proteins (20 µg) were diluted and boiled for 10 min in 2× Laemmli SDS buffer. Samples were electrophoresed on 10% SDS polyacrylamide gels and electroblotted onto 0.2 µm Bio-Rad nitrocellulose membranes using a Bio-Rad trans-blot electrophoretic cell and reagents (Bio-Rad Life Science, Segrate, Italy). The primary antibodies (anti-OB

(A-20) and anti-OB-R (M-18) affinity-purified rabbit polyclonal antibodies; Santa Cruz Biotechnology Inc.) were diluted 1 : 1000 in a solution containing 2% BSA, 0.01% NaN_3 in PBS and were incubated for 2 h at ~20°C and rinsed three times with PBS plus 0.05% Tween 20. Anti-β-actin antibody (ab8226; ABCAM, Cambridge, UK) was used to normalise the sample loading. The secondary antibody reactions were performed using Immun-Star goat anti-rabbit or goat anti-mouse AP Detection Kit reagents for western blot and ChemiDoc MP imager (Bio-Rad). Adipose tissue lysate was used as a positive sample and the negative control was swim-up sperm lysate immunodepleted with anti-OB or anti-OB-R after immunoprecipitation with protein A-G agarose.

Ob and Ob-R mRNA detection

Total RNA from equine adipose tissue, ejaculated spermatozoa after swim-up and immature spermatozoa from epididymides was isolated using TRIZOL reagent (Invitrogen Life Technologies Italia, Monza, Italy) following the manufacturer's protocol and according to Das *et al.* (2010). After treating the samples with DNase, RNA concentration and purity were measured using a NanoDrop Spectrophotometer (NanoDrop ND1000; Thermo scientific, Wilmington, DE, USA). Complementary DNA was synthesised from 500 ng of total RNA using TaqMan reverse transcription reagents (Applied Biosystems Italia, Monza, Italy). Conditions used were 25°C for 5 min, 42°C for 30 min and 85°C for 5 min. Qualitative PCR was performed using 1 µL of the obtained cDNA in 25 µL final volume with Jumpstart Taq ReadyMix under the following conditions: initial denaturation at 94°C for 2 min, 35 cycles at 94°C for 30 s (denaturation), 60°C for 30 s (annealing), 72°C for 2 min (elongation) and final elongation at 72°C for 5 min. PCR products were analysed by gel electrophoresis and visualised using an UV Gel Doc trans-illuminator (Bio-Rad). Equine-specific oligonucleotide primers were designed based on NCBI *Equus caballus* available sequences or on mammal multi-aligned sequences. Primers were used at 300 nM final concentration and their sequences are as follows: glycerhaldehyde-3-phosphate dehydrogenase (*GAPDH*): forward 5′-AGATC AAGAAGGTGGTGAAG-3′ and reverse 5′-TTGTCATACC AGGAAATGAGC-3′ (product size: 170 bp); leptin receptor (*Ob-R*): forward 5′-TCCAAGTCACATCTGGTGGA-3′ and reverse 5′-GGTAAAAGTGTTGGGCTGGA-3′ (product size: 154 bp); leptin (*Ob*): forward 5′-GCACTGTGGACCCCTG TGC-3′ and reverse 5′-TGGAGGAGACTGACTGCGTG-3′ (product size: 180 bp). Equine adipose tissue was employed as a positive control.

Experiment 2: capacitation and hyperactivation of equine spermatozoa assessed by motility, fluorescent staining and apoptosis

Sperm culture media

In this study, modified Whittens non-capacitating medium (MW; 100 mM NaCl, 4.7 mM KCl, 1.2 mM $MgCl_2$, 5.5 mM glucose anhydrous, 22 mM 2-[4-(2-hydroxyethyl)piperazin-1-yl]ethanesulfonic acid buffer (HEPES), 4.8 mM lactic acid hemicalcium salt and 1.0 mM pyruvic acid; Travis *et al.* 2004) was used. To obtain capacitating conditions, non-capacitating MW base medium was supplemented with 25 mM $NaHCO_3$ and 7 mg mL^{-1} BSA. This medium was called capacitating medium (CM). For both media the final pH was 7.25.

Another medium used in this study was FF. Follicular fluid was drawn from preovulatory follicles of mares' ovaries during oestrus collected at the local abattoir. Assessment of the diameter of the follicle (~4.5 cm) along with visual analysis of the presence of uterine endometrial folds and the value of circulating progesterone (<1 ng mL^{-1}) confirmed that mares were in oestrus. Pooled FF was centrifuged (1300*g*, 10 min, room temperature) to remove cells and then frozen at −80°C until P assays were performed. Progesterone concentration was determined on pooled FF using a quantitative test based on the enzyme-linked fluorescent assay (ELFA) technique (Mini-Vidas; bioMérieux Italia S.p.A., Florence, Italy; Anckaert *et al.* 2002).

Other media employed in this study were: CM supplemented with 10 ng mL^{-1} recombinant human OB (Sigma), CM supplemented with 200 ng mL^{-1} P (Sigma) and CM supplemented with 10 ng mL^{-1} OB and 200 ng mL^{-1} P.

Recombinant human OB was used because, after multiple sequence alignment studies, this OB was most similar to horse OB.

Semen preparation

Preparation of fresh semen was performed as previously reported (McPartlin *et al.* 2009) with some modifications. Sperm motility and concentration of each sample diluted in pre-warmed non-capacitating MW and kept at 37°C were analysed by computer-assisted semen analysis (CASA). A customised CASA system was assembled with an Olympus BX 51 microscope fitted with a warming stage, negative-phase contrast optics (20× objective and 10× ocular) and a Basler (model A6021–2; Sintak S.r.l., Corsico, Mi, Italy) video camera interfaced with a computer to digitise and analyse the image. The software used for image acquisition and analysis was Image-Pro Plus 5.1-Media Cybernetics (Immagini and Computer, Bareggio, Milano, Italy).

The instrument setting for computerised semen analysis is reported in Table 1.

An aliquot of 5 µL of diluted semen was pipetted into a pre-warmed 20-µm depth counting chamber (Cell-Vu Chambers; Fertility Technologies Inc., IMV, Piacenza, Italy). Sperm motility

Table 1. Instrument setting for computerised semen analysis

Parameter	Value
Number of frames to analyse	20 frames
Sampling frequency	30 frames s^{-1}
Minimum sampling points for motility	1 point
Minimum sampling points for velocity	3 points
Maximum velocity	150 µm s^{-1}
Threshold velocity	8 µm s^{-1}
Minimum sampling points for calculating AHL	7 points
Minimum velocity for calculating AHL	20 µm s^{-1}
Minimum linearity for calculating AHL	3.5 µm
Pixel scale	0.688 µm per pixel
Cell size range	4–15 pixel

was assessed within 20 s. For each sample, 10 microscope fields were analysed. Some parameters were measured directly on the digital images (velocity parameters and movements of the head) whilst others were calculated from the measurements, e.g. straightness of movement and the percentage of motile or progressively motile spermatozoa. The cell track was reconstructed on sequential digital images by the accompanying software.

Apoptotic rate

The percentage of apoptotic spermatozoa was assessed using an annexin-V-FITC apoptosis detection kit (Sigma Aldrich Chemical, Milano, Italy) following the manufacturers' instructions. Samples were analysed every 2 h from 0 h to 6 h of incubation under capacitating conditions: (1) CM, (2) FF, (3) CM supplemented with OB (10 ng mL^{-1}), (4) CM supplemented with P (200 ng mL^{-1}) or (5) CM supplemented with OB+P (10 ng mL^{-1} and 200 ng mL^{-1}, respectively). Reactions were performed on 500 µL of semen. Three hundred spermatozoa were analysed using a combination of 488/560 nm emission. Spermatozoa at the early stage of apoptosis stained positively only for the annexin V-FITC, necrotic spermatozoa for propidium iodide (PI) and annexin V-FITC and live spermatozoa did not stain positively for either PI or annexin V-FITC.

Capacitation of spermatozoa

Pooled samples of ejaculated spermatozoa from three stallions, in triplicate, were centrifuged in 15-mL conical tubes at 100*g* for 1 min at 37°C to remove particulate matter and dead spermatozoa. The supernatant was transferred to a 14-mL round-bottom centrifuge tubes and centrifuged at 600*g* for 5 min at 37°C. The pellet of pooled spermatozoa was resuspended in CM to a final concentration of 10×10^6 spermatozoa mL^{-1} and 500-µL aliquots were incubated for 6 h in polyvinyl alcohol-coated 5-mL round-bottom tubes (Holmquist 1982) at 37°C in a humidified air atmosphere.

Hyperactivation of spermatozoa

Hyperactivation of spermatozoa resuspended in CM was induced by incubation for an additional 6 h in different media: (1) CM (control, CTR), (2) FF, (3) CM supplemented with OB (10 ng mL^{-1}), (4) CM supplemented with P (200 ng mL^{-1}) or (5) CM supplemented with OB+P (10 ng mL^{-1} and 200 ng mL^{-1}, respectively). For each condition the final cell concentration was standardised to 1×10^6 spermatozoa mL^{-1} and sperm motility was analysed by CASA every 2 h from 0 h to 6 h of incubation. In addition to the percentage of motile spermatozoa, five motility parameters were evaluated: the average path velocity (VAP, µm s^{-1}; the average velocity of the smoothed cell path), the straight-line velocity (VSL, µm s^{-1}; the average velocity measured in a straight line from beginning to end of the track), the amplitude of lateral head displacement (ALH, µm; the mean width of head oscillations), the straightness (STR, %; the average value of the ratio VSL/VAP × 100) and the linearity index (LIN, %; the average value of the ratio VSL/VCL × 100).

First, a dose-response study on the effects of recombinant human OB on spermatozoa was performed in order to identify the best concentration of this hormone to be used for the subsequent experiments. Spermatozoa were incubated in CM supplemented with OB at different concentrations, from 0 to 50 ng mL^{-1} at 5 ng mL^{-1} increments. Sperm motility assessment, fluorescent staining (FITC-conjugated peanut agglutinin and propidium iodide (FITC–PNA/PI)) for viability and acrosome reaction and apoptotic rate evaluation were performed every 2 h from 0 h to 6 h after treatments.

The following experiments were performed using OB at 10 ng mL^{-1} based on the optimal results obtained for motility, viability, acrosome reaction and the lower response of apoptotic rate (data not shown).

Fluorescent staining (FITC–PNA/PI) for viability and acrosome reaction

FITC-conjugated peanut agglutinin (FITC–PNA) was used to determine the acrosome status of viable spermatozoa under all the conditions of hyperactivation tested: (1) CM, (2) FF, (3) CM supplemented with OB (10 ng mL^{-1}), (4) CM supplemented with P (200 ng mL^{-1}) and (5) CM supplemented with OB+P (10 ng mL^{-1} and 200 ng mL^{-1}, respectively). Propidium iodide staining was used to detect apoptotic spermatozoa. FITC–PNA intensely labelled the acrosome region of acrosome-reacted spermatozoa (green), whereas PI stained the head of dead spermatozoa (red). Evaluation was performed every 2 h from 0 h to 6 h of incubation. Briefly, 500 µL of semen were diluted in HEPES–BSA solution (130 mM NaCl, 4 mM potassium chloride, 14 mM fructose, 10 mM HEPES, 1 mM calcium chloride, 0.5 mM magnesium chloride, 0.1% BSA) to reach the concentration of 15×10^6 spermatozoa mL^{-1}. Samples were then incubated with 2.5 µL propidium iodide (1 µg mL^{-1}) and 2.5 µL FITC–PNA (1 µg mL^{-1}) at 37°C for 5 min under light-proof conditions. Spermatozoa were fixed in 10% formalin solution. Three hundred spermatozoa per slide were immediately examined using an Olympus BX 51 microscope equipped with DMU filter set using a simultaneous combination of excitation and emission filters at 488/650 nm at 100× magnification.

Experiment 3: in vitro *fertilisation*

Recovery and maturation of oocytes

Ovaries were obtained during the natural reproductive season (from March to August) immediately after slaughter, maintained at 30°C in PBS supplemented with antibiotics (100 IU mL^{-1} penicillin and 100 µg mL^{-1} streptomycin sulfate) and processed within 6 h of slaughtering. Cumulus–oocyte complexes (COCs) were harvested by scraping the surface of obvious follicles. Only compact cumulus oocytes (CCOs) with at least three layers of cumulus cells were assigned for *in vitro* maturation (IVM). CCOs were washed three times in basic TCM199 medium with Earle's salts, buffered with 4.43 mM HEPES, supplemented with 10% fetal bovine serum and 25 µg mL^{-1} gentamicin (M199). IVM was performed following the method previously described (Dell'Aquila *et al.* 2003). Medium TCM-199 with Earle's salts, buffered with 4.43 mM HEPES and 33.9 mM sodium bicarbonate and supplemented with 0.1 g L^{-1} L-glutamine, 2 mM sodium pyruvate, 2.92 mM calcium-L-lactate pentahydrate (Fluka 21175 Serva Feinbiochem GmbH and Co, Milano, Italy) and 50 µg mL^{-1} gentamicin was used. pH was adjusted to 7.18

and the medium was filtered through 0.22-μm filters (Lida Manufacturing Corp, Dix Hills, NY, USA) and stored at 4°C until use (for a maximum of 1 week). On the day of IVM, the medium was further supplemented with 20% (v/v) fetal calf serum. Then, gonadotrophins (10 μg mL^{-1} ovine FSH and 20 μg mL^{-1} ovine LH) and 1 μg mL^{-1} 17β-oestradiol were added. The medium was re-filtered and equilibrated for 1 h under 5% CO_2 in air before use. Compact COCs were washed three times in the culture medium and groups of up to 10 COCs were placed in 400 μL of medium per well of a four-well dish (Nunc Intermed, Euroclone, Milano, Italy), covered with pre-equilibrated lightweight paraffin oil and cultured for 29 h at 38.5°C under 5% CO_2.

The protocol for oocyte maturation was standardised in our laboratory and, as reported by Lange-Consiglio *et al.* (2009), the maturation rate of compact cumulus oocytes reached 43–45%.

In vitro *fertilisation*

Spermatozoa (10×10^6 mL^{-1}) were pre-incubated for 6 h in CM, then diluted to 1×10^6 spermatozoa mL^{-1} with: (1) CM, (2) FF, (3) CM supplemented with OB (10 ng mL^{-1}), (4) CM supplemented with P (200 ng mL^{-1}) or (5) CM supplemented with OB+P (10 ng mL^{-1} and 200 ng mL^{-1}, respectively). A sample of semen was pre-incubated in non-capacitating medium for 6 h and then diluted in each of the five media mentioned above and used for IVF.

Five mature mare oocytes were transferred into droplets of 100 μL of each sperm suspension and incubated for 18 h at 38.5°C in 5% CO_2. Oocytes were then transferred into Dulbecco's Modified Eagle Medium: Nutrient Mixture F-12 (DMEM/F-12) for three days to evaluate the rate of embryo development. For each experimental condition, a sperm-free control was performed to assess parthenogenesis. The presence of two pronuclei and a sperm tail before cleavage were evaluated, on a sample of oocytes, at the end of IVF by aceto–orcein stain (1% orcein in 45% acetic acid, followed by aceto-glycerol (glycerol 20%, acid acetic 20%, distilled water 60%)). Moreover, cleavage was evaluated by Hoechst staining on a sample of oocytes after 24 h of co-incubation with spermatozoa.

Oocytes were considered fertilised if one or more decondensing sperm heads or pronuclei were observed, or if they cleaved to the two-cell stage. Degenerating oocytes containing no chromatin or fragmented chromatin, and oocytes that failed to mature to metaphase II were not counted in the assessment of fertilisation rates.

Statistical analysis

The experiments on semen were repeated three times on pooled ejaculates from three stallions. The values reported represent the mean values. The IVF study was repeated four times. Data were analysed by one-way ANOVA with post-test using standard parametric methods through a system of linear model analysis of variance. When significant differences ($P < 0.05$) were detected, the Student–Newman–Keuls method was applied to assess all pair-wise multiple comparisons.

The statistical analyses were carried out using GraphPad Instat 3.00 for Windows (GraphPad Software, La Jolla, CA, USA).

Results

Experiment 1: detection of OB and OB-R on equine spermatozoa by immunocytochemistry, western blot analysis and molecular biology

Leptin OB and OB-R localisation and expression in equine spermatozoa

OB and OB-R were weakly detected in ejaculated spermatozoa in the post-acrosomal region and in the middle piece of equine spermatozoa (Fig. 1*a*). The adipose tissue, used as positive control, stained positively for both OB and OB-R (Fig. 1*b*). The negative controls demonstrated no immunoreactivity.

At mRNA level, *Ob* was detected in ejaculated spermatozoa but reverse transcription–polymerase chain reaction (RT-PCR) failed to detect signal for the *Ob-R* transcripts in the same samples (Fig. 1*c*). *Ob* and *Ob-R* expression was confirmed in immature spermatozoa collected from the head of the epididymis (Fig. 1*d*).

Western blot analysis

The presence of OB protein in equine spermatozoa was also investigated by western blotting. A single band at 16 kDa was observed in the lysate obtained from equine sperm samples, corresponding to that observed in the adipocyte extract used as positive control (Fig. 2*a*). Some weakly immunoreactive bands associated with different isoforms were obtained for OB-R. For this protein, one main band corresponding to the molecular weight of 90 kDa was also found (Fig. 2*b*).

Experiment 2: capacitation and hyperactivation of equine spermatozoa assessed by motility, fluorescent staining and apoptosis

To evaluate the effects of P in our experimental settings, we measured the levels of P in FF. The mean concentration of P evaluated by quantitative test was 200 ng mL^{-1}.

Apoptotic rate

There was no effect on the apoptotic rate of spermatozoa after 6 h of incubation in FF, OB or P when compared with those in CM, demonstrating no cytotoxic effect (Table 2).

Hyperactivation of spermatozoa

The addition of different media to stallion spermatozoa at 0 h induced an immediate change in motility. This change was characterised by the decrease ($P < 0.05$) of VSL, STR and LIN, increase of AHL ($P < 0.05$) and onset of circling motion. After 6 h incubation in the tested media, spermatozoa were slower compared with those incubated in CM medium, showing a further decrease ($P < 0.05$) in VSL, STR and LIN. (Table 3).

Fluorescent staining (FITC–PNA/PI) for viability and acrosome reaction and apoptosis

Immunofluorescent patterns of vitality and acrosome reaction staining of equine spermatozoa are shown in Table 4. As determined by FITC–PNA/PI staining, at the beginning of incubation on average 66.1%, 61.6%, 61.11%, 60.3% and 60.8% of viable spermatozoa were detected in CM, FF, CM

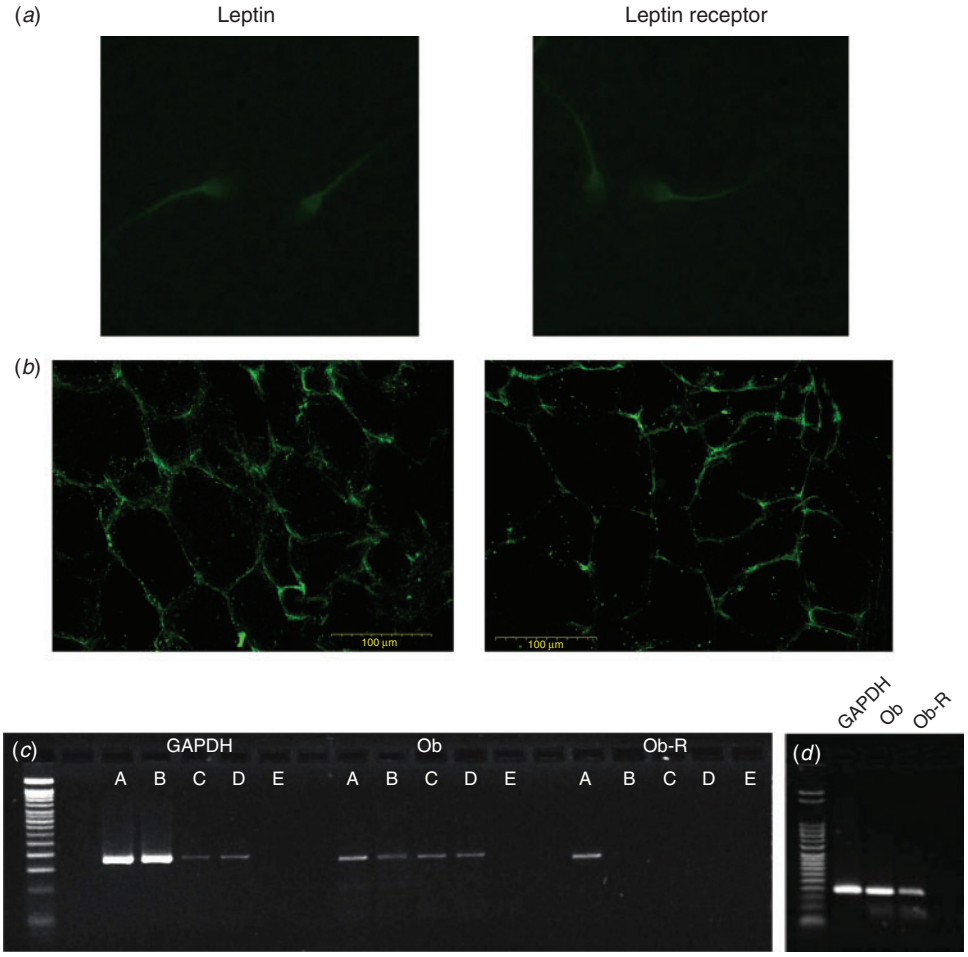

Fig. 1. Immunocytochemistry and molecular expression of leptin (OB) and leptin receptor (OB-R). (*a*) Immunolocalisation in the post-acrosomal region and in the tail in equine ejaculated spermatozoa. (*b*) Immunolocalisation of OB and OB-R in equine adipose tissue used as control. Magnification 20×. (*c*) *Ob* and *Ob-R* expression at mRNA level in equine spermatozoa. Signal for *GAPDH* (employed as reference gene) and leptin transcripts observed in: A, adipose tissue (positive control); B, total ejaculate; C, spermatozoa after swim-up; D, spermatozoa after swim-up and following 6 h of incubation with exogenous leptin; E, blank. (*d*) *GAPDH*, *OB* and *OB-R* transcripts observed in immature spermatozoa from head of epididymis. Marker: 100 bp.

with OB, CM with P and CM with OB+P, respectively, with no significant difference between media. Following 6 h incubation, sperm viability progressively decreased to 48.8%, 26.3%, 14.3%, 29.7% and 25.5%, respectively. The effects in each sample differed significantly from the control.

The initial percentage of AR in live equine spermatozoa at Time 0 of incubation was 10.7%, 11.4%, 9.2%, 10.5% and 12.7% in CM, FF, CM with OB, CM with P and CM with OB+P, respectively. No significant difference was found between the different culture conditions. After 6 h of incubation, the number of capacitated spermatozoa, expressed as live acrosome-reacted (AR), increased significantly ($P < 0.05$) reaching the percentages of 44.6%, 35.3%, 46.1% and 44.8% respectively in FF, CM with OB, CM with P and CM with OB+P. In CM, the percentage of AR spermatozoa remained constant until the last time point. In FF the highest percentage of live AR spermatozoa was achieved after 4 h of incubation, when the percentage of dead spermatozoa was lower. The incidence of AR spermatozoa in the OB-treated sample was lower and significantly different from FF, P and OB combined with P.

Experiment 3: in vitro *fertilisation*

Fertilisation was confirmed by either pronuclear formation (Fig. 3) or cleavage to the two-cell stage. The fertilisation rates obtained were 51% ± 4.83% (26/51 oocytes) for IVF with FF, 46.15% ± 3.18% (24/52) with P and 43.64% ± 3.63% (24/55) with OB+P. No fertilisation was achieved using OB (0/55) or CM (0/42). Our IVF setting only allowed for the attainment of eight-cell stage embryos, which were obtained when combining the capacitating conditions with the induction of hyperactivation. The eight-cell stage embryos were produced in four independent replicates at the following rates: 18.7 ± 1.9% using FF, 17.1% ± 1.15 with P and 16.7% ± 0.51 with OB+P. Spermatozoa incubated in OB alone and in the other conditions (in CM

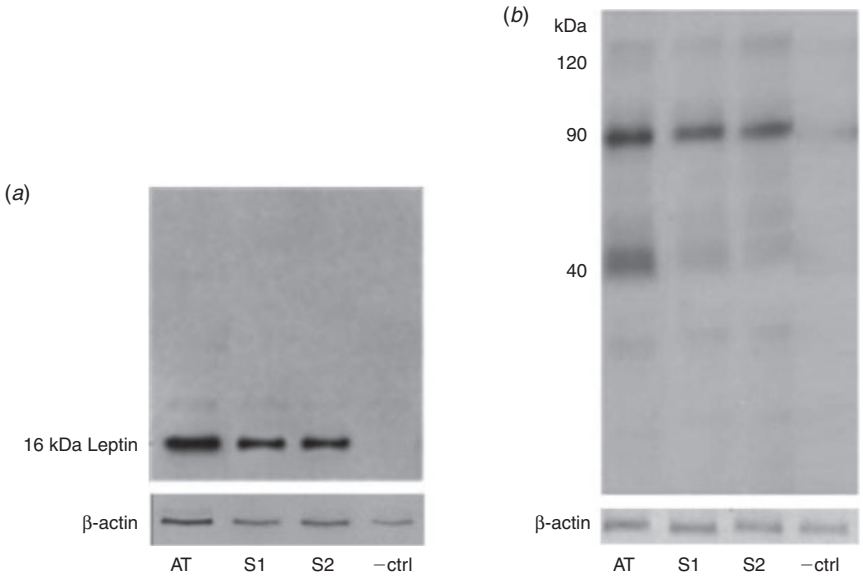

Fig. 2. Western blot to assess the presence of (*a*) OB and (*b*) OB-R on two horse sperm samples (S1, S2). Adipose tissue (AT) lysate was used as positive control and sperm lysate immunodepleted of OB or OB-R was employed as negative control (−ctrl). β-actin represents the reference marker.

Table 2. Percentage of apoptotic spermatozoa after exposure to different capacitation media

Data are expressed as mean ± s.e.m. Different small letter superscripts (^{a,b,c}) indicate statistically significant differences ($P < 0.05$) between rows. Different capital letter superscripts (^{A,B,C,D}) indicate statistically significant differences ($P < 0.05$) between columns. CM, capacitating medium; FF, follicular fluid; P, progesterone; OB, leptin

Time of exposure (h)	CM	CM + FF	CM + P	CM + OB	CM + OB+P
0	16 ± 0.6^{acA}	18 ± 0.4^{bA}	16 ± 0.6^{acA}	15 ± 0.3^{aA}	17 ± 0.6^{cA}
2	17 ± 0.5^{aAB}	16 ± 1.1^{aA}	16 ± 0.3^{aA}	18 ± 1.7^{aA}	17 ± 0.7^{aA}
4	18 ± 0.8^{aB}	17 ± 1.3^{aA}	$18. \pm 1.7^{aA}$	23 ± 2.3^{bB}	19 ± 0.6^{aB}
6	21 ± 0.7^{aC}	18 ± 0.4^{aA}	17 ± 0.8^{bcA}	25 ± 2.9^{dB}	20 ± 0.5^{abB}

alone, or in non-capacitating medium supplemented with FF, OB, P or OB+P), did not fertilise oocytes (Table 5, Fig. 4) as demonstrated by the Hoechst staining. These data are net of the rate of parthenogenesis that was ~6% in each experimental condition, as calculated on test sample oocytes.

Discussion

In this study, we investigated whether OB and OB-R were detectable in equine spermatozoa. Immunocytochemical analysis detected the presence of OB and OB-R in the post-acrosomal region, as well as in the middle piece of equine spermatozoa. Antibody specificity was supported by the positive controls on equine adipose tissues. The western blot analysis supported this result. At the molecular level, however, the expression of *Ob-R* was only confirmed in ejaculated spermatozoa, leading us to speculate that *Ob-R* transcription stops during sperm maturation. This suggests that the presence of protein is mainly due to the translation process occurring during the earlier stages of spermatogenesis. The expression of *Ob-R* found in immature spermatozoa collected from the head of the epididymis confirmed our hypothesis.

The expression pattern of one isoform at 90 kDa, observed in this study, is different from that reported for pig spermatozoa by Aquila *et al.* (2008), who observed different isoforms, and by De Ambrogi *et al.* (2007), who demonstrated one isoform at 382 bp, although Aquila *et al.* (2008) claim that the pattern of OB-R expression is species-specific.

To our knowledge, this is the first study reporting the presence of OB and OB-R mRNA in equine ejaculated spermatozoa. Aquila *et al.* (2005*b*) were the first to demonstrate direct production of OB by human ejaculated spermatozoa, indicating that spermatozoa are effective in secreting OB, despite their supposed inability to translate transcripts. In contrast to Grunewald *et al.* (2005), Aquila *et al.* (2005*a*) proposed that some of these transcripts could encode for proteins that are essential in early embryo development. More recently, the presence of OB mRNA was also detected in bull spermatozoa (Abavisani *et al.* 2011), supporting the idea that spermatozoa are able to transcribe *Ob* and translate it.

As demonstrated in pig spermatozoa, OB affects both the capacitation and acrosome reactions through its receptor (Aquila *et al.* 2008). After detecting OB and OB-R in ejaculated spermatozoa by immunocytochemistry and gene expression, we investigated its effect alone or in combination with P in the challenging settings of equine IVF to gain a deeper understanding of the involvement of OB in equine IVF. Results were then compared with those obtained when *in vitro* capacitation was induced using FF conditions.

Based on analysis of the motion parameters currently used to define hyperactivated motility in other species (Mortimer and

Table 3. Stallion sperm hyperactivation in different capacitation media at two set times

Data are expressed as mean ± s.e.m. Different small letter superscripts (^{a,b}) indicate statistically significant differences ($P < 0.05$) between 0 h and 6 h in each medium. Different capital letter superscripts (^{A,B}) indicate statistically significant differences ($P < 0.05$) at 6 h between CM and other media. CM, capacitating medium; FF, follicular fluid; P, progesterone; OB, leptin; VAP, average path velocity; VSL, straight-line velocity; AHL, average lateral head; STR, straightness; LIN, linearity index

Medium employed	VAP (μm s^{-1})		VSL (μm s^{-1})		AHL (μm)		STR (%)		LIN (%)	
	0 h	6 h	0 h	6 h	0 h	6 h	0 h	6 h	0 h	6 h
CM	141.5 ± 4.8^{a}	124.2 ± 9.2^{bA}	87.4 ± 9.4^{a}	67.6 ± 5.3^{bA}	6.1 ± 0.2^{a}	6.3 ± 0.8^{bA}	61.8 ± 0.3^{a}	54.0 ± 0.5^{bA}	34.3 ± 0.3^{a}	29.1 ± 0.1^{bA}
FF	167.3 ± 13.8^{a}	110.1 ± 9.5^{bB}	66.9 ± 6.9^{a}	40.5 ± 4.1^{bB}	7.6 ± 0.4^{b}	10.4 ± 0.9^{bB}	40.0 ± 0.7^{a}	36.7 ± 0.4^{bB}	19.7 ± 0.1^{a}	$17.2 \pm 0.2b^{B}$
CM + P	161.1 ± 5.6^{a}	113.4 ± 4.3^{bB}	63.2 ± 5.3^{a}	42.3 ± 4.0^{bB}	7.4 ± 0.6^{b}	9.4 ± 0.8^{bB}	39.2 ± 1.3^{a}	38.2 ± 1.5^{aB}	21.3 ± 0.7^{a}	$19.4 \pm 0.2b^{B}$
CM + OB	135.0 ± 6.2^{a}	115.6 ± 10.1^{bB}	85 ± 5.8^{a}	47.7 ± 3.8^{bB}	8.0 ± 0.5^{b}	9.9 ± 0.5^{bB}	63.0 ± 0.2^{a}	41.2 ± 0.2^{bB}	31.0 ± 0.2^{a}	$23.0 \pm 0.1b^{B}$
CM + OB+P	164.2 ± 4.2^{a}	112.2 ± 5.9^{bB}	64.3 ± 3.2^{a}	43.4 ± 4.2^{bB}	7.2 ± 0.6^{b}	10.4 ± 1.0^{bB}	38.6 ± 0.3^{a}	37.7 ± 0.8^{aB}	22.5 ± 0.5^{a}	$18.9 \pm 0.5b^{B}$

Table 4. Fluorescent staining (FITC–PNA) for acrosome reaction (AR) in different capacitation media

Data are expressed as mean ± s.e.m. Different small letter superscripts (^{a,b,c}) indicate statistically significant differences ($P < 0.05$) between rows. Different capital letter superscripts (^{A,B,C,D}) indicate statistically significant differences ($P < 0.05$) between columns. CM, capacitating medium; FF, follicular fluid; P, progesterone; OB, leptin

Type of spermatozoa	Time of exposure (h)	CM	CM + FF	CM + P	CM + OB	CM + OB+P
Viable	0	66.1 ± 3.5^{aA}	61.6 ± 4.3^{aA}	60.3 ± 3.4^{aA}	61.1 ± 4.2^{aA}	60.8 ± 2.9^{aA}
	2	62.1 ± 4.7^{aAC}	52.7 ± 3.6^{bA}	54.6 ± 2.9^{bA}	49.4 ± 3.6^{bB}	51.7 ± 3.7^{bA}
	4	54.2 ± 4.6^{aBC}	26.9 ± 3.2^{bB}	28.3 ± 3.1^{bB}	34.3 ± 2.8^{bC}	27.4 ± 4.1^{bB}
	6	48.8 ± 2.7^{aB}	26.3 ± 5.6^{bB}	29.7 ± 3.7^{bB}	14.3 ± 1.7^{bD}	25.5 ± 3.5^{bB}
Viable with AR	0	10.7 ± 2.0^{aA}	11.4 ± 1.2^{aA}	10.7 ± 1.6^{aA}	9.2 ± 2.1^{aA}	12.7 ± 1.8^{aA}
	2	14.6 ± 2.6^{aA}	15.4 ± 2.6^{aA}	18.5 ± 3.6^{aB}	15.9 ± 1.7^{aB}	16.7 ± 1.4^{aB}
	4	16.0 ± 4.1^{aA}	48.4 ± 1.7^{bB}	47.4 ± 1.8^{bcC}	25.3 ± 2.9^{dC}	35.6 ± 1.5^{eC}
	6	15.8 ± 5.0^{aA}	44.6 ± 2.6^{bB}	46.4 ± 2.0^{bC}	35.0 ± 3.0^{cD}	44.8 ± 1.9^{bD}
Dead	0	10.7 ± 1.7^{aA}	13.6 ± 3.0^{aA}	12.7 ± 1.6^{aA}	12.5 ± 1.9^{aA}	13.0 ± 1.0^{aA}
	2	9.2 ± 0.8^{aA}	17.3 ± 1.7^{bcA}	13.5 ± 1.6^{bA}	16.3 ± 2.1^{bcA}	17.9 ± 1.9^{cB}
	4	12.2 ± 1.0^{aAC}	12.9 ± 1.4^{aA}	13.7 ± 1.7^{abA}	16.0 ± 1.7^{abA}	17.0 ± 1.7^{bB}
	6	15.3 ± 2.9^{aBC}	14.3 ± 3.7^{aA}	11.6 ± 1.0^{aA}	27.0 ± 2.9^{bB}	16.1 ± 1.9^{aAB}
Dead with AR	0	12.4 ± 2.1^{aA}	13.4 ± 1.3^{abA}	16.4 ± 1.9^{abA}	17.1 ± 1.6^{bA}	13.5 ± 1.2^{abA}
	2	14.0 ± 2.0^{aAC}	14.7 ± 2.8^{aA}	13.4 ± 1.0^{aAC}	18.4 ± 2.9^{aA}	13.6 ± 0.7^{aA}
	4	17.6 ± 2.3^{aBC}	11.8 ± 1.5^{bA}	10.7 ± 2.0^{bBC}	24.3 ± 2.9^{cB}	20.0 ± 1.8^{aB}
	6	20.1 ± 1.4^{aB}	14.8 ± 3.0^{bA}	10.6 ± 1.7^{bBC}	23.7 ± 2.0^{cB}	13.5 ± 1.1^{bA}

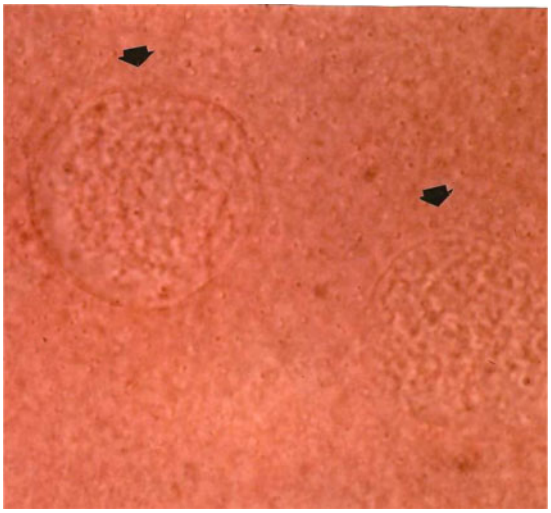

Fig. 3. Acteo–orcein stain showing presence of two pronuclei. The arrow at the left indicates the female pronucleus and the arrow at the right the male pronucleus.

Mortimer 1990; Suarez *et al.* 1992; Ho and Suarez 2001; Marquez and Suarez 2004, 2007; Baumber and Meyers 2006; Marquez *et al.* 2007), incubation with FF, OB, P or OB+P significantly affected stallion sperm motility. Stallion spermatozoa can be defined as hyperactivated when VSL <46.5 μm s^{-1}, STR <46.6% and LIN <20.2% are detected (McPartlin *et al.* 2009). As shown in this study, sperm tracks shortened, became more curved and the decrease in VSL, LIN and STR was consistent with the acquisition of hyperactivation.

Although the ability of FF to induce capacitation and motility changes has already been established, as well as the potential of P to increase the permeability of the plasma membrane to calcium (Thérien and Manjunath 2003), there is no evidence of the involvement of OB in equine sperm hyperactivation and fertilisation. Despite a claim by Li *et al.* (2009) that OB had no significant effect on ejaculated human sperm motility, our study suggests a regulatory role of OB signalling in sperm motility. This hypothesis comes from the expression of OB-R observed in the middle piece of equine spermatozoa, which is the region that mainly contributes to sperm motility.

Table 5. Development to eight-cell stage embryos

Data are expressed as mean ± s.e.m. Values labelled with different letters are statistically different ($P < 0.05$). CM, capacitating medium; FF, follicular fluid; P, progesterone; OB, leptin; non-CM, non-capacitating medium

Replicate	CM (%)	CM + FF (%)	CM + P (%)	CM + OB (%)	CM + OB+P (%)	Non CM + FF (%)	Non CM + P (%)	Non CM + OB (%)	Non CM + OB+P (%)
1	0/10 (0.0)	4/19 (21.1)	3/18 (16.7)	0/22 (0.0)	5/29 (17.2)	0/11 (0.0)	0/12 (0.0)	0/13 (0.0)	0/11 (0.0)
2	0/12 (0.0)	4/24 (16.7)	5/27 (18.5)	0/25 (0.0)	4/25 (16.0)	0/10 (0.0)	0/14 (0.0)	0/10 (0.0)	0/12 (0.0)
3	0/13 (0.0)	4/21 (19.1)	3/19 (15.8)	0/18 (0.0)	4/24 (16.7)	0/10 (0.0)	0/12 (0.0)	0/11 (0.0)	0/13 (0.0)
4	0/13 (0.0)	3/17 (17.7)	4/23 (17.4)	0/20 (0.0)	3/18 (16.7)	0/12 (0.0)	0/9 (0.0)	0/10 (0.0)	0/11 (0.0)
Average	0.0 ± 0.0	18.65 ± 1.9[a]	17.1 ± 1.2[a]	0.0 ± 0.0	16.7 ± 0.5[a]	0.0 ± 0.0	0.0 ± 0.0	0.0 ± 0.0	0.0 ± (0.0)

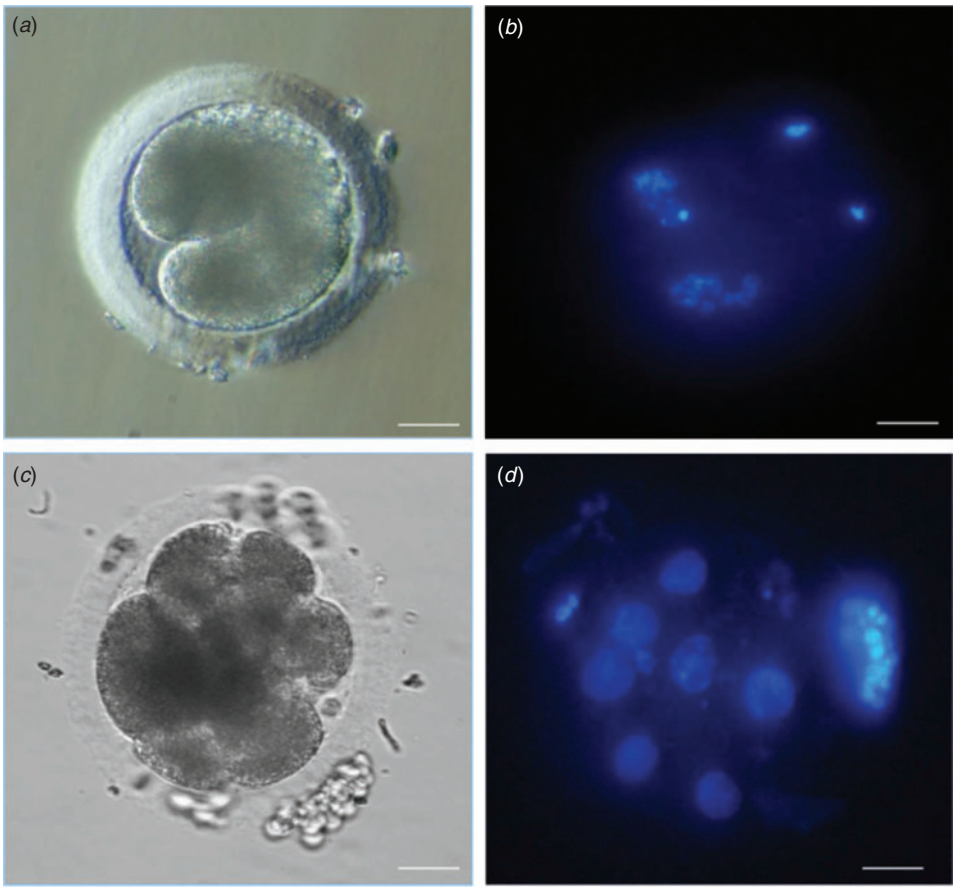

Fig. 4. Representative *in vitro* fertilised mare oocytes. (*a*) Light microscopy of two-cell stage embryos (Day 1). (*b*) Hoechst 33258 staining showing two pronuclei. (*c*) Light microscopy of eight-cell stage embryo (Day 3). (*d*) Hoechst 33258 staining showing eight pronuclei. Original magnification 20×. Scale bars represent 20 µm.

Capacitation is not only associated with hyperactivation, but also with the acquired capability of spermatozoa to undergo the acrosome reaction after binding to the zona pellucida. Following incubation in FF, in CM supplemented with OB, P or OB+P, the number of capacitated spermatozoa (expressed as live acrosome-reacted) increased significantly ($P < 0.05$). After 6 h of incubation, these percentages reached 44.6% for FF, 35.3% for OB, 46.1% for P and 44.8% for OB+P. Conversely, in CM alone, the rate of AR spermatozoa remained constant over time. According to Cheng *et al.* (1998), P alone or combined with OB increased the proportion of physiological AR spermatozoa to the same level as FF, in contrast to the effects of OB alone. Moreover, our results showed that spermatozoa pre-incubated in CM for 6 h and then exposed to fertilising medium supplemented with FF, P or OB+P for 18 h, were able to fertilise oocytes, leading to eight-cell stage embryo development at the rate of 18.7%, 17.1% and 16.7%, respectively. On the other hand, spermatozoa in medium supplemented with OB did not fertilise any oocytes.

It can be argued that P facilitated IVF by promoting both hyperactivation and the acrosome reaction. Many studies report that this hormone, secreted by cumulus cells and contained in FF, induces AR in human (Meizel and Turner 1991; Baldi *et al.* 1998), mouse (Roldan *et al.* 1994), boar (Melendrez *et al.* 1994), stallion (Meyers *et al.* 1995; Cheng *et al.* 1998), golden hamster (Llanos and Anabalón 1996), dog (Brewis *et al.* 2001) and caprine (Somanath *et al.* 2000) spermatozoa. Progesterone also affects human sperm capacitation (Foresta *et al.* 1992; Uhler *et al.* 1992; Luconi *et al.* 1995) and increases the ability of mouse spermatozoa to respond to the zona pellucida (Roldan *et al.* 1994). Steroid effects are mediated by proteins acting as receptors on the cell surface (Meizel and Turner 1991). The acrosome reactions produced by the exposure of capacitated spermatozoa to P could explain the rate of penetration in our IVF setting. Thus, because neither incubation of spermatozoa in capacitation conditions alone nor the treatment of non-capacitated spermatozoa with P supported IVF in our experiments, these results additionally support the hypothesis that the pre-incubation step in capacitation medium is required for the activation of functional receptors evoked by P binding. As reported by McPartlin *et al.* (2009), these results support the hypothesis that capacitation and hyperactivation are separate and independent events. Regarding OB, our results are in agreement with those reported for capacitation and acrosome reaction in pig spermatozoa (Aquila *et al.* 2008), although the rate of AR spermatozoa was lower compared with that obtained with P. The AR rate was calculated on live spermatozoa after OB treatment, highlighting the effect of OB compared with the control. In any case, after IVF no sperm penetration occurred and, therefore, no embryo was obtained.

It has been demonstrated that pig seminal plasma contains a significant amount of OB and that this amount is lower in FF (Lackey *et al.* 2002). As spermatozoa leave seminal plasma during transit in the female reproductive tract, they are exposed to decreased OB concentrations. Aquila *et al.* (2008) speculated that the high OB concentrations in seminal plasma might contribute to maintenance of spermatozoa in a quiescent metabolic condition. Conversely, the low OB concentrations in the secretions of the female pig reproductive tract (Gregoraszczuk *et al.* 2004) could induce sperm activation by facilitating their capacitation and acquisition of fertilising ability. Previous results from our laboratory indicate that supplementation with OB in the range between 10 and 1000 ng mL^{-1} increases the maturation rate of equine oocytes and enhances the fertilisation rate after intracytoplasmic sperm injection (ICSI), thus confirming the stimulatory effect of OB on oocyte quality and fertilisation rate after ICSI (Lange-Consiglio *et al.* 2009). Based on this information, OB supplementation would be expected to have a positive influence in standard equine IVF. Since no embryos were obtained, this hypothesis remains open to question. It is possible to speculate that although previous experiments suggested an optimal concentration of 10 ng mL^{-1} (data not shown), this dosage was not able to support oocyte fertilisation in the co-culture system. Recently, we evaluated OB levels in mare preovulatory FF (Lange-Consiglio *et al.* 2013) and, in that case, concentrations ranged between 3.36 and 5.72 ng mL^{-1} in adult Standardbred and draft mares, respectively, but, by the dose response in this study, the same concentrations did not activate equine spermatozoa *in vitro*. It remains to be seen whether interaction between the OB-R on spermatozoa and the OB produced by the female genital tract drives fertilisation *in vivo*.

In conclusion, in this study we induced hyperactivation and acrosome reaction in equine spermatozoa by FF, OB, P and OB+P. We obtained eight-cell stage embryos by using FF, P or OB+P. Interestingly, the supplementation of CM with OB in our IVF conditions did not help oocyte fertilisation. Based on these results, we can speculate that P, but not OB, is the key factor in FF to achieve IVF.

This finding may indicate that equine OB is specifically involved in the improvement of ooplasmic maturity (Lange-Consiglio *et al.* 2009), even though during co-culture with spermatozoa no effects were seen on the external layers of the oocyte (corona radiata, intercellular matrix, zona pellucida and oolemma), which are involved in sperm penetration, nor were effects seen on spermatozoa. This observation is a significant finding, as OB produced no toxic effects as demonstrated in our previous study of apoptosis. Nevertheless, it is important not to rule out the potential action of OB, nor its possible involvement in sperm functions other than those studied, such as sperm–zona pellucida binding and zona pellucida-induced acrosome reaction.

This study confirms the difficulties in achieving appropriate capacitation and hyperactivation of stallion spermatozoa *in vitro*. It supports the hypothesis that capacitation and hyperactivation are required for successful IVF in horses and, for the first time, it demonstrates the presence of *Ob* and *Ob-R* mRNA and their proteins in equine spermatozoa. Further studies are required to determine the role of these molecules.

Acknowledgements

We sincerely thank Professor S. Arrighi and Dr G.P. Bosi of the VESPA Department, Università degli Studi di Milano, for their assistance in immunocytochemical techniques.

References

Abavisani, A., Baghbanzadeh, A., Shayan, P., and Dehghani, H. (2011). Leptin mRNA in bovine spermatozoa. *Res. Vet. Sci.* **90**, 439–442. doi:10.1016/J.RVSC.2010.07.009

Anckaert, E., Mees, M., Schiettecatte, J., and Smitz, J. (2002). Clinical validation of a fully automated 17beta-oestradiol and progesterone assay (VIDAS) for use in monitoring assisted reproduction treatment. *Clin. Chem. Lab. Med.* **40**, 824–831. doi:10.1515/CCLM.2002.143

Aquila, S., Gentile, M., Middea, E., Catalano, S., and Andò, S. (2005*a*). Autocrine regulation of insulin secretion in human ejaculated spermatozoa. *Endocrinology* **146**, 552–557. doi:10.1210/EN.2004-1252

Aquila, S., Gentile, M., Middea, E., Catalano, S., Morelli, C., Pezzi, V., and Andò, S. (2005*b*). Leptin secretion by human ejaculated spermatozoa. *J. Clin. Endocrinol. Metab.* **90**, 4753–4761. doi:10.1210/JC.2004-2233

Aquila, S., Rago, V., Guido, C., Casaburi, I., Zupo, S., and Carpino, A. (2008). Leptin and leptin receptor in pig spermatozoa: evidence of their involvement in sperm capacitation and survival. *Reproduction* **136**, 23–32. doi:10.1530/REP-07-0304

Baldi, E., Luconi, M., Bonaccorsi, L., and Forti, G. (1998). Non-genomic effects of progesterone on spermatozoa: mechanisms of signal transduction and clinical implications. *Front. Biosci.* **3**, D1051–D1059.

Baumber, J., and Meyers, S. A. (2006). Hyperactivated motility in rhesus macaque (*Macaca mulatta*) spermatozoa. *J. Androl.* **27**, 459–468. doi:10.2164/JANDROL.05107

Bezard, J. (1992). *In vitro* fertilization in the mare. In 'Proceedings of the International Scientific Conference on Biotechnics in Horse Reproduction, Cracow, Poland. p. 12. (Agricultural University of Cracow: Cracow.) [Abstract]

Blackmore, P. F., Beebe, S. J., Danforth, D. R., and Alexander, N. (1990). Progesterone and 17 alpha-hydroxyprogesterone. Novel stimulators of calcium influx in human sperm. *J. Biol. Chem.* **265**, 1376–1380.

Brewis, I. A., Morton, I. E., Moore, H. D., and England, G. C. (2001). Solubilized zona pellucida proteins and progesterone induce calcium influx and the acrosome reaction in capacitated dog spermatozoa. *Mol. Reprod. Dev.* **60**, 491–497. doi:10.1002/MRD.1114

Chehab, F. F., Lim, M. E., and Lu, R. (1996). Correction of the sterility defect in homozygous obese female mice by treatment with human recombinant leptin. *Nat. Genet.* **12**, 318–320. doi:10.1038/NG0396-318

Cheng, F. P., Fazeli, A. R., Voorhout, W. F., Marks, A., Bevers, M. M., and Colenbrander, B. (1996). Use of peanut agglutinin to assess the acrosomal status and the zona pellucida-induced acrosome reaction in stallion spermatozoa. *J. Androl.* **17**, 674–682.

Cheng, F. P., Fazeli, A. R., Voorhout, W. F., Tremoleda, J. L., Bevers, M. M., and Colenbrander, B. (1998). Progesterone in mare follicular fluid induces the acrosome reaction in stallion spermatozoa and enhances *in vitro* binding to the zona pellucida. *Int. J. Androl.* **21**, 57–66. doi:10.1046/J.1365-2605.1998.00096.X

Das, P. J., Paria, N., Gustafson-Seabury, A., Vishnoi, M., Chaki, S. P., Love, C. C., Varner, D. D., Chowdhary, B. P., and Raudsepp, T. (2010). Total RNA isolation from stallion sperm and testis biopsies. *Theriogenology* **74**, 1099–1106. doi:10.1016/J.THERIOGENOLOGY.2010.04.023

De Ambrogi, M., Spinaci, M., Galeati, G., and Tamanini, C. (2007). Leptin receptor in boar spermatozoa. *Int. J. Androl.* **30**, 458–461.

De Placido, G., Alviggi, C., Clarizia, R., Mollo, A., Alviggi, E., Strina, I., Fiore, E., Wilding, M., Pagano, T., and Matarese, G. (2006). Intrafollicular leptin concentration as a predictive factor for *in vitro* oocyte fertilisation in assisted reproductive techniques. *J. Endocrinol. Invest.* **29**, 719–726. doi:10.1007/BF03344182

Dell'Aquila, M. E., Albrizio, M., Maritato, F., Minoia, P., and Hinrichs, K. (2003). Meiotic competence of equine oocytes and pronucleus formation after intracytoplasmic sperm injection (ICSI) as related to granulosa cell apoptosis. *Biol. Reprod.* **68**, 2065–2072. doi:10.1095/BIOLREPROD.102.009852

Ellington, J. E., Ball, B. A., and Yang, X. (1993). Binding of stallion spermatozoa to the equine zona pellucida after co-culture with oviductal epithelial cells. *J. Reprod. Fertil.* **98**, 203–208. doi:10.1530/JRF.0.0980203

Emiliozzi, C., Cordonier, H., Guérin, J. F., Ciapa, B., Benchaïb, M., and Fénichel, P. (1996). Effects of progesterone on human spermatozoa prepared for *in vitro* fertilisation. *Int. J. Androl.* **19**, 39–47. doi:10.1111/J.1365-2605.1996.TB00433.X

Flesch, F. M., Colenbrander, B., van Golde, L. M., and Gadella, B. M. (1999). Capacitation induces tyrosine phosphorylation of proteins in the boar sperm plasma membrane. *Biochem. Biophys. Res. Commun.* **262**, 787–792. doi:10.1006/BBRC.1999.1300

Foresta, C., Rossato, M., Mioni, R., and Zorzi, M. (1992). Progesterone induces capacitation in human spermatozoa. *Andrologia* **24**, 33–35. doi:10.1111/J.1439-0272.1992.TB02605.X

Galantino-Homer, H. L., Visconti, P. E., and Kopf, G. S. (1997). Regulation of protein tyrosine phosphorylation during bovine sperm capacitation by a cyclic adenosine 3′,5′-monophosphate-dependent pathway. *Biol. Reprod.* **56**, 707–719. doi:10.1095/BIOLREPROD56.3.707

González-Fernández, L., Macıas-Garcıa, B., Loux, S. C., Varner, D. D., and Hinrichs, K. (2013). Focal adhesion kinases and calcium/calmodulin-dependent protein kinases regulate protein tyrosine phosphorylation in stallion sperm. *Biol. Reprod.* **88**, 138. doi:10.1095/BIOLREPROD.112.107078

Graham, J. K. (1996). Methods for induction of capacitation and the acrosome reaction of stallion spermatozoa. *Vet. Clin. North Am. Equine Pract.* **12**, 111–117.

Gregoraszczuk, E. L., Ptak, A., Wojtowicz, A. K., Gorska, T., and Nowak, K. W. (2004). Oestrus cycle-dependent action of leptin on basal and GH or IGF-I stimulated steroid secretion by whole porcine follicles. *Endocr. Regul.* **38**, 15–21.

Grunewald, S., Paasch, U., Glander, H. J., and Anderegg, U. (2005). Mature human spermatozoa do not transcribe novel RNA. *Andrologia* **37**, 69–71. doi:10.1111/J.1439-0272.2005.00656.X

Ho, H. C., and Suarez, S. S. (2001). An inositol 1,4,5-trisphosphate receptor-gated intracellular Ca^{2+} store is involved in regulating sperm hyperactivated motility. *Biol. Reprod.* **65**, 1606–1615. doi:10.1095/BIOLREPROD65.5.1606

Holmquist, L. (1982). Surface modification of Beckman Ultra-Clear centrifuge tubes for density gradient centrifugation of lipoproteins. *J. Lipid Res.* **23**, 1249–1250.

Jope, T., Lammert, A., Kratzsch, J., Paasch, U., and Glander, H. J. (2003). Leptin and leptin receptor in human seminal plasma and in human spermatozoa. *Int. J. Androl.* **26**, 335–341. doi:10.1111/J.1365-2605.2003.00434.X

Kaláb, P., Pěknicová, J., Geussová, G., and Moos, J. (1998). Regulation of protein tyrosine phosphorylation in boar sperm through a cAMP-dependent pathway. *Mol. Reprod. Dev.* **51**, 304–314. doi:10.1002/(SICI)1098-2795(199811)51:3<304::AID-MRD10>3.0.CO;2-2

Kirkman-Brown, J. C., Punt, E. L., Barratt, C. L., and Publicover, S. J. (2002). Zona pellucida and progesterone-induced Ca21 signalling and acrosome reaction in human spermatozoa. *J. Androl.* **23**, 306–315.

Lackey, B. R., Gray, S. L., and Henricks, D. M. (2002). Measurement of leptin and insulin-like growth factor-I in seminal plasma from different species. *Physiol. Res.* **51**, 309–311.

Lampiao, F., and du Plessis, S. S. (2008). Insulin and leptin enhance human sperm motility, acrosome reaction and nitric oxide production. *Asian J. Androl.* **10**, 799–807. doi:10.1111/J.1745-7262.2008.00421.X

Lange Consiglio, A., Dell'Aquila, M. E., Fiandanese, N., Ambruosi, B., Cho, Y. S., Bosi, G., Arrighi, S., Lacalandra, G. M., and Cremonesi, F. (2009). Effects of leptin on *in vitro* maturation, fertilisation and embryonic cleavage after ICSI and early developmental expression of leptin (Ob) and leptin receptor (ObR) proteins in the horse. *Reprod. Biol. Endocrinol.* **7**, 113. doi:10.1186/1477-7827-7-113

Lange-Consiglio, A., Arrighi, S., Fiandanese, N., Pocar, P., Aralla, M., Bosi, G., Borromeo, V., Berrini, A., Meucci, A., Dell'aquila, M. E., and Cremonesi, F. (2013). Follicular fluid leptin concentrations and expression of leptin and leptin receptor in the equine ovary and *in vitro*-matured oocyte with reference to pubertal development and breeds. *Reprod. Fertil. Dev.* **25**, 837–846. doi:10.1071/RD12188

Leclerc, P., de Lamirande, E., and Gagnon, C. (1996). Cyclic adenosine 3′,5′monophosphate-dependent regulation of protein tyrosine phosphorylation in relation to human sperm capacitation and motility. *Biol. Reprod.* **55**, 684–692. doi:10.1095/BIOLREPROD55.3.684

Li, H. W., Chiu, P. C., Cheung, M. P., Yeung, W. S., and O, W. S. (2009). Effect of leptin on motility, capacitation and acrosome reaction of human spermatozoa. *Int. J. Androl.* **32**, 687–694. doi:10.1111/J.1365-2605.2008.00931.X

Llanos, M. N., and Anabalón, M. C. (1996). Studies related to progesterone-induced hamster sperm acrosome reaction. *Mol. Reprod. Dev.* **45**, 313–319. doi:10.1002/(SICI)1098-2795(199611)45:3<313::AID-MRD8>3.0.CO;2-V

Luconi, M., Bonaccorsi, L., Krausz, C., Gervasi, G., Forti, G., and Baldi, E. (1995). Stimulation of protein tyrosine phosphorylation by platelet-activating factor and progesterone in human spermatozoa. *Mol. Cell. Endocrinol.* **108**, 35–42. doi:10.1016/0303-7207(95)92576-A

Marquez, B., and Suarez, S. S. (2004). Different signalling pathways in bovine sperm regulate capacitation and hyperactivation. *Biol. Reprod.* **70**, 1626–1633. doi:10.1095/BIOLREPROD.103.026476

Marquez, B., and Suarez, S. S. (2007). Bovine sperm hyperactivation is promoted by alkaline-stimulated Ca^{2+} influx. *Biol. Reprod.* **76**, 660–665. doi:10.1095/BIOLREPROD.106.055038

Marquez, B., Ignotz, G., and Suarez, S. S. (2007). Contributions of extracellular and intracellular Ca^{2+} to regulation of sperm motility: release of intracellular stores can hyperactivate CatSper1 and CatSper2 null sperm. *Dev. Biol.* **303**, 214–221. doi:10.1016/J.YDBIO.2006.11.007

McPartlin, L. A., Suarez, S. S., Czaya, C. A., Hinrichs, K., and Bedford-Guaus, S. J. (2009). Hyperactivation of stallion sperm is required for successful *in vitro* fertilisation of equine oocytes. *Biol. Reprod.* **81**, 199–206. doi:10.1095/BIOLREPROD.108.074880

Meizel, S. (1997). Amino acid neurotransmitter receptor/chloride channels of mammalian sperm and the acrosome reaction. *Biol. Reprod.* **56**, 569–574. doi:10.1095/BIOLREPROD56.3.569

Meizel, S., and Turner, K. O. (1991). Progesterone acts at the plasma membrane of human sperm. *Mol. Cell. Endocrinol.* **77**, R1–R5. doi:10.1016/0303-7207(91)90080-C

Melendrez, C. S., Meizel, S., and Berger, T. (1994). Comparison of the ability of progesterone and heat-solubilised porcine zona pellucida to initiate the porcine sperm acrosome reaction *in vitro*. *Mol. Reprod. Dev.* **39**, 433–438. doi:10.1002/MRD.1080390412

Meyers, S. A., Overstreet, J. W., Liu, I. K., and Drobnis, E. Z. (1995). Capacitation *in vitro* of stallion spermatozoa: comparison of progesterone-induced acrosome reactions in fertile and subfertile males. *J. Androl.* **16**, 47–54.

Meyers, S. A., Liu, I. K., Overstreet, J. W., Vadas, S., and Drobnis, E. Z. (1996). Zona pellucida binding and zona-induced acrosome reactions in horse spermatozoa: comparisons between fertile and subfertile stallions. *Theriogenology* **46**, 1277–1288. doi:10.1016/S0093-691X(96)00299-3

Mortimer, S. T., and Mortimer, D. (1990). Kinematics of human spermatozoa incubated under capacitating conditions. *J. Androl.* **11**, 195–203.

Murase, T., and Roldan, E. R. (1996). Progesterone and the zona pellucida activate different transducing pathways in the sequence of events leading to diacylglycerol generation during mouse sperm acrosomal exocytosis. *Biochem. J.* **320**(Pt 3), 1017–1023.

Palmer, E., Bézard, J., Magistrini, M., and Duchamp, G. (1991). *In vitro* fertilisation in the horse. A retrospective study. *J. Reprod. Fertil. Suppl.* **44**, 375–384.

Roldan, E. R., Murase, T., and Shi, Q. X. (1994). Exocytosis in spermatozoa in response to progesterone and zona pellucida. *Science* **266**, 1578–1581. doi:10.1126/SCIENCE.7985030

Somanath, P. R., Suraj, K., and Gandhi, K. K. (2000). Caprine sperm acrosome reaction: promotion by progesterone and homologous zona pellucida. *Small Rumin. Res.* **37**, 279–286. doi:10.1016/S0921-4488(99)00148-0

Suarez, S. S., Dai, X. B., DeMott, R. P., Redfern, K., and Mirando, M. A. (1992). Movement characteristics of boar sperm obtained from the oviduct or hyperactivated *in vitro*. *J. Androl.* **13**, 75–80.

Tardif, S., Dubé, C., and Bailey, J. L. (2003). Porcine sperm capacitation and tyrosine kinase activity are dependent on bicarbonate and calcium but protein tyrosine phosphorylation is only associated with calcium. *Biol. Reprod.* **68**, 207–213. doi:10.1095/BIOLREPROD.102.005082

Tesarik, J., Moos, J., and Mendoza, C. (1993). Stimulation of protein tyrosine phosphorylation by a progesterone receptor on the cell surface of human sperm. *Endocrinology* **133**, 328–335.

Thérien, I., and Manjunath, P. (2003). Effect of progesterone on bovine sperm capacitation and acrosome reaction. *Biol. Reprod.* **69**, 1408–1415. doi:10.1095/BIOLREPROD.103.017855

Thomas, T. (2004). The complex effects of leptin on bone metabolism through multiple pathways. *Curr. Opin. Pharmacol.* **4**, 295–300. doi:10.1016/J.COPH.2004.01.009

Travis, A. J., Tutuncu, L., Jorgez, C. J., Ord, T. S., Jones, B. H., Kopf, G. S., and Williams, C. J. (2004). Requirements for glucose beyond sperm capacitation during *in vitro* fertilisation in the mouse. *Biol. Reprod.* **71**, 139–145. doi:10.1095/BIOLREPROD.103.025809

Uhler, M. L., Leung, A., Chan, S. Y., and Wang, C. (1992). Direct effects of progesterone and antiprogesterone on human sperm hyperactivated motility and acrosome reaction. *Fertil. Steril.* **58**, 1191–1198.

Visconti, P. E., Bailey, J. L., Moore, G. D., Pan, D., Olds-Clarke, P., and Kopf, G. S. (1995). Capacitation of mouse spermatozoa. I. Correlation between the capacitation state and protein tyrosine phosphorylation. *Development* **121**, 1129–1137.

Zhang, Y., Proenca, R., Maffei, M., Barone, M., Leopold, L., and Friedman, J. M. (1994). Positional cloning of the mouse obese gene and its human homologue. *Nature* **372**, 425–432. doi:10.1038/372425A0

Lange-Consiglio et al. Reproductive Biology and Endocrinology (2015) 13:65
DOI 10.1186/s12958-015-0064-6

REPRODUCTIVE BIOLOGY AND ENDOCRINOLOGY

RESEARCH Open Access

Platelet concentrate in bovine reproduction: effects on *in vitro* embryo production and after intrauterine administration in repeat breeder cows

Anna Lange-Consiglio[1], Nadia Cazzaniga[1], Rosangela Garlappi[2], Chiara Spelta[3], Claudia Pollera[4], Claudia Perrini[1] and Fausto Cremonesi[1,5*]

Abstract

Background: A repeat breeder cow (RBC) can be defined as an animal that after 3 or more inseminations cannot get pregnant because of fertilization failure or early embryonic death. If no cause is identified precisely, inadequate uterine receptivity is responsible for implantation failures. Since a large number of identified molecular mediators, such as cytokines, growth factors and lipids have been postulated to be involved in early feto-maternal interaction, in this study a different approach to the treatment of RBC syndrome has been employed using a platelet concentrate (PC) that contains a significant amount of growth factors accumulated in its α-granules.

Methods: Three explorative studies were performed. Initially, PC was supplemented in the *in vitro* embryo culture medium to study its effect on embryo-development. After the pilot study, 4 RBCs were treated with intrauterine administration of PC to evaluate proliferative potential of endometrium by immunohistochemical expression of the antigen Ki-67. Lastly, the effect of intrauterine administration of PC at 48 hrs after artificial insemination in RBCs was evaluated.

Results: The *in vitro* results show that 5 % of PC and 5 % of fetal calf serum (FCS) increase the rate of blastocysts compared with the control containing 10 % FCS only (43.04 % vs 35.00 % respectively). The immunohistochemical study shows more proliferating nuclei in the treated uterine horn compared to the control one. After intrauterine insemination in RBCs, the percentage of pregnant cows in the control group was 33.33 % compared to 70 % of the treated animals.

Conclusion: We suppose that when embryo descends in uterus could find a more appropriate environment for nesting and subsequent pregnancy.

Keywords: Repeat breeder cows, Embryos, Platelet concentrate, Intrauterine administration

Background

Unexplained infertility, the so called repeat breeder cow (RBC) syndrome, involves a heterogeneous group of sub-fertile cows, with no anatomical abnormalities and infections of the reproductive tracts, nor estrous cycle alterations. A repeat breeder is defined as a cow that fails to become pregnant after 3 or more inseminations as a consequence of either fertilization failure or early embryonic death [1].

The etiology of RBC syndrome is multi-factorial and unclear. The normal uterine environment promotes normal embryonic development but subclinical disorders compromise the survival of the embryo resulting in RBC syndrome. The RBCs are characterized by early embryonic loss [2], that decreases the conception rates [3, 4]. In some cases, the transfer of non-RBC donated embryos into RBC surrogates increased RBC pregnancy rate, indicating that the lower conception rate of RBCs is determined at early stages of embryo development [3]. The problem could be the embryo but also the

* Correspondence: fausto.cremonesi@unimi.it
[1]Large Animal Hospital, Reproduction Unit, Università degli Studi di Milano, Via dell'Università 6, 26900 Lodi, Italy
[5]Department of Veterinary Science for Animal Health, Production and Food Safety, Università degli Studi di Milano, 20133 Milan, Italy
Full list of author information is available at the end of the article

oviductal and/or uterine environment. Ferreira *et al.* [5] provided evidence that RBC syndrome is associated with oocyte quality and that this negative effect is enhanced during summer heat stress, but it is general opinion that the successful implantation requires also a complex sequence of signaling events that are crucial to the establishment of pregnancy. In human medicine there is a proportion of women with 'unexplained' infertility in whom pregnancies fail before they are clinically recognized. Koot *et al.* [6] underline that this infertility could occur as a result of a malfunction of the endometrial-embryo 'dialogue' after the early phases of implantation. Indeed, the uterus is responsible for two-thirds of failures whilst the embryo for only one-third [7, 8]. A large number of molecular mediators, under the influence of ovarian hormones, have been postulated to be involved in this early embryo-maternal interaction. These mediators embrace a large number of inter-related molecules including adhesion molecules, cytokines, growth factors, lipids and others [9, 10]. Many treatments have been proposed for prevention of RBC syndrome at both herd and individual level. These include, for example, nutritional supplements and assisted reproductive techniques, such as *in vitro* embryo production and embryo transfer. Commonly, therapies in use include hormonal treatments with progestins, GnRH, exogenous gonadotrophins and prostaglandins [1]. However, in view of the embryo-maternal interaction a different approach to the treatment of RBC syndrome could be found using platelet concentrate (PC). Platelets contain significant quantities of growth factors (accumulated in their α-granules), chemokines and cytokines and also active metabolites [11], that act in a paracrine manner on different cell types like myocytes [12], mesenchymal stem cells of different sources [13], condrocytes [14, 15], osteoblasts [16], fibroblasts [17]. Moreover, several *in vitro* studies have shown a direct dose–response influence of many growth factors on cell migration, cell proliferation, and matrix synthesis [18–20]. Transforming growth factor β1 (TGF-β1) and TGF-β2, platelet derived growth factors (PDGF-AA, PDGF-BB, PDGF-AB), insulin-like growth factor 1 (IGF-I), epidermal growth factor (EGF), vascular endothelial growth factor (VEGF), fibroblast growth factor (FGF) and hepatocyte growth factor (HGF) are very important for regeneration processes. Indeed, these growth factors act synergistically to increase the infiltration of neutrophils and macrophages, to promote angiogenesis, fibroplasia, matrix deposition and, ultimately, re-epithelialization, inducing the consequent tissue regeneration [21]. Lastly, it is known the anti-inflammatory property of PC by the presence of anti-inflammatory agents including HGF [22].

In this context, the uterine administration of PC may be useful in peri-implantation, or in the healing process of clinically silent endometrial injuries because many cytokines act as intermediary links in the materno-fetal relationship including decidualization (in the women), implantation, placentation, embryogenesis and fetal growth [23]. Moreover, since pro-inflammatory factor transcripts in bovine endometrial epithelial cells are elevated in case of subclinical or clinical endometritis [24], we hypothesized that an early administration of PC, after artificial insemination (AI) and before the descent of the blastocyst in the uterus, could improve the uterine microenvironment for embryo implantation and counteract eventual subclinical endometritis.

Methods

Materials

Chemicals were obtained from Sigma Chemical (Milan, Italy) and tissue culture plastic dishes from Euroclone (Milan, Italy) unless otherwise specified.

Experimental Design

This study was based on three experiments as summarized in Table 1. The first experiment was to evaluate the effect of PC on *in vitro* embryo production by replacing fetal calf serum (FCS) with PC to establish whether this product is able to support embryo development. The second experiment evaluated the endometrium immunohistochemically, after *in vivo* PC administration, using Ki-67 as a marker of cell proliferation. The third *in vivo* experiment evaluated embryo implantation and development in RBCs following intrauterine administration of PC at 48 h after artificial insemination (AI).

Animals and repeat breeder syndrome diagnosis

All procedures were performed according to approved animal care and use protocols of the institutional ethics committee and to good veterinary practice for animal welfare as to European directive 2010/63/UE. Moreover, written farmers' consent was obtained at the beginning of the study.

The study was performed between January and April to reduce the influence of climate (*i.e.* a hot and humid climate, heavy rain, heat stress). Indeed, in the Italian environment late winter is probably the most stable period, with a low rain rate and temperature between 0 and 10 °C. A total of 64 animals Holstein Friesians in which pregnancy had not been achieved despite 3 or more inseminations were enrolled in this study. Ultrasound examination was performed in each cow to detect any reproductive pathology (like ovarian cysts, pyometra, abscess…) that would result in exclusion of cows from the experiment because not considered RBCs. For each cow, on the day of the estrus, cervical mucus was tested and samples of cervical mucus were collected aseptically by swab (Equi-Vet, Kruuse, Marslev, Denmark). Bacteriological examinations were performed as reported by Gani *et al.* [25].

Table 1 Experimental design

Experiments	N° samples	Parameter evaluated
1 *In vitro*: effect of different amounts of PC on embryo development	705 oocytes	• Rate of embryos • Total cell numbers per blastocyst
2 *In vivo*: evaluation of endometrial cell proliferation, after *in vivo* PC administration	4 RBCs	Microscopic nuclear count of cells expressing Ki-67
3 *In vivo*: embryo implantation and development after intrauterine administration of PC	30 Treated RBCs 30 Control RBCs	Rate of pregnancy

The RBCs were 385 ± 12.5 days in milking, had a weekly milk production of 128.6 ± 0.7 kg, 6.05 ± 4.84 previous inseminations (minimum of 3 and maximum of 23 inseminations per animal), and were on lactation number 2.7 ± 0.2.

Preparation of Platelet Concentrate (PC)

Blood was obtained from 8 donor cows, at the forty days in milking because in this period the circulating platelet counts is higher than other periods (data not shown), in good health, free from infection that had not received medication during the previous two months. The collection of blood and the preparation of PC, with the method of double centrifugation, were performed as reported by Lange-Consiglio *et al.* [26]. Briefly, after surgical scrub preparation of a few centimetres of skin around the subcutaneous mammary vein, 450 ml of blood was collected in *ad hoc* Terumo blood bags (Terumo Srl, Rome, Italy) containing CPDA-1 by using the 16 gauge needle provided with the bags. The bags were transported at +4 °C to the laboratory within 2 hrs of collection and immediately processed. All separation steps to produce PC were performed under a horizontal laminar flow hood in aseptic conditions. To prepare the PC, the blood was drawn into sterile Falcon tubes of 50 ml each. The tubes were centrifuged at 100xg for 30 min. This caused separation of the blood into three components: red blood cells at the lowest level, 'buffy coat' comprised in the middle layer, and platelet-rich plasma (PRP) in the upper layer. Afterward, the PRP was carefully aspirated and distributed in new 50 ml tubes and centrifuged again at 1500xg for 10 min to obtain the platelet pellet and the poor platelet plasma (PPP) at the upper layer. Afterwards, two thirds of the volume of PPP was aspirated for later use and the pellet mixed in the residual PPP volume to allow for platelet count before the final dilution with PPP to obtain PC at a standard concentration of $1x10^9$ platelet/ml. All platelet counts on peripheral blood, PRP and PC were performed by an automatic hematology analyser HeCo Vet SEAC (Florence, Italy).

At the end of the process, PC was pooled and prepared at a standard concentration of 1×10^9 platelet/ml. The total volume of PC was aliquoted into 10 ml usage doses that were stored in syringes. To release platelet derived factors, three cycles of freezing at −80 °C and thawing at 37 °C were performed [27]. Syringes containing PC dose were kept frozen at −20 °C until use. The same pool of PC obtained from donor cows was used in all experiments and in all animals in an heterologous way meaning that it was employed in cows different from donor cows.

For supplementation in *in vitro* cultured embryos, to prevent coagulation and clot formation, a fibrinogen free PC was prepared as reported by Mojica-Henshaw *et al.* [28]. Briefly, after thawing, pooled PC was centrifuged at 4000 g for 20 min, and the supernatant was collected and was manufactured by adding calcium chloride (20 % w/v) at a ratio of 1:100. After allowing the product to form a clot overnight at 4 °C, the coagulated product was centrifuged at 4000 g for 20 min, and the supernatant was collected to obtain fibrinogen free PC.

Experiment 1: effect of PC on *in vitro* embryo production

The *in vitro* embryo production consisted of 3 steps: *in vitro* maturation of oocytes (IVM), *in vitro* fertilization (IVF) and *in vitro* culture of embryo (IVC) performed on a monolayer of cumulus cells. These steps were carried out as reported by Lange-Consiglio *et al.* [29]. Briefly, cumulus–oocyte complexes (COCs) were collected from ovaries obtained from an abattoir by aspirating follicles 2–8 mm in diameter and washing them twice in preincubated (38.5 °C, 5 % CO_2 in air) TCM 199-HEPES buffered culture medium supplemented with 10 % FCS.

IVM was performed for 24 h in TCM 199 Earl's Salt medium supplemented with 10 % FCS, 5 μg/ml LH (Lutropin, Bioniche, Canada), 0.5 μg/ml FSH (Folltropin, Bioniche, Canada), 0.2 mM sodium pyruvate, 10 μg/ml gentamycin and 1 mg/ml estradiol 17β. Cultures were in 70 μl droplets (up to 20 oocytes/droplet) of the medium under oil, at 38.5 °C in 5 % CO_2.

IVF was performed in Tyrode's-albumin-lactate-pyruvate (TALP) medium containing 2 mM penicillamine, 1 mM hypotaurine, 250 mM epinephrine and 20 μg/ml heparin. Frozen–thawed semen was prepared by Percoll gradient (Amersham Pharmacia Biotec, Upsala, Sweden). In a 15 ml conic tube, 1 ml Percoll 90 % was added followed by 1 ml Percoll 45 %. Semen was thawed at 37 ° C for 30 sec, placed on the top of the Percoll

gradient and centrifuged for 30 min at 300 xg. After removal of the supernatant, 4 ml TALP medium were added and the sample centrifuged again for 2 min at 200 xg to remove excess Percoll.

Semen (10^7 spermatozoa/ml) was co-incubated with matured oocytes for 18 h at 38.5 °C in 5 % CO_2. At the end of gametes co-culture, the cumulus cells were completely removed and evaluation of segmentation was carried out from the first day of embryo culture (considering as day zero the day of insemination) when embryos were equally divided into three different embryo culture media: 1) standard embryo culture medium (TCM-199) with 10 % of FCS; 2) standard medium supplemented with 5 % FCS and 5 % PC; 3) standard medium supplemented with 10 % PC. The percentage of embryos developing to blastocyst stage was evaluated daily up to day 7 after fertilization. Some blastocysts, as reported in Table 2, were stained with Hoechst 33342 (10 μg/ml) for 10 min, and total cell numbers were counted under an epifluorescence microscope to estimate embryo quality. Hoechst 33342 dye was excited at 353–365 nm while the emission wavelength was set at 460 nm.

Experiment 2: immunohistochemical analysis of endometrium after *in vivo* PC administration

Four RBCs, belonging to the group previously described, culled by owner decision were used to test the effect of PC on endometrial cell proliferation. On the ninth day of diestrous stage, 10 ml of PC were administered into uterine horn ipsy-lateral (two cows) or contra-lateral (two cows) to the corpus luteum, maintaining the opposite horn as a control. After PC administration, a Foley catheter was inserted in the control horn and the balloon was inflated to prevent passage of PC and create the control environment. Our previous study (data not shown) demonstrated that insertion of a Foley catheter for 3 days does not alter the normal histological appearance of endometrium. These cows were slaughtered 3 days after the treatment (on the twelfth day of diestrus stage) and the 4 uteri were evaluated macroscopically for differences between the treated and the control horns. For each horn, samples of middle/cranial portion were collected in formalin solution and were examined immunohistochemically for expression of the nuclear antigen Ki-67, a marker of cell proliferation, using the ABC-peroxidase method as reported by Turner *et al.* [30]. Briefly, the tissue was fixed in 4 % buffered formalin, dehydrated, and embedded in paraffin. Sections 4 μm thick were mounted on aptes (3-aminopropyl triethoxy silane, Sigma) coated slides, dewaxed, and rehydrated. Sections were immunostained using the standard ABC technique with the rabbit antihuman/horse polyclonal antibody to Ki-67 (Dako Italia, S.p.A., Milan. Italy) used at 1:50 dilution. Ki-67 antibody is directed against different epitopes of the proliferation-related antigen and can be used on fixed sections. Endogenous peroxidase activity was blocked using 3 % hydrogen peroxide. Pretreatment with microwaving in sodium citrate buffer, pH 6, was used. Non-specific primary antibody binding was blocked using fetal calf serum at a dilution of 1:20 for the ABC Ki-67. The primary antibody was applied for 18 hrs at +4 °C and washed in buffered saline. An antirabbit biotinylated secondary antibody (Insight Biotechnology Limited, Wembley Middlesex, UK) was applied at 1:200 dilution for 30 min at room temperature, followed by washes and then by application of the horseradish peroxidase streptavidin complex (Dako) at 1:400 dilution for 30 min. The anti-rabbit secondary antibody is an affinity-purified polyclonal antibody with well-characterized specificity for rabbit IgG. Colour development was with metal enhanced diaminobenzidine (DAB) (Pierce and Warriner Ltd, Chester, UK) applied for 15 min. The slides were lightly counterstained with Mayer emallume. The sections were viewed under a photomicroscope Olympus BX51 and nuclear count was performed on each section, at the level of endometrial epithelial cells, as number of positive cells to detect the entity of cell proliferation. Three different sections per cow and 4 microscopy fields for each section were counted.

Table 2 Number of blastocysts at 7 days in three different culture media and total cell number per blastocysts

Medium	N° of blastocysts at 7 days (%)	N° of embryos observed	Total cell numbers per blastocyst
CTR (10 % FCS)	84/240 (35.00 ± 1.72)[a]	29	104.6 ± 10.5[a]
FCS 5 % + PC 5 %	99/230 (43.04 ± 1.42)[b]	31	123.4 ± 8.3[b]
PC 10 %	64/235 (27.23 ± 1.39)[c]	34	98.7 ± 6.4[c]

The number are expressed as mean ± standard deviation (SD)
Different small letters superscript (a, b) in the same column indicate statistically different comparisons ($P < 0.05$)

Experiment 3: *in vivo* effectiveness of intrauterine administration of PC at 48 h after AI in RBCs

This experiment was carried out in 2 farms, managed in a cubicle yard. Sixty RBCs were randomly allocated into two groups: "treated group" (N = 30) that received intrauterine administration of PC 48 hrs after AI and "control group" (N = 30), that received no treatment in addition to AI. Treated group were characterized by 6.0 ± 5.19 inseminations prior to the enrollment in the study while control cows showed 6.1 ± 4.49 inseminations.

Cows displaying estrus in either group were submitted for insemination. The semen from the same bull was

used for insemination in each group, eliminating the "bull" effect in the results of fertility.

All the cows were blood sampled for progesterone assay at day 0 (day of insemination), and then 4 and 8 days after insemination (respectively T0, T4 and T8). At 48 hrs after insemination, 10 ml of PC at 1 x 10^9 platelet/ml were administered into the uterus in the cows in the treated group. This time was supposed to be ideal after AI not to disturb spermatozoa progression and before the embryo reaches the uterus. Ten ml of PC were administrated following previous study (data not shown) in which this volume proved to be evenly distributed along the uterine horns without signs of excessive distension allowing to reach the deepest portion of the organ. Ultrasound examination for pregnancy diagnosis was performed in all cows 32 days after insemination and confirmed at 60 days.

Bacteriological examination of cervical mucus

Bacteriological investigations were performed to detect aerobic and anaerobic microorganisms, such as *Trueperella pyogenes, Haemophylus sommni, Staphylococcus sp., Streptococcus sp., Enterobacteriaceae*, *Prevotella sp., Fusobacterium spp*. Each sample was plated on blood agar (agar with 5 % sheep blood, Sintak, Italy) for isolated colonies. The plates were incubated for 24–48 hrs in aerobic and anaerobic conditions at 37° ± 2 °C. Identification of bacteria was based on colonial morphology, Gram staining, and biochemical tests such as catalase, oxidase, coagulase according to the guidelines of the Bergey's manual of Systematic Bacteriology and the standard bacterial procedure of CLSI (Clinical and Laboratory Standards Institute) and confirmed by API-System (bioMerieux, France).

Intrauterine administration of platelet concentrate

After thawing and warming at 38 °C, the syringes of PC were connected to a sterile disposable intrauterine cannula, so that samples could be delivered through the vestibule, the vagina and the cervix to reach deep into the uterine horn ipsi-lateral to the newly formed corpus luteum. Plastic catheters with atraumatic ends were used. Ten ml of PC were administrated to cows in the treatment group 48 hrs after insemination.

Progesterone assay

Plasma samples were obtained by jugular venipuncture (2-5 ml). Blood was collected in heparinized tubes and centrifuged at 1000xg for 10 min. The plasma concentration of progesterone was assessed using a quantitative automated method based on the enzyme-linked fluorescent assay (ELFA) technique (Mini-Vidas; bioMérieux Italia S.p.A., Florence, Italy.

Statistical analysis

The collection efficiency of platelets for each PC was analyzed using the following formulas [31]:

$$\text{efficiency for platelet collection} = \frac{\text{platelet count/µl in PC x volume of PC}}{\text{platelet count in whole blood/µl x volume of whole blood}}$$

The statistical analysis of the data collected during the study, except for bacteriological data, was conducted using chi-square test. For all tests, differences were considered statistically significant when $P \leq 0.05$. The data were analyzed using the "Software GraphPad Instat 3.00 for Windows" (La Jolla, CA, USA).

Results

Platelet collection efficiency and product sterility test

The platelet collection efficiency for the PCs was 10.9 ± 2.3 %, indicating that 10.9 ± 2.3 ml of PC at the concentration of 1x10^9 platelet/ml were obtained from 100 ml of blood.

The bacterial sterility test performed on the PC produced in the laboratory has always given negative results, confirming that the experimentation has been performed in accordance with the appropriate standards of laboratory sterility.

Experiment 1: effect of PC on *in vitro* embryo production

During three experiments, 168 ovaries were processed, 705 oocytes were collected, with an average of 4.2 oocytes collected per ovary. The results related to the culture of embryos in the standard medium (CTR) show that the rate of cleavage of three replicates is 66.80 ± 2.07.

Results related to embryo culture show that the rate of blastocyst development was statistically significant different ($P < 0.001$) among all the three media tested and the best embryo production rate and quality was achieved in the culture medium supplemented with 5 % PC and 5 % FCS (Table 2).

Experiment 2: immunohistochemical analysis of endometrium after *in vivo* PC administration

No macroscopic alterations were observed in any of the uterine samples. Immunohistochemical examination for the unmasking of the nuclear antigen Ki-67 showed that in all animals there were statistically more proliferating nuclei in the treated uterine horn compared to the control one (Table 3 and Fig. 1).

Table 3 Microscopic nuclear count of cells expressing nuclear antigen Ki-67 protein in control (CTR) and treated (TRT) uterine horns of 4 cows in different sections and different microscopic fields

1		2		3		4	
Uterine horn		Uterine horn		Uterine horn		Uterine horn	
CTR	TRT	CTR	TRT	CTR	TRT	CTR	TRT
2 ± 0.7^{a}	12 ± 0.2^{b}	1 ± 0.2^{a}	10 ± 0.6^{b}	5 ± 2.9^{a}	18 ± 2.3^{b}	14 ± 3.8^{a}	40 ± 4.2^{b}

Legend: CTR Control; TRT Treated. The number are expressed as mean ± standard deviation (SD)
Different small letters superscript (a, b) in the same line indicate statistically different comparisons ($P < 0.05$)

Experiment 3: *in vivo* effectiveness of intrauterine administration of PC at 48 hrs after AI in RBCs

The clinical aspect of the uterus in all animals during the clinical examination at the estrous stage appeared normal in size, without presence of drains and with adequate, clear and stringy estrous mucus.

Progesterone values did not differ from those expected in a normal estrous cycle. Indeed, these values were lower than 1 ng/ml during peri-estrus and then increased gradually at day +4 as a result of ovulation and further increased at day +8 post insemination (Table 4). The percentage of pregnant cows in the control group was of 33.33 % (10/30) compared to 70 % (21/30) of the treated animals. The difference in pregnancy rates between the treated group and the control group was statistically significant ($P < 0.05$; Table 4). There was no correlation between treatment results and number of past inseminations before this study and characterizing the status of the enrolled RBCs ($P = 0.62$). All treated and control RBCs diagnosed as pregnant gave birth to normal offsprings.

Microbiological results

No significant bacterial growth was observed in any of the cervical mucus samples obtained from cows of both experimental groups. The microorganism *Aerococcus viridans* was isolate only from one cow.

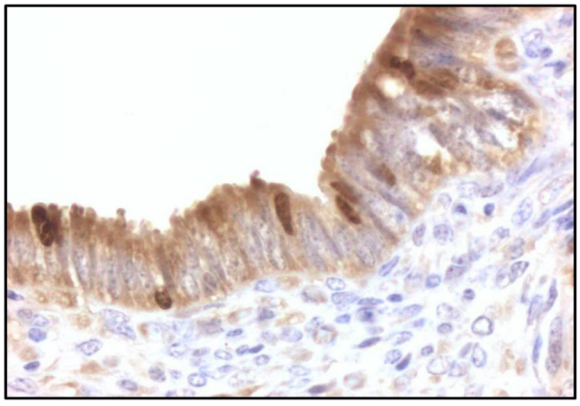

Fig. 1 Immunohystochemical analysis. Nuclear positivity to Ki-67 protein. Magnification 100x

Discussion

Studies in humans and in other mammals have shown that cytokines and growth factors are produced by the pre-implantation embryo and cells of the reproductive tract, even if the exact combinations required for successful implantation are not yet fully understood [23]. Based on the current knowledge of the regenerative effect of PC due to its high growth factor and cytokine content [22], this study proposes a novel therapeutic approach. Autologous PC is known to accelerate the healing process in human medicine, and has been used in maxillofacial surgery, muscle and/or tendon repair, and reversal of skin ulcers [21]. In veterinary medicine there are few clinical reports of the use of PC. It has been mainly used for promoting equine tendon repair [32], but there are some reports of its use in intestinal wound healing in pigs [33], in a large cutaneous lesion in a dog [34] and in bovine mastitis in which it was used in heterologous way [26]. In all cases PC or platelet rich plasma showed a clear regenerative potential.

For this reason, in this preliminary investigation, we performed three explorative studies *in vitro* and *in vivo*. Only one paper [35] described the effects of platelet rich plasma on morula and blastocysts *in vitro* production. In our study and in our experimental conditions (*i.e.* platelet concentration at 1x 10^{9}/ml), at first we studied the effect of PC on *in vitro* embryo development using two different percentages (respectively 5 % and 10 %) of PC as a partial or complete replacement of FCS. The rate of blastocyst production and the total cells number of the blastocysts were statistically increased in the medium with 5 % PC and 5 % FCS when compared to both the control and medium with 10 % PC. Platelets release many growth factors, including FGF, TGF-6, PDGF and EGF [36, 37] that can stimulate bovine embryo development [38, 39]. Indeed, Munson *et al.* [40] demonstrated that TGF-6 and PDGF act synergistically to promote proliferation of both bovine trophoblastic cells and endometrial epithelial cells during *in vitro* culture. Moreover, EGF *in vivo* is produced by endometrial cells and its receptors have been detected in the embryo itself, where EGF acts through the phosphorylation of membrane proteins as a mitogen, promoting DNA and RNA synthesis. As pregnancy progresses, the increased production of EGF enhances trophoblast differentiation [41], promoting cell attachment and embryo

Table 4 Results of *in vivo* effectiveness of intrauterine administration of PC 48 h after AI in RBCs

		Progesterone value (ng/ml)					
	N°cows	T0	T4	T8	Pregnant (%)	Not Pregnant (%)	Delivery (%)
Control	30	0.40 ± 0.21^{a}	2.63 ± 0.96^{a}	7.75 ± 2.21^{a}	10 (33.33)[a]	20 (66.67)[a]	10 (100)
Treated	30	0.40 ± 0.17^{a}	3.12 ± 0.85^{a}	8.33 ± 2.14^{a}	21 (70.00)[b]	9 (30.00)[b]	21 (100)

Different small letters superscript (a, b) in the same column indicate statistically different comparisons ($P < 0.05$)

development [23]. Fibronectin and other glycoproteins are also released from platelets after aggregation, and Larson *et al.* [42] discovered that a serum-free medium supplemented with fibronectin provides the extracellular matrix required by the embryo to develop to the blastocyst stage during *in vitro* culture. In a speculative interpretation, the embryo culture systems supplemented with PC may have provided TGF-6, PDGF and the matrix of extracellular fibronectin necessary to support the development of embryo during *in vitro* culture, thus replicating the uterine microenvironment appropriate for embryo growth, viability, and for cytokine secretion [23]. It is possible that the low rate of embryos obtained in the medium with 10 % PC, compared to control, results from an excess of factors that may have had an inhibitory effect on the embryo development.

This *in vitro* study provided a useful starting point for the pre-clinical investigation in order to use PC in *in vivo* trials. Immunohistochemical examination of uterine samples from animals slaughtered 3 days after PC treatment showed that there was more expression of the nuclear antigen Ki-67 in samples from treated uterine horns compared to the controls. Cell proliferation is not enough indicative for uterine health but Ki-67 is expressed in the nuclei of proliferating cells. In tissues with a high proliferative rate it is expressed in all cell cycle phases except for the resting or G0 phases [43, 44] and reaches a maximum level during G2 and M [45]. Since Ki-67 is significantly more expressed in samples from treated uterine horns, it may be supposed that the growth factors released by platelets in the PC may have an effect on endometrial cell proliferation.

After these preliminary studies, the *in vivo* administration of PC into the uterus of RBCs at 48 hrs after insemination was performed.

The gynecological clinical status and the progesterone analysis performed in this study ensured that pregnancy losses in enrolled animals were not caused by abnormal ovarian cycles, an important condition for classification of cows as RBC, as reported by Gustafsson *et al.* [46]. The progesterone analysis also allowed us to exclude hypoluteinism as a possible cause of repeat breeding. In fact, all animals showed progesterone values exceeding the 2 ng/ml threshold both at day +4 and +8 post-insemination [47]. Moreover, bacteriological examination performed on cervical mucus confirmed the absence of bacterial infections in the genital tract, as the only isolated microorganism was *Aerococcus viridans,* a bacterium not recognized as a uterine pathogen.

In the *in vivo* study, there were more pregnant cows in the treated group compared to the control group. This suggests that the *in vivo* intrauterine administration of PC 48 hrs after insemination, time supposed to be ideal after AI not to disturb spermatozoa progression and before the embryo reaches the uterus, could make the uterine environment favorable to embryo implantation. This may be the effect of platelet growth factors on regeneration and/or the healing of clinically silent endometrial abnormalities. Furthermore, PC should enrich the uterine environment with factors necessary for embryo development. Uterine glands produce a glycoprotein-rich secretion, which is believed to support the embryo during the pre-implantation period [48]. In addition to providing nutrition for the conceptus, this secretion contains a complex array of growth factors and cytokines. Katagiri and Takahashi [49] reported that RBCs show abnormalities in the growth factor-cytokine network - specifically in endometrial EGF concentrations. Cyclic cows have two peaks of EGF concentrations on days 2–4 and 13–14 of the oestrous cycle, but these peaks are lost or diminished in about 70 % of RBCs [49]. The EGF family could act on the trophectoderm promoting cell attachment and embryo development [23]. Since PC contains EGF, treatments targeting the endometrial growth factor regulatory network may be an effective way to deal with RBCs when uterine problems limit the production of this or other growth factors.

Conclusions

The preliminary data regarding the administration of PC into the uterus of animals at 48 hrs after insemination produced very encouraging results in RBCs. From our data, we hypothesize that PC, whose content is known, enriches the uterine environment with factors necessary for embryo development and counteracts eventual subclinical endometritis by its anti-inflammatory properties. The obtained results in our three different explorative studies are very interesting. This research could offer a new therapeutic strategy for RBC syndrome and also open the possibility for using PC in future embryo-transfer programs in both human and veterinary medicine as a vehicle to transfer embryos at the time of transplantation, with the aim of improving the uterine environment for implantation.

Abbreviations
AI: artificial insemination; EGF: Epidermal Growth Factor; FCS: Fetal Calf Serum; FGF: Fibroblast Growth Factor; HGF: Hepatocyte Growth Factor; IGF-I: Insulin-like Growth Factor 1; IVC: *in vitro* Culture of Embryo; IVF: *in vitro* Fertilization; IVM: *in vitro* Maturation; PC: Platelet Concentrate; PDGF-AA: PDGF-BB, PDGF-AB, Platelet Derived Growth Factors; RBC: Repeat Breeder Cow; TGF-β1: Transforming Growth Factor β1; TGF-β2: Transforming Growth Factor β2; VEGF: Vascular Endothelial Growth Factor.

Competing interests
All authors declare that there is no financial or non-financial competing interest that could be perceived as prejudicing the impartiality of the reported research.

Authors' contributions
ALC is responsible for the study concept and participated in designing the study, performed the *in vitro* study, collected and interpreted data performing statistical analysis, wrote and reviewed the manuscript and approved the final version. NC performed the *in vitro* study, collected and interpreted data, wrote the manuscript and approved the final version. RG and CS performed the *in vivo* study, collected and interpreted data, and approved the final version. CP and CP took part in collecting and interpreting data and approved the final version. FC is responsible for the study concept and participated in designing the study, performed the *in vivo* study, collected and interpreted data, revised and approved the final version of manuscript.

Acknowledgements
We sincerely thank Dr Pietro Riccaboni and Dr Marco Rondena of the DIVET Department, Università degli Studi di Milano, for their assistance in immunohistochemical techniques.

Author details
[1]Large Animal Hospital, Reproduction Unit, Università degli Studi di Milano, Via dell'Università 6, 26900 Lodi, Italy. [2]Private practitioner, 26833Merlino, Milan, Italy. [3]Private practitioner, 27100 Pavia, Italy. [4]Department of Veterinary Science and Public Health, Università degli Studi di Milano, 20133 Milan, Italy. [5]Department of Veterinary Science for Animal Health, Production and Food Safety, Università degli Studi di Milano, 20133 Milan, Italy.

Received: 20 April 2015 Accepted: 9 June 2015
Published online: 19 June 2015

References

1. Perez-Marin CC, Molina Moreno L, Vizuete CG. Clinical approach to the repeat breeder cow syndrome. A Bird's-Eye View of Veterinary Medicine. 2011;18:337–62.
2. Gustafsson H, Larsson K. Embryonic mortality in heifers after artificial insemination and embryo transfer: differences between virgin and repeat breeder heifers. Res Vet Sci. 1985;39:271–4.
3. Ferreira RM, Ayres H, Chiaratti MR, Rodrigues CA, Freitas BG, Meirelles FV, et al. Heat stress and embryo production in high-producing dairy cows. Acta Sci Vet. 2010;38:s277–315.
4. Yusuf M, Nakao T, Ranasinghe RB, Gautam G, Long ST, Yoshida C, et al. Reproductive performance of repeat breeders in dairy herds. Theriogenology. 2010;73:1220–9.
5. Ferreira RM, Ayres H, Chiaratti MR, Ferraz ML, Araújo AB, Rodrigues CA, et al. The low fertility of repeat-breeder cows during summer heat stress is related to a low oocyte competence to develop into blastocysts. J Dairy Sci. 2011;94:2383–92.
6. Koot YEM, Boomsma CM, Eijkemans MJC, Lentjes EGW, Macklon NS. Recurrent pre-clinical pregnancy loss is unlikely to be a 'cause' of unexplained infertility. Hum Reprod. 2011;26:2636–41.
7. Simon C, Moreno C, Remohi J, Pellicer A. Cytokines and embryo implantation. J Reprod Immunol. 1998;39:117–31.
8. Ledee-Bataille N, Lapree-Delage G, Taupin JL, Dubanchet S, Frydman R, Chaouat G. Concentration of leukaemia inhibitory factor (LIF) in uterine flushing fluid is highly predictive of embryo implantation. Hum Reprod. 2002;17:213–8.
9. Lessey BA, Damjanovich L, Coutifaris C, Castelbaum A, Albelda SM, Buck CA. Integrin adhesion molecules in the human endometrium. correlation with the normal and abnormal menstrual cycle. J Clin Invest. 1992;90:188–95.
10. Simon C, Martin JC, Pellicer A. Paracrine regulators of implantation. Baillière's Best Pract Res Clin Obstet Gynaecol. 2000;14:815–26.
11. Macaulay IC, Carr P, Gusnanto A, Ouwehand WH, Fitzgerald D, Watkins NA. Platelet genomics and proteomics in human health and disease. J Clin Invest. 2005;115:3370–7.
12. Mazzocca AD, McCarthy MB, Chowaniec DM, Dugdale EM, Hansen D, Cote MP, et al. The positive effects of different platelet-rich plasma methods on human muscle, bone, and tendon cells. Am J Sports Med. 2012;40:1742–9.
13. Cho HS, Song LH, Park SY, Sung MC, Ahn MW, Song KE. Individual variation in growth factor concentrations in platelet-rich plasma and its influence on human mesenchymal stem cells. Korean J Lab Med. 2011;31:212–8.
14. Drengk A, Zapf A, Stürmer EK, Stürmer KM, Frosch KH. Influence of platelet-rich plasma on chondrogenic differentiation and proliferation of chondrocytes and mesenchymal stem cells. Cells Tissues Organs. 2009;189:317–26.
15. Van Buul GM, Koevoet WL, Kops N, Bos PK, Verhaar JA, Weinans H, et al. Platelet-rich plasma releasate inhibits inflammatory processes in osteoarthritic chondrocytes. Am J Sports Med. 2011;39:2362–70.
16. Graziani F, Ivanovski S, Cei S, Ducci F, Tonetti M, Gabriele M. The in vitro effect of different concentrations on osteoblasts and fibroblasts. Clin Oral Implants Res. 2005;16:456–60.
17. Anitua E, Sánchez M, del Mar ZM, de la Fuente M, Prado R, Orive G, et al. Fibroblastic response to treatment with different preparations rich in growth factors. Cell Prolif. 2009;42:162–70.
18. Thomopoulos S, Harwood FL, Silva MJ, Amiel D, Gelberman RH. Effect of several growth factors on canine flexor tendon fibroblast proliferation and collagen synthesis in vitro. J Hand Surg. 2005;30:441–7.
19. Costa MA, Wu C, Pham BV, Chong AK, Pham H-M, Chang J. Tissue engineering of flexor tendons: optimization of tenocyte proliferation using growth factor supplementation. Tissue Eng. 2006;12:1937–43.
20. Haupt JL, Donnelly BP, Nixon AJ. Effects of platelet-derived growth factor-BB on the metabolic function and morphologic features of equine tendon in explant culture. Am J Vet Res. 2006;67:1595–600.
21. Anitua E, Andia I, Ardanza B, Nurden P, Nurden AT. Autologous platelets as a source of proteins for healing and tissue regeneration. Thromb Haemost. 2004;91:4–15.
22. Bendinelli P, Matteucci E, Dogliotti G, Corsi MM, Banfi G, Maroni P, et al. Molecular basis of anti-inflammatory action of platelet rich plasma on human chondrocytes: mechanisms of NF-kB inhibition via HGF. J Cell Physiol. 2010;225:757–66.
23. Castro-Rendón WA, Castro-Álvarez JF, Guzmán-Martinez C, Bueno-Sanchez JC. Blastocyst-endometrium interaction: intertwining a cytokine network. Braz J Med Biol Res. 2006;39:1373–85.
24. Fischer C, Drillich M, Odau S, Heuwieser W, Einspanier R, Gabler C. Selected pro-inflammatory factor transcripts in bovine endometrial epithelial cells are regulated during the oestrous cycle and elevated in case of subclinical or clinical endometritis. Reprod Fertil Develop. 2010;22:818–29.
25. Gani MO, Amin MM, Alam MGS, Kayesh MEH, Karim MR, Samad MA, et al. Bacterial flora associated with repeat breeding and uterine infections in dairy cows. Bangl J Vet Med. 2008;6:79–86.
26. Lange-Consiglio A, Spelta C, Garlappi R, Luini M, Cremonesi F. Intramammary administration of platelet concentrate as an unconventional therapy in bovine mastitis: first clinical application. J Dairy Sci. 2014;97:1–8.
27. Zimmermann R, Arnold D, Strasser E, Ringwald J, Schlegel A, Wiltfang J, et al. Sample preparation technique and white cell content influence the detectable levels of growth factors in platelet concentrates. Vox Sang. 2003;85:283–9.
28. Mojica-Henshaw MP, Jacobson P, Morris J, Kelley L, Pierce J, Boye M, et al. Serum-converted platelet lysate can substitute for fetal bovine serum in human mesenchymal stromal cell cultures. Cytotherapy. 2013;15:1458e–68e.
29. Lange-Consiglio A, Maggio V, Pellegrino L, Cremonesi F. Equine bone marrow mesenchymal or amniotic epithelial stem cells as feeder in a model for the in vitro culture of bovine embryos. Zygote. 2012;20:45–51.
30. Turner HE, Nagy ZS, Esiri MM, Wass JAH. The enhanced peroxidase one step method increases sensitivity for detection of Ki-67 in pituitary tumours. Clin Pathol. 1999;52:624–6.
31. Weibrich G, Kleis WK, Hitzle WE, Hafner G. Comparison of the platelet concentrate collection system with the plasma-rich-in growth factors kit to produce platelet rich plasma: a technical report. Int J Oral Max Imp. 2005;29:118–23.

32. Rindermann G, Cislakova M, Arndt G, Carstanjen B. Autologous conditioned plasma as therapy of tendon and ligament lesions in seven horses. J Vet Sci. 2010;11:173–5.
33. Fresno L, Fondevila D, Bambo O, Chacaltana A, García F, Andaluz A. Effects of platelet-rich plasma on intestinal wound healing in pigs. Vet J. 2010;185:322–7.
34. Kim JH, Park C, Park HM. Curative effect of autologous platelet-rich plasma on a large cutaneous lesion in a dog. Vet Dermatol. 2009;20:123–6.
35. Thibodeaux JK, Del Vecchio RP, Broussard JR, Dickey JF, Hansel W. Stimulation of development of in vitro-matured and in vitro-fertilized bovine embryos by platelets. J Anim Sci. 1993;71:1910–6.
36. Siess W. Molecular mechanisms of platelet activation. Physiol Rev. 1989;69:58–168.
37. Whal SM, McCartney-Francis N, Mergenhager SE. Inflammatory and immunomodulatory roles of TGF-β. Immunol Today. 1989;10:258–61.
38. Larson RC, Ignotz GG, Currie WB. Transforming growth factor and basic fibroblast growth factor synergistically promote early bovine embryo development during the fourth cell cycle. Mol Reprod Develop. 1992;33:432–5.
39. Larson RC, Ignotz GG, Currie WB. Platelet derived growth factor (PDGF) stimulates development of bovine embryos during the fourth cell cycle. Development. 1992;115:821–6.
40. Munson L, Wilkinson JE, Bechtel M. Transforming growth factor-6 (TGF-(3) and platelet-derived growth factor (PDGF) are synergistic mitogens for bovine trophoblastic and endometrial epithelial cells. Biol Reprod. 1992;46 Suppl 1:S67.
41. Kliman HJ, Feinberg RF, Haimowitz JE. Human trophoblast-endometrial interactions in an in vitro suspension culture system. Placenta. 1990;11:349–67.
42. Larson RC, Ignotz GG, Currie WB. Effect of fibronectin on early embryos development in cows. J Reprod Fertil. 1992;96:289–97.
43. Brown DC, Gatter KC. Monoclonal antibody Ki-67: its use in histopathology. Histopathology. 1990;17:489–503.
44. McCormick D, Chong H, Hobbs C, Datta C, Hall PA. Detection of the Ki-67 in fixed and wax embedded sections with the monoclonal antibody MIB1. Histopathology. 1993;22:355–60.
45. Sasaki K, Murakami T, Kavasaki M, Takahasashi M. The cell cycle associated change of the Ki-67 reactive nuclear antigen expression. J Cell Physiol. 1987;133:579–84.
46. Gustafsson H, Emanuelson U. Has a repeat breeder cow in the present lactation a higher risk to become a repeat breeder in the next lactation? Proceding of the 14th international congress on animal reproduction, vol. 15:26. Sweden: Stockholm; 2000. p. 100.
47. King SG, Dobson H, Royal MD, Christley RM, Murray RD, Routly JE, et al. Identification of inadequate maternal progesterone concentrations in nulliparous dairy heifers and treatment with human chorionic gonadotrophin. Vet Rec. 2013;173:450–7.
48. Burton GJ, Watson AL, Hempstock J, Skepper JN, Jauniaux E. Uterine glands provide histiotrophic nutrition for the human fetus during the first trimester of pregnancy. J Clin Endocrinol Metab. 2002;87:2954–9.
49. Katagiri S, Takahashi Y. Changes in EGF concentrations during estrous cycle in bovine endometrium and their alterations in repeat breeder cows. Theriogenology. 2004;62:103–12.

CELLULAR REPROGRAMMING
Volume 17, Number 6, 2015

DOI: 10.1089/cell.2015.0029

Peculiarity of Porcine Amniotic Membrane and Its Derived Cells: A Contribution to the Study of Cell Therapy from a Large Animal Model

Anna Lange-Consiglio,[1] Bruna Corradetti,[2] Sabrina Bertani,[1] Valentina Notarstefano,[2] Claudia Perrini,[1] Maria Giovanna Marini,[2] Silvana Arrighi,[3] Giampaolo Bosi,[3] Angelo Belloli,[4] Davide Pravettoni,[4] Valentina Locatelli,[4] Fausto Cremonesi,[1,3] and Davide Bizzaro[2]

Abstract

The aim of this work was to provide, for the first time, a protocol for isolation and characterization of stem cells from porcine amniotic membrane in view of their potential uses in regenerative medicine. From three samples of allanto-amnion recovered at delivery, the amniotic membrane was stripped from overlying allantois and digested with trypsin and collagenase to isolate epithelial (amniotic epithelial cells [AECs]) and mesenchymal cells, respectively. Proliferation, differentiation, and characterization studies by molecular biology and flow cytometry were performed. Histological examination revealed very few mesenchymal cells in the stromal layer, and a cellular yield of AECs of 10×10^6/gram of digested tissue was achieved. AECs readily attached to plastic culture dishes displaying typical cuboidal morphology and, although their proliferative capacity decreased to the fifth passage, AECs showed a mean doubling time of 24.77 ± 6 h and a mean frequency of one fibroblast colony-forming unit (CFU-F) for every 116.75 plated cells. AECs expressed mesenchymal stem cell (MSC) mRNA markers (*CD29, CD166, CD90, CD73, CD117*) and pluripotent markers (*Nanog* and *Oct 4*), whereas they were negative for *CD34* and *MHCII*. Mesodermic, ectodermic, and endodermic differentiation was confirmed by staining and expression of specific markers. We conclude that porcine amniotic membrane can provide an attractive source of stem cells that may be a useful tool for biomedical research.

Introduction

Two essential factors are needed for successful stem cell therapy research—a good animal model and an effective and sustainable source of stem cells. The use of animals in science and research is well documented and practiced (Doherty et al., 2008). However, the evolutionary gap between humans and many of the applied animal models (such as rodents) has always hampered direct application of the knowledge gained from animals to human therapy (Vodicka, et al., 2005). Ideally, preclinical animal model studies replicate the pathogenesis of the relevant human disease so that therapeutic intervention in the animal model mimics the intended clinical application. In this regard, the pig offers many advantages because it shows many similarities to humans in aspects of anatomy and physiology, nutrition and metabolism, histology, immunology, and pharmacokinetics (Swindle et al., 2012). Moreover, with the substantially improved knowledge of the structure and function of the pig genome in the last two decades, it has been shown that this animal shares a high sequence and chromosomal structure homology with humans (Lunney, 2007).

The similarities between pigs and humans make this animal model a valuable tool for evaluation of the safety, feasibility, dosage, engraftment, or toxicity of transferred mesenchymal stem cells (MSCs) (Casal and Haskins, 2006). For practical application of MSCs in regenerative medicine, some aspects of the stem cell reservoir must be considered: large numbers of cells must be harvested in an inexpensive and noninvasive way, without risk to the donor, and these cells must retain a high ability to proliferate and differentiate *in vitro* (Carlin et al., 2006). The most used and best-

[1]Large Animal Hospital, Reproduction Unit, Università degli Studi di Milano, Lodi, Italy.
[2]Department of Life and Environmental Sciences, Università Politecnica delle Marche, Ancona, Italy.
[3]Department of Health, Animal Science and Food Safety, Università degli Studi di Milano, Milan, Italy.
[4]Large Animal Hospital, Clinic for Ruminants and Pigs, Università degli Studi di Milano, Lodi, Italy.

characterized source of adult MSCs is bone marrow (BM), but collection of BM requires an invasive procedure. Moreover, the proliferative and differentiation potential of BM-MSCs is limited due to the donor age and the number of *in vitro* passages (Digirolamo et al., 1999; Guillot et al., 2007; Majors et al., 1997).

Placenta has been proposed as a more suitable candidate for the derivation of MSCs both in human and in veterinary medicine. It includes several tissues, such as umbilical cord blood (Chang et al., 2006; Grewal et al., 2003; Kang et al., 2013; Kern et al., 2006), Wharton jelly (Corradetti et al., 2011; Cremonesi et al., 2008; Hoynowski et al., 2007; Iacono et al., 2012; La Rocca et al., 2009; Lovati et al., 2011; Passeri et al., 2009; Weiss et al., 2008), amniotic membrane (Corradetti et al., 2013; Filioli Uranio et al., 2011; Lange Consiglio et al., 2012; Miki and Strom, 2006; Muttini et al., 2013; Parolini and Soncini, 2004; Rutigliano et al., 2013), and amniotic fluid (Chen et al., 2011; Corradetti et al., 2013; Dev et al., 2012; Gao et al., 2014; Iacono et al., 2012; Lovati et al., 2011; Parolini et al., 2009; Steigman and Fauza, 2007). These tissues could provide a large number of cells without risks to the donor in an inexpensive and noninvasive way, because they are discarded at delivery.

In addition, it is known that human MSCs from extrafetal tissues possess a higher proliferation ability and differentiation potential and a longer telomere length compared to cells derived from adult tissues (Kern et al., 2006; Kögler et al., 2004). Specifically, MSCs isolated from amnion are thought to be in an intermediate stage between embryonic and adult stem cells (De Coppi et al., 2007; Delo et al., 2006; Gucciardo et al., 2009; In't Anker et al., 2004) and are known to prevent rejection of the fetus due to their low immunogenicity and immunomodulatory characteristics (Evangelista et al., 2008; Wang, et al. 2006).

In veterinary medicine, presumptive stem cells have been identified in the epithelial and/or stromal portions of the amnion in canine (Filioli Uranio et al., 2011), equine (Lange Consiglio et al., 2012), bovine (Corradetti et al., 2013), ovine (Muttini et al., 2013), and feline (Rutigliano et al., 2013) species. In this regard, some studies have already demonstrated the clinical relevance of amniotic stem cells. Lange-Consiglio et al. (2012, 2013a, b) isolated equine MSCs from the amniotic membrane as an alternative to BM-MSCs and demonstrated their superior efficacy for the treatment of spontaneous tendon injuries in horses, showing only 4% of relapses of the tendon defect in comparison to BM-MSCs (23.08%).

In swine, MSCs have been isolated from other extrafetal tissues such as Wharton jelly (Carlin et al., 2006), umbilical cord blood (Kumar et al., 2007), and amniotic fluid (Chen et al., 2011). The authors of these studies worked with placental tissues and, although the results confirmed that the isolated cells had stem cell properties, the collection of Wharton jelly and amniotic fluid was invasive, occurring, as it did, from the embryonic disc or from early or mid stage of gestation with sows under general anesthesia. In addition, it was only possible to collect a small amount (2 mL) of umbilical cord blood after delivery (Kumar et al., 2007).

The aim of the study reported here was to isolate, for the first time, presumptive MSCs from porcine amniotic membrane (a usually discarded tissue) at delivery and to characterize these cells in terms of morphology, proliferative and differentiation potential, colony-forming unit (CFU) capability, and expression of stemness markers.

Materials and Methods

Materials

Chemicals were obtained from Sigma-Aldrich Chemical (Milan, Italy) unless otherwise specified, and tissue culture plastic dishes were purchased from Euroclone (Milan, Italy).

Tissue collection

In this study, after approval by the Ethical Committee of the University of Milan and written owner's consent, all procedures were conducted following standard veterinary practice and in accordance with 2010/63 EU directive on animal protection and Italian Law (D.L. No. 116/1992). Allanto-amniotic membranes and mesamnions were collected at delivery from three normal full-term pregnant sows. A mean of four allanto-amniotic membranes and four mesamnions were collected from each sow. Mesamnion, generally found just after delivery adhering to the back of piglet, is where the two chorio-amniotic folds meet and fuse, thus connecting the amniotic membrane with the chorion, as shown in Figure 1A. In pigs, as in cattle, the mesamnion persists until parturition in such a way that offspring are generally born without covering membranes (Hyttel et al., 2011).

Samples for histology were fixed immediately as described in the following section. Other samples were kept at 4°C in calcium- and magnesium-free phosphate-buffered saline (PBS-CMF) (Euroclone), supplemented with 100 U/mL of penicillin, 100 μg/mL streptomycin (Sigma) and 1 μg/mL amphotericin B (Sigma), and processed within 12 h of harvesting.

Histology of allanto-amnion and mesamnion

Paraffin embedding and preparation of histologic sections. For each sow, fragments of the four allanto-amnions and four mesamnions were fixed in 10% formalin for 48–72 h at 4°C. Tissues were dehydrated in a graded series of ethanol and embedded in paraffin. Tissue blocks were cut at 5- to 7-μm thickness using a microtome (Microm International GmbH, Walldorf), and sections were dewaxed and stained for general morphological purposes.

Hematoxylin & Eosin and Periodic Acid Schiff staining. Serial sections were stained either using a routine Hematoxylin & Eosin method for precise anatomical information or with Periodic Acid Schiff (PAS) staining technique to describe better the major tissue types in the specimens. PAS-positive structures stain magenta. Sections were examined under an Olympus BX51 photomicroscope connected to a digital camera and DP-soft (Olympus, Italy) for computer-assisted image acquisition and processing.

Isolation of amniotic mesenchymal and epithelial stem cells

The allanto-amniotic membranes collected were stripped mechanically from the overlying allantois to obtain the thin, transparent amniotic membranes. Then, pools of the amniotic membranes and pools of the mesamnions of each sow (4–5 grams of tissue for every type of membrane) were made.

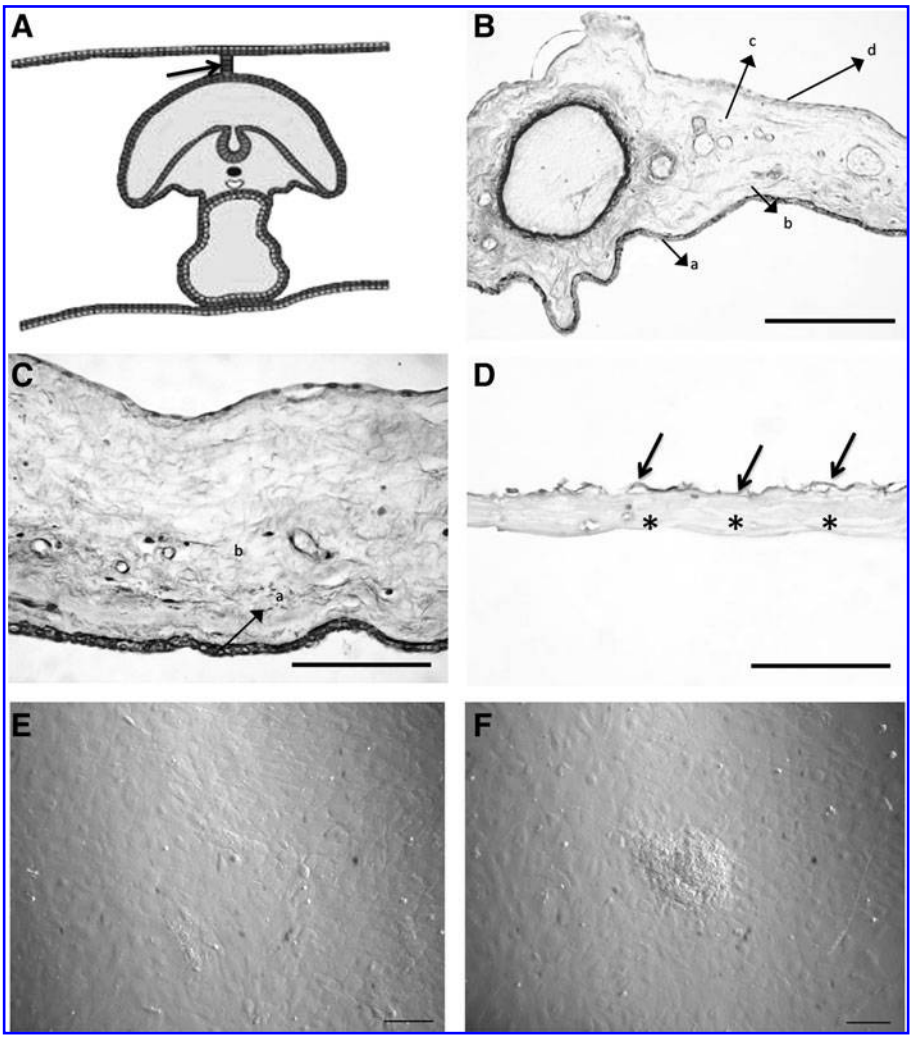

FIG. 1. Histology of swine fetal adnexa, PAS reaction. (**A**) Schematic drawing of the extraembryonic membranes in the early pig embryo, indicating how the mesamnion (arrow) forms (redrawn from Vejlsted, 2010). (**B**) Within the allanto-amnion, it is possible to appreciate four layers: (**a**) Amniotic epithelial layer of cuboidal cells; (**b**) amniotic mesenchymal layer; (**c**) allantois mesenchymal layer; (**d**) allantois epithelial layer of flattened cells. (**C**) Higher magnification of the allanto-amnion to demonstrate epithelial and stromal layers of amnion. (**D**) Mesamnion. The modified amniotic epithelium (arrows) is lying above the amniotic mesenchymal layer (asterisks). Observe the paucity of cells present in the mesenchymal components both of allanto-amnion and of the mesamnion. Scale bars: **B**, 200 μm; **C**, 100 μm; **D**, 40 μm. (**E**) Morphology of monolayer amnion-derived epithelial cells. (**F**) Clusters of AECs. Scale bar, 20 μm.

Membranes of each pool were cut into small pieces and digested enzymatically for 9 min at 37°C in a PBS solution containing 2.4 U/mL dispase (Becton Dickinson and Company, Italy).

Cell isolation was performed as previously reported (Lange Consiglio et al., 2012). Briefly, after a resting period of 5–10 min at room temperature in High-Glucose Dulbecco's Modified Eagle Medium (HG-DMEM; Celbio-Corning) supplemented with 10% heat-inactivated fetal bovine serum (FBS; Sigma) and 2 mM L-glutamine (Sigma), fragments were digested with 0.93 mg/mL collagenase type I (Sigma) and 20 μg/mL DNase (Roche, Mannheim, Germany) for $\approx$3 h at 37°C. The amniotic fragments were then removed, and cells were filtered using a 100-μm cell strainer (Sigma) before being collected by centrifugation at 200 $\times$ *g* for 10 min. In this way, amniotic mesenchymal cells (AMCs) were obtained. Meanwhile, the amnion fragments not digested by collagenase were collected in the strainer and further incubated twice with 0.05% trypsin (Sigma) at 37°C for 45 min to isolate amniotic epithelial cells (AECs). AECs were collected by filtration and centrifugation, as described above.

Culture, expansion, and cell count

Soon after isolation, the number of viable cells was counted using the Trypan Blue dye exclusion method (Sigma). Cells were plated at a density of 1×10^5 cell/cm^2 in T75 flasks (Euroclone). Cultures were established in HG-DMEM supplemented with 10% FBS, 10 ng/mL epidermal growth factor (EGF; Sigma), 1% penicillin (100 UI/mL) and streptomycin 100 μg/mL, 0.25 μg/mL amphotericin B, and 2 mM L-glutamine. Cell cultures were maintained in an incubator (SANYO CO2 Incubator, MCO-15AC), at 38.5°C,

in a humidified atmosphere (90%) with 5% CO_2. The medium was replaced after 72 h to eliminate nonadherent cells. Cell cultures were maintained changing the medium twice a week. After reaching confluence, corresponding to approximately 80% of the flask surface [passage 0 (P0)], the primary culture was detached from the bottom of the flask with 0.05% trypsin and 0.02% EDTA in phosphate buffer (Celbio-Corning) at 37°C for 2–3 min and seeded for subculture at 1×10^4 cell/cm^2.

Immunocytoscreen

AECs and AMCs were tested for immunoreactivity against Vimentin (mouse monoclonal, clone Vim V9; Dako, Glostrup, Denmark) and PanCytokeratin (mouse monoclonal, clone A1E; Santa Cruz Biotechnology, Santa Cruz, CA, USA). Cultured AECs and AMCs were fixed in Cytoscreen solution (Hospitex Diagnostics, Milan, Italy) for 48 h and then cytocentrifuged on Superfrost Plus slides (Thermo Scientific, Menzel GmbH & Co., KG, Braunshweig, Germany) and air-dried.

Briefly, for the immunocytochemistry procedure, primary antibodies (anti-Vimentin: 1/100; anti-PanCytokeratin: 1/200) diluted in Tris-buffered saline with Tween 20 (TBST) were applied and incubated overnight at 4°C. Secondary antibodies, conjugated with horseradish peroxidase (HRP), were added and incubated for 30 min at room temperature. The peroxidase reaction was developed for 10 min using diaminobenzidine (DAB), following the manufacturer's instructions (ImpactDAB, Vector Labs Inc., Burlingame, CA, USA) and blocked with deionized water. Cells were considered positive for Vimentin and PanCytokeratin when the presence of intracytoplasmic stain was observed. Negative controls for the target antigens were performed by replacing the primary antibodies with irrelevant antibodies from the host species in which the immunoglobulins were developed [rabbit immunoglobulin (Ig) fraction normal X093 and mouse IgG_1 X0931; Dako]. Negative controls in which the primary antibody was replaced with a buffer solution (TBST) alone were also performed.

Proliferation rate and CFU assay

Proliferation rate and CFU assay were determined as previously reported (Lange-Consiglio et al., 2012). Doubling time (DT) was assessed from P1 to P5, CFU assays were performed at P0 plating cells at different densities (100, 250, 500, and 1000 cells/cm^2). Colonies formed by 16–20 nucleated cells were counted under a BX71 inverted microscope (Olympus).

Flow cytometry

AECs were analyzed by flow cytometry to determine the percentage of pluripotent- (Oct-4) and mesenchymal- (CD73) associated markers after isolation (P0). Primary antibodies were purchased from Abcam (Cambridge, UK; goat polyclonal antibody Oct-4) and Santa Cruz Biotechnology Inc. (Texas, USA; rabbit polyclonal CD73). Secondary antibodies included donkey anti-goat IgG-AlexaFluor-488 and goat anti-rabbit IgG- AlexaFluor-488 (Abcam, Cambridge, UK). Staining procedure was performed as previously reported (Corradetti et al., 2011). Cells (1×10^6 cells / mL) were labeled with anti-CD73 in PBS with 3% of bovine serum albumin (BSA) (BDH; VWR International Ltd, Poole, UK) for 45 min at room temperature in the dark, followed by washing in cold PBS and final incubation with the secondary antibodies (1:250) for 30 min at room temperature in the dark.

For evaluation of Oct-4, cells (2×10^6 cells / mL) were fixed in 0.01% paraformaldehyde (in PBS) at 4°C for 15 min, washed in 3% BSA (in PBS), and then treated to promote permeability for 10 min at room temperature in 1% Triton-X 100 (in PBS). After incubation, cells were washed twice in ice-cold PBS and analyzed using a Millipore Guava easyCyte™ Single Sample Flow Cytometer. A minimum of 10,000 cells was acquired for each sample and analyzed in the FL1 channel. All analyses were based on control cells incubated with isotype-specific IgGs to establish background signal. Off-line analyses of the flow cytometry standard (FCS) files were performed using Weasel software v.2.5 (http://en.bio-soft.net/other/weasel.html).

In vitro *differentiation*

To assess their potential to undergo mesodermic (osteogenic and adipogenic), ectodermic (neurogenic), and endodermic (pancreatic) differentiation, AECs were expanded up to P3 and then seeded at a density of 3×10^3 cell/cm^2. Cells plated at the density of 1.5×10^3 cells/cm^2 were used as control (noninduced cells). When 80% confluence was achieved, the differentiation procedure began. Controls (or the uninduced cells) were cultured for the same time as the differentiation protocol in growth medium.

Osteogenic differentiation. To induce osteogenic differentiation, cells were incubated in HG-DMEM supplemented with 10% FBS, 100 U/mL penicillin, 100 μg/mL streptomycin, 0.25 μg/mL amphotericin B, 2 mM L-glutamine, 10 mM β-glycerophosphate (Sigma), 0.1 μM dexamethasone (Sigma), and 250 μM ascorbic acid (Sigma). Osteogenic differentiation was performed by incubating cells for 3 weeks at 38.5°C and 5% CO_2. The medium was changed twice a week for 3 weeks. Bone was used as positive control.

Adipogenic differentiation. Adipogenic differentiation was performed by stimulating cells with three cycles of induction/maintenance for a 21-day period. The adipogenesis induction medium was composed of HG-DMEM supplemented with 10% FBS, 100 U/mL penicillin, 100 μg/mL streptomycin, 0.25 μg/mL amphotericin B, 2 mM L-glutamine, 10 μg/mL insulin (Sigma), 150 μM indomethacin (Sigma), 1 μM dexamethasone, and 500 μM 3-isobutyl-methylxanthine (IBMX; Sigma). The adipogenesis maintenance medium was composed of HG-DMEM supplemented with 10% FBS and 10 μg/mL insulin. Adipose tissue was used as positive control.

Neurogenic differentiation. Neurogenic differentiation was performed with a 24-h preinduction in a medium composed of HG-DMEM supplemented with 20% FBS and 1 mM β-mercaptoethanol (Sigma) (Mitchell et al., 2003). Then, neurogenic induction was performed with a medium composed of HG-DMEM supplemented with 2% FBS, 2% dimethyl sulfoxide (Sigma), and 200 μM butylated hydroxyanisole (Sigma). Cells were maintained in this medium for 3 days. Spinal cord was used as positive control.

Table 1. Oligonucleotide Sequences Used for PCR Analysis and Their Description

	Gene	*Forward (F) and reverse (R) primers*	*Annealing temperature*	*Size cDNA*
Housekeeping gene	*GAPDH*	F, GCAAAGTGGACATTGTCGCCATCA R, AGCTTCCCATTCTCAGCCTTGACT	62°C	124 bp
Pluripotent markers	*Oct-4*	F, GTTCAGCCAAACGACCATCTG R, TCTCTGCCTTGCATATCTCCTG	62°C	140 bp
	Nanog	F, AACTTCACCAATGCCTGAG R, CTGATCTTCTGCTTCTTGACTG	58°C	234 bp
	Sox2	F, CAGCCCAGACCGAGTTAAGC R, ATCCGGGTGCTCCTTCATGT	63°C	214 bp
Mesenchymal markers	*CD117*	F, GGACCGAAGGAGGCACTTAC R, AACGGAACATCTCTGCTCGG	59°C	206 bp
	CD166	F, TGGTCACAGAGGACAACGT R, CCACGTGATGTTGCCATCTG	58°C	167 bp
	CD29	F, TAAGAGTGCCGTGACAACCG R: TTCAGAACCTGCCCATAGCG	64°C	154 bp
	CD90	F: GCTAACAGTCTTGCAGGTGG R, AGAAGTTGGTTCGAGAGCGG	64°C	212 bp
	CD73	F, ATTCGAGCAAGTGCGTCAAC R, TCGTAACCCAAGGCGTTCAT	64°C	193 bp
Hematopoietic marker	*CD34*	F, ACCAGAGCTACTCCCGAAAG R, TAAGGGTCTTCGCCCAGC	58°C	139 bp
Immunological markers	*MHC I*	F, TGGAGAGGAGCAGAGCTACAC R, CTGTCACTGCCTGCAGCCT	65°C	225 bp
	MHC II	F, CCTGCTCCCCTTACACACTG R, TGCAATAACCTCACCCGCTC	62°C	209 bp
Osteogenic markers	*BGLAP*	F, TCAACCCCGACTGCGACG R, TTGGAGCAGCTGGGATGATGG	63°C	204 bp
	OPN	F, TTGCTAAAGCCTGACCCATCT R, CGTCGTCCACATCGTCTGT	58°C	145 bp
Adipogenic markers	*ADIPQ*	F, TATGATGTCACCACTGGCAAATT R, TAGAGGAGCACAGAGCCAGAG	60°C	185 bp
	LEP	F, AGCCTTTCGACCATCAAGCA R, CAACTTGTGTTGCGTGGGAG	63°C	100 bp
Neurogenic markers	*GFAP*	F, ATCGAGATCGCCACCTACAG R: CAGGCTGGTTTCTCGGATCT	58°C	102 bp
	NES	F, CAGGAGAAACAGGGCCTACA R, GCTCCAACTTAGGGTCCAAGA	58°C	193 bp
Pancreatic markers	*INS*	F, AGGCCTTCGTGAACCAGCAC R, GAGGGAACAGATGCTGGTGC	62°C	233 bp
	PDX-1	F, AAGGCTCACGCGTGGAAAAGG R, CATGCGGCGGTTTTGGAACC	62°C	229 bp

F, forward; R, reverse; *GAPDH*, glyceraldehyde-3-phosphate dehydrogenase; *BGLAP*, osteocalcin; *OPN*, osteopontin; *ADIPQ*, adiponectin; *LEP*, leptin; *GFAP*, glial fibrillary acidic protein; *NES*, nestin; *INS*, insulin; *PDX-1*, pancreatic and duodenal homeobox 1.

Pancreatic differentiation. Expanded AECs at P3 were induced to differentiate by a three-step protocol (Gao et al., 2008). In step 1, the cell monolayer was treated for 24 h with HG-DMEM supplemented with 10% FBS and 10^{-6} M retinoic acid (Sigma); then the medium was changed with HG-DMEM with only 10% FBS for 2 days. In step 2, the cells were detached with 0.25% trypsin–EDTA and seeded in extracellular matrix (ECM) gel- (Euroclone) coated 60-mm plates. The medium was switched to Low-DMEM, supplemented with 10% FBS, 10 mmol/L nicotinamide (Sigma), and 20 ng/mL EGF (Sigma) for 6 days. In step 3, to mature the insulin-producing cells, the low-glucose medium was supplemented with 10% FBS and 10 nmol/L exendin-4 (Sigma) for 6 days. As a control group, the cells were cultured in Low-DMEM containing only 10% FBS.

To confirm differentiation toward the osteogenic, adipogenic, and neurogenic lineages, conventional von Kossa, Oil Red O, and Nissl stainings were performed, respectively, whereas pancreatic differentiation was monitored by observation of three-dimensional, islet-like cell cluster formation. Gene expression of specific differentiation markers was evaluated.

Gene expression analysis (RT-PCR)

Qualitative PCR analysis was performed to evaluate the expression of specific MSC-, pluripotent-, histocompatibility-, and hematopoiesis -associated markers at P0, P1, P3, and P5 and to confirm differentiation. Total RNA was isolated from cells using TRIzol® Reagent (Invitrogen, Carlsbad, CA, USA)

according to manufacturer's instructions. RNA concentration and purity were measured using a NanoDrop Spectrophotometer (NanoDrop ND1000, Wilmington, DE, USA). The cDNA was synthesized from 1 μg of total RNA using the iScript retrotranscription kit (Bio-Rad Laboratories), and a qualitative PCR reaction was performed using the Taq DNA Polymerase recombinant commercial kit (Invitrogen Life Technologies). All amplification reactions were performed using a T1 Thermocycler (Biometra). The conditions of the amplification reaction were: 94°C for 2 min (initial denaturation); 94°C for 30 sec (denaturation); 58–65°C (temperature depending on the melting temperature of primers) for 30 sec (annealing); 72°C for 30 sec (extension); 72°C for 10 min (final elongation). Denaturation, annealing, and extension steps were repeated 32 times.

Primer design. Swine-specific oligonucleotide primers were designed using open source PerlPrimer software v. 1.1.17, based on available NCBI *Sus scrofa* sequences or on mammalian multialigned sequences. Primers were designed across an exon–exon junction to avoid DNA amplification. Table 1 lists the primers used to characterize AECs and confirm their multidifferentiation potential. *GAPDH* (glyceraldehyde-3-phosphate dehydrogenase) was used as a reference gene.

Statistical analysis

Statistical analysis was performed using GraphPad Instat 3.00 for Windows (GraphPad Software, La Jolla, CA, USA). Three replicates for each experiment (growth curve, DT, and CFU) were performed and the results are reported as mean ± standard deviation (SD). One-way analysis of variance (ANOVA) for multiple comparisons by Student–Newman–Keuls multiple comparison tests was used. CFU comparisons among different cell plating densities inside each group were analyzed. Differences were considered statistically significant for p values <0.05.

Results

Histological analysis, cell collection, and morphology

Figure 1, B and C, shows that different contiguous tissues can be distinguished within the allanto-amnion—amniotic epithelial layer, amniotic mesenchymal layer, allantoic mesenchymal layer, and allantoic epithelial layer. The amnion consisted of cuboidal epithelial cells in the epithelial layer (Fig. 1B, Ca) and of stromal cells in the underlying mesenchymal layer (Fig. 1B, Cb). The adjacent allantoic membrane was composed of mesenchymal tissue (Fig. 1B, Cc) covered by the flattened allantoic epithelium (Fig. 1B, Cd). The amniotic and allantoic counterparts were separated mechanically for further analyses. At the time of membrane collection, a thin membrane was harvested from the backs of piglets. On the basis of histologic analysis and of its positioning, this membrane was thought to be the mesamnion (Fig. 1D). Both the allanto-amnion and the mesamnion showed a paucity of cells in their mesenchymal components. Actually, no cells were obtained from the stromal layer of the amnion or the mesamnion, and only the amnion epithelial layer proved to be an efficient source of cells to be plated and maintained in culture (AECs). A concentration of 10×10^6 cells/gram of digested tissue was obtained after digestion and viability of the isolated cells was higher than 95%. AECs showed a typical polygonal morphology (Fig. 1E). Cell colonies, observed since the first culture steps, demonstrated an ability to organize into three-dimensional structures and to form clusters (Fig. 1F).

Immunocytoscreen

AECs were strongly positive for PanCytokeratin and negative for Vimentin (Fig. 2A, B).

Proliferation analysis

Figure 3A shows the growth curve for AECs at P1, P3, and P5. AECs showed a growth curve, with an initial lag phase of few hours and a further intense log phase of 2–12 days at P1 and P3. At P5, AECs showed a slow lag phase (about 4 days) and a less intensive log phase. Statistically significant differences ($p < 0.05$) in DT were identified between the passages studied (see asterisks in Fig. 3B). After P1, the proliferation rate increased; indeed, the values decreased at P2 and remained constant until P3. The mean DT value was 24.77 ± 6 h. A statistically significant increase ($p < 0.05$) in fibroblast CFUs (CFU-F) frequency was observed, reflecting the increase of plating density (Table 2).

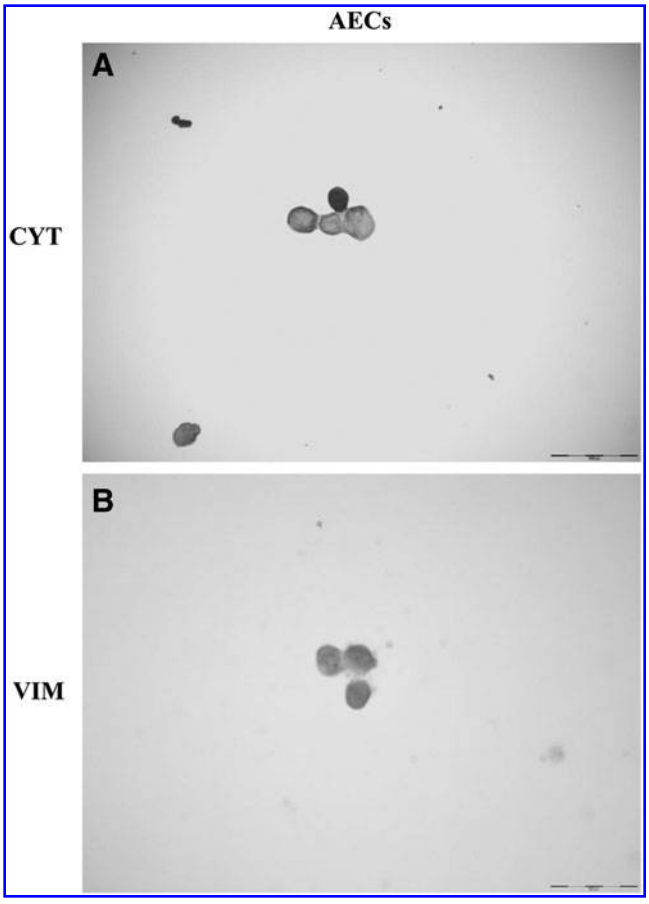

FIG. 2. Immunocytoscreen results. Immunolocalization of cytokeratins (CYT) and vimentin (VIM) in AECs (**A**, **B**). Scale bars, 15 μm.

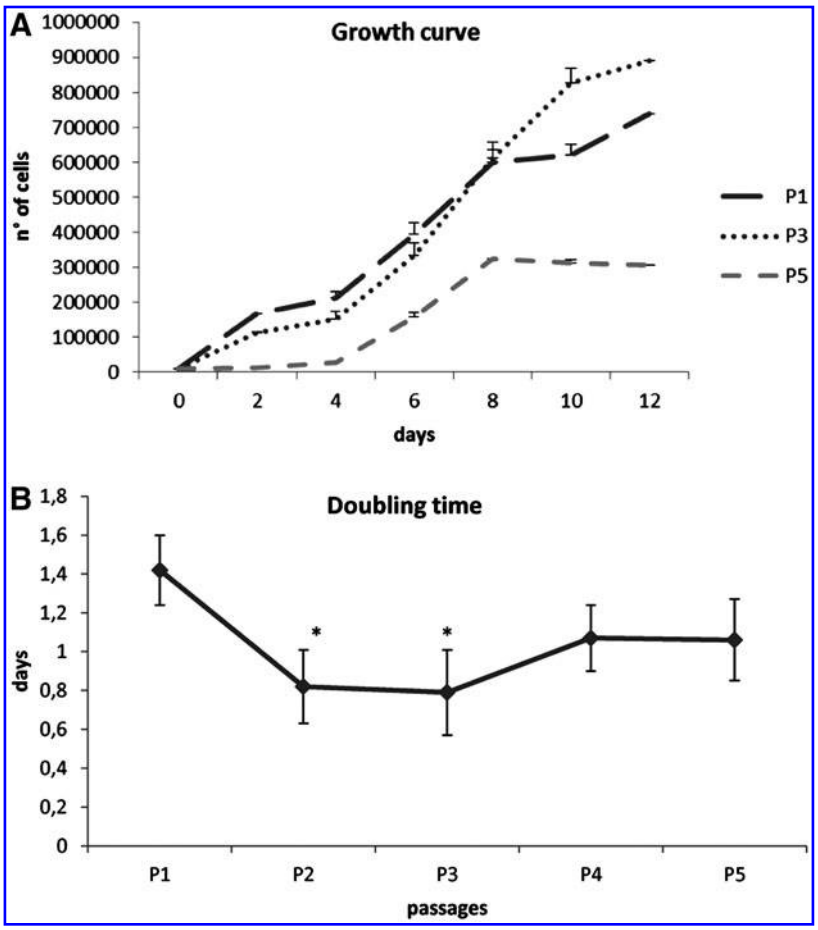

FIG. 3. Proliferative potential. (**A**) Growth curve of AECs at P1, P3, and P5. (**B**) Doubling time of AECs at different passages during cell culture. Statistically significant differences were observed in doubling time means between the passages studied (*$p < 0.05$).

Flow cytometry analysis

Flow cytometry analysis was assessed to evaluate the homogeneity of the cell population and to identify the subset of pluripotent or mesenchymal cells. The cell population tested resulted homogeneously composed of CD73- and Oct-4–positive cells, as reported in Figure 4.

In vitro *differentiation*

At P3, AECs were shown to be plastic and able to undergo osteogenic, adipogenic, neurogenic, and pancreatic differentiation. After 21 days of induction, the osteogenic differentiation of AECs was confirmed by Von Kossa staining, which highlighted calcium precipitates. Moreover, cells modified their morphology and increased their size. The control sample did not stain and did not develop a mineralized matrix. The osteogenic induction was further verified through RT-PCR analysis of osteogenesis-associated markers expression—osteocalcin (*BGLAP*) and osteopontin (*OPN*). Induced cells expressed *OPN* and *BGLAP*, whereas control cells did not. Bone was used as positive control for the expression of osteogenic markers (Fig. 5A).

After 3 weeks of induction, AECs demonstrated differentiation ability. Indeed, after adipogenic induction, the Red Oil O staining showed intracellular lipid vacuoles that were not present in control AECs maintained in standard medium. RT-PCR for the expression of adipogenic markers such as adiponectin (*ADIPQ*) and leptin (*LEP*) confirmed adipogenic induction. Adipose tissue was used as positive control (Fig. 5B).

After 3 days of neurogenic induction, stimulated cells acquired a typical neuronal morphology and stained positively for Nissl, whereas uninduced cells did not. The analysis of neurogenic expression markers, such as the glial fibrillary acidic protein (*GFAP*) and nestin (*NES*) confirmed the neurogenic induction. Spinal cord was used as positive control (Fig. 5C).

After 15 days of induction, AECs changed their typical epithelial shape and gradually organized large three-dimensional colonies (Fig. 5D), reminiscent of typical

TABLE 2. COLONY-FORMING UNIT ASSAY OF AMNIOTIC EPITHELIAL CELLS AT PASSAGE 0

Density cells/cm²	*Total cells*	*CFU-F*	*1 CFU-F each*
100	950	54 ± 0	17.59[a]
250	2375	218 ± 1.53	10.89[b]
500	4750	Confluence	
1000	9500	Confluence	

Different superscripts (a, b) indicate statistically different comparisons ($p < 0.05$) between cell densities in each group.
CFU-F, fibroblast colony-forming units.

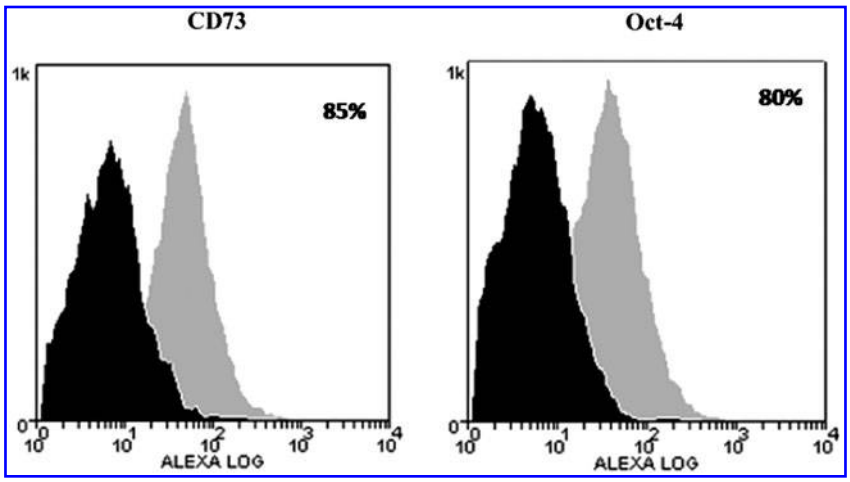

FIG. 4. Flow cytometry analysis of antigen expression with Alexafluor-488 labeled antibodies: Oct-4 and CD73. Histograms represent relative number of cells vs. fluorescence intensity (FL1). Black histograms indicate background fluorescence intensity of cells labeled with isotype control antibodies only; grey histograms show positivity to the studied antibodies.

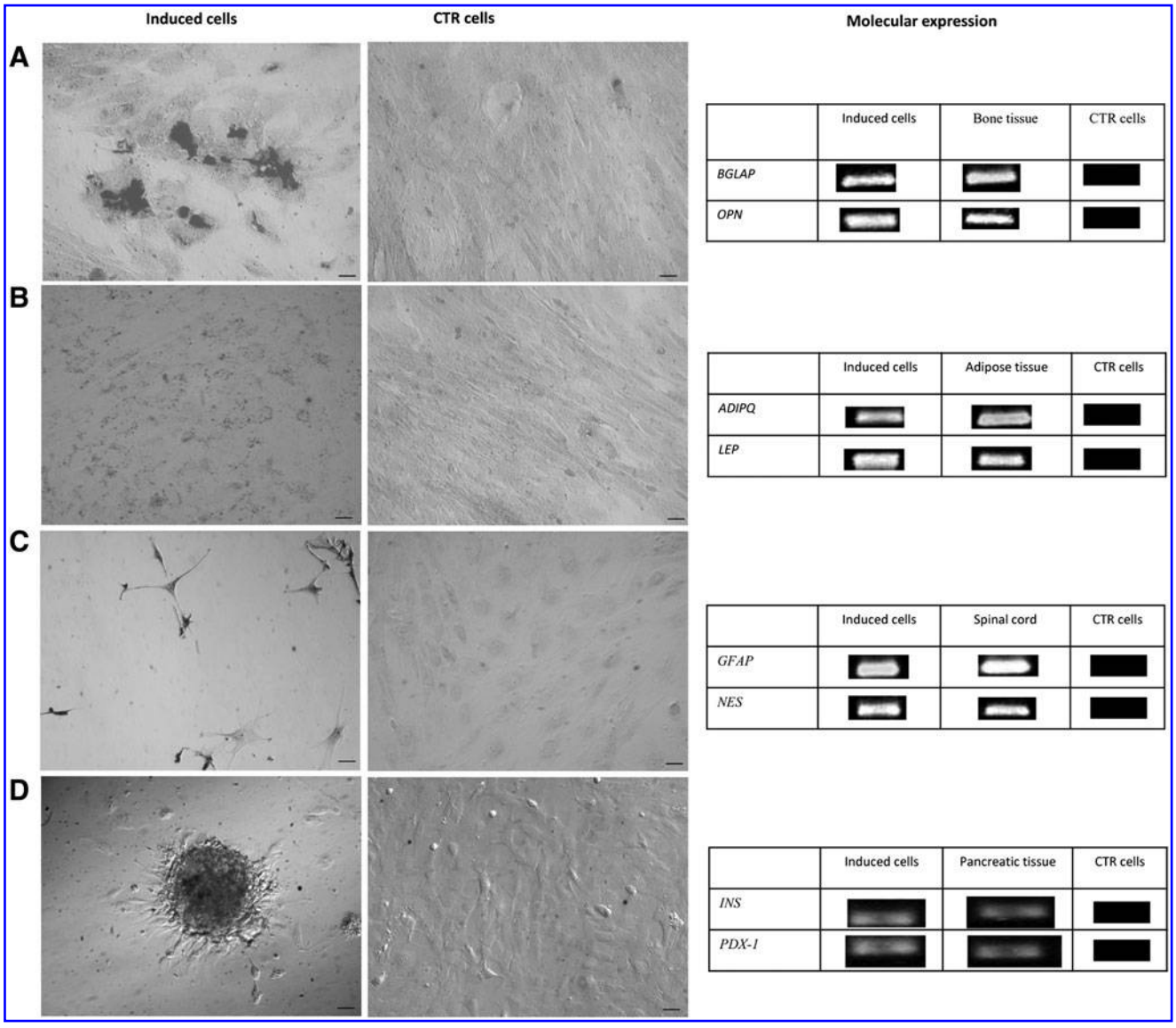

FIG. 5. Differentiation potential. (**A**) Osteogenic differentiation: Von Kossa staining on induced and control (CTR) AECs, and osteogenesis-associated marker expression. (**B**) Adipogenic differentiation: Oil Red O staining in induced and CTR AECs, and adipogenesis-associated marker expression. (**C**) Neurogenic differentiation: Nissl staining in induced and CTR AECs, and neurogenic marker expression. (**D**) Pancreatic differentiation: AECs organized large three-dimensional colonies reminiscent of typical pancreatic islets *in vitro* and pancreatic marker expression Scale bars, 20 μm. See text for acronyms of the different markers.

pancreatic islets *in vitro*. Expression of insulin and pancreatic and duodenal homeobox 1 (*PDX-1*) mRNA transcripts were detected by RT-PCR.

Evaluation of marker expression by RT-PCR

To characterize amniotic stem cells, RT-PCR analysis was performed on cells at different passages (P0, P1, P3, P5). As shown in Figure 6, cells expressed mesenchymal-associated markers (*CD166*, *CD117, CD29, CD90, CD73*), embryonic-associated markers (*Nanog, Oct-4, Sox2*), and the immunological marker *MHC-I*. They did not express *MHC-II* nor the hematopoietic marker *CD34* from P0 to P5. Of particular interest is the *CD117* expression that decreased from P0 to P5,

Discussion

The advantage of using amniotic membrane for production of stem/progenitor cells in human and animal species is the availability of the large amount of these tissues and the noninvasive collection procedure at birth. Because the amniotic membrane is an extrafetal tissue, we conjectured that amniotic cells with the potential to be primitive mesenchymal cell types might also exist in full-term porcine amnion. Moreover, considering the similarity between pigs and humans, the chance to characterize porcine stem cells from this source could be helpful in experimental cell-based therapies.

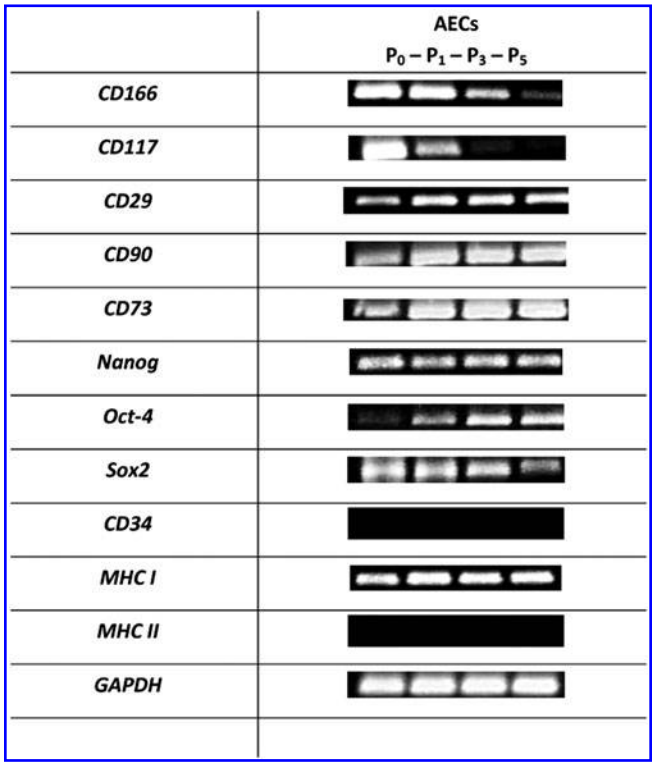

FIG. 6. RT-PCR analysis. Specific gene expression in AECs from P0 to P5 of mesenchymal (*CD166*, *CD117, CD29, CD90, CD73*), pluripotent (*Nanog, Oct-4, Sox2*), hematopoietic (*CD34*) and histocompatibility (*MHC-I* and *MHC-II)* mRNA markers. *GAPDH* was used as reference gene.

The aim of this study was to isolate and characterize presumptive stem cells from the porcine amniotic membrane, suggested in several studies to be an optimal source of pluripotent/multipotent stem cells in a variety of veterinary species (Corradetti et al., 2013; Filioli Uranio et al., 2011; Lange Consiglio et al., 2012; Muttini et al., 2013; Rutigliano et al., 2013). Usually, two cell types are harvested from this tissue—amniotic epithelial and mesenchymal cells. In contrast to findings in other species, in the present study we were able to isolate only AECs from the amniotic membrane; the mesenchymal layer of amniotic membrane contained few stromal cells. Concerning the mesamnion, few epithelial cells and no stromal cells could be retrieved. For this reason, only amniotic AECs were expanded, characterized, and differentiated. After digestion, large numbers of AECs with greater than 95% viability (optimal value in terms of plating efficiency and cellular growth) were obtained. Positivity to cytokeratin and negativity to vimentin confirmed that isolated cells were epithelial cells.

When cultured, AECs demonstrated strong adherence to plastic dishes and developed epithelial polygonal morphology over time. Adherence is a fundamental property of cultured stem cells (Dominici et al., 2006). When AECs were kept in culture, small cell clusters or spheroid structures developed, showing that these cells lacked contact-inhibited cell growth and continued to proliferate after reaching 100% surface confluence, forming aggregates overlying the monolayer of confluent cells. Other investigators have reported that the monolayer of amniotic cells may support the growth and lack of differentiation in amniotic cells forming the spheroid structures, possibly playing the role of an autologous feeder layer and providing secreted factors (Miki et al., 2010).

The proliferation study showed that AECs reached high plating efficiency and had a high proliferation rate *in vitro* until P3, when AECs showed a growth curve with a lag phase of few hours and an intensive log phase of 12 days. Moreover, the DT value at P3 was 19 h. These data are in agreement with those obtained by other researchers who reported a high proliferation rate of human (Miki et al., 2010; Soncini et al., 2007), equine (Lange-Consiglio et al., 2012), bovine (Corradetti et al., 2013), and feline (Rutigliano et al., 2013) amniotic cells. After this period, the proliferation rate decreased.

During the different subcultures, the time required to remove adherent cells from a culture surface using trypsin increased reaching a maximum of about 20 min. It is likely that prolonged treatment with trypsin degrades membrane proteins, causing alterations in the cells' ability to adhere to the plate. Indeed, at P5 the lag phase was 4 days. For this reason, in this preliminary study, cell expansion could not be continued beyond P5. This problem, which can be circumvented by use of other techniques for cell detachment (for example using scrapers), does not affect the potential therapeutic use of these cells because in regenerative medicine cells are usually used at P3. Indeed, this passage is considered the best passage to obtain homogeneity of cells and to prevent aging in the plate that would lead to epigenetic changes in gene expression related to *in vitro* culture (Lange-Consiglio et al., 2012).

Swine AECs also showed the ability to produce clones and revealed the typical expression pattern expected for

cultured stem cells (Dominici et al., 2006) when analyzed by RT-PCR and flow cytometry. It has been demonstrated in both human (Manuelpillai et al., 2011; Marongiu et al., 2010; Miki et al., 2010; Soncini et al., 2007) and animal MSCs (Chen et al., 2011; Corradetti et al., 2013; Lange-Consiglio et al., 2012; Lovati et al., 2011; Iacono et al., 2012) that pluripotent- and mesenchymal-associated markers are expressed. In our results, the same expression pattern occurred, with the exception of *CD117*, which decreased substantially from P0 to P5, as reported in some other studies (Meirelles et al., 2003, 2006). The isolated cells are epithelial cells, but they expressed MSC markers. Bilic et al. (2008) reported that human AECs had an antigenic expression profile characteristic of culture-expanded MSCs and could co-express epithelial and mesenchymal cell markers (Sakuragawa et al., 2004).

In fact, it has been reported that the amnion-derived cells have not completely differentiated into the epithelial or mesenchymal phenotype; another explanation is that the epithelial–mesenchymal transition may occur in the amniotic membrane (Bilic et al., 2008; Sakuragawa et al., 2004). Expression of the hematopoietic marker *CD34* was not found at any passage. This result was expected, and it confirmed that isolated cells do not belong to a hematopoietic lineage.

To assess the usefulness of porcine AECs for cell therapy, expression of markers related to cell immunogenicity, including *MHC-I* and *MHC-II,* was also evaluated. At each passage studied, AECs were negative for *MHC-II* and positive for *MHC-I*, consistent with previous reports (Corradetti et al., 2013; Lange-Consiglio et al., 2012), thus reinforcing the role of the amniotic membrane as an allogenic source for cell-based therapies in pigs.

Differentiation data confirmed the high plasticity of these cells that can differentiate into mesodermic (osteogenic and adipogenic), ectodermic (neurogenic), and endodermic lineages. After 21 days of induction, mineral deposits were confirmed by Von Kossa staining and by the expression of *BGLAP* and *OPN*. These results suggest that these cells reached a mature osteogenic differentiation, as *BGLAP* and *OPN* genes are associated to the matrix maturation and mineralization phases (Raouf and Seth, 2000). Stimulated AECs were also able to undergo adipogenic differentiation confirmed by expression of *LEP* and *ADIPQ* (regarded as intermediate and late markers of adipocyte differentiation). Moreover, AECs acquired a neuron-like morphology and expressed specific neuronal markers expression (*GFAP* and *NES)* after *in vitro* induction. The morphological changes and the marker expression confirmed that the cell population comprised neuronal precursor stem cells (Lendahl et al., 1990), as observed for amniotic-fluid derived MSCs in the same species (Zheng et al., 2010). Regarding the pancreatic differentiation, morphological and molecular studies suggest that the differentiation occurred, but further study will be needed to confirm the ability of these induced cells to secrete insulin.

This work allowed the isolation, characterization, and differentiation of stem cells derived from the epithelial layer of the amniotic membrane in pigs. Altogether, our findings suggest that porcine amniotic membrane is a reliable source of presumptive AECs, displaying intermediate features between adult and embryonic stem cells, and could have a wide clinical application because of their low immunogenicity and high differentiation potential. Only epithelial cells were isolated here, but the amniotic epithelium layer, while originating from the trophectoderm as with other parts of fetal membranes, has the peculiarity of being continuous with the epiblast (Vejlsted, 2010). For this reason, it may probably preserve some of the characteristics of the epiblast (Miki et al., 2006), such as *Nanog* and *Oct4* expression.

Conclusion

The advantages of this study are the source of cells (amniotic membrane) and the pig as an animal model. Collection of the amnion, in comparison to embryonic and adult tissues, does not pose ethical issues, and its retrieval at term is a noninvasive procedure. One of the most important criteria when choosing an animal model is its relevance to human conditions. Over the years, a huge amount of information, mostly conducted on standard laboratory animals such as rodents, has been generated. When new therapies for human use are designed using this data, they often fail, particularly if the metabolism of xenobiotics of interest is different.

Aside from nonhuman primates, the pig is the species that shares the closest evolutionary resemblance to humans (Verma et al., 2011); thus, its human-like physiology means that data obtained in this species are highly relevant for human-related therapeutic research. In addition to the potential use of porcine amniotic cells as candidates in auto/allo/xenogenic transplantation, these AECs are widely available and could also be used to evaluate the safety and efficacy of cell therapies.

Acknowledgment

This study was supported by grants from Università degli Studi di Milano and Università Politecnica delle Marche, Ancona, Italy.

Author Disclosure Statement

The authors declare that no conflicting financial interests exist.

References

Bilic, G., Zeisberger, S.M., Mallik, A.S., Zimmermann, R., and Zisch, A.H. (2008). Comparative characterization of cultured human term amnion epithelial and mesenchymal stromal cells for application in cell therapy. Cell Transplant. 17, 955–968.

Carlin, R., Davis, D., Weiss, M., Schultz, B., and Troyer, D. (2006). Expression of early transcription factors Oct-4, Sox-2 and Nanog by porcine umbilical cord (UC) matrix cells. Reprod. Biol. Endocrinol. 6, 4–8.

Casal, M., and Haskins, M. (2006). Large animal models and gene therapy. Eur. J. Hum. Genet. 14, 266–272.

Chang, Y.J., Shih, D.T.B., Tseng, C.P., Hsieh, T.B., Lee, D.C., and Hwang, SM. (2006). Disparate mesenchyme-lineage tendencies in mesenchymal stem cells from human bone marrow and umbilical cord blood. Stem Cells 24, 679–685.

Chen, J., Lu, Z., Cheng, D., Peng, S., and Wang, H. (2011). Isolation and characterization of porcine amniotic fluid-derived multipotent stem cells. PLoS One 6, e19964.

Corradetti, B., Lange-Consiglio, A., Barucca, M., Cremonesi, F., and Bizzaro, D. (2011). Size-sieved subpopulations of mesenchymal stem cells from intervascular and perivascular equine umbilical cord matrix. Cell Prolif. 44, 330–342.

Corradetti, B., Meucci, A., Bizzaro, D., Cremonesi, F., and Lange Consiglio, A. (2013). Mesenchymal stem cells from amnion and amniotic fluid in the bovine. Reproduction 145, 391–400.

Cremonesi, F., Violini, S., Lange Consiglio, A., Ramelli, P., Ranzenigo, G., and Marian, P. (2008). Isolation, in vitro culture and characterization of foal umbilical cord stem cells at birth. Vet. Res. Commun. 32 (Suppl 1), 139–142.

De Coppi, P., Bartsch, G. Jr., Siddiqui, M.M., Xu, T., Santos, C.C., Perin, L., Mostoslavsky, G., Serre, A.C., Snyder, E.Y., Yoo, J.J., Furth, M.E., Soker, S., and Atala, A. (2007). Isolation of amniotic stem cell lines with potential for therapy. Nat. Biotechnol. 25, 100–106.

Delo, D.M., De Coppi, P., Bartsch, G.Jr., and Atala, A. (2006). Amniotic fluid and placental stem cells. Methods Enzymol. 419, 426–438.

Dev, K., Giri, S.K., Kumar, A., Yadav, A., Singh, B., and Gautam, S.K. (2012). Derivation, characterization and differentiation of buffalo (*Bubalus bubalis*) amniotic fluid derived stem cells. Reprod. Domest. Anim. 47, 704–711.

Digirolamo, C.M., Stokes, D., and Colter, D. (1999). Propagation and senescence of human marrow stromal cells in culture: A simple colony-forming assay identifies samples with the greatest potential to propagate and differentiate. Br. J. Haematol. 107, 275–281.

Doherty, M.K., Beynon, R.J., and Whitfield, P.D. (2008). Proteomics and naturally occurring animal diseases: Opportunities for animal and human medicine. Proteomics Clin. Appl. 2, 135–141.

Dominici, M., Le Blanc, K., Mueller, I., Slaper-Cortenbach, I., Marini, F., Krause, D., Deans, R., Keating, A., Prockop, D.J., and Horwitz, E. (2006). Minimal criteria for defining multipotent mesenchymal stromal cells. The International Society for Cellular Therapy position statement. Cytotherapy 8, 315–317.

Evangelista, M., Soncini, M., and Parolini, O. (2008). Placenta-derived stem cells: New hope for cell therapy? Cytotechnology 58, 33–42.

Filioli Uranio, M., Valentini, L., Lange Consiglio, A., Caira, M., Guaricci, A.C., Guaricci, A.C., Catacchio, C.R., Ventura, M., Cremonesi, F., and Dell'Aquila, M.E. (2011). Isolation, proliferation, cytogenetic, and molecular characterization and in vitro differentiation potency of canine stem cells from foetal adnexa: A comparative study of amniotic fluid, amnion, and umbilical cord matrix. Mol. Reprod. Dev. 78, 361–373.

Gao, F., Wu, D.Q., Hu, Y., Jin, G.X., Li, G.D., Sun, T.W., and Li, F.J. (2008) In vitro cultivation of islet-like cell clusters from human umbilical cord blood-derived mesenchymal stem cells. Transl. Res. 151, 293–302.

Gao, Y., Zhu, Z., Zhao, Y., Hua, J., Ma, Y., and Guan, W. (2014). Multilineage potential research of bovine amniotic fluid mesenchymal stem cells. Int. J. Mol. Sci. 15, 3698–3710.

Grewal, S.S., Barker, J.N., Davies, S.M., and Wagner, J.E. (2003). Unrelated donor hematopoietic cell transplantation: Marrow or umbilical cord blood? Blood 101, 4233–4244.

Gucciardo, L., Lories, R., Ochsenbein-Kolble, N., Done, E., Zwijsen, A., and Depresta, J. (2009). Fetal mesenchymal stem cells: Isolation, properties and potential use in perinatology and regenerative medicine. BJOG 116, 166–172.

Guillot, P.V., Gotherstrom, C., Chan, J., Kurata, H., and Fisk, N.M. (2007). Human first-trimester fetal MSC express pluripotency markers and grow faster and have longer telomeres than adult MSCs. Stem Cells 25, 646–654.

Hoynowski, S.M., Fry, M.M., Gardner, B.M., Leming, M.T., Tucker, J.R., Black, L., Sand, T., and Mitchell, K.E. (2007). Characterization and differentiation of equine umbilical cord-derived matrix cells. Biochem. Biophys. Res. Commun. 362, 347–353.

Hyttel, P., Kamstrup, K.M., and Hyldig, S. (2011). From hatching into fetal life in the pig. Acta Scientiae Veterinariae 39 (Suppl 1), 203–221.

Iacono, E., Brunori, L., and Pirrone, A. (2012). Isolation, characterization and differentiation of mesenchymal stem cells from amniotic fluid, umbilical cord blood and Wharton's jelly in the horse. Reproduction 143, 455–468.

In't Anker, P.S., Scherjon, S.A., Kleijburg-van der Keur, C., De Groot Swings, G.M., Claas, F.H., Fibbe, W.E., and Kanhai, H.H. (2004). Isolation of mesenchymal stem cells of fetal or maternal origin from human placenta. Stem Cells 22, 1338–1345.

Kang, J.G., Park, S.B., Seo, M.S., Kim, H.S., Chae, J.S., and Kang, K.S. (2013). Characterization and clinical application of mesenchymal stem cells from equine umbilical cord blood. J. Vet. Sci. 14, 367–371.

Kern, S., Eichler, H., Stoeve, J., Kluter, H., and Bieback, K. (2006). Comparative analysis of mesenchymal stem cells from bone marrow, umbilical cord blood, or adipose tissue. Stem Cells. 24, 1294–1301.

Kögler, G., Sensken, S., Airey, J.A., Trapp, T., Müschen, M., Feldhahn, N., Liedtke, S., Sorg, R.V., Fischer, J., Rosenbaum, C., Greschat, S., Knipper, A., Bender, J., Degistirici, O., Gao, J., Caplan, A.I., Colletti, E.J., Almeida-Porada, G., Müller, H.W., Zanjani, E., and Wernet, P.A (2004). New human somatic stem cell from placental cord blood with intrinsic pluripotent differentiation potential. J. Exp. Med. 200, 123–135.

Kumar, B.M., Yoo, J.G., and Ock, S.A. (2007). In vitro differentiation of mesenchymal progenitor cells derived from porcine umbilical cord blood. Mol. Cells. 24, 343–350.

La Rocca, G., Anzalone, R., Corrao, S., Magno, F., Loria, T., Lo Iacono, M., Di Stefano, A., Giannuzzi, P., Marasà, L., Cappello, F., Zummo, G., and Farina, F. (2009). Isolation and characterization of Oct-4+/ HLA-G+ mesenchymal stem cells from human umbilical cord matrix: Differentiation potential and detection of new markers. Histochem. Cell Biol. 131, 267–282.

Lange Consiglio, A., Corradetti, B., Bizzaro, D., Magatti, M., Ressel, L., Tassan, S., Parolini, O., and Cremonesi, F. (2012). Characterization and potential applications of progenitor-like cells isolated from horse amniotic membrane. J. Tissue Eng. Regen. Med. 6, 622–635.

Lange-Consiglio, A., Corradetti, B., Meucci, A., Perego, R., Bizzaro, D., and Cremonesi, F. (2013a). Characteristics of equine mesenchymal stem cells derived from amnion and bone marrow: In vitro proliferative and multilineage potential assessment. Equine Vet. J. 45, 737–744.

Lange-Consiglio, A., Tassan, S., Corradetti, B., Meucci, A., Perego, R., Bizzaro, D., and Cremonesi, F. (2013b). Investigating the efficacy of amnion-derived compared with bone marrow-derived mesenchymal stromal cells in equine tendon and ligament injuries. Cytotherapy 15, 1011–1020.

Lendahl, U., Zimmerman, L.B., and McKay, R.D. (1990). CNS stem cells express a new class of intermediate filament protein. Cell. 60, 585–595.

Lovati, A.B., Corradetti, B., Lange Consiglio, A. Recordati, C., Bonacina, E., Bizzaro, D., and Cremonesi, F. (2011). Comparison of equine bone marrow-, umbilical cord matrix and

amniotic fluid-derived progenitor cells. Vet. Res. Commun. 35, 103–121.

Lunney, J.K. (2007). Advances in swine biomedical model genomics. Int. J. Biol. Sci. 3, 179–184.

Majors, A.K., Boehm, C.A., Nitto, H., Midura, R.J., and Muscheler, G.F. (1997). Characterization of human bone marrow stromal cells with respect to osteoblastic differentiation. J. Orthop. Res. 15, 546–557.

Manuelpillai, U., Moodley, Y., Borlongan, C.V., and Parolini, O. (2011). Amniotic membrane and amniotic cells: Potential therapeutic tools to combact tissue inflammation and fibrosis? Placenta 32, (Supp l4), 320–325.

Marongiu, F., Gramignoli, R., Sun, Q., Tahan, V., Miki, T., Dorko, K., Ellis, E., and Strom, S.C. (2010). Isolation of amniotic mesenchymal stem cells. Curr. Protoc. Stem Cell Biol. (Suppl 12), 1E.5.1–1E.5.11.

Meirelles, L. da S., and Nardi, N.B. (2003). Murine marrow-derived mesenchymal stem cell: Isolation, in vitro expansion, and characterization. Br. J. Haematol. 123, 702–711.

Meirelles, L. da S., Chagastelles, P.C., and Nardi, N.B. (2006). Mesenchymal stem cells reside in virtually all post-natal organs and tissues. J. Cell Sci. 119, 2204–2213.

Miki, T., Marongiu, F., Dorko, K., Ellis, E.C., and Strom, S.C. (2010). Isolation of amniotic epithelial stem cells. Curr. Protoc. Stem Cell Biol. 12, 1E.3.1–1E.3.10.

Miki, T., and Strom, S. (2006). Amnion-derived pluripotent/multipotent stem cells. Stem Cell Rev. 2, 133–142.

Mitchell, K.E., Weiss, M.L., Mitchell, B.M., Martin, P., Davis, D., Morales, L., Helwig, B., Hildreth, T., and Troyer, D. (2003). Matrix cells from Wharton's jelly form neurons and glia. Stem Cells 21, 50–60.

Muttini, A., Valbonetti, L., Abate, M., Colosimo, A., Curini, V., Mauro, A., Berardinelli, P., Russo, V., Cocciolone, D., Marchisio, M., Mattioli, M., Tosi, U., Podaliri Vulpiani, M., and Barboni, B. (2013). Ovine amniotic epithelial cells: In vitro characterization and transplantation into equine superficial digital flexor tendon spontaneous defects. Res.Vet. Sci. 94, 158–169.

Parolini, O., and Soncini, M. (2004). Human placenta: A source of progenitor/stem cells. J. Reproduktionsmed Endokrinol. 2, 117–126.

Parolini, O., Soncini, M., Evangelista, M., and Schmidt, D. (2009). Amniotic membrane and amniotic fluid-derived cells: Potential tools for regenerative medicine? Regen. Med. 4, 275–291.

Passeri, S., Nocchi, F., Lamanna, R., Lapi, S., Miragliotta, V., Giannessi, E., Abramo, F., Stornelli, M.R., Matarazzo, M., Plenteda, D., Urciuoli, P., Scatena, F., and Coli, A. (2009). Isolation and expansion of equine umbilical cord-derived matrix cells (EUCMCs). Cell Biol. Int. 33, 100–105.

Raouf, A., and Seth, A. (2000). Ets transcription factors and targets in osteogenesis. Oncogene 19, 6455–6463.

Rutigliano, L., Corradetti, B., Valentini, L., Bizzaro, D., Meucci, A., Cremonesi, F., and Lange-Consiglio, A. (2013). Molecular characterization and in vitro differentiation of feline progenitor-like amniotic epithelial cells. Stem Cell Res. Ther. 4, 133.

Sakuragawa, N., Kakinuma, K., Kikuchi, A., Okano, H., Uchida, S., Kamo, I., Kobayashi, M., and Yokoyama, Y. (2004). Human amnion mesenchyme cells express phenotypes of neuroglial progenitor cells. J. Neurosci. Res. 78, 208–214.

Soncini, M., Vertua, E., Gibelli, L., Zorzi, F., Denegri, M., Alberini, A., Wengler, G.S., and Parolini, O. (2007). Isolation and characterization of mesenchymal cells from human fetal membranes. J. Tissue Eng. Regen. Med. 1, 296–305.

Steigman, S.A., and Fauza, D.O. (2007). Isolation of mesenchymal stem cells from amniotic fluid and placenta. Curr. Protoc. Stem Cell Biol. 1E.2.1–1E.2.12.

Swindle, M.M., Makin, A., Herron, A.J., Clubb, F.J, Jr., and Frazier, K.S. (2012) Swine as models in biomedical research and toxicology testing. Vet. Pathol. 49, 344–356.

Vejlsted, M. (2010). Gastrulation, body folding and coelom formation. In: *Essentials of Domestic Animals Embryology*. P. Hyttel, F. Sinowatz, M. Vejlsted, eds. (Saunders/Elsevier, Edinburgh, London, New York, Oxford, Philadelphia, St. Louis, Sydney, Toronto) pp. 79–95.

Verma, N., Rettenmeier, A.W., and Schmitz-Spanke, S. (2011). Recent advances in the use of *Sus scrofa* (pig) as a model system for proteomic studies. Proteomics 11, 776–793.

Vodicka, P., Smetana, K.Jr., Dvorankova, B., Emerick, T., Xu, Y., Ourednik, J., Ourednik, V., and Motlik, J. (2005). The miniature pig as an animal model in biomedical research. Ann. N.Y. Acad. Sci. 1049, 161–171.

Wang, M., Yoshida, A., Kawashima, H., Ishizaki, M., Takahashi, H., and Hori, J. (2006). Immunogenicity and antigenicity of allogeneic amniotic epithelial transplants grafted to the cornea, conjunctiva, and anterior chamber. Invest. Ophthalmol. Vis. Sci. 47, 1522–1532.

Weiss, M.L., Anderson, C., Medicetty, S., Seshareddy, K.B., Weiss, R.J., VanderWerff, I., Troyer, D., and McIntosh, K.R. (2008). Immune properties of human umbilical cord Wharton's jelly-derived cells. Stem Cells 26, 2865–2874.

Zheng, Y.M., Zhao, X.E., and An, Z.X. (2010). Neurogenic differentiation of EGFP gene transfected amniotic fluid-derived stem cells from pigs at intermediate and late gestational ages. Reprod. Domest. Anim. 45, e78–e82.

Address correspondence to:
Prof. Fausto Cremonesi
Università degli Studi di Milano
Large Animal Hospital
Reproduction Unit
Via dell'Università 6
26900, Lodi, Italy

E-mail: fausto.cremonesi@unimi.it

CELLULAR REPROGRAMMING
Volume 18, Number 2, 2016

DOI: 10.1089/cell.2015.0062

Research Article

Does the Bovine Pre-Ovulatory Follicle Harbor Progenitor Stem Cells?

Anna Lange-Consiglio,[1] Alessio Romaldini,[2] Alessio Correani,[2] Bruna Corradetti,[2] Paola Esposti,[1] Maria Francesca Cannatà,[2] Claudia Perrini,[1] Maria Giovanna Marini,[2] Davide Bizzaro,[2] and Fausto Cremonesi[1,3]

Abstract

Recent studies have revealed the presence of a mesenchymal stem cell (MSC) population in human and in gilt granulosa cells (GCs), thus increasing the interest in identifying the same population in the bovine species. We first isolated GCs by scraping from bovine preovulatory follicles and then tested several different media to define the ideal conditions to select granulosa-derived stem cells. Although expressing MSC-associated markers, none of the media tested proven to be efficient in selecting MSC-like cells that were able to differentiate into mesodermic or ectodermic lineages. We performed another experimental approach exposing cells to a chemical stress, such as lowering of pH, as a system to select a more plastic population. Following the treatment, granulosa-specific granulose markers [follicle-stimulating hormone receptor (*FSHR*), follistatin (FST), and leukemia inhibitory factor receptor (*LIFR*)] were lost in bovine GCs, whereas an increase in multi- (*CD29*, *CD44*, *CD73*) and pluripotent (*Oct-4* and *c-Myc*) genes was noticed. The stress allowed up-regulation of tumor necrosis factor-α and interleukin-1β expression and the dedifferentiation of GCs, which was demonstrated by differentiation studies. Indeed, pH-treated cells were able to differentiate into the mesodermic and ectodermic lineages, thus suggesting that the chemical stress allows for the selection of cells that are more prone to adjust and respond to the environmental changes.

Introduction

As in humans, mesenchymal stem cells (MSCs) have also been harvested successfully in veterinary medicine from adult tissues, such as bone marrow (Arnhold et al., 2007; Fortier et al., 1998; Kern et al., 2006; Mitchell et al., 2003; Ringe et al., 2002; Smith et al., 2003; Vidal et al., 2006, 2008) and adipose tissue (Kern et al., 2006, Vidal et al., 2008). MSCs have been derived mainly from bone marrow in cattle, as described by Bosnakovski et al. (2005, 2006). Adult stem cells currently are the most used stem cell type for clinical applications (Trounson et al., 2011), but their isolation usually requires invasive techniques for sampling that are not devoid of complications. Moreover, their culture and expansion *in vitro* are time consuming, and the cells obtained display an ability to proliferate and differentiate that is inversely proportional to the age of the donor and to the number of *in vitro* passages (Vidal et al., 2011). Adult tissues are not satisfactory because of the low yield of stem cells that can be obtained, thus representing a strong limitation for the therapeutic application of these cells in veterinary and human medicine.

On the basis of these considerations, the interest of clinicians in finding alternative sources of multipotent cells has increased over the past years. MSCs from the fetal adnexa have been reported as a potential tool to overcome some of these limitations, opening up new prospects for the development of regenerative medicine (Lange-Consiglio et al., 2012). Also in bovine species, MSCs have been obtained from umbilical cord blood (Raoufi et al. 2011) and amnion and amniotic fluid (Corradetti et al., 2013). Recently, other research groups have suggested granulosa cells (GCs) as a promising adult source of MSCs in humans (Kossowska-Tomaszczuk et al., 2009) and in gilts (Mattioli et al., 2012). The investigation of Kossowska-Tomaszczuk et al. (2009) refers to luteinizing GCs recovered from preovulatory follicles of patients treated for oocyte retrieval. Mattioli et al.

[1]Large Animal Hospital, Reproduction Unit, Università degli Studi di Milano, Lodi, Italy.
[2]Department of Life and Environmental Sciences, Università Politecnica delle Marche, Ancona, Italy.
[3]Department of Veterinary Science for Animal Health, Production and Food Safety, Università degli Studi di Milano, Milan, Italy.

(2012) compared GCs retrieved from growing follicles before the preovulatory gonadotropin surge, and hence before luteinization (*e.g.*, in a condition of active proliferation and before the final differentiation) with those obtained from preovulatory follicles. In both studies, cells expressed MSC-associated markers and were able to differentiate into different cell types not present within the follicles, thus suggesting their potential use in cell-based therapy. Moreover, Mattioli et al. (2012) demonstrated that luteinizing GCs have more efficient osteogenic potential compared to GCs isolated from growing follicles.

GCs represent a readily available source from which to isolate cells easily, relying on the well-established techniques for oocyte retrieval used in assisted reproduction. This has increased our interest in identifying a MSC-like population in the bovine species, considering that ovaries can be easily collected in slaughterhouses due to the absence of their commercial value. In this context, the present study was designed to define a suitable protocol to select GCs with MSC-associated features in terms of morphology, specific markers, and differentiative potential from bovine preovulatory follicles.

Material and Methods

Samples were collected from bovine species slaughtered in a slaughterhouse (INALCA, Ospedaletto Lodigiano, Lodi, Italy) under legal regulations. Chemicals were obtained from Sigma-Aldrich Chemical (Milan, Italy) unless otherwise specified, and tissue culture plastic dishes were purchased from Euroclone (Milan, Italy).

Collection of ovaries and cells isolation

Bovine GCs employed in this study were isolated from ovaries collected from slaughterhouses. The age, genealogy, physiological status, and race were unknown for the animals. The transport of the gonads to the laboratory occurred in a portable thermos maintained at a temperature of 30°C in physiological saline solution (0.9% NaCl) supplemented with kanamycin (150 mg/liter). This temperature was maintained at a constant level from the beginning of ovary collection and during the time needed to reach the laboratory. In the laboratory, the ovaries were washed repeatedly in physiological saline solution supplemented with antibiotics; they were maintained in a thermos for the period of sampling to avoid thermal shock.

GCs were isolated from the bovine ovaries by scraping (Mattioli et al., 2012). Briefly, follicles with a diameter between 0.8 and 1.2 cm were opened using a scalpel blade, and GCs were gently scraped away from the internal face of the follicle wall. The material collected by scraping was deposited into 50-mL tubes containing Tissue Culture Medium (TCM)-HEPES (Sigma) supplemented with 1 mM pyruvic acidic (Sigma), 2.2 grams/liter of sodium bicarbonate (Sigma), 100× penicillin/streptomycin (Sigma), and 10% fetal calf serum (FCS; Sigma). The tubes were left at room temperature until the oocytes sedimented under gravity to the bottom of the tubes. The deposited portion was aspirated and plated on a gridded Petri plate (100 × 15 mm) to select and discharge oocytes. This procedure was performed using a stereomicroscope (model SZX-ILLK200, Olympus) with a 40× enlargement equipped with a heating plate set at 38°C. The GCs were pooled, washed in TCM-HEPES through two successive centrifugations (200 × *g* for 5 min at room temperature), counted in a Burker chamber, and used in the following experiments.

Experimental design

GCs were collected from bovine preovulatory follicles by scraping, cultured in different media or exposed to acid conditions (pH 5.7), induced to differentiate to mesodermic and ectodermic lineages, and analyzed by qualitative and quantitative PCR. All experiments were performed in triplicate.

GC isolation and culture

At first, GCs isolated by scraping were randomly allocated to five different culture media with the basic medium (MB) consisting of High-Glucose Dulbecco's Modified Eagle Medium (HG-DMEM) supplemented with 10% FCS, 100 IU/mL penicillin, 100 μg/mL streptomycin, 0.25 μg/mL amphotericin B, and 2 mM L-glutamine. This medium was chosen because it is the most commonly used for the isolation of MSCs (Wang et al., 2004). The other conditions included MB supplemented with 0.1% epidermal growth factor (MB + EGF) (Mattioli et al., 2012), MB supplemented with 0.02% leukemia inhibitory factor (MB + LIF) (Kossowska-Tomaszczuk et al., 2009), and MB supplemented with only 2% FCS (2%-MB), as reported by Solmesky et al. (2009), to perform *in vitro* isolation of stem cells, and MB supplemented with 0.02% LIF (MB + LIF) and 0.014 μL/mL β-mercaptoethanol (MB + LIF + BME), as reported by Marshall et al. (2001) for culturing *in vitro* embryonic stem cells.

This protocol was modified in our study because BME was maintained only for passage 1 (P1) and then removed from the culture medium. For each condition, cells cultures were established in an atmosphere of 5% CO_2 and 90% humidity and at a temperature of 38.5°C. Medium was replaced 72 h after isolation to remove nonadherent cells. Adherent cells were detached with 0.05% trypsin-EDTA (EuroClone) just prior to reaching confluence (80%) and then reseeded for culture maintenance. Cells were expanded for three passages, at which point they were analyzed for the expression of specific markers by qualitative and quantitative PCR and were tested for multidifferentiative potential.

In a second step, GCs isolated by scraping were divided into two portions: One was cryopreserved and used as a control [day 0 (d0)] and the second one was exposed to acidic conditions (pH 5.7) and was observed constantly for 7 days to assess the viability and morphological changes (d7). The acidic treatment was performed for 25 min at pH 5.7 and at 37°C (Hjelmeland et al., 2011). After that, cells were centrifuged and the pellet was resuspended in DMEM/F12 medium supplemented with LIF and B27. The cellular suspension was seeded at a density of 1×10^5 cell/cm^2 in T25 flasks.

In vitro *differentiation*

GCs from each condition were seeded at the density of 3×10^3 cells/cm^2 for differentiation in adipogenic, osteogenic, and neurogenic lineages. Cells plated at a density of 1.5×10^3 cells/cm^2 were used as control. For the first 3–4 days, the cells

were incubated with basic medium to allow adhesion; at 60–70% of confluence, they were induced to differentiate.

Osteogenic differentiation. This was assessed by incubating cells for up to 3 weeks at 38.5°C under 5% CO_2 in medium composed of HG-DMEM medium supplemented with 10% FBS, 100 IU/mL penicillin, 100 mg/mL streptomycin, 0.25 mg/mL amphotericin B, 2 mM L-glutamine, 10 mM β-glycerophosphate, 0.1 mM dexamethasone, and 250 mM ascorbic acidic. Noninduced control cells were cultured for the same time period in standard control medium (HG-DMEM supplemented with 10% FCS, 100 IU/mL penicillin, 100 mg/mL streptomycin, 0.25 mg/mL amphotericin B, and 2 mM L-glutamine). Osteogenesis was assessed by conventional von Kossa staining using 1% silver nitrate and 5% sodium thiosufate, which allowed detection of calcium deposits.

Adipogenic differentiation. Near-confluent cells were cultured through three cycles of induction/maintenance to stimulate adipogenic differentiation. Each cycle consisted of feeding the GCs for 3 days with supplemented adipogenesis induction medium, followed by culture for another 3 days (38.5°C, 5% CO_2) in supplemented adipogenic maintenance medium. The induction medium consisted of HG-DMEM supplemented with 10% FCS, 100 IU/mL penicillin, 100 mg/mL streptomycin, 0.25 mg/mL amphotericin B, 2 mM L-glutamine, 10 mg/mL insulin, 150 mM indomethacin, 1 mM dexamethasone, and 500 mM 3-isobuty-l-methylxanthine. The maintenance medium consisted of HG-DMEM supplemented with 10% FCS and 10 mg/mL insulin. Noninduced control cells were cultured for the same time period in standard control medium. Adipogenesis was assessed using conventional Oil Red O staining (0.1% in 60% isopropanol) to detect lipid droplets.

Neurogenic induction. This was performed by culturing cells for 24 h in preinduction medium consisting of HG-DMEM, 20% FCS, and 1 mM BME (Mitchell et al., 2003; Seo et al., 2009). Neural induction was performed by switching to a medium composed of DMEM plus 2% FCS, 2% dimethylsulfoxide, and 200 mM butylated hydroxyanisole for 3 days (Woodbury et al., 2000). Noninduced control cells were cultured for the same time period in standard medium. Neurogenic differentiation was demonstrated by conventional Nissl staining (0.1% Cresyl Violet solution) to detect increase of Nissl bodies.

Molecular biology study

Qualitative PCR analysis was performed to evaluate the expression of specific granulosa-, MSC-, pluripotent-, histocompatibility- and hematopoiesis-associated markers to confirm the differentiation that occurred and the stress induced by the acidic treatment. RNA was isolated using TRIzol® Reagent (Invitrogen, Carlsbad, CA, USA) according to the protocol indicated by the manufacturer. RNA concentration and purity were measured using a NanoDrop spectrophotometer (NanoDrop ND1000, Wilmington, DE, USA). Complementary DNA (cDNA) was synthesized from 300 ng of total RNA using the PrimeScript RT reagent kit (Takara Bio, Otsu-Shi, Japan). Gene expression evaluation was performed using specific sequences. Bovine-specific oligonucleotide primers were designed using open source

TABLE 1. OLIGONUCLEOTIDE SEQUENCES USED FOR MOLECULAR ANALYSIS

	Genes	*Forward*	*Reverse*	*Annealing temperature*	*Size cDNA (bp)*
Markers of pluripotency	*Oct4*	CACACTAGGATATACCCAGGC	GGAGATATGCAAGGCAGAGA	60°C	177
	c-Myc	GCGCCGCATTCGCGAAACTT	TGAGGGGCATCGCTGCAAGC	58°C	214
Markers of multipotency	*CD73*	AAGGTTCCTGTGGTCCAGGCCT	TGCATTCTCGAAAGCGGCAGGA	68°C	260
	CD29	GTTGGTTCTGCAGTTACGATCAG	AACCAAACCCAATTCGGAAGTC	52°C	203
	CD44	AACAGTAGGAGAAGGTGTGG	TCATGAACTGGTCTTGGGTC	61°C	166
	MHC I	GATCTCACTGACCTGGCA	CTGAGGAGGTTCCCATCTC	60°C	199
	MHC II	CCTCGCTTGCCTGAATTTGC	ACAGGTGCCGACTGATGC	53°C	266
Hematopietic marker	*CD34*	CCTGAAGCTAAATGAGACCT	AACTTTCTGTCCTGTTGGTC	58°C	173
Markers of granulosa cells	*FSHR*	TGGTCCTGTTCTACCCCATCA	GAAGAAATCCCTGCGGAAGTT	58°C	83
	FST	CTCTGCCAGTTCATGGAGGACC	GGCCAATCCAATAGATCTGCCC	63°C	651
	LIFR	TGGCAGTACACATTGTCCCC	TCCCGCAAAAACAACCGTTC	60°C	145
Markersof differentiation	*LEP*	CAATGACATCTCACACACGCAG	CGGCCAGCAGGTGGAGAAG	55°C	212
	PPARγ	CGCACTGGAATTAGATGACAGC	CACAATCTGTCTGAGGTCTGTC	55°C	214
	BGLAP	TCGGGCAAAGGCGCAGCCTTC	GCAGGGCTGCAAGCTCTAGACG	55°C	231
	SPP1	CGCCGATCTAACGTTCAGAGTC	GACTCTCAATCAGATTGGAATGC	55°C	199
	SPARC	CTGGTCACGCTGTACGAGAG	CGGTGTGAGACAGGTACCCGT	55°C	232
	GFAP	GGCACCTTGAGGCAGAAGCTC	CTCCTGGAGCTCCCGCACCT	60°C	195
Markers of inflammation	*TNF-α*	ACATACCCTGCCACAAGGC	TGGGGACTGCTCTTCCCTCT	60°C	259
	IL-1β	TGCAGCTGGAGGAAGTAGAC	GTCGGGCATGGATCAGACAA	60°C	338
Housekeeping gene	*GAPDH*	ATGAGATCAAGAAGGTGGTG	CCAAATTCATTGTCGTACCAG	60°C	190

MHC I, major histocompatibility complex class I; *MHC II*, major histocompatibility complex class II; *FSHR*, follicle-stimulating hormone receptor; *LIFR*, leukemia inhibitory factor receptor; *LEP*, leptin; *PPARγ*, peroxisome proliferator-activated receptor gamma; *BGLAP*, bone gamma-carboxyglutamate protein; *SPP1*, osteopontin; *SPARC*, secreted protein acidic and rich in cysteine; *GFAP*, glial fibrillary acidic protein; *TNF-α*, tumor necrosis factor-α; *IL-1β*, interleukin-1β; *GAPDH*, glyceraldehyde 3-phosphate dehydrogenase.

PerlPrimer software (v. 1.1.17), based on available National Center for Biotechnology Information (NCBI) *Bos taurus* sequences or on mammalian multialigned sequences. Primers were designed across an exon–exon junction to avoid DNA amplification. Primers sequences and characteristics are reported in Table 1. The bovine glyceraldehyde 3-phosphate dehydrogenase gene (*GAPDH*) was employed as a reference gene in each sample to standardize the results by eliminating variation in messenger RNA (mRNA) and cDNA quantity and quality.

Conventional qualitative PCR was performed using 1 μL of the cDNA obtained in a 25-μL final volume with recombinant Taq DNA polymerase (Invitrogen, Life Technologies, Monza, Italy). Amplified PCR products were electrophoresed on a 1.8% agarose gel with ethidium bromide.

For quantitative PCR, one single representative gene per set of markers (*CD73*, *FSHR*, and *Oct-4*) was chosen to evaluate the selection efficiency of any culture condition used in this study. In addition, the expression of tumor necrosis factor-α (*TNF-*α) and interleukin-1β (*IL-1*β) was evaluated to confirm cellular stress induced by acidic treatment. Analyses were carried out with the SYBR (a fluorescent intercalating agent, able to bind the DNA in double-stranded conformation) method, in the MyiQ™ Single-Color Real-Time PCR Detection System (BioRad, Hercules, CA, USA). Triplicate PCR reactions were carried out for each analyzed sample. Reactions were set on a strip in a final volume of 25 μL by mixing, for each sample, 1 μL of cDNA, 12.5 μL of 2× concentrated SYBR® Select Master Mix (Applied Biosystems, Foster City, CA, USA), 1 μM forward primer, 1 μM of reverse primer, and Milli-Q water.

Immunocytochemical characterization of Oct-4

To test the expression of the Oct-4 marker, primary antibody was purchased from Abcam (Cambridge, MA, USA), whereas Alexa Fluor 488–conjugated secondary antibody and goat serum were from Life Technologies (Carlsbad, CA, USA). All products were used following the manufacturer's instructions.

For immunostaining, GCs after isolation (control cell) and GCs cultured in MB + LIF were fixed in 4% paraformaldehyde (PFA) for 10 min at room temperature and washed three times in phosphate-buffered saline (PBS). After fixation, cells were permeabilized for 15 min at room temperature in 0.25% Triton-X 100 diluted in PBS and washed three times in PBS. After washing, cells were blocked using 10% goat serum in PBS for 30 min at room temperature. Cells were incubated with primary antibodies (1:200 dilution) overnight at 4°C. After washing three times, cells were incubated with secondary antibodies conjugated to Alexa Fluor 488 (1:250 dilution) for 1 h. Finally, for nuclear staining, cells were incubated for 15 min with Hoechst 33342 (1 mg/mL; Sigma) diluted 1:100 in PBS. Images were captured on a BX51 microscope (Olympus, Japan). A negative control was performed without the primary antibodies. The positive control was carried out on bovine *in vitro* embryos produced routinely in our laboratory as described by Lange-Consiglio et al. (2010).

Statistical analysis

For quantitative PCR data, nonparametric tests were used. The Mann–Whitney U-test was employed to compare two groups (treated vs. untreated). Results were considered statistically significant if $p < 0.05$.

Results

GCs yield and morphology

From each ovary, about 2 million GCs were isolated with an 80% viability evaluated by Trypan Blue dye exclusion. Cells were plated and selected on the basis of their ability to adhere to plastic. Observation under microscopy revealed the presence of cells with epithelial morphology when cultured in MB (Fig. 1A), with atypical morphology in LIF + BME (Fig. 1B), whereas they displayed fibroblast-like morphology when cultured under other conditions (Fig. 1C–E). After pH treatment, in the next 7 days of culture, cells displayed morphological changes compared to initial epithelial morphology and a progressive vacuolization (Fig. 2). After acidic treatment, the number of viable cells immediately decreased 50%. During the following 7 days of culture, the viability of the remaining cells was further reduced 40%.

Molecular analysis of GCs

Table 2 shows expression of GCs studied in different culture conditions. These cells expressed mesenchymal

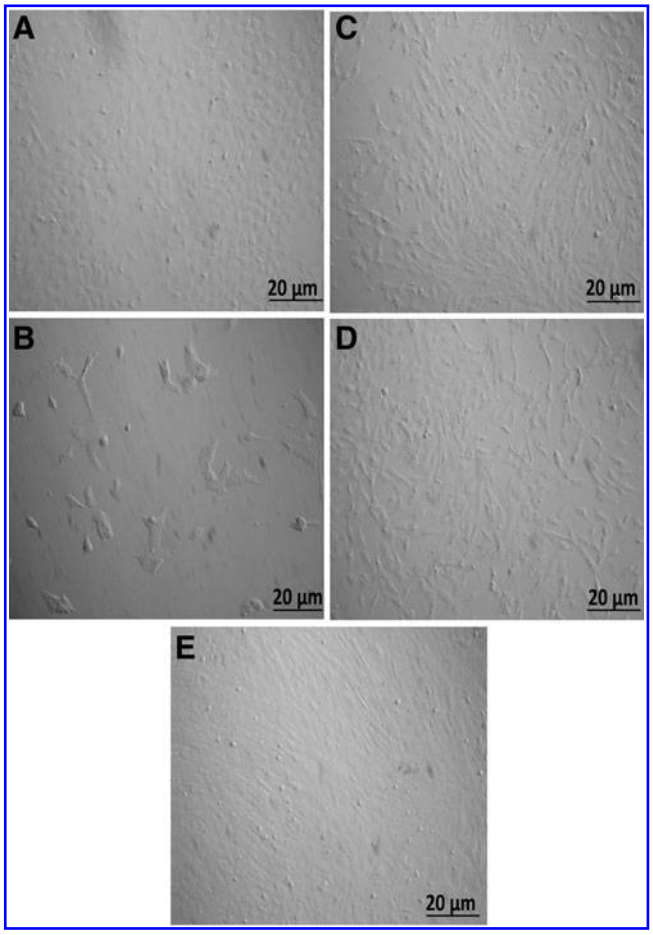

FIG. 1. Morphology of cells cultured in different culture conditions: (**A**) MB; (**B**) MB with LIF and BME; (**C**) MB with EGF; (**D**) MB with LIF; (**E**) BM with 2% of FCS. Scale bars, 20 μm; magnification, 20×.

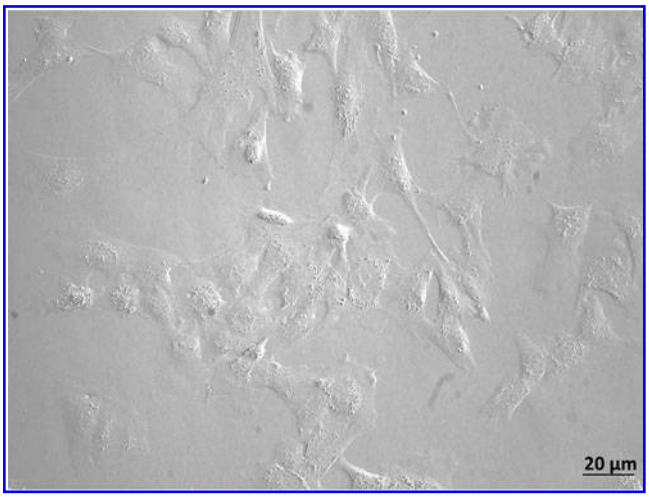

FIG. 2. Morphology of cells isolated from bovine preovulatory follicles and exposed to a chemical stress (d7) display a progressive vacuolization. Scale bar, 20 μm; magnification, 20×.

(*CD29*, *CD44*, *CD166*, and *CD73*) and pluripotent (*Oct-4* and *c-Myc*) markers and lacked *CD34* marker expression. For these markers, no differences induced by the culture conditions were observed compared to P0, except for *CD166*, whose expression was not detected at P0. On the other hand, changes in the granulosa-associated markers were detected in the different culture conditions. Specifically, follicle-stimulating hormone receptor (*FSHR*) was expressed only at P1 when cells were cultured in MB, MB + EGF, MB + LIF, and MB + LIF + BME. Cells cultured in 2% MB expressed *FSHR* over the passages studied. Follistatin (*FST*) expression was observed in all of the conditions and passages, but disappeared at P3 in MB + LIF + BME.

qPCR results highlighted differences in the expression of *FSHR* between cells cultured in different conditions (Fig. 3). In MB + LIF and MB + EGF, *FSHR* expression was found about 10 times less compared to the baseline (P0). *Oct-4* expression reached the maximum expression in MB + LIF medium (157.8 ± 65.07) and the minimum expression in 2% MB and MB (0.83 ± 0.38 and 1.73 ± 0.27, respectively). A relatively high value was recorded also in MB + EGF and MB + LIF + BME (4.1 ± 1.1 and 39.7 ± 13.6). The expression level of *CD73* was found higher in MB (49.7 ± 23.19) and MB + LIF + BME (29.75 ± 19.87). The lowest expression of *CD73* was registered in 2% MB, showing a 1.37- (± 0.44) fold increase.

GCs before and after acidic treatment expressed *Oct-4*, *C-Myc*, *CD73*, *CD29*, *CD44*, *MHC I*, *MHC II*, and granulosa-associated markers (*FST* and *LIFR*), but not *CD34*. The main difference found between d0 and d7 was the loss of *FSHR* expression (Fig. 4A). Considerable differences in gene expression were observed in GCs before and after acidic treatment (Fig. 4B). In particular, *FSHR* expression was found significantly decreased in treated cells at d7. Further indications supporting the efficacy of the treatment were provided by the loss of other granulosa markers (*i.e.*, *FST* and *LIFR*) and the increase of *Oct-4* and *CD29* compared to untreated cells (d0). Decreased expression of *MHC I* and *MHC II* in d7 was also observed. In addition, as a response to the acidic treatment, in bovine GCs expression of inflammatory markers, such as *TNF-α* and *IL-1β*, was found to be significantly upregulated at d7 compared to d0, with a 7.02- (± 0.2) and 21.26- (± 0.25) fold increase (Fig. 5; $p < 0.05$ and $p < 0.001$, respectively).

In vitro *differentiation*

GCs cultured in different conditions did not show any ability to differentiate (data not shown). On the other hand, GCs treated with an acidic pH were easily induced into the adipogenic, osteogenic, and neurogenic lineages. After 18 days of induction, the presence of intracellular lipid vacuoles was determined by Oil Red O staining (Fig. 6A). After 21 days in osteogenic media, extracellular mineral deposits were demonstrated by von Kossa staining (Fig. 6B). Interestingly, cells induced to differentiate toward the neurogenic lineage acquired the typical neuronal morphology with

Table 2. Gene Expression Analysis Using RT-PCR in Granulosa Cells in Different Culture Conditions

Colture condition	*Passage*	GAPDH	OCT4	C-MYC	CD44	CD29	CD166	CD34	CD73	FSHR	FST
Baseline	P0	✓	✓	✓	✓	✓	✗	✗	✓	✓	✓
MB	P1	✓	✓	✓	✓	✓	✓	✗	✓	✓	✓
	P3	✓	✓	✓	✓	✓	✓	✗	✓	✗	✓
	P5	✓	✓	✓	✓	✓	✓	✗	✓	✗	✓
2%-MB	P1	✓	✓	✓	✓	✓	✓	✗	✓	✓	✓
	P3	✓	✓	✓	✓	✓	✓	✗	✓	✓	✓
	P5	✓	✓	✓	✓	✓	✓	✗	✓	✓	✓
MB + EGF	P1	✓	✓	✓	✓	✓	✓	✗	✓	✓	✓
	P3	✓	✓	✓	✓	✓	✓	✗	✓	✗	✓
	P5	✓	✓	✓	✓	✓	✓	✗	✓	✗	✓
MB + LIF	P1	✓	✓	✓	✓	✓	✓	✗	✓	✓	✓
	P3	✓	✓	✓	✓	✓	✓	✗	✓	✗	✓
	P5	✓	✓	✓	✓	✓	✓	✗	✓	✗	✓
MB + LIF + BME	P1	✓	✓	✓	✓	✓	✓	✗	✓	✓	✓
	P3	✓	✓	✓	✗	✓	✗	✗	✓	✗	✗
		190 bp	177 bp	214 bp	166 bp	203 bp	755 bp	173 bp	260 bp	83 bp	651 bp

GAPDH, glyceraldehyde 3-phosphate dehydrogenase; *FSHR*, follicle-stimulating hormone receptor; *FST*, follistatin; MB, basic medium; EGF, epidermal growth factor; LIF, leukemia inhibitory factor; BME, β-mercaptoethanol.

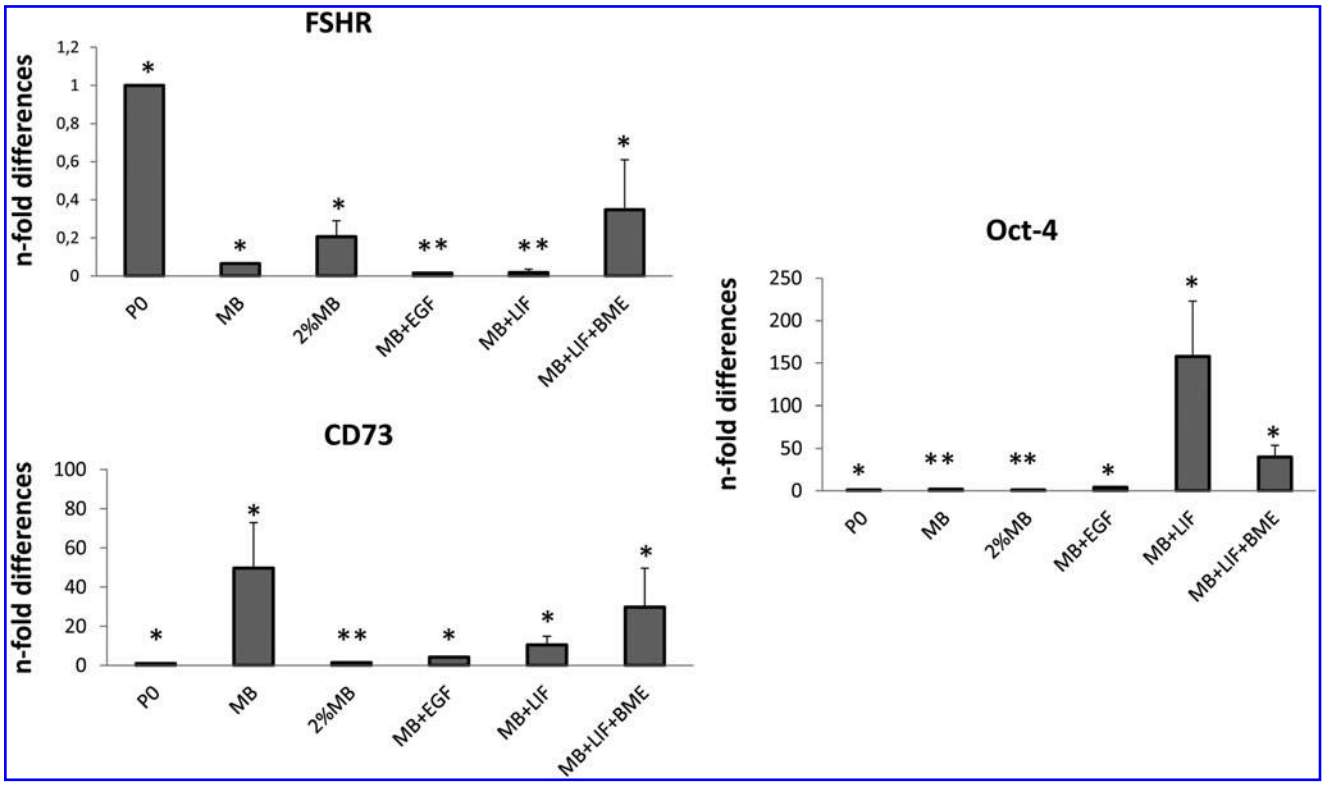

FIG. 3. Quantitative RT-PCR analysis for the expression of multipotent (*CD73*), pluripotent (*Oct-4*), and granulosa-specific (*FSHR*) markers in cells cultured under different conditions (MB, 2% MB, MB + EGF, MB + LIF, MB + LIF + BME) at P3. Expression levels were normalized to the reference gene (*GAPDH*). Data are represented as fold change compared with expression observed in P0. Values are mean ± standard deviation (SD) ($n = 3$). Asterisks depict highly significant (**$p < 0.01$) differences.

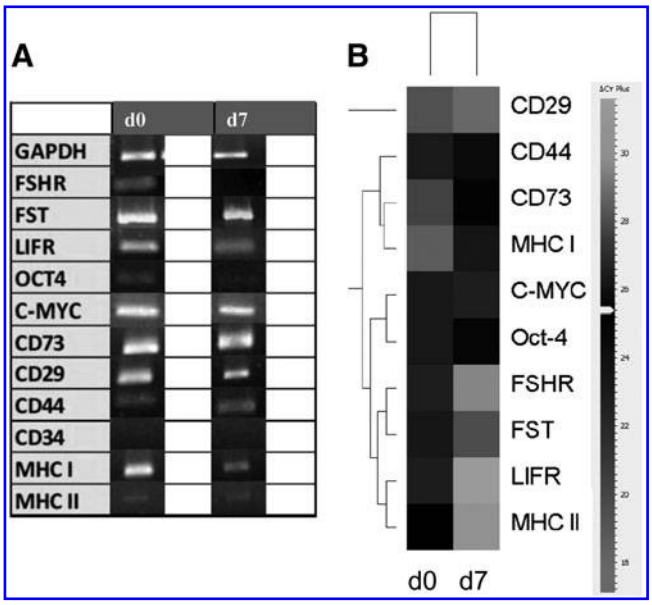

FIG. 4. Qualitative (**A**) and quantitative (**B**) RT-PCR analysis for the expression of specific granulosa (*LIF-R, FSHR, FST*)-, MSC (*CD73, CD29, CD44*)-, pluripotent (*Oct-4, c-Myc*)-, histocompatibility (*MHC I* and *MHC II*)-, and hematopoiesis (*CD34*)-associated markers in cells before (d0) and after (d7) acidic treatment. (**B**) Quantitative data are reorganized in a heat map. Representing the intensity of the gene expression: black refers to the higher level of expression and white refers to the lowest level of expression.

axon- and dendrite-like processes and were positive for Nissl staining of Nissl bodies (Fig. 6C). Uninduced cells were maintained in culture for the same period of each differentiation protocol time and used as a negative control. They were negative for all of the staining performed. Differentiation was confirmed by molecular analysis through the use of specific markers, including leptin (LEP) and peroxisome proliferator-activated receptor gamma (PPARγ) for adipogenic differentiation, bone gamma-carboxyglutamate protein (BGLAP), osteopontin (SPP1), and secreted protein acidic and rich in cysteine (SPARC) for osteogenic differentiation, and glial fibrillary acidic protein (GFAP) for neurogenic differentiation.

In cells induced to undergo adipogenesis the expression of *PPARγ* but not *LEP* was revealed in induced cells, whereas control cells did not express the genes tested. Following osteogenesis induction, *BGLAP* was not expressed in induced cells. Qualitative PCR did not allow for the discrimination between induced and uninduced cells when the expression of *SSP1* and *SPARC* was assessed (Fig. 6B). For this reason, qPCR was performed to determine the levels of expression of these two markers in induced cells compared to their respective uninduced controls. The expression of osteogenesis-associated genes quantitatively confirmed the induction. *SPP1* expression increased 2.17- (±0.09) fold ($p < 0.05$), whereas a slight but statistically significant ($p < 0.05$) increase (1.45 ± 0.085) in *SPARC* expression was found compared to the uninduced counterparts (Fig. 7). The expression of *GFAP* confirmed the neurogenic differentiation.

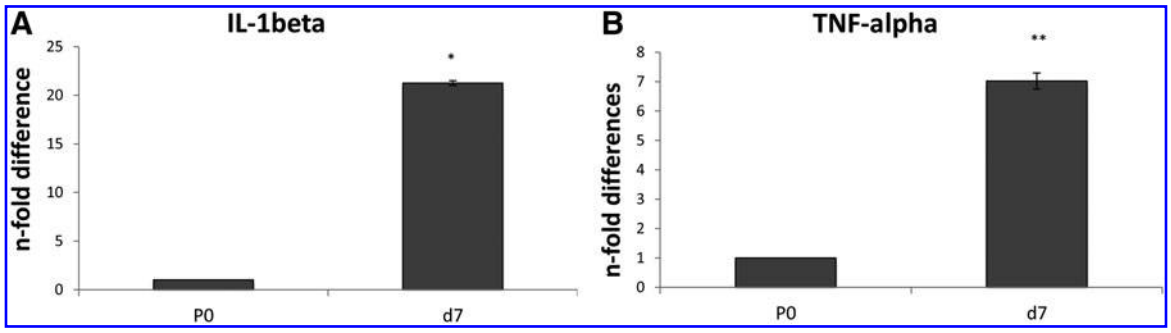

FIG. 5. Quantitative RT-PCR analysis for the expression of inflammatory markers such as *TNF-α* and *IL-1β* in GCs before (d0) and after acidic treatment (d7). Expression levels were normalized to the reference gene (*GAPDH*). Values are mean ± standard deviation (SD) ($n=3$). Asterisks depict highly significant (**$p<0.01$) and significant (*$p<0.05$) differences compared to d0.

Immunocytochemical characterization of Oct-4

Immunopositivity to Oct-4 was detected in GCs cultured in MB + LIF and in bovine embryos used as a positive control. GCs after collection, used as a control, were negative (Fig. 8).

Discussion

The purpose of this study was to identify a new source of stem cells that were easy to collect and able to comply with the requirements of regenerative medicine on a large scale. On the basis of recently published studies in humans (Kossowska-Tomaszczuk et al., 2009) and gilts (Mattioli et al., 2012), GCs represent an alternative source of MSCs.

To reach our goal, we tested different culture conditions and evaluated their efficacy in selecting MSCs from a cell population obtained from the follicle. Once isolated, GCs have been characterized on the basis of the minimal criteria defined by the International Society for Stem Cell Therapy to define MSCs (Dominici et al., 2006). According to results obtained in humans (Kossowska-Tomaszczuk et al., 2009) and gilts (Mattioli et al., 2012), cells adhered to a plastic dish and expressed a pattern of mesenchymal (*CD44*, *CD29*, *CD166*, *CD73*) and pluripotency (*Oct-4*, *c-Myc*) genes, with

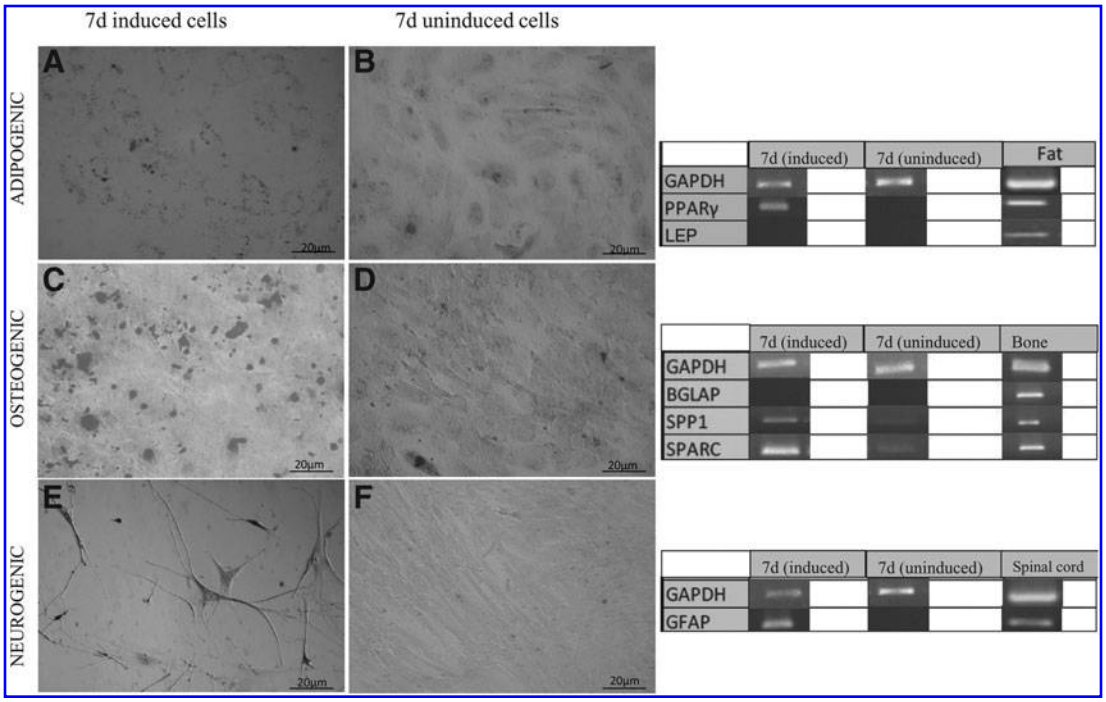

FIG. 6. Differentiative potential. (**A**) Adipogenic differentiation: Oil Red O staining in induced and control cells at d7 and adipogenesis-associated marker expression. (**B**) Osteogenic differentiation: Von Kossa staining on induced and control cells d7 and osteogenesis-associated markers expression. (**C**) Neurogenic differentiation: Nissl staining in induced and control cells d7 and neurogenic marker expression. Scale bars, 20 μm. Magnification, 20×. (*Right panel*) Specific gene expression in induced and control cells. *BGLAP*, *SPP1*, and *SPARC* mRNA were investigated for osteogenesis; *PPARY* and *LEP* for adipogenesis; and *NES* and *GFAP* for neurogenesis. *GAPDH* was employed as reference gene. Bone, adipose tissue, and spinal cord were used as positive controls.

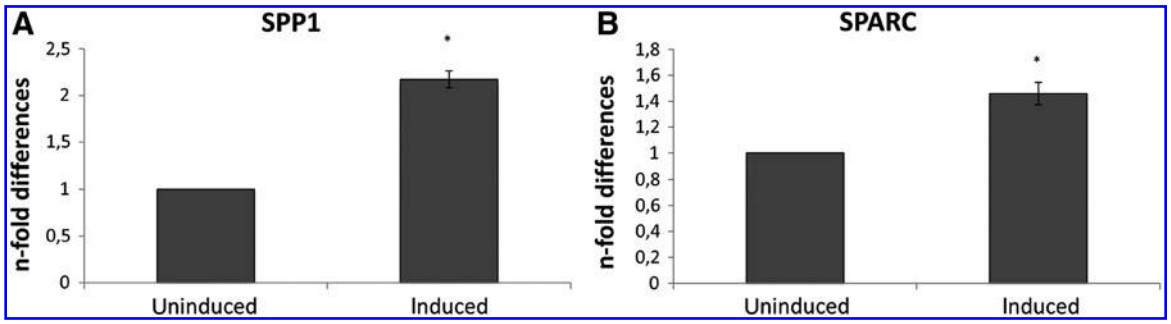

FIG. 7. Quantitative RT–PCR analysis for the expression of osteogenesis-associated genes such as *SPP1* (**A**) and *SPARC* (**B**). Data are represented as fold change compared with expression observed in P0. Values are mean ± standard deviation (SD) ($n=3$). Asterisks depict highly significant (**$p<0.01$) or significant (*$P<0.05$) differences compared to uninduced cells.

no expression of the hematopoietic *CD34* and the functional marker *FSHR*. The levels of expression of *CD73*, *Oct-4*, and *FSHR* were also confirmed quantitatively, showing the reduction of specific granulosa markers and the upregulation of MSC-associated genes.

In addition to molecular characterization by RT-PCR, the high level of Oct-4 in GCs cultured in MB + LIF was also detected by immunocytochemistry. Contrary to data reported for humans (Kossowska-Tomaszczuk et al., 2009) and gilts (Mattioli et al., 2012), however, despite inducing a MSC-like phenotype in bovine GCs, none of the culture conditions tested was efficient in selecting a plastic cell population. In fact, cells exposed to each condition were not able to differentiate into adipogenic, osteogenic, and neurogenic lineages. To date, the expression of *FST*, a protein broadly secreted by GCs in the ovary, was never found to be downregulated, as we would expect it to be for cells retaining/acquiring a stem cell–associated phenotype. The *FST* gene continued to be switched

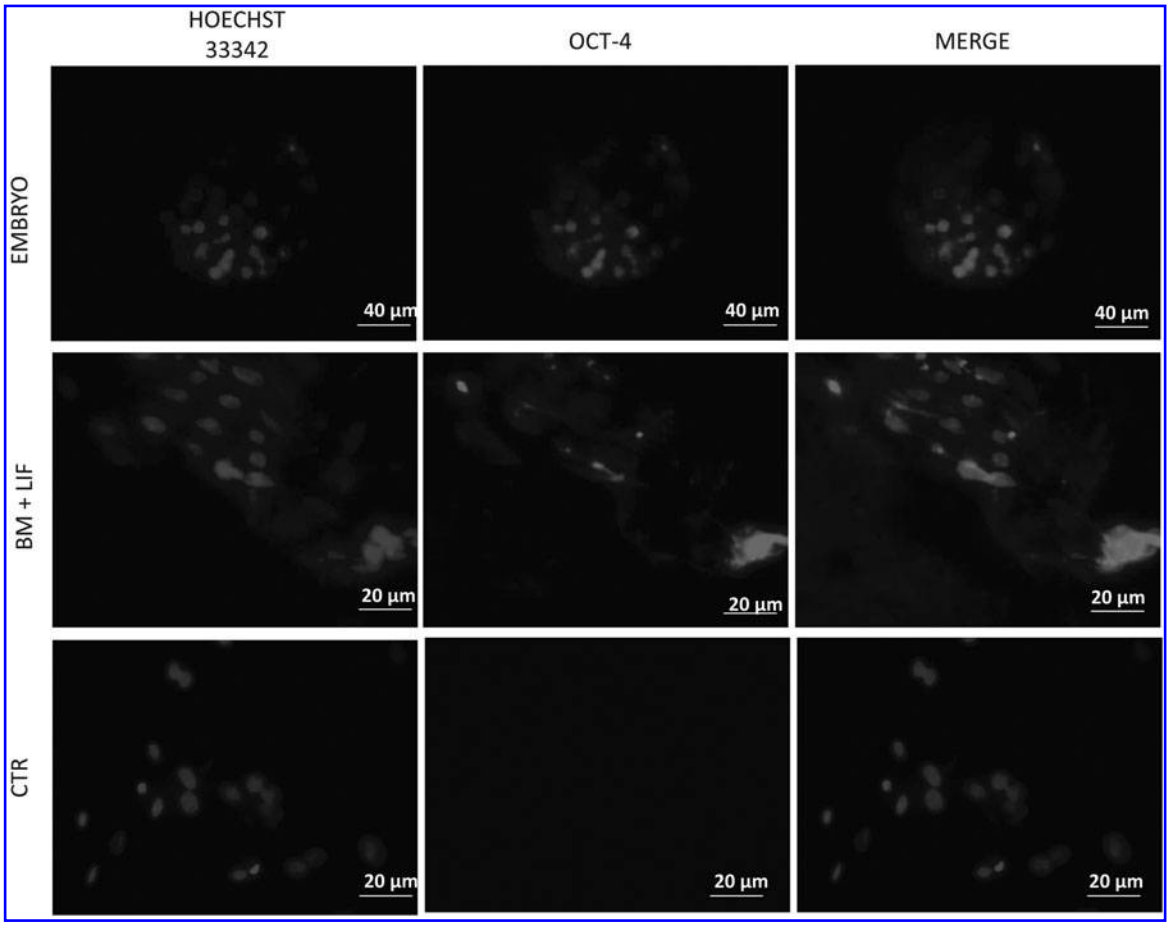

FIG. 8. Photomicrographs of immunostaining of bovine GCs labeled with antibodies against antigens for Oct-4. Magnification, 40×; scale bar, 20 μm. Magnification for embryos: 20×; scale bar, 40 μm. CTR, control.

''on'' in the genetic pattern of GCs, even if they were grown under different culture conditions. Its expression probably indicates an incomplete dedifferentiation to mesenchymal cells and the maintenance of a strong epigenetic imprinting that prevented GCs from differentiating. This epigenetic imprinting could be the reason of failed differentiation.

On the basis of our findings, it is reasonable to assume that GCs isolated in our study and maintained in different conditions can be considered progenitors of GCs; the only exception was those kept in MB + LIF + BME that lost expression of *CD44* and *CD166*. The discrepancy in the differentiation outcome observed between the present study and that reported by Mattioli et al. (2012) and Kossowska-Tomaszczuk et al. (2009) is difficult to explain considering that GCs were isolated from the internal side of the preovulatory follicle and, thus, from the periantral layer, as reported by Mattioli et al. (2012). Erickson (2000) postulated that stem cells could be located in the periantral layer of granulosa. As such, this method could be the most appropriate for the collection of multipotent stem cells from granulosa compared to the aspiration protocol performed by Kossowska-Tomaszczuk et al. (2009).

On the basis of our negative results to detect stem cells in preovulatory follicles, we decided to expose GCs to chemical stress by lowering the pH in culture to elucidate whether acidic stress could influence the phenotype and, eventually, help with the selection of more plastic cells. In plants, drastic environmental changes have been reported to convert mature somatic cells (for example, dissociated carrot cells) into immature blastema cells, from which a whole plant structure, including stalks and roots, develops in the presence of auxins (Thorpe, 2007). In our study, molecular analysis revealed significant differences between the cells before and after the acidic treatment. In particular, 7d cells showed a significant decrease of expression of granulosa-specific markers (*FSHR, FST, LIF-R*), with a concomitant increase in the pluripotency-associated marker *Oct-4*. Chiou et al. (2008) also reported the upregulation of *Oct-4* in these conditions. The loss of *FSHR* could be explained with the lack of its ligand (FSH) in the culture media, which is in agreement with the findings obtained by Kossowska-Tomaszczuk et al. (2009), focusing on human GCs isolated from the ovarian follicles of infertile patients and cultured in the presence of LIF.

Changes in gene expression can be further justified by hypothesizing that the chemical stress is able to induce either a cell dedifferentiation or a strong selection of progenitor cells. Changes in the external environment (including the pH reduction) have been previously associated with a specific phenotype acquired by cells exposed to them, as in the case of ovary cells and cancer cells (Tannock and Rotin, 1989). Moreover, when cultured in acidic conditions, cells lose the expression of the immunogenic markers (*MHC I* and *MHC II*), confirming their more undifferentiated state. MSCs have been reported to be immuno-privileged cells, with no or low expression of those markers (Hass et al., 2011).

Differentiation studies further corroborated such observations. pH-treated cells were induced toward the mesodermic (adipogenic and osteogenic) and ectodermic (neurogenic) lineages. Oil Red O, von Kossa, and Nissl staining, respectively, demonstrated differentiation, which was further confirmed by molecular analysis. For adipogenesis, we investigated the expression of *PPARγ*and *LEP*; however, only the first one was expressed in differentiated cells. The expression of *PPARγ* suggests a preadipocytic commitment of cells (Corradetti et al., 2013), which is further confirmed by the lack of *LEP*, a marker regarded as an intermediate and late marker. The expression of *GFAP* in induced cells suggests that astrocyte differentiation occurred, as previously reported for bovine and equine amniotic-derived cells (Corradetti et al., 2011, 2013; Lange-Consiglio et al., 2012).

Osteogenesis was assessed investigating the osteogenic-specific markers BGLAP, SPP1, and SPARC. All of these markers were expressed in induced cells, with the exception of only *BGLAP*. This might be explained considering that *BGLAP* is expressed in terminally differentiated osteoblasts (Wagner et al., 2011). Surprisingly, the expression of *SPP1* and *SPARC* was detected also in the negative controls (7d uninduced cells), although with a lower expression level compared to induced cells. We hypothesized that the expression of these markers (*SPP1* and *SPARC*) in negative controls can be due to the role they play in inflammation. Indeed, these markers are mainly involved in the immune response to an inflamed environment (Lund et al., 2009; Xu et al., 2013), as is the case of the acidic treatment. The upregulation of *TNF-α* and *IL-1β* expression confirmed our hypothesis. In particular, *SPARC* levels are significantly correlated with inflammation (Xu et al., 2013) and *SPP1* is strikingly upregulated at sites of inflammation and tissue remodeling, because it promotes the migration of inflammatory cells to the wound site and functions as a proinflammatory cytokine (Lee et al., 2012).

Conclusions

Results obtained from this work demonstrated that none of the culture conditions employed in this study allowed for the selection of the stem cell population within GCs isolated by scraping. The stress induced by the acidic treatment on bovine GCs endorsed the selection of the more plastic cells, which were the only ones able to respond to stimuli and adjust to a more rigid environment. Thus, compared to the freshly isolated cells, selected cells showed an increased expression of the pluripotent marker *Oct-4* and were able to differentiate into mesodermic and ectodermic lineages. The acquired phenotype of those cells can be also explained as a consequence of the activation of an inflammatory process, able to determine de-differentiation or nuclear reprogramming in GCs (Lee et al., 2012). Further studies are required to understand better the effect of the acidic treatment and the consequent stress induced by it at molecular level. Moreover, different approaches will be required to discover a possible stem cell niche in bovine pre-ovulatory follicle.

Acknowledgments

This study was supported by grants from Università degli Studi di Milano and Università Politecnica delle Marche, Ancona, Italy. The authors wish to thank Prof. Fulvio Gandolfi and Dott.ssa Georgia Pennarossa (Department of Veterinary Science Animal Health and Food Safety, Univerità degli Studi di Milano, Italy) for providing the reagent and protocol for Oct-4 immunocytochemical detection.

Author Disclosure Statement

The authors declare that there are no conflicts of interest.

Author contributions: Anna Lange-Consiglio is responsible for the study concept and participated in designing the study, performed the *in vitro* study, collected and interpreted data performing statistical analysis, wrote and reviewed the manuscript, and approved the final version; Alessio Romaldini performed the molecular study, collected and interpreted data, and approved the final version; Alessio Correani performed the molecular study, collected and interpreted data, and approved the final version; Bruna Corradetti performed the molecular study, collected and interpreted data, wrote and reviewed the manuscript, and approved the final version; Paola Esposti took part in collecting and interpreting data and approved the final version; Maria Francesca Cannatà took part in collecting and interpreting data and approved the final version; Claudia Perrini took part in collecting and interpreting data and approved the final version; Maria Giovanna Marini took part in collecting and interpreting data and approved the final version; Davide Bizzaro took part in collecting and interpreting data and approved the final version; Fausto Cremonesi is responsible for the study concept and participated in designing the study, interpreted data, and revised and approved the final version of the manuscript.

References

Arnhold, S.J., Goletz, I., Klein, H., Stumpf, G., Beluche, L.A., Rohde, C., Addicks, K., and Litzke LF. (2007). Isolation and characterization of bone marrow-derived equine mesenchymal stem cells. Am. J. Vet. Res. 68, 1095–1105.

Bosnakovski, D., Mizuno, M., Kim, G., Takagi, S., Okumura, M., and Fujinaga, T. (2005). Isolation and multilineage differentiation of bovine bone marrow mesenchymal stem cells. Cell Tissue Res. 319, 243–253.

Bosnakovski, D., Mizuno, M., Kim, G., Takagi, S., Okumura, M., and Fujinaga, T. (2006). Chondrogenic differentiation of bovine bone marrow mesenchymal stem cells (MSCs) in different hydrogels: Influence of collagen type II extracellular matrix on MSC chondrogenesis. Biotechnol. Bioeng. 93, 1152–1163.

Chiou, S.H., Yu, C.C., Huang, C.Y., Lin, S.C., Liu, C.J., Tsai, T.H., Chou, S.H., Chien, C.S., Ku, H.H., and Lo, J.F. (2008). Positive correlations of Oct-4 and Nanog in oral cancer stem-like cells and high-grade oral squamous cell carcinoma. Clin. Cancer Res. 14, 4085–4095.

Corradetti, B., Lange-Consiglio, A., Barucca, M., Cremonesi, F., and Bizzaro, D. (2011). Size-sieved subpopulations of mesenchymal stem cells from intervascular and perivascular equine umbilical cord matrix. Cell Prolif. 44, 330–42.

Corradetti, B., Meucci, A., Bizzaro, D., Cremonesi, F., and Lange Consiglio, A. (2013). Mesenchymal stem cells from amnion and amniotic fluid in the bovine. Reproduction 145, 391–400.

Dominici, M., Le Blanc, K., Mueller, I., Slaper-Cortenbach, I., Marini, F., Krause, D., Deans, R., Keating, A., Prockop, D.J., and Horwitz, E. (2006). Minimal criteria for defining multipotent mesenchymal stromal cells. Cytotherapy 8, 315–317.

Erickson, G. (2000). The graafian follicle: A functional definition. In: *Ovulation: Evolving Scientific and Clinical Concepts*. Adashi, E.Y., ed. (Springer-Verlag, New York), pp. 31–48.

Fortier, L.A., Nixon, A.J., Williams, J., and Cable, C.S. (1998). Isolation and chondrocytic differentiation of equine bone marrow-derived mesenchymal stem cells. Am. J. Vet. Res. 59, 1182–1187.

Hass, R., Kasper, C., Böhm, S., and Jacobs, R. (2011). Different populations and sources of human mesenchymal stem cells (MSC): A comparison of adult and neonatal tissue-derived MSC. Cell Commun. Signal. 9, 12.

Hjelmeland, A.B., Wu, Q., Heddleston, J.M., Choudhary, G.S., MacSwords, J., Lathia, J.D., McLendon, R., Lindner, D., Sloan, A., and Rich, J.N. (2011). Acidic stress promotes a glioma stem cells phenotype. Cell Death Differ. 18, 829–840.

Kern, S., Eichler, H., Stoeve, J., Klüter, H., and Bieback, K. (2006). Comparative analysis of mesenchymal stem cells from bone marrow, umbilical cord blood, or adipose tissue. Stem Cells 24, 1294–1301.

Kossowska-Tomaszczuk, K., De Geyter, K.C., De Geyter, M., Martin, I., Holzgreve, W., Scherberich, A., and Zhang, H. (2009). The multipotency of LGC collected from mature ovarian follicles. Stem Cells 27, 210–219.

Lange-Consiglio, A., Maggio, V., Pellegrino, L., and Cremonesis, F. (2010). Equine bone marrow mesenchymal or amniotic epithelial stem cells as feeder in a model for the in vitro culture of bovine embryos. Zygote 20, 45–51.

Lange-Consiglio, A., Corradetti, B., Bizzaro, D., Magatti, M., Ressel, L., Tassan, S., Parolini, O., and Cremonesi, F. (2012). Characterization and potential applications of progenitor-like cells isolated from horse amniotic membrane. J. Tissue Eng. Regen. Med. 6, 622–635.

Lee, J., Sayed, N., Hunter, A., Au, K.F., Wong, W.H., Mocarski, E.S., Pera, R.R., Yakubov, E., and Cooke, J.P. (2012). Activation of innate immunity is required for efficient nuclear reprogramming. Cell 151, 547–558.

Lund, S.A., Giachelli, C.M., and Scatena, M. (2009). The role of osteopontin in inflammatory processes. J. Cell Commun. 3, 311–322.

Marshall, V.S., Waknitz, M.A., and Thomson, J.A. (2001). Isolation and maintenance of primate embryonic stem cells. Methods Mol. Biol. 158, 11–18.

Mattioli, M., Gloria, A., Turriani, M., Berardinelli, P., Russo, V., Nardinocchi, D., Curini, V., Baratta, M., Martignani, E., and Barboni, B. (2012). Osteo-regenerative potential of ovarian granulosa cells: An in vitro and in vivo study. Theriogenology 77, 1425–1437.

Mitchell, K.E., Weiss, M.L., and Mitchell, B.M. (2003). Matrix cells from Wharton's jelly form neurons and glia. Stem Cells 21, 50–60.

Raoufi, M.F., Tajik, P., Dehghan, M.M., Eini, F., and Barin, A. (2011). Isolation and differentiation of mesenchymal stem cells from bovine umbilical cord blood. Reprod. Domest. Anim. 46, 95–99.

Ringe, J., Kaps, C., Schmitt, B., Büscher, K., Bartel, J., Smolian, H., Schultz, O., Burmester, G.R., Häupl, T., and Sittinger, M. (2002). Porcine mesenchymal stem cells. Induction of distinct mesenchymal cell lineages. Cell Tissue Res. 307, 321–327.

Seo, M.S., Jeong, Y.H., Park, J.R., Park, S.B., Rho, K.H., Kim, H.S., Yu, K.R., Lee, S.H., Jung, J.W., Lee, Y.S., and Kang, K.S. (2009). Isolation and characterization of canine umbilical cord blood-derived mesenchymal stem cells. J. Vet. Sci. 10, 181–187.

Smith, R.K., Korda, M., Blunn, G.W., and Goodship, A.E. (2003). Isolation and implantation of autologous equine mesenchymal stem cells from bone marrow into the superfi-

cial digital flexor tendon as a potential novel treatment. Equine Vet. J. 35, 99–102.

Solmesky, L.J., Abekasis, M., Bulvik, S., and Weil, M (2009). Bone morphogenetic protein signaling is involved in human mesenchymal stem cell survival in serum-free medium. Stem Cells Dev. 18, 1283–1292.

Tannock, I.F., and Rotin, D. (1989). Acidic pH in tumors and its potential for therapeutic exploitation. Cancer Res. 49, 4373–4384.

Thorpe, T. (2007). A history of plant tissue culture. Mol. Biotechnol. 37, 169–180.

Trounson, A., Thakar, R.G,, Lomax, G., and Gibbons, D. (2011). Clinical trials for stem cell therapies. BMC Med. 9, 52–59.

Vidal, M.A., Kilroy, G.E., Johnson, J.R., Lopez, M.J., Moore, R.M., and Gimble, J.M. (2006). Cell growth characteristics and differentiation frequency of adherent equine bone marrow-derived mesenchymal stromal cells: Adipogenic and osteogenic capacity. Vet. Surg. 35, 601–610.

Vidal, M.A., Robinson, S.O., Lopez, M.J., Paulsen, D.B., Borkhsenious, O., Johnson, J.R., Moore, R.M., and Gimble, J.M. (2008). Comparison of chondrogenic potential in equine mesenchymal stromal cells derived from adipose tissue and bone marrow. Vet. Surg. 37, 713–724.

Vidal, M., Walker, N.J., Napoli, E., and Borjesson, D.L. (2011). Evaluation of senescence in mesenchymal stem cells isolated from equine bone marrow, adipose tissue and umbilical cord tissue. Stem Cells Dev. 21, 273–283.

Wagner, E., Luther, G., Zhu, G,, Luo, Q., Shi, Q., Kim, S.H., Gao, J.L., Huang, E., Gao, Y., Yang, K., and Wang, L. (2011). Review article: Defective osteogenic differentiation in the development of osteosarcoma. Sarcoma http://dx.doi.org/10.1155/2011/325238.

Wang, H., Hung, S., Peng, S., Lai, C., and Chena, C. (2004). Mesenchymal stem cells in the Warthon's jelly of the human umbilical cord. Stem Cells 22, 1330–1337.

Woodbury, D., Schwarz, E.J., Prockop, D.J., and Black, I.B. (2000). Adult rat and human bone marrow stromal cells differentiate into neurons. J. Neurosci. Res. 61, 364–370.

Xu, L., Ping, F., Yin, J., Xiao, X., Xiang, H., Ballantyne, C.M., Wu, H., and Li, M. (2013). Elevated plasma sparc levels are associated with insulin resistance, dyslipidemia, and inflammation in gestational diabetes mellitus. PLoS One 8: e81615.

Address correspondence to:
Prof. Fausto Cremonesi
Università degli Studi di Milano
Large Animal Hospital
Reproduction Unit,
Via dell'Università 6
26900, Lodi, Italy

E-mail: fausto.cremonesi@unimi.it

Marini et al. Reproductive Biology and Endocrinology (2016) 14:58
DOI 10.1186/s12958-016-0195-4

Reproductive Biology and Endocrinology

RESEARCH Open Access

Effects of platelet-rich plasma in a model of bovine endometrial inflammation *in vitro*

Maria Giovanna Marini[1], Claudia Perrini[2], Paola Esposti[2], Bruna Corradetti[1], Davide Bizzaro[1], Pietro Riccaboni[3], Eleonora Fantinato[3], Giuseppe Urbani[4], Giorgio Gelati[4], Fausto Cremonesi[2] and Anna Lange-Consiglio[2*]

Abstract

Background: Endometritis reduces fertility and is responsible for major economic losses in beef and dairy industries. The aim of this study was to evaluate an alternative therapy using platelet-rich plasma (PRP). PRP was tested *in vivo*, after bovine intrauterine administration, and *in vitro* on endometrial cells.

Methods: Bovine endometrial cells were cultured until passage (P) 10 with 5 % or 10 % PRP. Effect of PRP on endometrial cell proliferation and on the expression of genes [prostaglandin-endoperoxide synthase 2 (*COX2*), tumor protein p53 (*TP53*), oestrogen receptors (*ER-α* and *ER-β*), progesterone receptor (*PR*) and *c-Myc*] involved in the regulation of oestrus cycle and fetal-maternal interaction were evaluated. Moreover, to evaluate the ability of PRP to counteract inflammation, 10 and 100 ng/ml of bacterial endotoxin lipopolysaccharide (LPS) were used to inflame endometrial cells *in vitro* for 1, 6, 12, 24 and 48 h. The expression of genes such as interleukin 1β (*IL-1β*), interleukin-8 (*IL-8*), inducible nitric oxide synthase (*iNOS*), prostaglandin-endoperoxide synthase 2 (*COX2/PTGS2*), and the release of PGE-2, IL-1β and IL-8 were evaluated.

Results: *In vivo* treatment with PRP increased the detection of PR. *In vitro*, 5 % PRP at passage 5 increased proliferation rate and induced a significant increase in the expression of all studied genes. Furthermore, the results revealed that 10 ng/ml of LPS is the most effective dose to obtain an inflammatory response, and that PRP treatment significantly down regulated the expression of pro-inflammatory genes.

Conclusion: This study lays the foundations for the potential treatment of endometritis with PRP *in vivo*.

Keywords: Cattle, Endometrial cells, Platelet-rich plasma, LPS, gene expression

Background

The wall of the uterus consists of endometrium, myometrium and perimetrium (tunica serosa). The bovine endometrium is a complex tissue that comprises the tunica mucosa (lamina epithelialis and lamina propria consisting of loose connective tissue) and the tunica submucosa of the uterus. In the lamina propria, neutrophils and lymphocytes are commonly detectable. The endometritis is characterized by an increase number of inflammatory cells associated to epithelial erosion and/or necrosis and diffuse oedema of endometrium [1]. Meta-analysis studies show that endometritis reduces pregnancy rate by 16 % [2]. The economic losses related to this disease are substantial and associated with a great impact on the economy to drop in milk yield and calves, and treatment costs [3]. Approximately, 80 % to 100 % of cows have intrauterine bacterial contamination in the first two weeks postpartum. In most cases, clinical disease does not develop, as the normal uterus is able to clear a bacterial infection efficiently [4]. In 10 %-20 % of cows, however, the infection is not controlled and may lead to chronic uterine inflammation [1, 5]. It is commonly accepted that the development of uterine infection depends on the immune response of the cow, as well as species and number of bacteria [1]. Economically, important uterine diseases in cattle are commonly

* Correspondence: anna.langeconsiglio@unimi.it
[2]Large Animal Hospital, Reproduction Unit, Università degli Studi di Milano, Via dell'Università 6, 26900 Lodi, Italy
Full list of author information is available at the end of the article

associated with bacterial infection by *Escherichia coli*, *Trueperella pyogenes*, *Fusobacterium necrophorum* or *Prevotella* species [1, 5–8]. The most significant pathogenic bacteria responsible for uterine infection are *E. coli*, which produce an endotoxin lipopolysaccharide (LPS) that is present in their cell wall.

Establishment of uterine bacterial infection may also depend on metabolic disease, although the specific mechanisms are still not clear or by endocrine environment, that affects the likelihood of bacteria elimination [9–11].

The inflammatory response is a complex process involving many signalling cascades. In the genital tract, the initial response of the endometrium against infection is dependent on innate immunity and mucosal defence systems [3, 12]. The uterine immune response is provided at the cellular level, by uterine leukocytes and polymorphonuclear cells that are the cells phagocytizing and clearing bacteria [13]. In horse, at the molecular level, cytokines have a significant role in the recruitment of inflammatory cells [14]. In cattle, interleukin-6 and TNF-α stimulate the production of antimicrobial peptides that assist in the elimination of pathogenic bacteria [15, 16]. Moreover, bovine endometrial epithelial and stromal cells can respond to bacterial LPS through the Toll-like receptor (TLRs) [17]. Activated TLRs subsequently stimulate the production of pro-inflammatory cytokines and chemokines [18].

Literature on the treatment of endometritis in cattle is extensive and at times inconsistent. Specifically, uterine disease treatments aim at reverting inflammatory changes that impair fertility, whilst enhancing uterine defence and repair [19]. In cows, many therapeutic agents and procedures have been developed to treat endometritis, including systemic or intrauterine administration of antibiotics [20–22], or administration of PGF2α and its analogue [20–24]. The intrauterine infusion of antiseptics (e.i. Lugol's solution) has been tested although side-effects on future fertility of the cows have been reported [23, 25]. Furthermore, approaches using proteolytic enzymes [21], administration of estradiol [26, 27] or GnRH [28] have also been described. Even if all these treatments show some effects on uterine healing, no definitive results can be extrapolated from published clinical trials.

Platelet-rich plasma (PRP) is an emerging therapeutic application in tissue regeneration and engineering due to its enrichment in growth factors with mitogenic and anti-inflammatory potential [29, 30]. In particular, PRP is a concentration of platelets (3-5 fold the plasma baseline level) containing transforming growth factor β1 (TGF-β1) and TGF-β2, platelet derived growth factors (PDGF-AA, PDGF-BB, PDGF-AB), insulin-like growth factor 1 (IGF-I), epidermal growth factor (EGF), vascular endothelial growth factor (VEGF), fibroblast growth factor (FGF) and hepatocyte growth factor (HGF) that are very important for regeneration processes. Indeed, these growth factors act synergistically to increase the infiltration of neutrophils and macrophages, to promote angiogenesis, fibroplasia, matrix deposition and, ultimately, re-epithelialization, inducing the consequent tissue regeneration [29]. Lastly, the presence of anti-inflammatory molecules, including HGF [31] also confers on PRP the ability to suppress inflammatory process.

In this context, the specific aim of this study was to investigate the effect of PRP *in vivo* and *in vitro*, on a model of healthy or LPS stressed bovine endometrial cells. *In vivo*, the progesterone receptor (PR) expression was detected immunohistochemically. The steroid hormone progesterone (P4) plays a key role in reproductive events associated with establishment and maintenance of pregnancy. Conceptus growth and development require the action of P4 on the uterus to regulate endometrial function, including conceptus-maternal interactions, pregnancy recognition, and uterine receptivity to implantation [32]. Indeed, low P4 concentrations have been implicated as a causative factor in the low pregnancy rates observed in high-yielding dairy cows [33]. *In vitro*, genes involved in the regulation of oestrous cycle, in pro-inflammatory process and the release of some cytokines were evaluated.

Methods

Experimental design

This study was based on three experiments. The first experiment evaluated the endometrium histologically and immunohistochemically, after *in vivo* PRP administration, using PR receptor as a marker of cell receptivity. The second experiment evaluated the effect of a 5 % and 10 % concentration of PRP in culture medium, on *in vitro* endometrial cell proliferation and on the expression of some genes involved in the regulation of oestrous cycle and fetal-maternal interaction, to establish whether it is able to improve the functions of this cell line. The genes included prostaglandin-endoperoxide synthase 2 (*COX2* or *PTGS2*), tumor protein p53 (*TP53*), oestrogen receptors (*ER-α* and *ER-β*), progesterone receptor (*PR*) and v-myc avian myelocytomatosis viral oncogene homolog (*c-Myc*). The third *in vitro* experiment evaluated the ability of PRP to counteract an *in vitro* model of inflammation by stressing endometrial cells with LPS at different times and concentrations. Expression of pro-inflammatory genes and release of some cytokines were evaluated.

Materials

Chemicals were obtained from Sigma-Aldrich Chemical (Milan, Italy) unless otherwise specified. LPS was

purchase by Sigma-Aldrich Chemical (E. coli 0:111B4; L2630 catalog number). Tissue culture plastic dishes were purchased from Euroclone (Milan, Italy).

Animals

All procedures were performed according to approved animal care and use protocols of the institutional ethics committee and to good veterinary practice for animal welfare as to European directive 2010/63/UE. Written farmers' consent was obtained at the beginning of the study.

From a group of Holstein Friesian, animals at 150-180 days in milking belonging to a 180 cows dairy farm located in North Italy, 14 cows bearing a well-developed corpus luteum (CL) diagnosed by B-mode ultrasound evaluation of the ovaries, were selected. They received an i.m. luteolytic dose of PGF2α to synchronize the estrous cycle. All animals ($n = 10$) showed estrous signs in the following 96 hours and at that time bacteriological and cytological analyses, trans rectal and vaginal palpation, and sonography of the reproductive tract were conducted to exclude genital diseases. These animals were enrolled for the first study.

Endometrial samples for *in vitro* study were collected from slaughtered bovines under legal regulations

Preparation of platelet-rich plasma

Collection of blood

Blood was obtained from two donor cows at forty days in milking, as this is the period the circulating platelet count is higher than other periods (data not shown). These animals were in good health, free from infectious diseases and they did not receive medication during the previous two months. The collection of blood and the preparation of PRP, with the method of double centrifugation, were performed as reported by Lange-Consiglio et al. [34]. After surgical scrub preparation of a few centimeters of skin around the subcutaneous mammary vein, 450 ml of blood was collected in *ad hoc* Terumo blood bags (Terumo Srl, Rome, Italy) containing citrate-phosphate-dextrose-adenine (CPDA-1) using the 16-gauge needle provided with the bags. The bags were transported at 4 °C to the laboratory within 2 h of collection and immediately processed.

Double centrifugation method

All separation steps were performed under a horizontal laminar flow hood in aseptic conditions. To prepare the PRP, the blood was drawn into sterile Falcon tubes of 50 mL each (EuroClone SpA, Milan, Italy). The tubes were centrifuged at 100 x g for 30 min at 4 °C. This caused separation of the blood into three components: red blood cells at the lowest level, "buffy coat" in the middle layer, and platelet rich plasma (PRP) in the upper layer. Afterward, the PRP was carefully aspirated and distributed in new 50-ml tubes and centrifuged again at 1,500 x g for 10 min at 4 °C to obtain the platelet pellet and the poor platelet plasma (PPP) on the upper layer. Afterward, two-thirds of the volume of PPP was aspirated for later use and the pellet mixed in the residual PPP volume to allow for platelet count before the final dilution with PPP to obtain PRP at a standard concentration of 1×10^9 platelets/ml [34]. All platelet counts on peripheral blood and PRP were performed using a HeCo Vet automatic hematology analyzer (SEAC, Florence, Italy). The total amount of PRP obtained for each donor was aliquoted in 10 ml ready-to-use doses that were stored in syringes. The syringes were then frozen at −80 °C and thawed at 37 °C three times [35] to allow the release of platelet-derived factors. The PRP was subjected to aerobic and anaerobic bacteriological examination to verify its sterility. Syringes containing the PRP dose were kept frozen at −20 °C until use.

Experiment 1: *in vivo* effect of intrauterine administration of PRP

At day 4 post estrus, all previously selected animals were checked by ultrasound for the presence of a newly formed CL and were randomly divided in two groups. Seven cows were treated with PRP while the other seven animals were enrolled as control (CTR). Physiological solution (0.9 % NaCl) was used as placebo for these latter. Ten ml of PRP or ten ml of physiological solution were aseptically infused into the uterus by a disposable sterile catheter included in a protective sheath guided into the cervix by manipulation per rectum. To prevent transfer of vaginal flora into the uterine lumen, the protective sheath was removed just after cervix penetration and the catheter was hence introduced into corpus uteri where PRP was infused.

Endometrial biopsy

Endometrial biopsies were collected using a stainless steel Hauptner equine endometrial biopsy instrument as previously described by Chapwanya et al. [15] and Katagiri and Takahashi [36]. Samples were obtained just before treatment at day 4 post estrus (T0) and 7-day post treatment, that is at day 11 post estrus (T1). Briefly, after cleaning the base of tail, perineum and external genitalia, animals were given caudal epidural anesthesia (4–5 ml 2 % of lidocaine). Afterwards, the biopsy instrument included in a protective sheath was introduced into the uterus through the cervix by manipulation per rectum. Once the cervix was passed, and the protective sheath ruptured, the tip of the biopsy instrument inside the uterus was identified using the hand per rectum. Then, with the help of the hand in the rectum, the medial uterine wall was gently pressed into the instrument jaws and biopsies were taken from the dorsomedial aspect of one

horn just anterior to the bifurcation. Biopsies for histology were gently removed from the biopsy instrument with a fine gauge needle and transferred to a vial of fixation solution. All biopsies were processed by the same operator. The samples were performed for histological and immunocytochemical studies.

Histological and immunohistochemical examinations

Samples were routinely formalin-fixed (10 % buffered formalin) for 48-72 hours and paraffin-wax embedded. Four-micrometer thick sections were stained with hematoxylin and eosin (HE), while others were prepared on poly-L-lysine–coated glass slides for immunohistochemistry to detect the presence of PR.

The immunohistochemical staining of all samples was performed using the avidin–biotin–peroxidase complex procedure with a commercial immunoperoxidase kit (Vectastain Standard Elite; Vector Laboratories, Inc., Burlingame, CA, USA).

Tissue sections were immersed in a pre-heated solution at 94 °C of Dewax and HIER Buffer H (Thermo Fischer Scientific, Lab Vision Corporation, Fremont, CA, USA) diluted 1:15 with deionized water for 40 minutes. This solution is designed to simultaneously dewax and perform heat induced epitope retrieval.

Endogenous peroxidase was blocked using 1 % hydrogen peroxide in Tris buffer for 45 min.

Sections were incubated for 18 hours at 4 °C with anti-PR (Thermo Fischer Scientific, Lab Vision Corporation, Fremont, CA, USA) mouse monoclonal antibodies diluted 1:400. After incubation with the secondary biotinylated anti-mouse immunoglobulin (diluted 1:200; Vector Laboratories, Inc.) for 30 min, the avidin–biotin–peroxidase complex method (Vector Laboratories, Inc.) was performed. Positive staining was visualized with 3.3-diaminobenzidine-4 HCl (Vectastain, Vector Laboratories, SK-4100) and nuclei were counterstained with Mayer's hematoxylin. Diluent negative control sections were produced by omission of the primary antibody.

Evaluation of histological and immunohistochemical data

Tissue samples were evaluated in order to assess the absence of pathological lesions.

The immunohistochemically stained tissue slides were examined using standard light microscopy. Three randomly selected areas were evaluated per section. The staining results were independently scored semi quantitatively by different blinded operators at 400X magnification. The results of PR protein expression were assessed by categorizing immunoreaction of epithelial cells, muscular layer and glandular cells into five groups according to the percentage of positive cells. These group were: 0) no positive cells; 1) <1 % of positive cells; 2) from 1 % to 10 %; 3) from 11 % to 33 %; 4) from 34 % to 66 % and 5) from 67 % to 100 % [37]. The intensity of labeling was graded as: weak positive staining (W); moderate positive staining (M); intense positive staining (I) and scored as follows: W = 1, M = 2, I = 3. A total score was conferred adding together the positive cells percentage score and the intensity of immunolabeling score [37].

Experiment 2: effect of different concentrations of PRP on *in vitro* endometrial cells proliferation and gene expression

Tissue collection and cell isolation

Fresh bovine uteri were collected from three different cows at the slaughterhouse intended for human consumption and unrelated to our experiments. Samples were obtained from healty normal-cycling cows at diestrus stage (middle-late luteal phase). Only uteri belonging to cows with an obvious corpus luteum on the ovary were used for endometrial fragment collection and ensuing cell culture.

Endometrial samples were kept at 4 °C in saline solution supplemented with 4 μg/ml amphotericin B, 100 IU/ml penicillin-100 μg/ml streptomycin and processed within 2 h. Endometrial stromal cells were obtained according to the protocol described by Donofrio et al., [38]. Briefly, the endometrium was digested in 25 ml of sterile filtered Hanks' buffered salt solution supplemented with 50 mg collagenase II, 100 mg bovine serum albumin, and 10 mg DNase I for 90 minutes at 38.5 °C in a shaking bath. Then, cells were filtered with an 80-μm filter, centrifuged at 300 x g for 10 minutes, and washed twice in PBS. Before seeding, the total number of viable cells was evaluated by the exclusion method staining with trypan blue and using a Bürker chamber.

Cells expansion

A pool of endometrial stromal cells cultures from three different cows was established in Dulbecco's Modified Eagle's Medium high glucose (HG-DMEM) supplemented with 10 % FBS, 100 UI/ml penicillin–100 μg/ml streptomycin, 0.25 mg/ml amphotericin B and 2 mM L-glutamine (standard complete medium). For maintenance of cultures, cells were plated in 75 cm^2 flasks (SPL Cell culture flask 70025) at up to $1x10^5$ cells/cm^2 and incubated at 38.5 °C with 5 % CO_2 in a humidified atmosphere. To remove non-adherent cells, the medium was replaced for the first time after 48 h. Adherent cells were detached with 0.05 % trypsin-EDTA just prior to reaching confluence (80 %) and then reseeded for culture maintenance at the density of $1x10^4$ cells/cm^2.

Proliferation studies

All data are representative of three independent experiments.

Doubling time (DT) DT for passages 1–10 (P1 and P10) was assessed plating $9x10^3$ cells into six-well tissue culture plates. Every 4 days cells were trypsinized, counted and reseeded at the same density. Mean DT was calculated from day 0 to day 4. The DT value was obtained for each passage according to the formula DT = CT/CD, where CT represents the culture time and CD = log (Nc/No)/$\log_2$ represents the number of cell generations (Nc represents the number of cells at confluence, No represents the number of seeded cells).

Growth curves To obtain growth curves at P1, P5 and P10 endometrial cells were plated at the density of $9x10^3$ cells into six-well tissue culture plates. Every two days, over the 12 days of culture, cells from one well of each plate were detached and counted.

In vitro effect of PRP on endometrial gene expression

In this study, culture medium was replaced for the first time after 48 h to remove non-adherent cells and changed with complete standard medium supplemented with two different concentrations of PRP, 5 % and 10 %, as a FBS substitute. Control cells were grown in complete standard medium supplemented with 10 % FBS. The cells were expanded for 10 passages, which was the last time point included in our study. Cells from each well were then collected to evaluate mRNA expression of genes involved in the regulation of oestrous cycle and fetal-maternal interaction by quantitative real-time PCR. The genes evaluated were prostaglandin-endoperoxide synthase 2 (*COX2*), tumor protein p53 (*TP53*), oestrogen receptors (*ER-α* and *ER-β*) and progesterone receptor (*PR*). The expression of *c-Myc* was also evaluated.

Molecular characterization of endometrial cells was performed at passages 1, 3, 5 and 10 by qualitative PCR. Data were obtained from three replicates.

Experiment 3: *In vitro* effect of PRP after LPS treatment on gene expression

P5 endometrial cells were plated in six well plates at a density of 50,000 cells/well in DMEM standard complete medium containing two different concentration of LPS, 10 ng/ml and 100 ng/ml. Evaluation of the expression of genes involved in inflammation was performed at 1, 6, 12, 24 and 48 h. The LPS concentrations were chosen on the base of results of Herath et al. [39] that demonstrated level of LPS around 100 ng/ml in cows with clinical endometritis. Supernatants were collected and stored at -20 °C until being used for ELISA to measure PGE-2, IL-1β and IL-8.

To study the *in vitro* effect of PRP in cells inflammed with LPS, endometrial cells were treated with 10 ng/ml LPS and 5 % PRP for 1, 6, 12, 24 and 48 h. At each time point, the expression of same genes was analyzed. Data were obtained from three replicates.

Molecular characterization

Total RNA was extracted from endometrial cells using TRI Reagent Solution (Life Technologies, Monza, Italy). Samples were then treated with DNase in order to eliminate DNA contamination. RNA concentration and purity were measured by Nanodrop Spectrophotometry (NanodropH ND1000). The quality and integrity of the total RNA extracted were verified by electrophoresis on a 1.5 % (w/v) agarose gel. The cDNA was synthesized from total RNA (200 ng) using the PrimeScript RT reagent Kit (Takara Bio). Gene expression evaluation was performed using bovine specific sequences. Oligonucleotide primers were designed using open source PerlPrimer software v. 1.1.17 based on available NCBI *Bos taurus* sequences or on mammal multi-aligned sequences. Primers were designed across an exon–exon junction in order to eliminate genomic DNA amplification and their sequence conditions and the references used are shown in Table 1.

Qualitative PCR analysis was performed in a 25 μl final volume with Taq DNA Polymerase recombinant commercial kit (Invitrogen Life Technologies) under the following conditions: initial denaturation at 94 °C for 2 minutes, 32 cycles at 94 °C for 30 seconds (denaturation), 55–60 °C for 30 seconds (annealing), 72 °C for 30 seconds (elongation) and final elongation at 72 °C for 10 minutes. For conventional PCR, primers were used at 200 nM final concentrations.

Quantitative PCRs were performed with SYBR green method in a MyiQ iCycler thermal cycler (Biorad). PCR reactions were carried out in triplicate for each sample. The reactions were set on a strip in a final volume of 25 μl by mixing, for each sample, 1 μl of cDNA, 12.5 μl of 2X concentrated SYBR Premix Ex Taq II (Takara Bio) containing SYBR Green as a fluorescent intercalating agent, 0.2 μg forward primer, 0.2 μg of reverse primer and MQ water. PCR efficiencies were tested and found to be close to 1. The thermal profile for all reactions was 30 seconds at 95 °C and then 40 cycles of 5 seconds at 95 °C, 30 seconds at 60 °C. Fluorescence monitoring occurred at the end of each cycle. Efficiency of amplification for each primer was monitored through the analysis of serial dilution. Additional dissociation curve analysis was performed and in all cases showed a single peak. The data thus obtained were analyzed using the iQ5 optical system software version 2.0 (BioRad). The expression of each gene was normalized to the reference gene glyceraldehyde-3-phosphate dehydrogenase (*GAPDH*) (internal control) in order to standardize the results by eliminating variation in cDNA quantity.

Table 1 Oligonucleotide sequences used for RT-PCR analysis

Marker	Forward 5'-3'	Reverse 5'-3'	T annealing	bp
Interleukin-1β (IL-1β)	TGCAGCTGGAGGAAGTAGAC	GTCGGGCATGGATCAGACAA	60	338
Interleukin 8 (IL-8)	ACATACCCTGCCACAAGGC	TGGGGACTGCTCTTCCCTCT	57	146
Inducible nitric oxide synthase (iNOS)	GGACCTCAACAAAGCCCTGA	CCTTGACCCAATAGCTGCCA	60	293
Prostaglandin-endoperoxide synthase 2 (COX2)	CATGGGTGTGAAAGGGAGGAA	AAAGACGTCAGGCAGAAGGG	60	700
Tumor protein p53 (TP53)	CCTAGGAGCACTAAGCGAGC	GCCCCTCTCTCTTGAGCATT	55	268
Oestrogen receptor alpha (ERα)	AGGGAAGCTCCTATTTGCTCC	CGGTGGATGTGGTCCTTCTCT	55	234
Oestrogen receptor beta (ERβ)	GCTTCGTGGAGCTCAGCCTG	AGGATCATGGCCTTGACACAG	55	262
Progesterone receptor (PR)	GAGAGCTCATCAAGGCAATTGG	CACCATCCCTGCCAATATCTTG	55	227
v-myc avian myelocytomatosis viral oncogene homolog (c-Myc)	GCGCCGCATTCGCGAAACTT	TGAGGGGCATCGCTGCAAGC	58 °C	214
Glyceraldehyde-3-phosphate dehydrogenase (GAPDH)	ATGAGATCAAGAAGGTGGTG	CCAAATTCATTGTCGTACCAG	60	190

Such gene was identified among others used as endogenous control genes based on previous studies focusing on endometrial gene expression [40]. Relative gene expressions were presented with the $2^{-\Delta\Delta Ct}$ method [41].

Protein release by ELISA

Protein release (PGE-2, IL-1β and IL-8) was measured in cell-free supernatants obtained by centrifugation at 250 x g for 5 min and stored at −80 °C until measurement. Protein production was assessed according to the manufacturers' instructions (Bovine PGE-2 MBS737103, MyBioSource; Bovine IL-1β Screening Set ESS0027, Thermo Fisher Scientific; CXCL8/IL-8 DuoSet DY208, R&D Systems). The Human CXCL8/IL-8 DuoSet was previously validated for measurement of bovine IL-8 [42]. The limits of detection for PGE-2, IL-ß and IL-8 were 1.0, 20.1 and 14.3 pg/ml, respectively.

Results are expressed in pg/ml.

Statistical analysis

Statistical analysis was performed using GraphPad Instat Software version 3.00 for Windows (La Jolla, CA, US). For proliferation data, three replicates for each experiment were performed. Results are reported as mean ± standard deviation (SD). One-way analysis of variance (ANOVA) for multiple comparisons by Student-Newman-Keuls multiple comparison tests was used.

Immunohistochemical data were analyzed by unpaired Student's *t*-test.

For cytokines, statistical differences were determined using ANOVA followed by Dunnett's multiple comparison test, the Tukey–Kramer multiple comparisons test or unpaired t test.

Differences were considered statistically significant for P values < 0.05.

For quantitative PCR data, non-parametric tests were used. The Mann-Whitney U-test was employed to compare two groups (treated vs untreated). Results were considered significant if the value of P was < 0.01.

Results

Experiment 1: *in vivo* effectiveness of intrauterine administration of PRP

Histological examination

No pathological alterations were detected in any of the examined biopsies. All the samples were covered by a columnar simple epithelial monolayer. A moderately large amount of uterine glands was dispersed in the stroma. Scattered rare lymphocytes were also detectable in the stroma. Neither fibrosis nor hemorrhages were present.

Immunohistochemical evaluation

Positive nuclei to PR were brown-stained, while negative nuclei were blue stained by hematoxylin counterstain. Diluent negative controls showed no immunoreaction.

The PR immunoreactivity was evaluated separately in the surface epithelial cells, glandular epithelium and smooth muscle cells. The total scores are listed in Table 2.

PR expression has been detected in all these uterine compartments (Fig. 1). Treated animals in T1 showed the highest PR receptor score in glandular epithelium and smooth muscle cells compared to T0 ($P < 0.05$). In T1 control animals, glandular epithelium and smooth muscle cells obtained the same high average score that is not statistically different compared to T0 ($P > 0.05$).

Experiment 2: effect of different percentages of PRP on *in vitro* endometrial cells proliferation and gene expression

Cells isolation and expansion

Cells were selected on their ability to adhere to plastic. For endometrial cells, initial viability was >80 %. Cells displayed the typical fibroblast-like morphology (Fig. 2a). The molecular biology study on the isolated cells confirmed their endometrial nature due to the expression of *ER-α*, *ER-β*, *PR* and *TP53* (Fig. 2b).

Proliferation studies

The DT value at P1 and P2 were similar between the cells grown in presence of 5 % PRP, 10 % PRP and 10 % FBS. After P2, for endometrial cells grown in presence of 5 % PRP, the proliferative ability increased until P5 while for cells grown in presence of 10 % PRP, the proliferative ability decreased and then remained constant until P10. No difference in the DT value for endometrial cells grown in presence of 10 % FBS were found over the passages studied (Fig. 3a). The mean DT value for endometrial cells grown in presence of 5 % PRP was 1.96 ± 0.31 days, while it was 4.64 ± 1.52 and 2.20 ± 0.22 days for endometrial cells grown with 10 % PRP and FBS 10 %, respectively.

Endometrial cells cultured with 5 % of PRP, at P1 showed a growth curve with an initial lag phase of 2 days and a subsequent long log phase of 8 days. At P5, endometrial cells demonstrated a growth curve with an initial lag phase similar to that observed for P1, continues with a log phase of 4 days followed by a stationary phase of 4 days. Finally, after 10 days in culture, a death phase was observed. At P10, endometrial cells showed a growth curve with an initial lag phase longer than that registered for endometrial cells at P5 (2-8 days) and subsequent log phase shorter than that observed for P5 (2 days) (Fig. 3b).

In vitro effect of PRP on endometrial gene expression

Endometrial cells were cultured in presence of two different concentrations of PRP (5 % and 10 %) until passage 10, and mRNA expression of genes involved in the regulation of oestrous cycle and fetal-maternal interaction was measured by quantitative PCR. PRP 5 % at P5 had a significant effect on the expression of endometrial genes when compared to the expression levels of untreated cells (Fig. 4a-f). The results showed a statistically significant increase ($P < 0.01$) in the expression of all studied genes at P5 in cells cultured in

Table 2 Total score for PGR expression in bovine according to the surface epithelial cells, glandular epithelium and smooth muscle cells

		Surface epithelium		Glandular epithelium		Smooth muscle	
	Subject	T0	T1	T0	T1	T0	T1
SALINE CTR	2	5	3.5	8	5	3	4.5
	4	8	4	8	8	6.5	6.5
	8	3	4	3	8	4	7.5
	9	8	7.5	7.5	8	5.5	7.5
	10	3	2	4	4	4	7
	11	4	4	5	4	5	4.5
	14	4	4	6	7	6	4
Average score		5.0±2.2[a]	4.1±1.7[a]	5.9±2.0[a]	6.3±1.9[a]	4.4±1.1[a]	5.8±1.66[a]
PRP	1	5	3.5	5.5	6.5	4	7.5
	3	3.5	0	4.5	7	2.5	6.5
	5	2	6.5	3.5	8	2.5	7
	6	8	8	7.5	8	8	7.5
	7	7.5	8	8	8	6	6.5
	12	5	5	6	7	3	7
	13	4	6	5	7	5	6.5
Average score		5.0±2.1[a]	5.3±2.8[a]	5.7±1.6[a]	7.4±0.6[b]	4.4±2[a]	6.9±0.4[b]

Legend: average score represent mean ± standard deviation. Different small letters superscripts (a,b) indicate statistically different comparisons ($P<0.05$) between T0 and T1

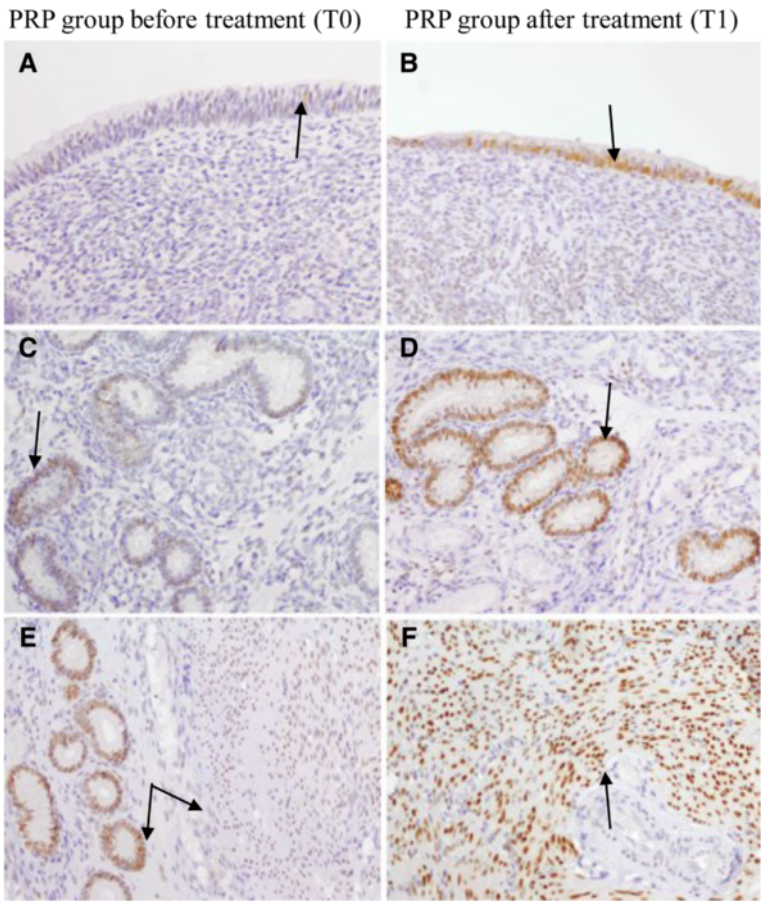

Fig. 1 Immunohistochemical PR expression in uterine biopsies (20x, Haematoxylin counterstain). Figures in the left column are of PRP group treated at T0 while in the right column are of PRP group treated at T1. Arrows show the following results. Uterine surface epithelium showing: (**a**) weak positivity involving scattered cells (score W1); (**b**) and marked positivity in the majority of the epithelial cells (score I5). Glandular epithelium with (**c**) weak and diffuse immunostaining (score W4); (**d**) intense and diffuse imunostaining scored as I5. Smooth muscle cells with (**e**) moderate and diffuse immunolabeling (score M5). The same score is detectable in the close glandular epithelium. (**f**) Intense and diffuse immunohistochemical expression in smooth muscle cells (score I5)

presence of 5 % PRP compared to 10 % PRP or 10 % FBS. In particular, *ER-α* expression increased 9-fold (±0.66), *ER-β* expression increased 260-fold (±6.8), *PR* expression increased 5.44-fold (±0.85), *TP53* expression increased 5.56-fold (±0.52) and *COX2* expression increased 15.74-fold (±0.78). The expression of *c-Myc* increased of 22-fold (±0.24). At P10, a decrease in the expression of all the evaluated genes was observed, with the only exception on TP53, whose expression remains constant.

Experiment 3: in vitro effect of PRP after LPS treatment on gene expression

Endometrial cells at P5 were cultured with or without 10 ng/ml or 100 ng/ml LPS for 1, 6, 12, 24, and 48 h, and mRNA expression of pro-inflammatory genes was evaluated by qPCR. The results are summarized in Fig. 5a,c,e,g for 10 ng/ml and Fig. 5b,d,f,h for 100 ng/ml. Treatment with PRP did not alter *GAPDH* mRNA expression, which was included as a reference gene. The results revealed that the 10 ng/ml concentration of LPS between 1 h and 12 h is the most effective dose to induce an over-expression of pro-inflammatory genes in bovine endometrial cells.

A significant increased ($P < 0.01$) expression of *IL-1β* (18.65 ± 0.32), *iNOS* (208.17 ± 0.18) and *COX2* (99.84 ± 0.31) was observed immediately (1 h) after LPS treatment compared to untreated cells. Expression of *IL-8* was significantly higher ($P < 0.01$) at 6 h and 12 h (10.55 ± 0.29 and 10.22 ± 0.12 respectively) after LPS treatment compared to untreated cells. Within 48 h, all genes returned nearly to baseline.

The PRP treatment had a significant effect ($P < 0.01$) on the endometrial gene expression of these genes when

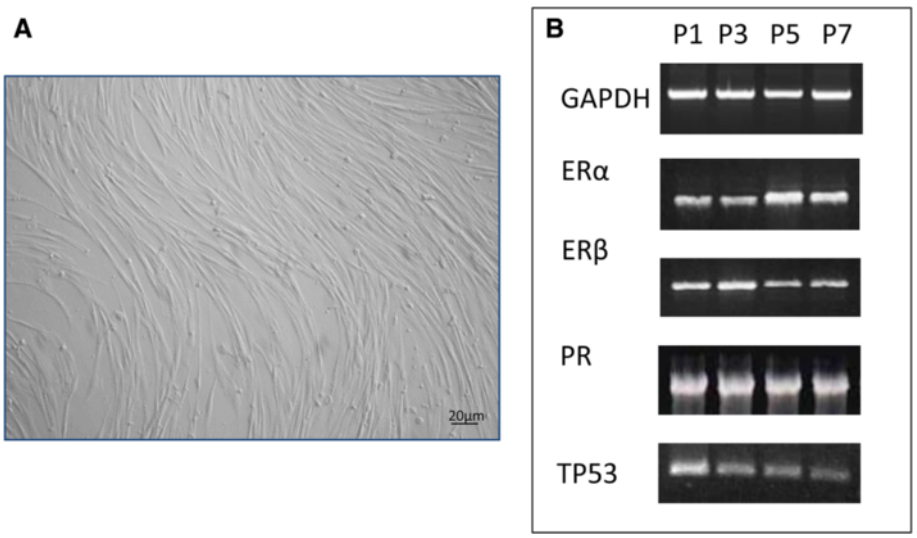

Fig. 2 (**a**) Cell morphology. Monolayer of endometrial cells. Scale bar: 20 μM. Magnification 20X. (**b**) Molecular characterization of endometrial cells at diestrus stage. Qualitative PCR analysis for the expression of genes that influencing pre-implantation conceptus development (*ERα, ERβ* and *PR*)

compared to the levels of expression found in the LPS (10 ng/ml) treated cells (Fig. 6a-d). The mRNA expression of the pro-inflammatory cytokine *IL-1β* was found significantly lower compared to untreated cells, passing from 18.65 ± 0.32 to 0.59 ± 0.16 ($P < 0.01$), immediately 1 h after PRP treatment. The mRNA expression of the pro-inflammatory chemokine *IL-8* was significantly lower ($P < 0.01$) with values decreasing at 1 h, 6 h and 12 h after PRP treatment to 0.33 ± 0.14, 1.37 ± 0.31 and 2.23 ± 0.16, respectively, compared to untreated cells. A significant reduction ($P < 0.01$) in the expression levels of *iNOS* (from 208.17 ± 0.18 it fell to 1.66 ± 0.04) and *COX2* (from 99.84 ± 0.31 it fell to 7 ± 0.07) was found compared to untreated cells 1 h after treatment with PRP.

Protein release

The results of the release of PGE-2 for endometrial cells treated by PRP at P5 are shown graphically in Fig. 7a. The release of PGE-2, IL-1β and IL-8 by endometrial cells stimulated with 10 ng/ml of LPS and treated with 5 % PRP at different time (1, 6, 12, 24 and 48 h) are shown graphically in Fig. 7 b,c,d). In endometrial cells (CTR), the concentrations of IL-1β and IL-8 were below the limits of detection of the assay. The endometrial cells responded to 5 % of PRP with release of 5000 ± 480 pg/ml of PGE-2 that is statistically different ($P < 0.05$) compared to CTR (330 ± 30 pg/ml). The treatment with 10 ng/ml of LPS induced release of PGE-2 and IL-1β at 1 h (30000 ± 2490 and 2500 ± 220 pg/ml, respectively). The greater release of IL-8 was at 6 h (150 ± 13 ng/ml).

The PRP was able to counteract the action of LPS and significantly ($P < 0.05$) decreased the production of PGE-2, IL-1β and IL-8 mainly between the first and the 24[a] h.

Discussion

In the present study, the effect of PRP has been investigated *in vivo* on healthy animals (without endometrial infection) and in an *in vitro* model where bovine endometrial cells were stressed with LPS. After *in vivo* application, our results delineate a trend showing that, *in vivo*, PR expression was detected with a similar average score in all the animals at T0. At T1 in epithelial cells, PR average scores in control and PRP animals remain unchanged. In glandular epithelium and smooth muscle cells, at T1, PR expression increases in PRP animals. These results have to be further explored but may indicate that PRP might be helpful in maintaining and/or increasing the number of progesterone receptors in uterine tissues. In our *in vitro* experiment, bovine endometrial cells were cultured with two different concentrations of PRP (5 % and 10 %) and mRNA levels of different genes were quantified and compared to control cells, cultured with 10 % FBS only. Various research groups have studied the use of PRP as a supplement of cell culture [43–45] demonstrating that PRP increases cell proliferation. PRP confirmed this effect also on endometrial cells, mainly at the concentration of 5 %. This concentration of PRP sustained the shortest population doubling time at P5 while the highest concentration (10 %) inhibited proliferation rate, leading to speculate that this effect may be due to an excess of growth factors. This data was confirmed by growth curve study with 5 % of PRP at different passages. According to this, at P5, 5 % of PRP induced an intensive endometrial cells proliferation. Regarding gene expression, the presence of 5 % of PRP at P5 induced also an up-regulation of the expression of *COX2*, *TP53*, *ER-α*, *ER-β* and *PR*. To test the release of

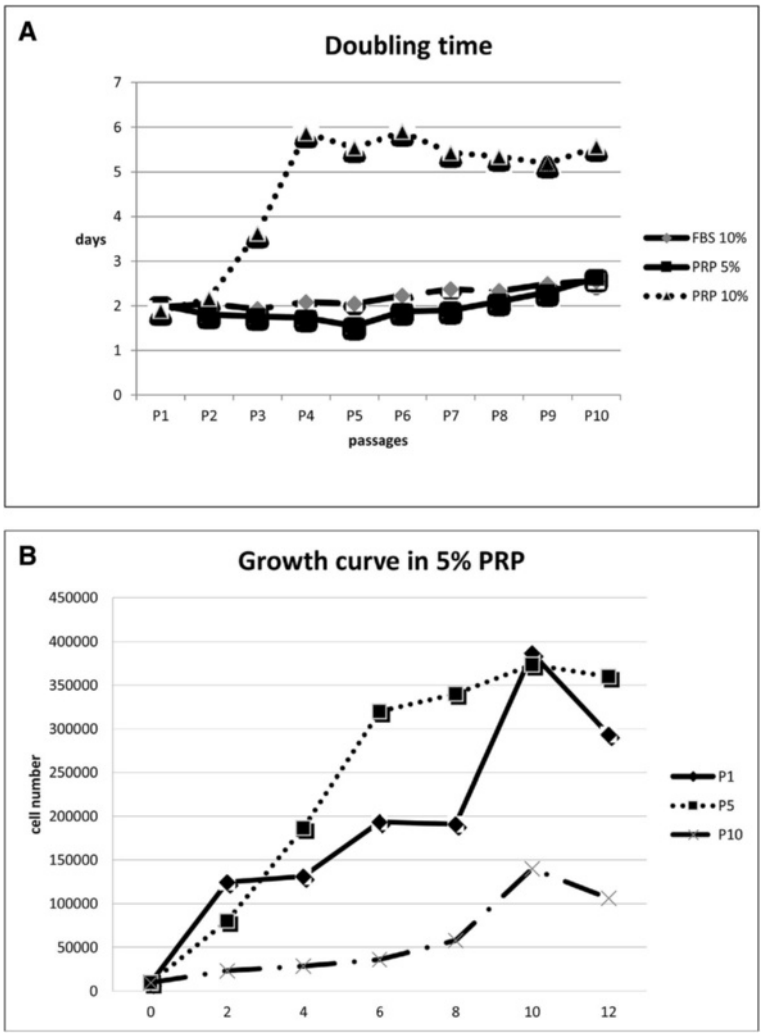

Fig. 3 Proliferation studies. (**a**) Doubling time at different passages during cell culture in different culture conditions (5 % PRP and 10 % FBS). (**b**) Growth curve at P1, P5 and P10 for endometrial cells cultured with 5 % PRP

some proteins, we evaluated the secretion of prostaglandin E2 (PGE2). Indeed, it is known that in the bovine uterus, COX2 converts arachidonic acid to prostaglandin H2, which is then converted, by PGE synthase and PGF synthase, to PGE-2 [46]. In these cells, PGE-2 production was modulated in parallel with *COX2* expression in all conditions. This is the first study reporting the effects of PRP on the proliferation and gene expression of bovine endometrial cells *in vitro* and further studies are required to elucidate the mechanisms through which the PRP up-regulates these genes. Although, the molecular mechanisms involved in this up-regulation are not clear, is conceivable that PRP-derived growth factors play an important role. Indeed, the expression of *c-Myc*, that was up-regulated in this study and which is involved in cell proliferation and growth, is activated by EGF that is a component of PRP [29].

In our study, we even further tested the hypothesis that PRP has anti-inflammatory properties and is able to influence gene expression of pro-inflammatory factors in an *in vitro* model of inflammation. To develop an *in vitro* cell culture system with stressed cells and to study gene response, endometrial cells were exposed to the bacterial endotoxin LPS before and after the treatment with PRP. Exposure of endometrial cells to 10 ng/ml LPS resulted in marked changes in the expression of pro-inflammatory genes that was reduced by the addition of 5 % of PRP. The presence of PRP ameliorated the LPS-induced molecular changes in endometrial cells as they increased the levels of gene expression of *IL-1β*, *IL-8*, *iNOS* and *COX2* expression. In parallel with gene expression, the release of some proteins was studied confirming the observations regarding gene regulations. LPS demonstrates to be capable of

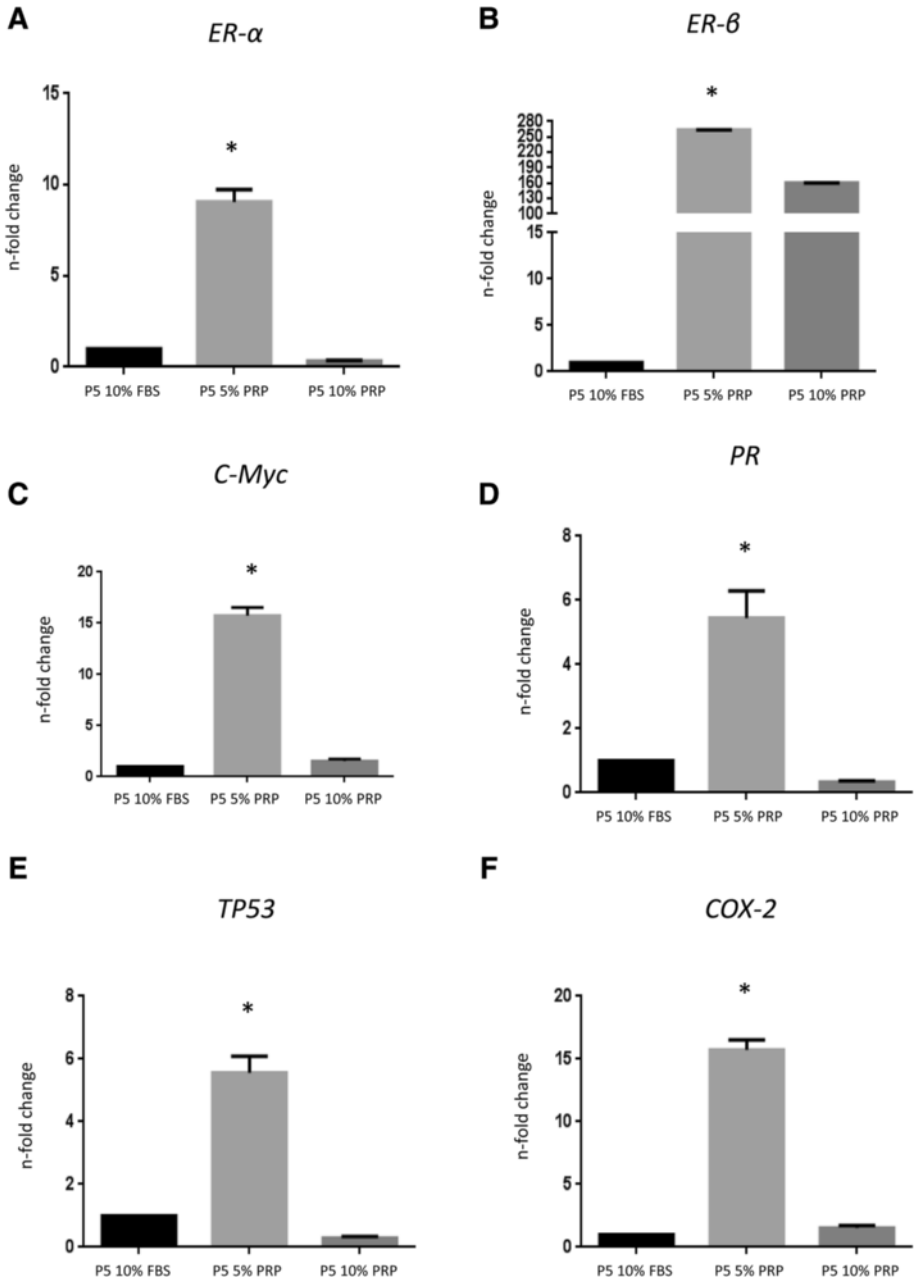

Fig. 4 Quantitative PCR analysis for the expression of genes involved in the regulation of oestrus cycle and fetal-maternal interaction like: (**a**, **b**) oestrogen receptors (*ERa* and *ERβ*), (**c**) *c-Myc*, (**d**) progesterone receptor (*PR*), (**e**) tumor protein p53 (*TP53*), and (**f**) prostaglandin-endoperoxide synthase 2 (*COX2*) in cells cultured in presence of 5 % PRP. Also the expression of is reported. Expression levels normalized to the reference gene. Data are represented as fold-change compared with expression observed in cells cultured in presence of 10 % FBS. Values are mean ± SD ($n = 3$). Asterisk depict highly significant (*, $P < 0.01$) differences compared to cells cultured in presence of 10 % FBS

inducing the release of PGE-2, IL-1β and IL-8 whose pick were obtained 1 h and 12-24 h, after stimulation with LPS. PRP reduce the release of these proteins-and the maximum modulatory activity was observed immediately after 1 h for PGE-2 and IL-1β, and between 12 h and 24 h for IL-8. Therefore, our results indicated consistent anti-inflammatory effect of PRP.

How can we explain these results? Recent literature demonstrates the healing potential of autologous platelet-rich plasma in human medicine, including maxillofacial surgery, dental implant surgery, orthopedic surgery, bone reconstruction, muscle and tendon repair, reversal of skin ulcers, retinal hole repair in eye surgery, and cosmetic surgery [29]. In veterinary medicine, little

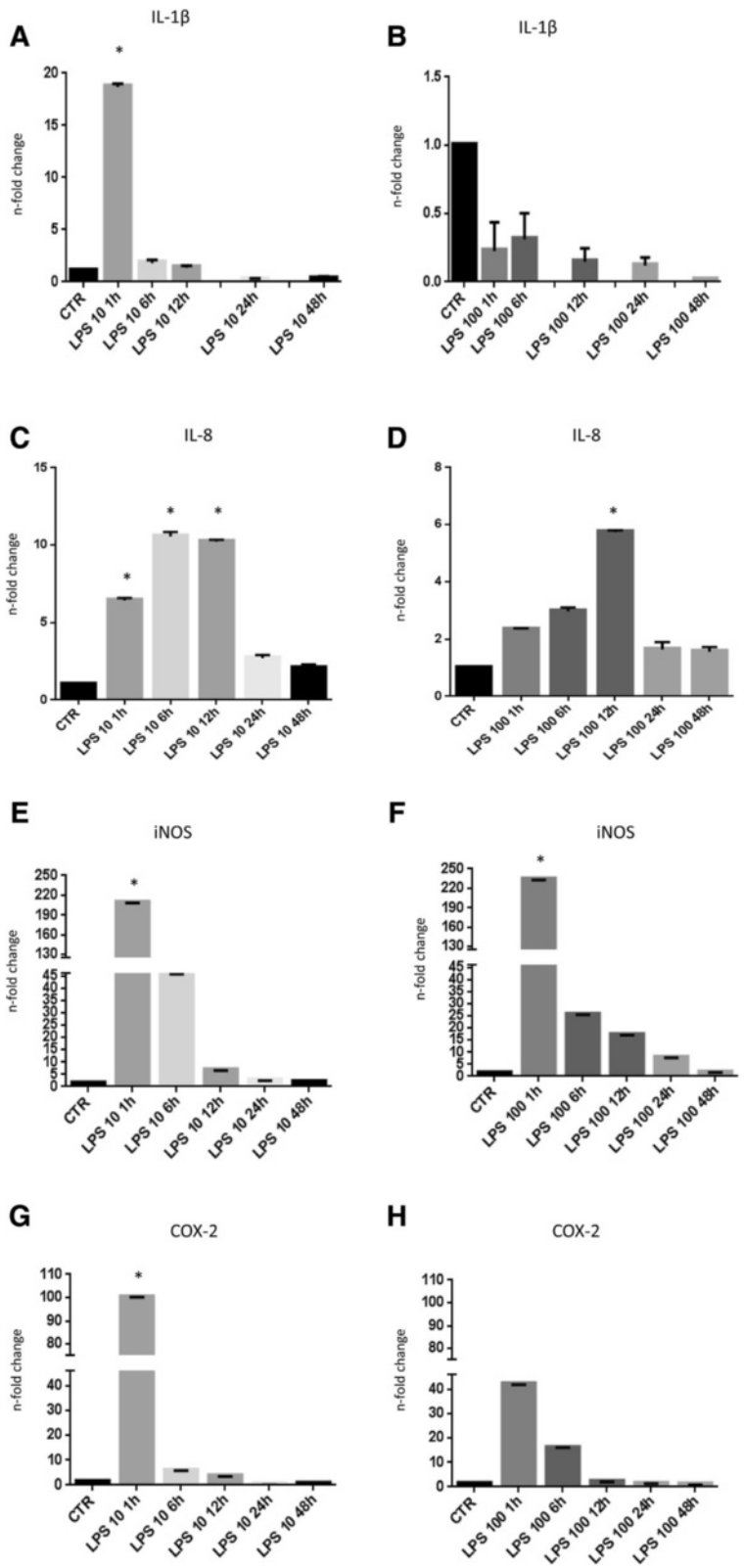

Fig. 5 Quantitative PCR analysis for the expression of pro-inflammatory markers such as *IL-1β*, *IL-8*, *iNOS* and *COX2* in cells cultured in presence of 10 (**a**, **c**, **e**, **g**) or 100 ng/ml LPS (**b**, **d**, **f**, **h**). Expression levels normalized to the reference gene *GAPDH*. Data are represented as fold-change compared with expression observed in untreated cells. Values are mean ± SD ($n = 3$). Asterisk depict highly significant (*, $P < 0.01$) differences compared to untreated cells

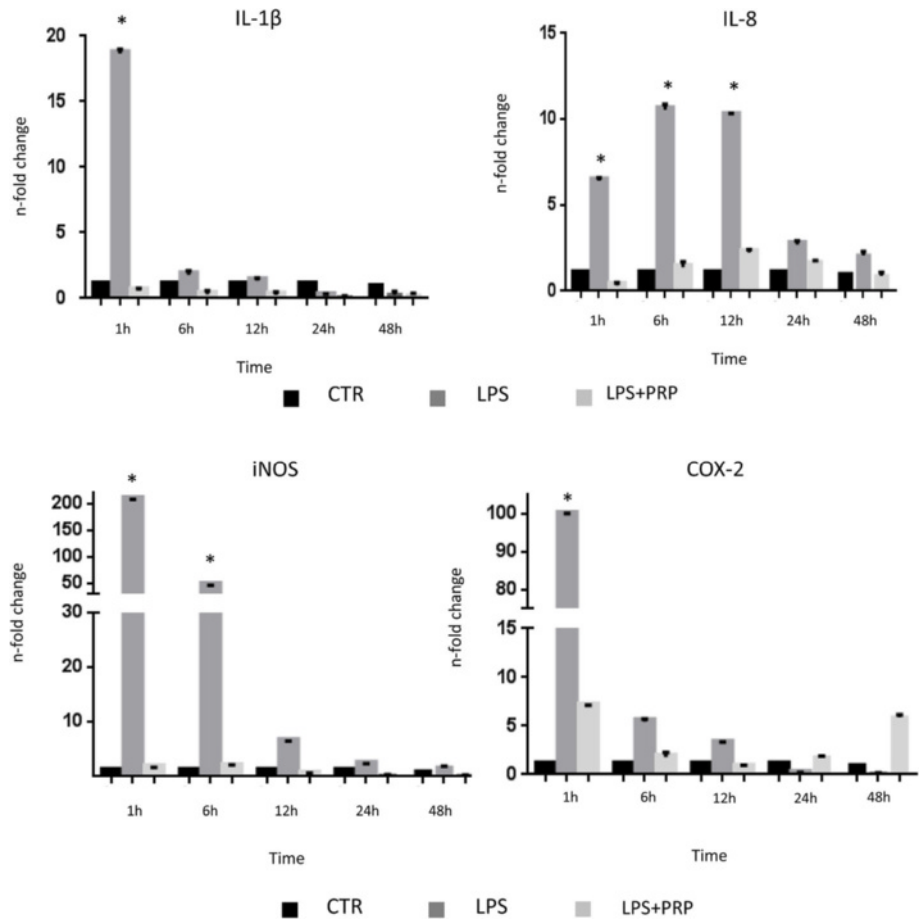

Fig. 6 Quantitative PCR analysis for the expression of pro-inflammatory markers such as *IL-1β*, *IL-8*, *iNOS* and *COX2* in cells cultured in presence of 10 ng/ml of LPS and 5 % PRP. Expression levels normalized to the reference gene *GAPDH*. Data are represented as fold-change compared with expression observed in untreated cells (CTR). Values are mean ± SD ($n = 3$). Asterisk depict highly significant (*, $P < 0.01$) differences compared to untreated cells

clinical information exists about its application. PRP is mainly used for equine tendon repair [47] although its application has also been reported for intestinal wound healing in pigs [48] and for the treatment of a large cutaneous lesion in a dog [49]. Recently, our group has proposed its use as an alternative therapy for bovine mastitis and for repeat breeder cows syndrome, showing promising results [32, 50]. Indeed, in acute mastitis, the treatment with only PRP did not show statistically significant differences compared to antibiotic alone or treatment with PRP combined to antibiotic, but it was better than the use of only antibiotic for chronic mastitis [32]. In repeat breeder treatment, after intrauterine administration of PRP the percentage of pregnant cows was 70 % compared to control group, treated with physiological solution, where the rate was 33.33 %. Moreover, immunohistochemical study, by the nuclear antigen Ki-67, a marker of cell proliferation, showed more proliferating nuclei in the treated uterine horn, after three days of administration, compared to the control one [50]. In tissues with a high proliferative rate, Ki-67 is expressed in all cell cycle phases except for the resting or G0 phases [51, 52] and reaches a maximum level during G2 and M [53]. Since Ki-67 was significantly more expressed in uterine horns treated with PRP, Lange-Consiglio et al. [50] supposed that the growth factors released by platelets in the PRP might have had an effect on endometrial cell proliferation. Indeed, in all treated horns there were statistically more proliferating nuclei compared to the controls. Also in our *in vitro* study, PRP induce cell proliferation confirming these previous results [50], but a longer *in vitro* culture time (P5) is necessary to stimulate a good proliferation rate. It is difficult to explain the different times of PRP efficacy between *in vivo* and *in vitro* study, probably they are mainly due to the different doses used.

After the study with PRP on repeat breeder cows, our group tried to test the effect of PRP on *in vitro* endometrial stressed cells by LPS. Results showed that LPS

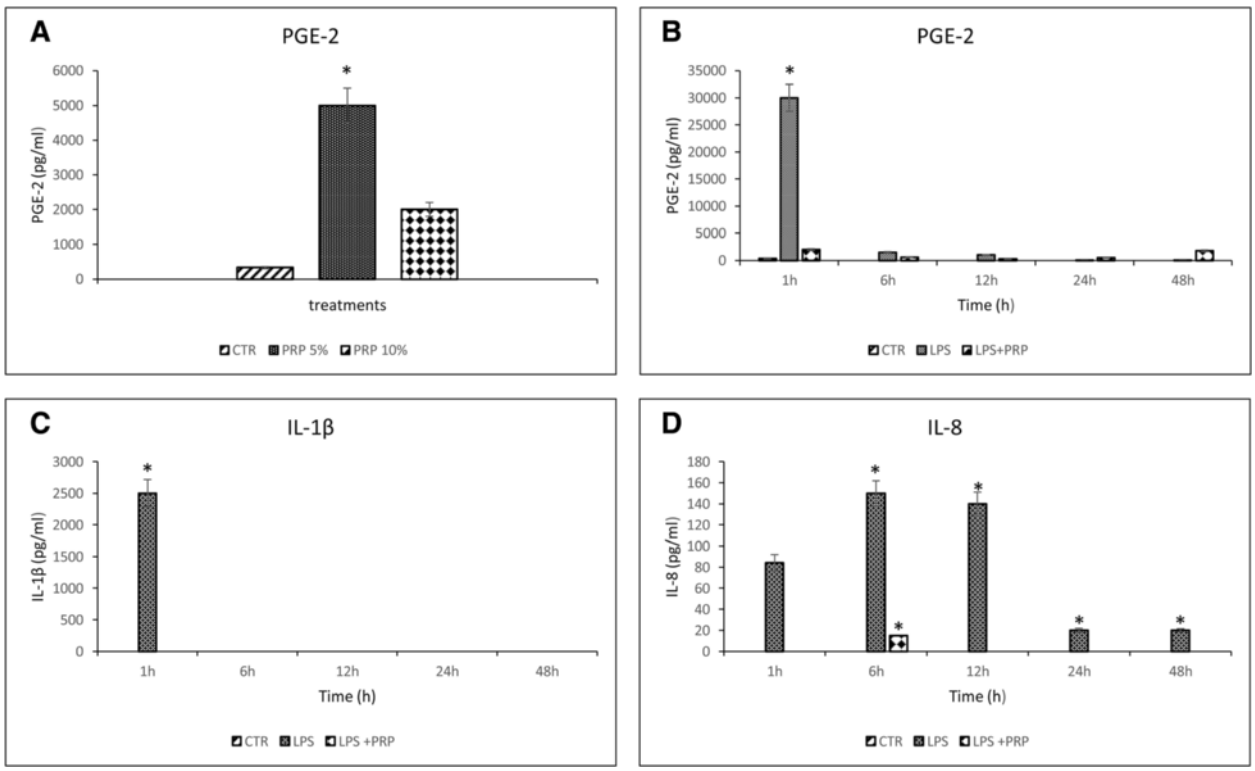

Fig. 7 Effect of 5 % PRP at P5 on release of PGE-2 (**a**) and effect of LPS and PRP on release of PGE-2 (**b**), IL-1β (**c**) and IL-8 (**d**) in endometrial cells. Each value represents the mean ± SD of three samples. Values labeled with asterisk are statistically different ($P < 0.05$) compared to untreated cells (CTR)

provoked a rapid increase in endometrial mRNA expression and release of IL-1β and IL-8. Previous studies have shown that bovine endometrium expresses the TLR-4/CD14/MD-2 receptor complex in both epithelial and stromal cells [17, 18, 54]. This is a key component of the innate immune system, which is necessary to detect LPS. Subsequent activation of TLR4 triggers the production of cytokines, particularly IL-1β and chemokine IL-8 in bovine endometrium. Accordingly, after LPS treatment, we found an immediate rapid rise in *IL-1β* expression, which had already peaked by 1 h, and had been followed by a rise in *IL-8* expression, with a significant up-regulation at 6 h and 12 h. These waves of cytokine gene activation, short for *IL-1β* and prolonged for *IL-8* until 12 h, are supported by data of DeForge and Remick [55] that studied the kinetics of these cytokines in LPS-stimulated human whole blood as an *ex vivo* model of sepsis. LPS also induces an inflammatory response characterized by the increased expression of *iNOS* and *COX2* and stimulates the secretion of PGE, as demonstrated also by Herath et al. [56]. Prostaglandins, produced by the uterine endometrium, have multiple roles in endometrial function [46]. Indeed, they are key regulators of several reproductive events, including estrous cycle, implantation, pregnancy maintenance and parturition. The release of PGE-2 induced by 5 % of PRP could support these events. In addition, PGE has an important role in the mammalian immune response, acting through prostaglandin E receptors 2 and 4 (PTGER2 and PTGER4) to control inflammation [3]. Instead, the intensive LPS-induced PGE secretion by endometrial cells may impair fertility. In fact, this has been suggested as a pathogenic mechanism after uterine bacterial infection, which could result in an extended luteal phase and thus contribute to an impaired reproductive performance. According to this, *COX2* was greatly up-regulated in the present study by LPS. Regarding the inducible iNOS, it is the main isoenzyme governing the production of NO, and it is considered an important mediator of cellular interactions and a potent regulator of many local processes [57]. iNOS is typically expressed at the sites of inflammation, produces large amounts of NO for a prolonged time and is usually related to the activation of pro-inflammatory macrophages [58]. In this context, our findings showed a significantly higher expression of *iNOS* in cells cultured in presence of LPS. This gene returned nearly to baseline within 48 h, supporting the idea that the inflammatory process is controlled by negative feedback regulation in order to eliminate excessive tissue inflammation and damage [59].

The treatment with 5 % of PRP, after LPS action, down-regulated the expression of all pro-inflammatory genes. The inhibition of NF-kB (nuclear factor kappa-light-chain-enhancer of activated B cells) activation could be a possible mechanism through which PRP exerted these anti-inflammatory effects. Within mammalian cells, including endometrial cells, NF-kB is present in an inactive status [60]. It regulates more than 150 genes, including those involved in inflammation and other immune responses [61]. Upon phosphorylation, it translocates into the nucleus [62] by the interaction of specific receptors on the surface of a cell, and it triggers the inflammatory cascade. In particular, LPS is reported to bind the surface antigen CD44 and induce the translocation of the phosphorylated Nf-kB to the nuclei leading to the increase of pro-inflammatory gene levels [63]. Numerous studies demonstrated that PRP inhibited the translocation of NF-kB to the nucleus [31, 64]. Between different growth factors, indeed, the HGF is described to disrupt the transactivacting activity of NF-kB, with its retention in the cytosol [31].

Based on these results, it would be interesting to explore the mechanisms through which the PRP induces up-regulation of *COX2*, *TP53*, *ER-α*, *ER-β* and *PR* genes and to perform *in vivo* investigation on the potential application of PRP in the treatment of bovine endometritis. Indeed, considering the results obtained in our *in vivo* and *in vitro* studies, it might be possible to envisage treatment of endometritis with PRP combined with administration of exogenous P4. This combination, using intravaginal P4 devices, may improve the fertility in bovine with inadequate circulating P4 concentrations. In this way, at the same time, it would be possible to increase circulating P4 concentration and endometrial PR.

Conclusions

Although this study is performed on an *in vitro* model, our data indicates that PRP have strong effects on endometrial cells determining high proliferation rate and up-regulation of genes that play an important role in reproduction. The mechanisms through which the PRP up-regulates these genes is not yet clear, but it is conceivable that its growth factors are involved in these mechanisms. The results of the current investigation demonstrated that PRP is capable of effectively decrease gene expression of pro-inflammatory factors *IL-1β*, *I-L8*, *COX2* and *iNOS* after stimulation by LPS, prospecting its possible use in regenerative therapy in *in vivo* endometritis.

Abbreviations

c-Myc: v-myc avian myelocytomatosis viral oncogene homolog; DT: Doubling time; EGF: Epidermal growth factor; ERβ: Oestrogen receptor β; ERα: oestrogen receptor α; FBS: Fetal bovine serum; HG-DMEM: High glucose-Dulbecco's modified Eagle medium; iNOS: Inducible nitric oxide synthase; IL-1β: Interleukin 1 beta; IL-8: Interleukin 8; LPS: Lipopolysaccharide; P: Passage; PDGFs: Platelet-derived growth factors; PGE2: Prostaglandin E2; PGF2α: Prostaglandin F2α; PR: Progesterone receptor; PPP: Poor platelet plasma; PRP: Platelet-rich plasma; PTGS2 (o COX2): Prostaglandin-endoperoxide synthase 2; RT-PCR: Reverse transcriptase-polymerase chain reaction; TGF-β: Transforming growth factor β; TLRs: Toll-like receptor; TP53: Tumor protein p53 inducible protein3; VEGF: Vascular endothelial growth factor

Acknowledgements

Technical staff of the Large Animal Hospital of Università degli Studi di Milano is acknowledged for skilled assistance.

Funding

Funding for this research was provided by Università degli Studi di Milano and Università Politecnica delle Marche.

Availability of data and materials

"The datasets supporting the conclusions of this article are included within the article."

Authors' contributions

MGM performed the molecular study, collected and interpreted data performing statistical analysis, wrote and reviewed the manuscript and approved the final version. CP and PE performed the *in vitro* study (expansion and proliferation of endometrial cells, *in vitro* effect of PRP). BC and DB took part in collecting and interpreting data and approved the final version. EF and PR performed histological and immunohistochemical examinations. GU and GG performed the *in vivo* study. FC is responsible for the study concept and participated in designing the study, interpreted data, revised and approved the final version of manuscript. ALC is responsible for the study concept and participated in designing the study, organized and coordinated all experiments, prepared PRP, isolated endometrial cells, collected and interpreted data performing statistical analysis, wrote and reviewed the manuscript and approved the final version.

Competing interests

The authors declare that there are no conflicts of interest that could be perceived as prejudicing the impartiality of the reported research.

Consent for publication

Not applicable.

Ethics approval and consent to participate

All procedures were performed according to approved animal care and use protocols of the institutional ethics committee and to good veterinary practice for animal welfare as to European directive 2010/63/UE. Written farmers' consent was obtained at the beginning of the study.

Author details

[1]Department of Life and Environmental Sciences, Università Politecnica delle Marche, Ancona, Italy. [2]Large Animal Hospital, Reproduction Unit, Università degli Studi di Milano, Via dell'Università 6, 26900 Lodi, Italy. [3]Large Animal Hospital, Anatomo-Pathology Unit, Università degli Studi di Milano, Lodi, Italy. [4]Private Practitioner, Milano, Italy.

Received: 16 June 2016 Accepted: 3 September 2016
Published online: 13 September 2016

References

1. Sheldon IM, Lewis GS, LeBlanc S, Gilbert RO. Defining postpartum uterine disease in cattle. Theriogenology. 2006;65:1516–30.
2. Fourichon C, Seegers H, Malher X. Effect of disease on reproduction in the dairy cow: a meta-analysis. Theriogenology. 2000;53:1729–59.
3. Sheldon IM, Cronin J, Goetze L, Donofrio G, Schub HJ. Defining postpartum uterine disease and the mechanisms of infection and immunity in the female reproductive tract in Cattle. Reprod Biol Endocrinol. 2009;81:1025–32.
4. Mari G, Iacono E, Toni F, Predieri PG, Merlo B. Evaluation of the effectiveness of intrauterine treatment with formosulphathiazole of clinical endometritis in postpartum dairy cows. Theriogenology. 2012;78:189–200.
5. Le Blanc SJ, Duffield TF, Leslie KE, Bateman KG, Keefe GP, Walton JS, Johnson WH. Defining and diagnosing postpartum clinical endometritis and its impact on reproductive performance in dairy cows. J Dairy Sci. 2002;85:2223–36.

6. Olson JD, Ball L, Mortimer RG, Farin PW, Adney WS, Huffman EM. Aspects of bacteriology and endocrinology of cows with pyometra and retained fetal membranes. Am J Vet Res. 1984;45:2251–5.
7. Borsberry S, Dobson H. Periparturient diseases and their effect on reproductive performance in five dairy herds. Veterinary Record. 1989;124:217–9.
8. Gilbert RO, Shin ST, Guard CL, Erb HN, Frajblat M. Prevalence of endometritis and its effects on reproductive performance of dairy cows. Theriogenology. 2005;64:1879–88.
9. Le Blanc SJ. Interactions of metabolism, inflammation and reproductive tract in postpartum period in dairy cattle. Reprod Domest Anim. 2012;47 Suppl 5: 18–30.
10. Esposito G, Irons PC, Webb EC, Chapwanya A. Interactions between negative energy balance, metabolic diseases, uterine health and immune response in transition dairy cows. Anim Reprod Sci. 2014;144:60–71.
11. Mordaknd R, Stewart PA. Periparturient stress and immune suppression as a potential cause of retained placenta in highly productive dairy cows: examples of prevention. Acta Vet Scand. 2015;57:84.
12. Wira CR, Grant-Tschudy KS, Crane-Godreau MA. Epithelial cells in the female reproductive tract: a central role as sentinels of immune protection. Am J Reprod Immunol. 2005;53:65–76.
13. Gilbert R, Santos N, Galvão K, Brittin S, Roman H. The relationship between postpartum uterine bacterial infection (BI) and subclinical endometritis (SE). Journal Dairy Science. 2007;90 Suppl 1:469.
14. Woodward EM, Christoffersen M, Horohov D, Squires EL, Troedsson MH. The effect of treatment with immune modulators on endometrial cytokine expression in mares susceptible to persistent breeding-induced endometritis. Equine Vet J. 2015;47:235–9.
15. Chapwanya A, Meade KG, Doherty ML, Callanan JJ, Mee JF, O'Farrelly C. Histopathological and molecular evaluation of Holstein-Friesian cows postpartum: toward an improved understanding of uterine innate immunity. Theriogenology. 2009;71:1396–407.
16. Sheldon IM, Cronin J, Borges A. The postpartum period and modern dairy cow fertility: Part 1: Uterine function. Livest Sci. 2011;16:14–8.
17. Davies D, Meade KG, Herath S, Eckersall PD, Gonzalez D, White JO, Conlan RS, O'Farrelly C, Sheldon IM. Toll-like receptor and antimicrobial peptide expression in the bovine endometrium. Reprod Biol Endocrinol. 2008;6:53.
18. Akira S, Takeda K. Toll-like receptor signalling. Nat Rev Immunol. 2004;4:499–511.
19. Shams-Esfandabadi N, Shirazi A, Ghasemzadeh-nava H. Pregnancy rate following post-insemination intrauterine treatment of endometritis in dairy Cattle. Journal of Veterinary Medicine Series A. 2004;5:155–6.
20. Le Blanc SJ, Duffield TF, Leslie KE, Bateman KG, Keefe GP, Walton JS, Johnson WH. The effect of treatment of clinical endometritis on reproductive performance in dairy cows. J Dairy Sci. 2002;85:2237–49.
21. Drillich M, Raab D, Wittke M, Heuwieser W. Treatment of chronic endometritis in dairy cows with an intrauterine application of enzymes. A field trial. Theriogenology. 2005;63:1811–23.
22. Runciman DJ, Anderson GA, Malmo J. Comparison of two methods of detecting purulent vaginal discharge in postpartum dairy cows and effect of intrauterine cephapirin on reproductive performance. Aust Vet J. 2009;87: 369–78.
23. Heuwieser W, Tenhagen BA, Tischer M, Luhr J, Blum H. Effect of three programmes for the treatment of endometritis on the reproductive performance of a dairy herd. Veterinary Record. 2000;146:338–41.
24. Drillich M, Wittke M, Tenhagen BA, Unsicker C, Heuwieser W. Behandlung chronischer Endometritiden bei Milchkühen mit Cephapirin, Tiaprost oder einer Kombination aus beiden Wirkstoffen. Tierarztl Prax. 2005;33:404–10.
25. Knutti B, Kupfer U, Busato A. Reproductive efficiency of cows with endometritis after treatment with intrauterine infusions or prostaglandin injections, or no treatment. Journal of Veterinary Medicine Series A. 2000;47:609–15.
26. Pepper RT, Dobson H. Preliminary results of treatment and endocrinology of chronic endometritis in the dairy cow. Veterinary Record. 1987;120:53–6.
27. Sheldon IM, Noakes DE. Comparison of three treatments for bovine endometritis. Veterinary Record. 1998;142:575–9.
28. Janowski T, Zdunczyk S, Mwaanga ES. Combined GnRH and PGF2alpha application in cows with endometritis puerperalis treated with antibiotics. Reprod Domest Anim. 2001;36:244–6.
29. Anitua E, Andia I, Ardanza B, Nurden P, Nurden AT. Autologous platelets as a source of proteins for healing and tissue regeneration. Thromb Haemost. 2004;91:4–15.
30. Gentile P, Orlandi A, Scioli MG, Di Pasquali C, Bocchini I, Cervelli V. Concise review: adipose-derived stromal vascular fraction cells and platelet-rich plasma: basic and clinical implications for tissue engineering therapies in regenerative surgery. Stem Cells Transl Med. 2012;1:230–6.
31. Bendinelli P, Matteucci E, Dogliotti G, Corsi MM, Banfi G, Maroni P, Desiderio MA. Molecular basis of anti-inflammatory action of platelet-rich plasma on human chondrocytes: mechanisms of NF-kB inhibition via HGF. J Cell Physiol. 2010;225:757–66.
32. Lonergan P, O'Hara L, Forde N. Role of diestrus progesterone on endometrial function and conceptus development in cattle. Animal Reproduction. 2013;10:223–7.
33. Diskin MG, Morris DG. Embryonic and early foetal losses in cattle and other ruminants. Reprod Domest Anim. 2008; 43(suppl. 2):260–267
34. Lange-Consiglio A, Spelta C, Garlappi R, Luini M, Cremonesi F. Intramammary administration of platelet concentrate as an unconventional therapy in bovine mastitis: first clinical application. J Dairy Sci. 2014;97:6223–30.
35. Zimmermann R, Arnold D, Strasser E, Ringwald J, Schlegel A, Wiltfang J, Eckstein R. Sample preparation technique and white cell content influence the detectable levels of growth factors in platelet concentrates. Vox Sang. 2003;85:283–9.
36. Katagiri S, Takahashi Y. Changes in EGF concentrations during estrous cycle in bovine endometrium and their alterations in repeat breeder cows. Theriogenology. 2004;62:103–12.
37. Saruhan BG, Sağsoz H, Akbalik ME, Ketani MA. Distribution of estrogen receptor α and progesterone receptor B in the bovine oviduct during the follicular and luteal phases of the sexual cycle: an immunohistochemical and semi-quantitative study. Biotech Histochem. 2011;86:315–25.
38. Donofrio G, Franceschi V, Capocefalo A, Cavirani S, Sheldon IM. Bovine endometrial stromal cells display osteogenic properties. Reprod Biol Endocrinol. 2008;6:65.
39. Herath S, Williams EJ, Lilly ST, Gilbert RO, Dobson H, Bryant CE, Sheldon IM. Ovarian follicular cells have innate immune capabilities that modulate their endocrine function. Reproduction. 2007;134:683–93.
40. Walker CG, Meier S, Mitchell MD, Roche JR, Littlejohn M. Evaluation of real-time PCR endogenous control genes for analysis of gene expression in bovine endometrium. BMC Mol Biol. 2009;10:100.
41. Kenneth JL, Thomas DS. Analysis of relative gene expression data using real-time quantitative PCR and the $2-\Delta\Delta CT$ Method. Methods. 2001;25:402–8.
42. Rinaldi M, Ceciliani F, Lecchi C, Moroni P, Bannerman DD. Differential effects of alpha1-acid glycoprotein on bovine neutrophil respiratory burst activity and IL-8 production. Vet Immunol Immunopathol. 2008;126:199–210.
43. Akeda K, An HS, Okuma M, Attawia M, Miyamoto K. Platelet-rich plasma stimulates porcine articular chondrocyte proliferation and matrix biosynthesis. Osteoarthritis Cartilage. 2006;14:1272–80.
44. Duan J, Kuang W, Tan J, Li H, Zhang Y, Hirotaka K, Tadashi K. Differential effects of platelet rich plasma and washed platelets on the proliferation of mouse MSC cells. Mol Biol Rep. 2011;38:2485–90.
45. García-Martínez O, Reyes-Botella C, Díaz-Rodríguez L, De Luna-Bertos E, Ramos-Torrecilla J, Vallecillo-Capilla MF. Effect of platelet-rich plasma on growth and antigenic profile of human osteoblasts and its clinical impact. J Oral Maxillofac Surg. 2012;70:1558–64.
46. Parent J, Fortier MA. Expression and contribution of three different isoforms of prostaglandin E synthase in the bovine endometrium. Biol Reprod. 2005;73:36–44.
47. Georg R, Maria C, Gisela A, Bianca C. Autologous conditioned plasma as therapy of tendon and ligament lesions in seven horses. J Vet Sci. 2010;11: 173–5.
48. Fresno L, Fondevila D, Bambo O, Chacaltana A, García F, Andaluz A. Effects of platelet-rich plasma on intestinal wound healing in pigs. Vet J. 2010;185: 322–7.
49. Kim JH, Park C, Park HM. Curative effect of autologous platelet-rich plasma on a large cutaneous lesion in a dog. Vet Dermatol. 2009;20:123–6.
50. Lange-Consiglio A, Cazzaniga N, Garlappi R, Spelta C, Pollera C, Perrini C, Cremonesi F. Platelet concentrate in bovine reproduction: effects on in vitro embryo production and after intrauterine administration in repeat breeder cows. Reprod Biol Endocrinol. 2015;13:65.
51. Brown DC, Gatter KC. Monoclonal antibody Ki-67: its use in histopathology. Histopathology. 1990;17:489–503.
52. McCormick D, Chong H, Hobbs C, Datta C, Hall PA. Detection of the Ki-67 in fixed and wax embedded sections with the monoclonal antibody MIB1. Histopathology. 1993;22:355–60.
53. Sasaki K, Murakami T, Kavasaki M, Takahasashi M. The cell cycle associated change of the Ki-67 reactive nuclear antigen expression. J Cell Physiol. 1987; 133:579–84.

54. Herath S, Lilly ST, Santos NR, Gilbert RO, Goetze L, Bryant CE, White JO, Cronin J, Sheldon IM. Expression of genes associated with immunity in the endometrium of cattle with disparate postpartum uterine disease and fertility. Reprod Biol Endocrinol. 2009;7:55.
55. DeForge LE, Remick DG. Kinetics of TNF, IL-6, and IL-8 gene expression in LPS-stimulated human whole blood. Biochem Biophys Res Commun. 1991; 15:18–24.
56. Herath S, Fischer DP, Werling D, Williams EJ, Lilly ST, Dobson H, Bryant CE, Sheldon IM. Expression and function of Toll-like receptor 4 in the endometrial cells of the uterus. Endocrinology. 2006;147:562–70.
57. Förstermann U, Sessa WC. Nitric oxide synthases: regulation and function. Eur Heart J. 2012;33:829–37.
58. Barański W, Kaleczyc J, Zduńczyk S, Podlasz W, Długołęcka-Malinowska E, Janowski T. Distribution of CD14+ macrophages, CD4+, CD8+ lymphocytes and mRNA expression of inducible nitric oxide synthase in the endometrium of repeat breeding cows. Pol J Vet Sci. 2013;16:443–51.
59. Swangchan-Uthai T, Lavender CRM, Cheng Z, Fouladi-Nashta AA, Wathes DC. Time course of defense mechanisms in bovine endometrium in response to lipopolysaccharide. Biol Reprod. 2012;87:1–13.
60. Cronin JG, Turner ML, Goetze L, Bryant CE, Sheldon IM. Toll-like receptor 4 and MYD88-dependent signaling mechanisms of the innate immune system are essential for the response to lipopolysaccharide by epithelial and stromal cells of the bovine endometrium. Biology Reproduction. 2012;86:1–9.
61. Pahl HL. Activators and target genes of Rel/NF-kappaB transcription factors. Oncogene. 1999;18:6853–66.
62. Roman-Blas JA, Jimenez SA. NF-kappaB as a potential therapeutic target in osteoarthritis and rheumatoid arthritis. Osteoarthritis Cartilage. 2006;14:839–48.
63. Taraballi F, Corradetti B, Minardi S, Powel S, Cabrera F, Van Eps JL, Weiner BK, Tasciotti E. Biomimetic collagenous scaffold to tune inflammation by targeting macrophages. J Tissue Eng. 2016;7:1–13.
64. Andia I, Maffulli N. Platelet-rich plasma for managing pain and inflammation in osteoarthritis. Nat Rev Rheumatol. 2013;9:721–30.

Theriogenology xxx (2016) 1–10

Contents lists available at ScienceDirect

Theriogenology

journal homepage: www.theriojournal.com

Isolation, molecular characterization, and *in vitro* differentiation of bovine Wharton jelly–derived multipotent mesenchymal cells

Anna Lange-Consiglio [a], Claudia Perrini [a], Alessia Bertero [b], Paola Esposti [a], Fausto Cremonesi [a,*], Leila Vincenti [b]

[a] Reproduction Unit, Large Animal Hospital, Università degli Studi di Milano, Lodi, Italy
[b] Department of Animal Science, Università degli Studi di Torino, Torino, Italy

ARTICLE INFO

Article history:
Received 12 July 2016
Received in revised form 21 September 2016
Accepted 23 September 2016

Keywords:
Bovine
Wharton jelly
Stromal cell
Characterization

ABSTRACT

Extrafetal tissues are a noncontroversial and inexhaustible source of mesenchymal stem cells that can be harvested noninvasively at low cost. In the veterinary field, as in man, stem cells derived from extrafetal tissues express plasticity, reduced immunogenicity, and have high anti-inflammatory potential making them promising candidates for treatment of many diseases. Umbilical cord mesenchymal cells have been isolated and characterized in different species and have recently been investigated as potential candidates in regenerative medicine. In this study, cells derived from bovine Wharton jelly (WJ) were isolated for the first time by enzymatic methods, frozen/thawed, cultivated for at least 10 passages, and characterized. Wharton jelly–derived cells readily attached to plastic culture dishes displaying typical fibroblast-like morphology and, although their proliferative capacity decreased to the seventh passage, these cells showed a mean doubling time of 34.55 ± 6.33 hours and a mean frequency of one colony-forming unit fibroblast like for every 221.68 plated cells. The results of molecular biology studies and flow cytometry analyses revealed that WJ-derived cells showed the typical antigen profile of mesenchymal stem cells and were positive for CD29, CD44, CD105, CD166, Oct-4, and c-Myc. They were negative for CD34 and CD14. Remarkably, WJ-derived cells showed differentiation ability. After culture in induced media, WJ-derived cells were able to differentiate into osteogenic, adipogenic, chondrogenic, and neurogenic lines as shown by positive staining and expression of specific markers. On polymerase chain reaction analysis, these cells were negative for *MHC-II* and positive for *MHC-I*, thus reinforcing the role of extrafetal tissue as an allogenic source for bovine cell–based therapies. These results provide evidence that bovine WJ-derived cells may have the potential to differentiate to repair damaged tissues and reinforce the importance of extrafetal tissues as stem cell sources in veterinary regenerative medicine. A more detailed evaluation of their immunologic properties is necessary to better understand their potential role in cellular therapy.

1. Introduction

Increasing interest in veterinary stem cell therapy has led to research into new stem cell sources that can supply sufficient numbers of cells while minimizing risks to donors and recipients [1]. Extrafetal stem cells are being investigated for this purpose in large animals [2]. Extrafetal stem cells have been isolated from umbilical cord blood, amniotic fluid, amniotic membrane, umbilical cord matrix, yolk sac, and placenta [3–9]. It has been shown that they possess properties of mesenchymal stem cells (MSCs), and their application in regenerative medicine has increased

* Corresponding author. Tel.: +39 0250331150; fax: +39 0250331115.
E-mail address: fausto.cremonesi@unimi.it (F. Cremonesi).

0093-691X/$ – see front matter © 2016 Elsevier Inc. All rights reserved.
http://dx.doi.org/10.1016/j.theriogenology.2016.09.042

over the past few years [10]. These studies show that umbilical cord, previously considered as a biomedical waste, is a source of stem cells with promising therapeutic applications in man and in livestock species.

The umbilical cord provides an inexhaustible source of stem cells and presents few, if any, ethical concerns. Indeed, umbilical cord can be collected after parturition because it is considered a waste tissue. In addition, the process of obtaining the cord tissue is relatively simple and noninvasive. Mesenchymal stem cells have been isolated from different compartments of the umbilical cord in different species. In particular, they were obtained invasively, by a surgical intrauterine approach, from umbilical cord blood of sheep [11,12]; noninvasively at the time of birth in the horse [13]; in cattle, after caesarean section delivery [14]; and from canine and feline fetuses at birth [15,16]. In 2006, for the first time in veterinary medicine, MSCs from cordon matrix, called Wharton jelly (WJ), were obtained from porcine umbilical cord [17]. Wharton jelly is the embryonic mucous connective tissue lying between the amniotic epithelium and the umbilical vessels [18]. It encloses the yolk sac, which is the source of primordial germ cells and the first hematopoietic stem cells [18]. Extraembryonic tissues, which originate from the hypoblast and the trophectoderm, do not participate in gastrulation; therefore, they are less differentiated than adult somatic tissues such as bone marrow or adipose tissue [2]. Wharton jelly is a rich source of MSCs [19–21]. Recently, primitive MSCs were isolated from the umbilical cord matrix in caprine [22,23], canine [24], and equine species [4,13,25]. These cells show specific markers of pluripotency and MSCs markers and are able to differentiate into adipogenic, chondrogenic, osteogenic, and neurogenic tissues [2]. The similarities in growth kinetics and expression of markers of pluripotency indicate their close resemblance to embryonic stem cells [26]. These markers, found in mouse and human embryonic stem cells, include the POU (Pit/Oct/Unc) domain-containing protein Oct-4, Sox-2, and Nanog. Some authors have shown that human umbilical cord matrix expresses low levels of transcription factors that play a central role in the regulation of pluripotency and self-renewal [18]. In contrast, however, Carlin et al. [17] showed that cells derived from porcine umbilical cord matrix express markers of embryonic lineage Oct-3/4, Sox-2, and Nanog. Contrary to observations in adult MSCs, WJ MSCs share properties unique to fetal-derived MSCs, such as more rapid proliferation and greater *ex vivo* expansion capabilities [18,27]. Moreover, they have high potential to be differentiated *in vitro* [28], they express human leukocyte antigen-class I surface markers but do not express human leukocyte antigen-class II markers [29], and they are immunosuppressive in mixed lymphocyte assays by inhibition of T-cell proliferation [30,31]. For these reasons, these cells have raised interest for their potential uses in cell and gene therapy, cloning, virological, and biotechnological studies [32].

Despite the importance of bovine species as models for *in vivo* studies, little is known about bovine MSCs. So far, they have been derived from umbilical cord blood [14], bone marrow [33,34], and amniotic membrane or amniotic fluid [8]. To date, only one article on isolation and characterization of MSCs from bovine umbilical cord matrix [32] has been published, but these cells were isolated by migration techniques and not by classical enzymatic digestion. The mechanical and enzymatic disaggregation of the tissue avoids problems of selection by migration, but perhaps more importantly, yields a higher number of cells more representative of the whole tissue in a shorter time. However, as well as the primary explant technique selecting on the basis of cell migration, the dissociation technique selects cells resistant to disaggregation but still capable of attachment [35].

The isolation of bovine MSCs from fetal adnexa is an interesting prospect because of the potential for these cells to be used for biotechnological applications. For the first time, we isolated, by enzymatic methods, presumptive MSCs from bovine WJ and were able to characterize them in terms of morphology, specific mesenchymal or pluripotent markers, proliferative and differentiation potential.

2. Materials and methods

2.1. Materials

Chemicals were obtained from Sigma Chemical (Milan, Italy) and tissue culture plastic dishes from Euroclone (Milan, Italy) unless otherwise specified.

2.2. Tissue collection

This study was approved by the Ethical Committee of the University of Milan, and written owner consent was given. All procedures were conducted following standard veterinary practice and in accordance with 2010/63 EU directive on animal protection and Italian Law (D.L. No. 116/1992).

Fresh bovine umbilical cords were obtained after full-term births.

Bovine umbilical cords ($n = 3$) were obtained from three cows after normal-term pregnancies with spontaneous parturition in accordance with veterinary practice standard. Before the cows stood up breaking the cord, a surgical tape was placed at the calf junction, and a second tie was tightened at approximately 30 or 40 cm from the first. The tie-limited cord portion was cut away with scissors. The harvested segment of the cord was washed twice in sterile saline solution and kept at 4 °C in saline solution supplemented with 4 μg/mL amphotericin, 100 UI/mL penicillin, and 100 μg/mL streptomycin and processed within 12 hours of collection.

2.3. Isolation and culture of WJ-derived cells

At the laboratory, the loose amnion was removed from the exterior of the cords, and the cords were incised longitudinally to expose and remove umbilical vessels (arteries and veins). The remaining WJ-containing tissue was minced into small pieces using scissors. The tissue was digested in high glucose-Dulbecco's Modified Eagle medium (HG-DMEM) supplemented with 1 mg/mL collagenase type I at 38.5 °C for 8 hours. After incubation, collagenase was inactivated by diluting 1:1 with HG-DMEM supplemented with 10% fetal calf serum (FCS). The digested suspension was filtered on an 80-μm strainer, centrifuged

at ×300*g* for 10 minutes, and washed twice in PBS. Before seeding, cells were counted using a Burker chamber with the trypan blue dye exclusion assay. WJ cell cultures were established in HG-DMEM standard medium composed of 10% FCS, penicillin (100 UI/mL)–streptomycin (100 μg/mL), 0.25 μg/mL amphotericin B, 2 mM L-glutamine, and 10 ng/mL EGF. Cultures were established at a density of 1×10^5 cells/cm^2 in T75 culture flasks. The flasks were incubated at 38.5 °C with 5% CO_2 and 90% humidity. The medium was replaced after 72 hours to remove non-adherent cells and then replaced twice weekly until cells reached approximately 80% confluence. Cells were then detached with 0.05% trypsin-EDTA, counted, and redistributed into new culture flasks at a density of 1×10^4 cells/cm^2 to maintain and expand the culture for 10 passages (P).

2.4. Cryopreservation and thawing

Cells at P3 were cryopreserved. Briefly, the confluent cultures were treated with 0.05% trypsin-EDTA and washed by centrifugation (×200*g* at 4 °C, for 5 minutes) with cell culture medium supplemented with 10% FCS to neutralize trypsin-EDTA. The cell pellet obtained was resuspended in precooled (4 °C) cryopreservation media in 1-mL cryovials. The cryopreservation medium was 90% (v:v) FCS and 10% DMSO. The cryovials were maintained at −80 °C overnight and then plunged into liquid nitrogen (−196 °C). After a minimum of 1 month of cryopreservation, the cells were thawed in a water bath at 37 °C. The cells were diluted in culture medium and centrifuged twice at ×200*g* for 10 minutes. The cell pellet was resuspended in culture medium and plated in T25 culture flasks. Aliquots of these cells were kept to evaluate the cell viability using Burker hemocytometer chamber and the trypan blue dye exclusion method, under phase-contrast microscopy (Nikon Eclipse Ti, Tokyo, Japan). After thawing, other aliquots were used for population doubling studies or expanded until P3 to evaluate specific MSC marker expression and multipotent differentiation capacity in comparison to freshly isolated cells.

2.5. Proliferation rate and colony-forming unit assay

Proliferation of MSCs was determined as previously reported [6]. Doubling time (DT) from P 1 to 10 was assessed by plating 9×10^3 cells into six-well tissue culture plates. Every 4 days, cells were trypsinized, counted, and reseeded at the same density. Mean DT was calculated from Days 0 to 4. The DT value was obtained for each P according to the formula $DT = CT/CD$, where CT represents the culture time and $CD = \log(N_c/N_o)/\log 2$ represents the number of cell generations (N_c represents the number of cells at confluence, N_o represents the number of seeded cells). Data representative of three independent experiments are reported.

To obtain the cell proliferation growth curve, cells at P0, P3, and P5 were seeded into six-well tissue culture dishes at a density of 1×10^3 cells/cm^2. Every 2 days, until 14 days of culture, one of the six wells was trypsinized, and cells were counted using the trypan blue dye exclusion method with a Burker chamber.

Colony-forming unit (CFU) assays were performed at P0 on freshly isolated cells at different densities (100, 250, 500, and 1000 cells/cm^2). Cells were plated in six-well plates for 2 weeks in HG-DMEM standard medium. Then, colonies were fixed for 1 hour with 4% formalin and stained with 1% methylene blue for 15 minutes in 10 mM borate buffer at room temperature. Colonies formed by 16 to 20 nucleated cells were counted under a BX71 microscope (Olympus Italia, Srl, Milano, Italy).

2.6. Osteogenic, adipogenic, chondrogenic, and neurogenic cell differentiation

All the differentiation tests were performed when cells reached P3.

For osteogenic differentiation, cells were placed in plastic six-well plates at a density of 28×10^3 cells/well. After the cells had adhered to the plastic, the inducer medium was added to the plate for 21 days and refreshed every 3 days. The medium was composed of HG-DMEM, 10% FCS, penicillin (100 UI/mL)–streptomycin (100 μg/mL), 0.25 μg/mL amphotericin B, 200 mM L-glutamine, 0.25 mM ascorbic acid, 10 mM β-glycerophosphate, and 0.1 μM dexamethasone [36]. Osteogenic differentiation was confirmed by positive staining of the extracellular calcium matrix using Von Kossa staining.

For adipogenic differentiation, cells were placed in plastic six-well plates at a density of 28×10^3 cells/well. After the cells had adhered to the plastic, the inducer medium and the maintaining medium were added alternately, every 3 days for a total of 21 days. The inducer medium was composed of HG-DMEM, 10% FCS, penicillin (100 UI/mL)–streptomycin (100 μg/mL), 0.25 μg/mL amphotericin B, 200 mM L-glutamine, 0.1% insulin, 0.1 μM dexamethasone, and 1% indomethacin. The maintaining medium was composed of HG-DMEM, 10% FCS, penicillin (100 UI/mL)–streptomycin (100 μg/mL), 0.25 μg/mL amphotericin B, and 0.1% insulin [36]. Adipogenic differentiation was confirmed by positive staining of the lipid structures using Oil Red O staining.

For chondrogenic differentiation, cells were cultured in DMEM low glucose, containing 100 U/mL penicillin, 100 μg/mL streptomycin, 0.25 μg/mL amphotericin B, 2 mM/L L-glutamine, 100 nM dexamethasone, 50 μg/mL L-ascorbic acid 2-phosphate, 1 mM sodium pyruvate (BDH, Atlanta, USA), 40 μg/mL proline, ITS (insulin 5 μg/mL, transferrin 5 μg/mL, selenous acid 5 ng/mL), and 5 ng/mL transforming growth factor-β3 (Peprovet, DBA Italia, 100-36E). Chondrogenic differentiation was assessed after incubating cells for up to 3 weeks [37]. Differentiation was evaluated by Alcian blue staining.

For neurogenic differentiation, cells were placed in plastic six-well plates at a density of 28×10^3 cells/well. After the cells had adhered to the plastic, the preinducer medium was administrated to the plates for 1 day, followed by administration of inducer medium for 7 days. The preinducer medium was composed of HG-DMEM, 20% FCS, penicillin (100 UI/mL)–streptomycin (100 μg/mL), 0.25 μg/mL amphotericin B, and 0.0007% β-mercaptoethanol [15,38]. The inducer medium was composed of HG-DMEM, 2% FCS, penicillin (100 UI/mL)–streptomycin (100 μg/mL),

Table 1
Oligonucleotide sequences used for reverse transcription polymerase chain reaction analysis.

Markers	Forward (5′→3′)	Reverse (5′→3′)	Annealing *T*	Product length
Integrin β-1 (*CD29*)	GTTGGTTCTGCAGTTACGATCAG	AACCAAACCCAATTCGGAAGTC	52 °C	203
CD44 antigen (*CD44*)	AACAGTAGGAGAAGGTGTGG	TCATGAACTGGTCTTGGGTC	61 °C	166
Endoglin (*CD105*)	ACAAGTCTTGCAGAAACAGTC	GATGTCTGGAGAGTCAGCTC	61 °C	182
ALCAM (*CD166*)	GTATTTATTGCCTTCAGGTCCT	TCTACCAGGGAGCATTTATAGTC	59 °C	755
Octamer-binding transcription factor 4 (*Oct-4*)	CACACTAGGATATACCCAGGC	GGAGATATGCAAGGCAGAGA	60 °C	177
v-myc avian myelocytomatosis viral oncogene homolog *(c-Myc*)	GCGCCGCATTCGCGAAACTT	TGAGGGGCATCGCTGCAAGC	58 °C	214
CD34 molecule (*CD34*)	CCTGAAGCTAAATGAGACCT	AACTTTCTGTCCTGTTGGTC	58 °C	173
CD14 molecule (*CD14*)	TCCGAAGCCTGACTGGTCTA	TGTCGGCTCCCTTGAGAAAC	56 °C	104
Major histocompatibility complex I (*MHC-I*)	GATCTCACTGACCTGGCA	CTGAGGAGGTTCCCATCTC	60 °C	199
Major histocompatibility complex II (*MHC-II*)	CCTCGCTTGCCTGAATTTGC	ACAGGTGCCGACTGATGC	53 °C	299
Bone gamma-carboxyglutamate (Gla) protein (*BGLAP*)	TCGGGCAAAGGCGCAGCCTTC	GCAGGGCTGCAAGCTCTAGACG	55 °C	231
Secreted phosphoprotein 1 (*SPP1*)	CGCCGATCTAACGTTCAGAGTC	GACTCTCAATCAGATTGGAATGC	55 °C	199
Secreted protein acidic and rich in cysteine (*SPARC*)	CTGGTCACGCTGTACGAGAG	CGGTGTGAGACAGGTACCCGT	55 °C	232
Leptin (*LEP*)	CAATGACATCTCACACACGCAG	CGGCCAGCAGGTGGAGAAG	55 °C	212
Peroxisome proliferator-activated receptor (*PPAR-γ*)	CGCACTGGAATTAGATGACAGC	CACAATCTGTCTGAGGTCTGTC	55 °C	199
Collagen type 1, alpha I (*COL1A1*)	CGCGGATTTGTTGCTGCTTGC	AGGTCCCATCAGCCCCATTGGT	55 °C	269
Aggrecan (*ACAN*)	CGCTGTCTCGCCAAGTGTATGG	CGGTTCAGGGATGCTGACACTC	60 °C	175
Glial fibrillary acidic protein (*GFAP*)	GGCACCTTGAGGCAGAAGCTC	CTCCTGGAGCTCCCGCACCT	60 °C	195
Nestin (*NES*)	ACCACTGAGCAGTTCCAGCTGG	TTGCAGGTGTCTGCAGCCGT	55 °C	187
Glyceraldehyde-3-phosphate dehydrogenase (*GAPDH*)	ATGAGATCAAGAAGGTGGTG	CCAAATTCATTGTCGTACCAG	60 °C	190

Abbreviation: T, temperature.

0.25 μg/mL amphotericin B, 1% DMSO, and 0.36 mg/mL butylated hydroxyanisole [39]. Neurogenic differentiation was confirmed by positive staining of the Nissl substance and granules, using Nissl staining.

For each differentiation experiment, a control group was performed by seeding cells at lower density (9.5×10^3 cells/well) and feeding with HG-DMEM standard medium. These cells were stained using the same protocol as the treated cells. At the end of the differentiations, aliquots of non-stained cells were harvested and stored at −80 °C for further molecular analysis.

2.7. RNA extraction and reverse transcription polymerase chain reaction analysis

Expression of specific MSC (*CD29*, *CD44*, *CD105*, *CD166*), pluripotent (*Oct-4* and *c-Myc*), and hematopoietic (*CD34, CD14, CD45*) markers was investigated by reverse transcription polymerase chain reaction (RT-PCR) analysis on fresh and thawed undifferentiated cells at P3. To evaluate whether cells could be well tolerated by the host once transplanted, expression of the major histocompatibility complex class I (*MHC-I*) and II (*MHC-II*) was assessed. Total RNA was extracted from bovine WJ-derived cells using Trizol reagent (Invitrogen, Monza, Italy), followed by DNase treatment according to the manufacturer's specifications. RNA concentration and purity were measured using a NanoDrop ND1000 spectrophotometer (*NanoDrop* Technologies, Wilmington, DE, USA). cDNA was synthesized from 500 ng total RNA, using the iScript retrotranscription kit (Bio-Rad Laboratories, Hercules, CA, USA). Conventional PCR was performed in a 25-mL final volume with DreamTaq DNA Polymerase (Fermentas, St. Leon Rot, Germany) under the following conditions: initial denaturation at 95 °C for 2 minutes, 32 cycles at 95 °C for 30 seconds (denaturation), 55 °C to 63 °C for 30 seconds (annealing), 72 °C for 30 seconds (elongation), and final elongation at 72 °C for 10 minutes.

For differentiation experiments, total RNA was extracted from undifferentiated (control cells) and from induced WJ-derived cells, and RT-PCR analysis was performed as described previously. Bovine adult tissues (bone, adipose tissue, cartilage, and spinal cord) were used as positive controls for assessing the expression of *BGLAP*, *SPP1*, and *SPARC* for osteogenic differentiation; peroxisome proliferator-activated receptor-gamma (*PPAR-γ*) and leptin (*LEP*) for adipogenesis; collagen type 2α1 (*COL2A1*) and aggrecan (*ACAN*) for chondrogenesis; and glial fibrillary acidic protein (*GFAP*) and nestin (*NES*) for neurogenesis. Bovine-specific oligonucleotide primers were designed using open-source PerlPrimer software version 1.1.17, based on available NCBI *Bos taurus* sequences or on mammal multialigned sequences. Primers were designed across an exon–exon junction to avoid DNA amplification. Primers were used at 300 nM final concentrations. Their sequences and the conditions used to amplify each gene are presented in Table 1. *GAPDH* was used as a reference gene.

2.8. Flow cytometry

WJ-derived cells were analyzed by flow cytometry to determine the percentage of mesenchymal (CD105, CD166), hematopoietic (CD34), and immunogenic (MHC-II) markers after isolation (P0). For CD105, CD166, and CD34, primary mouse monoclonal antibodies and secondary antibodies rabbit antimouse fluorescein isothiocyanate were used. For MHC-II, primary rat monoclonal antibody and secondary rabbit antirat fluorescein isothiocyanate were used. Staining was performed as previously reported [40]. Cells (1×10^6 cells/mL) were labeled with primary antibodies in PBS with 3% of BSA (BDH; VWR International Ltd, Poole, UK) for 45 minutes

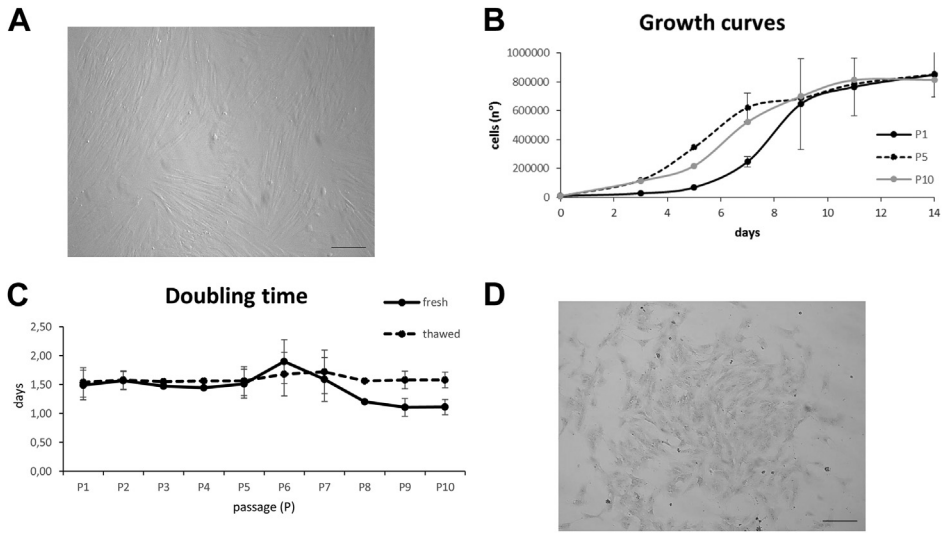

Fig. 1. Cell characteristics. (A) Monolayer of Wharton jelly (WJ)-derived cells; magnification × 20; scale bar = 20 μm. (B) Growth curve at P1, P5 and P10. (C) Doubling times for both fresh and thawed cells. (D) Colony of WJ-derived cells for CFU study; magnification × 20; scale bar = 20 μm.

at room temperature in the dark, followed by washing in cold PBS and a final incubation with secondary antibodies (1:50) for 30 minutes at room temperature in the dark. After incubation, cells were washed twice in ice-cold PBS and analyzed using a Millipore Guava easyCyte Single Sample Flow Cytometer. A minimum of 10,000 cells was acquired for each sample and analyzed in the FL1 channel.

The negative pattern was examined by applying the same cell suspension with the first incubation, and the result was included on the global compensation, to exclude autofluorescence. A 488-nm filter was used in each analysis.

Offline analyses of the flow cytometry standard files were performed using Weasel software version 2.5 (http://en.bio-soft.net/other/WEASEL.htmL).

2.9. Statistical analysis

Statistical analysis was performed using GraphPad Instat 3.00 for Windows (GraphPad Software, La Jolla, CA, USA). Three replicates were performed for each experiment (DT and CFU) and the results reported as mean ± standard deviation (SD). One-way ANOVA for multiple comparisons by Student-Newman-Keuls multiple comparison tests was used. $P < 0.05$ was considered as significant.

3. Results

3.1. Cell morphology

The cellular yield was approximately 3×10^6 cells/g of minced WJ. The initial viability was greater than 95%.

Cells were selected purely on their ability to adhere to plastic. Isolated cells readily attached to plastic culture dishes. Colonies started to appear within the first 2 days, reaching confluence after 5 days. Wharton jelly–derived cells were a morphologically homogeneous population of fibroblast-like cells in all passages of cell culture (Fig. 1A).

After thawing (at P3), viability was 80%. Wharton jelly–derived cells conserved their fibroblast-like shape.

3.2. Proliferation studies

Wharton jelly–derived cells were able to proliferate, reaching confluence up to 10 passages.

At P1, the growth curve showed an initial lag phase of 3 to 4 days longer than that seen in the other passages and a subsequent log phase until 14 days. The WJ-derived cells showed more extensive proliferation at P5, but the intensity of proliferation was similar in all passages in the final culture days (Fig. 1B).

DT remained constant until the seventh passage, then decreased significantly ($P < 0.05$) until P10. The mean DT was 1.44 ± 0.24 days or 34.55 ± 6.33 hours (Fig. 1C).

After thawing, the mean DT was 1.59 ± 0.06 days or 38.21 ± 1.68 hours (Fig. 1C) with no statistical difference compared to fresh cells.

The number of cell colonies formed was counted at P0 on fresh cells. These cells were able to form an average of 1 CFU-F (Fig. 1D) for 221.68 ± 3.86 seeded cells. The highest number of colonies was found at the greatest density of seeding (Table 2).

Table 2
Colony-forming unit (CFU) assay.

Density cells/cm^2	Total cells	CFU	One CFU each
100	950	1.5 ± 0.71^a	633.33
250	2375	22.33 ± 5.17^b	106.36
500	4750	57.92 ± 4.31^c	82.01
1000	9500	146.15 ± 2.78^c	65.00

Different small letter superscripts (a, b, c) indicate statistically different comparisons ($P < 0.05$) between cell densities in the WJ group.

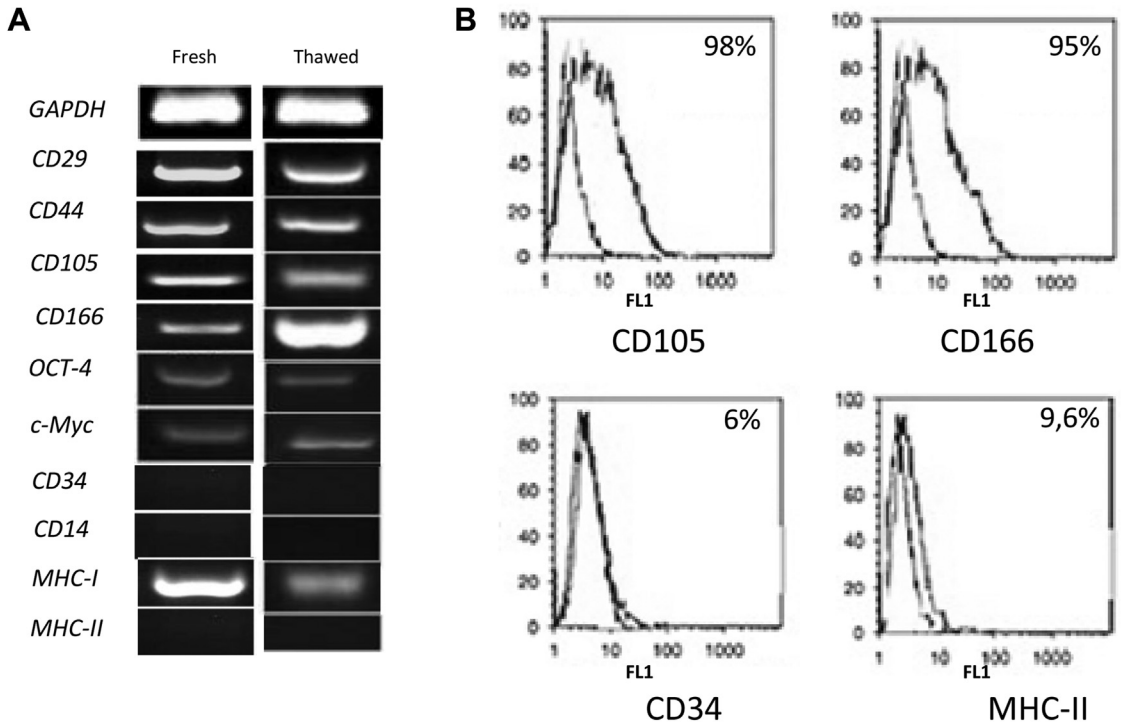

Fig. 2. (A) Reverse transcription polymerase chain reaction analysis of mesenchymal (*CD29*, *CD44*, *CD105*, and *CD166*), pluripotent (*Oct-4* and *c-Myc*), hematopoietic (*CD34* and *CD14*) specific gene expression on WJ–derived fresh and thawed cells. Major histocompatibility complex (*MHC*) I and II gene expression is also reported. *GAPDH* was used as the reference gene. (B) Flow cytometry analysis of the expression of mesenchymal (CD105 and CD166), hematopoietic (CD34) and immunogenic (MHCII) markers. Histograms represent relative number of cells versus fluorescence intensity (FL1). Black histograms indicate background fluorescence intensity of cells labeled with isotype control antibodies only gray histograms show positivity to the studied antibodies.

3.3. Molecular characterization

As shown by RT-PCR, WJ-derived cells expressed MSC markers (*CD29*, *CD44, CD105, CD166*) and lacked hematopoietic ones (*CD34* and *CD14*) from P0 to P10. *MHC-I* expression was present, whereas *MHC-II* was not. Moreover, undifferentiated MSCs were found to express *Oct-4* and *c-Myc,* essential transcription factors for maintaining the primitive pluripotent state of embryonic stem cells. After thawing, cells studied at P3 expressed the same MSC-mRNA markers such as *CD29, CD44, CD105, CD166, Oct-4*, *c-Myc*, and *MHC-I*, as freshly isolated cells, but not *CD34*, *CD14*, and *MHC-II* (Fig. 2A).

3.4. Flow cytometry analysis

Flow cytometry was used to evaluate the homogeneity of the cell population and to identify the subset of mesenchymal, hematopoietic, and immunogenic cells. The cell populations tested were all $CD105^{+}$ and $CD166^{+}$, but negative for CD34 and MHC-II, as shown in Figure 2B.

3.5. Differentiation assay

The results of all differentiation assays are shown in Figure 3.

3.5.1. Osteogenic differentiation potential

After 21 days of induction, osteogenic differentiation was confirmed by von Kossa staining. The control (non-induced cells) was negative for von Kossa staining. RT-PCR analysis of *SPP1* and *SPARC* mRNA expression confirmed osteogenic induction, but *BGLAP* was not expressed in induced cells.

3.5.2. Adipogenic differentiation potential

Cells were able to undergo adipogenic differentiation, as demonstrated by the development of positive staining for Oil Red O after 3 weeks of culture in adipogenic induction medium. Control cells, maintained in regular control medium, showed no lipid deposits. RT-PCR analysis of *PPAR-γ* and *LEP* mRNA expression confirmed adipogenic induction.

3.5.3. Chondrogenic differentiation potential

Differentiation was identified by marked deposition of glycosaminoglycans in the matrix, stained with Alcian blue. The presence of COL2A1 and ACAN mRNA confirmed chondrogenic induction for this cell population.

3.5.4. Neurogenic differentiation potential

After 3 days of induction, neurogenic differentiation was confirmed by the morphology of the cells. The WJ-derived cells adopted the typical morphology of neural cells with dendrite-like processes. The presence of *GFAP* mRNA

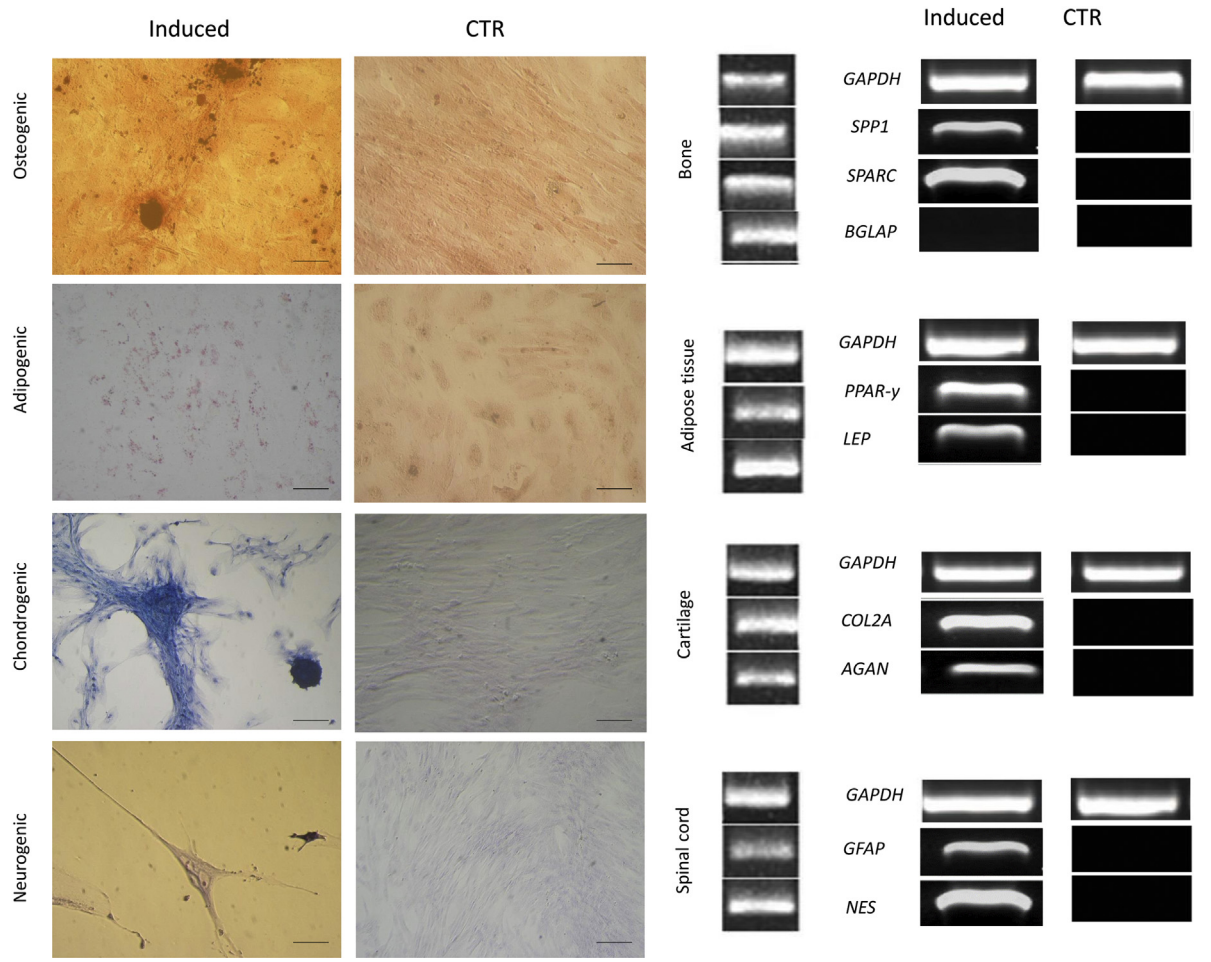

Fig. 3. Staining of differentiated and control (CTR) (un-differentiated) WJ–derived cells and respective molecular expression. Osteogenic induced cells were evaluated for von Kossa staining and reverse transcription polymerase chain reaction (RT-PCR) analysis of *SPP1*, *SPARC*, and *BGLAP*. Adipogenic induced cells were evaluated for Oil Red O–stained cytoplasmic neutral lipids and RT-PCR of *PPAR-γ* and *LEP*. Chondrogenic induced cells were evaluated for Alcian blue staining and RT-PCR of *COL2A1* and *ACAN*. Neurogenic induced cells were evaluated for Nissl staining and RT-PCR of *NES* and *GFAP*; magnification: × 20; scale bar = 20 μm. *GAPDH* was employed as reference gene. Bone, adipose tissue, cartilage, and spinal cord were used as positive controls.

suggested that under these culture conditions, WJ-derived cells were induced to differentiate into glial cells. RT-PCR analysis of bovine adult tissues (bone, adipose tissue, cartilage, and spinal cord) showed expression of the specific studied genes.

The frozen-thawed cells were able to differentiate toward the same lineages as freshly isolated cells (data not shown).

4. Discussion

This work allowed the isolation, characterization, and differentiation of bovine stem cells derived from WJ. Our findings suggest that this tissue is a reliable source of presumptive stem cells, displaying intermediate features between adult and embryonic stem cells. These cells have wide potential clinical applications because of their low immunogenicity and high differentiation potential. After digestion, large numbers of WJ-derived cells with greater than 95% viability (optimal value in terms of plating efficiency and cellular growth) were obtained. When cultured, these cells demonstrated strong adherence to plastic dishes and developed fibroblast-like morphology over time. Adherence is a fundamental property for the culture of stem cells [41]. The proliferation studies showed that WJ-derived cells reached high plating efficiency and had a high proliferation rate *in vitro* until P10, demonstrating a growth curve with a lag phase of few hours and an intensive log phase of 12 days. Moreover, the mean value of DT for 10 passages was 34.55 hours. During this intensive proliferation, the cells maintained their morphological characteristics. These data are in agreement with those obtained by other researchers who reported a high proliferation rate of human [37,42], equine [6], bovine [8], and feline [43] extrafetal derived cells. It is very difficult to compare these data with those obtained from Cardoso et al. [32] because that study only reported the number of cells per milliliter found at different passages and the DT value was not calculated.

Bovine WJ-derived cells also showed the ability to produce clones. When seeded at different densities, they were able to form clones with a frequency that increased with the cell-seeding density, suggesting paracrine signaling between cells at P0 [44]. Moreover, WJ-derived cells showed a typical expression pattern expected for cultured stem cells [41] when analyzed by RT-PCR. Indeed, these cells expressed a pattern of mesenchymal (*CD29*, *CD44, CD105, CD73*, *CD166*) and pluripotency (*Oct-4*, *c-Myc*) genes with no expression of the hematopoietic *CD34.* The pluripotency genes are essential transcription factors for maintaining the primitive pluripotent state of embryonic stem cells. These data confirm the results obtained in equine, canine, and bovine WJ [6,8,24,32,45–47] where pluripotent- and mesenchymal-associated markers were expressed.

For the first time, the expression of *MHC-I* and *MHC-II,* related to cell immunogenicity, was also evaluated to assess the usefulness of bovine WJ-derived cells for cell therapy. At each passage, these cells were negative for *MHC-II* and positive for *MHC-I*, consistent with findings of previous publications [6,8]. These findings reinforce the role of the extrafetal tissue as an allogenic source for cell-based therapies in cattle. It is important to underline that RT-PCR alone is not useful for characterizing WJ-derived cells and that quantitative analyses are needed to make meaningful statements about their gene expression. Flow cytometry provides useful quantitative data on the percentage of cell reactivity. Indeed, we showed that greater than 90% cells were positive for CD105 and CD73, whereas less than 10% were positive for CD34 and MHC-II. These data confirm the mesenchymal nature of isolated cells and the lack of immunogenicity and underline the homogeneity of this cell line.

The capacity of MSCs to differentiate into a variety of cell types (adipocytes, osteocytes, and chondrocytes) [48,49] has aroused interest in cell and gene therapy. Bovine WJ-derived cells, obtained by enzymatic digestion, were able to differentiate into osteocytes, adipocytes, chondrocytes, and neuron-like cells in the same way as cells obtained by nonenzymatic digestion [32]. This suggests that these cells are capable of differentiation into multiple germ layers, an essential characteristic also observed in the pig [17], dog [24], horse [4], and chicken [50]. After 21 days of induction, mineral deposits were confirmed by von Kossa staining and by the expression of *SPP1* and *SPARC* but not of *BGLAP*. This might be because *BGLAP* is expressed in terminally differentiated osteoblasts [51]. When stimulated to differentiate toward the adipogenic lineage, bovine WJ-derived cells were positive for Oil Red O staining and expressed genes involved in lipid biosynthesis and storage. mRNAs for *PPAR-γ*, crucial for the preadipocyte commitment [52], and *LEP*, as late marker of adipocyte differentiation, were detected. The potential of bovine WJ-derived cells to undergo chondrogenesis was confirmed by positive Alcian blue staining and identification of markers commonly associated with the chondrocyte phenotype such as collagen type II and aggrecan, the most essential cartilage proteoglycan and key markers of chondrocyte differentiation [53]. *ACAN* expression was demonstrated, whereas a basal level of *COL2A1* was detected. The low expression of *COL2A1* might be related to the culture conditions in this study because chondrogenic differentiation of MSCs in monolayer culture appears to be dose dependent and time dependent in relation to the bioactive factors used [32,33]. GFAP and nestin, markers expressed in neuronal precursor stem cells, have been detected in WJ-derived cells. The expression of both markers is probably related to the ability of these cells to differentiate either toward the glial cell lineage, as previously shown by Miki et al. [54] for 95% of cells isolated from human amnion, or toward neurogenic line as previously observed in pigs [55].

Whatever the reason, this cell line converted into a typical neuron-like morphology when appropriately induced.

Our findings suggest that, in agreement with reports of other researchers in several species [6,45–47,56], bovine WJ represents an alternative source of progenitor cells that can be obtained by enzymatic methods for use in cell-based therapies. In our study, the digestion of tissue did not result in a reduced cellular viability or degradation of cellular surface receptors or alteration of cellular function as reported by Jeschke et al. [57].

Moreover, after thawing, the cryopreserved cells had a high level of viability (80%) and could be successfully expanded and differentiated. This demonstrates that bovine umbilical cord matrix cells can tolerate freezing without loss of functional integrity in terms of morphology, presence of specific stemness markers, and differentiation potential, although renewal capacity was slightly lower than that observed in freshly isolated cells.

In conclusion, these data confirm that bovine WJ contains a niche of MSCs. However, further investigation, including preclinical studies and further study of immunologic properties, is needed to better understand their role in cellular therapy before *in vivo* applications of WJ-derived cells are considered. To date, there is only a single literature report of transplantation of caprine WJ-derived cells for wound healing, which showed promising effects [23]. The findings of this study reinforce the emerging importance of extraembryonic tissues for derivation of cells that may be ideal tools in veterinary regenerative medicine.

Acknowledgments

This work was supported by grants from Università degli Studi di Milano and by “Bando ricerca scientifica 2011, Sezione innovazione tecnologica, Approcci metodologici per la valorizzazione della razza Piemontese, Cassa di Risparmio di Cuneo”.

Author contributions: A.L.-C. designed the study; performed isolation cells; acquired, analyzed, and interpreted data; and wrote the article. C.P. performed proliferation study, molecular characterization, and approved the final version of manuscript. A.B. performed cytofluorimetric analyses and approved the final version of manuscript. P.E. performed differentiation study and approved the final version of manuscript. F.C. designed the study, analyzed and interpreted data, and revised the manuscript. L.V. conceived and designed the study,

collected the umbilical cords, analyzed and interpreted data, and wrote the article.

Competing interests

The authors declare that there are no conflicts of interest that could be perceived as prejudicing the impartiality of the reported research.

References

[1] Marcus-Sekura C, Richardson JC, Harston RK, Sane N, Sheets RL. Evaluation of the human host range of bovine and porcine viruses that may contaminate bovine serum and porcine trypsin used in the manufacture of biological products. Biologicals 2011;39:359–69.
[2] Cremonesi F, Corradetti B, Lange Consiglio A. Fetal adnexa derived stem cells from domestic animal: progress and perspectives. Theriogenology 2011;75:1400–15.
[3] In't Anker PS, Scherjon SA, Kleijburg-van der Keur C, Noort WA, Claas FHJ, Willemze R, et al. Amniotic fluid as a novel source of mesenchymal stem cells for therapeutic transplantation. Blood 2003;102:1548–9.
[4] Lange-Consiglio A, Corradetti B, Rutigliano L, Cremonesi F, Bizzaro D. *In vitro* studies of horse umbilical cord matrix-derived cells and labeling efficiency with magnetic resonance contrast agents. Open Tissue Eng Regen Med J 2011;4:120–33.
[5] Yadav PS, Mann A, Singh V, Yashveer S, Sharma RK, Singh I. Expression of pluripotency genes in buffalo (Bubalus bubalis) amniotic fluid cells. Reprod Domest Anim 2011;46:705–11.
[6] Lange-Consiglio A, Corradetti B, Bizzaro D, Magatti M, Ressel L, Tassan S, et al. Characterization and potential applications of progenitor-like cells isolated from horse amniotic membrane. J Tissue Eng Regen Med 2012;6:622–35.
[7] Mann A, Yadav RP, Singh J, Kumar D, Singh B, Yadav PS. Culture, characterization and differentiation of cells from buffalo (Bubalus bubalis) amnion. Cytotechnology 2012;65:23–30.
[8] Corradetti B, Meucci A, Bizzaro D, Cremonesi F, Lange-Consiglio A. Mesenchymal stem cells from amnion and amniotic fluid in the bovine. Reproduction 2013;145:391–400.
[9] Mançanares CAF, Oliveira VC, Oliveira LJ, Carvalho AF, Sampaio RV, Mançanares ACF, et al. Isolation and characterization of mesenchymal stem cells from the yolk sac of bovine embryos. Theriogenology 2015;84:887–98.
[10] Abdulrazzak H, Moschidou D, Jones G, Guillot PV. Biological characteristics of stem cells from foetal, cord blood and extraembryonic tissues. J R Soc Interface 2010;7 Suppl 6:S689–706.
[11] Hall JG, Martin PL, Wood S, Kurtzberg J. Unrelated umbilical cord blood transplantation for an infant with beta-thalassemia major. Am J Pediatr Hematol Oncol 2004;26:382–5.
[12] Fuchs JR, Hannouche D, Terada S, Zand S, Vacanti JP, Fauza DO. Cartilage engineering from ovine umbilical cord blood mesenchymal progenitor cells. Stem Cells 2005;23:958–64.
[13] Koch TG, Heerkens T, Thomsen PD, Betts DH. Isolation of mesenchymal stem cells from equine umbilical cord blood. BMC Biotechnol 2007;7:26.
[14] Raoufi MF, Tajik P, Dehghan MM, Eini F, Barin A. Isolation and differentiation of mesenchymal stem cells from bovine umbilical cord blood. Reprod Domest Anim 2011;46:95–9.
[15] Seo MS, Jeong YH, Park JR, Park SB, Rho KH, Kim HS, et al. Isolation and characterization of canine umbilical cord blood-derived mesenchymal stem cells. J Vet Sci 2009;10:181–7.
[16] Brólio MP, Vidane AS, Zomer HD, Wenceslau CV, Ozório JJ, Martins DS, et al. Morphological characterization of the progenitor blood cells in canine and feline umbilical cord. Microsc Res Tech 2012;75:766–70.
[17] Carlin R, Davis D, Weiss M, Schultz B, Troyer D. Expression of early transcription factors Oct-4, Sox-2 and Nanog by porcine umbilical cord (PUC) matrix cells. Reprod Biol Endrocrinol 2006;4:8.
[18] Troyer DL, Weiss ML. Concise review: Wharton's Jelly-derived cells are primitive stromal cell population. Stem Cells 2008;26:591–9.
[19] Lee MW, Choi J, Yang MS, Moon YJ, Park JS, Kim HC, et al. Mesenchymal stem cells from cryopreserved human umbilical cord blood. Biochem Biophys Res Commun 2004;320:273–8.
[20] Nekanti U, Mohanty L, Venugopal P, Balasubramanian S, Totey S, Ta M. Optimization and scale-up of Wharton's jelly-derived mesenchymal stem cells for clinical applications. Stem Cell Res 2010;5:244–54.
[21] Seshareddy K, Troyer D, Weiss ML. Method to isolate mesenchymal-like cells from Wharton's jelly of umbilical cord. Methods Cell Biol 2008;86:101–19.
[22] Babaei H, Moshrefi M, Golchin M, Nematollahi-Mahani SN. Assess the pluripotency of caprine umbilical cord Wharton's jelly mesenchymal cells by RT-PCR analysis of early transcription factor nanog. Iran J Vet Surg 2008;3:57–66.
[23] Azari O, Babaei H, Derakhshanfar A, Nematollahi-Mahani SN, Poursahebi R, Moshrefi M. Effects of transplanted mesenchymal stem cells isolatedfrom Wharton's jelly of caprine umbilical cordon cutaneous wound healing; histopathological evaluation. Vet Res Commun 2011;35:211–22.
[24] Filioli Uranio M, Valentini L, Lange-Consiglio A, Caira M, Guaricci A, L'abbate A, et al. Isolation, proliferation, cytogenetic, and molecular characterization and in vitro differentiation potency of canine stem cells from foetal adnexa: a comparative study of amniotic fluid, amnion, and umbilical cord matrix. Mol Reprod Dev 2011;78:361–73.
[25] Reed SA, Johnson SE. Equine umbilical cord blood contains a population of stem cells that express Oct4 and differentiate into mesodermal and endodermal cell types. J Cell Physiol 2007;215:329–36.
[26] Pappa K, Anagnou N. Novel sources of fetal stem cells: where do they fit on the developmental continuum? Regen Med 2009;4:423–33.
[27] Weiss ML, Anderson C, Medicetty S, Seshareddy KB, Weiss RJ, VanderWerff I, et al. Immune properties of human umbilical cord Wharton's Jelly-derived cells. Stem Cells 2008;26:2865–74.
[28] Hartmann I, Hollweck T, Haffner S, Krebs M, Meiser B, Reichart B, et al. Umbilical cord tissue-derived mesenchymal stem cells grow best under GMP-compliant culture conditions and maintain their phenotypic andfunctional properties. J Immunol Methods 2010;363:80–9.
[29] La Rocca G, Anzalone R, Corrao S, Magno F, Loria T, Lo Iaconno M, et al. Isolation and characterization of Oct-4+/HLA-G+ mesenchymal stem cells from human umbilical cord matrix: differentiation potential and detection of new markers. Histochem Cell Biol 2009;131:267–82.
[30] Francese R, Fiorina P. Immunological and regenerative properties of cord blood stem cells. Clin Immunol 2010;136:309–22.
[31] Anzalone R, Lo Iacono M, Corrao S, Magno F, Loria T, Cappello F, et al. New emerging potentials for human Wharton's jelly mesenchymal stem cells: immunological features and hepatocyte-like differentiative capacity. Stem Cells Dev 2010;19:423–38.
[32] Cardoso TC, Ferrari HF, Garcia AF, Novais JB, Silva-Frade C, Ferrarezi MC, et al. Isolation and characterization of Wharton's jelly-derived multipotent mesenchymal stromal cells obtained from bovine umbilical cord and maintained in a defined serum-free three-dimensional system. BMC Biotechnol 2012;12:18.
[33] Bosnakovski D, Mizuno M, Kim G, Takagi S, Okumura M, Fujinaga T. Isolation and multilineage differentiation of bovine bone marrow mesenchymal stem cells. Cell Tissue Res 2005;319:243–53.
[34] Bosnakovski D, Mizuno M, Kim G, Ishiguro T, Okumura M, Iwanaga T, et al. Chondrogenic differentiation of bovine bone marrow mesenchymal stem cells in pellet cultural system. Exp Hematol 2004;32:502–9.
[35] Freshney RI. Culture of animal cells. A manual of basic technique. Third edition. New York: Wiley-Liss. A John Wiley & Sons, Inc., Publication; 1994.
[36] Romanov YA, Svintsitskaya VA, Smirnov VN. Searching for alternative sources of postnatal human mesenchymal stem cells: candidate MSC-like cells from umbilical cord. Stem Cells 2003;21:105–10.
[37] Soncini M, Vertua E, Gibelli L. Isolation and characterization of mesenchymal cells from human fetal membranes. J Tissue Eng Regen Med 2007;1:296–305.
[38] Mitchell KE, Weiss ML, Mitchell BM. Matrix cells from Wharton's jelly form neurons and glia. Stem Cells 2003;21:50–60.
[39] Woodbury D, Schwarz EJ, Prockop DJ. Adult rat and human bone marrow stromal cells differentiate into neurons. J Neurosci Res 2000;61:364–70.
[40] Corradetti B, Lange-Consiglio A, Barucca M, Cremonesi F, Bizzaro D. Size-sieved subpopulations of mesenchymal stem cells from intervascular and perivascular equine umbilical cord matrix. Cell Prolif 2011;44:330–42.
[41] Dominici M, Le Blanc K, Mueller I, Slaper-Cortenbach I, Marini F, Krause D, et al. Minimal criteria for defining multipotent mesenchymal stromal cells. The International Society for Cellular Therapy position statement. Cytotherapy 2006;8:315–7.

[42] Miki T, Marongiu F, Ellis E, Strom C. Isolation of amniotic epithelial stem cells. Curr Protoc Stem Cell Biol 2010;Chapter 1:Unit 1E.3.
[43] Rutigliano L, Coradetti B, Valentini L, Bizzaro D, Meucci A, Cremonesi F, et al. Molecular characterization and in vitro differentiation of feline progenitor-like amniotic epithelial cells. Stem Cell Res Ther 2013;4:133.
[44] Sarugaser R, Lickorish D, Baksh D, Hosseini MM, Davies JE. Human umbilical cord perivascular (HUCPV) cells: a source of mesenchymal progenitors. Stem Cells 2005;23:220–9.
[45] Lovati AB, Corradetti B, Lange Consiglio A, Recordati C, Bonacina E, Bizzaro D, et al. Comparison of equine bone marrow-, umbilical cord matrix and amniotic fluid-derived progenitor cells. Vet Res Commun 2011;35:103–21.
[46] Iacono E, Brunori L, Pirrone A, Pagliaro PP, Ricci F, Tazzari PL, et al. Isolation, characterization and differentiation of mesenchymal stem cells from amniotic fluid, umbilical cord blood and Wharton's jelly in the horse. Reproduction 2012;143:455–68.
[47] Chen J, Lu Z, Cheng D, Peng S, Wang H. Isolation and characterization of porcine amniotic fluid-derived multipotent stem cells. PLoS One 2011;6:e19964.
[48] Pittenger MF, Mackay AM, Beck SC, Jaiswal RK, Douglas R, Mosca JD, et al. Multilineage potential of adult human mesenchymal stem cells. Science 1999;284:143–7.
[49] Sekiya I, Vuoristo JT, Larson BL, Prockop DJ. In vitro cartilage formation by human adult stem cells from bone marrow stroma defines the sequence of cellular and molecular events during chondrogenesis. Proc Natl Acad Sci U S A 2002;99:4397–402.
[50] Khatri M, O'Brien TD, Sharma JM. Isolation and differentiation of chicken mesenchymal stem cells from bone marrow. Stem Cells Dev 2009;18:1485–92.
[51] Wagner E, Luther G, Zhu G, Luo Q, Shi Q, Kim SH, et al. Review article: defective osteogenic differentiation in the development of osteosarcoma. Sarcoma 2011;2011:325238.
[52] Tontonoz P, Hu E, Graves RA, Budavari AI, Spiegelman BM. mPPARg2: tissue-specific regulator of an adipocyte enhancer. Genes Dev 1994;8:1224–34.
[53] Han Y, Lefebvre V. L-Sox5 and Sox6 drive expression of the aggrecan gene in cartilage by securing binding of Sox9 to a far-upstream enhancer. Mol Cell Biol 2008;28:4999–5013.
[54] Miki T, Lehmann T, Cai H, Stolz DB, Strom SC. Stem cell characteristics of amniotic epithelial cells. Stem Cells 2005;23:1549–59.
[55] Zheng YM, Zhao XE, An ZX. Neurogenic differentiation of EGFP gene transfected amniotic fluid-derived stem cells from pigs at intermediate and late gestational ages. Reprod Domest Anim 2010;45:e78–82.
[56] Iacono E, Cunto M, Zambelli D, Ricci F, Tazzari PL, Merlo B. Could fetal fluid and membranes be an alternative source for Mesenchymal Stem Cells (MSCs) in the feline species? a preliminary study. Vet Res Commun 2012;36:107–18.
[57] Jeschke MG, Gauglitz GG, Phan TT, Herdon DN, Kita K. Umbilical cord lining membrane and Wharton's jelly-derived mesenchymal stem cells: the similarities and differences. Open Tissue Eng Regen Med J 2011;4:21–7.

Title: MicroRNA mediated regulation and role of PI3K-Akt pathway in bovine oocyte developmental competence

Authors: Gabriella Mamede Andrade[1§]; Juliano Coelho da Silveira[1§]; Claudia Perrini[1,2]; Maite Del Collado[1]; Samuel Gebremedhn[3]; Dawit Tesfaye[3]; Flávio Vieira Meirelles[1*]; Felipe Perecin[1*]

[1] Veterinary Medicine Department, Faculty of Animal Sciences and Food Engineering, University of Sao Paulo, Av. Duque de Caxias Norte 225, 13635-900, Pirassununga, SP, Brazil.

[2] Large Animal Hospital, Reproduction Unit, Università degli Studi di Milano, Via dell'Università 6, 26900, Lodi, Italy.

[3] Institute for Animal Sciences (ITW), University of Bonn, Bonn, Germany.
[§*] Equal contributors.

ABSTRACT

Ovarian follicle encloses oocytes in a microenvironment throughout its growth and competence acquisition. MicroRNAs were identified in follicular cells and shown to be active during intra-follicular communication regulating cellular processes. To determine cellular origin of follicular miRNAs we screened 348 miRNAs in granulosa cells and cumulus-oocyte complexes (COCs) and their derived extracellular vesicles (EVs). Bioinformatics analyses revealed that PI3K-Akt pathway was highly regulated by exclusive microRNAs. To investigate whether miRNAs could influence oocyte quality, we individualized follicles and recovered follicular cells (FCs) and COCs, that were individually cultured in order to pool follicular cells based on oocyte competence to reach the blastocyst stage. We found levels of PI3K-Akt signalling pathway components in FCs correlating with oocyte competence. This miRNA-modulated pathway was downregulated in FCs of lower quality oocytes, indicated by increased levels of *PTEN* and decreased levels of *PTEN* regulators bta-miR-494 and bta-miR-20a. Using PI3K-Akt responsive genes we showed decreased *FOXO3a* levels in lower quality groups inferring changes in cell cycle progression and oxidative response. MicroRNA expression profiles were used as tool to identify molecular pathways involved in oocyte competence. The distinct levels of PI3K-Akt pathway components in FCs from follicles carrying oocytes with distinct developmental competences validated this strategy.

INTRODUCTION

The success of *in vitro* production of bovine embryos is closely associated with oocyte quality[1,2] . The oocyte's competence to reach the blastocyst stage is progressively acquired during follicle growth[3], and is the result of interactions between external factors and the follicular microenvironment[4]. The ovarian follicle is composed of three cell types besides the oocyte; theca, granulosa, and cumulus cells, along with a basement membrane and follicular fluid. Each one of these cell types plays an active role in oocyte differentiation and regulation[5]. Due to its complexity, currently there is no reliable method to measure oocyte competence prior to phenotype analysis following fertilization.

Several morphological, ultrastructural, and metabolic criteria have been used to predict oocyte competence. These morphological criteria remain subjective and in some cases invasive and/or poorly correlated with oocyte competence. Identification of other relevant biomarkers to accurately predict oocyte quality is of primary interest[6]. The appropriate interplay between oocyte and follicular cells (FCs) is indispensable for proper folliculogenesis, oocyte development, and progression to ovulation, as well as subsequent embryo development[7]. Hence, understanding the different signalling pathways in FCs that modulate the oocyte competence is important for unravelling the key intracellular events driving oocyte competence acquisition.

The mechanisms governing cellular communication within ovarian follicles were first studied and described using paracrine agents (oocytes-secreted factors)[8] and observing the exchange of small molecules through gap junctions[9]. Recently, it was demonstrated that exchanges of bioactive molecules across FCs may occur within the follicular environment, potentially influencing the oocyte, via cell-secreted vesicles[10] or through transzonal projections[11]. As a result, such mechanisms, among others, allow the intra-follicular flow of molecules such as proteins, mRNAs, and miRNAs.

MicroRNAs are naturally occurring small non-coding RNAs that act as key posttranscriptional regulators of gene expression following base pair interactions with the 3'-untranslated region (3'UTR) of target protein-coding genes[12]. miRNAs have been linked to the regulation of genes involved in tissue development and differentiation. In mammals, miRNAs are predicted to control the activity of more than 60% of all protein-coding genes and participate in the regulation of many cellular processes[13]. Recently, miRNAs were reported as regulators of different genes associated with follicle selection in sheep and oocyte developmental competence in bovines and equines[14,15,10]. Therefore, the determination of miRNA expression profiles in models including ovarian follicles and cellular communication within this microenvironment may lead to the discovery of molecular pathways involved in the acquisition of oocyte competence.

The phosphatidylinositol-3-kinase/protein kinase B (PI3K-Akt) pathway plays a key role in cellular responses to cell proliferation, apoptosis, DNA repair, and protein synthesis. Accumulating evidence suggests that PI3K-Akt is associated with ovarian function, including recruitment of primordial follicles, granulosa proliferation, corpus luteum survival, and oocyte maturation[16,17,18]. There are several functions of PI3K-Akt regulators, including the upregulation of Akt activity by its phosphorylation as a result of PI3K upregulation and downregulation by PTEN (phosphatase homologous to tensin). Additionally, there are experimental indications that miRNAs are also involved in the regulation of PI3K-Akt, representing an additional layer of complexity in the regulating system of this pathway[19]. Specifically, some miRNAs, such as miR-494 and miR-20a, have been shown to have modulatory effects on *PTEN* levels and thus, on downstream genes of the PI3K-Akt pathway[20,21].

Here, we investigated the levels of miRNAs in FCs following isolation and culture. Granulosa cells (GCs) and cumulus-oocyte-complexes (COCs) were cultured in order to allow the identification of miRNAs in individual cell types as well as in their secreted extracellular vesicles (EVs). Bioinformatics analyses of miRNAs identified in different follicular cell types and EVs indicate that the PI3K-Akt pathway to be regulated by miRNAs uniquely expressed in GCs, COCs and in their respective EVs. Therefore, we tested the hypothesis that oocyte competence is associated with alterations in levels of PI3K-Akt pathway components and their regulatory miRNAs during follicle development. For this,, we dissected ovarian follicles and retrieved FCs and COCs. We placed the COCs in individual droplets and tracked maturation and parthenogenetic development until the blastocyst stage was reached. Then we further determined the levels of PI3K-Akt components in previously collected FCs from the originated follicles, relating them to the oocyte's competence to mature and support early development. We determined the levels of PI3K-Akt downstream genes related to different cellular processes (i.e. protein synthesis, DNA repair, cell cycle progression, and apoptosis), as well as the levels of *PTEN*-regulators bta-miR-494 and bta-miR-20a. Our results demonstrated that the PI3K-Akt pathway is regulated by different miRNAs detected in FCs, and as a result, potentially driving oocyte competence.

RESULTS

To find new pathways involved in oocyte competence acquisition without disrupting the oocyte, we used FCs and EVs to perform miRNA profiling after stimulating with FSH. FCs from immature follicles (3-6 mm in diameter) were exposed to physiological levels of FSH in culture in order to mimic follicle

development, and the cells were subsequently used to determine miRNA profiles. As a result, we identified different miRNAs present in GCs and COCs. Interestingly, these specific miRNAs were found to regulate similar pathways. EVs derived from FCs in culture media were equally used to determine miRNA profiles and identify specifically regulated pathways. In both the FCs and their EVs, the PI3K-Akt pathway appeared to be highly regulated by miRNAs. Based on that observation, we investigated the levels of PI3K-Akt family members in a retrospective model, with respect to oocyte competence. In order to do so, we used FCs collected from immature follicles (3-6 mm in diameter). PI3K-Akt levels of the selected members were altered in FCs and were correlated with oocyte competence.

miRNA profiles of FCs

A total of 326 miRNAs were detected (<37 Ct, in at least 2 out of 3 samples of each group), of which 302 were detected in both GCs and COCs (Supplementary Table S1.A). Ten of these miRNAs showed increased levels ($p < 0.05$) in COCs, let7a-3p, miR-128, miR-15b, miR-196b, miR-342, miR-411a, miR-497, miR-502b, miR-542-5p, and miR-592, and one showed increased levels ($p > 0.05$) in GCs: miR-454. Additionally, specific miRNA signatures were identified in GCs and COCs. Eight out of 326 miRNAs were specifically present in GCs while 16 only appeared in COCs (Table 1).

Cell type	miRNA	Ct value	miRNA	Ct value
GCs	bta-miR-367	35.43	bta-miR-543	34.69
	bta-miR-449a	33.13	bta-miR-653	35.33
	bta-miR-451	28.47	bta-miR-759	35.18
	bta-miR-539	35.43	bta-miR-875	36.60
COCs	bta-miR-105a	30.58	bta-miR-329b	35.32
	bta-miR-126-3p	30.35	bta-miR-365-5p	30.41
	bta-miR-137	35.15	bta-miR-369-5p	31.30
	bta-miR-142-3p	34.70	bta-miR-371	34.57
	bta-miR-200a	35.04	bta-miR-374b	28.44
	bta-miR-218	35.96	bta-miR-495	35.89
	bta-miR-219-5p	35.83	bta-miR-544b	32.18
	bta-miR-329a	36.06	bta-miR-562	33.65
EVs origin	**miRNA**	**Ct value**	**miRNA**	**Ct value**
GCs	bta-miR-125b	34.84	bta-miR-370	35.66
	bta-miR-130b	34.92	bta-miR-502b	36.14
	bta-miR-132	36.45	bta-miR-760-3p	33.40
	bta-miR-154b	34.08	bta-miR-885	34.97
	bta-miR-155	35.06	bta-miR-143	34.95
	bta-miR-27a-5p	27.27	bta-miR-197	34.26
	bta-miR-29d-5p	34.36		
COCs	bta-let-7e	32.83	bta-miR-16b	33.10
	bta-let-7f	34.45	bta-miR-187	34.26
	bta-let-7i	34.61	bta-miR-210	33.86
	bta-miR-1	35.61	bta-miR-25	35.07
	bta-miR-100	34.27	bta-miR-26a	33.81
	bta-miR-101	35.30	bta-miR-30c	36.50
	bta-miR-106a	34.41	bta-miR-339b	35.12
	bta-miR-124b	34.84	bta-miR-346	33.54
	bta-miR-125a	34.18	bta-miR-378b	34.98
	bta-miR-129	34.66	bta-miR-425-3p	29.46
	bta-miR-133a	32.78	bta-miR-453	34.95
	bta-miR-145	33.29	bta-miR-665	31.20
	bta-miR-149-3p	30.64	bta-miR-874	33.87

	bta-miR-149-5p	33.14	bta-miR-877	32.88
	bta-miR-15a	33.60	bta-miR-940	28.43

Ct value represents the group average.

MiRNA profiles of follicular EVs isolated from culture media

EVs recovered from GCs and COCs culture media were used for RNA isolations and subsequent real-time PCR amplifications of 348 mature bovine miRNAs was performed. Real-time PCR analysis revealed 67 detectable miRNAs (<37 Ct and detected in at least 2 samples of each group), of which 24 were common between EVs from the two FC types (Supplementary Table S1.B). Two miRNAs (miR-127 and miR-433) showed higher levels ($p < 0.05$) in GC-EVs and other two miRNAs (miR-631 and miR-323) higher levels ($p < 0.05$) in COC-EVs. Specific miRNA signatures were identified in GCs and COCs EVs. Thirteen out of 67 miRNAs in EVs were specifically detected in GCs, while 30 only appeared in COCs (Table 1).

Bioinformatics analyses of miRNAs

Bioinformatics analyses were performed to identify the pathways regulated by miRNAs and potentially involved in follicle development and acquisition of oocyte competence. MicroRNAs that were specific to each cell type or EV origin were used to determine cellular pathways. We performed a bioinformatics analysis on bovine miRNAs using human miRNA sequences that are homologous to bovine miRNAs (Supplementary Table S2), and the great homology between miRNAs and 3'UTR of the target genes (Supplementary Table S3). Additionally, we grouped miRNAs according to their cellular origin and, using the mirpath analysis package from DIANA tools (http://diana.imis.athena-innovation.gr/DianaTools), we identified the regulated pathways. The analysis of 8 miRNAs, specifically detected in GCs, showed their role in the regulation of 69 pathways. The analysis of 16 miRNAs, specifically identified in COC cells, showed their role in the regulation of 94 pathways. Regarding the differences in miRNA expressions between the two cell types, the ones showing increased expression levels in GC cells play a role in the regulation of 19 pathways, while the ten showing increased expression levels in COC cells play a role in the regulation of 68 pathways. In addition, 13 specific EV miRNAs from GCs were shown to regulate 58 pathways. Moreover, 30 specific COC-EV miRNAs were shown to be involved in the regulation of 102 pathways. Finally, regarding miRNAs differently expressed depending on the EVs types, those with increased expression levels in GC-EVs were shown to regulate 14 pathways, while those found in COC-EVs, play a role in the regulation of 13 pathways.

We selected the most relevant pathways regulated by exclusive miRNAs of both the different FCs and EV types, which are shown in Figure 1. Different genes were shown to be regulated by specific miRNAs in the different cells and EV types. Therefore, specific miRNAs are modulating important cellular processes, including many signalling pathways such as the PI3K-Akt pathway. Interestingly, the PI3K-Akt signalling pathway appears to be controlled by miRNAs from different origins. There are 70 and 111 genes belonging to the PI3K-Akt shown to be regulated by specific miRNAs from GC and COCs, respectively.

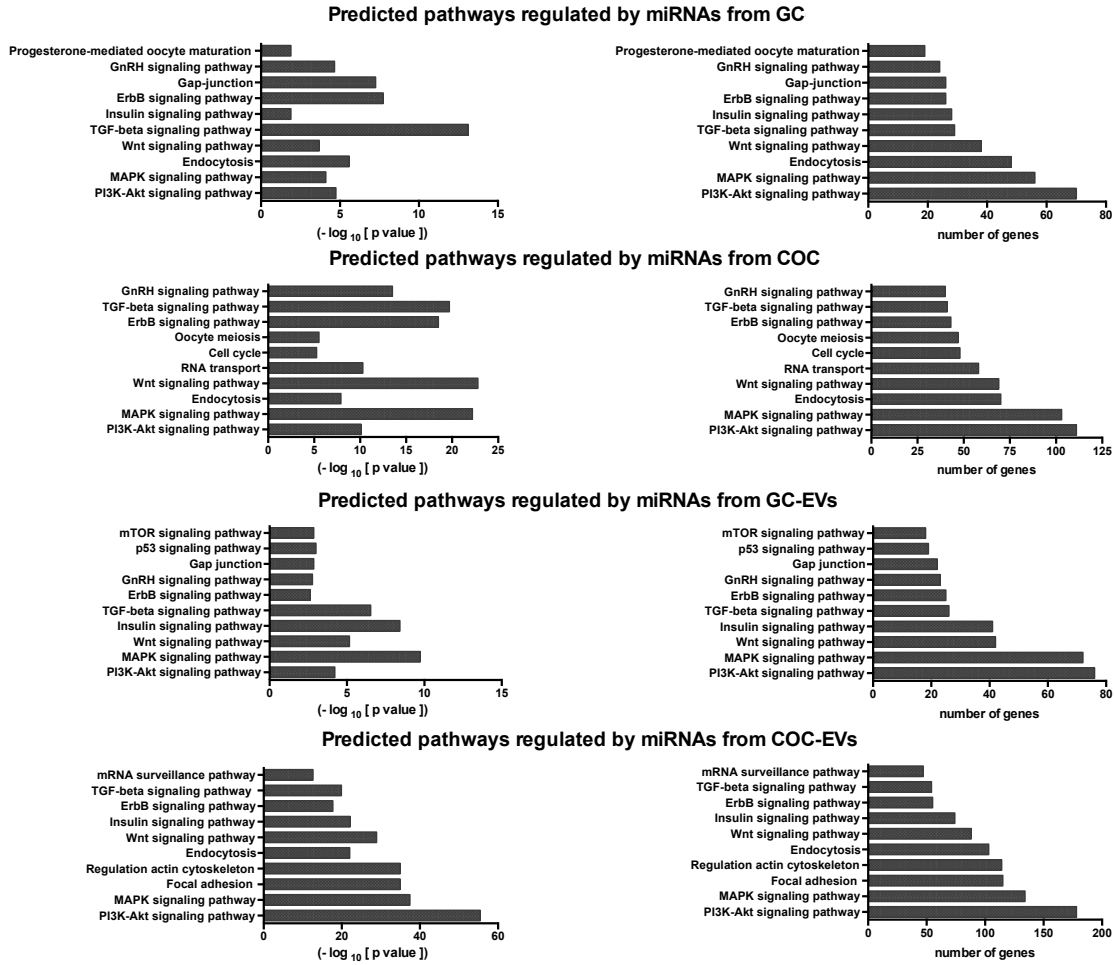

Similarly, different miRNAs from EVs also target PI3K-Akt pathway components with GC- and COC-derived EVs carrying 13 and 30 specific miRNAs that are known to regulate 76 and 178 genes, respectively, showing the relevance of this signalling pathway during follicular development. After determining the regulation of the PI3K-Akt pathway using bioinformatics analyses, we identified which of the 67 specific miRNAs in each of the groups showed strong evidence of targeting genes from the PI3K-Akt pathway using the miRTarBase tool. The results were as follows: CG (8 miRNAs), COC (16 miRNAs), GC-EV (13 miRNAs), and COC-LV (30 miRNAs). A total of 23 miRNAs, out of the 67 specifically identified in both FCs and EVs, showed strong evidence (after experimental validation) of interaction with PI3K-Akt pathway components (Figure 2).

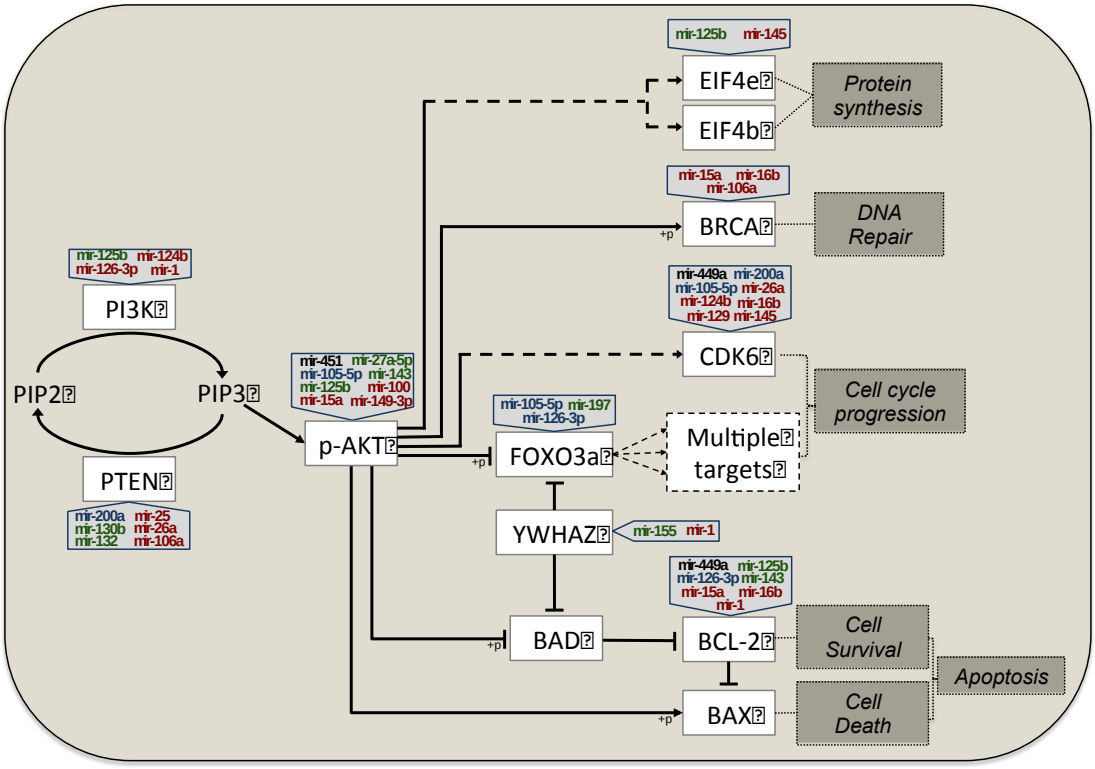

Individual oocyte competence and developmental rates

A total of 174 oocytes were collected and activated. Among these oocytes, 63.79% cleaved and 29.31% reached the blastocyst stage (Supplementary Table S4). Only routines with blastocyst/cleaved rates both higher than 35% were used in the following experiments.

Analysis of PTEN and PI3K transcripts and p-Akt protein levels in FCs in relation to oocyte competence

Since miRNAs present in GCs, COCs, and their respective EVs are predicted to be involved in the regulation of genes within the PI3K-Akt signalling pathway, we decided to investigate the mRNA levels corresponding to the main molecules within this pathway. mRNA levels of *PTEN* (a negative effector of the PI3K-Akt pathway) and *PI3K* (a positive effector) were determined in FCs of NC, CNB, and BL groups. Relative abundance of *PTEN* was significantly lower ($p < 0.05$) in FCs originated from follicles containing oocytes capable of generating blastocysts *in vitro* compared to those observed in FCs originated from follicles containing oocytes which could not reach this stage (Figure 3A). PTEN is responsible for converting PIP3 to PIP2 and maintaining low levels of PIP3, an Akt activator. Although *PI3K* levels appear to be increased in CNB and BL samples, no statistical differences among the oocyte quality groups were detected (Figure 3B). PI3K is responsible for converting PIP2 to PIP3 and therefore, is an important activator of this pathway.

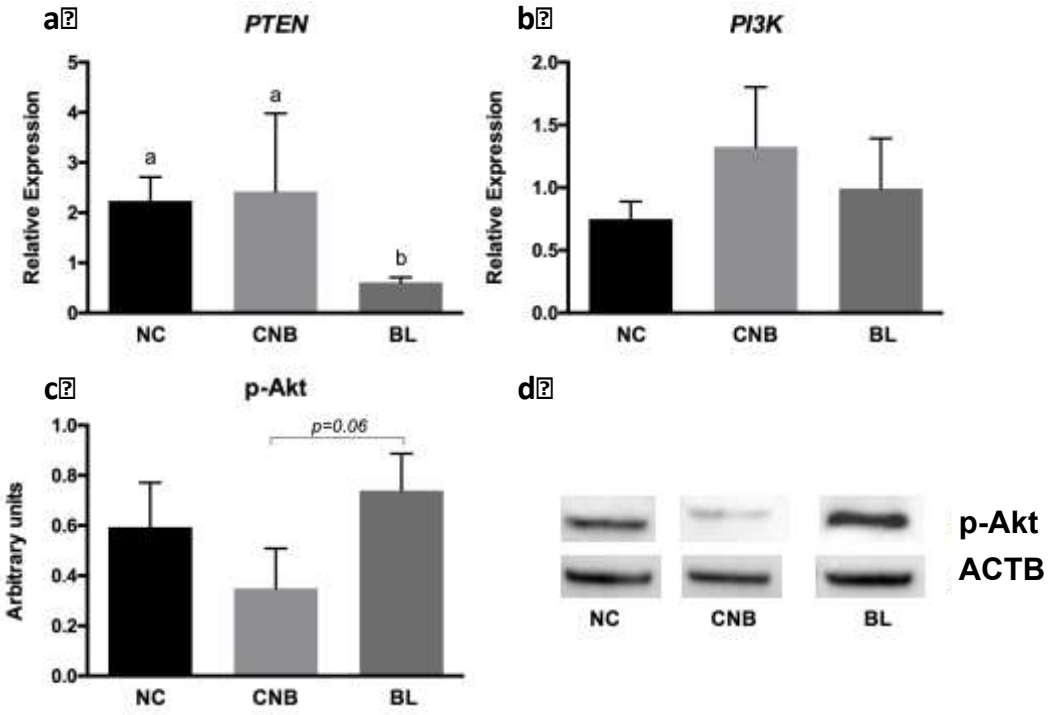

PI3K-Akt signalling pathway is modulated by the levels of PTEN and PI3K, which are responsible for Akt activation. In order to understand how the PI3K-Akt pathway influences oocyte competence, we evaluated the levels of phosphorylated Akt protein (p-Akt) in FCs within the distinct oocyte quality groups. Western blot analysis revealed increased levels of p-Akt ($p < 0.06$) in FCs originated from follicles that generated blastocysts (Figure 3C and 3D).

miRNA-494 and miR-20a analysis in FCs in relation to oocyte competence

We investigated the levels of bta-miR-494 and bta-miR-20a, two validated regulators of *PTEN* in humans and bovine, respectively[22,21]. The miR-494 presents a validated and conserved binding site across mammalian species, including bovine, using TargetScan (http://www.targetscan.org/). Additionally, bta-miR-20a was recently validated as a regulator of *PTEN* in bovine granulosa cells [21]. Relative levels of bta-miR-494 and bta-miR-20a were significantly higher ($p < 0.05$) in FCs derived from follicles in which the oocytes cleaved, regardless of subsequent blastocyst generation (CNB and BL), than in follicles in which the oocytes did not cleave (NC) (Figure 4A and 4B). Additionally, we performed a luciferase assay to demonstrate that miR-494 can regulate the *PTEN* by binding to its 3'UTR. Our results demonstrated that granulosa cells containing the vector with the wild copy of the *PTEN* 3'UTR have decreased firefly luciferase activity after transfection of the miR-494 mimic compared to the control and mutant construct, suggesting that miR-494 is a validated regulator of *PTEN* (Figure 4C).

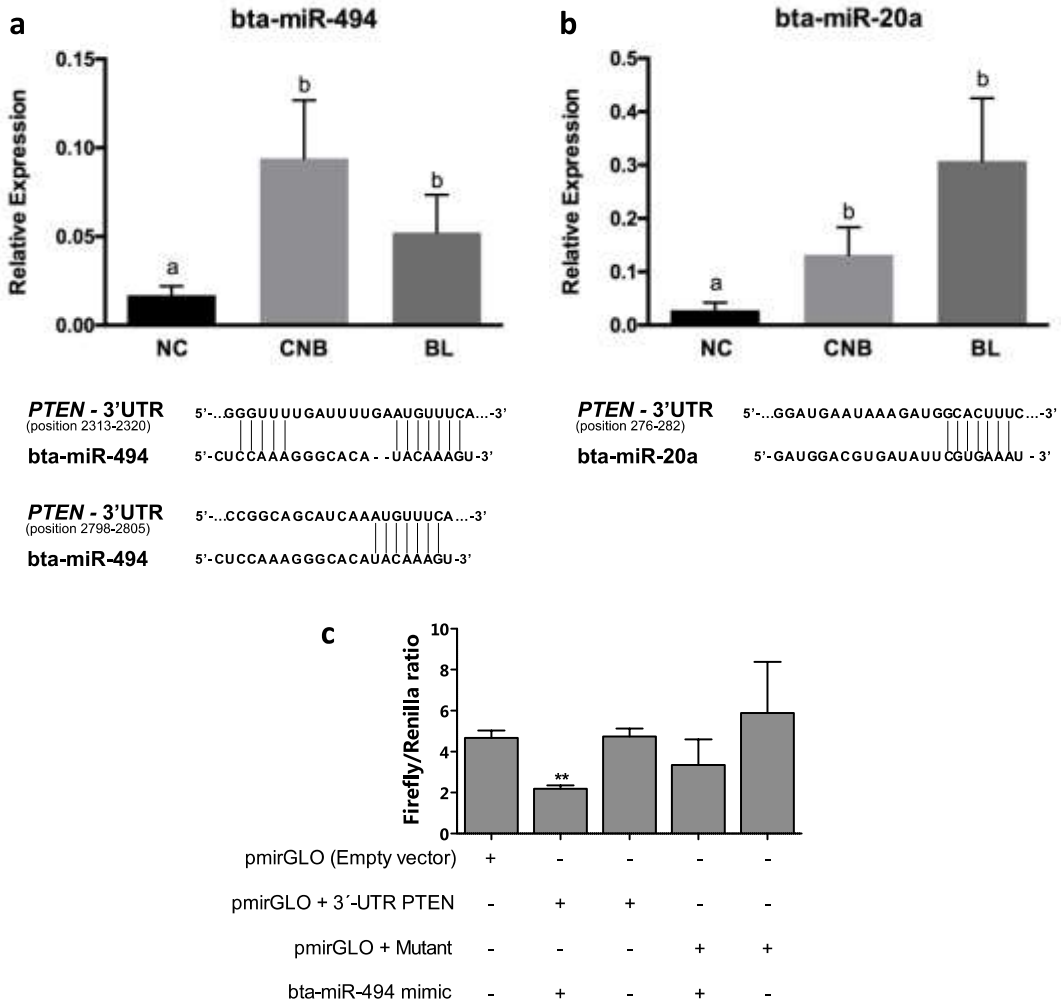

Analysis of PI3K-Akt regulated genes in FCs according to oocyte competence

The PI3K-Akt signalling pathway can lead to different cellular effects, including changes in protein synthesis, DNA repair, cell cycle progression, apoptotic signalling etc.. In order to identify the mechanisms by which PI3K-Akt regulation is influencing oocyte competence, we chose to analyse downstream genes related to different cellular effects using RT-PCR.

We analysed the mRNA levels of 8 genes (*BAX*, *BCL2*, *BRCA*, *CDK6*, *EIF4b*, *EIF4e*, *FOXO3a,* and *YWHAZ*) in FCs of different oocyte competence groups (Figure 5). Among these genes, only *BAX* and *FOXO3a* showed statistical differences between the competence groups. *BAX* levels were increased ($p < 0.05$) in the BL group although the ratio between *BAX/BCL-2* transcript levels did not differ among the groups. Similarly, *FOXO3a* mRNA levels were significantly increased ($p < 0.05$) in the BL and CNB groups compared to NC, inferring a possible FOXO3a-dependent cell cycle progression response.

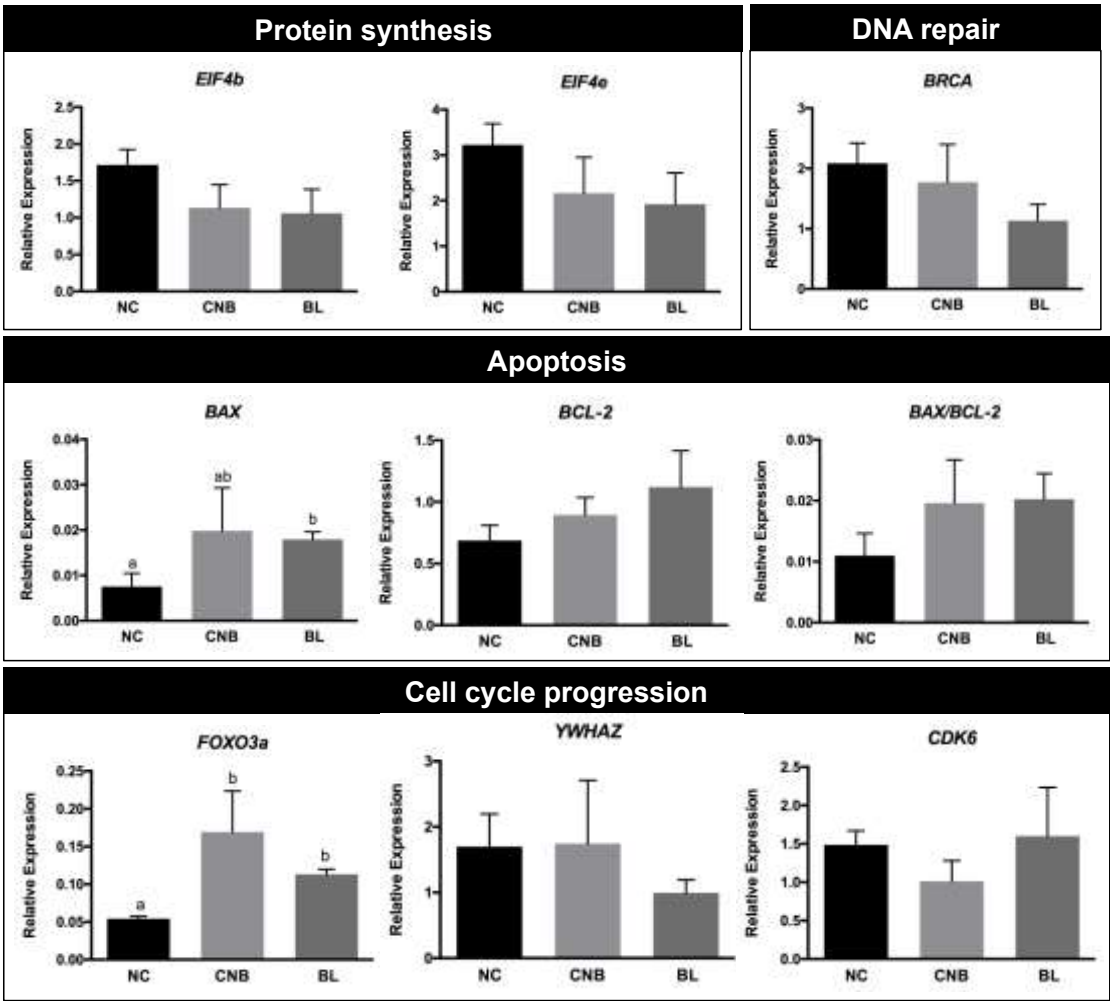

DISCUSSION

Ovarian follicle development and oocyte competence acquisition are complex events that result from the interaction between FCs, such as theca, granulosa, and cumulus, and the oocyte. MiRNA-controlled pathways related to oocyte meiosis and to the Wnt, TGF-beta, ErbB, Insulin, PI3K-Akt, and MAPK signalling pathways have been identified in bovine FCs (theca cells and GCs) and have been associated with follicular development[23]. Exosomal and non-exosomal miRNAs present in follicular fluid can control important pathways involved in oocyte quality[15]. Recently, miRNAs controlling the proliferation and cell cycle of GCs were identified in metabolic pathways downstream of the PI3K-Akt pathway[24]. Herein, we utilised a novel approach to identify pathways associated with oocyte competence. Initially, we determined the levels of miRNAs in GCs and COCs as well as in their respective EVs, 48 h after *in vitro* exposure to physiological levels of FSH in order to mimic the follicle environment. Functional analysis of the identified miRNAs indicate the modulation of the PI3K-Akt signalling pathway regardless of follicle compartment (GCs, COCs or its EVs) that originated the miRNAs.

In order to test if the components of this pathway can serve as predictors of oocyte quality, we dissected ovarian follicles, stored FCs, and individually activated oocytes to evaluate their developmental competences. *In vitro* parthenogenetic development allowed us to pool FCs in different groups using retrospective method, depending on oocyte competences, for subsequent RNA and protein experiments. Our

results demonstrated that the main members of the PI3K-Akt signalling family displayed different levels of expression or amounts of protein depending on oocyte quality. In addition, we investigated genes regulated by PI3K-Akt and observed an increase in *FOXO3a* levels suggesting the existence of mechanisms governing the modulation of cell-cycle progression, protection to oxidative stress, and anti-apoptotic response.

Regarding miRNAs differently expressed among cell and EV types, according to miRTarBase (http://mirtarbase.mbc.nctu.edu.tw/index.php), only one that was found to increase in COC cells, miR-15b, has strongly been validated in previous bovine studies. In mouse GCs, miR-15b is negatively controlled by FSH[25]. Some of these miRNAs, such as miR-342 or miR-542-5p, which showed increased levels in COCs in this study, were recently identified in EVs from bovine follicular fluid by Navakanitworakul and collaborators[26], displaying increased levels of expression in large follicles compared to small follicles. Additionally, miR-433 was increased in GC-EVs in our study, was linked to induction of senescence in ovarian cancer cells. Moreover, cells with high miR-433 expression level release this miRNA into growth media via exosomes, promoting a bystander effect[27].

Several miRNAs detected in the present study are exclusively found in GCs and COCs cells or their respective EVs (Tables 2 and 3) and have been described as key molecules for the regulation of the PI3K-Akt signalling pathway[20,19]. Examples of specific GC miRNAs related to PI3K-Akt signalling are miR-105[28], miR-126[29], and miR-200a[30]. Similarly, COC miRNAs associated with this pathway are miR-449[31] and miR-451[32,33]. Although most studies have been done in humans and are related to reproductive diseases, it has been unequivocally demonstrated that miRNA-dependent regulation of the PI3K-Akt signalling pathway is necessary for the correct gene balance governing this pathway, and eventually, reproductive success.

Oocyte growth and follicle development rely on the regulation of pathways involved in cell proliferation and survival, such as the PI3K-Akt signalling pathway[34]. Stimulation of PI3K promotes phosphorylation of Akt, resulting in follicle survival and activation of growth. Alternatively, this pathway is suppressed under the action of PTEN[35]. PTEN is involved in converting PIP3 to PIP2, and high levels of PTEN are responsible for decreasing the Akt pathway activity, consequently reducing cell proliferation[34,36]. In the present study, we detected high levels of PTEN mRNA and low levels of p-Akt protein in FCs from poor oocyte quality groups, suggesting that the PI3K-Akt signalling pathway is less active in these follicles. In addition, we observed decreased levels of bta-miR-494 and bta-miR-20a, two validated modulators of PTEN, in FCs of poor oocyte quality groups. The inhibition of PTEN in human ovary *in vitro* results in the increased activation of primordial follicles, but compromises the development of growing follicles[35]. In murine ovary, the deletion of PTEN in mouse oocytes resulted in pan-ovarian follicle activation and premature oocyte depletion, whereas disruption of granulosa cell-specific PTEN did not affect the initiation of follicle growth but increased GC proliferation and enhanced ovulation[37,17]. Down-regulation of PTEN was also caused by the up-regulation of miR-494 (a conserved miRNA among mammals) in human bronchial cells, demonstrating the importance of this mechanism in controlling PTEN levels[22]. Furthermore, we validate the interaction between miR-494 and the PTEN using the luciferase assay for the wild-type or the mutant 3'UTR. As predicted by bioinformatics analysis the presence of bta-miR-494 and the wild-type 3'UTR sequence reduced the levels of luciferase activity compared to control and the PTEN

mutant sequence. Therefore, these results demonstrate that bta-miR-494 is regulating the levels of *PTEN* in follicular cells. Similar analysis were performed for bta-miR-20a, which was validated as a regulator of PTEN in granulosa cells[21]. Thus, our results demonstrated that *PTEN* levels are regulated by the increase in miR-494 and miR-20a in follicles harbouring competent oocytes. Additionally, these results suggest that multiple miRNAs regulating the same mRNA target are necessary to induce a physiological response such as upregulation of AKT, which was observed in cells obtained from follicles associated with higher quality oocytes.

Thus, our data demonstrated that the components of the PI3K-Akt pathway such as PTEN, bta-miR-494, bta-miR-20a and p-Akt are associated, in the follicular environment, with the developmental potential and oocyte quality. The experimental model adopted in this study allowed us to evaluate the molecular profile of the PI3K-Akt pathway in follicular cells of low oocyte competence follicles (LCO, i.e., Non-Cleaved or Cleaved Non Blastocyst groups) and high oocyte competence (HCO; i.e. Bastocyst group). LCO follicular cells have a molecular profile marked by an increase in PTEN expression, lower expression of bta-miR-494, and decreased amounts of p-Akt, which indicates lower activity of the PI3K-Akt pathway. On the contrary, the HCO group has different indicator levels, confirming the increased activity of the PI3K-Akt pathway in this group. These two molecular profiles were associated with extreme oocyte competence, and based on previously described functions of the PI3K-Akt pathway in follicular environments, we can assume that these oocyte competence extremes are related to the regulation of cell proliferation, protection from oxidative stress, and apoptosis blockage in the FCs, as discussed below.

The PI3K-Akt signalling pathway, besides being involved in cell proliferation and survival, plays a role in apoptosis, protein synthesis, cell cycle, angiogenesis, DNA repair, and metabolic pathways etc., as reviewed by Lai and colaborators[38]. In the present study, we analysed the mRNA levels of genes related to different cellular processes, such as *BAX* and *BCL-2* (apoptosis), *BRCA* (DNA repair), *EIF4b* and *EIF4e* (protein synthesis), *FOXO3a* and *YWHAZ* (cell cycle progression), and *CDK6* (FOXO-independent cell cycle progression) in order to find, which intracellular events mediate the relation between the PI3K-Akt signalling pathway and oocyte ability to develop. We observed differences in the transcript levels of *FOXO3a* and *BAX* between FC groups, associated with different oocyte capacities of development.

Here, we found that *FOXO3a* levels are increased in FCs of higher quality oocytes. Transcription factor FOXO3a plays an important role in ovarian activity[39], and when activated, has broad anti-proliferative and pro-apoptotic cellular effects. Besides these effects, FOXO3a protects quiescent cells from oxidative stress[40]. In addition, FOXO3a has been reported to also protect mouse oocytes against oxidative stress[41]. The effects induced by FOXO3a elevations may also vary depending on the signal integration and associated factors, and may differ from triggering cell death to promoting survival by expression of oxidative stress resistance factors[42]. Since this study does not include the testing of other factors involved in FOXO3a regulation levels, apart from the p-Akt protein and the levels of *FOXO3a*, we cannot specify the final effects associated with FOXO3a in the FCs. However, since different levels of *FOXO3a* were found in FCs associated with oocyte competence, we can consider that the Akt-FOXO3a interaction acts in such cases by adjusting the regulation of oxidative stress response, cell proliferation, and leads to apoptosis by either favouring (in HCO) or preventing (in LCO) the acquisition of competence. We also assume that in the HCO group, the Akt-FOXO3a interaction promotes the transcription of

FOXO3a (since it acts as an enhancer for its own transcription), which could contribute to the regulation of ROS scavengers, and that Akt, being able to inhibit FOXO3a, allows a final proliferative and anti-apoptotic response in high competence follicles.

Another gene that displayed differences in expression levels among the developmental competence groups was *BAX*, which increased in the higher quality group. *BCL2* and *BAX* are anti-apoptotic and pro-apoptotic genes, respectively, which serve as markers for apoptosis identification in ovarian tissues[43]. Oocyte competence may be related to events linked to apoptosis, and it has been suggested that early apoptosis signals in the oocyte[44] or in GCs[45] are positively correlated with oocyte competence, suggesting the involvement of apoptotic processes in follicular and oocyte development. The pro-apoptotic or anti-apoptotic effects of *BCL-2* and *BAX* genes depend on protein-protein interactions. The BAX protein can form homodimers or heterodimers with BCL-2. The increase in the proportion of BAX homodimers in relation to BAX-BCL-2 heterodimers determines the triggering of cell death through apoptosis. So, the ratio *BAX/BCL-2* is the main indicator of the apoptotic process[46,47]. In this study, the *BAX/BCL-2* ratios showed no statistical differences among oocyte quality groups, and therefore, there is no clear evidence in our results that this ratio regulates the acquisition of oocyte competence, as previously suggested by Yang et al[48]. The homodimerisation of BAX and its translocation to the mitochondria to trigger apoptosis is under the direct influence of the p-Akt protein[49]. The p-Akt phosphorylates the BAX protein and regulates its activity, so phosphorylation of BAX prevents its translocation to mitochondria and induces its maintenance in the cytoplasm as an heterodimer through its association with BCL-2, preventing apoptosis. In the results described in this study, the BL group, besides displaying higher *BAX* levels, also has elevated p-Akt. Therefore, there is evidence that, in these cells, the elevation of *BAX* did not lead to higher incidence of apoptosis due to its low activity resulting from the phosphorylation induced by p-Akt. Furthermore, in the CNB group, *BAX* is elevated in the FCs, but not p-Akt, which may suggest a higher probability of apoptosis, even if the *BAX/BCL-2* ratio does not increase. Finally, the p-Akt also has effects on the control of apoptosis through the regulation of BCL-2 availability. BCL-2 and its associated death promoter (BAD) form heterodimers, precluding BCL-2 to be available to form heterodimers with BAX. Phosphorylation of BAD by p-Akt leads to the isolation of BAD per 14-3-3 proteins family, and the consequential anti-apoptotic effect[50]. Therefore, p-Akt, acting by either phosphorylation and sequestration of BAD or by phosphorylation of BAX, and its maintenance in the cytoplasm triggers the anti-apoptotic response within cells.

The mechanisms involved in the acquisition of oocyte competence have not yet been completely elucidated. The acquisition of oocyte competence is a multifactorial process, and while some basic processes are well known, such as the progression of meiosis and migration of cortical granules, some intracellular processes related to molecular events that lead to the formation of an oocyte capable of supporting development are still unclear. Several factors influence oocyte quality and regulate competence acquisition. However, an adequate follicular microenvironment is a key factor towards successful follicle growth, oocyte maturation and fertilisation, early embryo development, and even full-term development, allowing the generation of a healthy product[4]. In conclusion, our study demonstrated that miRNAs expressed in different compartments of the ovarian follicle microenvironment potentially regulate the PI3K-Akt signalling pathway.

Using a retrospective developmental competence model, we investigated whether the PI3K-Akt pathway could be associated with oocyte quality. This model allowed to compare the molecular profile of the PI3K-Akt signalling pathway members in FCs associated with LCO (i.e. in the FCs of the NC or CNB groups) and HCO (i.e. in FCs of the BL group). We were able to identify a molecular landscape formed by the PI3K-Akt pathway in FCs consisting of lower *PTEN* levels, higher p-Akt, *FOXO3a*, bta-miR-494, bta-miR-20a, and *BAX* levels, leading to high oocyte developmental potential (Figure 6). This molecular landscape is compatible with cellular responses related to oxidative stress protection, cell proliferation, and blockage of apoptosis, suggesting that these PI3K-Akt-induced cellular responses contribute to oocyte competence acquisition during oogenesis.

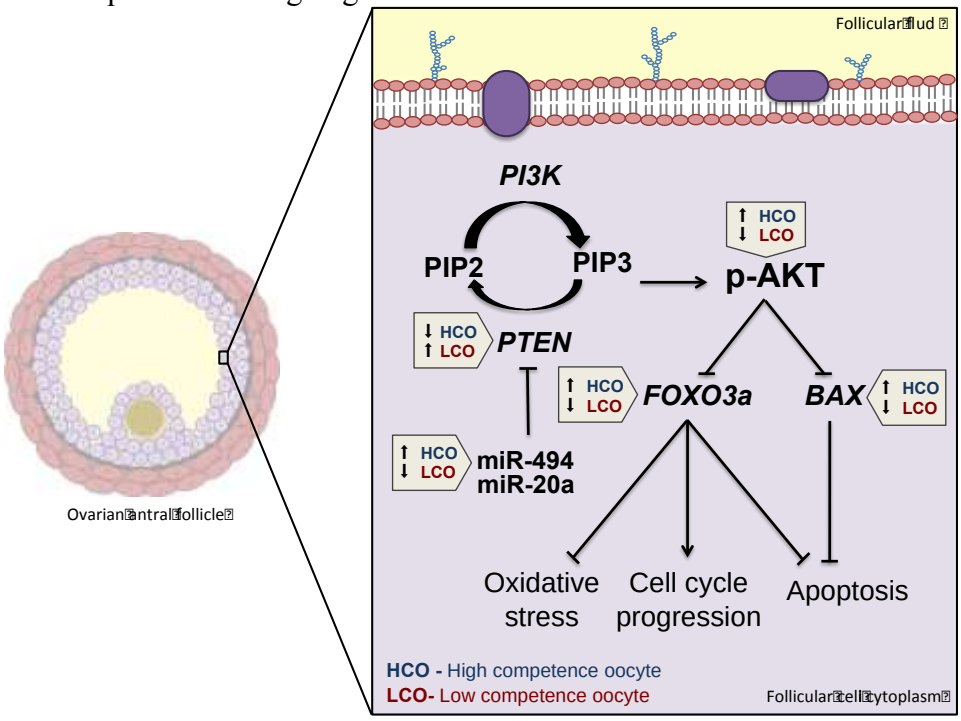

MATERIAL AND METHODS

This study was approved by the University of São Paulo Research Ethics Committee (Protocol number 14.1.674.74.0). Experiments were conducted in accordance with International Guiding Principles for Biomedical Research Involving Animals (Society for the Study of Reproduction). Unless otherwise stated, the reagents and culture media used were purchased from Sigma-Aldrich Chemical Company (St. Louis, MO, USA).

This study consists of two experiments (Figure 7). In the first experiment, we determined the miRNA profiles in GCs and COCs as well as in their respective EVs (GC-EVs and COC-EVs) and identified the pathways regulated by miRNAs exclusively expressed in each group. In the second experiment, ovarian follicles were dissected and loose FCs were stored, while COCs were subjected to *in vitro* maturation (IVM) and embryo development after parthenogenetic activation. The oocyte's ability to mature and sustain development until reaching the blastocyst stage after parthenogenetic activation was evaluated and used as the criteria to group FCs according to oocyte competence, retrospectively. FCs were used to investigate the PI3K-Akt components levels.

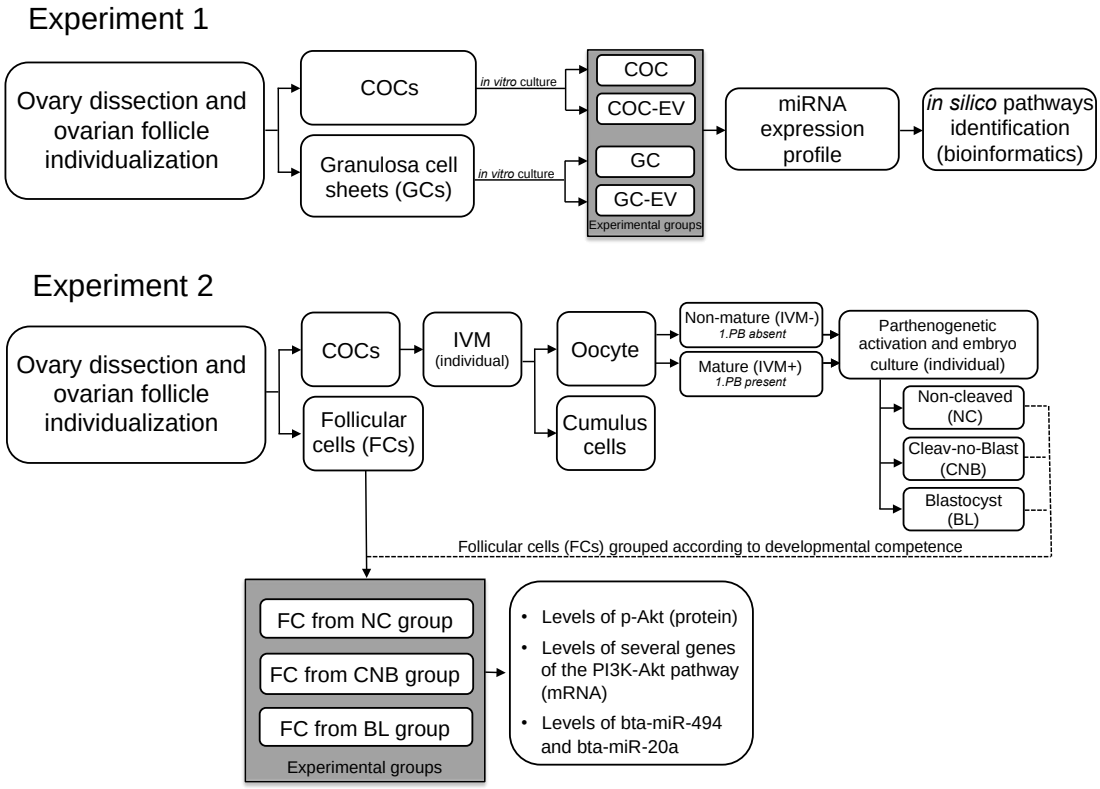

Experiment 1: Granulosa and cumulus-oocyte complex culture to identify miRNAs origin inside follicular environment

In order to identify the miRNAs present in different compartments of the ovarian follicles, as well as the contribution of miRNAs transiting within the follicular environment in EVs, three routines of bovine ovarian follicles were dissected and the follicular components were separated. Following follicle rupture, we identified and separated COCs and loose GCs before placing them in independent culture plates. After culturing the cells, the culture media were collected and RNAs were isolated from both the cells and respective EVs. Bioinformatics analyses were performed to identify metabolic pathways regulated by miRNAs in the different cell types and respective EVs. Additional and detailed information related to material and methods for experiment 1 can be found in the Supplementary material and methods.

Follicular dissection and cellular recovery

Ovaries were recovered from slaughterhouses. Follicles, ranging between 3 and 6 mm in diameter, were dissected and ruptured with 18G needles under a stereomicroscope. After rupture, COCs and loose GCs were collected for further experiments.

GC and COC cultures

After the follicle rupture, loose GCs and COCs were collected under the stereomicroscope using pipettes. The cell culture system was based on the protocol developed by Portela et al.[51] adapted from Gutiérrez et al[52]. At the end of the culture period our aim was to obtain cells similar to growing follicle cells. Both the cells and medium were collected 48 h after the FSH treatment and stored at -80 ˚C until RNA extraction.

EV isolation

EVs were isolated from GCs and COCs culture media using differential centrifugation and ultracentrifugation steps (modified from Crescitelli[53]). In order to determine the EVs size, 6 pellets (3 from GC-EVs and 3 from COC-EVs) were analysed using the Nanosight (Malvern, UK) instrument (Supplementary Figure S1). A second set of pellets was diluted in TRI-reagent BD (Molecular Research Center, Inc.) before storage at -80 ^{o}C.

RNA extraction

Total RNA (mRNAs and miRNAs) was extracted from three of each sample using a TRI-reagent or TRI-reagent BD (Molecular Research Center, Inc.) according to the manufacturer's instructions with some modifications.

GC, COC, and EV screening for miRNAs by RT-PCR

Briefly, the reverse transcription reaction was carried out with 100 ng of total RNA using the miScript PCR Starter Kit (Qiagen, Venlo & Limburg, the Netherlands) according to the manufacturer's instructions. The levels of 348 miRNAs and 3 housekeeping genes (miR-99b, RNU1, and RNU43) were investigated by RT-PCR using miScript SYBR Green PCR Kit (Qiagen, Venlo & Limburg, the Netherlands) with specific primers to miRNAs (Supplementary Table S5). Samples were analysed in triplicates and only miRNAs with Ct value under 37 and detected in at least 2 out of 3 samples in each group were considered as present.

Bioinformatics analyses of miRNAs according to cellular origin

Bioinformatics analyses were performed to identify miRNA-controlled pathways in FCs. As bioinformatics tools are based on human sequences the homology between bovine and human miRNA sequences were determined using miRBase, the homology of miRNA-gene interactions was identified using TargetScan. Additionally, pathway identification was performed using DIANA tools. The validation of target genes was accomplished using miRTarBase.

Experiment 2: Retrospective oocyte development competence model

In order to determine the levels of PI3K-Akt members in FCs of follicles containing oocytes with distinct development capacities, we developed an experimental model based on individual maturation of oocytes and culture of embryos. After maturation and embryo development, FCs were grouped according to oocyte competence. Prior to oocyte maturation, ovarian follicles were dissected, FCs (regardless of cell types) were obtained after centrifugation of follicular fluid and stored for further use, and COCs collected for individual IVM and embryo culture after parthenogenetic activation. At the end of the IVM, oocytes were denuded and classified depending on the presence or absence of first polar body in mature (IVM+) or non-mature (IVM-) ones, respectively. Regardless of the maturation status, denuded oocytes were individually activated parthenogenetically and placed in a droplet for embryo development *in vitro*. Embryos (zygotes) from the IVM+ group without signs of embryonic cleavages were classified as 'non-cleaved' (NC group). Embryos that started development (cleaved) but stopped before reaching the blastocyst stage were classified as 'cleaved non-blastocyst' (CNB group), while those who had reached the blastocyst stage composed the 'blastocyst' group (BL group).

FCs from NC, CNB, and BL groups were used to determine the levels of PI3K-Akt members in samples from follicles containing oocytes with different developmental capacities. Additional and detailed information related to material and methods for experiment 2 can be found in Supplementary material and methods.

Oocyte maturation, parthenogenetic activation, and single embryo culture

After follicle rupture, COCs were collected for single embryo culture as described in supplementary materials and methods and FCs were collected, washed by centrifugation (600 x *g*) to remove the follicular fluid, and immediately placed in liquid nitrogen for future analyses of the PI3K-Akt pathway components to retrospectively determine the follicle of origin. The oocyte maturation, parthenogenetic activation and single embryo culture procedure allowed us to classify oocytes and their respective FCs, according to their development competence.

RNA and protein extractions

Total RNA, including small RNA molecules, and proteins were extracted using either TRI-reagent or TRI-reagent BD (Molecular Research Center, Inc.) according to the manufacturer's instructions with some modifications. RNA concentrations were measured using a NanoDrop 2000 (Thermo Scientific) according to the manufacturer's protocol. Proteins were precipitated from the organic phase left from TRI reagent lysis and dissolved in 20 µL of 8 M urea.

Determination of mRNA and miRNA expressions by RT-PCR

Briefly, the reverse transcription reaction was carried out with 30 ng of total RNA per gene using a *High Capacity* cDNA reverse transcription kit (*Life Technologies*) according to the manufacturer's instructions. PCR amplification was performed with the resulting cDNA using sequence-specific forward and reverse oligonucleotide primers in custom-prepared plates for the indicated genes (Supplementary Table S6). Relative quantification of transcripts was determined by qPCR using ABI-7500 (Applied Biosystems).

For the miRNA-494 and miR-20a study, RT-PCR was performed with using miScript SYBR Green PCR Kit (Qiagen, Venlo & Limburg, the Netherlands), primer specific to miRNA target (Supplementary Table S5), and 0.1 µL cDNA. Real-time PCRs were performed using ABI-7500 (Applied Biosystems). The assays were analysed in quadruplicates and only the Ct values under 35 were considered.

Target gene validation using luciferase reporter assay

To experimentally validate the miRNA-mRNA interaction between bta-miR-494 and the PTEN gene, we constructed a plasmid vector with a fragment of the 3´-UTR harboring the conserved binding sites of bta-miR-494 (wild type construct) or fragment with mutant variants of the miRNA binding sequences (Mutant construct) inserted between the *SacI and XhoI* restriction sites downstream of pmirGLO Dual-Luciferase miRNA Target Expression Vector (Promega, Madison, USA). Plasmids were amplified and sequenced to verify the presence and absence of miRNA binding sites in the wild type and mutant constructs, respectively. Sub-confluent cells were co-transfected with either the wild type construct or the mutant construct in the presence or absence of bta-miR-494 mimic using lipofectamine 2000 transfection reagent (Invitrogen, Darmstadt, Germany). After 24 h, treated cells were lysed and shaking for 15 min. The activity of firefly luciferase and renilla was determined using Dual-

Glo luciferase assay kit (Promega, Madison, WI, USA) followed by luciferase assay reagent (LAR) and Stop & Glo reagent. Data was calculated as the ratio of firefly luciferase to renilla activity and compared with the group transfected with only empty vector.

Akt protein detection and quantitation by western blotting

Samples were separated on 12% SDS-polyacrylamide gels. The antibodies used was p-Akt1/2/3 antibody (Ser 473), a rabbit polyclonal IgG from Santa Cruz Biotechnology, at a 1:200 dilution (catalogue number SC-101629), a HRP-labelled anti-rabbit IgG (catalogue number #7074S - Cell Signaling) in TBST containing 1% BSA and a HRP labelled mouse monoclonal anti-beta-actin (ACTB) antibody (catalogue number A3854 - Sigma-Aldrich) to normalize the data. Blots treated with Clarity^{TM} Western ECL substrate (Bio-Rad) to visualise the proteins.

Statistical analyses

Data are displayed as means ± SEM of replicate samples. Statistical analyses were performed using the SAS 9.3 Software (SAS Institute). To assess statistical differences, ANOVA was performed respecting normality and homoscedasticity premises. Means were compared by Duncan test. When ANOVA premises were not satisfied, data were compared by Kruskal-Wallis test. Unless differently stated, a level of 5% was considered significant.

REFERENCES

1 Sirard, M. A. *et al.* The use of genomics and proteomics to understand oocyte and early embryo functions in farm animals. *Reproduction*, 117-129 (2003).

2 Lonergan, P., Rizos, D., Gutierrez-Adan, A., Fair, T. & Boland, M. P. Oocyte and embryo quality: Effect of origin, culture conditions and gene expression patterns. *Reproduction in Domestic Animals* **38**, 259-267, doi:10.1046/j.1439-0531.2003.00437.x (2003).

3 Mermillod, P. *et al.* Factors affecting oocyte quality: Who is driving the follicle? *Reproduction in Domestic Animals* **43**, 393-400, doi:10.1111/j.1439-0531.2008.01190.x (2008).

4 Krisher, R. L. In Vivo and In Vitro Environmental Effects on Mammalian Oocyte Quality. *Annual Review of Animal Biosciences, Vol 1* **1**, 393-417, doi:10.1146/annurev-animal-031412-103647 (2013).

5 Combelles, C. M. H., Holick, E. A., Paolella, L. J., Walker, D. C. & Wu, Q. Q. Profiling of superoxide dismutase isoenzymes in compartments of the developing bovine antral follicles. *Reproduction* **139**, 871-881, doi:10.1530/rep-09-0390 (2010).

6 Sirard, M. A. & Assidi, M. Screening for Oocyte Competence. *Oocyte Physiology and Development in Domestic Animals*, 191-206 (2013).

7 Gilchrist, R. B., Lane, M. & Thompson, J. G. Oocyte-secreted factors: regulators of cumulus cell function and oocyte quality. *Human Reproduction Update* **14**, 159-177, doi:10.1093/humupd/dmm040 (2008).

8 Buccione, R., Vanderhyden, B. C., Caron, P. J. & Eppig, J. J. FSH-induced expansion of the mouse cumulus oophorus in vitro is dependent upon a

specific factor (s) secreted by the oocyte. *Developmental biology* **138**, 16-25 (1990).
9 Downs, S. M. The influence of glucose, cumulus cells, and metabolic coupling on ATP levels and meiotic control in the isolated mouse oocyte. *Developmental Biology* **167**, 502-512, doi:10.1006/dbio.1995.1044 (1995).
10 da Silveira, J. C., Veeramachaneni, D. N. R., Winger, Q. A., Carnevale, E. M. & Bouma, G. J. Cell-Secreted Vesicles in Equine Ovarian Follicular Fluid Contain miRNAs and Proteins: A Possible New Form of Cell Communication Within the Ovarian Follicle. *Biology of Reproduction* **86**, doi:10.1095/biolreprod.111.093252 (2012).
11 Macaulay, A. D. *et al.* The Gametic Synapse: RNA Transfer to the Bovine Oocyte. *Biology of Reproduction* **91**, doi:10.1095/biolreprod.114.119867 (2014).
12 Cortez, M. A. *et al.* MicroRNAs in body fluids-the mix of hormones and biomarkers. *Nature Reviews Clinical Oncology* **8**, 467-477, doi:10.1038/nrclinonc.2011.76 (2011).
13 Friedman, R. C., Farh, K. K. H., Burge, C. B. & Bartel, D. P. Most mammalian mRNAs are conserved targets of microRNAs. *Genome Research* **19**, 92-105, doi:10.1101/gr.082701.108 (2009).
14 Donadeu, F. X., Schauer, S. N. & Sontakke, S. D. Involvement of miRNAs in ovarian follicular and luteal development. *Journal of Endocrinology* **215**, 323-334, doi:10.1530/joe-12-0252 (2012).
15 Sohel, M. M. H. *et al.* Exosomal and Non-Exosomal Transport of Extra-Cellular microRNAs in Follicular Fluid: Implications for Bovine Oocyte Developmental Competence. *Plos One* **8**, doi:10.1371/journal.pone.0078505 (2013).
16 Adhikari, D. & Liu, K. Molecular Mechanisms Underlying the Activation of Mammalian Primordial Follicles. *Endocrine Reviews* **30**, 438-464, doi:10.1210/er.2008-0048 (2009).
17 Reddy, P. *et al.* Oocyte-specific deletion of Pten causes premature activation of the primordial follicle pool. *Science* **319**, 611-613, doi:10.1126/science.1152257 (2008).
18 Makker, A., Goel, M. M. & Mahdi, A. A. PI3K/PTEN/Akt and TSC/mTOR signaling pathways, ovarian dysfunction, and infertility: an update. *Journal of Molecular Endocrinology* **53**, R103-R118, doi:10.1530/jme-14-0220 (2014).
19 Xu, M. & Mo, Y. Y. The Akt-associated microRNAs. *Cellular and Molecular Life Sciences* **69**, 3601-3612, doi:10.1007/s00018-012-1129-8 (2012).
20 Luo, X., Dong, Z., Chen, Y., Yang, L. & Lai, D. Enrichment of ovarian cancer stem-like cells is associated with epithelial to mesenchymal transition through an miRNA-activated AKT pathway. *Cell Proliferation* **46**, 436-446, doi:10.1111/cpr.12038 (2013).
21 Andreas, E. *et al.* MicroRNA 17–92 cluster regulates proliferation and differentiation of bovine granulosa cells by targeting PTEN and BMPR2 genes. *Cell and Tissue Research*, 1-12 (2016).
22 Liu, L. H., Jiang, Y. G., Zhang, H. Y., Greenlee, A. R. & Han, Z. Y. Overexpressed miR-494 down-regulates PTEN gene expression in cells transformed by anti-benzo(a)pyrene-trans-7,8-dihydrodiol-9,10-epoxide. *Life Sciences* **86**, 192-198, doi:10.1016/j.lfs.2009.12.002 (2010).

23 Zielak-Steciwko, A. E. *et al.* Expression of microRNAs and their target genes and pathways associated with ovarian follicle development in cattle. *Physiological Genomics* **46**, 735-745, doi:10.1152/physiolgenomics.00036.2014 (2014).
24 Gebremedhn, S. *et al.* MicroRNA-183-96-182 Cluster Regulates Bovine Granulosa Cell Proliferation and Cell Cycle Transition by Coordinately Targeting FOXO1. *Biology of Reproduction* **94**, doi:10.1095/biolreprod.115.137539 (2016).
25 Yao, N. *et al.* A network of miRNAs expressed in the ovary are regulated by FSH. *Frontiers in Bioscience* **14**, 3239-3244, doi:10.2741/4047 (2009).
26 Navakanitworakul, R. *et al.* Characterization and Small RNA Content of Extracellular Vesicles in Follicular Fluid of Developing Bovine Antral Follicles. *Scientific Reports* **6**, doi:10.1038/srep25486 (2016).
27 Weiner-Gorzel, K. *et al.* Overexpression of the microRNA miR-433 promotes resistance to paclitaxel through the induction of cellular senescence in ovarian cancer cells. *Cancer Medicine* **4**, 745-758, doi:10.1002/cam4.409 (2015).
28 Shen, G. *et al.* MicroRNA-105 suppresses cell proliferation and inhibits PI3K/AKT signaling in human hepatocellular carcinoma. *Carcinogenesis* **35**, 2748-2755, doi:10.1093/carcin/bgu208 (2014).
29 Kim, W. *et al.* miR-126 contributes to Parkinson's disease by dysregulating the insulin-like growth factor/phosphoinositide 3-kinase signaling. *Neurobiology of Aging* **35**, 1712-1721, doi:10.1016/j.neurobiolaging.2014.01.021 (2014).
30 Becker, L. E., Takwi, A. A. L., Lu, Z. X. & Li, Y. The role of miR-200a in mammalian epithelial cell transformation. *Carcinogenesis* **36**, 2-12, doi:10.1093/carcin/bgu202 (2015).
31 Yao, Y. L. *et al.* MiR-449a exerts tumor-suppressive functions in human glioblastoma by targeting Myc-associated zinc-finger protein. *Molecular Oncology* **9**, 640-656, doi:10.1016/j.molonc.2014.11.003 (2015).
32 Tian, Y. *et al.* MicroRNA miR-451 downregulates the PI3K/AKT pathway through CAB39 in human glioma. *International journal of oncology* **40**, 1105-1112 (2012).
33 Li, H.-Y., Zhang, Y., Cai, J.-H. & Bian, H.-L. MicroRNA-451 inhibits growth of human colorectal carcinoma cells via downregulation of Pi3k/Akt pathway. *Asian Pacific Journal of Cancer Prevention* **14**, 3631-3634 (2013).
34 Wang, L.-Q. *et al.* Regulation of primordial follicle recruitment by cross-talk between the Notch and phosphatase and tensin homologue (PTEN)/AKT pathways. *Reproduction, Fertility and Development* (2014).
35 McLaughlin, M., Kinnell, H. L., Anderson, R. A. & Telfer, E. E. Inhibition of phosphatase and tensin homologue (PTEN) in human ovary in vitro results in increased activation of primordial follicles but compromises development of growing follicles. *Molecular Human Reproduction* **20**, 736-744, doi:10.1093/molehr/gau037 (2014).
36 Maehama, T. & Dixon, J. E. The tumor suppressor, PTEN/MMAC1, dephosphorylates the lipid second messenger, phosphatidylinositol 3,4,5-trisphosphate. *Journal of Biological Chemistry* **273**, 13375-13378, doi:10.1074/jbc.273.22.13375 (1998).
37 Fan, H. Y., Liu, Z. L., Cahill, N. & Richards, J. S. Targeted disruption of Pten in ovarian granulosa cells enhances ovulation and extends the life span of

luteal cells. *Molecular Endocrinology* **22**, 2128-2140, doi:10.1210/me.2008-0095 (2008).
38 Lai, K., Killingsworth, M. & Lee, C. Gene of the month: PIK3CA. *Journal of clinical pathology* **68**, 253-257 (2015).
39 Brenkman, A. B. & Burgering, B. M. T. FoxO3a eggs on fertility and aging. *Trends in Molecular Medicine* **9**, 464-467, doi:10.1016/j.molmed.2003.09.003 (2003).
40 Kops, G. *et al.* Forkhead transcription factor FOXO3a protects quiescent cells from oxidative stress. *Nature* **419**, 316-321, doi:10.1038/nature01036 (2002).
41 Di Emidio, G. *et al.* SIRT1 signalling protects mouse oocytes against oxidative stress and is deregulated during aging. *Human Reproduction* **29**, 2006-2017, doi:10.1093/humrep/deu160 (2014).
42 Neri, C. Role and therapeutic potential of the pro-longevity factor FOXO and its regulators in neurodegenerative disease. *Frontiers in Pharmacology* **3**, doi:10.3389/fphar.2012.00015 (2012).
43 Driancourt, M. A. & Thuel, B. Control of oocyte growth and maturation by follicular cells and molecules present in follicular fluid. A review. *Reproduction Nutrition Development* **38**, 345-362, doi:10.1051/rnd:19980401 (1998).
44 Li, H. J. *et al.* Early apoptosis is associated with improved developmental potential in bovine oocytes. *Animal Reproduction Science* **114**, 89-98, doi:10.1016/j.anireprosci.2008.09.018 (2009).
45 Feng, W. G. *et al.* Effects of follicular atresia and size on the developmental competence of bovine oocytes: A study using the well-in-drop culture system. *Theriogenology* **67**, 1339-1350, doi:10.1016/j.theriogenology.2007.01.017 (2007).
46 Marx, D. *et al.* Differential expression of apoptosis associated genes bax and bcl-2 in ovarian cancer. *Anticancer Research* **17**, 2233-2240 (1997).
47 Raisova, M. *et al.* The Bax/Bcl-2 ratio determines the susceptibility of human melanoma cells to CD95/Fas-mediated apoptosis. *Journal of Investigative Dermatology* **117**, 333-340, doi:10.1046/j.0022-202x.2001.01409.x (2001).
48 Yang, M. Y. & Rajamahendran, R. Expression of Bcl-2 and Bax proteins in relation to quality of bovine oocytes and embryos produced in vitro. *Animal Reproduction Science* **70**, 159-169, doi:10.1016/s0378-4320(01)00186-5 (2002).
49 Gardai, S. J. *et al.* × Phosphorylation of Bax Ser184 by Akt Regulates Its Activity and Apoptosis in Neutrophils. *Journal of Biological Chemistry* **279**, 21085-21095 (2004).
50 Pugazhenthi, S. *et al.* Akt/protein kinase B up-regulates Bcl-2 expression through cAMP-response element-binding protein. *Journal of Biological Chemistry* **275**, 10761-10766, doi:10.1074/jbc.275.15.10761 (2000).
51 Portela, V. M., Zamberlam, G. & Price, C. A. Cell plating density alters the ratio of estrogenic to progestagenic enzyme gene expression in cultured granulosa cells. *Fertility and Sterility* **93**, 2050-2055, doi:10.1016/j.fertnstert.2009.01.151 (2010).
52 Gutierrez, C. G., Campbell, B. K. & Webb, R. Development of a long-term bovine granulosa cell culture system: Induction and maintenance of estradiol production, response to follicle-stimulating hormone, and morphological

characteristics. *Biology of Reproduction* **56**, 608-616, doi:10.1095/biolreprod56.3.608 (1997).
53 Crescitelli, R. *et al.* Distinct RNA profiles in subpopulations of extracellular vesicles: apoptotic bodies, microvesicles and exosomes. *Journal of extracellular vesicles* **2** (2013).

ACKNOWLEDGEMENTS
The authors like to thank the staff and students at the LMMD for all their help with the sample collections and laboratory procedures. This work was supported by grants from FAPESP (grant 2014/21034-3; grant 2014/22887-0; grant 2013/08135-2 and grant 2012/50533-2). The funders had no role in study design, data collection and analysis, decision to publish, or preparation of the manuscript.

AUTHOR CONTRIBUTIONS
G.M.A., J.C.S., F.V.M., and F.P designed the study; G.M.A and J.C.S. collected the samples; G.M.A., C.P., M.D.C., S.G. performed the experiments; G.M.A, J.C.S. and F.P analysed the data; G.M.A., J.C.S., D.T., and F.P. wrote the manuscript. All the authors discussed the results and reviewed the manuscript.

COMPETING INTERESTS
The authors declare no competing financial interests.

FIGURE LEGENDS
Figure 1. Most relevant pathways regulated by exclusive miRNAs of granulosa cells and cumulus-oocyte complexes and respective extracellular vesicles. Represented by graphics of number of genes and enrichment factor in granulosa cells (GCs), cumulus-oocyte complexes (COCs), and extracellular vesicles (GC-EVs and COC-EVs).
Figure 2. Schematic representation of the PI3K-Akt pathway. Solid lines indicate direct interactions, dashed lines indicate multiple step interactions, lines ending with arrowheads indicate stimulation, lines ending in bar indicate blockage, and the symbol 'p' indicates phosphorylation. Except for *BAD*, genes (enclosed in white boxes), other genes had their mRNA levels (*PI3K, PTEN, FOXO3a, YWHAZ, BCL-2, BAX, CDK6, BRCA, EIF4e, or EIF4b*) or protein levels (p-Akt) determined in ovarian follicular cells associated with different oocyte competences. Pentagons indicate bovine miRNAs exclusively identified in granulosa cells (GC; black) and in cumulus-oocyte complexes (COC; blue); or identified in GC-derived EVs (red) and in COC-derived EVs (green). Only miRNAs validated with strong evidence of interaction with the target gene are depicted.
Figure 3. PI3K-Akt components levels in oocyte quality groups. Relative expression of (**A**) *PTEN* and (**B**) *PI3K* mRNAs and (**C, D)** levels of phosphorylated Akt protein (p-Akt) in follicular cells of non-cleaved (NC), cleaved non-blastocyst (CNB), and blastocyst (BL) groups of oocyte quality. **C.** Normalized levels of p-Akt obtained from western blotting analyses. **D.** Representative protein bands of p-Akt (~ 60 kDa) and Actin B (ACTB; 42 kDa) from western blotting analyses. Bars depict means and error bars depict standard errors of the means. Differences were statistically significant when $p < 0.05$.

Figure 4. Relative levels of bta-miR-494 and bta-miR-20a in follicular cells. (A) Relative levels of bta-miR-494 in non-cleaved (NC), cleaved non-blastocyst (CNB), and blastocyst (BL) groups. Bovine miRNA-494 and its validated target *PTEN*. Bioinformatics analysis of the 3'UTR of *PTEN* indicated two conserved target sites among mammals. (B) Relative levels of bta-miR-20a in non-cleaved (NC), cleaved non-blastocyst (CNB), and blastocyst (BL) groups. (C) Luciferase assay of the bovine *PTEN* 3'UTR in granulosa cells. The firefly luciferase activity was evaluated in cells transfected the empty pmirGLO vector, the vector with the wild type *PTEN* 3'UTR insert, the vector with the mutated construct insert and evaluated by the transfection of the bta-miR-494 mimic. Different letters indicate $p<0.05$. ** indicate $p<0.01$.
Figure 5. Relative expression of mRNAs of genes responsible for the PI3K-Akt downstream cellular effects in non-cleaved (NC), cleaved non-blastocyst (CNB) and blastocyst (BL) groups. Bars depict means and error bars depict standard errors of the means. Different superscripts (a, b) indicate significant differences ($p < 0.05$).
Figure 6. Schematic representation of the PI3K-Akt signalling pathway model and cellular responses in ovarian follicular cells (FCs) associated with high (HCO) or low (LCO) competent oocytes. In this study, HCO were represented by FCs from the BL group while LCO were represented by FCs from either the CNB or the NC group or a combination of both. Pentagons indicate if a given component of the pathway was upregulated (upward arrow) or downregulated (downward arrow) in FCs of LCO and HCO. Lines ending with arrowheads indicate stimulation, whereas lines ending with bars indicate blockage.
Figure 7. Flowchart of the experiments 1 and 2 showing the formation of experimental groups and subsequent analysis. **COC** - cumulus-oocyte complex; **GC** - granulosa cells; **EVs** - extracellular vesicles; **FCs** follicular cells (granulosa and cumulus may be included); **IVM** - oocytes after IVM that did not showed the presence of the first polar body (1.CP); **IVM** - oocytes after IVM that showed the presence of the 1.CP; **NC** - embryos (or zygotes) derived through IVM, oocytes that did not undergo cleavage after parthenogenetic activation; **CNB** - embryos that underwent cleavage after parthenogenetic activation but did not reach the blastocyst stage; **BL** - blastocyst; **p-Akt** - phosphorylated Akt protein.

SUPPLEMENTARY FIGURE LEGENDS

Supplementary Fig. S1. Extracellular vesicle (EV) characterization by nanoparticle tracking analysis (NTA) and western blot. EV size was validated using Nanosight equipment (Malvern) and analysed with the NanoSight NTA Software v3.1. Videos were acquired at camera level 14 and room temperature (25 °C) using 50 nm, 100 nm, and 150 nm calibration beads (Malvern) in order to check size accuracy. Samples were introduced manually. Samples were analysed by recording between three and five 30 s videos. EVs were diluted at 1:500 in PBS. Vesicles size was defined as the mode and the mean determined from the acquired videos. **A**. EV size mode with standard deviation bars; **B**. Nanosight analysis showing EV concentration. **C**. NTA results of one representative COC-EVs sample showing concentration and size **D**. NTA results of one representative GC-EVs sample showing concentration and size. In order to investigate the EVs contents, we performed a western blotting analysis using the same methods than those described in Materials and Methods but with Alix (SC-49267) and CD63 (SC-15363) as primary antibodies. Western blot analysis

demonstrated the presence of ALIX and CD63 in EVs isolated from COC and GC culture media. Protein detection in EVs originated from COCs is low due to the low amount of EVs isolated from these cells. **E**. Western blotting demonstrating the detected bands for ALIX and; **F.** for CD63.

SUPPLEMENTARY TABLES

Supplementary Table S1. A complete list of miRNAs identified in bovine granulosa cells (GCs) and cumulus-oocyte complexes (COCs) with their respective Ct values and standard deviations.

Supplementary Table S2. Homology between bovine and human miRNA sequences (5'-3'). Bold letters indicate a mismatch.

Supplementary Table S3. Homology of interaction between miRNAs and 3'UTR of the target genes in bovines and humans.

Supplementary Table S4. Routines of individual parthenogenetic bovine embryo development displaying blastocyst/cleaved rates higher than 35%.

Supplementary Table S5. Mature bovine miRNA sequences present in the profiler plate.

Supplementary Table S6. Bovine primer sequences used in the RT-PCR amplification.

Acknowledgements

First, I would like to thank Prof. Cremonesi and Dr. Lange-Counsiglio for welcoming me in their laboratory of the Reproduction Unit: they taught me all the abilities that I used in preparing this thesis and have enriched my professional experience.

I thank all the collaborators who participated in the experiments contained in this thesis, without which certain results would not be obtained.

I thank the professor Perecin for welcoming me for six months in his laboratory, to allow me to do this work experience abroad and conduct experiments part of a scientific work.

Eventually, I thank all the students attending the laboratory of Reproduction Unit that led along with me all the experiments that bring to the essential results in the drafting of this thesis.